Universitat Politècnica de València
Departamento de Máquinas y Motores Térmicos

Study of the degradation of new lubricant oil formulations with the design and demands of current and future engines

Doctoral Thesis
Presented by:
Antonio García Barberá
Supervised by:
Dr. Bernardo Tormos Martínez

València, January 2022

Doctoral Thesis

Study of the degradation of new lubricant oil formulations with the design and demands of current and future engines

Presented by: Antonio García Barberá
Supervised by: Dr. Bernardo Tormos Martínez

Tribunal:

President: Dr. Raúl Payri Marín
Secretary: Dr. Lino Montoro Moreno
Vocal: Dr. José Martín Herreros

External Evaluators:

Dr. José Martín Herreros
Dr. José Torres Farinha
Dr. Yesid Antonio Gómez Estrada

València, January 2022

Resumen

El análisis de los aceites lubricantes de motor, englobado dentro de las tareas realizadas en el Oil Condition Monitoring (OCM), resulta ser una herramienta poderosa con la cual se es capaz de extraer información de utilidad. Por este motivo, en esta Tesis se decidió explotar este campo realizando un estudio en profundidad centrado en tres aspectos: mejorar las técnicas y protocolos ya existentes, desarrollar procedimientos propios acorde con las necesidades y requisitos del momento y, para terminar, poner en valor la información obtenida del análisis de los lubricantes mediante el uso de tratamientos estadísticos y quimiométricos. Bajo estas tres premisas, se ha desarrollado toda la tarea de investigación de esta Tesis.

En primer lugar, en relación con el análisis de los aceites lubricantes, se realizó un estudio acerca de la degradación de cuatro formulaciones de aceites lubricantes. En este estudio se analizaron aspectos propios de los aceites como: su viscosidad cinemática, oxidación, nitración, caída de los aditivos antioxidantes, etc. así como parámetros de desgaste de motor (monitorizando la presencia de metales). Como resultado de este estudio fue posible encontrar limitaciones en las técnicas actuales, lo cual condujo a realizar mejoras y/o adaptaciones de estas técnicas para conseguir obtener la información deseada.

A continuación, debido a la disponibilidad de una cantidad de datos considerable, fruto del trabajo realizado durante todo el tiempo de duración de la Tesis, se decidió emplear toda ella para conseguir extraer la máxima información posible gracias al uso de tratamientos estadísticos y quimiométricos. Este trabajo, nuevo en la línea, se dividió en dos vertientes: la primera focalizada en el conjunto de datos de los aceites ya caracterizados (procedentes del estudio de la degradación de los aceites) y la otra parte en encontrar sinergias entre las técnicas espectroscópicas (FT–IR y NIR) y los ensayos de caracterización de los lubricantes. Como resultado de ello, se obtuvieron relaciones entre parámetros que anteriormente no se tenían presentes, así como modelos predictivos de propiedades de los lubricantes a partir del análisis de sus espectros.

Por último, el siguiente aspecto tratado en esta Tesis es una consecuencia de la necesidad de, en ciertas situaciones, disponer de información acerca de uno o varios parámetros de una determinada forma y con un grado de precisión elevado. El caso en cuestión analizado en la Tesis está relacionado con la cuantificación de hollín en el aceite

lubricante. Respecto a la cuantificación del hollín se requirió encontrar una técnica que fuera capaz de aportar información de una forma rápida y, además, poder detectar pequeños cambios. Esta técnica fue la espectroscopia Ultravioleta-Visible, con la cual se diseñó un protocolo analítico que permitiera trabajar con muestras de aceites lubricante con muy poco uso y, por ende, poca cantidad de hollín disuelta, consiguiendo resultados muy satisfactorios en periodos de tiempo cortos.

El presente documento de Tesis se encuentra redactado en dos idiomas: en español y en inglés. Principalmente el documento se encuentra redactado en inglés para hacer especial énfasis en aquellas labores de investigación desarrolladas en esta etapa, así como los resultados derivados de los diferentes estudios realzados. Mientras que, la parte confeccionada en español hace referencia a aquellos aspectos más descriptivos del documento de Tesis.

Resum

L'anàlisi dels olis lubrificants de motor, englobat dins de les tasques realitzades en el Oil Condition Monitoring (OCM), resulta ser una eina poderosa amb la qual s'és capaç d'extraure informació d'utilitat. Per aquest motiu, en aquesta Tesi es va decidir explotar aquest camp realitzant un estudi en profunditat centrat en tres aspectes: millorar les tècniques i protocols ja existents, desenvolupar procediments propis d'acord amb les necessitats i requisits del moment i, per a acabar, posar en valor la informació obtinguda de l'anàlisi dels lubrificants mitjançant l'ús de tractaments estadístics i quimiomètrics. Sota aquestes tres premisses, s'ha desenvolupat tota la tasca d'investigació d'aquesta Tesi.

En primer lloc, en relació a l'anàlisi dels olis lubrificants, es va realitzar un estudi sobre la degradació de quatre formulacions d'olis lubrificants. En aquest estudi es van analitzar aspectes propis dels olis com: la seua viscositat cinemàtica, oxidació, nitració, caiguda dels additius antioxidants, etc. així com paràmetres de desgast de motor (monitorant la presència de metalls). Com a resultat d'aquest estudi va ser possible trobar limitacions en les tècniques actuals, la qual cosa va conduir a realitzar millores i/o adaptacions d'aquestes tècniques per a aconseguir obtindre la informació desitjada.

A continuació, a causa de la disponibilitat d'una quantitat de dades considerable fruit del treball realitzat durant tot el temps de duració de la Tesi, es va decidir emprar tota ella per a aconseguir extraure la màxima informació possible gràcies a l'ús de tractaments estadístics i quimiomètrics. Aquest treball, nou en la línia, es va dividir en dos vessants: la primera focalitzada en el conjunt de dades dels olis ja caracteritzats (procedents de l'estudi de la degradació dels olis) i l'altra part a trobar sinergies entre les tècniques espectroscòpiques (FT–IR i NIR) i els assajos de caracterització dels lubrificants. Com a resultat d'això, es van obtindre relacions entre paràmetres que anteriorment no es tenien presents així com models predictius de propietats dels lubrificants a partir de l'anàlisi dels seus espectres.

Finalment, el següent aspecte tractat en aquesta Tesi és una conseqüència de la necessitat de, en unes certes situacions, disposar d'informació sobre un o diversos paràmetres d'una determinada forma i amb un grau de precisió elevat. El cas en qüestió analitzat en la Tesi està relacionat amb la quantificació de sutge (soot en anglès). Respecte a la quantificació del soot es va requerir trobar una tècnica que fora capaç

d'aportar informació d'una forma ràpida i, a més, poder detectar xicotets canvis. Aquesta tècnica va ser l'espectroscòpia Ultravioleta-Visible, amb la qual es va dissenyar un protocol analític que permetera treballar amb mostres d'olis lubrificant amb molt poc ús i, per tant, poca quantitat de soot dissolta, aconseguint resultats molt satisfactoris en períodes de temps curts.

El present document de Tesi es troba redactat en dos idiomes: en espanyol i en anglès. Principalment el document es troba redactat en anglès per a fer especial èmfasi en aquelles labors d'investigació desenvolupades en aquesta etapa així com els resultats derivats dels diferents estudis realitzats. Mentre que, la part confeccionada en espanyol, fa referència a aquells aspectes més descriptius del document de Tesi.

Abstract

The analysis of engine lubricating oils, encompassed within the tasks carried out in Oil Condition Monitoring (OCM), is a powerful tool with which it is possible to extract useful information. For this reason, in this Thesis, it has been decided to exploit this field by carrying out an in-depth study focusing on three aspects: improving existing techniques and protocols, developing our own procedures in accordance with current needs and requirements and finally, adding value to the information obtained from the analysis of lubricants through the use of statistical and chemometric treatments. All the research work in this Thesis has been carried out under these three premises.

Firstly, in relation to the analysis of lubricating oils, a study was carried out on the degradation of four lubricating oil formulations. This study analysed aspects of the oils, such as their kinematic viscosity, oxidation, nitration, antioxidant additives depletion, etc., and engine wear parameters (monitoring the presence of metals). Thanks to this study, it was possible to find limitations in the current techniques, which led to improvements and/or adaptations of these techniques in order to obtain the desired information.

Next, due to the availability of a considerable amount of information resulting from the work carried out throughout the Thesis, it was decided to use all of these data to extract as much information as possible, thanks to the use of statistical and chemometric treatments. This work, new in the research line, was divided into two parts: the first focused on the dataset of oils already characterised (from the study of oil degradation) and the other on finding synergies between spectroscopic techniques (FT–IR and NIR) and lubricant characterisation tests. As a result, relationships between previously unknown parameters were obtained and also predictive models of lubricant properties based on the analysis of their spectra.

Finally, the next aspect dealt with in this Thesis is a consequence of the need, in certain situations, to have information about one or more parameters in a particular form and with a high degree of accuracy. The case in question analysed in the Thesis is related to the quantification of soot. Concerning soot quantification, it was necessary to find a technique capable of providing information quickly and, in addition, detecting small changes. This technique was Ultraviolet-Visible spectroscopy, with which an analytical protocol was designed to work with samples of lubricating

oils with very little use and, therefore, with a small amount of dissolved soot, achieving very satisfactory results in short periods of time.

This Thesis document is written in two languages: Spanish and English. The document is mainly written in English to place special emphasis on the research work carried out at this stage and the results derived from the different studies carried out. The part written in Spanish refers to the more descriptive aspects of the Thesis document.

– All sorts of things can happen when you're open to new ideas and playing around with things. –
Stephanie Kwolek

A todos aquellos que se preocuparon y se preocupan por mí y me han acompañado en este viaje.

Agradecimientos

Con estas líneas me gustaría expresar mi más sincero agradecimiento a todos mis compañeros de camino que han hecho posible que durante el transcurso de esta aventura no me desviase de la senda marcada y llegase a buen puerto.

En primer lugar, quería hacer mención a mi tutor y director de tesis Bernardo Tormos, por toda la confianza depositada en mí y la paciencia y compresión que me ha mostrado durante todos estos años. Y, en segundo lugar, al instituto CMT-Motores Térmicos de la Universitat Politècnica de València por permitirme formar parte de la gran familia de profesionales que componen este prestigioso centro de investigación, haciendo una mención especial a Francisco Payri y José María Desantes por aceptarme y facilitarme todos los recursos necesarios para el desarrollo de mis Tesis doctoral. En esta misma línea quiero agradecer a Vicente Macián, director de la línea de Ingeniería de Mantenimiento, por recibirme como uno más dentro del grupo de trabajo. No me gustaría terminar antes sin agradecer al resto de compañeros que se han visto involucrados, por suerte o por desgracia, en diferentes tareas y trabajos realizados durante esta etapa: Santiago, Juanma, Figo, Fito, Toni, José, Daniel, Omar, Valentín y Vicentón. Así como el personal de gestión y administración del instituto: Amparo, Haby, Elena, Elvira, Carmina y Ricardo.

My most sincere gratitude to Professor Athanasios Tsolakis, who received me at the School of Mechanical Engineering of the University of Birmingham during my research stay, taking into account the global pandemic situation that modified the route plan. Despite this, the time I enjoyed with him and his group was most enriching. In addition, taking advantage of the opportunity, I thank you for your warm welcome to the great people with whom I shared residence and WhatsApp group.

A continuación, me gustaría agradecer a todas aquellas personas que han compartido despacho conmigo: Leo y Guillermo, y a las aquellas con las que disfruté tiempo de laboratorio: Juan Pablo, Álex, Jorge (tanto en su etapa de TFG como de TFM), Miquel, Juan Diego y Carlos. Y, de entre todos ellos nombrar a Antonio y a Sophia, con los que compartí penas y glorias, luces y sombras durante estos años, lo cual nos hizo mejorar y afianzar nuestra amistad. A todos ellos, gracias.

Por último, pero no menos importante, a toda mi familia y seres queridos que no han dejado nunca de apoyarme y animarme a lograr todos mis propósitos vitales. Gran parte de lo qué soy y cómo soy se lo debo a ellos. Gracias por estar siempre ahí.

Espero no haberme dejado a nadie por el camino, no fue mi intención. Todo aquel que se sienta alegre por verme completar esta etapa significa que de una forma u otra ha influenciado a que se produzca, que no les quepa duda de que una fracción de este trabajo se la debo a todos (sin lugar a duda).

Table of Contents

Index of Figures

Index of Tables

Nomenclature

Latin

ΔH	Variación de Entalpía
A	Factor de frecuencia o pre-exponencial
$Abs.$	Absorbance
C	Concentration
c_p	Calor específico
E	Energía
E_a	Energía de Activación
EP	Endpoint o Punto Final en español
EQP	Equivalence Point o Punto de Equivalencia en español
f	Coeficiente de Fricción
F	Constante de Faraday, 96487 C/mol
F_N	Fuerza Normal
g	Aceleración de la gravedad
h	Espesor de la película de aceite lubricante
H	Número de Hersey
i	Intensidad de la corriente, en amperes
I	Intensity of the light in the detector
I_0	Intensity of the light source
k	Constante de velocidad de la reacción
KV	Viscosidad Cinemática
l	Longitud
L	Thickness of the medium or path lenght
M_r	Masa molecular, g/mol
n	Engine speed

n_e	Número de electrones
p	Presión
Q	Cantidad de carga, cuyas unidades son Coulombs
r	Coordenada de transcurso de la reacción
r	Correlation coefficient
r	Radio
R	Constante de los Gases Ideales
R	Rugosidad superficial
R^2	Coefficient of determination
RSD	Relative Standard Deviation
S	Gradiente de velocidades o Shear Rate
$S_{aparente}$	Velocidad de cizallamiento aparente
t	Tiempo
T	Periodo
T	Temperatura
$Trn.$	Transmittance
v	Velocidad
v	Velocidad de reacción

Greek

α	Coeficiente de relación de la viscosidad con la presión
β	Coeficiente de relación de la viscosidad con la temperatura
γ	Tensión Superficial
δ	Disminución logarítmica de la amplitud
ϵ	Molar Absorption Coefficient
η	Viscosidad Dinámica
θ	Ángulo de giro o Crank angle
κ	Conductividad térmica
λ	Longitud de onda
ν	Viscosidad Cinemática
ν	Frecuencia
$\bar{\nu}$	Número de onda
ρ	Densidad
τ	Cizalladura o esfuerzo cortante

Acronyms

AA	Compuestos aromáticos

ACEA	Association des Constructeurs Europeens d'Automobiles European Automobile Manufacturers Association
AF	Aditivos Anti–espumantes
AFNOR	Association française de Normalisation
AO	Aditivos Antioxidantes
API	American Petroleum Institute
ASTM	American Society for Testing and Materials
ATIEL	Association Technique de l'Industrie Européenne des Lubrifiants
ATR	Attenuated Total Reflectance
AW	Aditivos Anti–desgaste o Antiwear additives
BDC	Bottom Dead Center
BMEP	Brake Mean Effective Pressure
BTSA	Bench Top Soot Analyzer
CAD	Crank Angle Degree
CEC	Coordinating European Council
CFD	Computational Fluid Dynamics
CI	Compression Ignition engine
CIDI	Compression Ignition Direct Injection
COC	Cleveland Open Cup
CNG	Compressed Natural Gas
DD	Aditivos Detergentes y Dispersantes
DI	Direct Injection engine
DIN	Deutsches Institut für Normung
DOC	Catalizador de Oxidación Diesel o Diesel Oxidation Catalyst
DPF	Filtro antipartículas Diesel o Diesel Particulate Filter
EEV	Energy Efficient Vehicles
EGR	Recirculación de Gases de Escape o Exhaust Gas Recirculation
EOLCS	Engine Oil Licensing and Certification System
EP	Aditivos de Extrema-presión
EPR	Electron Paramagnetic Resonance
ETG	Etilenglicol
FID	Flame Ionization Detector
FM	Aditivos Modificadores de Fricción
FT–IR	Fourier–Transform Infrared
GC	Gas Chromatography

GCD	Gas Chromatographic Distillation
GPF	Filtro antipartículas Gasolina o Gasoline Particulate Filter
GPR	Gaussian Process Regression
HATR	Horizontal Attenuated Total Reflectance
HC	Hydrocarbons o Hidrocarburos
HP–EGR	High Pressure loop EGR
HRTEM	High Resolution Transmission Electron Microscopy
ICE	Internal Combustion Engine o Motor de Combustión Interna
ICP–OES	Inductively Coupled Plasma Optical Emission Spectroscopy
ILSAC	International Lubricant Standardization and Approval Committee
IP	Injection Pressure
IP	Institute of Petroleum
ISF	Insoluble Fraction
ISO	International Organisation for Standardisation
ISO-VG	International Standards Organization Viscosity Grade
IUPAC	International Union of Pure and Applied Chemistry
IV	Índice Viscosidad
JIS	Japanese Industrial Standards
JPI	Japan Petroleum Institute
JSA	Japanese Standards Association
KF	Karl Fischer
LOD	Limit of Detection
LP–EGR	Low Pressure loop EGR
LR	Linear Regressions
LVEO	Low Viscosity Engine Oils
MARS	Monotone Advection and Reconstruction Scheme
MCIA	Motor de Combustión Interna Alternativo
MDA	Aditivos Desactivadores de Metales
MoI	Fuel Mass of Injection
MS	Mie Scattering
MVIN	Medium Viscosity Index Naphthenic
M–UV	Middle Ultraviolet
N	Compuestos nafténicos
NIR	Near–Infrared

NN	Número de Neutralización
NOx	Óxidos de Nitrógeno
N–UV	Near Ultraviolet
ODI	Período de Cambio de Aceite o Oil Drain Interval
OCM	Oil Condition Monitoring
OEM	Fabricante de Equipo Original o Original Equipment Manufacturer
P	Compuestos parafínicos
PAG	Polialquilenglicol
PAO	Polialfaolefina
PCA	Principal Component Analysis
PES	Photoelectron Spectroscopy
PG	Propilenglicol
PIO	Poli-interna-olefina
PISO	Pressure Implicit with Splitting of Operators
PLS	Partial Least Squares
PM	Material Particulado o Particulate Matter
PPD	Aditivos Depresores del Punto de Fluidez o Pour Point Depresant
RMSE	Root Mean Square Error
RPD	Ratio of Predictive Deviation
RS	Rayleigh Scattering
S	Hidrocarburos saturados
SAE	Society of Automotive Engineers
SCR	Reducción Catalítica Selectiva o Selective Catalytic Reduction
SEM	Scanning Electron Microscopy
SEP	Standard Error of Performance
SI	Sistema Internacional de Unidades
SI	Spark Ignition engine
SiE	Soot in Exhaust
SiO	Soot in Oil
SOF	Soluble Organic Fraction
SoI	Start of Injection
SOx	Óxidos de Azufre
SP2	Single–Particle soot Photometer
SVM	Support Vector Machine

TAN	Número Total Ácido o Total Acid Number
TBN	Número Total Básico o Total Basic Number
TDC	Top Dead Center
TGA	Termogravimetría analítica
TPO	Temperature–Programmed Oxidation
UHC	Hidrocarburos sin quemar o Unburned Hydrocarbons
UV	Ultraviolet
UV–Vis	Ultraviolet–Visible
VII	Aditivos Mejoradores del Índice de Viscosidad o Viscosity Index Improvers
Vis	Visible
ZDDP	Dialquil-ditiofosfato de zinc

Chapter 1

Introducción

Contents

1.1 Antecedentes y contexto

El estudio del comportamiento de los aceites lubricantes de baja viscosidad, LVEOs (del inglés Low Viscosity Engine Oils), es un trabajo de larga trayectoria realizado dentro del grupo de investigación de Ingeniera del Mantenimiento (se realizaron un total de 5 fases distintas). Este estudio se basaba en determinar dos aspectos derivados del uso de estas formulaciones de lubricantes: por una parte, ver su influencia sobre el consumo de combustible [2, 6–8] y, por otro lado, comprobar que estas formulaciones de baja viscosidad no produjeran daños en los motores [1, 3–5]. Por la parte que atañe a esta Tesis, los trabajos se centraron en completar el estudio del comportamiento de nuevas formulaciones con los grados API CK-4 y FA-4 en aceites 5W30 (en la fase cuarta) y 10W30 (en la fase quinta). De este modo se consigue completar este estudio, aportando una visión global completa acerca del comportamiento tribológico estos aceites de baja viscosidad.

Sin embargo, el resto de los temas que se abordan en esta Tesis han sido campos nuevos desarrollados íntegramente desde el inicio para así, al final del periodo de investigación, dejar como legado al instituto una serie de herramientas nuevas y provechosas que antes no se disponían. Los temas a los cuales se está haciendo mención son:

- El primero de ellos está relacionado con un nuevo campo de investigación que se está empezando a implementar en el CMT-Motores Térmicos relacionado con la aplicación de protocolos quimiométricos aplicados a los aceites lubricantes de motor. Esta línea fue desarrollada como una de las consecuencias de la situación pandémica generada por el COVID-19, lo cual permitió destinar tiempo al tratamiento de datos procedentes del análisis de los aceites lubricantes por lo que se decidió ponerlos en valor realizando un estudio de este tipo.

- Mientras que, el tema restante, está relacionado con el hollín, en especial en el hollín presente en el aceite lubricante. El grupo de investigación de Ingeniería del Mantenimiento no disponía de conocimientos extensos sobre este tema que, en la actualidad despierta tanto interés. Es por esa razón que se decidió invertir parte del tiempo de investigación en desarrollar una labor de desarrollo e implementación de las diversas técnicas existentes para la cuantificación de dicho contaminante. Además, no sólo el estudio de las técnicas existentes fue corroborado (y en algunos casos, ciertas técnicas fueron adaptadas a los nuevos aceites de baja viscosidad) sino que también se pudo desarrollar unos protocolos

propios con técnicas alternativas que permiten cuantificar también la concentración de hollín en el aceite.

De modo que, estos dos nuevos temas de investigación que se han desarrollado en esta Tesis puedan servir como punto de partida para futuros estudios y tesis doctorales que se realicen en la línea en los siguientes años.

1.2 Motivación y preguntas de investigación

Esta Tesis ha intentado dar respuesta a las siguientes preguntas que, hoy en día, resultan aún despertar interés motivando a buscar una solución e incentivando a la investigación. Estas tres preguntas o inquietudes que se están haciendo referencia son:

- Actualmente, se están empleando aceites lubricantes de baja viscosidad con el objetivo de mejorar la eficiencia de los motores desde un punto de vista del consumo de combustible, pero las nuevas formulaciones ya empleadas y aquellas que están siendo desarrolladas han sido estudiadas principalmente desde un enfoque centrado en mejorar la eficiencia del consumo de combustible. No obstante, el efecto que tiene el uso de estas formulaciones en aspectos como su comportamiento en motor y las tasas del desgaste de este junto con las tareas de mantenimiento asociadas, han sido aspectos que no se han tenido presentes. Por esa razón, existe la necesidad de analizar cómo afectan las nuevas formulaciones en estos tres aspectos anteriormente citadas: comportamiento de las formulaciones, desgaste del motor y mantenimiento, de modo que se establezca que ninguno de los tres esté penalizado o quede por fuera de valores aceptables.

- Desde el punto de vista del OCM (Oil Condition Monitoring), cada vez es necesario disponer de información de forma rápida y precisa. Como consecuencia de ello, se están destinando esfuerzos en el estudio de técnicas aptas para el análisis de aceites lubricantes que permitan extraer información del estado de los lubricantes de la forma anteriormente mencionada: rápida y precisa. Motivado por esta corriente de estudio, se han empezado a estudiar las ventajas que presentan las técnicas espectroscópicas, las cuales son técnicas que, desde un punto de vista operacional, extraen una gran cantidad de información con unos costos de operación y tiempo bajos. A pesar de ello, aún queda mucho por

explotar en este campo tal y como ha mostrado el hecho de la aplicación de la quimiometría en conjunción con las técnicas espectroscópicas. Resulta pues muy interesante desarrollar esta sinergia entre estos dos bloques de conocimiento dado que, tal y como se está comprobando, permiten extraer una cantidad aún mayor de información acerca del estado y comportamiento de los aceites lubricantes.

- Por último, existe otra inquietud vinculada con el tema de la contaminación excesiva de los aceites lubricantes por parte del hollín. Como consecuencia de cumplir los bajos niveles de emisiones contaminantes, los constructores de motores han implementado una serie de mecanismos y tecnologías para conseguir alcanzar los niveles estipulados por las normativas y leyes. No obstante, un efecto derivado de esta mejora a la hora de emitir emisiones menos nocivas para el medio ambiente ha resultado en una degradación y contaminación acelerada de los aceites lubricantes empleados reduciendo su periodo de vida útil y generando problemas en los motores. De entre ellos, el hollín es el agente más relevante, por lo que existe la necesidad de mejorar su detección y cuantificación, en especial, ser capaces de discernir pequeñas variaciones en el contenido de hollín presente en el aceite lubricante. Gracias a ello, se podrá conocer, en periodos de tiempo relativamente cortos, los valores de hollín que contiene el aceite lubricante de modo que se pueda estimar, a un cierto tiempo vista, los niveles que se alcanzarán, así como su ratio. Por esa razón, es conveniente realizar una investigación relacionada con este problema actual y que, de acuerdo con las tendencias mostradas en los últimos años, cada vez cobrará mayor relevancia en el sector de la automoción.

Como consecuencia de plantearse estas tres preguntas se ha despertado el interés de brindar un poco más de información para así contribuir con esta Tesis a resolverlas.

1.3 Objetivos y alcance de la Tesis

Esta Tesis doctoral, desarrollada en el instituto CMT-Motores Térmicos, ha centrado su estudio en el análisis de los aceites lubricantes de motor con el propósito de caracterizar mejor su comportamiento e incrementar su conocimiento acerca de ellos. Por consiguiente, en el marco actual, el sistema de estudio se focaliza sobre los aceites lubricantes de baja viscosidad y es, precisamente sobre este sistema, dónde se desarrolla el presente documento.

Los objetivos marcados para esta Tesis fueron los siguientes:

- Estudiar, bajo condiciones de uso real, el comportamiento de las nuevas formulaciones de aceites lubricantes de motor de baja viscosidad que van a aparecer en el mercado con el propósito de conocer cuál es su desempeño atendiendo a los valores de parámetros característicos reportados por las analíticas realizadas sobre las diferentes muestras de lubricante recogidas en la prueba de campo. En esta prueba de campo se emplearán vehículos de trabajo pesado (considerado diferentes tecnologías de motorización y combustibles al uso: diésel y GNC), los cuales usarán estas nuevas formulaciones por un periodo de tiempo especificado marcado por un límite de 30000 kilómetros.
- Avanzar en el procedimiento de obtención de información procedente de los análisis tradicionales de los aceites lubricantes gracias a la implementación de procesos quimiométricos y estadísticos. En este aspecto, el uso de este tipo de herramientas brinda la oportunidad de extraer una cantidad de información útil a partir de diferentes tipos de datos: numéricos, espectrales, etc., por lo que en esta Tesis se plantea aplicar este tipo de procedimientos a los aceites lubricantes de motor.
- Por último, elaborar un plan de análisis de aceite lubricante focalizado a la determinación del contenido de hollín presente. Para ello se diseñará un organigrama de técnicas analíticas disponibles capaces de facilitar dicho parámetro estructuradas en función de los requisitos y limitaciones de cada técnica para, de este modo, seleccionar qué técnica se adapta mejor a las circunstancias del análisis. Además, impulsado por la necesidad de poder detectar pequeñas variaciones de hollín en el lubricante, desarrollar nuevas metodologías alrededor de este tema resulta de interés debido a las exigencias de disponer de información cada vez más precisa y en un tiempo menor.

1.4 Estructura y planteamiento de la Tesis

El documento final de la Tesis, el cual ha sido redactado durante toda esta fase de investigación, está compuesto por un total de siete capítulos. En cada capítulo se aborda una tarea en particular, mostrando todo el proceso de investigación: desde su planteamiento hasta la obtención de los resultados y conclusiones. De acuerdo con conseguir cumplir los objetivos planteados en la sección 1.2 *Objetivos y alcance de la Tesis* de esta Tesis, la estructura del documento es la siguiente:

- **Capítulo 2**:
  En esta primera parte de la Tesis se intenta contextualizar el estudio, explicando qué es un aceite lubricante y cuáles son sus principales características físicoquímicas que se requieren conocer para comprender mejor este trabajo de investigación.

- **Capítulo 3**:
  En este capítulo es dónde se exponen aquellas técnicas y procedimientos que permite caracterizar los aceites lubricantes, dejando expuestos aspectos relacionados con la aplicación de una serie de adaptaciones y mejoras (en aquellos momentos dónde fuese necesario y posible) realizadas sobre las técnicas analíticas y protocolos de caracterización de los lubricantes, en especial, para su mejora adaptación y rendimiento a la hora de analizar las nuevas formulaciones de aceites lubricantes.

- **Capítulo 4**:
  El capítulo 4 se trata de la exposición de los resultados obtenidos del trabajo de investigación sobre el comportamiento de las nuevas formulaciones de aceites lubricantes de baja viscosidad. En este capítulo, a partir de los datos e información recopilada, se expondrán los aspectos más relevantes del desempeño de estas formulaciones y las conclusiones que se pueden extraer de dicho trabajo.

- **Capítulo 5**:
  Este capítulo se ha destinado a exponer la potencialidad de la quimiometría aplicada al estudio de los aceites lubricantes de motor. Para ello, se parte de toda la información recabada en el capítulo anterior (Capítulo 3), la cual sirve como base para poder desarrollar este trabajo. Concretamente, este trabajo es un estudio inicial (el cual puede y debe encarecidamente seguir desarrollándose) dónde se ha realizado una primera incursión al empleo de la quimiometría aplicada al análisis de los aceites lubricantes de motor para la predicción de parámetros característicos de dichos sistemas. Además, para aportar un valor extra a este estudio, se han barajado fuentes de datos e información diversas: desde los resultados extraídos de técnicas clásicas de análisis de lubricantes hasta datos más complejos como los espectros de los lubricantes.

- **Capítulo 6**:
  El penúltimo capítulo está dedicado a la investigación acerca de la cuantificación del hollín en el aceite lubricante de motor. Esta investigación se centró en conseguir conocer el bench mark de las técnicas

existentes capaces de aportar esta información poniéndolas a prueba hasta intentar llegar a su máximo potencial y, además, desarrollar nuevos protocolos con técnicas alternativas que satisfagan los requisitos actuales de rápida obtención de datos para cambios muy pequeños en la cantidad de hollín presente en el aceite lubricante.

- **Capítulo 7**:
  En este último capítulo es dónde se reúnen y prestan las conclusiones derivadas de los diferentes trabajos realizados en esta Tesis para así discutir en profundidad sobre cada uno de ellos y, posteriormente, proponer las líneas futuras de investigación que puedan darse.

Siguiendo esta propuesta de Tesis, se ha intentado mostrar todo el trabajo realizado y los resultados obtenidos de una forma que facilitase su comprensión siguiendo un orden lógico que, durante su lectura, permitiese generar un hilo argumental que le confiriera unidad al conjunto.

Cabe destacar que, en esta Tesis, se ha decidido realizar una parte en español y el resto en inglés. Esto es debido al tipo de contenido de cada una de ellas y a su aportación al campo de estudio. Así, de acuerdo con esto, en el documento se encuentra que:

- El Capítulo 2, que es un capítulo introductorio que contextualiza la matriz o sistema de estudio, los lubricantes, se ha redactado en español por su carácter descriptivo.

- El Capítulo 3, por su parte, está redactado en ambos idiomas. La primera sección, redactada en español, atiende al contenido más descriptivo referente a las propiedades típicas de los lubricantes. Mientras que, la parte destinada a la detección y cuantificación de agentes contaminantes en aceites lubricantes ha sido preparada en inglés ateniendo a que, más adelante en el documento de Tesis, se ha destinado un capítulo entero (concretamente el Capítulo 6) a uno de los contaminantes expuestos: el hollín. Por esa razón, para facilitar el vínculo entre estos dos capítulos, se decidió preparar este contenido en inglés.

- El resto de los capítulos, del Capítulo 4 al Capítulo 7, están completamente escritos en inglés debido a su interés y relevancia, ya que son capítulos dónde se recogen los resultados experimentales y conclusiones obtenidas por los trabajos de investigación realizados.

Del conjunto del documento se extrae la idea de la intención de que aquellas partes escritas en inglés se han realizado con el claro objetivo de dar una mayor difusión y transmisión de los conocimientos obtenidos durante toda la investigación llevada a cabo durante la Tesis. Esto no implica un menosprecio de la parte escrita en español, sino simplemente que se ha dado más énfasis a aquellas aportaciones de gran impacto a través de su redacción en una lengua de transmisión del conocimiento como es el inglés.

Bibliography

[1] V. Macián, B. Tormos, S. Bastidas, and T. Pérez. Improved fleet operation and maintenance through the use of low viscosity engine oils: Fuel economy and oil performance. *Eksploatacja i Niezawodność*, 22(2), 2020.

[2] V. Macián, B. Tormos, V. Bermúdez, and L. Ramírez. Assessment of the effect of low viscosity oils usage on a light duty diesel engine fuel consumption in stationary and transient conditions. *Tribology International*, 79:132–139, 2014.

[3] V. Macián, B. Tormos, G. Miró, and T. Pérez. Assessment of low-viscosity oil performance and degradation in a heavy duty engine real-world fleet test. *Proceedings of the Institution of Mechanical Engineers, Part J: Journal of Engineering Tribology*, 230(6):729–743, 2016.

[4] V. Macián, B. Tormos, S. Ruíz, and G. Miró. Low viscosity engine oils: Study of wear effects and oil key parameters in a heavy duty engine fleet test. *Tribology International*, 94:240–248, 2016.

[5] V. Macián, B. Tormos, S. Ruiz, G. Miró, and T. Pérez. Evaluation of low viscosity engine wear effects and oil performance in heavy duty engines fleet test. In *International Powertrain, Fuels & Lubricants Meeting*. SAE International, jan 2014.

[6] V. Macián, B. Tormos, S. Ruíz, and L. Ramírez. Potential of low viscosity oils to reduce CO_2 emissions and fuel consumption of urban buses fleets. *Transportation Research Part D: Transport and Environment*, 39:76–88, 2015.

[7] B. Tormos, B. Pla, S. Bastidas, L. Ramírez, and T. Pérez. Fuel economy optimization from the interaction between engine oil and driving conditions. *Tribology International*, 138:263–270, 2019.

[8] B. Tormos, L. Ramírez, J. Johansson, M. Björling, and R. Larsson. Fuel consumption and friction benefits of low viscosity engine oils for heavy duty applications. *Tribology International*, 110:23–34, 2017.

Chapter 2

Aceites lubricantes: degradación y contaminación

Contents

2.1 Introducción

En este capítulo se darán las bases para comprender la complejidad de un aceite lubricante de motor: empezando por explicar los elementos que lo conforman y, qué efectos tienen estos elementos en el aceite lubricante final. Como en los nuevos MCIA los aceite lubricantes sufren una elevada demanda de prestaciones y rendimiento, por lo que se trata de un elemento a tener presente a la hora de diseñar un MCIA.

Por motivaciones de diferente índole (medio ambiental, económico, social, legislativas, etc.) los nuevos MCIA cada vez tienden a ser más limpios desde el punto de vista de la emisión de contaminantes. Lo que sucede es que, para conseguir los niveles bajos de contaminantes que se proponen, es necesario aplicar ciertas tecnologías de combustión y de postratamiento (EGR, SCR, DPF, entre otras) a los motores y el uso de nuevos combustibles. Aunque tiene un efecto positivo en los motores, tiene ciertas contraprestaciones por lo que respecta al aceite lubricante.

Por consiguiente, en este capítulo se explicará cómo los nuevos MCIA exigen más prestaciones a los aceites lubricantes teniendo en cuenta aspectos relacionados con la contaminación y degradación del mismo.

2.2 Composición y características principales de los aceites lubricantes

El aceite lubricante se trata de una mezcla líquida formada por dos grandes elementos: base y aditivos, la combinación de los cuales define un producto final con una serie de características y propiedades definidas para un cierto entorno y condiciones de trabajo en las cuáles el fluido deberá actuar realizando una serie de tareas concretas. Para poder cumplir con todo ello, los dos elementos que constituyen la formulación del aceite deben estar bien definidos, dado que ambos poseen una relación de complementariedad, es decir: las propiedades que permite alcanzar por si solo la base evita el uso de aditivos específicos, mientras que si la base no reúne o presenta una o unas propiedades que se desean en el fluido final es necesario la incorporación de otros compuestos (aditivos) que permitan conseguir y alcanzar las prestaciones deseadas en el producto final.

2.2.1 Composición de un aceite lubricante

Centrando el foco sobre la base dado que se trata de el componente principal, el que se encuentra en mayor proporción (entre el 70% y 90% aproximadamente); existen varias categorías de bases que se emplean en la formulación de un aceite lubricante. En la Tabla 2.1 se muestran los diferentes grupos de bases atendiendo a la clasificación generada por la American Petroleum Institute (API) en su documento "Engine Oil Licensing and Certification System" (EOLCS) [32], la cual describe un conjunto de 5 categorías de bases lubricantes distintas (sin tener en consideración los procesos requeridos para la obtención de la base en sí).

Table 2.1. *Propiedades principales de los diferentes grupos de fluidos base para aceites lubricantes.*

Clasificación API	Con. Saturados	Con. Aromáticos	Con. Azufre	Índ. Viscosidad
Grupo I	<90% (65-85%)	>10% (15-35%)	>0.03%	80 a ⩽120
Grupo II	⩾90% (93->99%)	⩽10% (<1-7%)	⩽0.03%	80 a ⩽120
Grupo III	⩾90% (95->99%)	⩽10% (<1-5%)	⩽0.03%	⩾120
Grupo IV	Polialfaolefinas (PAO)			
Grupo V	El resto no incluido en los grupos anteriores			

En una primera observación, los grupos mostrados en la tabla superior (Tabla 2.1) presentan dos procedencias: una cuyo origen es el crudo de petróleo (el cual posee una variabilidad tal y como se observa en la Figura 2.1) y otro dónde se trata de un producto de síntesis. A partir del crudo de petróleo, cuya composición elemental es: carbono (83–87%), hidrógeno (10–14%), nitrógeno (0.1–2.0%), oxígeno (0.1–1.5%), azufre (0.5–6.0%) y trazas de metales (<0.1%), se obtienen los grupos I, II y el III. Los HC presentes en el crudo de petróleo (los cuales abarcan HC de pocos átomos de carbonos hasta 100) pertenecen, básicamente, a tres familias: HC cuya estructura química es de tipo parafínica, nafténica o aromática. En consecuencia, la distribución de estas tres en la composición del crudo hace posible diferenciar varias familias de crudo las cuales poseerán una serie de características distintivas del resto [65, 70]. En la Figura 2.1 se han delimitado una serie de regiones con el objetivo de enunciar la variedad de crudo que se obtiene:

Para facilitar la comprensión del diagrama anterior, la información se ha organizado en la Tabla 2.2, en la cual se muestra la composición de los diferentes crudos atendiendo a su contenido en hidrocarburos: saturados (S), aromáticos (AA), parafínicos (P) y nafténicos (N).

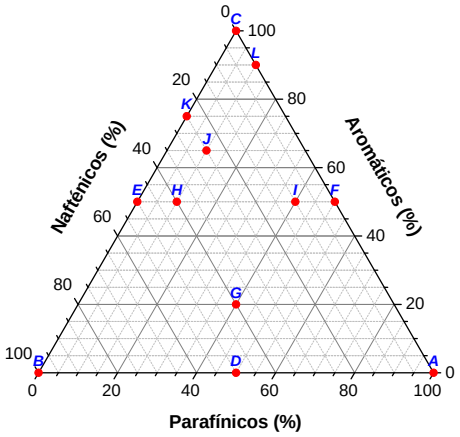

Figure 2.1. *Diagrama ternario de los diferentes tipos de crudos.*

Table 2.2. *Composición de los diferentes tipos de crudos de petróleo.*

Concentración HC		Tipo	Sección	Conc. Azufre
S>50% AA<50%	P>N y P>40%	Parafínico	A-D-G-I-F	<1%
	P⩽40% y N⩽40%	Parafínico–Nafténico	G-H-I	<1%
	P<N y N>40%	Nafténico	B-D-G-H-E	<1%
S⩽50% AA⩾50%	P>10%	Aromático Intermedio	F-I-H-J-L	>1%
	P⩽10% y N>25%	Aromático–Nafténico	E-H-J-K	<1%
	P⩽10% y N⩽25%	Aromático Pesado	K-J-L-C	>1%

Conociendo la riqueza de composición del crudo de petróleo con el que se pueden preparar las bases de aceites minerales, no es de extrañar que la base que derive de un cierto crudo posee una propiedades fisicoquímicas propias (ver Tabla 2.3).

Ahora bien, a partir de un crudo, para obtener una base se requiere la realización de una serie de procesos físicos y químicos que permitan alcanzar el producto deseado: realizando protocolos de extracción comunes como la destilación y extracción selectiva mediante disolventes (entre otros) o, por otro lado, alternativas más complejas que emplean procesos catalíticos. Independientemente de la ruta de obtención de los grupos minerales, del I al III, se puede esbozar un diagrama acerca de la distribución de las tres grandes familias de HC en cada uno de ellos [54]. Atendiendo a esto, en la Figura 2.2

Table 2.3. *Propiedades de las tres grandes familias de estructuras químicas de los hidrocarburos.*

Característica	HC Parafíncos	HC Nafténicos	HC Aromáticos
Ind. Viscosidad	Alta	Baja	Baja
Densidad	Baja	Baja	Alta
Pour Point	Alta	Baja	Baja
Volatilidad	Baja	Media	Alta
Flash Point	Alta	Baja	Baja/Media
Estab. a la Oxidación	Alta	Alta	Baja
Estab. Térmica	Baja	Baja/Media	Alta

se han representado las composiciones de cada uno de los grupos involucrados en este apartado:

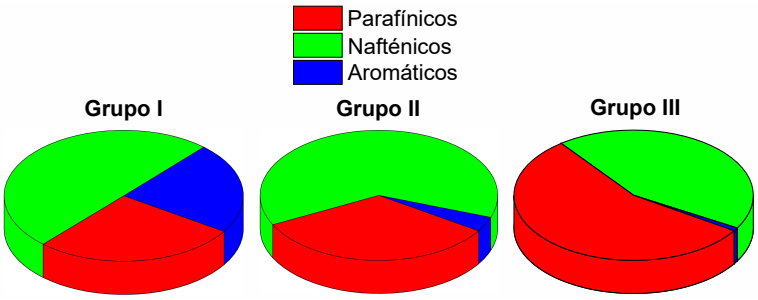

Figure 2.2. *Composición de las diferentes bases minerales.*

Dejando a un lado a los grupos minerales, ahora es turno de explicar el resto de grupos: Grupo IV y Grupo V. Como ya se introdujo anteriormente, los aceites de base sintética aglutina al Grupo IV (ver Figura 2.3) mientras que el Grupo V es un compendio de todas aquellas bases que no han estado consideradas en los cuatro grupos anteriores [50, 68].

Entrando un poco mas en detalle en cada tipo de base de aceite, cada una de ellas presenta una serie de propiedades fisicoquímicas derivadas de la propia estructura química que presentan los diferentes componentes (moléculas) que la conforman. Según la proporción de los diferentes compuestos que pueda contener la base en cuestión, las propiedades que ésta reúne son diferentes [57, 59, 75]. En consecuencia, a modo de descripción; se procederá a enunciar cada una de las diferentes bases:

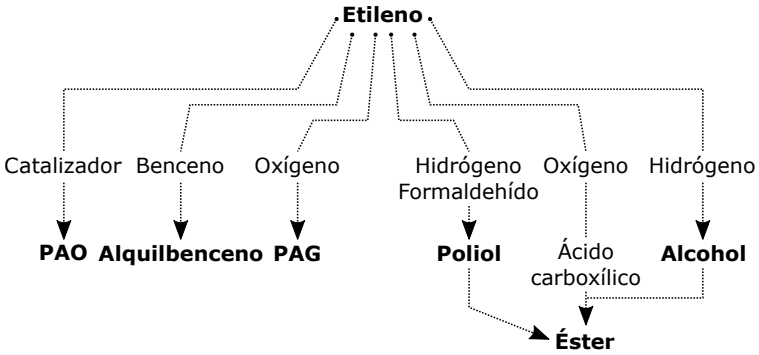

Figure 2.3. *Diagrama de obtención de las diferentes bases sintéticas a partir del etileno.*

- **Grupo I**: Este tipo de bases se obtienen a partir de tratar el crudo de petróleo con una serie de disolventes con el propósito de separar selectivamente sus componentes químicos de interés, este proceso se conoce como extracción o refinado mediante disolventes. La extracción mediante disolventes se basa en las afinidades de solubilidad de los diferentes compuestos que conforman el crudo de petróleo con los disolventes en cuestión, de este modo es posible separar y desechar aquellas moléculas aromáticas (moléculas policíclicas) y ceras que no son deseadas. Como producto final, la base generada mediante este proceso presenta un alto IV (índice de Viscosidad) y un contenido de HC saturados alto (dentro de los límites propios de la técnica, dado que la proporción de compuestos aromáticos puede oscilar entre el 10% y el 40%) e igual que azufre (tanto en forma libre como formando parte de un compuesto). Este tipo de base de aceite presenta una buena solvencia y propiedades antioxidantes propias. Por esa razón resultan interesantes dado que permite la solubilidad de aditivos en sí y extiende la vida del aceite gracias a su resistencia a la oxidación.

- **Grupo II**: Estas bases se producen por hidrotratamiento del crudo de petróleo, lo cual favorece una extracción más efectiva de ceras, componentes aromáticos y de azufre. Durante su producción, como consecuencia de la misma, se generan nuevos compuestos que en origen no se encontraban en la materia prima. Los IV que muestran estas bases son similares a los del Grupo I, entre 80 y 120. Dentro de este grupo, se podría distinguir un pequeño subgrupo el cual se podría llamar Grupo II^{+} (siguiendo las pautas API/ATIEL, pero no siendo

reconocido como un grupo oficial). Este subgrupo se obtiene mediante un proceso más severo, lo cual permite obtener un fluido con unos IV más acotados: donde el límite inferior se encuentra alrededor de los 100-115 hasta alcanzar los 120, todo ello manteniendo prácticamente invariable la composición en comparación con el Grupo II.

- **Grupo III**: Ahora, gracias a la realización de una hidroprocesado más exhaustivo del crudo, hidrocracking; donde además se realiza una etapa catalítica de desparafinación (eliminación de ceras), es posible eliminar aquella fracción de HC cíclicos que permanecían en la composición de la base del Grupo II. Durante su producción, como consecuencia de los procedimientos y fases que se le realizan a los productos, se generar nuevos compuestos que en origen no se encontraban en la materia prima. De hecho, la cantidad de nuevos compuestos que se generan durante toda la etapa de procesado para la obtención de este grupo es tal, que el producto final dista mucho del de partida. De igual forma que en el grupo anterior, existe una variante de este grupo llamada Grupo III$^+$. Esta distinción "+" afecta al hecho de que los IV en este grupo están en el límite superior (valores más elevados) de las pautas que estipula la API además de subir los valores de IV inferiores recayendo en valores de 130-140. No obstante, las especificaciones acerca del contenido de azufre y de HC saturados de este Grupo III$^+$ permanecen invariables, tomando como referencia los valores de dichos parámetros en el grupo oficial del que deriva.

- **Grupo IV**: Este grupo se obtiene por vía sintética a partir del etileno, a partir del cual se obtiene una α-olefina y esta a su vez, mediante reacciones de oligomerización (condensación o unión de varias unidades de construcción denominadas monómeros) se va extendiendo hasta conformar el esqueleto del HC saturada para terminar con un proceso de hidrogenación que garantice la no-insaturación de la molécula. Como resultado se obtiene una base cuya composición presenta una estructura química única y bien definida: se tratan de alcanos de cadena extendida con pocas ramificaciones del esqueleto carbono-carbono de longitud de 6 átomos de carbono o más llegando hasta 12 (lo más común es encontrarse con estructuras de 10 carbonos, deceno), siendo además alcanos completamente saturados, es decir sin dobles enlaces ni estructuras aromáticas. La homogeneidad de su composición es tal que solo existen despreciables cantidades de insaturados y compuestos policílicos aromáticos y trazas de impurezas (como nitrógeno, azufre entre otras). Así pues, como consecuencia de su composición, sus

propiedades son muy diferentes al resto de grupos anteriores. Estas bases se caracterizan por presentar poca variación de su viscosidad con la temperatura (alta retención de su viscosidad), por lo que no es de extrañar que los IV que abarcan sean elevados (superior a 135, en general) aunque se pueden modular abarcando valores de IV desde los 125 llegando a sobrepasar los 200. Además, como consecuencia de la estructura química de las moléculas de olefinas que la componen, la resistencia de la base frente a la oxidación y a la temperatura son excelentes [60].

- **Grupo V**: En este grupo se reúnen todas aquellas bases que no se han visto reflejadas en los cuatro grupos anteriores, siendo pues bases de origen: nafténico, ésteres (de origen natural o sintético), siliconas, poliglicoles y otros, pero de entre ellos los de mayor peso son las bases nafténicas, por lo que no es raro encontrarse que a este grupo se lo conozca también como Medium Viscosity Index Naphthenic o bien por sus siglas MVIN. Como la variedad de compuestos químicos que existen en este grupo es considerable, el espectro de propiedades que los aceites de esta base pueden reunir es importante por lo que no es aconsejable aportar valores generalistas para el Grupo V.

- **Grupo VI**: Este grupo está compuesto por lo que se conoce como PIOs, poli-interna-olefinas. Se trata de un nuevo grupo, del año 2003, que solo es reconocido por ATIEL en Europa (por lo que no se trata de un grupo principal según API). Se caracteriza por ser una base sintética compuesta por HC de larga cadena principal alifática (cadena abierta) en la cual se distribuyen de forma aleatoria ramificaciones. Esta diferencia con las PAOs se debe al oligómero de partida, una n-olefina interna. Estas moléculas son más complejas de oligomerizar, por lo que se requieren más pasos en su síntesis: fase de reacción, fase de neutralizacion, fase de hidrogenación y fase de destilación [60].

La base empleada en un aceite lubricante da un punto de partida a las propiedades finales que se desea alcanzar en el producto final, pero para poder lograrlas se requiere incorporar en dicha base una serie de aditivos que aporten nuevas características o bien potencien/minimicen aquellas ya existentes en la base. De modo que, gracias a la conjunción o sinergia entre la base y los aditivos se consigue obtener un aceite lubricante apto para el desempeño de un determinado trabajo sujeto a unas exigencias concretas. En la Tabla 2.4 se muestran la relevancia que tiene cada una de las dos, base y aditivos, de la formulación de un aceite lubricante en sus propiedades finales.

Table 2.4. *Influencia de las propiedades de un aceite lubricante como consecuencia de la base o la aditivación empleada en su formulación.*

Propiedad	**Base**	**Paquete de aditivos**
Viscosidad	Principal	Secundario
Ind. Viscosidad	Principal	Principal
Estab. Térmica	Principal	-
Poder disolvente	Principal	-
Liberación del aire	Principal	-
Volatilidad	Principal	-
Flujo a baja temp.	Principal	Principal
Estab. oxidación	Principal	Principal
Dispersancia	Secundario	Principal
Demulsividad	Secundario	Principal
AW/EP	Secundario	Principal

No obstante, en una primera aproximación, se podría clasificar los aditivos en dos grupos: uno referente a aquellos aditivos los cuales influencian sobre las propiedades físicas y químicas de las bases y otro tipo relacionado con aquellos aditivos que interaccionan principalmente con las superficies metálicas. Pero, en la gran mayoría de casos, esta distinción queda ambigua debido a que los aditivos no suelen mostrar una de esas dos facetas individualmente, sino que más bien actúan en ambas campos a la vez (aunque sí preferentemente en uno de ellos) pero realizando diferentes tareas. Así pues, es necesario conocer qué tipo de aditivos forman parte de la formulación de un fluido lubricante y cual es su proporción. Por consiguiente, los diferentes aditivos que pueden contener los aceites lubricantes se clasifican según función o desempeño: existen aditivos que se incorporan para controlar la degradación del aceite lubricante, para modificar su viscosidad, para mejorar su lubricidad y por último para mantener un control de la contaminación que experimenta el aceite lubricante durante su periodo de uso. Dentro de cada una de estas cuatro familias existen una variedad de aditivos [24, 55, 68]:

- Para el conjunto de aditivos englobados bajo la descripción de **control de la degradación del aceite** se incluyen todos aquellos que implican una mejora por lo que respecta a la estabilidad química del aceite lubricante. Por esa razón, dentro de esta modalidad se encuentran [12]:

- En primer lugar los *aditivos detergentes* y los *aditivos dispersantes*. Como su nombre indican se incorporan en la formulación del aceite lubricante con el objetivo limpiar y neutralizar aquellas impurezas que aparecen en el aceite lubricante y que derivan al final en la formación de depósitos no deseados en los motores. Tales impurezas, como la carbonilla, partículas de suciedad, lodos u otra serie de materiales insolubles, gracias a estos aditivos no se combinan entre sí formando aglomerados o agregados que, debido a su tamaño, precipiten y se depositen en zonas calientes del motor, regiones sensibles a que se produzcan este tipo de fenómenos. Este tipo de aditivos se combinan con este tipo de sustancias arrancándolas de las superficies a las cuales se encuentran adheridas o bien disgregan los aglomerados facilitando que se mantengan en suspensión y viajen en compañía del aceite lubricante [75].

- El siguiente tipo serían aquellos aditivos que se encargan de retrasar la degradación de la base que constituye el aceite lubricante como consecuencia de su reacción, a altas temperaturas, con el oxígeno u otros agentes oxidantes. Este tipo de aditivos se llaman *aditivos antioxidantes* y se encargaran pues de evitar los dos posibles mecanismos de degradación del aceite lubricante: la reacción de las moléculas de oxigeno con las del lubricante y/o la descomposición de las moléculas de la base por altas temperaturas. De entre estos dos mecanismos, el que más efecto y relevancia tiene para el caso de los aceites lubricantes es el mecanismo de oxidación. Este proceso es un proceso radicalario compuesto por 3 fases: iniciación, propagación y terminación. En la fase de iniciación, es dónde se produce un aumento en el número de radicales libres (especies químicas con uno o varios electrones desapareados) debido a la reacción de las moléculas del aceite lubricante con el oxígeno. A continuación, la etapa de propagación consiste en la aparición de reacciones en las que intervienen los radicales y, por último, la etapa de terminación en la que los radicales se recombinan dando lugar a compuestos más estables o bien son consumidos por inhibidores radicalarios y por ende el proceso se termina al quedar consumidos dichos radicales. Los radicales más importantes en los aceites lubricantes son aquellos derivados de grupos alquilo (simbolizados por R·) y peróxido (ROO·). Así pues, atendiendo a la diferente estructura química de los radicales mayoritarios, el mecanismo de actuación es diferente. Por esa razón existen varios tipos de aditivos antioxidantes: AO primarios y AO secundarios. Los primeros son

conocidos como radical scavengers (por su nombre en inglés) y se caracterizan por ser aditivos de rápida acción. Se caracterizan por interrumpir la propagación del proceso de oxidación del aceite lubricante gracias a que son capaces de reaccionar con las especies radicalarias en sus primeras fases de generación. El siguiente tipo son AO que se encargan de reaccionar con los radicales de tipo peróxido dando como resultado productos no-reactivos y estables. Independientemente del tipo de AO que se emplee, la virtud común de todos ellos es que se tratan de aditivos con una gran afinidad por los radicales libres (especies químicas de alta reactividad) que aparecen en el aceite lubricante, por lo que éstos se movilizan combinándose con los radicales libres para neutralizarlos impidiendo que se propague la degradación del aceite lubricante.

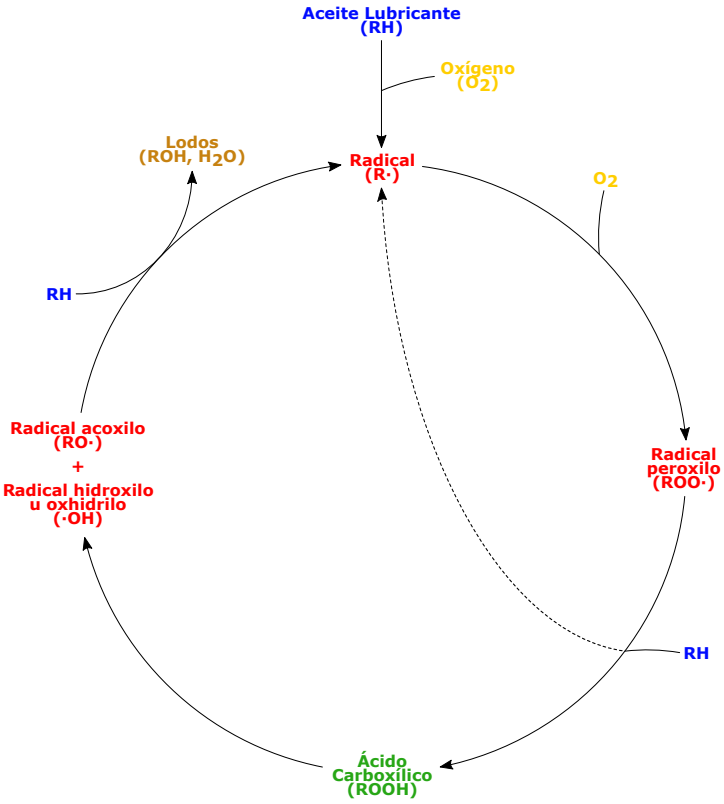

Figure 2.4. *Mecanismo de oxidación de un aceite lubricante. Los AO primarios atacan a las especies RO· y ·OH, mientras que los AO secundarios rompen el mecanismo al reaccionar con los radicales ROO·.*

- En tercer lugar se encuentran los *inhibidores de corrosión y herrumbre*. Su tarea principal es limitar la corrosión de los metales y la formación de herrumbre dentro del motor. Estos aditivos pueden ser capaces de realizar dos acciones: en primera instancia se encargan de neutralizar aquellas especies ácidas que puedan aparecer en el aceite lubricante, mientras que la segunda hace referencia a la generación una capa o película protectora que se adsorba (principalmente mediante mecanismos de fisisorción, adsorción física entre la superficie adsorbente y el adsorbato) y aísle las superficies metálicas de los posibles agentes ácidos. Como resultado se forma esa capa de aditivos, densamente empaquetados, que permite delimitar las dos regiones o fases que están en contacto: la superficie del metal y aceite lubricante. Algunos de estos inhibidores, son capaces de realizar estas dos tareas o al menos una de ellas, estando además (en algunos casos) predispuestos a proteger ciertos metales debido a estar diseñados para proteger preferentemente un metal en cuestión. Este grupo, a su vez, se puede dividir en dos atendiendo al metal que protege: existen aditivos anti-herrumbre los cuales se centran en proteger las superficies de hierro y aditivos pasivadores de metales no-ferrosos.

- El último grupo, el cuál se podría considerar como una variante de un inhibidor de corrosión; son los conocidos como *desactivadores de metales* (también llamados como MDA de las siglas en inglés de Metal Deactivating Agents). Dentro de los MDA existen tres modelos o tipos: aquellos compuestos que generar un film protector al metal, compuestos que atrapan metales (agentes quelantes) y eliminadores de azufre. El primer tipo, tiene como objetivo principal formar una capa de protección en las superficies metálicas no-ferrosas de igual forma que lo hace los aditivos anteriores: generando una capa de pasivación que protege la superficie de metal expuesta al aceite lubricante. De este modo, estos aditivos previenen que los átomos expuestos de la superficie se disuelvan en el aceite lubricante, dado que al combinarse con ellos provocan que la reactividad de la superficie metálica se reduzca. El siguiente grupo, los agentes quelantes, son moléculas orgánicas afines por los iones metálicos (cationes, iones con carga positiva). Este tipo de moléculas generan un espacio o entorno químico el cual es apto para combinarse con dichos iones. En esta región existen orientados ciertos grupos químicos que son capaces de interactuar con estos iones y/o formar enlaces de coordinación, de este modo,

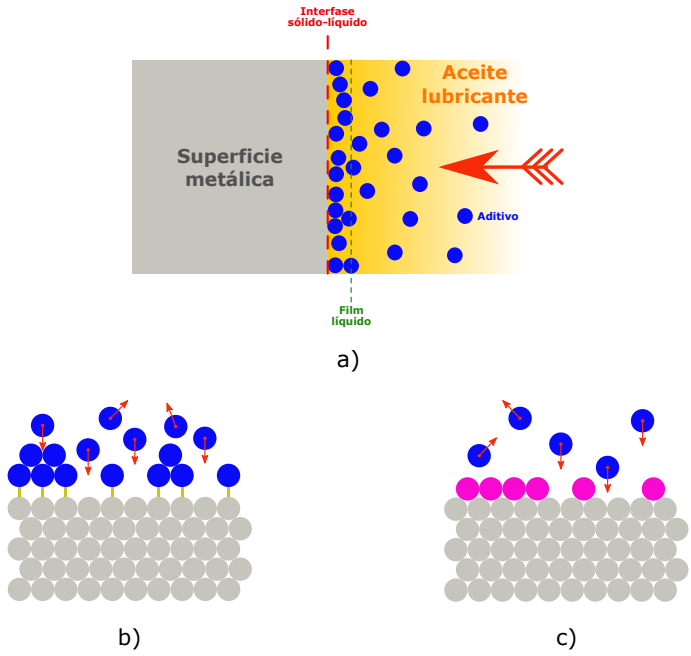

Figure 2.5. *Diferentes mecanismos de adsorción a superficies: a) Proceso superficial de adsorción entre la superficie del metal y los aditivos que migran hacia la interfase sólido-líquido, b) Fisisorción y c) Quimisorción.*

aquellos iones presentes en el aceite son secuestrados por este tipo de aditivos. La efectividad de ellos se debe a que al reaccionar con los iones metálicos, mediante una reacción de complejación, se forma un compuesto mas estable: un compuesto de coordinación. Por último, los eliminadores de azufre (en inglés, sulfur scavenger) son moléculas capaces de reaccionar con el azufre presente formando enlaces estables y así integrándolos en su estructura molecular.

- El siguiente conjunto son aquellos aditivos que afectan a la **viscosidad**. En esta división existen dos tipos: los Modificadores o Mejoradores del IV (representados por las siglas VII, Viscosity Index Improvers) y los Depresores del Punto de Fluidez (más conocidos como, PPD, Pour Point Depresant).

  – Los *VII* son aditivos que se encargan de modificar el comportamiento de la viscosidad del aceite lubricante a altas temperaturas, provocando que la variación del valor de este parámetro sea lo

menos posible. En consecuencia, se trata de favorecer el hecho de que el aceite lubricante sea capaz de retener un cierto rango de valores de viscosidad independientemente de la temperatura en la que se encuentre. Por otro lado, los PPD son aditivos que actúan en condiciones de baja temperatura teniendo como objetivo favorecer la fluidez (reducir su viscosidad) del aceite lubricante en esas condiciones. Ambos aditivos de este grupo son aditivos basados en polímeros y/o en copolímeros, unos especiales para trabajar en condiciones de altas temperaturas y otros para baja, radicando este hecho en su naturaleza química (estructura y composición). Los VII son polímeros de cadena larga (alta peso molecular) los cuales tienen la característica de que dependiendo a la temperatura a la que se encuentren, su solubilidad en la base del aceite lubricante varía: la disposición que adoptan este tipo de polímeros recibe el nombre conformación de "ovillo de lana" (random coil en inglés), la cual se debe a las interacciones entre los grupos funcionales de los monómeros interaccionan entre si debido a la aparición de fuerzas débiles que provocan que toda la estructura esté más o menos cohesionada. Estas fuerzas son fácilmente superadas por la temperatura, debido a que al aumentar la temperatura, la cadena polimérica obtiene una cierta libertad estructural (gana flexibilidad). Como consecuencia de este fenómeno, el empaquetamiento en forma de ovillo se expande. Este cambio conformacional induce que, la solvatación de estos polímeros por moléculas del aceite lubricante varíe en función de la temperatura modificando así la viscosidad del aceite lubricante: a bajas temperaturas el empaquetamiento es más denso, por lo que la cantidad de moléculas de aceite alrededor del polímero es baja y por ende la viscosidad no se ve comprometida. Pero, a altas temperaturas la estructura de estos polímeros ocupa un mayor volumen y la cantidad de moléculas de aceite lubricante que lo rodean es mayor dando lugar a un aumento de la viscosidad (ver Figura 2.6) [14].

– Los *PPD* por su parte, se encargan de evitar que aquellos componentes constituyente de la base de aceite empleada empiecen a cristalizar como consecuencia de la bajada de la temperatura. La formación de cristales es un proceso que se produce en dos etapas: la inicial es conocida como nucleación y es donde se forman los primeros cuerpos sólidos (partícula cristalina inicial) que actuarán como germen de crecimiento de un cristal, mientras que la siguiente

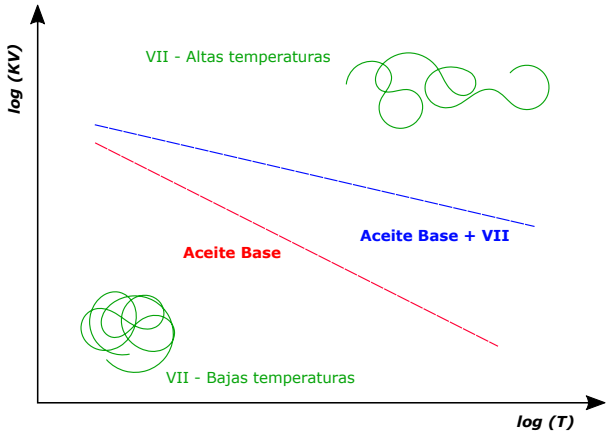

Figure 2.6. *Efecto de los VII sobre la variación de la viscosidad del aceite lubricante en relación con su estructura en función en unas condiciones de temperatura dadas.*

fase ya es la del crecimiento del cristal en sí. Los PPD evitan la formación de cristales interponiéndose en la interfase núcleo sólido-aceite, de este modo se interrumpe el crecimiento.

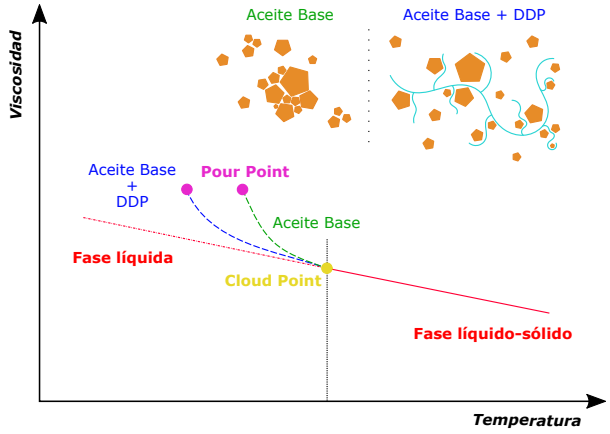

Figure 2.7. *En el gráfico se han representado los puntos de Punto de Enturbiamiento o de Niebla (o en inglés Cloud Point) en amarillo y los Puntos de Fluidez (Pour Point) en rosa. Se puede apreciar como con la adición de PPD a la composición del aceite lubricante, el Punto de Fluidez se alcanza a temperaturas más bajas que si no se hubieran empleado.*

- El otro grupo existente son los **aditivos mejoradores de la lubricidad**, cuyo propósito es mejorar el comportamiento del aceite lubricante mejorando aspectos que condicionan su lubricidad. En este grupo se encuentran: los aditivos Modificadores de Fricción (FM de Friction Modifiers), aditivos Anti-desgaste (representados por las siglas AW de Antiwear) y aditivos de Extrema-presión (EP). Cada uno entra en jugo en diferentes condiciones de lubricación, ver Figura 2.8, en dónde se tiene en consideración el Coeficiente de Fricción (μ) y el Número de Hersey (H) (Ecuación 2.1):

$$H = \frac{\eta \cdot U}{F_N} \tag{2.1}$$

En dónde se tiene en consideración los siguientes elementos: la viscosidad dinámica (η), la velocidad de deslizamiento relativo (U) entre las superficies involucradas y por último, la carga normal aplicada (F_N) en dichas. Por lo que, analizando la relación entre Coeficiente de Fricción (f) y el Número de Hersey (H) es posible determinar cual es el régimen de lubricación y por consiguiente, cual aditivo interviene para evitar la fricción entre las superficies metálicas con movimiento relativo.

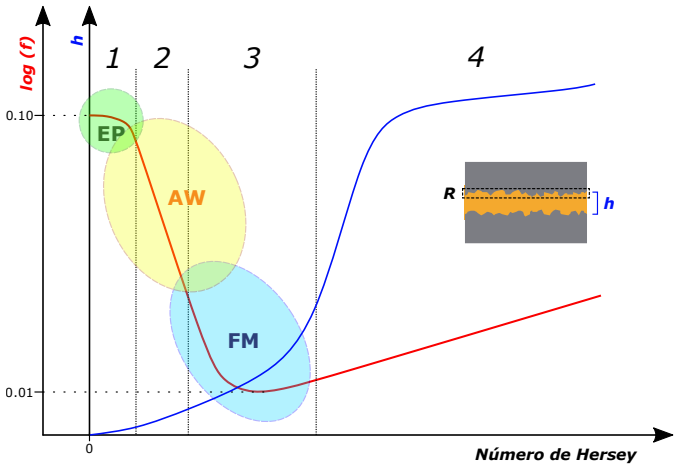

Figure 2.8. *Curva de Stribeck–Hersey dónde se han resaltado las zonas de trabajo de los aditivos mejoradores de lubricidad atendiendo al régimen de lubricación: 1) Lubricación Límite ($h \longrightarrow 0$), 2) Lubricación Mixta ($h \cong R$), 3) Lubricación Elasto-Hidrodinámica ($h > R$) y 4) Lubricación Hidrodinámica ($h >> R$). Estas diferentes situaciones se dan lugar en función de la relación entre el espesor de la película de aceite (h) y la rugosidad de la superficie (R).*

  - Los primeros, los *FM* son aditivos que favorecen la reducción de la fricción entre dos superficies lubricadas debido a que este tipo de aditivos altera la lubricidad de la base empleada en la formulación del aceite lubricante. De este modo, los FM evitan que tenga lugar entre estas superficies el fenómeno antideslizante (stick-slip) el cual induce a procesos de desgaste en el motor. Los FM se pueden organizar en 2 variedades si se tiene en consideración cómo trabajan: en primer lugar se encuentran los FM los cuales actúan de forma mecánica, FM que generan películas protectoras (bien sea mediante mecanismos de adsorción o por reacciones triboquímicas) y por último aquellos FM basados en polímeros y compuestos organometálicos.
  - Pasando a los aditivos restantes, los *aditivos Anti-desgaste* (AW) y los *aditivos de Extrema-presión* (EP); se podrían describir conjuntamente debido a su comportamiento similar. Estos dos aditivos se caracterizan por estar compuestos por elementos que son formadores de films (películas finas de bajo espesor) que, debido al carácter polar de la estructura química; se adhieren a las superficies metálicas evitando así que entren en contacto y se produzcan procesos abrasivos. Aunque la forma que tienen estos dos aditivos de hacer frente a los fenómenos de desgaste es muy similar, la diferencia entre ambos radica en las condiciones en las que trabajan: en aquellas zonas de motor dónde las exigencias permiten que la película de aceite lubricante es suficiente como garantizar una correcta lubricación, son los aditivos AW los que entran en acción debido a que la estabilidad de la película protectora no es del todo crucial debido al espesor de aceite lubricante que existe (por esa razón, lo más común es que los aditivos AW generen films mediante procesos de fisisorción). Pero, cuando las condiciones de trabajo son tales que pueden llegar a romper la película de aceite lubricante, se requiere que se forme un film protector muy estable. Para conseguirlo, se requieren que entre los aditivos y las superficies se formen enlaces químicos, es decir que se forme una capa aditivo-metal por un mecanismo de quimisorción. Es pues, que los aditivos EP presentan moléculas que son capaces de formar capas muy estables gracias mediante este mecanismo de quimisorción.

- El último grupo es aquel que tiene por objetivo mantener un **control sobre los contaminantes** que pueden aparecer en los aceites lubricantes. Por consiguiente, existen aditivos que tienen una

actividad polivalente y otros que son específicos a cierto tipo de agentes contaminantes. Esto se debe como consecuencia del diseño del aditivo, o bien los que reaccionan por afinidad con el contaminante (el cual pasa a ser su elemento target o diana) o bien aquellos que por interacciones físicas son capaces de interactuar con cualquier sustancia ajena al aceite lubricante que posea o se le pueda inducir una propiedad que pueda ser aprovechada por este tipo de aditivos para sustraerlos de la matriz de aceite lubricante. Teniendo esto en cuenta, se pueden describir varias tipologías de aditivos que son capaces de desempeñar este tipo de tarea: aditivos detergentes y dispersantes y aditivos anti-espumantes.

- Los primeros aditivos son los *aditivos detergentes y dispersantes* (comúnmente simbolizados mediante DD) esos aditivos se encargan de evitar que los contaminantes sólidos que va acumulando el aceite lubricante (por ejemplo, el hollín, cenizas, etc.) se reúnan formando aglomerados y en consecuencia, empiecen a precipitar y depositarse en el interior del motor. Para prevenir la coagulación de los contaminantes y garantizar que los contaminantes insolubles permanezcan en suspensión y viajen en compañía del aceite lubricante, estos aditivos generalmente poseen estructuras químicas con carácter anfifílico o anfipático: una parte polar (hidrófila) y otra apolar (hidrófoba). La primera de ellas es la parte afín o la que es atraída por los contaminantes, mientras que la otra prefiere permanecer en contacto con el aceite lubricante. Así que esta diferencia de comportamiento provoca que se formen construcciones llamadas micelas, las cuales se basan en ser estructuras que delimitan una región dentro de una matriz en las cuales están disueltas. Las micelas en el aceite lubricante lo que hacen es separar los contaminantes de la base del aceite lubricante, es decir, lo encapsulan: la parte polar es la que se reorganiza envolviendo las partículas contaminantes mientras que la apolar (que es más oleofílica) se orienta hacia la base [71]. Una forma de diferenciar entre aditivos detergentes y dispersantes es observando su composición química dado que ambos poseen una moléculas donde una mitad es polar y la otra apolar pero la intensidad de ese carácter polar/apolar es diferente. En los detergentes el carácter polar es mas marcado que en los dispersantes, mientras que en los disertantes es el carácter apolar (dado que poseen una parte hidrófoba con mayor relevancia). Esta diferencia de comportamiento se plasma en su solubilidad en aceite, dado que cuanto más polar sea la molécula más difícil será de disolver ésta

en la matriz de la base de aceite. Además, los dispersantes no generan cenizas (son aditivos ashless) mientras que los detergentes son formulados junto a iones metálicos [13]. Como consecuencia de ello, se puede describir brevemente cada uno de estos dos tipos:

* Los aditivos dispersantes se unen, físicamente, a contaminantes (que presentan carácter polar) para evitar que éstos vayan coagulando dando pie a partículas de mayor tamaño y así poder mantenerlos disueltos. Esta virtud se la es conferida por su propia estructura: la parte polar se fija a la superficie del contaminante favoreciendo que el aditivo lo rodee por completa. Como consecuencia, quedan orientadas hacia el exterior (hacia la fase compuesta por el aceite) la parte apolar. Al quedar aislado el contaminante, éste no puede unirse con ningún otro, pero no solo por que esté rodeado por las moléculas de aditivo, sino que debido al tamaño de la parte apolar del dipersante, la separación entre contaminantes es grande. Esto se debe a que aparecen fuerzas repulsivas (para ser más precisos, fenómenos de impedimento estérico) entre las partes apolares de diferentes núcleos. Para entender mejor este hecho es mejor observar la Figura 2.9.

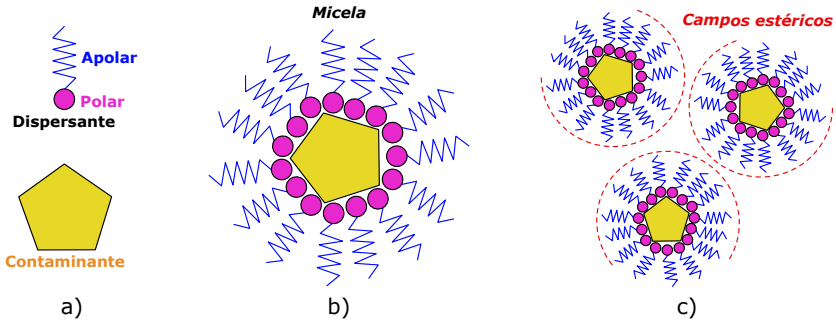

Figure 2.9. *Representación del comportamiento de una aditivo dispersante: a) En esta parte se representan los dos elementos que entran en juego, b) Formación de la estructura de micela al ser rodeado por moléculas de dispersante el contaminante y c) Espacio mínimo que ocupan cada una de las micelas.*

* Por otro lado, los aditivos detergentes son aquellos que están especialmente diseñados para trabajar en condiciones más severas que los anteriores: altas temperaturas y con ratios de generación de lodos y depósitos de sustancias insolubles importantes. Es por esa razón que estos aditivos están

compuestos por varios componentes: un metal (por ejemplo: Al, Zn, Ba y Ca), uno o varios grupos aniónicos (como serían los grupos carboxilatos, sulfonatos, tiofosfonatos, fenatos y salicilicatos) y un conjunto oleofílico (ver Figura 2.10). A la vista de los elementos, queda claro el hecho de que los aditivos detergentes son aditivos con carácter tensioactivo (también llamados empleando el anglicismo surfactante), son sales metálicas capaces de disolverse en matrices apolares [8].

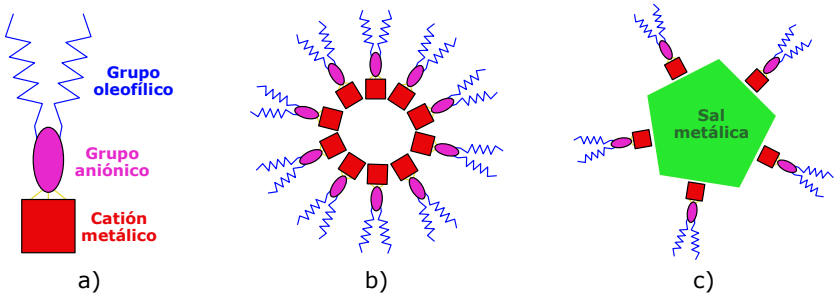

Figure 2.10. *La imagen a) representa la estructura típica de un tensioactivo, estructura de la cual derivan los dos tipos de detergentes siguientes, b) se trata de un aditivo detergente neutro, mientras que la c) es una detergente overbased.*

La forma de obtener este tipo de aditivos es relativamente sencilla, simplemente se trata de combinar un ácido orgánico con un metal mediante una reacción ácido-base. Pero, en función de como se realice esta síntesis, se pueden generar dos tipos de productos: detergentes neutros (simbolizados por RMR en la reacción 2.2) o detergentes overbased ($RMR(n-1)M(OH)_2$, ver reacción 2.3). Los primeros son aquellos dónde los dos elementos se encuentran en proporciones estequiométricas, mientras que los segundos existe un exceso de la base inorgánica.

$$2RH + M(OH)_2 \rightarrow RMR + 2H_2O \tag{2.2}$$

$$2RH + nM(OH)_2 \rightarrow RMR(n-1)M(OH)_2 + 2H_2O \tag{2.3}$$

En las reacciones anteriores se observa como el ácido orgánico (RH) reacciona con la base inorgánica ($M(OH)_2$) dando lugar

a un tipo de detergente según el ratio con el que se balancee la reacción.

- Los aditivos anti-espumantes (AF por el nombre que reciben en inglés de anti-foam o defoamant agents) son los encargados de inhibir la formación de burbujas (ya sean de aire o de gases de la combustión) y espumas en el aceite lubricante. Para conseguirlo, estos aditivos provocan una reducción de la tension superficial del aceite lubricante para así facilitar la liberación de los gases disueltos que pueda contener. La formación de espumas es un problema importante dado que tiene efectos negativos en el aceite lubricantes: reducen su poder lubricante (aumentado la fricción entre los elementos internos del motor), debido al contacto entre gases-aceite lubricante la oxidación se ve magnificada y dan pie a que se favorecen procesos de pitting o cavitación además de corrosión en superficies metálicas (en especial cuando el gas que forma la espuma son gases de combustión). Ahora bien, existen dos tipos de espumas que pueden darse o producirse en los aceites lubricante: primeramente se encuentra a espuma superficial la cual, según su nombre indica, es aquella que se acumula progresivamente en la superficie del aceite lubricante (zona de separación aire-aceite). Y la siguiente es aquella referente a las pequeñas burbujas de gas disueltas en la matriz del aceite lubricante permaneciendo durante largo tiempo (llegando incluso a formar dispersiones estables). El primer caso es el mas sencillo de tratar con este tipo de aditivos, mientras que le segundo depende más de las propiedades inherentes de la base de aceite empleada [80].

Estos aditivos son los más representativos que se pueden encontrar en los aceites lubricantes de motor, aunque no son los únicos. También existes aditivos como: tintes, biocidas, aditivos para evitar la atomización del lubricante (antimisting), agentes demulsificantes entre otros.

En conclusión, el binomio formado por la base y los aditivos conforma un producto final que reúne una serie de características y propiedades concretas. Para el caso de un aceite lubricante, las proporciones entre los diferentes elementos que lo constituyen es variada y dependiente de cada uno de los elementos que entran en juego y del aceite lubricante que se quiere conseguir. Centrándose en los aceites lubricantes para MCIA, donde se promedia que la base constituye aproximadamente del 80% del total del aceite lubricante, la proporción destinada al paquete aditivos se descompone o desglosa en:

- Los aditivos VII y los PPD, suelen aparecer en proporciones de alrededor del 0–15% y 0–2%, respectivamente, del total del peso en la composición del aceite.

- Por lo que el porcentaje restante, que oscila entre un 10% y un 15% se distribuye de la siguiente forma:

  - Los dispersantes son los mayoritarios en este grupo, llegando a alcanzar valores de 55–60%.
  - El siguiente aditivo que les siguen son los detergentes con valores en torno a 15–20%.
  - Con unos valores comprendidos entre el 8% y el 12% se encuentras los aditivos AW.
  - Los aditivos FM presentan un valor aproximado que ronda el 4%.
  - Ahora existe cierta variedad por lo que respecta a los aditivos AO, dado que están muy condicionados por las exigencias que se le va a pedir al aceite lubricante. Por esa razón el abanico es más amplio: entre el 3% y el 12%.
  - Al final queda una porción remanente por cumplir, <2%–15%, dónde se encuentran el resto de aditivos requeridos para un aceite lubricante en concreto. En este cómputo se podrían encontrar aditivos muy específicas para ciertas situaciones, por esa razón este conjunto puede tener muy poca relevancia hasta incluso llegar a ser casi una quinta parte de esta sección.

2.2.2 Características principales de los aceites lubricantes

Ahora, teniendo en cuenta cómo se formula y para qué sirve cada uno de los elementos constituyentes de un aceite lubricante, es momento de dar paso a exponer cuáles son las propiedades deseadas en un aceite lubricante. Las propiedades de un aceite lubricante están relacionadas con las diferentes tareas que éste realiza (Figura 2.11). Dichas tareas abarcan, más allá de su función primordial de reducir el rozamiento entre elementos que presentan movimiento relativos; otras funciones que son de especial importancia para un buen funcionamiento de un MCIA:

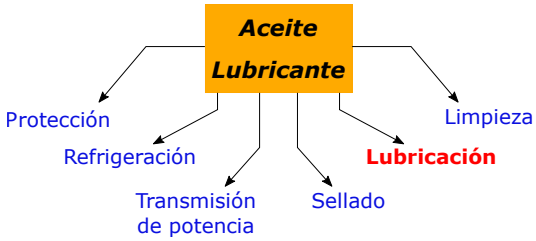

Figure 2.11. *Diagrama de las diferentes tareas y funciones que realiza un aceite lubricante en un MCIA.*

- La primera de ellas y la mas fácilmente reconocible es la **lubricación**. Esta función es necesaria para conseguir reducir la fricción y el desgaste de los componentes móviles de un MCIA al separar sus superficies entre sí. El aceite lubricante se dispone entre ambas superficies generando una película que hace que el coeficiente de rozamiento entre las superficies que separa se vea reducido. Gracias a esta separación física, la resistencia al movimiento (fricción) y los fenómenos de desgaste disminuyen, además de el beneficio de reducción de ruido dentro del motor que deriva de una correcta y eficiente lubricación.

- En los MCIA, existe una generación de calor la cual requiere ser gestionada para que el motor trabaje en condiciones óptimas. Teniendo en cuenta este hecho, el aceite lubricante es uno de los elementos que entran en juego para la **refrigeración** en un motor, en especial en aquellas regiones dónde el sistema de refrigeración (entendiéndolo como el conjunto formado por: fluido refrigerante, bomba, controladores de temperatura, intercambiador de calor, ventilador y conducciones) no puede llegar. Siendo pues en esas zona dónde el aceite lubricante, a medida que fluye absorbe esa energía (calor) para luego transportarla para que así sea disipada y evacuada.

- **Limpieza**, otro aspecto de los aceites lubricantes. Hace referencia al poder que tiene el aceite lubricante para mantener los contaminantes en suspensión en su seno y luego ser capaz de transportarlos hasta los sistemas de separación y extracción de contaminantes (como por ejemplo los filtros). De este modo se puede eliminar aquellas sustancias indeseadas en el motor prolongando su vida útil.

- La **protección** está relacionada con los procesos de degradación (corrosión) que pueden darse en un MCIA debido al entorno ácido que

se genera como resultado de la formación de subproductos procedentes del proceso de combustión del combustible. Estos productos poseen comportamiento ácido, por lo que son agentes de corrosión de aquellos elementos susceptibles a ser corroídos. Es pues que los aceites lubricantes poseen ciertas sustancias disueltas que se encargan de reducir el impacto de estas sustancias: ya sea neutralizándolas o bien recubriendo las superficies sensibles a los ácidos.

- Por último, según la construcción y diseño de los MCIA, el **sellado** es un parámetro que se requiere aportar. El aceite lubricante es capaz rellenar el espacio existente entre dos elementos, de modo que las dos regiones que cada uno delimitan queden aisladas evitando la comunicación y/o paso de fluidos. Gracias a esto, es posible mejorar la eficiencia y rendimiento de estos motores. Un caso dónde esta propiedad es muy importante es en el sellado de la cámara de combustión.

Para garantizar que el aceite lubricante sea capaz de realizar todas estas tareas, éste debe reunir una serie de propiedades [67]. Para el caso de estudio que se plantea en esta tesis, las propiedades que más interés suscitan son aquellas que se engloban bajo los dos primeros grupos. Así pues, extrayendo las más importantes, se procederá a describirlas de forma clara:

- Viscosidad: La viscosidad es el aspecto más importante y descriptivo por lo que respecta a un aceite lubricante, dado que es el que determina el espesor de la película lubricante y su comportamiento: altas viscosidades implican espesores de película mayores y viceversa, en general. Pero hay que tener en cuenta que si el espesor es bajo las superficies involucradas pueden entrar en contacto, mientras que si el espesor es excesivo, el mismo lubricante genera fricción extra por sí (pérdida de energía) que se opone al movimiento. Siendo tal la importancia de la viscosidad, es necesario conocer en que condiciones de temperatura, presión y esfuerzo de cortante (o de cizalla) va a trabajar el aceite lubricante, dado que estos tres elementos condicionan al valor de la viscosidad. La viscosidad se puede entender como la oposición de un fluido a fluir, es decir, se trata de la resistencia interna que ejercen las moléculas del fluido entre ellas mismas cuando se deslizan entre sí [77].

  - *Viscosidad Dinámica*: La viscosidad dinámica (también llamada como viscosidad absoluta) se simboliza mediante la letra griega η y se define como la resistencia al flujo de un fluido cuando es alterado por fuerza. Para comprender mejor esta propiedad, resulta práctico

observar la Figura 2.12 en dónde se representa dos superficies (A y B) separadas una cierta distancia (z) y a una de ellas se le comunica una fuerza tangencial (τ) provocando que se produzca un deslizamiento.

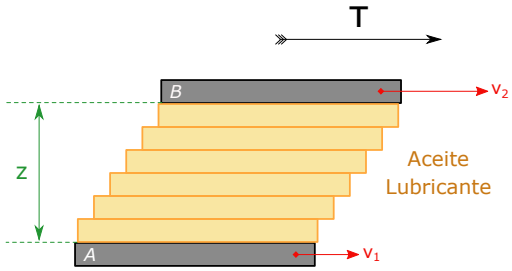

Figure 2.12. *Representación del fenómeno del perfil de velocidades de la película de lubricante entre dos superficies que se mueven a dos velocidades diferentes: la velocidad de la superficies* A *(v_1) es menor que la de la superficie* B *(v_2).*

Como consecuencia de esta fuerza, cada una de las superficies se desplazan a distintas velocidades. Esto es debido a la resistencia que ejerce cada una de las capas infinitesimales que conforman la película en dónde la transmisión de este esfuerzo entre ellas cada vez pierde energía. Como resultado se genera un gradiente de velocidad de corte o cizalla (S) (Ecuación 2.4):

$$S = \frac{dv}{dz}; \left[\frac{m/s}{m} = s^{-1}\right] \tag{2.4}$$

De la expresión anterior se extrae el hecho de que la capa de aceite lubricante más próxima a la superficie B es la capa que más rápida se moverá mientras que a medida que se avance transversalmente por el aceite lubricante se apreciará como la velocidad es menor (atendiendo al hecho de que la velocidad v_1 es menor que la velocidad v_2).

De forma matemática, lo que sucede se puede escribir en forma de la siguiente Ecuación 2.5 en dónde se tiene en consideración el esfuerzo cortante (τ) y el gradiente de velocidad de cizalla (S):

$$\eta = \frac{\tau}{S}; \left[\frac{N/m^2}{s^{-1}} \equiv Pa \cdot s\right] \tag{2.5}$$

Es pues esta expresión la forma en que se entiende la Viscosidad Dinámica (η), la cual es la relación entre τ y S. Su unidades (según el SI) son Pascal por segundo ($Pa{\cdot}s$). No obstante, cuando se habla de la viscosidad dinámica de un aceite lubricante, esta se expresa en unidades del sistema cegesimal: Centipoise (cP, la cual es derivada del Poise P, que es 100 veces mayor). Para determinar el valor de la viscosidad dinámica se debe emplear un reómetro, dispositivo que es capaz de proporcionar un esfuerzo de cizallamiento para una velocidad de corte determinada (a una cierta temperatura de interés).

– *Viscosidad Cinemática*: Obtener el valor de la viscosidad dinámica suele ser un poco más complejo que no la Viscosidad Cinemática (υ). Esta forma de comprender la viscosidad hace referencia o se define como la medida de la resistencia interna inherente de un fluido al flujo (cuando no se imparte ninguna fuerza externa excepto la gravedad). La medida de la viscosidad cinemática se realiza en unas condiciones más sencillas: no se requiere aplicar ningún esfuerzo al fluido de estudio y se trabaja en condiciones de presión atmosférica. Además, si se conoce la densidad del fluido que se está estudiante (ρ) es posible obtener el valor de la viscosidad dinámica de acuerdo con la Ecuación 2.6:

$$\upsilon = \frac{\eta}{\rho}; \left[\frac{Pa \cdot s}{kg/m^3} \equiv \frac{N \cdot s \cdot m^3}{m^2 \cdot kg} = \frac{m^2}{s} \right] \tag{2.6}$$

De acuerdo con la Ecuación 2.6, el cálculo es sencillo, pero hay que tener presentes en qué condiciones: presión y temperatura, se ha realizado la medida, dado que todos los elementos de la expresión están influenciados por estos dos factores. Para el caso de la viscosidad cinemática, sus unidades son m^2/s (según el SI), pero se suele emplear un submúltiplo: los mm^2/s los cuales son equivalentes a Centistokes (cSt)

Indistintamente de la viscosidad que se emplee para caracterizar a un aceite lubricante, la propiedad en sí depende de la temperatura (T), de la presión (p) y del esfuerzo cortante (τ), principalmente. El efecto de cada uno de los tres factores anteriores sobre la viscosidad es un tema de interés que aún no se ha llegado a resolver en su totalidad debido a la complejidad del problema. Si se presta atención a la evolución de la viscosidad con la temperatura, se observa que son inversamente proporcionales (cuando una crece la otra decrece y viceversa), pero la

forma con la que ambas se relacionan (en las temperaturas que suelen rondar dentro de un MCIA, 0-150°C) se puede plasmar mediante la Ecuación 2.7 [63]:

$$\eta(T) = A \cdot e^{B/T} \tag{2.7}$$

En esta ecuación de tipo Arrhenius, los parámetros A y B son unas constantes que deben determinarse de forma empírica y son específicas de cada fluido. No obstante, se pude obtener el valor de la viscosidad a una determinada temperatura siempre que se tenga información del aceite lubricante a otra temperatura (T_i). De este modo, se puede emplear la siguiente formula (Ecuación 2.8):

$$\eta(T) = \eta_{T_i} \cdot e^{-\beta(T-T_i)} \tag{2.8}$$

En la Ecuación 2.8, β es un factor que muestra la dependencia de la viscosidad con la temperatura, el cual es propio de cada aceite lubricante (Ecuación 2.9) y suele presentar valores de 0.05–0.07°C^{-1}, siempre que se tome las temperaturas de referencia de 40°C y 100°C siguiendo las pautas dictadas por la ISO (que fueron adoptadas por las organizaciones más relevantes: API, ASTM y SAE).

$$\beta = 1 - \left(\frac{\eta_{100^\circ C}}{\eta_{40^\circ C}}\right)_p \tag{2.9}$$

Si se grafica la relación viscosidad-temperatura se obtendría una respuesta como la de la Figura 2.13. Pero no sólo es la temperatura un factor relevante que afecta a la viscosidad, tal y como se ha avanzada en unas lineas anteriores, la presión también tiene un papel importante [24]. En este caso, se observa que al aumentar la presión sobre el aceite lubricante este experimenta un incremento de su viscosidad, estando ese incremento condicionado por la composición química del aceite lubricante [68]. El comportamiento se puede describir mediante la Ecuación 2.10 que se muestra a continuación:

$$\eta(p) = \eta_{p_{atm}} \cdot e^{\alpha(p-p_{atm})} \tag{2.10}$$

En ella se tiene en consideración la viscosidad a presión atmosférica $\eta_{p_{atm}}$, la cual presenta un valore de 1 bar (p_{atm}). De modo que, conociendo la presión p a la cual se requiere obtener el valor de la viscosidad ($\eta(p)$),

empleando esta expresión es fácilmente calculable. Pero es necesario conocer el valor del coeficiente de dependencia de la viscosidad con la presión, simbolizado en la ecuación como α. Este coeficiente se obtiene a partir de la siguiente expresión, Ecuación 2.11, presentado un rango de valores que abarca desde $1.4{\cdot}10^{-8}$ Pa^{-1} hasta más de $5.0{\cdot}10^{-8}$ Pa^{-1}:

$$\alpha = 1\frac{1}{\eta_p}\left(\frac{\partial \eta_p}{\partial p}\right)_T \tag{2.11}$$

Según esta ecuación (Ecuación 2.10), la dependencia de la viscosidad con la presión sigue un comportamiento lineal. La forma más común de representar esta tendencia de comportamiento es como se ha representado en la Figura 2.13.

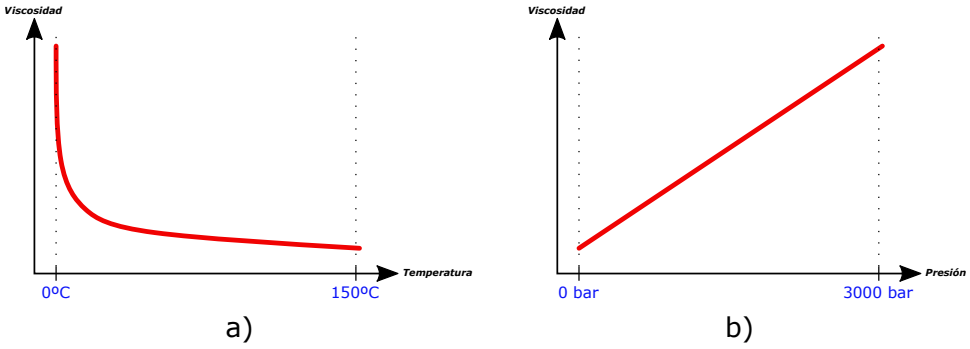

Figure 2.13. *Variación de la viscosidad en función de la temperatura (a) y en función de la presión (b), ambas enmarcadas en aquellos valores que comúnmente se pueden encontrar en un funcionamiento normal en un MCIA.*

A pesar de definir cómo se comporta el aceite lubricante, por lo que respecta a su viscosidad, en función de la temperatura y presión, el esfuerzo cortante (τ) es también importante. Al aplicar una cierta carga sobre un aceite lubricante, al tratarse de un fluido con un comportamiento pseudo-plástico, altos ratios o tasas de cizallado provocan que su viscosidad se vea disminuida. En la Figura 2.14 se muestra cómo es el comportamiento de este tipo de fluido no-newtoniano (fluido con viscosidad estructural):

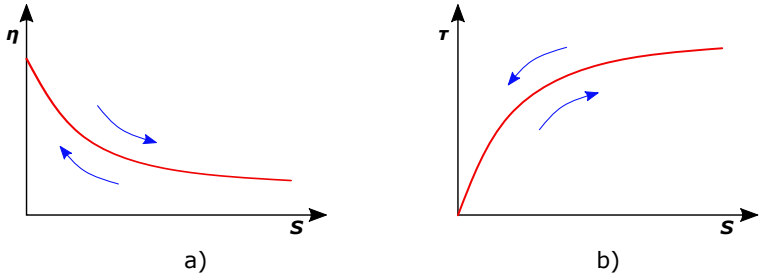

Figure 2.14. *El comportamiento de un fluido pseudo-plástico tiene la virtud de poder recuperar, generalmente, su estado inicial cuando se le retira el esfuerzo que está experimentando (S), conociéndose este fenómeno como tixotropía. En el gráfico a) se ha representado la variación del la viscosidad dinámica (η) y en el b) el esfuerzo cortante (τ).*

No obstante, existen diferencias de comportamiento según el ratio de cizallado: en primer lugar, el aceite lubricante se comporta como un fluido newtoniano (la viscosidad no depende del esfuerzo cortante aplicado) cuando se encuentra con valores por debajo de 10^5-10^6 s^{-1}, pero al superar este umbral se produce una caída de la viscosidad debido a que en ese momento el aceite lubricante se comporta como un fluido no-newtoniano [52, 69].

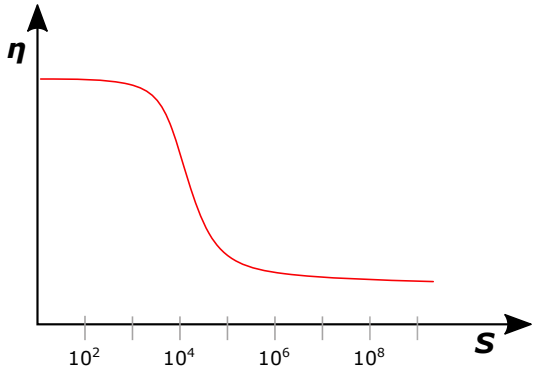

Figure 2.15. *Viscosidad de un aceite lubricante dónde se aprecia el cambio de comportamiento de fluido newtoniano a no-newtoniano dentro del rango de cizallado (S) de un MCIA: 10^3 a 10^7 s^{-1}.*

Este comportamiento diferente se debe a que un aceite lubricante no se trata de un fluido simple. Un aceite lubricante debido a su formulación,

compuesta por una base y un paquete de aditivos, se trata de una matriz muy compleja. Como consecuencia de ello, la organización de las moléculas de sus constituyentes es muy rica, debido al gran número de combinaciones que se pueden adoptar, dando lugar a que este tipo de fluidos se comporten de la forma plasmada en la Figura 2.15 [52]. No obstante, este comportamiento puede perderse llegados al punto en el cual esta estructura no se puede recuperar debido a que el cizallado es tan severo que es capaz de romper las moléculas del aceite lubricante, provocando que el carácter tixotrópico del aceite lubricante se pierda (dicho de otra forma, que el aceite lubricante no recupera el valor de viscosidad original).

Para cerrar el apartado de la viscosidad, en el ámbito de los aceites lubricantes, existe una parámetro conocido como Índice de Viscosidad (IV). El IV permite cuantificar el cambio de la viscosidad que experimenta un determinado fluido como resultado de una variación de la temperatura. Dicha de otra forma, el IV indica la sensibilidad o comportamiento de un fluido concreto respecto a la temperatura: altos valores de IV significa que la temperatura tiene un bajo impacto sobre la viscosidad, y viceversa. Este índice es adimensional (no presenta unidades) y se obtiene experimentalmente a partir de observar el comportamiento de un aceite lubricante a dos temperaturas de referencia: 40°C y 100°C. Fijadas las temperaturas de control, es momento de escoger cuáles son los aceites lubricantes representativos (referencia) de IV bajos y cuáles de IV altos, dado que se emplearán para comparar el aceite lubricante problema que se desea determinar su IV (es una medida relativa). La forma de proceder es mediante comparación de las viscosidades a 40°C de aceites referencia cuya viscosidad cinemática a 100°C sean la misma que la que presenta el aceite lubricante problema. En la actualidad, los aceites lubricantes presentan valores de IV superiores a 100 debido al desarrollo y la mejora de los aditivos que incorporan y de la calidad de las bases empleadas.

- Densidad: La densidad (ρ) se trata de una propiedad intensiva de los materiales, lo cual implica que su valor no está condicionada con el tamaño del material. Se define como el cociente entre la masa (m) y el volumen (V) tal y como se muestra en la Ecuación 2.12:

$$\rho = \frac{m}{V}; \left[\frac{kg}{m^3}\right] \tag{2.12}$$

Igual como sucedía con la viscosidad, la densidad también depende de la temperatura, por lo que se debe tener en cuenta a qué temperatura se realiza la medición, aunque la temperatura (T) no es el único elemento que condiciona el valor de la densidad, dado que la presión (p) y la viscosidad del fluido son también agentes que alterna a la densidad del fluido en cuestión. Para el caso de estudio, los aceites lubricantes, la densidad es un parámetro que se queda en segundo plano (en relación a la importancia que presenta la viscosidad). Pero, no obstante, sí resulta un parámetro útil para ciertos casos: el primero sería para brindar información acerca de la composición del aceite lubricante (dado que se trata de una propiedad aditiva), el siguiente para poder calcular la viscosidad dinámica a partir de la cinemática (ver Ecuación 2.6) y luego para poder conocer la relación entre masa y volumen.

Una forma de expresar la densidad, específicamente para aceites lubricantes y productos derivados del crudo de petróleo, es emplear lo que se conoce como densidad API (acuñada por el American Petroleum Insitute). Esta escala paralela de densidad está realcionada con la densidad (ρ) mediante la Ecuación 2.13, dónde se tiene en cuenta la densidad relativa del aceite a 15.6°C (lo que equivale a 60°F) frente al agua (d_W^O):

$$^\circ API = \frac{141.5}{d_w^o} - 131.5 \tag{2.13}$$

Así pues, según la formula anterior: cuanto mas grados API posea una aceite lubricante, menor será su densidad, y viceversa. Los valores de densidad que suelen presentar los aceites lubricantes son: 850-980 kg/m^3 o lo que es equivalente a 34.6-12.6 °API.

- Propiedades físicas relacionadas con condiciones limitantes: Para el caso de aceite lubricante de motor, existen una serie de propiedades físicas muy concretas que depende de una serie de temperaturas. En dichas temperaturas, el aceite lubricante presenta un comportamiento muy particular, dado que en ellas se producen cambios de fase en el aceite lubricante. Los fenómenos en cuestión son característicos y aparecen en el siguiente orden de temperaturas (ver Figura 2.16):

  A continuación se enuncian cada uno de ellos, desde el de más baja temperatura hasta llegar al de mayor:

  - El punto de más baja temperatura es conocido como *Pour Point*, aunque en español se llama Punto de Fluidez o de Congelación. Se

Figure 2.16. *Distribución de los puntos característicos de un aceite en función de la temperatura.*

trata de la temperatura mínima en la cual el aceite es capaz de fluir libremente (solo por la acción de la gravedad). En esa determinada temperatura lo que sucede es que las moléculas de aceite lubricante ya no son capaces de moverse con libertad como consecuencia de que éstas empiezan a reunirse y organizándose entre ellas (dado que se trata de un patrón energético más estable), lo cual deriva en un aumento de la viscosidad y densidad del mismo. Si se sobrepasa esta temperatura puede llegar el punto donde esas estructuras (cristales) se extiendan y el aceite lubricante se solidifique. Este parámetro es importante, dado que delimita a que temperatura el aceite puede ser bombeado por el sistema de lubricación de un MCIA. Para poder caracterizar este punto, la ASTM en su norma D97 ha descrito y normalizado el ensayo.

- A una temperatura mayor, se encuentra lo que se conoce como *Cloud Point*. En esa temperatura, es dónde se inicia la aparición de las primeras partículas sólidas. Estas partículas sólidas provienen de aquellas sustancias que poseen una temperatura de solidificación más alta dentro de la matriz del aceite lubricante (como por ejemplo sería el caso de las parafinas). Visualmente lo que se aprecia es que el aceite lubricante empieza a presentar cierta turbidez como consecuencia de estas partículas solidas que se separan del resto del aceite lubricante líquido. De igual modo que en el Pour Point, existe unas condiciones y procedimiento de ensayo propias reunidas en la ASTM D2500.
- Al cambiar de un registro de temperaturas bajas hacia unas altas, empiezan a aparecer fenómenos de *Volatilidad*, ya que cuando un aceite lubricante es calentado es susceptible a sufrir fenómenos de evaporación. La volatilidad de un aceite lubricante depende de su composición, ya que cada uno de los componentes que lo constituyen presenta su propia presión de evaporación condicionada por la estructura molecular de cada uno de ellos. De modo que

un aceite lubricante con un ratio de volatilidad elevado indica que sus componentes se evaporan con facilidad: primero se evaporan sus fracciones más ligeras (que poseen una presión de evaporación elevada) y luego las más pesadas, lo cual provoca una pérdida de material que deriva en que el aceite lubricante experimenta cambios en su comportamiento. Esta pérdida de materia en función de la temperatura se puede conocer a partir del test de volatilidad de Noack (DIN 51581, CEC L40-T-87, ASTM D5800) [34] o mediante Destilación por Cromatografía de Gases (GCD por el nombre que recibe en inglés, Gas Chromatographic Distillation) [33]. No obstante, también se puede conocer la volatilidad de un acetite lubricante estudiando las curvas de destilación (ver Figura 2.17).

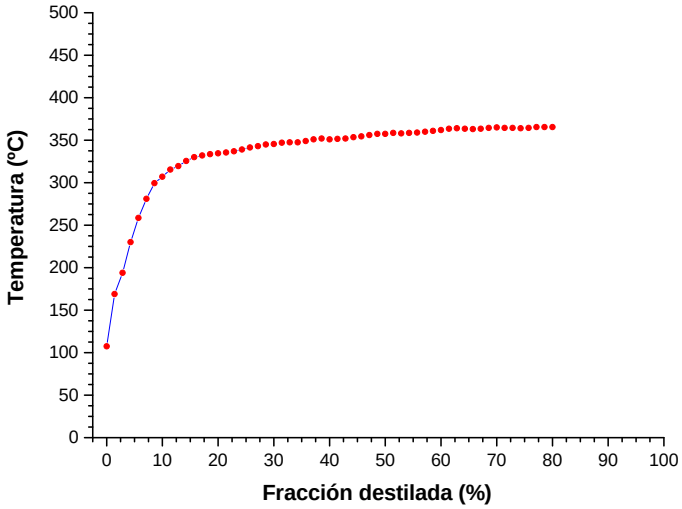

Figure 2.17. *Curva de destilación de un aceite lubricante 5W30 a presión atmosférica.*

– El *Flash Point* o Punto de Inflamación en español es la temperatura mínima a la cual la superficie de un aceite lubricante expuesto a una fuente de calor libera la cantidad suficiente de vapores como para que estos puedan prender al aplicar un aporte extra de energía. Dicho de otra forma, a cierta temperatura los componentes más volátiles empiezan a evaporarse de modo que si a dichos vapores se les acerca una foco caliente estos se inflaman. La generación de vapores inflamables no es suficiente como para poder sostener la llama en el tiempo, por lo que es una llama que se extingue con

rapidez (la llama es consumida muy rápidamente, por lo que parece un flash). Para determinar el Flash Point existen dos alternativas: la primera es realizando el ensayo, calentado y agitando la muestra de aceite lubricante a analizar, en una recipiente (copa) abierto (Cleveland Open Cup o método COC, reflejado en la norma ASTM D92) o bien en uno cerrado (Pensky–Martens Closed Cup test, estipulado de acuerdo con el estándar ASTM D93).

  - Si se prosigue calentando la muestra de aceite lubricante, es posible alcanzar lo que se conoce como *Fire Point* o, en español, Punto de Ignición. El Fire Point se define como la temperatura mínima que se requiere para que un aceite lubricante genera un flujo o caudal de vapores suficientes como para que al prenderlos (mediante el uso de un foco caliente) éstos combustionen y generen una llama que se sostenga en el tiempo una vez iniciada la quema (se considera que la llama es estable si perdura al menos 5 segundos). En este momento el ratio de generación de vapores y el ratio de consumo de dichos están balanceados, por lo que la llama no cesa.

- Contaminación por Aire y Agua: Otro aspecto importante de un aceite lubricante es su comportamiento frente a la entrada de aire y agua, dos elementos que suelen estar presentes o en contacto íntimo con el aceite lubricante. Como consecuencia de la aparición de estos dos elementos en el aceite lubricante, este debe ser capaz de intentar separarse de ellas evitando la mezcla. Así que, teniendo en cuenta esto, es posible determinar tres tipos diferentes de comportamiento de un lubricante: la capacidad de liberación del aire disuelto, la resistencia a la formación de espumas y la última la demulsibilidad.

  - La *Liberación o Expulsión del Aire* hace referencia al característica que tiene el aceite lubricante por expulsar el aire disuelto que se encuentra en su interior (que a presión atmosférica puede llegar a valores del 8%). Esta capacidad de liberar este aire está influenciado por la tension superficial (γ) del aceite lubricante, dado que la liberación de éste se realiza transportando la burbuja a través del aceite hasta llegar a la superficie (interfase que separa el aire y el aceite lubricante). La presencia de aire en el aceite es algo no deseado dado que favorece la producción de fenómenos de: oxidación al maximizar el contacto entre ambos, cavitación e incrementa la compresibilidad del aceite. Si se desea determinar este parámetro, solo se requiere seguir las pautas de operación marcadas en la norma DIN 51381 o bien en la ASTM D3427.

  - La *Espumación* determina la tendencia que tiene un aceite lubricante en formar espumas, entendiendo por espuma una gran cantidad de gas en un pequeño volumen de líquido. El aceite lubricante, al no tratarse de un líquido monocomponente puro, tiene tendencia a formar espumas. Por esa razón, este debe ejercer cierta resistencia a la formación de espumas (o en su defecto, debe eliminarlas de forma sencilla y/o rápida) ya que ellas son causantes de varios problemas importantes en un MCIA como: pérdidas por sobrepresiones, desbordamiento y derrame, fenómenos de cavitación y fallos mecánicos derivados de una mala lubricación (película protectora de aceite no eficiente al no disponer de la cantidad de fluido requerida). En MCIA, donde las condiciones para formar espumas son las más propicias: altas velocidades que provocan una gran agitación del volumen de aceite en el cárter.
  - La última tiene que ver con la presencia de agua en el aceite lubricante. La *Demulsibilidad* hace mención a la capacidad de un aceite lubricante de separar el agua que pueda contener. En un MCIA, el agua puede aparecer por problemas con el sistema de refrigeración o bien se trata de aquella agua procedente de la reacción de combustión del combustible y se va acumulando progresivamente en el cárter (especialmente si el aceite no alcanza la temperatura óptima de trabajo, cuando el tiempo de trabajo del MCIA es corto). Pero esta agua puede existir en un aceite de varias formas: en primer lugar está el agua disuelta (difícil de eliminar) y la otra es aquella que no lo está dado que aparece en forma de una fase extra (de gran o pequeño volumen) en la matriz del aceite lubricante. Esta segunda es la que tiene relación con la demulsibilidad. Debido al propio funcionamiento de un MCIA, el aceite lubricante se encuentra en continuo movimiento (bombeo, agitación, trasiego, etc.) lo que provoca que cuando ingresa un cierto volumen de agua en su interior, este se divide en porciones mas pequeñas: se forma un emulsión. Esta emulsión es algo no deseado en un aceite dado que da pie a procesos de corrosión, desgaste, entre otros. Por esa razón el aceite lubricante debe ser capaz separar esa agua.

- Estabilidad Térmica: El aceite lubricante puede absorber calor, lo cual puede conllevar a que se produzcan reacciones químicas que alteren al lubricante afectando de este modo a su estabilidad. Por esa razón, el aceite lubricante debe ser capaz de resistir el estrés o carga térmica

para evitar su termólisis (descomposición térmica). Esta propiedad recae casi únicamente sobre la base empleada [73], dado que los cambios producidos por el paquete de aditivos no tiene un efecto substancial sobre la estabilidad térmica. La estabilidad térmica es una propiedad que depende de varios factores: temperatura y presión de operación y tiempo de exposición a esas condiciones, principalmente [39].

- Acidez y Basicidad: Estas dos propiedades, antagónicas entre sí; aportan información muy importante por lo que respecta a la calidad de un aceite lubricante: la acidez aporta información del grado de refino de la base empleada en la formulación (relacionada con la cantidad de azufre presente) mientras que la basicidad viene modulada por el paquete de aditivos. Esta pareja viene expresada por dos parámetros de importante relevancia, por lo que respecta a los aceites lubricantes: el Número Total Ácido (TAN, del inglés Total Acid Number) y el Número Total Básico (TBN, Total Basic Number), ambos parámetros expresados en unidades de Número de Neutralización (NN). El NN se trata de la cantidad (en miligramos, mg) de base estándar, en este caso el Hidróxido de Potasio (KOH), requerida para neutralizar un gramo de aceite lubricante.

  - El control del *Número ácido* es una forma de monitorizar la degradación del aceite lubricante. Esto se debe a que, como resultado de los productos derivados de la reacción de oxidación, por la contaminación de los subproductos de la combustión y las altas temperaturas, el aceite lubricante adquiere cierto carácter ácido. Es pues cuando el valor de TAN es elevado, cuando el aceite lubricante provoca ataques ácidos sobre aquellos metales susceptibles a ser corroídos (como por ejemplo el cobre y el plomo). No obstante, debido a la variedad de componentes que aportan acidez al aceite: ácidos orgánicos, derivados y productos clorados o de azufre, nitratos y nitroderivados entre otros, la medición del TAN no es suficiente como para predecir el carácter corrosivo del aceite lubricante.
  - El parámetro complementario para determinar cómo de corrosivo es un aceite lubricantes es aquel que determina su *Número básico*. El grado de basicidad, representado por el TBN, esta relacionado con el contenido de aditivos con carácter básico (aditivos neutralizadores de ácidos, como los aditivos detergentes, overbased, y aditivos dispersantes) que existen en un aceite lubricante para la protección del MCIA. Cuando el aceite lubricante es fresco (no se ha usado) el valor del TBN elevado, disminuyendo

este pues a medida que avanza su uso. Por lo que, según la velocidad de disminución del valor de TBN; es un indicador de la capacidad de protección (frente al desgaste y la corrosión inducida por las especies ácidas) que aún retiene el aceite lubricante.

- Carácter limpiador: Un aceite lubricante debe ser capaz de evitar, o por lo menos minimizar, la formación de depósitos o cúmulos de contaminantes e impurezas dentro de un MCIA pudiendo cargar éstos en su seno y conducirlos a sus respectivos puntos de eliminación. Este aspecto del lubricante está íntimamente relacionada con los aditivos detergentes y dispersantes (DD) que posee en su formulación, aunque ciertas bases ya poseen propiedades de este tipo en origen. En un inicio, el poder limpiador del aceite lubricante es alto pero, a lo largo del intervalo de cambio del aceite (ODI, Oil Drain Interval), se consume a medida que acumula uso. Como esta propiedad se le es conferida, la magnitud de esta depende de las condiciones a las cuales deberá enfrentarse el aceite lubricante: tipo y diseño de motor, combustible, condiciones ambientales y de trabajo, etc. En esta pareja, cada uno se encarga de contribuir a este carácter limpiador del aceite lubricante:

  - Los aditivos detergentes, gracias a que reducen la tension superficial del aceite lubricante, favorecen que el aceite moje (humecte) de forma eficiente las superficies metálicas.
  - Por otro lado, los aditivos dispersantes aportan la formación y estabilidad de suspensiones de partículas sólidas, de modo que éstas queden distribuidas en el aceite lubricante de forma individual.

  Como resultado final de la comunión entre estos dos efectos, se genera una propiedad de mayor impacto: el poder de limpieza.

- Estabilidad Química: Básicamente, la estabilidad química de una aceite lubricante está relacionada con su oxidación. Por esa razón se busca conseguir un aceite lubricante que reúna una gran estabilidad ya que, en un MCIA, el aceite está bajo condiciones de estrés importantes: altas temperaturas, continuo movimiento, contacto con el aire y otros gases, entre otras circunstancias que pueden derivar en su deterioro. Sea cual sea el detonante de la oxidación del aceite lubricante, esta lo que deriva es en una alteración del aceite lubricante a diferentes niveles: provoca que aumente su viscosidad, favorece la aparición de sedimentos y depósitos y lo vuelve más corrosivo (modifica su acidez). Para evitar esta degradación, el aceite lubricante se prepara empleando bases de

calidad y, si es menester, un paquete de aditivos especialmente diseñado y seleccionado para evitar que los mecanismo iniciadores de una oxidación anómala del aceite se den lugar.

- Protección contra la corrosión y el óxido: En un aceite lubricante, puede darse le caso de que se produzca una entrada de agua: o bien pequeños volúmenes o bien uno grande. Independientemente del caso, lo que relevante es que la presencia de agua en el aceite provoca que el aceite lubricante pierda efectividad a la hora de generar la película lubricante (dado que no moja las superficies involucradas de una forma que garantice su separación) y por consiguiente de evitar que esa agua que viaja con el aceite no ataque a la parte expuesta de las superficies metálicas que se queda en los fallos o discontinuidades de la película. Las medidas que se adoptan para conseguir un aceite capaz de proteger frente a la corrosión es actuar justamente en el foco dónde tiene lugar: en el conjunto metal-agua-aceite lubricante. Para ello, lo que se hace intentar que el contacto entre el agua y el metal sea mínimo (reducir el ángulo de contacto) mediante aditivos incorporados en el aceite lubricante que son capaces de formar películas hidrofóbicas sobre la superficies metálicas. Ahora bien, no solamente el agua es el causante de esta corrosión, la presencia de ácidos en el aceite también lo provoca (pero es más, el agua actúa como catalizador de estas reacciones de generación de especies ácidas). Es por eso que el paquete de aditivos de un aceite lubricante se completa con sustancias o compuestos químicos capaz de neutralizar estos ácidos y/o proteger las superficies metálicas evitando su exposición a estos elementos o entornos agresivos.

Una vez conocidas las principales propiedades que debe reunir un aceite lubricante para poder ser empleado en un MCIA sujeto a unas condiciones de trabajo y entorno determinadas, las propiedades deben estar preestablecidas y definidas en unos cánones, tanto de valores permitidos como de tipos de ensayos habilitantes para determinar dichos valores. Para ello, estos estándares recogen cómo se debe describir cada propiedad y determinan bajo qué condiciones (normalizadas) se deben realizar las pertinentes medidas para poder obtener el valor de la propiedad que reúne el aceite lubricante: ya sea un aceite nuevo o bien una muestra de un aceite lubricante en uso. Existen normas centradas sobre la calidad del aceite lubricante, las cuales se encargan de controlar que el aceite que se formule cumpla los requisitos que se requieren para desempeñar el trabajo que se le exija. Entre este primer tipo, se encuentran un determinado grupo de organismos que regulan la calidad de los aceites lubricantes, como son: la American Petroleum Institute (API),

la Society of Automotive Engineers (SAE), la Association des Constructeurs Europeens d'Automobiles European Automobile Manufacturers Association (ACEA), la Association Technique de l'Industrie Européenne des Lubrifiants (ATIEL), la American Automobile Manufacturers Association (AAMA) y la Japanese Automotive Standards Organization (JASO). Mientras que, por otra parte, hay un grupo de normas que se especializan en la metodología que se debe seguir para caracterizar de forma correcta a un aceite lubricante. En este caso, los organismos que gestionan los ensayos y certifican su validez y vigencia correspondiente son: la American Society for Testing and Materials (ASTM), el Deutsches Institut für Normung (DIN), la International Organisation for Standardisation (ISO), el Coordinating European Council (CEC), el Energy Institute (IP, siglas de su anterior nombre Institute of Petroleum) y el International Lubricant Standardization and Approval Committee (ILSAC). A pesar de ser dos ámbitos diferentes, se han formado algunas fusiones o colaboraciones entre algunas agencias con el objetivo de formar un órgano con mayor peso. Este el caso del EOLCS (Engine Oil Licensing and Certification System) compuesto por: ILSAC, API, SAE y ASTM.

2.3 Exigencias de los Motores de Combustión Interna Alternativos

Un Motor de Combustión Interna (ICE, Internal Combustion Engine) hace referencia a aquellos motores, conjunto de elementos mecánicos, que desarrollan potencia (energía mecánica) directamente a partir de los gases de combustión (fluido operante o activo) derivados de la reacción de combustión de un combustible que se produce en su interior (energía térmica o calorífica). Un tipo de ICE son los llamados Motores de Combustión Interna Alternativos, MCIA, los cuales se caracterizan por ser un tipo de motor térmico que presenta un movimiento alternativo de sus elementos mecánicos para, empleando el estado térmico del fluido comprensible que lo traviesa, generar un trabajo. Por lo que, para garantizar un buen funcionamiento del motor; es importante tener un sistema de lubricación eficiente que sea capaz de garantizar que todo el conjunto de elementos mecánicos (ver Figura 2.18) funcionen de forma correcta [56].

Entre las variedad de diseños y construcciones de los MCIA, los elementos más influyente por lo que respecta al sistema de lubricación que debe presentar el motor son:

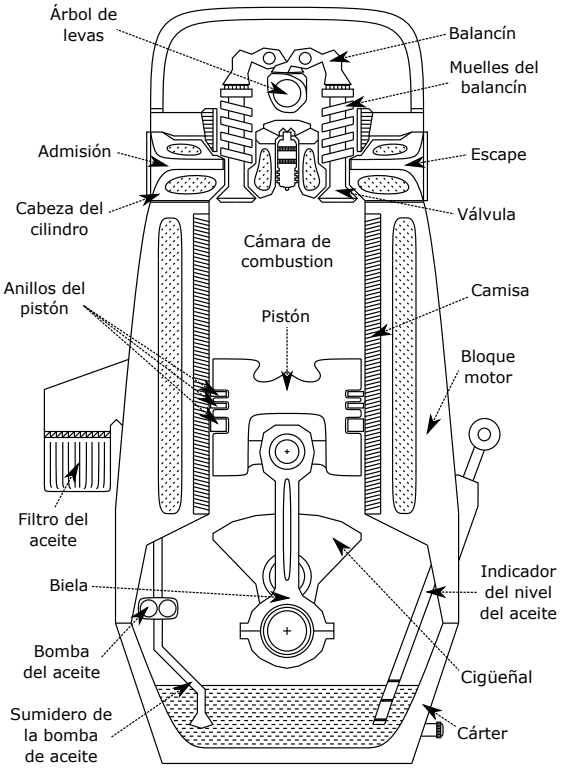

Figure 2.18. *Vista transversal de un MCIA.*

- El primer aspecto es el ciclo de combustión, dado que se pueden encontrar motores de 2-tiempos o de 4-tiempos. No obstante, la mayoría de motores (en el ámbito de la automoción) sigue la configuración de 4-tiempos, por lo que este aspecto se ha generalizado.

- El siguiente aspecto está relacionada con la construcción del motor. Este aspecto, puramente mecánico, se centra en escoger entre tres configuraciones: tronco, pistón o cruzado.

- El tercer punto sería si el motor requiere un sistema de sobrealimentación o bien trabajar en aspiración natural.

- Y el último sería aquel directamente centrado sobre el sistema de lubricación, dado que es propio y distintivos de cada motor.

En un MCIA, existen tres tipos de diferentes de sistema de lubricación, los cuales están adecuados de acuerdo con las condiciones de trabajo de aquellos elementos internos del motor que requieren ser lubricados. Así pues, estas variedades son las siguientes [17]:

- Lubricación por Cuchara y Salpicadura: También se conoce como Lubricación por Barboteo, cuyo principio es emplear un componente del motor que presente un giro rápido para poder favorecer la salpicadura del aceite lubricante. El caso más común es aquel que consiste en un sistema compuesto por una biela en cuya cabeza hay una cuchara, la cual, al sumergirse en el cárter, recoge cierto volumen de aceite lubricante. Luego esta cantidad de aceite, por la inercia que le transmite el movimiento de la biela, es capaz de llegar a: una parte del lubricante penetra en el cojinete de la misma biela para lubricarlo y otra parte es proyectada contra las paredes internas del cilindro y el cárter para que, por gravedad, avance a través de un sistema de canales hacia el cigüeñal y es sistema de distribución. Este tipo de lubricación está abandonada en los motores modernos debido a que se trataba de una forma de lubricar poco eficiente, aunque fue ampliamente usada con anterioridad en motores que presentaban regímenes de funcionamiento lentos. Actualmente, aún se puede encontrar este tipo de lubricación en ciertas regiones de un MCIA como la falda del pistón.

- Lubricación Forzada o a Presión: En este tipo de lubricación, se emplea un sistema específico de bombas y conducciones que obligan al aceite lubricante a llegar a aquellas regiones de interés que se desean lubricar (con una presión y caudal adecuados) para que, una vez realizada su tarea, fluya hacia el cárter en dónde se vuelve a realizar el ciclo. Anexo a este conjunto de bombas y canales, existe una serie de filtros o sistemas de depuración que extraen del aceite cualquier contaminante que puede llevar consigo de modo que se devuelva al circuito libre de ellos y, además un sistema de refrigeración si la situación lo requiere. Este tipo de lubricación es la que más beneficios aporta al motor, dado que garantiza una correcta lubricación en función de las condiciones de trabajo bajo las que está sujeto el motor en un determinado momento.

- Lubricación por Mezcla: Se trata de una lubricación dónde interviene dos componentes: aceite lubricante (componente minoritario de la mezcla) y el propio combustible (componente mayoritario), los cuales requieren ser mezclados o bien de forma directa (durante el repostaje) o bien por separado (mediante una bomba dosificadora). Se encuentra en

motores de dos tiempos y de carburación, en los cuales la mezcla aire-combustible se forma en el carburador. De esta forma, el aceite entra en compañía con la mezcla aire-combustible durante la admisión, para que una vez dentro de la cámara de combustión, el aceite se deposita (parcialmente) en las paredes internas de cárter y posteriormente en las del cilindro. En estos motores es el pistón el que se encarga de comprimir el fluido operante en el cárter dado que es este el único caso dónde se pone el aire carburado en contacto con el conjunto sistema-biela y en condiciones de lubricarlo. Por lo que se trata de un sistema de lubricación que consume aceite lubricante, dado que o bien se pierde a través del escape o bien se quema dentro del cilindro.

Debido a la complejidad que presenta los MCIA: este tipo de maquinaria poseen un gran número de elementos que se encuentran en contacto con otros y además en continuo movimiento. Es por eso, que los anteriores tipos de modos de lubricación pueden ser combinados adecuándolo para cada situación de modo que el conjunto global del motor esté perfectamente lubricado. Pero además, el funcionamiento del aceite lubricante se ve comprometido por el mero hecho de que la reacción de combustión se realiza en el interior del motor, por lo que a la difícil tarea anterior se le debe sumar: temperaturas elevadas, entorno con presencia de contaminantes, altos esfuerzos de cizallamiento, sobrepresiones, tipo y calidad del combustible, largos períodos de uso, ambientes corrosivos, presencia de gases de combustión, etc. En la Figura 2.19 se han mostrado los principales problemas que se producen en los elementos lubricados en un MCIA así como el rango de temperaturas en las que suelen trabajar ciertas regiones conflictivas:

Observando la Figura 2.19, se han coloreado las diferentes regiones térmicas que se producen en un MCIA. Estas regiones dependen de varios factores como: el tamaño del motor, condiciones de funcionamiento, combustible empleado, etc. por lo que según la configuración del motor, éstas pueden varias de forma significativa [72]. Así pues, a modo general, se puede encontrar las siguientes zonas:

- Las regiones más calientes son las coloreados con colores rojizos: la mayor de ellas, resaltadas en rojo, experimentan temperaturas $\sim$350°C. En estas zonas, pistón y válvulas, se favorece la formación de depósitos. Mientras que las coloreadas en naranja presentan temperaturas entre 200–300°C los fenómenos de desgaste son los más destacables.
- En un rango intermedio de temperaturas se encuentran: el conjunto biela-cigüeñal y el sistema de lubricación. El primero, de un color rosa,

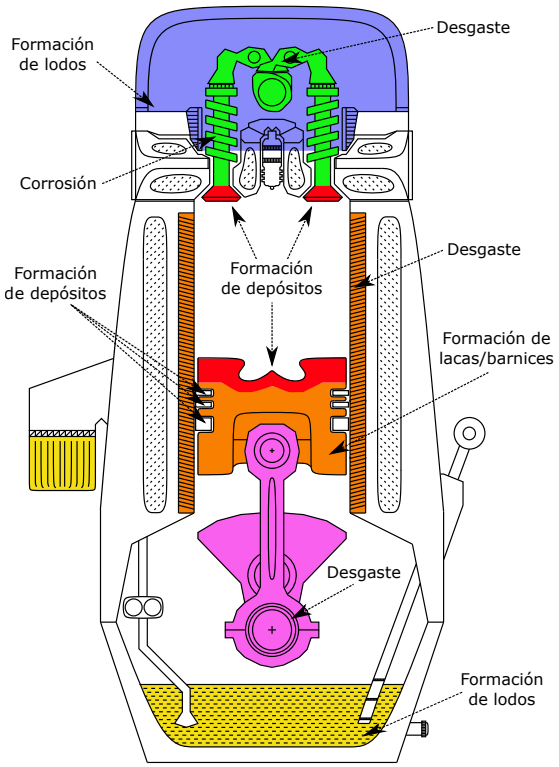

Figure 2.19. *Regiones de exigencia térmica y localización de fenómenos degradativos del motor.*

experimenta temperaturas de 80 a 150°C y fenómenos de desgaste. Por parte del sistema de lubricación, coloreado en amarillo simbolizando temperaturas de 90–120°C, los problemas que pueden aparecer son la formación de lodos en el fondo del cárter como resultado de todos los contaminantes que arrastra tras de sí el aceite lubricante. Además, el aceite lubricante también puede experimentar otros problemas como: incrementos de la viscosidad, estabilidad al cizallamiento y pérdidas de volumen por un consumo excesivo del mismo.

- Y, para terminar, las regiones térmicas más frías son: con 40–70°C (verde) el conjunto de árbol de levas y los balancines, y con 40–50°C la culata (azul). Estas temperaturas son propicias para que empiecen a sedimentar productos que deriven en la formación de lodos, los cuales pueden inducir fenómenos de corrosión y desgaste.

Debido a esta variedad, en cada uno de los sistemas que conforma un MCIA existen una serie de elementos o componentes que pueden llegar a entrar en contacto con el sistema de lubricación y pasar a combinarse y mezclarse con el aceite lubricante. En el siguiente diagrama, Figura 2.20, se han esquematizado aquellos contaminantes más comunes en los aceites lubricantes así como el sistema de procedencia por dónde han podido ingresar en el aceite:

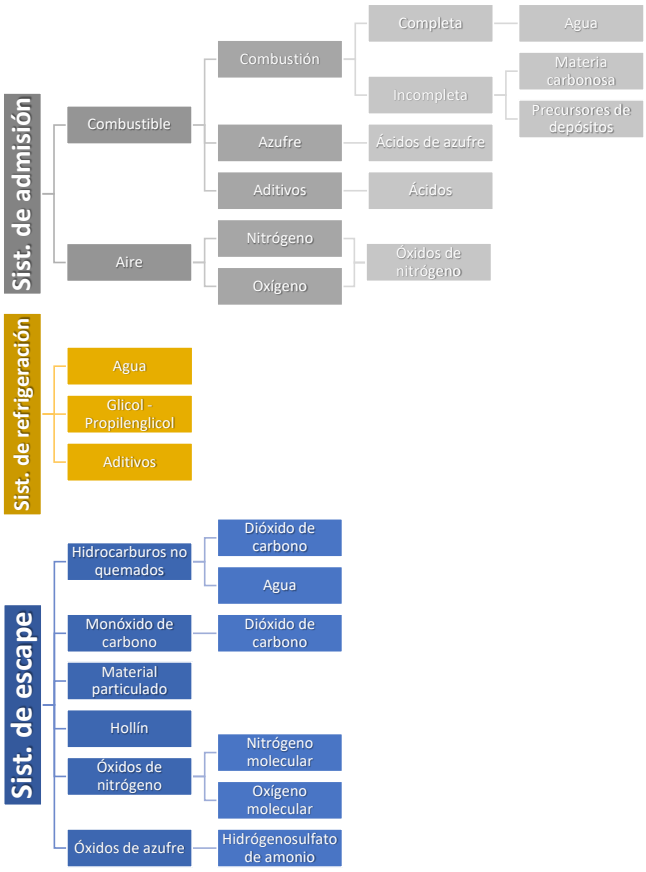

Figure 2.20. *Contaminantes de los aceites lubricantes, elementos susceptibles a formar parte o combinarse con el aceite lubricante.*

De acuerdo con la Figura 2.20, la diversidad de posibilidad de generar focos de degradación y contaminación del aceite lubricante son muy considerables. No obstante, siguiendo el esquema de la Figura 2.20, una vez detectado el elemento (anómalo al aceite lubricante) que genera el problema, se puede

seguir en sentido inverso el esquema para así buscar en qué sistema y dónde se localiza en centro del fallo.

En la actualidad, los MCIA se enfrentan a unas serie de desafíos o retos orientados a conseguir una optimización energética junto con una reducción (a límites muy severos) de sus emisiones contaminantes [6]. Esta imposición deriva en el desarrollo de nuevos motores, los cuáles son más respetuosos con el medio ambiente: tanto atendiendo a ser motores que presentan un menor consumo de combustible como a los niveles de emisiones que generan. No obstante, las estrategias que se siguen están orientadas a conseguir ambos aspectos: un buen rendimiento con un bajo impacto medioambiental [37]. Para conseguirlo, se está actuando en tres aspectos diferentes: sobre nuevas tecnológicas de combustión, el empleo de nuevos combustibles que generen combustiones más limpias y por último en el aspecto relacionada con todos los proceso de postratamiento de las emisiones de los ICE [2, 49].

Sea cual sea el campo dónde se desarrolle trabajo, se requerirá analizar como afectará al resto, dado que les tres campos: combustión, combustible y postratamiento, están interconectados [40]. Por consiguiente, se requiere una inversión en: experimentación, diagnóstico y simulación, para poder llegar a buen puerto y conseguir las metas marcadas. De este modo, los constructores (OEM, Original Equipment Manufacturer) deben intentar cumplir con las legislaciones expuestas por los organismos competentes. La legislación vigente en Europa es muy estricta por lo que respectos a las emisiones contaminantes. De hecho, si se observa cada una de las diferentes normas, normas EURO, que se han ido redactando con el paso de los años, se puede apreciar como cada vez los limites permitiros son cada vez más pequeños (ver Tabla 2.5) [19–22, 58].

Table 2.5. *Límites de emisiones de motores diésel según las distintas normas Euro.* [a] *hace referencia a que los valores marcados contienen tanto al NOx como HC, mientras que* [b] *solo afecta a motores de inyección directa.*

Normativa	Fecha de aprobación	Fecha de implantación	NOx (g/km)	PM (g/km)
Euro - I	01/Julio/1992	03/Diciembre/1992	0.97^{a}	0.1400
Euro - II	01/Enero/1996	01/Enero/1997	$0.90^{a,b}$	0.1000
Euro - III	01/Enero/2000	01/Enero/2001	0.50	0.0500
Euro - IV	01/Enero/2005	01/Enero/2006	0.25	0.0250
Euro - V	01/Septiembre/2009	01/Enero/2011	0.18	0.0050
Euro - VI	01/Septiembre/2014	01/Septiembre/2015	0.08	0.0045

La presión legislativa, a todos los niveles: local regional, nacional e internacional, es un indicativo del interés social que despierta el impacto

que ejerce sobre el medio ambiente las emisiones de gases contaminantes que se arrojan a la atmósfera. Por ese motivo, ha aparecido una corriente de conciencia global que ha provocado que se estén dedicando esfuerzos en poder mejorar aquellos aspectos de los MCIA que permitan cumplir con dichas normas (en especial, las más actuales [66]). Las soluciones que se han encontrado para tal problema se pueden organizar en: soluciones activas y soluciones pasivas. Las primeras son aquellas que provocan cambios o ajustes tanto en el motor como en sus componentes, mientras que las segundas se centran en el sistema de escape. Concretamente, las soluciones pasivas implican el uso de dispositivos que se incorporan al sistema de escape para que las emisiones, antes de ser vertidas a la atmósfera, cumplan con los niveles estipulados [36, 38]. De acuerdo con su descripción, han sido bautizadas como sistemas de postratamiento de gases de escape, pero aunque en un principio estos sistemas no deben alterar al motor, en realidad sí son responsables de alguna modificación o ajuste en alguno de los aspectos (en especial, la admisión y combustión de forma notoria). A continuación se proporciona un listado de aquellas acciones más importantes:

- Por lo que respecta al **sistema de inyección**, la acción se centra en inyectores de nueva generación que permitan poder alcanzar mayores presiones de inyección con unos tamaños (diámetros) de orifico menores. Pero además, la posibilidad de diseñarlos con varios grupos (coronas) de orificios que se accionen de forma independiente y con una geometría (del spray) distinta. Y si esto no fuera poco, los sistemas de doble inyección (2 inyectores funcionando de forma síncrona, según necesidades) también presenta buenos resultados [53].

- Otra opción que se plantea afecta a las **válvulas**. Se está buscando una flexibilidad en su accionamiento de modo que se puede adecuar su apertura/cierre según las condiciones de funcionamiento, desactivar ciertos cilindros y realizar ciclos alternativos.

- En los nuevos motores que se están diseñando se busca que sean capaces de presentar una **relación de compresión variable** que se ajuste a las condiciones de funcionamiento y al combustible que se esté empleando. De modo que, llegados el momento, esto facilite el paso de poder aunar varias acciones, como seria los nuevos modos de combustión, para conseguir un beneficio mayor.

- Mejora e implementación de nuevos sistemas de **recirculación de gases de escape** (EGR) [1].

- Como la tendencia que se está siguiendo es la fabricación de motores más reducidos y sobrealimentados, la evolución de las **técnicas de sobrealimentación** es pues un punto de estudio importante.

- El **postratamiento de gases de escape** es un aspecto con especial relevancia, dado que se trata del último estadio dónde se puede actuar antes de que el motor expulse al exterior los subproductos de la combustión. Por ende, la investigación en este campo, buscando nuevos materiales y configuraciones de fases y tecnologías para la transformación/captura/eliminación de las emisiones está continuamente evolucionando.

- Por lo que respecta a los **combustibles**, se están mejorando las propiedades de los combustibles tradicionales para poder adecuarlos acorde con las necesidad que están requiriendo los nuevos motores, pero también se están desarrollando y probando nuevos combustibles alternativos. Lo que se busca en los combustibles es que su combustión sea más limpia y que el poder calorífico sea lo más alto posible.

- Desarrollo de **técnicas avanzadas de control** del motor.

- Nuevos **modos de combustión** que permitan una combustión y funcionamiento del motor, desde el punto de vista de desempeño del trabajo y desde el punto de vista medioambiental, más eficiente [3, 51].

A pesar del buen propósito que tiene todos estos trabajos [28], por lo que respecta al aceite lubricante, el resultado de algunos de ellos deriva en unas condiciones más severas y unas demandas más exigentes sobre él. Dependiendo según como sean, se puede producir una pérdida o destrucción de aceite lubricante. Este hecho está relacionado con la combustión, dado que las altas temperaturas que se dan durante el proceso, provocan que parte del aceite lubricante se queme. La cantidad de lubricante que se pierde por esta vía depende de: en primera instancia de la temperatura que se alcanza en la combustión (y el tiempo en que están vigentes), luego los elementos que conforman la cámara de combustión, la mezcla aire-combustible para la combustión y la volatilidad del propio aceite lubricante. Cualquier elemento o agente que altere alguno de estos puntos derivará en un efecto sobre el aceite lubricante.

De todo el listado anterior, las acciones que tiene un mayor impacto sobre el aceite lubricantes son: la recirculación de gases de escape y el postratamiento de los gases de escape, principalmente. Estos dos recursos

son los actores con mayor peso que intervienen en una degradación pronta del aceite lubricante en un MCIA debido a que, a pesar de estar orientados a reducir las emisiones contaminantes (en especial en motores diésel), generan unas demandas mayores (más exigentes) tanto al propio motor como al aceite lubricante.

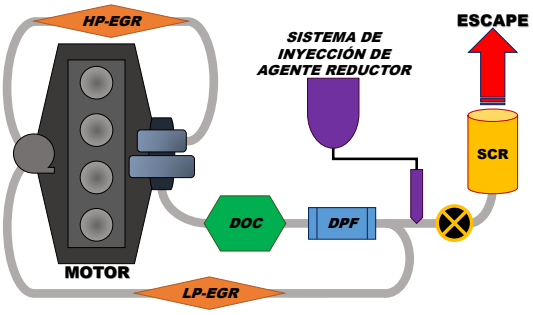

Figure 2.21. *Esquema de la distribución de los diferentes sistemas de postratamiento de los gases de escape en un motor diésel de automoción.*

En la Figura 2.21, se han esquematizado los elementos más importantes y relevantes que conforman el sistema de prostratamiento en un MCIA. De entre ellos destacan: el catalizador de oxidación (DOC), el filtro de partículas (DPF), el catalizador de reducción selectivo (SCR) y el sistema de recirculación de los gases de escape (EGR). Cada uno de ellos, por una vía u otra, tienen una cierta influencia sobre el aceite lubricante. De modo que, para comprender mejor cómo puede darse esta influencia y cómo es esa, es requerido primeramente conocer el papel que desempeñan y cómo funcionan estos distintos elementos:

- Catalizador de Oxidación (DOC): Se trata de un sistema que se incorpora al sistema de escape de un MCIA con el objetivo de transformar ciertos componentes de las emisiones de escape (que presentan cierto toxicidad y peligrosidad, tanto para los seres vivos como para el medio ambiente) [18]. El DOC emplea una serie de catalizadores metálicos, catalizadores que son específicos para llevar a cabo la transformación de aquellas sustancias químicas peligrosas en otras con un menor índice de peligrosidad. En este sistema, los compuestos químicos de los gases de escape que requieren ser convertidos son: los hidrocarburos sin quemar (UHC) (ver reacción 2.14) y el el monóxido de carbono (CO) (ver reacción 2.15) [61].

$$C_xH_{2y} + (x + y/2)O_2 \rightarrow xCO_2 + yH_2O \tag{2.14}$$

$$2CO + O_2 \rightarrow 2CO_2 \tag{2.15}$$

El resultado final de esta transformación catalítica son subproductos de oxidación: agua (H_2O) y dióxido de carbono (CO_2), con una peligrosidad menor a la de sus predecesores. En la siguiente figura, Figura 2.22, se muestra un esquema de la construcción de un DOC dónde se aprecia el monolito en el cual se depositan los compuestos reactivo que se emplean como catalizadores de las diferentes reacciones de oxidación:

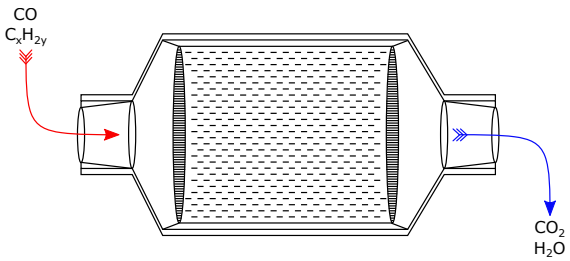

Figure 2.22. *Diagrama de un DOC dónde se aprecia la entrada de gases provenientes del motor (coloreados en rojo) y los mismos gases una vez reaccionados con el catalizador pertinente (coloreado en azul).*

Pero por contraposición también genera la reacción de oxidación del dióxido de azufre (SO_2) y del monóxido de nitrógeno (NO), las cuales son reacciones no deseadas:

$$2SO_2 + O_2 \rightarrow 2SO_3 \Rightarrow SO_3 + H_2O \rightarrow H_2SO_4 \tag{2.16}$$

$$2NO + O_2 \rightarrow 2NO_2 \tag{2.17}$$

Como resultado de la oxidación del SO_2 y su posterior combinación con el agua generada como producto de la reacción de combustión, puede producir de ácido sulfúrico (H_2SO_4) tal y como se muestra en la reacción 2.16. Mientras que la siguiente reacción, la reacción de oxidación del monóxido de nitrógeno (2.17), genera un producto gaseosos de mayor toxicidad e irritante: NO_2. Para evitar esta reacciones secundarias, es necesario emplear un sistema extra que se encargue de la destrucción de estos productos [7].

- Filtro de Partículas (DPF): El DPF consiste en un filtro monolítico cerámico poroso, entre un 35–50%, compuesto por un entramado de canales paralelos de pequeño diámetro (reducida sección transversal, 10 y 25 μm) por los cuales se les hace fluir, en sentido longitudinal, los gases de escape con el propósito de retener en los canales aquellas partículas que los gases pueden llevar consigo. La naturaleza y composición de las partículas, material particulado (PM) que el DPF es capaz de separa de los gases de escape es variada: hollín/materia carbonosa, hidrocarburos, sulfatos, agua y cenizas. Para poder retener las partículas, el monolito posee una configuración de sellado de los canales (en sus extremos) de forma alternativa para que de este modo, el gas se vea forzado a travesar las paredes de los canales y así favorecer que en dichas paredes se queden adheridas las partículas. Con este sistema, se consiguen una eficiencias de filtrado cercanas al 95% [30]. En la Figura 2.23 se ha representado un esquema de uno de los tipos de DPF más utilizados, "wall-flow":

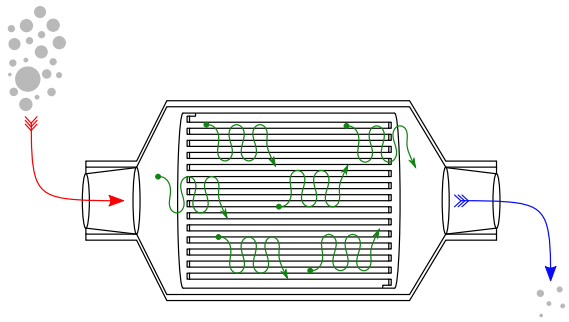

Figure 2.23. *Diagrama de un DPF, tipo wall-flow, dónde se aprecia la entrada de materia particulada (PM), el cual al pasara a través del filtro cerámico, se eliminan gran parte de las partículas, en especial las más grandes.*

No obstante, los DPFs deben reunir otra serie de características para poder ser utilizados. Estos requerimientos adicionales son: poder soportar elevadas temperaturas de operación, sus materiales de construcciones debe presentar una gran resistencia térmica (choque térmico) y mecánica, gran poder y rendimiento de filtración con un bajo coste de mantenimiento (gran capacidad de acumular partículas), no generar nuevas emisiones y por último ser capaces de aceptar la posibilidad de interactuar con otros sistemas de regeneración (compatiblidad) [16].

Por uso, la acumulación de residuos en los canales provoca que éstos queden obstaculizados provocando una caída del rendimiento del filtro, es decir, el filtro se colmata. Este problema provoca que el paso de gas a través de los poros del se vea perjudicado, por lo que empiezan a tener lugar contrapresiones de escape que afectan negativamente al funcionamiento del motor: dificulta de renovación de gases y aumenta el consumo de combustible [74]. Con el propósito de evitar la colmatación del filtro, se realizan una serie de estrategias de regeneración para conseguir eliminar esos depósitos dentro de los canales del filtro y así restituirlos [15, 26]. Esos procesos de regeneración, que deben estar controlados con el fin de evitar fallos en el DPF [78], son procesos de oxidación que requieren altas temperaturas (500–600°C). Para conseguir las condiciones óptimas para la regeneración del DPF, son requeridas una serie de vías que permitan alcanzar esas temperaturas:

- La primera vía consiste en aportar la energía suficiente (calor) al DPF de forma directa para lograr la regeneración térmica del filtro. Esta vía recibe el nombre de *regeneración activa*, dado que se actúa de forma directa sobre el DPF. Concretamente, la forma más extendida de proceder en este tipo de regeneración es o bien alterando los protocolos de inyección del motor, o bien dotar al DPF de un sistema de calentamiento propio. El primero de estos dos es el protocolo más usado, dónde se realiza una modificación del mapa de inyecciones para incluir una serie de de post-inyecciones (inyecciones tardías al final de la etapa de expansión) que buscan que el calor liberado en la combustión pase al sistema de escape llegando hasta el DPF. Si esto no fuera posible, existe la opción de realizar una inyección extra de forma directa en el sistema de escape [10]. El inconveniente de aportar por esta vía el calor necesario para conseguir las temperaturas necesarias es el hecho de emplear combustible, el cual no realiza ningún trabajo mecánico, y de ser un protocolo agresivo para el DPF (estrés térmico).
- La otra opción es alterar el mecanismo de oxidación de las partículas mediante la búsqueda de rutas oxidativas que requieren temperaturas de iniciación más bajas. Esta forma de proceder es conocida como "regeneración pasiva", dado que busca la regeneración del DPF se realice de forma automática en las temperaturas normales que se encuentran en el sistema de escape. Para poder lograr esta auto-oxidación, existen varios procedimientos: funcionalizar la superficie del filtro cerámico con

un catalizador específico, emplear combustibles que contengan aditivos de oxidación (llamados Fuel Borne Catalyst) o aportar una especie oxidante al DPF. La opción más sencilla es la última, dado que la configuración más extendidas de los sistemas de postratamiento es colocar el DPF después del DOC. Como consecuencia de esta disposición, es posible emplear el NO_2 como dicho agente oxidante [27, 35]. Empleando este gas, se consiguen temperaturas de inicio alrededor de los 250–300°C.

Ambas modalidades de regeneración pueden ser combinadas para conseguir regeneraciones más controladas y que garanticen la integridad y funcionalidad del DPF, ampliando así su vita útil. En conclusión, a pesar de ser una sistema con altos rendimiento de filtrado, el DPF presenta el problema de requerir realizar procesos de regeneración y limpieza que restauren su funcionalidad, procesos que afectan al aceite lubricante [64].

- Catalizador de Reducción Selectivo (SCR): El SCR surgió por la necesidad de reducir la cantidad de ciertos compuestos de los gases de escape pero, debido a la abundancia de oxígeno en los gases, la vía de reducción catalítica convencional no podría llevarse a cabo. Así pues, estos sistemas tiene como objetivo la disminución de la concentración en las emisiones de un MCIA de óxidos de nitrógeno (NOx) [29]. Para conseguirlo, el SCR hace uso de una serie de reacciones químicas que emplean un agente líquido con propiedades reductoras que se mezcla con los gases de escape. La construcción de un SCR está compuesta por varios elementos tal y como se muestra en la Figura 2.24:

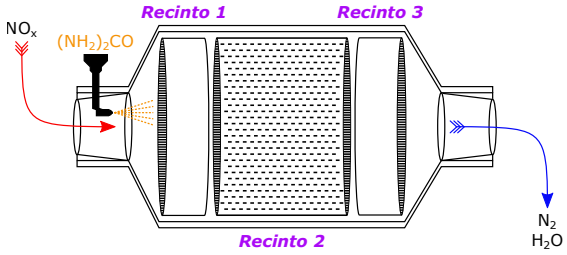

Figure 2.24. *Diagrama de un SCR, en el cual se han representado los diferentes compartimentos dónde se realizan cada una de las tres fases del proceso catalítico de los gases de escape.*

En el interior del SCR, básicamente, se encuentran una serie de sustratos cerámicos sobre los cuales se han depositado una serie de óxidos de metales de transición (por ejemplo, vanadio y titanio) que favorecen la reacción de transformación de los NOx. Como se observa en la Figura 2.24, existen varias zonas diferenciadas en el sistema. Esto se debe a que en cada una de ellas se produce una de las etapas del proceso de reducción catalítica: en la primea sección se procede a la hidrólisis catalítica de la urea (reacción 2.18), a continuación tiene lugar la reducción de los NOx (ver reacciones 2.19, 2.20 y 2.21) y por último se realiza la oxidación del amoniaco (reacción 2.22).

$$(NH_2)_2CO + H_2O \rightarrow 2NH_3 + CO_2 \tag{2.18}$$

$$8NH_3 + 6NO_2 \rightarrow 7N_2 + 12H_2O \tag{2.19}$$

$$4NH_3 + 4NO_2 + O_2 \rightarrow 4N_2 + 6H_2O \tag{2.20}$$

$$2NH_3 + NO + NO_2 \rightarrow 2N_2 + 3H_2O \tag{2.21}$$

$$4NH_3 + 3O_2 \rightarrow 2N_2 + 6H_2O \tag{2.22}$$

El resultado final de todo el proceso es la conversión del más del 90% del NOx. A pesar del buen desempeños de este sistema requiere de unas condiciones de uso y de trabajo muy controladas:

- Con los problemas que puede derivar el uso masivo de amoniaco (NH_3), se emplea urea ($(NH_2)_2CO$) como fuente de amoniaco dado que se trata de un compuesto no toxico y biodegradable. Así pues, empleando disoluciones de urea en agua (del orden del 30–40%) se puede obtener amoniaco suficiente como para seguir con los procesos de reducción.
- Como la información de la urea es por vía catalítica, se requiere un elevado control sobre la cantidad que es inyectada dentro del sistema. Debido a que en ocasiones pueden producirse ciertos descontroles en la tase de inyección de urea, puede darse el caso de que se genere más amoniaco que el que se va a consumir. Cuando esto sucede se generan emisiones de amoniaco, lo cual no

es recomendable. Es por eso que para evitarlo, se incorporo una etapa de oxidación catalítica del amoniaco para así solucionar el problema.

– La relación molar entre el agente reductor (NH_3) y el NOx debe ser $\sim$0.9, por lo que se debe construir un catalizador lo bastantemente voluminosos como para favorecer el contacto entre los distintos elementos que entrenan en juego en el proceso (relacionado con os tiempos de residencia).

- Sistema de Recirculación de Gases de Escape (EGR): La recirculación de los gases de escape tiene como meta intentar minimizar la cantidad de NOx que emite un MCIA. Para ello, el funcionamiento de esta herramienta consisten en introducir en la cámara de combustión los gases que se han generado durante la combustión. Como resultado, se produce una dilución (que en ciertos casos puede llegar a ser del 50%) entre los gases de combustión con los gases frescos provenientes de la admisión. Así pues se consigue reducir la proporción óxigeno-combustible durante la combustión, lo que deriva en que esta combustión sea a más baja temperatura (llama más fría) [23, 41]. La recirculación de los gases de escape puede realizarse a través de dos vías:

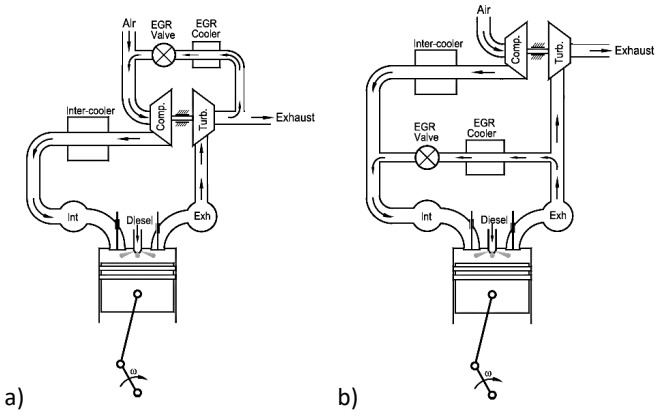

Figure 2.25. *Los dos sistemas EGR existentes: a) Se trata de un EGR de baja presión y b) Es un EGR de alta presión [79].*

– *EGR de baja presión*: este tipo de EGR se realiza desde la salida de la turbina hacia la entrada del compresor. (LP-EGR, low pressure loop EGR).

– *EGR de alta presión*: ahora la vía parte de la entrada de la turbina y prosigue hacia la salida del compresor. (HP-EGR, high pressure loop EGR).

En ambas modalidades de EGR se requiere de ajustes en el motor para poder producir un caudal que sea capaz de fluir por todo el sistema como consecuencia de la aparición de un gradiente de presión entre el escape y la admisión. Para ello se puede actuar en una de estas dos regiones: si es escoge el escape, es necesario provocar una contrapresión elevada mediante el uso de una turbina, mientras que si se escoge la otra opción, lo más sencillo es reducir (de forma local) la presión en la zona a través de sistemas con un venturi.

A pesar de ser una buena solución para la reducción de las emisiones contaminantes, el EGR tiene alguna serie de inconvenientes: los sistemas EGR provocan un estrés térmico al motor y además modifican toda la química del proceso de combustión [46]. Es por esa razón que, en ciertos casos, pesan más los problemas derivados del uso del EGR que los beneficios [4, 5]. De entre los inconvenientes más relevantes de este sistema es la generación de un aumento de las concentraciones de PM e UHC en los gases de escape [42–45], sin olvidar la contribución que tiene el EGR sobre la degradación y contaminación del aceite lubricante [47].

Por concluir, según todo los descrito en este apartado, queda claro que los nuevos MCIA presentan un alta demanda por lo que respeta a su desempeño tanta a lo que concierne a su rendimiento de trabajo que produce como a las emisiones que de ellos derivan. Como consecuencia de todo ello, ha quedado claro que el aceite lubricante también debe ser capaz de poder amoldarse a este nueva escena. Actualmente, el ámbito que concierne al aceite lubricante es muy exigente, por lo que se requiere tener en cuenta los tres pilares que determinan el rendimiento de un aceite lubricante (ver Figura 2.26).

Cada uno de estos tres aspectos o rasgos están relacionados con una serie de pautas que se dan lugar en un aceite lubricante:

- Por **degradación** se entiende como mecanismo por el cual se producen variaciones de las propiedades características de un aceite lubricante.
- La **contaminación** se trata de la presencia de especies ajenas dentro de la matriz del aceite lubricante. La presencia de dichos contaminantes puede acarrear al desarrollo de fenómenos de degradación del mismo aceite así como fallas en la lubricación del motor.

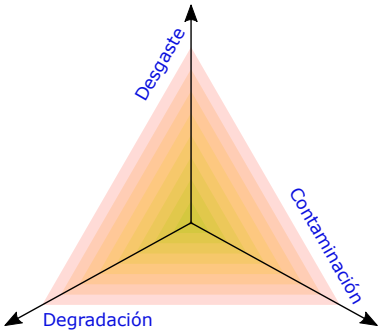

Figure 2.26. *Aspectos a tener en consideración a la hora de analizar/evaluar el comportamiento de una aceite lubricante para así mantener un seguimiento de la evolución de su estado.*

- Y por último, el **desgaste**. Se trata de un tipo de contaminación, la cual se basa solamente en aquellas partículas cuya procedencia es debida a la aparición de fenómenos de desgaste sufrido en el motor. Por esa razón, el desgaste se centra principalmente en las partículas metálicas.

En la siguiente tabla, Tabla 2.6, se muestra un ejemplo de los diferentes orígenes de los agentes detonantes de cada uno de los tres rasgos anteriormente citados así como una aproximación del grado de relevancia que cada uno de ellos tiene sobre el estado del aceite lubricante (y del motor) [11].

Table 2.6. *Orígenes y causantes de los diferentes rasgos relevantes del estado del aceite lubricante.*

Rasgo	**Causante**	**Impacto (%)**	
Degradación	Cambio de sus propiedades por uso	20.2	
Contaminación	Dilución por combustible	7.2	40.2
	Ingreso de líquido refrigerante	9.7	
	Subproductos de la combustión	12.1	
	Polvo/Suciedad	11.2	
Desgaste	Desgaste anormal	37.3	
Otro	Consumo excesivo de lubricante	2.3	

De modo que, si no se conoce y se estudia con detalle estos tres aspectos: degradación, contaminación y desgaste, difícilmente se podrá conocer cómo

se comportará el aceite lubricante postulado para realizar una determinada tarea.

2.4 Degradación del aceite lubricante

Por degradación se entiende el proceso por le cual el aceite lubricante experimente una variación por lo que respecta a sus propiedades físico-químicas, lo cual deriva en una reducción de su capacidad por desempeñar de forma correcta las tareas o funcionas por las fue formulado. Entre los diferentes factores que provocan la degradación del aceite lubricante como son: la exposición a temperaturas elevadas [31], elevados ratios de cizallamiento, atmósferas corrosivas (presencia de gases de combustión) y la presencia de elementos contaminantes, se le debe sumar aquellas tendencias a la hora del diseño de los nuevos MCIA. Los nuevos MCIA se caracterizan por: su alta potencia específica (alta potencia por unidad de desplazamiento), relaciones carrera del pistón/diámetro interno del cilindro elevadas, tamaños más reducidos y con un volumen de aceite menor, ODI más largos (por motivos de ahorro en el consumo de aceite) y por aquellos aspectos relacionados los requerimientos necesarios para incorporar los sistemas de control de emisiones contaminantes. Así pues, bajo estas condiciones, los parámetros o variables físico-químicas del aceite lubricante empleados para determinar el grado de degradación que éste ha experimentado son: su viscosidad, el grado de oxidación/nitración, el carácter ácido/básico que presente y por último el agotamiento del paquete de aditivos.

2.4.1 Viscosidad y densidad

La viscosidad y la densidad son dos parámetros que se encuentran relacionados, pero son dos propiedades físicas diferentes: la primera indica la fluidez de un material, mientras que la segunda se trata de la relación entre el peso de una sustancia y el volumen que ocupa. Por ende, cuando se analiza su dependencia con la temperatura también muestran comportamientos diferentes (ver Figura 2.27) [62]:

A la vista de la Figura 2.27, se observa que la temperatura es una variable que conlleva una diferencia significativa entre el comportamiento de la viscosidad (simbolizada por la linea roja) y la densidad (representan por la linea azul). Por consiguiente, el comportamiento de ambos parámetros, cuando el aceite empiece a usarse y den comienzo los fenómenos de degradación también será distinto la variación que la viscosidad y la densidad registren [25].

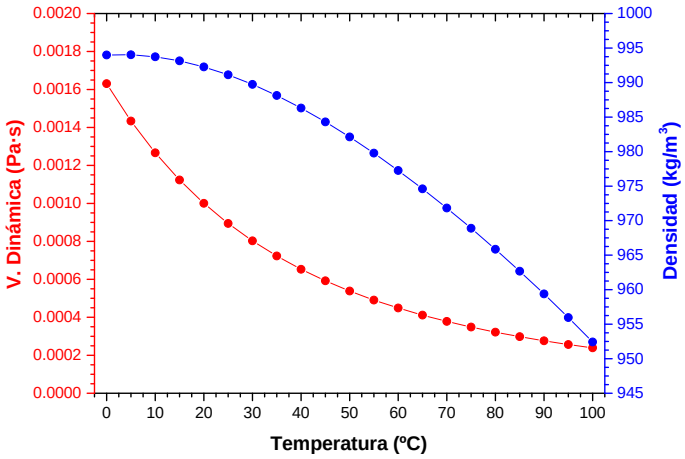

Figure 2.27. *Variación de la viscosidad dinámica (o viscosidad absoluto) y la densidad en función de la temperatura.*

Para el caso de la viscosidad, centrando el foco sobre la viscosidad cinemática, son varios los efectos a los cuales dicha viscosidad cinemática experimenta reacciones o alteraciones. Básicamente, se puede estructurar los efectos en dos grupos: uno que esté relacionado con modificaciones experimentadas en la composición del aceite lubricante y otro que trate aquellos elementos ajenos al aceite (contaminantes).

- Por lo que respecta a **cambios en el aceite lubricante**, se pueden producir efectos opuestos: unos que aumenten el valor de la viscosidad y otros que la reduzcan.

  – Aumento de la viscosidad: como consecuencia de los procesos de degradación oxidativa y térmica, el aceite lubricante experimenta cambios químicos (como podría ser las reacciones de polimerización) que provocan que su viscosidad aumente. Pero además, en este tipo de procesos, pueden llegar a formarse compuestos (por ejemplo: lodos, barnices, lacas, etc.) que también reportan un aumento de la viscosidad. Si las temperaturas son bastante elevadas, puede darse el caso de que el aceite empiece a evaporarse (primero aquellos componentes más volátiles), por lo que se genera un efecto de concentración que multiplica el peso de los problemas descritos en las lineas anteriores.

– Descenso de la viscosidad: por uso, puede darse el caso de que las condiciones de trabajo exijan tanto al aceite que, por un mecanismo u otro, provoquen la ruptura de las moléculas de la base que lo compone. Como consecuencia de ello se observa como la viscosidad desciende. Pero, además, en los aceite lubricante actuales, en su composición también se encuentran aditivos especialmente formulados para mejorar la viscosidad del aceite lubricante final, los aditivos VII. Este tipo de aditivos, de base polimérica, también pueden degradarse si se les somete a condiciones de alta cizalla, perdiendo así la capacidad de retener la viscosidad del aceite lubricante (ver Figura 2.28).

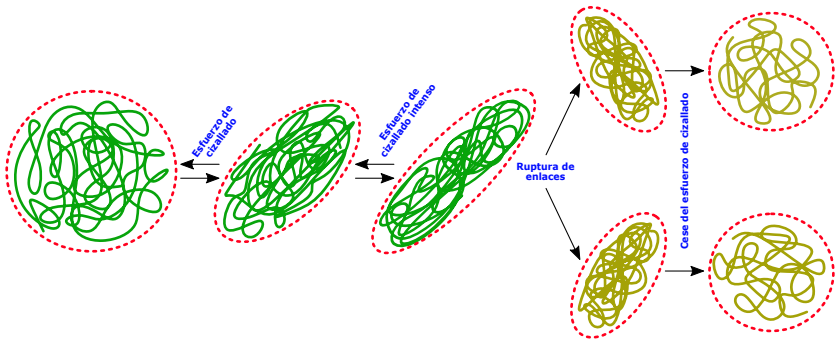

Figure 2.28. *Degradación de los aditivos VII por acción mecánica.*

- La presencia de **contaminantes** en el aceite lubricante también presenta esa dualidad, en función de la naturaleza del agente contaminante en sí. Entonces, es posible encontrar:

  – Aumento de la viscosidad: los contaminantes que poseen una viscosidad mayor que la del aceite que será su anfitrión, va a provocar que dicho valor aumente. Por consiguiente, aquellos contaminantes que entrarían en este grupo seria: el agua, aquella materia insoluble que pueda formarse, la carbonilla.

  – Descenso de la viscosidad: en este momento, exceptuando fallos o problemas muy graves, el contaminante que produce un descenso de la viscosidad es el combustible.

Ahora, para la densidad, el sentido (si aumenta o decrece) de evolución es el mismo que la viscosidad, pero cambia la magnitud del cambio producido.

2.4.2 Oxidación y nitración

La oxidación y la nitración de un aceite lubricante es una forma de comprender su grado de envejecimiento.

Por lo que respecta a la oxidación, se trata de un reacción química que involucra al aceite lubricante y un elemento oxidante para formar compuestos como: ésteres, cetonas, aldehídos o ácidos carboxílicos (todos ellos, compuestos con grupos carbonilo) entre otros. La oxidación en un MCIA se produce en dos regiones: en el cárter y en la cámara de combustión.

- En el cárter es donde se reúne la mayor cantidad de aceite lubricante y, más importante aún, una gran cantidad de oxígeno.
- La cámara de combustión es la otra región del motor dónde también entra en juego es sistema de lubricación. Esto se debe a las temperaturas que en ella se alcanzan: 200°C y 300°C, en promedio.

De modo que cada una de las zonas, reúnen uno de los dos componentes que favorecen la oxidación del aceite: o bien altas cantidades de agente oxidante (como en el caso el cárter) o bien elevadas temperaturas (alcanzadas durante la quema del combustible dentro de la cámara de combustión). Por lo que respecta al cárter, cuanto mayor cantidad de los elementos que entran en juego, aceite y oxigeno, estén en contacto entre sí, más fácilmente puede producirse la reacción entre ellos. Mientras que, la temperatura tiene un efecto potencionador dado que es una forma de aportar la energía suficiente como para superar el umbral energético (energía de activación, E_a) además de favorecer un incremento de la velocidad de la reacción (v). En la Figura 2.29 se ha esquematizado una reacción endotérmica:

En la cual su velocidad de reacción (v) se podría escribir según la siguiente expresión (Ecuación 2.23):

$$v = -\frac{d[A]}{dt} = -\frac{d[B]}{dt} = \frac{d[C]}{dt} = \frac{d[D]}{dt} = k \cdot [A]^m \cdot [B]^n \tag{2.23}$$

De acuerdo con la Ecuación 2.23, la constante de velocidad de la reacción (k) presenta la siguiente forma (ver Ecuación 2.24):

$$k = A \cdot e^{\frac{-E_a}{R \cdot T}} \tag{2.24}$$

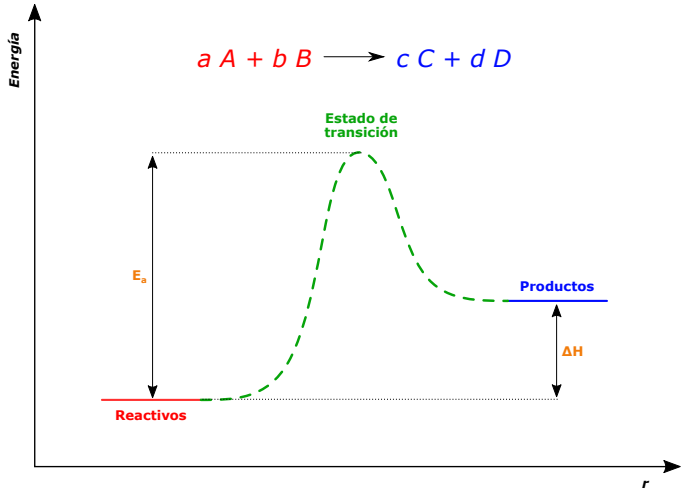

Figure 2.29. *Diagrama de energías de una reacción endotérmica, $\Delta H > 0$.*

En dónde: A se trata de un factor pre-exponencial, E_a es la energía de activación de la reacción, R es la constante de los gases ideales (cuyo valor es 8.31472 J/K·mol) y T es la temperatura (expresada en Kelvin). De modo que la temperatura es un factor que influye tanto en la energía de E_a como en la velocidad de la reacción tal y como se justifica con la Ecuación 2.25 (en condiciones de presión constante):

$$E_a = R \cdot T^2 \cdot \left(\frac{\partial ln(k)}{\partial T} \right)_p \tag{2.25}$$

Con todo esto queda claro el impacto de la temperatura sobre la termodinámica y la cinética de la reacción de oxidación. Pero, ni la presencia de oxígeno ni la temperatura son los únicos factores que condicionan la oxidación del aceite lubricante, dado que pueden intervenir otro tipo de agentes como: partículas metálicas (que tiene la capacidad de actuar como catalizador en ciertas etapas de la oxidación) y otros productos de degradación.

Así pues, la oxidación del aceite lubricante tiene un fuerte impacto sobre:

- La viscosidad, dado que la oxidación favorece los procesos de polimerización de la matriz del aceite lubricante.

- Una acidificación del lubricante y un desgaste corrosivo en el motor como consecuencia de la aparición de compuestos ácidos agresivos para ciertas superficies metálicas.

- Aparición de productos insolubles y material carbonoso indicativos de estados avanzados de la oxidación del lubricante. Lo cual se detecta fácilmente observando el aspecto: oscurecimiento del color y opacidad que adopta el aceite lubricante.

Por lo que concierne a la nitración, ésta es una reacción también oxidativa la cual tiene por agente oxidante los óxidos de nitrógeno (NOx). Por esa razón la nitración y la oxidación son dos procesos degradativos del aceite que se encuentra íntimamente conectados, tal como parece indicar la Figura 2.30:

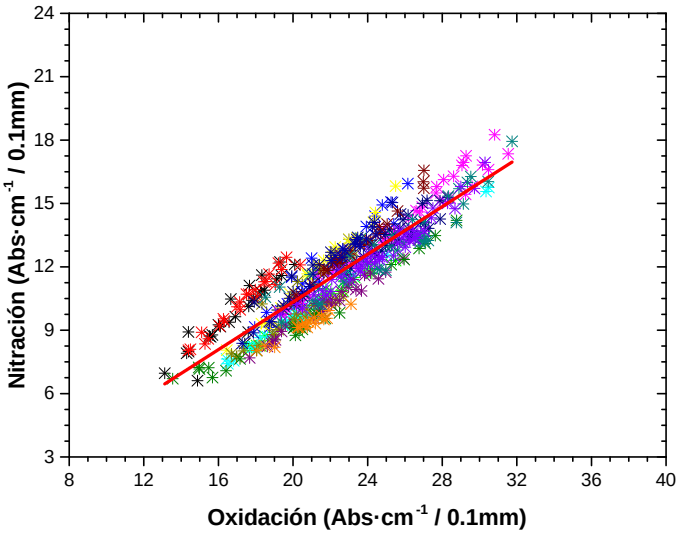

Figure 2.30. *Relación oxidación-nitración en aceites lubricantes. La determinación de ambos parámetros fue realizada mediante espectroscopia FT–IR.*

Pero ahora, el agente oxidante proviene como resultado de combustiones que emplean dosados (mezclas combustible-aire) pobres. Como consecuencia de este dosado, el balance entre los óxidos de nitrógeno y el oxígeno que pueden reaccionar con el aceite lubricante es favorable al primero de ellos dos. La incorporación de gases ricos en óxidos de nitrógeno: el óxido nítrico (NO) y el dióxido de nitrógeno (NO_2) principalmente, es debido al fenómeno de blow-by (ilustrado en la Figura 2.31):

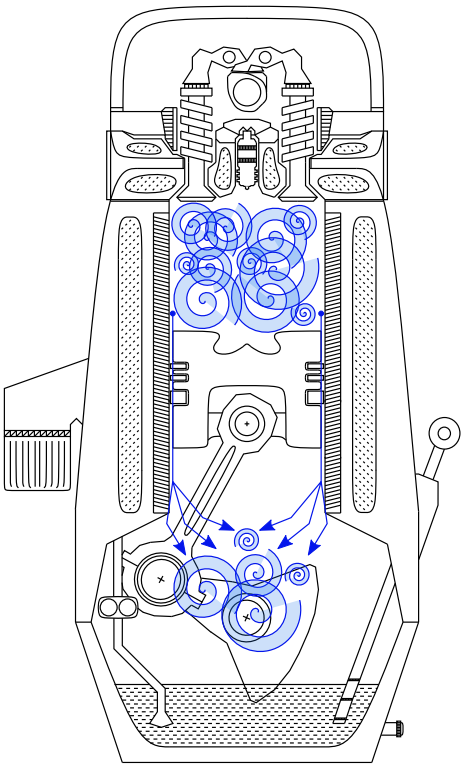

Figure 2.31. *Paso de los gases de combustión hacia el cárter debido al fenómeno de soplado (o blow-by).*

Estos gases, al encontrarse con el aceite lubricante reaccionan dando lugar a una reacción exotérmica (libera calor) que provoca la incorporación de grupos nitro (-NO_2) a las moléculas de base y ciertos aditivos del aceite. Pero existe una distinción, a tener en cuenta: si el aceite que reacciona es el que se localiza en el cárter, al encontrarse este a temperaturas relativamente bajas, la reacción de nitración no es tan agresiva. Como resultado se forman compuestos de nitrógeno inestables y organo-nitratos que, al ser especies tan inestables/reactivas, inmediatamente reaccionen con el oxígeno para oxidarse dando pie a la aparición de lodos y barnices. Pero si el aceite que reacciona es aquel que genera la película de la cámara de combustión, las condiciones son muy distintas y por consiguiente la reactividad también. En la cámara de combustión, región donde las temperaturas que se alcanzar son muy altas, las reacciones se producen con mayor velocidad. Pero, independientemente de la vía que se siga, al final el aceite degradado irá a acumularse en el cárter,

por lo que al fin se produce un proceso de acumulación constante de lodos y barnices derivado de la nitración.

Por concluir, ambos procesos: la oxidación y la nitración, son responsables de la limitación de la vida útil del lubricante y su contaminación con especies y compuestos que lo dañan de forma paulatina durante todo el tiempo de vida útil.

2.4.3 Total Acid Number (TAN) y Total Basic Number (TBN)

El TAN y el TBN son dos indicadores del estado del aceite lubricante los cuales entre ellos son dos parámetros antagónicos que describen un mismo fenómeno pero mediante aproximaciones diferentes: el TAN explica el fenómeno de la degradación como la aparición de compuestos con carácter ácido en el aceite, mientras que el TBN lo explica como el consumo de la reserva alcalina que posee el aceite lubricante como consecuencia de la aparición de especies ácidas derivadas de la degradación del aceite. En conclusión, si se registrara la evolución de ambos, TAN y TBN, en función del uso acumulado por el aceite lubricante, se observaría como los valores de TAN irían en aumento a consta de los de TBN (ver Figura 2.32).

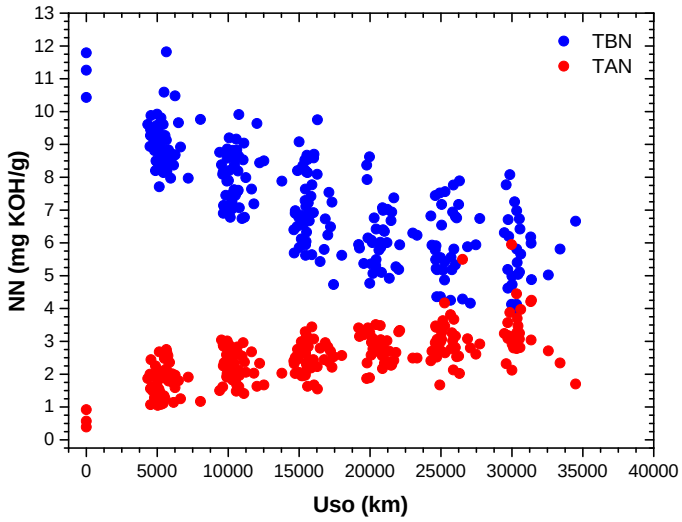

Figure 2.32. *Evolución del TAN y del TBN durante el ODI de un aceite lubricante.*

Tal y como se aprecia en la Figura 2.32, la tendencia de las evoluciones del TAN (linea de color rojo) y el TBN (de color azul) es la descrita. No obstante

existe un aspecto interesante, cerca del final del uso del aceite se observan como los valores de TAN y TBN llegan a cruzarse. De acuerdo con este hecho se puede extraer lo siguiente: antes de llegar al punto de cruce, el aceite aun poseía suficiente reserva alcalina como para neutralizar los ácidos que pudiera aparecer, pero llegado a sobrepasar el momento de cruce esto cambia. Después del cruce lo que sucede es que el grado de acidificación del aceite lubricante es muy importante, tanto que los aditivos del aceite destinados a contrarrestar los ácidos no son suficientes para poder neutralizar esos niveles. Esta inversión del comportamiento global del aceite lubricante es un caso extremo, o bien por un ODI muy largo o bien por una selección del aceite lubricante erróneo (exceptuando fallos graves repentinos).

Los nuevos MCIA, de acuerdo con el diseño y construcción que siguen, experimentan una carga térmica elevada para así poder alcanzar los rendimientos que se les pide. Esta carga es capaz de degradar (a través de reacciones de oxidación térmica, mayoritariamente) el aceite con facilidad, es por eso que los nuevos aceites lubricantes que se emplean en este tipo de motores poseen valores de TBN elevados para así evitar la pronta acidificación del aceite. A pesar de ello, en el aceite aparecen especies ácidas que son capaces de desempeñar tareas de desgaste corrosivo sobre ciertas superficies metálicas. Estas especies corrosivas se producen a medida que el motor está en funcionamiento pero, en función del régimen de trabajo y de las condiciones de entorno, la magnitud y la velocidad de la disminución del TBN puede ser muy diferente. Es por esa razón que también se mantiene bajo control los niveles de TAN en el aceite dado que, a la vista de los resultados, puede llegar el momento dónde se produzca un aumento abrupto y exponencial del valor de TAN lo cual conduciría a un desgaste corrosivo más severo.

2.4.4 Agotamiento del paquete de aditivos

Según los anteriores aspectos de la degradación que han sido expuesto, se puede extraer la idea de que los aditivos se trata de un tipo de medidas de control que, mediante su propio sacrificio (dado que son el primer elemento constituyente del lubricante en consumirse/destruirse), permiten prolongar y optimizar la funcionalidad del aceite lubricante. Tal es la relevancia que el paquete de aditivos posee, que cada conjunto está especialmente preparado para una determinada tarea y condiciones de uso que experimentará el aceite lubricante terminado que contenga dicha formulación.

Atendiendo a la variedad de aditivos que se emplean en la formulación de un aceite lubricante (enunciados ya en el capítulo 2.2.1 *Composición de*

un aceite lubricante), es complejo intentar enunciar un comportamiento del todo general por lo que respecta a la degradación del aceite lubricante. No obstante, se ha observado un fenómeno que afecta a todos (o por lo menos a la gran mayoría) de los aditivos que se emplean en la formulación de los aceites lubricantes: se trata del hecho de la disparidad a la hora de cuantificar los aditivos cuando se emplean varias técnicas o metodologías. En la Figura 2.33 se ha recopilada el caso de los aditivos anti-desgaste (AW), en especial del dialquil-ditiofosfato de zinc (ZDDP).

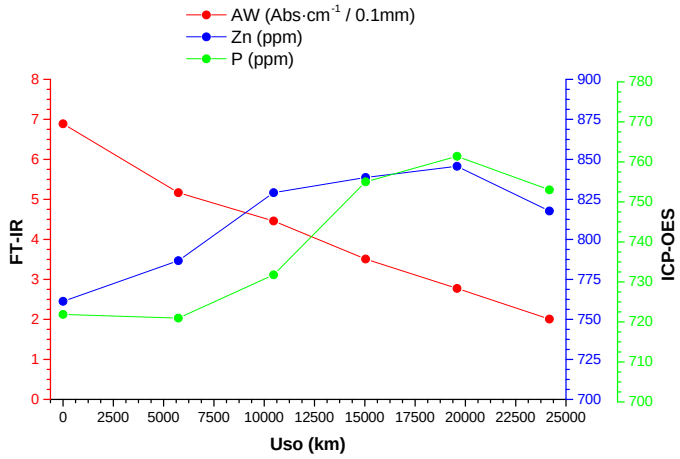

Figure 2.33. *Divergencias a la hora de cuantificar el ZDDP durante el ODI: la linea roja es la generada a partir de los estudios de FT–IR de diferentes muestras de aceite, mientras que el resto son los resultados que aporta el ICP acerca de la concentración de los metales que están presentes en el ZDDP, el cinc (de color azul) y el fósforo (verde).*

A la vista de la Figura 2.33, el ZDDP presenta un comportamiento (por lo que atañe a su degradación) opuesto según se estudie a través del FT–IR o a través del ICP–OES: si se acude a la primera técnica, el FT–IR, el comportamiento registrado de la evolución del contenido de ZDDP es el lógico que se espera obtener. Según el FT–IR, el ZDDP se consume a lo largo del ODI, mientras que de acuerdo con el ICP–OES se produce un incremento.

Esto parece una discordancia, pero no lo es. A simple vista no se puede extraer una conclusión acerca de la degradación del ZDDP, pero se se indaga un poco en el principio físico-químico en el que se sustenta cada técnica es posible extraer un juicio acerca del verdadero estado del aditivo: el FT–IR se centra en las vibraciones de ciertos grupos funcionales de naturaleza orgánica, los cuales son susceptibles de absorber cierto rango de frecuencias en su

estructura. Mientras que el ICP–OES se trata de un análisis elemental dónde se obtienen, las concentraciones de los elementos constituyentes (metálicos) del aditivo. Según esto, con el FT–IR se puede extraer si la molécula de aditivo aún retiene su integridad estructural y, en consecuencia, su funcionamiento. Mientras que con el ICP–OES se puede controlar que el paquete de aditivos, en su origen, cumple con las especificaciones e incluso, seguir un control acerca de las posibles reposiciones de aceite lubricante durante todo el ODI como consecuencias de pérdidas de volumen del mismo. Es por esa razón que cuándo se analiza el comportamiento de un aditivo, un aspecto del trabajo reside en determinar su concentración al inicio (aceite lubricante nuevo), durante y al final del periodo de uso.

En conclusión, se requiere un análisis crítico de la información que se obtiene acerca del paquete de aditivación, dado que cuando un aditivo es movilizado para contrarrestar un posible daño sobre el aceite, el aditivo es degradado: la molécula original del aditivo es alterada, lo cual puede con llevar a que cada porción o fragmento presente una inercia a permanecer en la matriz del aceite lubricante o bien será eliminada.

2.5 Contaminación del aceite lubricante

La contaminación, entendida como la presencia de elementos extraños (no pertenecientes) al aceite lubricante puede ser muy variada independientemente de su origen o fuente de generación o de procedencia. Entonces, considerando la variedad de especies (tanto en fase sólida, líquida como gaseosa) que son capaces de llegar a formar parte del aceite, resulta de utilidad distribuirlas acorde las diferentes zonas o regiones que son generadoras de dichas especies:

- El más fácil de asignar es el mismo motor. Así pues, este origen interno se clasifica en dos subapartados: el primero se debe al desgaste interno de los componentes mecánicos que constituyen al motor, los productos de los cuales y, el segundo, a la misma degradación del aceite lubricante.
- Además del origen interno, existe su foco antagónico, el exterior del motor. Este punto se centra en la entrada de contaminantes externos que son capaces de acceder al interior del motor por una vía u otra.
- Otra posible fuente de contaminantes es inherente al proceso de fabricación del motor, dado que siempre, por el mero hecho de construir un motor, se generan residuos (de mecanizado, de limpieza, pintura, etc.) que difícilmente son eliminados en su totalidad.

- Y la última posible contaminación del aceite lubricante puede asignarse a las tareas de mantenimiento que se deben realizar para el correcto funcionamiento del motor en cuestión.

Sea cual sea la procedencia del contaminante, un contaminante en el aceite siempre es un núcleo de incidencias indeseadas dado que es influyente sobre las prestaciones del aceite lubricante. Por eso se intenta, en primer lugar evitar que alcancen al aceite, si ya es tarde la otra opción es deshacerse de ellos o bien, si eliminarlos no es posible, mitigar su participación. Los contaminantes en un aceite lubricante pueden involucrarse tanto en afectar al lubricante en sí como a los elementos del motor que están en contacto íntimo con el aceite lubricante. A efectos prácticos, el impacto de los contaminantes es grande, por ejemplo: al perder prestaciones, el aceite lubricante ve recortada su vida útil. Por esa razón los tiempos de sustitución y reposición de aceite lubricante se ven recortados (se vuelven más frecuentes). Otro ejemplo seria la aparición y proliferación de residuos en cantidades reseñables, entre otros inconvenientes.

A continuación, centrando los esfuerzos en aquellos contaminantes que tiene un alto impacto en el comportamiento y propiedades del aceite lubricante, se procederá a desglosar cada uno de ellos. Así pues, los contaminantes que se explicarán son:

- El **hollín**, el cual se trata de un producto carbonoso derivado de la combustión del combustible.
- El propio **combustible** que es empleado puede alcanzar al aceite lubricante a través de varios caminos: fallos en los inyectores, combustiones incompletas o por soplado (blow-by).
- El **fluido refrigerante** puede alcanzar al aceite lubricante debido a la aparición de fugas internas en el sistema de refrigeración, las cuales vierten sus pérdidas en zonas del motor (como sería el cárter) en las cuales puede combinarse con el aceite lubricante que se encuentre.
- Y por último, los **metales de desgaste**. Estas partículas (en forma de metal nativo o en formato óxido) tienen su procedencia en los fenómenos de desgaste entre las partes metálicas que el aceite lubricante debería intentar separar para que no se generase fricción entre ellas.

2.5.1 Hollín y materia carbonosa

La materia carbonosa en un aceite lubricante es un contaminante común, siendo entre ellos el hollín (o soot en inglés) el más importante. El hollín, >95%

de carbono, es uno de los subproductos que se forman durante la combustión de combustible que es capaz de mezclarse con el aceite. Para conseguirlo, las opciones que pueden favorecer el contacto entre el aceite y el hollín son:

- De las que mayor cantidad de hollín introducen en el sistema de lubricación es mediante blow-by accede al cárter y se mezcla con el lubricante que allí reside.
- Otra opción es la deposición del hollín sobre el film de aceite expuesto en las paredes de la cámara de combustión. Según este camino, el hollín alcanza, por difusión, las paredes del cilindro dónde se encuentra el aceite lubricante y luego, durante el progreso de la carrera del pistón; es arrastrado hasta el cárter.
- Y la última opción, que reúne importancia según la tendencia de los OEMs, es debido a los sistemas EGR que introducen los gses de escape que ya contienen hollín. Por consiguiente, el aporte total de hollín al aceite lubricante aumenta.

Cuando el hollín se disuelve en el aceite, el primer fenómeno que sucede es el oscurecimiento de éste. Este cambio de coloración es indicativo de la presencia de hollín disuelto. Entonces, cuando se detecta hollín, el aceite lubricante ha experimentado una serie e cambios en su comportamiento como consecuencia de alojar en su interior dicho contaminante. A continuación se exponen aquellos efectos:

- El hollín puede generar dos efectos, o bien interviene sobre la base del aceite o bien sobre los aditivos empleados. Par el primer caso, la presencia de hollín provoca los siguientes fenómenos:
  - El más simple es, como ya se ha dicho, un cambio en su coloración.
  - El siguiente aspecto es un aumento en la viscosidad del aceite, favoreciendo que ahora el aceite contaminado genere películas protectoras de un espesor mayor.
  - Modifica la capacidad térmica del aceite lubricante cuando éste contiene en su interior una dispersión de hollín.
  - El hollín, al combinarse con el aceite, produce un aceite que es más conductor de la electricidad (pierde su carácter dieléctrico) quedando reflejado en el aumento de la constante dieléctrica.

- En relación con el paquete de aditivos, la influencia del hollín se observa en:
  - Uno de los principales es la pérdida de poder dispersante. Bajo estas situaciones de contaminación de hollín, el aceite lubricante sufre un consumo de los aditivos dispersantes y detergentes debido a la facilidad que posee el hollín de formar agregados (partículas de mayor tamaño) que, llegados a ciertos momentos, son capaces de formar depósitos y barros (sludge).
  - El hollín es un agente abrasivo muy eficiente, por lo que es capaz de provocar un rápido agotamiento de los aditivos anti-desgaste.

En conclusión, a la vista de los problemas que deriva la presencia de hollín en el aceite lubricante, no es de extrañar el continuo interés que despierta el campo: tanto de comprender como se forma el hollín durante la combustión, sino también como se gestiona a posteriori (se expulsa por a través de los gases de escape o permanece en el motor) y, por lo que respecta al aceite que consecuencias tienen la presencia de hollín en su comportamiento.

2.5.2 Combustible

La presencia de combustible en en aceite lubricante de motor es un problem de especial relevancia, sobre todo en los nuevos motores con los sistemas de postratamiento de las emisiones contaminares que poseen. En un principio, los agentes que pueden provocar que exista una transferencia de combustible hacia el aceite lubricante puede achacarse a varios aspectos: problemas mecánicos del motor como podrían ser fallos en los inyectores, fugas en el circuito de suministro de combustible, falta de estanqueidad y aislamiento de secciones del motor, etc. o bien, otro causante de la aparición de combustible en el aceite lubricante es debido a efectos derivados de combustiones no eficientes [9]. En cualquier caso, los problemas que la presencia de combustible en el lubricante produce son [48, 76]:

- Como el combustible, diésel o gasolina, posee una menor viscosidad que el aceite lubricante, al tener lugar la combinación entre ambos el resultado final es una mezcla con una viscosidad menor. Esta caída de la viscosidad puede traer consigo carencias a la hora del generar el film protector entre dos superficies. Al bajar la viscosidad del aceite, el espesor de la película que este genera es también menor llegando a ser muy preocupante en aquellas regiones de alta demanda: temperaturas y cargas elevadas.

- Si se produce una entrada de combustible, éste puede propiciar que bajo unas condiciones de temperatura concreta empiezan a generarse de vapores inflamables procedentes de las fracciones más volátiles del combustible. Dicho en otras palabras, el ingreso de combustible en el aceite provoca que su temperatura de flash point sea más baja. Un aceite lubricante posee una temperatura de inflamación de entorno a los 250°C, dado que en los aceites las fracciones más volátiles poseen temperatura de ebullición elevadas. Por contraposición, los combustibles poseen una temperatura de cambio de fase liquida a gaseosa más baja que el aceite lubricante. Así pues, si en el lubricante se encuentra disuelto combustible, la temperatura del flash point será menor. No obstante, la temperatura a la que el aceite lubricante se encuentra en el cárter en ocasiones es suficiente como para eliminar las fracciones volátiles del combustible contaminante, por lo que se consigue minimizar esa reducción de la temperatura del flash point.

- Si se produce dilución, eso implica que no todo el fluido que se está haciendo circular para lubricar el motor es aceite lubricante especifico. Según las exigencias que los nuevos MCIA piden a los aceites, éstos fueron mejorados mediante la incorporación de aditivos. De modo que si el aceite es diluido por combustible, la cantidad de aditivos que entra en juego es menor también y, como consecuencia, el rendimiento del aceite lubricante puede verse comprometido (acorde con del grado de dilución producido).

A pesar de todo, la dilución por combustible no suele alcanzar grandes consecuencias debido a que, siempre y cuando no se haya producido un fallo mecánico significante, no es un problema con grandes repercusiones debido a los niveles de dilución máximos que se encuentran (alrededor del 5%).

2.5.3 Fluido refrigerante

Por fluido refrigerante se entienden como aquellos fluidos que se encargan de extraer el calor excedente que se produce en un motor. En la actualidad, en un MCIA, los refringentes más comunes son aquellos compuestos por disoluciones acuosas de etilenglicol (ETG) o propilenglicol (PG) en proporción 1:1 (50% glicol : 50% agua). De entre los dos mencionados, el ETG es el más extendido debido a que posee mejores rendimientos a la hora de la transmisión de calor. Ahora bien, el agua se trata de un contaminante muy destructivo dado que afecta a facetas tanto químicas como físicas de los aceites lubricantes.

Tal es la problemática que deriva su presencia en el sistema de lubricación que es necesario prestar atención a las posibles puertas de entrada de agua: fuga del sistema de refrigeración, respiraderos, poros en los sellos o fenómenos de condensación (tanto del agua en forma de humedad del aire que toma el motor, como ea gua derivada de la reacción de combustión).

Una vez el agua se encuentra dentro del sistema de lubricación, puede adoptar varios estados: disuelta, emulsionada o libre.

- En la primera de ellas, el **agua disuelta**, las moléculas de agua se hallan mezcladas con el aceite. En este caso, las moléculas se distribuyen por todo el aceite de modo que queden dispersar de forma aislada con el objetivo de maximizar su solubilidad en la matriz orgánica.
- Si el aceite no es capaz de aceptar más agua (se encuentra baja una situación de saturación), el agua tiende a formar gotas de diámetro del orden de micras (glóbulos microscópicos). En estas condiciones esas pequeñas gotas de agua conforman un estado conocido como emulsión, nombre que se le es cedido a este tipo de agua: **agua emulsionada**.
- Y por último, si se sigue incorporando más agua al aceite se llega al punto donde el agua y el aceite lubricante forman dos fases diferenciadas.

Estas dos últimas formas de poder encontrar agua en el aceite lubricante son las más peligrosas y perjudiciales para un motor, dado que los efectos que tienen sobre los sistemas lubricados son muy peligrosos:

- Según su propiedad de fluido incompresible, el agua es capaz de desplazar al aceite en ciertas regiones del motor dónde la película protectora no es muy grande. En esas regiones, el agua ocupa se interfiere en la película provocando: en primer lugar se pierde la lubricidad de la zona por lo que aparecerán fenómenos de daño de superficies (desgaste abrasivo, adhesivo y fatiga) además de favorecer el ataque corrosivo de dichas superficies, en especial si éstas se componen de metales como cobre, plomo y hierro.
- El agua es un medio propicio para las reacciones de ataque a metales. Cuando un metal se oxida, esta capa de herrumbre actúa como segundo estado de degradación: el primero de ellos está relacionado con la formación de partículas (óxidos metálicos) los cuales actúan como agentes abrasivos y estabilizadores de emulsiones (favoreciendo que se forme una espuma estable), el siguiente es la pérdida de poder de

disipación del calor del aceite y disminución de la estabilidad química (convierte al aceite en una sustancia con mayor tendencia a oxidarse) y por último, aparición de depósitos.

- El agua tiene el poder de hidrolizar aquellos aditivos que poseen grupos susceptibles o afines al agua, lo cual provoca un agotamiento prematura del paquete de aditivos. Además, en gran parte de ellos, los productos de la degradación de los aditivos genera precursores o especies ácidas que se suman a la corrosión de aquellas aleaciones o piezas compuestas por metales blandos.

- El agua es un medio de cultivo para la proliferación de bacterias y microorganismos. La presciencia de este tipo de serie vivos en el aceite es del todo desaprovechosa dado que suelen emplear el aceite como sustento y medio de vida, por lo que a la vez que es degradado se contamina como resultado del metabolismos de los organismos que lo habita.

- Por último, existen regiones del motor que trabajan bajo unas condiciones de presión y temperatura que, cuando ingresa agua en dichas regiones, ésta llega evaporarse de forma casi instantánea retirando tras de si la película de lubricante que en esas zonas existían.

2.5.4 Metales de desgaste

En este apartado, se incluyen tanto las partículas propias originadas en el interior del motor (virutas metálicas) como aquellas que son incorporadas a él como el polvo. Sea cual sea la ruta a través de la cual estas partículas apareen en el aceite lubricante, siempre poseen el mismo efecto: actúan como agentes abrasivos que erosionan aquellas superficies. En este caso, un factor importante es el tamaño de partícula dado que en función de la relación entre su tamaño y el espesor de la película lubricante (film, en inglés), las presencia de estas partículas deriva en dos procesos distintos: si el tamaño de la partícula es equiparable al de la película de aceite, la partícula modifica el comportamiento y la eficiencia de la película por lo se inician procesos de desgaste. Pero si el diámetro de la partículas sobrepasa al espesor de la película de aceite, la partícula actúa como nexo de unión entre las superficies que separaba el aceite lubricante dando lugar pues a que las superficies involucradas sufran una erosión muy importantes.

Bibliography

[1] G. H. Abd-Alla. Using exhaust gas recirculation in internal combustion engines: a review. *Energy Conversion and Management*, 43(8):1027–1042, 2002.

[2] A. A. Abdel-Rahman. On the emissions from internal-combustion engines: a review. *International Journal of Energy Research*, 22(6):483–513, 1998. doi:10.1002/(SICI)1099-114X(199805)22:6<483::AID-ER377>3.0.CO;2-Z.

[3] A. K. Agarwal, D. K. Srivastava, A. Dhar, R. K. Maurya, P. C. Shukla, and A. P. Singh. Effect of fuel injection timing and pressure on combustion, emissions and performance characteristics of a single cylinder diesel engine. *Fuel*, 111:374–383, 2013.

[4] D. Agarwal, S. K. Singh, and A. K. Agarwal. Effect of exhaust gas recirculation (EGR) on performance, emissions, deposits and durability of a constant speed compression ignition engine. *Applied Energy*, 88(8):2900–2907, 2011.

[5] S. Aldajah, O. O. Ajayi, G. R. Fenske, and I. L. Goldblatt. Effect of exhaust gas recirculation (EGR) contamination of diesel engine oil on wear. *Wear*, 263(1-6):93–98, 2007.

[6] U. G. Alkemade and B. Schumann. Engines and exhaust after treatment systems for future automotive applications. *Solid State Ionics*, 177(26-32):2291–2296, 2006.

[7] J. L. Ambs and B. T. McClure. The influence of oxidation catalysts on no_2 in diesel exhaust. In *International Off-Highway & Powerplant Congress & Exposition*. SAE International, sep 1993. doi:10.4271/932494.

[8] W. J. Bartz. *Engine oils and automotive lubrication*. CRC Press, 2019.

[9] A. Behn, M. Feindt, G. Matz, S. Krause, and M. Gohl. Fuel transport across the piston ring pack: Measurement system development and experiments for online fuel transport and oil dilution measurements. *SAE Technical Paper*, (2015-24-2534), 2015.

[10] S. Bensaid, C. J. Caroca, N. Russo, and D. Fino. Detailed investigation of non-catalytic DPF regeneration. *The Canadian Journal of Chemical Engineering*, 89(2):401–407, 2011.

[11] B. Bhushan. *Modern tribology handbook*. CRC Press, 2000.

[12] M. Bohnet. *Ullmann's encyclopedia of industrial chemistry*. Wiley-VCH, 7th edition, 40 volume set edition, 2006.

[13] J. D. Burrington, J. K. Pudelski, and J. P. Roski. Challenges in detergents and dispersants for engine oils. In *Practical Advances in Petroleum Processing*, pages 579–595. Springer, 2006.

[14] M. J. Covitch and K. J. Trickett. How polymers behave as viscosity index improvers in lubricating oils. *Advances in Chemical Engineering and Science*, 5(02):134, 2015.

[15] Y. Cui, Y. Cai, R. Fan, Y. Shi, L. Gu, and et al. Effects of residual ash on dpf capture and regeneration. *International Journal of Automotive Technology*, 19(5):759–769, 2018.

[16] H. DaCosta, C. Shannon, and R. Silver. Thermal and chemical aging of diesel particulate filters. In *World Congress & Exposition*. SAE International, jan 2007. doi:10.4271/2007-01-1266.

[17] G. Dante. *Motores endotérmicos*. Omega, 3a edición edition, 1989.

[18] S. Dey and G. C. Dhal. Materials progress in the control of CO and CO_2 emission at ambient conditions: an overview. *Materials Science for Energy Technologies*, 2019.

[19] EU Directive. 98/69/EC of the European Parliament and of the Council of 13 October 1998 relating to measures to be taken against air pollution by emissions from motor vehicles and amending Council Directive 70/220/EEC. *Official Journal of the European Communities L*, 350(28):12, 1998.

[20] EU Directive. Directive 2005/55/EC of the European Parliament and of the Council of 28 September 2005 on the approximation of the laws of the Member States relating to the measures to be taken against the emission of gaseous and particulate pollutants from compression-ignition engines for use in vehicles, and the emission of gaseous pollutants from positive-ignition engines fuelled with natural gas or liquefied petroleum gas for use in vehicles. *Official Journal of the European Communities L*, 275:1–163, 2005.

[21] EU Directive. Regulation (EC) No 715/2007 of the European Parliament and of the Council of 20 June 2007 on type approval of motor vehicles with respect to emissions from light passenger and commercial vehicles (Euro 5 and Euro 6) and on access to vehicle repair and maintenance information. *Official Journal of the European Communities L*, 171:1–16, 2007.

[22] Directive Council. 91/441/EEC of 26 June 1991 amending Directive 70/220. *EEC on the approximation of the laws of the Member States relating to measures to be taken against air pollution by emissions from motor vehicles*, 1991.

[23] P. S. Divekar, X. Chen, J. Tjong, and M. Zheng. Energy efficiency impact of EGR on organizing clean combustion in diesel engines. *Energy Conversion and Management*, 112:369–381, 2016.

[24] A. Dorinson and K. C. Ludema. *Mechanics and chemistry in lubrication*, volume 9. Elsevier, 1985.

[25] B. Esteban, J. Riba, G. Baquero, A. Rius, and R. Puig. Temperature dependence of density and viscosity of vegetable oils. *Biomass and bioenergy*, 42:164–171, 2012.

[26] J. Fang, Z. Meng, J. Li, Y. Pu, Y. Du, and et al. The influence of ash on soot deposition and regeneration processes in diesel particular filter. *Applied Thermal Engineering*, 124:633–640, 2017.

[27] X. Feng, Y. Ge, C. Ma, J. Tan, L. Yu, and et al. Experimental study on the nitrogen dioxide and particulate matter emissions from diesel engine retrofitted with particulate oxidation catalyst. *Science of the Total Environment*, 472:56–62, 2014.

[28] M. Fiebig, A. Wiartalla, B. Holderbaum, and S. Kiesow. Particulate emissions from diesel engines: correlation between engine technology and emissions. *Journal of Occupational Medicine and Toxicology*, 9(1):6, 2014.

[29] B. Guan, R. Zhan, H. Lin, and Z. Huang. Review of state of the art technologies of selective catalytic reduction of NOx from diesel engine exhaust. *Applied Thermal Engineering*, 66(1-2):395–414, 2014.

[30] B. Guan, R. Zhan, H. Lin, and Z. Huang. Review of the state-of-the-art of exhaust particulate filter technology in internal combustion engines. *Journal of environmental management*, 154:225–258, 2015.

[31] J. A. Heredia-Cancino, M. Ramezani, and M. E. Álvarez-Ramos. Effect of degradation on tribological performance of engine lubricants at elevated temperatures. *Tribology International*, 124:230–237, 2018.

[32] American Petroleum Institute. *Engine oil licensing and certification system. API 1509 Eighteenth Edition*, 2019. https://www.api.org/ /media/Files/Certification/Engine-Oil-Diesel/Publications/150918thedition-06282019.pdf.

[33] ASTM International. *ASTM D2887-19 Standard test method for boiling range distribution of petroleum fractions by gas chromatography*, 2019. doi:10.1520/D2887-19AE01.

[34] ASTM International. *ASTM D5800-20 Standard test method for evaporation loss of lubricating oils by the Noack Method*. West Conshohocken, PA, 2020. doi:10.1520/D5800-20.

[35] E. Jiaqiang, L. Xie, Q. Zuo, and G. Zhang. Effect analysis on regeneration speed of continuous regeneration-diesel particulate filter based on NO_2 assisted regeneration. *Atmospheric Pollution Research*, 7(1):9–17, 2016.

[36] T. Johnson. Diesel engine emissions and their control. *Platinum Metals Review*, 52(1):23–37, 2008.

[37] T. Johnson and A. Joshi. Review of vehicle engine efficiency and emissions. *SAE International Journal of Engines*, 11(6):1307–1330, 2018.

[38] T. V. Johnson. Diesel emission control in review. *SAE international journal of fuels and lubricants*, 1(1):68–81, 2009.

[39] Ö Karacan, M. V. Kök, and U. Karaaslan. Dependence of thermal stability of an engine lubricating oil on usage period. *Journal of thermal analysis and calorimetry*, 55(1):109–114, 1999.

[40] W. Knecht. Diesel engine development in view of reduced emission standards. *Energy*, 33(2):264–271, 2008.

[41] N. Ladommatos, S. Abdelhalim, and H. Zhao. The effects of exhaust gas recirculation on diesel combustion and emissions. *International Journal of Engine Research*, 1(1):107–126, 2000.

[42] N. Ladommatos, S. M. Abdelhalim, H. Zhao, and Z. Hu. The dilution, chemical, and thermal effects of exhaust gas recirculation on diesel engine emissions - part 2: Effects of carbon dioxide. In *International Fuels & Lubricants Meeting & Exposition*. SAE International, may 1996. doi:10.4271/961167.

[43] N. Ladommatos, S. M. Abdelhalim, H. Zhao, and Z. Hu. The dilution, chemical, and thermal effects of exhaust gas recirculation on diesel engine emissions - part 3: Effects of water vapour. In *International Spring Fuels & Lubricants Meeting & Exposition*. SAE International, may 1997. doi:/10.4271/971659.

[44] N. Ladommatos, S. M. Abdelhalim, H. Zhao, and Z. Hu. The dilution, chemical, and thermal effects of exhaust gas recirculation on diesel engine emissions - part 4: Effects of carbon dioxide and water vapour. In *International Spring Fuels & Lubricants Meeting & Exposition*. SAE International, may 1997. doi:10.4271/971660.

[45] N. Ladommatos, S. M. Abdelhalim, Hua Zhao, and Z. Hu. The dilution, chemical, and thermal effects of exhaust gas recirculation on diesel engine emissions - part 1: Effect of reducing inlet charge oxygen. In *International Fuels & Lubricants Meeting & Exposition*. SAE International, may 1996. doi:10.4271/961165.

[46] T. Lattimore, C. Wang, H. Xu, M. L. Wyszynski, and S. Shuai. Investigation of EGR effect on combustion and PM emissions in a DISI engine. *Applied Energy*, 161:256–267, 2016.

[47] J. A. Leet, T. Friesen, and A. Shadbourne. EGR's effect on oil degradation and intake system performance. *SAE transactions*, pages 347–354, 1998.

[48] D. Ljubas, H. Krpan, and I. Matanović. Influence of engine oils dilution by fuels on their viscosity, flash point and fire point. *Nafta: exploration, production, processing, petrochemistry*, 61(2):73–79, 2010.

[49] A. C. Lloyd and T. A. Cackette. Diesel engines: environmental impact and control. *Journal of the Air & Waste Management Association*, 51(6):809–847, 2001.

[50] T. Mang and W. Dresel. *Lubricants and lubrication*. John Wiley & Sons, 2007.

[51] J. Martin, A. Boehman, R. Topkar, S. Chopra, U. Subramaniam, and H. Chen. Intermediate combustion modes between conventional Diesel and RCCI. *SAE International Journal of Engines*, 11(6):835–860, 2018.

[52] N. Marx, L. Fernández, F. Barceló, and H. Spikes. Shear thinning and hydrodynamic friction of viscosity modifier-containing oils. Part I: shear thinning behaviour. *Tribology Letters*, 66(3):92, 2018.

[53] B. Mohan, W. Yang, and S. kiang Chou. Fuel injection strategies for performance improvement and emissions reduction in compression ignition engines–A review. *Renewable and Sustainable Energy Reviews*, 28:664–676, 2013.

[54] R. M. Mortier, S. T. Orszulik, and M. F. Fox. *Chemistry and technology of lubricants*, volume 107115. Springer, 2010.

[55] Z. Pawlak. *Tribochemistry of lubricating oils*. Elsevier, 2003.

[56] F. Payri and J. M. Desantes. *Motores de combustión interna alternativos*. Editorial Universitat Politècnica de València, 2011.

[57] D. M. Pirro, M. Webster, and E. Daschner. *Lubrication fundamentals, revised and expanded*. CRC Press, 2016.

[58] EC Regulation. Regulation (EC) No 595/2009 of the European Parliament and of the Council of 18 June 2009 on type-approval of motor vehicles and engines with respect to emissions from heavy duty vehicles (Euro VI) and on access to vehicle repair and maintenance information and amending Regulation (EC) No 715/2007 and Directive 2007/46/EC and repealing Directives 80/1269/EEC, 2005/55/EC and 2005/78/EC. *Official Journal of the European Communities L*, 188, 2009.

[59] L. R. Rudnick. *Synthetics, mineral oils, and bio-based lubricants: chemistry and technology*. CRC press, 2005.

[60] L. R. Rudnick and R. L. Shubkin. *Synthetic lubricants and high-performance functional fluids, revised and expanded*. CRC Press, 1999.

[61] A. Russell and W. S. Epling. Diesel oxidation catalysts. *Catalysis Reviews*, 53(4):337–423, 2011.

[62] L. Severa, M. Havlíček, and V. Kumbár. Temperature dependent kinematic viscosity of different types of engine oil. *Acta Universitatis Agriculturae et Silviculturae Mendelianae Brunensis*, 57(4):95–102, 2009.

[63] L. Severa, M. Havlíček, and V. Kumbár. Temperature dependent kinematic viscosity of different types of engine oils. *Acta Universitatis Agriculturae et Silviculturae Mendelianae Brunensis*, 57(4):95–102, 2014.

[64] B. Song and Y. Choi. Investigation of variations of lubricating oil diluted by post-injected fuel for the regeneration of DPF and its effects on engine wear. *Journal of mechanical science and technology*, 22(12):2526–2533, 2008.

[65] J. G. Speight. *The chemistry and technology of petroleum*. CRC press, 2014.

[66] L. L. F. Squaiella, C. A. Martins, and P. T. Lacava. Strategies for emission control in diesel engine to meet Euro VI. *Fuel*, 104:183–193, 2013.

[67] G. W. Stachowiak and A. W. Batchelor. *Engineering tribology*. Butterworth-Heinemann, 2013.

[68] V. Stepina and V. Vesely. *Lubricants and special fluids*, volume 23. Elsevier, 1992.

[69] R. I. Taylor and B. R. de Kraker. Shear rates in engines and implications for lubricant design. *Proceedings of the Institution of Mechanical Engineers, Part J: Journal of Engineering Tribology*, 231(9):1106–1116, 2017.

[70] B. P. Tissot and D. H. Welte. *Petroleum formation and occurrence*. Springer Science & Business Media, 2013.

[71] M. Torbacke, Å. K. Rudolphi, and E. Kassfeldt. *Lubricants: introduction to properties and performance*. John Wiley & Sons, 2014.

[72] A. Torregrosa, P. Olmeda, J. Martín, and C. Romero. A tool for predicting the thermal performance of a diesel engine. *Heat transfer engineering*, 32(10):891–904, 2011.

[73] A. Tripathi and R. Vinu. Characterization of thermal stability of synthetic and semi-synthetic engine oils. *Lubricants*, 3(1):54–79, 2015.

[74] H. Wang, Y. Ge, J. Tan, L. Hao, L. Wu, and et al. Ash deposited in diesel particular filter: a review. *Energy Sources, Part A: Recovery, Utilization, and Environmental Effects*, 41(18):2184–2193, 2019.

[75] Q. J. Wang and Y. Chung. *Encyclopedia of tribology*. Springer, 2013.

[76] M. Wattrus. Fuel property effects on oil dilution in diesel engines. *SAE International Journal of Fuels and Lubricants*, 6(3):794–806, 2013.

[77] S. Wen and P. Huang. *Principles of tribology*. John Wiley & Sons, 2012.

[78] R. Zhan, Y. Huang, and M. Khair. Methodologies to control dpf uncontrolled regenerations. *SAE Transactions*, pages 431–444, 2006.

[79] M. Zheng, G. T. Reader, and J. G. Hawley. Diesel engine exhaust gas recirculation—-a review on advanced and novel concepts. *Energy conversion and management*, 45(6):883–900, 2004.

[80] U. Zoller. *Handbook of detergents, Part E: applications*. Surfactant Science. Taylor & Francis, 2008.

Chapter 3

Técnicas analíticas para el estudio de los aceites lubricantes

Contents

3.1 Introducción

El presente capítulo reúne las técnicas analíticas más importantes a la hora de analizar los aceites lubricantes de los MCIA con el objetivo de la realización de un diagnóstico del estado del motor a partir de los resultados obtenidos atendiendo a parámetros referentes a la degradación y contaminación del aceite lubricante (parámetros estrechamente relacionados) así como de desgaste del propio motor.

Estas herramientas que se presentarán se enmarcan dentro de lo que se conoce como Oil Condition Monitoring (OCM, por su nombre en inglés). Como su propio nombre indica, se trata de la aplicación de un sistema o protocolo de monitorizado del aceite lubricante del motor dónde se realizan controles del estado del aceite lubricante con el propósito de poder registrar sus condiciones y su comportamiento para así obtener también información relevante del estado del motor.

Así pues, el OCM es una herramienta muy útil, dado que permite obtener información del estado del MCIA simplemente a partir del análisis de su aceite lubricante. Es por esa razón que en este capítulo se procederá a explicar aquellas tareas incluidas en el OCM y el potencial que éstas reúnen a la hora de recabar datos relevantes del motor.

3.2 Propiedades inherentes de los aceites lubricantes

El primer conjunto de parámetros que deben extraerse del análisis del aceite lubricantes son aquellos derivados de su degradación. Por degradación se entiende como cualquier alteración del aceite lubricante, tanto física como química, que provoque una reducción de su capacidad de acción sobre alguna de las diferentes funciones que el aceite lubricante desempeña (lubricación, refrigeración, limpieza, protección y sellado).

Estas modificaciones, provocadas por las condiciones de trabajo y entorno a las cuales se somete al aceite lubricante, deben controlarse dado que el impacto sobre el aceite lubricante se puede agravar en función del efecto de diversos factores participantes: temperatura, estrés, presencia de agentes contaminantes, etc. Este hecho es importante en los MCIA, dado que cada vez éstos le exigen al aceite lubricante trabajar en condiciones más severas por lo que, si no se toman medidas (empleo de nuevas y mejores formulaciones de aceite lubricantes, mayor frecuencia de análisis, etc.), pueden provocar que

la degradación del aceite lubricante se acelere y/o agrave y produzca fallos o daños en el motor [135].

Una vez expuesta la relevancia de controlar la degradación del aceite lubricante, los factores indicativos que permiten conocer el grado y/o velocidad de degradación de un aceite lubricante son: la viscosidad, el grado de acidez y de basicidad, degradación y consumo de paquete de aditivos [127].

3.2.1 Viscosidad

La viscosidad es la característica más relevante de un aceite lubricante. Esto se debe a que en función de ésta las pérdidas por fricción, el rendimiento mecánico, la capacidad de carga y el gasto del fluido (para unas determinadas condiciones/situaciones y aplicaciones) se ven condicionadas. La viscosidad se puede expresar, dentro del ámbito de los aceites lubricantes, de dos formas: una de ellas es mediante la viscosidad absoluta o dinámica (η) o bien a través de la viscosidad cinemática (υ). En la Tabla 3.1 se muestran las diferentes unidades con las que se suelen expresar ambas viscosidades [105].

Table 3.1. *Unidades empleadas para expresar la viscosidad dinámica y la viscosidad cinemática.*

Sistema de unidades	Viscosidad dinámica	Viscosidad cinemática
S. Internacional (SI)	Poiseuille (PI) = Pa·s = 10 P	m^2/s
S. Cegesimal (CGS)	Poise (P)	Stokes (St)
	centi-Poise (cP)	centi-Stokes (cSt)
S. Técnico (MKgfS)	Kgf·s/m^2	m^2/s
S. Británico Inch-Pound-Second (IPS)	Reyn	sq in/s

De entre ellas, la viscosidad cinemática es más práctica de medir debido a la menor complejidad del sistema analítico. Para poder conocer el valor de la viscosidad existen diferentes opciones de dispositivos: viscosímetros capilares, viscosímetros de orificio, viscosímetros de oscilación, viscosímetros rotacionales, viscosímetros de cuerpo móvil y viscosímetros vibracionales. No obstante, de entre todas estas diferentes modalidades de viscosímetros, en este estudio se han empleado los viscosímetros capilares y el viscosímetro rotacional (concretamente el viscosímetro de tipo Stabinger, el cual se trata de una modificación del viscosímetro de Couette) [103, 104].

- **Viscosímetros capilares**: Este tipo de viscosímetros se basan en el caudal volumétrico de fluido que fluye, por influencia de la gravedad o

por la acción de una fuerza externa, a través de un agujero de diámetro pequeño conocido como capilar. Para la obtención del valor de la viscosidad cinemática (υ), se registra el tiempo de circulación requerido para que un cierto volumen de fluido pase por una serie de marcas de gradación (bajo unas ciertas condiciones de presión y temperatura). Los elementos básicos que conforman los viscosímetros capilares de vidrio son: un viscosímetro capilar de vidrio provisto de un depósito para el fluido y un capilar (de dimensiones conocidas) (Figura 3.1), un sistema para controlar la presión que se debe aplicar (si procede) y un sistema termostático para mantener el sistema a la temperatura que sea requerida [140].

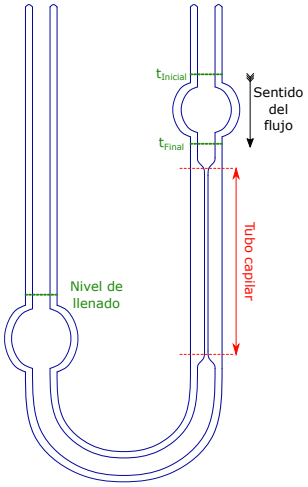

Figure 3.1. *Esquema de un viscosímetro de Ostwald, el cual se compone por un tubo en forma de U provisto de dos bulbos y un capilar.*

Este tipo de viscosímetros se caracterizan por ser instrumentos que trabajan con tensiones de cizallado bajas (entre 1 y 15 Pa para los viscosímetros que operan por acción de la gravedad o entre 1 hasta 50 Pa si se emplea una presión para generar el flujo). Además, la tasa de cizallamiento en estos viscosímetros oscila entre 1 y 20000 s^{-1} (tomando como referencia tiempos de flujo de entre 200 segundos y 800 segundos). De entre todas las variedades de viscosímetros que existen, se puede realizar una clasificación en tres grupos: viscosímetros de Ostwald modificados (para fluidos transparentes) (Tabla 3.2), viscosímetros de nivel suspendido (para fluidos transparentes) (Tabla 3.3) y viscosímetros de flujo inverso (para fluidos transparentes y opacos) (Tabla 3.4).

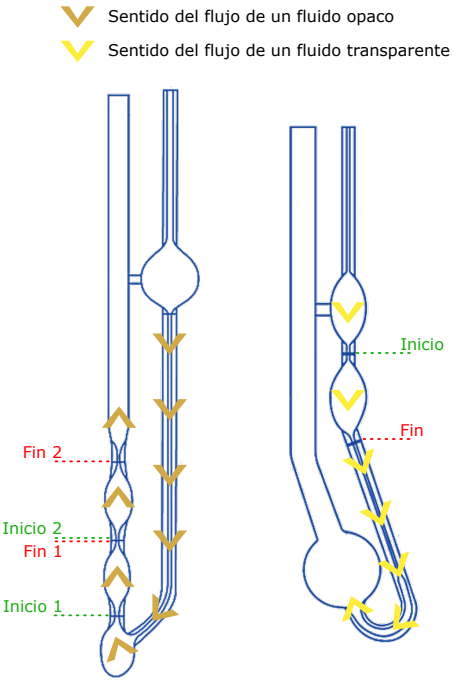

Figure 3.2. *Diagrama de funcionamiento de dos de los tipos de viscosímetros capilares de vidrio más usados para el análisis de aceites lubricantes.*

Table 3.2. *Tipos de viscosímetros de Ostwald modificados. Dentro de este grupo se encuentran aquellos viscosímetros de volumen constante a la temperatura a la que son llenados* [a] *y aquellos en los que, a la temperatura del ensayo, el volumen es constante* [b].

Tipo de viscosímetro	**Rango v (cSt)**
Cannon-Fenske [a]	0.5-20000
Zeitfuchs [b]	0.6-3000
SIL [b]	0.6-10000
Viscosímetro Semi-micro de Cannon-Manning [a]	0.4-20000
Tubo-U [b]	0.9-10000
Viscosímetro miniaturizados [b]	0.2-100
Pinkevitch [a]	0.6-17000

Table 3.3. *Tipos de viscosímetros de nivel suspendido.*

Tipo de viscosímetro	**Rango v (cSt)**
Ubbelohde	0.3-100000
Cannon-Ubbelohde	0.5-100000
BS/IP/SL	3.5-100000
BS/IP/SL (S)	1.05-10000
BS/IP/MSL	0.6-3000
FitzSimons	0.6-1200
Atlantic	0.7-5000
Viscosímetro Semi-micro de Cannon-Ubbelohde	0.4-20000

Table 3.4. *Tipos de viscosímetros de flujo inverso.*

Tipo de viscosímetro	**Rango v (cSt)**
Zeitfuchs de brazo cruzado	0.6-100000
Cannon-Fenske	0.4-20000
Lantz-Zeitfuchs	60-100000
VBS/IP/RF Tubo-U de flujo inverso	0.6-300000

Este tipo de viscosímetros, por lo que respecta a aceites lubricantes de motor, se encuentran sujetos a la norma ASTM D445 [87] la cual marca las pautas para poder obtener la viscosidad cinemática en fluidos newtonianos (tanto sean transparentes como si se tratan de opacos) a la temperatura que se haya decido realizar la medición.

Un avance de los viscosímetros capilares, los cuales normalmente se atemperan mediante su inmersión en un baño termostático, son los viscosímetros que emplean un sistema de calefacción-refrigeración a base de resistencias eléctricas o bien mediante sistemas de tipo Peltier (termoeléctrico). Independientemente del sistema empleado, los nuevos sistemas para la medición de la viscosidad, siendo rigurosos, no se ciñen exactamente a la norma ASTM D445 dado que difieren en el hecho de que solo se hace una sola determinación por muestra. No obstante, en función del control de la temperatura y del sistema de registro del flujo del fluido, existen sistemas que se acercan mucho a la norma ASTM mencionada de modo que la medida de la viscosidad prácticamente es la misma, se encuentra correlacionada.

Figure 3.3. *Viscosímetro semiautomático SimpleVIS+.*

Un sistema de esta nueva generación de viscosímetros es el viscosímetro SimpleVIS+ de CANNON Instrument Company (Figura 3.3). El SimpleVIS+ se trata de un viscosímetro de tipo Houillon semiautomático sujeto a la norma ASTM D7279 [83]. El equipo se compone, de forma muy breve, de los siguientes elementos: un tubo de borosilicato de tipo Houillon (tubo en forma de Z) encerrado dentro de un bloque de aluminio (ver Figura 3.4), sistema de calefacción eléctrica y ventilador para disipación del calor de alto rendimiento (elevado control de la temperatura ($\pm$ 0.05°C) para las temperaturas de ensayo estipuladas de 40°C y 100°C y un sistema óptico compuesto de led y fotodiodo enfrentados para la detección del flujo del fluido a través del tubo.

El SimpleVIS+, al basarse en un tubo capilar por flujo gravitacional, se encuentra sujeto a la ecuación de Hagen-Poiseuille 3.1:

$$\nu = \frac{\pi \cdot h \cdot g \cdot r^4 \cdot t}{8 \cdot l \cdot V} = cte \cdot t \tag{3.1}$$

Dónde: h diferencia de altura entre el frente de avance del fluido del capilar (mm), g aceleración de la gravedad (980.24 cm/s^2), r radio interno del capilar (mm), t tiempo de paso entre las marcas de control (s), l longitud de funcionamiento efectiva del tubo capilar (mm), V volumen calibrado localizado entre las marcas de registro de tiempo (cm^3). A la vista de la expresión, gran parte de los elementos que la constituyen pueden reunirse en una constante característica y propia del viscosímetro, por lo que simplemente con el registro del tiempo de flujo

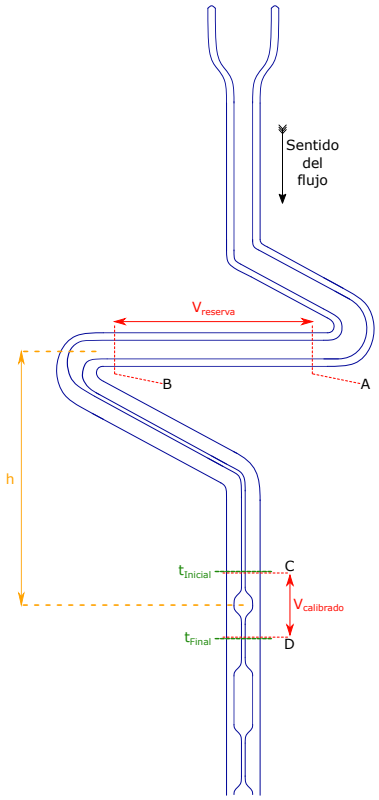

Figure 3.4. *Esquema de un tubo capilar para medir la viscosidad de fluidos, transparentes y opacos, de tipo Houillon.*

es posible determinar la viscosidad cinemática (ν) del fluido en cuestión [111].

El funcionamiento del SimpleVIS+ reside en el registro del avance del fluido a través de una serie de puntos de control o secciones específicas. Para su correcto uso, el modo de empleo de este viscosímetro de tipo Houillon es:

- En primer lugar, se vierte una cierta cantidad de fluido, concretamente 0.5 mililitros (una inyección por test/medición), directamente en el puerto o cáliz del tubo.
- Se deja avanzar el fluido a través del tubo de modo que el frente más avanzado alcance el punto C, momento dónde se empieza a registrar el tiempo de flujo. Cuándo sucede esto, se debe corroborar que la

cola del fluido se encuentra en una posición más avanzada respecto al punto A. Es por esa razón que la cantidad de fluido inyectada debe estar muy controlada.

– El fin de la medida tiene lugar cuándo el frente del fluido alcanza el punto D, punto donde se interrumpe el registro del tiempo. De igual forma que en el momento de inicio de la adquisición del tiempo de flujo, en alcanzar el punto D, la cola de la columna del fluido debe estar aguas atrás del punto B.

Siguiendo esta forma de trabajar, el SimpleVIS+ permite obtener una correcta medida directa de la viscosidad cinemática del fluido, en este caso, aceite lubricante (sin requerir de ninguna relación con datos o valores de viscosidad dinámica) en unos 3–5 minutos pudiéndose alcanzar un total de 20 mediciones de viscosidad por hora. Además, de acuerdo con las especificaciones y características técnicas del SimpleVIS+, cada medición presenta una precisión del <3% y una repetibilidad del <2%.

En un principio, el SimpleVIS+, se trata de un viscosímetro capaz de trabajar con una gran variedad de aceites: aceites minerales y aceites sintéticos, tanto formulaciones destinadas para lubricación de motores como para lubricación de engranajes (grados ISO-VG y grados SAE). Siendo además, su mayor ventaja la posibilidad de trabajar con aceites lubricantes nuevos (de aspecto trasparente) hasta aceites lubricantes usados (opacos). No obstante, este sistema tiene un par de inconvenientes: en primer lugar, el estado del tubo no se puede corroborar en ningún momento (exceptuando aquellas alarmas que emite el equipo) debido a que se encuentra encapsulado dentro del bloque de aluminio termostatizado por lo que resulta muy difícil acceder al tubo para el usuario del viscosímetro con el propósito de poder realizar una inspección o valoración, y la segunda se trata del sistema de detección del flujo. El sistema de detección se basa en un sistema que registra un cambio en la cantidad de luz (emitida por un led) que recibe un fotodiodo. Según lo descrito anteriormente, cualquier sustancia que se deposite en las paredes del tubo va a alterar la lectura dando pie a errores y falsos mensajes de alarma. En la Figura 3.5 se muestran dos imágenes del tubo del viscosímetro nuevo (izquierda) y tras ser usado para el análisis de muestras de aceites lubricantes usados (derecha), dónde se aprecia que las paredes internas del tubo quedan cubiertas por la materia carbonosa que este tipo de muestras contienen.

En conclusión, todo esto resulta propicio para el hecho de que las muestras sucias generen problemas o inconvenientes a la hora de emplear

Figure 3.5. *Foto del tubo tipo Houillon del SimpleVIS+ nuevo (izquierda) y tras ser usado en muestras de aceites lubricantes de motor usado (derecha).*

el SimpleVIS+, dado que cualquier tipo de suciedad: carbonilla (en especial), partículas de desgaste o elementos de otra índole es susceptible de depositarse en las paredes internas del tubo de Houillon confundiendo a los sensores e incluso llegando a obstruir el capilar aun siguiendo todos los protocolos (más o menos exhaustivos) de lavado dictados por el fabricante. Es por esa razón que, a la vista de la experiencia adquirida con este sistema, es preferible su uso únicamente para el caso de aceites lubricantes limpios.

- **Viscosímetros rotacionales**: Los viscosímetros rotacionales o rotativos son sistemas que se sustentan en el efecto de cizallamiento que experimenta un fluido contenido entre dos superficies con movimiento rotativo (rotor y estator). Dicho de otra forma, en estos equipos lo que se realiza es la aplicación de una fuerza o par conocidas para provocar un giro, a una velocidad angular definida (relacionada con la resistencia de un fluido al flujo), de una cuerpo sólido en un medio viscoso. De modo que, la medición de la fuerza aplicada necesaria para provocar el giro (a una determinada velocidad) permite conocer la viscosidad del fluido dado que ambas son proporcionales [41].

  Estos equipos son versátiles gracias a la variedad de combinaciones que se pueden realizar entre sus diferentes parámetros: velocidad de rotación,

dimensiones del rotor, espesor del fluido (distancia de separación entre rotor y estator) y fuerza de cizallamiento. Como consecuencia, se pueden realizar una gran variedad de mediciones: en estacionario, en continuo, a diferentes ratios de velocidad de cizallamiento, etc.

Como consecuencia de la versatilidad de diseños, existe una clasificación en cinco categorías atendiendo al par rotor-estator: los primeros son los viscosímetros de cilindros coaxiales (tanto en su versión de Couette como Searle) [126], el siguiente son los viscosímetros de cono y plato, el tercero son los de tipo cono–cilindro, el cuarto grupo son los viscosímetros concéntricos (o bien esferas o bien conos) y como quinto y último el de disco rotatorio.

Para cada tipo, la forma de obtener la viscosidad (viscosidad dinámica, η) es dependiente de la geometría del conjunto rotor–estator y la velocidad angular (Ω, en rad/s) a la que se realiza la medición. Para el primer caso, según la Figura 3.6, dónde se esquematiza el viscosímetro, la expresión matemática que relaciona ese esfuerzo cortante (τ) que experimenta el sistema en función de la viscosidad del fluido viene dado por la Ecuación 3.2:

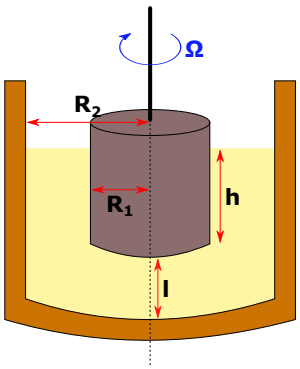

Figure 3.6. *Parámetros de un viscosímetro rotacional del tipo cilindro coaxial.*

$$\tau = \frac{4 \cdot \pi \cdot h \cdot \Omega \cdot \eta \cdot r_a^2 \cdot r_b^2}{r_a^2 - r_b^2} = cte \cdot \Omega \cdot \eta \tag{3.2}$$

El segundo, el viscosímetros de tipo cono y plato (Figura 3.7), la expresión que permite obtener el valor de la viscosidad dinámica es la siguiente:

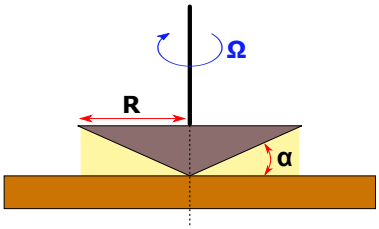

Figure 3.7. *Esquema de la zona de medida de un viscosímetro rotacional de cono y plato.*

$$\tau = 2 \cdot \pi \cdot \alpha \cdot \frac{R^3}{3} \cdot \Omega \cdot \eta = cte \cdot \Omega \cdot \eta \tag{3.3}$$

Para el caso del viscosímetro cono-cilindro, debido a su geometría más compleja (tal y como se aprecia en la Figura 3.8), la expresión resultante para la obtención de la viscosidad resulta ser también mas compleja:

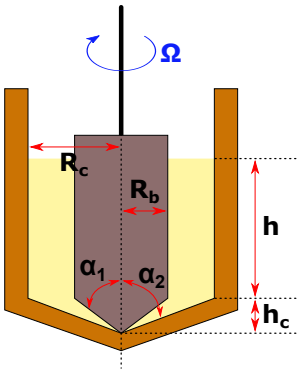

Figure 3.8. *Esquema de la zona de medida de un viscosímetro rotacional con un rotor cono–cilíndrico.*

$$\tau = \frac{4 \cdot \pi \cdot h}{\frac{1}{R_b^2} - \frac{1}{R_c^2}} \cdot \left(1 + \frac{\Delta h}{h}\right) \cdot \Omega \cdot \eta = cte \cdot \Omega \cdot \eta \tag{3.4}$$

Dónde Δh se trata:

$$\Delta h = \frac{h_c}{6 \cdot \cos^2 \alpha_1} \cdot \left(\frac{1}{\tan^2 \alpha_1} - \frac{1}{\tan^2 \alpha_2}\right) \cdot \left(\int_{\alpha_1}^{\alpha_2} \frac{1}{\sin^2 \alpha} \cdot d\alpha\right)^{-1} \tag{3.5}$$

El último caso, los viscosímetros que emplean un disco como rotor (detalles que se observan en la Figura 3.9), requieren una serie de consideraciones previas para poder obtener la viscosidad dinámica del fluido que se desee analizar:

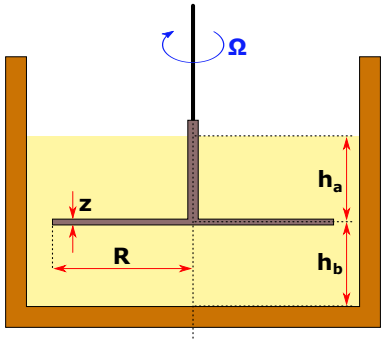

Figure 3.9. *Diagrama del viscosímetro de disco rotatorio.*

- En primer lugar, al tratarse de un disco, el espesor (z) es prácticamente irrelevante al compararlo con el radio del disco (R).
- El espesor de la capa de aceite, tanto por arriba (h_a) como por debajo (h_b) del disco es la misma: $h_a = h_b \equiv h$.

Realizando el ensayo de esta forma, se puede obtener la Ecuación 3.6:

$$\tau = \frac{\pi \cdot R^4}{h} \cdot \Omega \cdot \eta = cte \cdot \Omega \cdot \eta \tag{3.6}$$

Estos cinco son los tipos de viscosímetros rotatorios generales, aunque se han desarrollado una serie de modificaciones o adaptaciones de algunos de ellos acorde con unas determinadas necesidades o requisitos que han derivado en diseños concretos según que aplicación. Un caso de especial mención es el viscosímetro de Stabinger (el cual se rige bajo la norma ASTM D7042: Standard Test Method for Dynamic Viscosity and Density of Liquids by Stabinger Viscometer (and the Calculation of Kinematic Viscosity) [88]). El viscosímetro de Stabinger se sustenta a partir del viscosímetro de cilindros coaxiales de tipo Couette (ver Figura 3.10).

En este tipo de sistemas son tres los elementos que entran en juego: un cilindro estacionario, un cilindro rotatorio y el fluido a analizar dispuesto

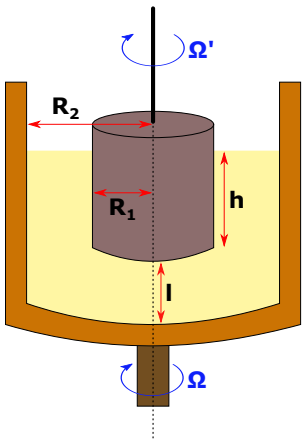

Figure 3.10. *Viscosímetro de cilindros coaxilaes o concéntricos de tipo Couette, dónde el cilindro interno es un cilindro estacionario (stator) y el externo es el rotor.*

entre los dos cilindros. Normalmente, la configuración más habitual es aquella dónde el cilindro exterior (en este caso, el rotor) es el que impone una acción, una tensión o estrés cortante (Ω), al fluido. A continuación, el fluido transmite dicho efecto al cilindro central, que en un principio se encuentra estático, el cual empieza a experimentar la influencia de dicha acción (transmitida por el fluido que lo rodea) pudiéndose así medir el par (Ω'). Este fenómeno es en el que se sustenta el principio de Couette.

Ahora, por lo que respecta al viscosímetro de Stabinger empleado, viscosímetro SVM3001 de Anton Paar (Figura 3.11), este sistema presenta una serie de adaptaciones y características que lo convierten en un sistema de especial interés para su uso y aplicación en el campo de los aceites lubricantes.

Centrándose en el aspecto involucrado en la medición de la viscosidad cinemática, la construcción de la celda de medición es un poco peculiar tal y como se puede observar en la Figura 3.12. En esta celda se combinan varios aspectos: el más importante es el diseño celda de medición compacta y de reducido tamaño que integra dos subsistemas dónde se mide la viscosidad dinámica y la densidad del fluido por separado (para a continuación calcular el valor de la viscosidad cinemática a partir de la Ecuación 2.6), y por otro lado, el control de la temperatura gracias a un bloque de cobre termostatizado mediante un sistema termoeléctrico de tipo Peltier que permite alcanzar un ancho rango de temperaturas (desde -20°C hasta los 135°C).

Figure 3.11. *Viscosímetro Stabinger SVM3001 de Anton Paar.*

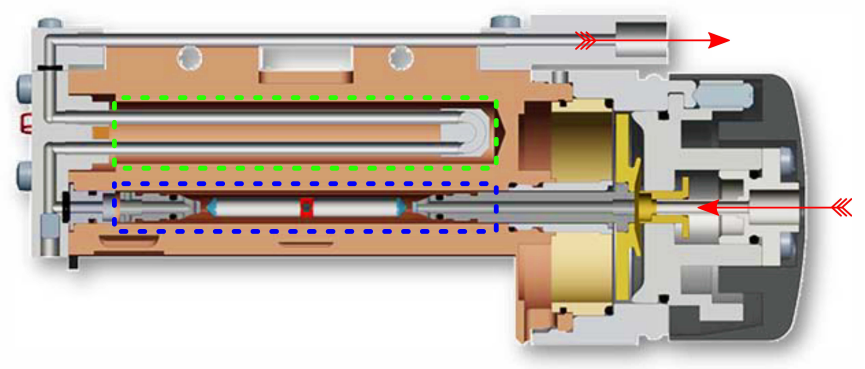

Figure 3.12. *Celda de medición de viscosidad (enmarcada en azul) y densidad (enmarcada en verde) del viscosímetro Stabinger SVM3001.*

La adaptación o versión del viscosímetro de tipo Couette en la que se sustenta el viscosímetro SVM3001 consiste en la miniaturización del sistema para la medición de la viscosidad (región resaltada en azul en la Figura 3.12). Para poder llevar a cabo esta reducción de dimensiones y obtener un sistema eficaz para la determinación de la viscosidad, la forma que tiene este sistema de trabajar es mediante el registro de la velocidad de rotación y frecuencia del cilindro exterior (n_2) y del rotor (cilindro interior) (n_1) y analizando su relación.

Así pues, en este viscosímetro, la parte del mecanismo rotatorio que inflige el movimiento (esfuerzo cortante) es el cilindro o tubo exterior, giro que se realiza a una velocidad constante. De este modo, el tubo comunica este giro al fluido y, debido a la acción de las fuerzas viscosas

del fluido, el movimiento del tubo circundante es capaz de impulsar al cilindro interior. Este cilindro interior es un componente que, debido a su reducido peso (normalmente suele ser un cilindro hueco), es capaz de sustentarse en el seno del fluido y girar en él con total libertad siempre estando centrado en el eje del cilindro exterior gracias a la acción de fuerzas centrífugas que lo empujan a ocupar dicha posición.

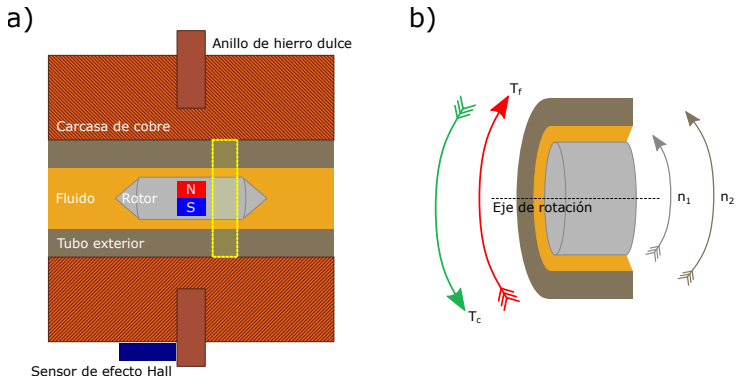

Figure 3.13. *Detalle del modo de trabajo del viscosímetro Stabinger: a) Esquema de la región de medida y b) Parámetros a considerar para la medición.*

Tal y como se aprecia en la Figura 3.13, el cilindro interior contiene un pequeño imán por lo que, cuando éste se encuentra en movimiento, el campo magnético de dicho imán también lo está. Como consecuencia, dentro de la celda se genera un campo magnético alterno o oscilante (CMO), es decir, que su orientación varia. El hecho relevante de este fenómeno radica en que dicho campo, generado por este imán, si se genera en el interior de un material conductor de electricidad (en este caso es la carcasa de cobre circundante) induce corrientes parásitas que se oponen a su origen, en este caso al impulso provocado por las fuerzas de cizallamiento del fluido, y provocan que el giro del cilindro interior se ralentice. De modo que en estos sistemas existen dos fenómenos que se oponen: uno de fuerza impulsoras de cizallamiento del fluido (Ecuación 3.7) y otro de frenado provocado por la corriente inducida (Ecuación 3.8).

$$T_c = K_c \cdot \eta \cdot (n_2 - n_1) \tag{3.7}$$

$$T_f = K_f \cdot n_1 \tag{3.8}$$

Una vez se alcanza el equilibrio de fuerzas entre la acción acelerante (o impulsora) y la de freno (o retardante), el cilindro interior alcanza una cierta velocidad de giro debido a que los momentos de aceleración o conducción (T_c) y el de frenado (T_f) se igualan. Siendo pues esta velocidad del cilindro interior la que se corresponde con la viscosidad dinámica del fluido (Ecuación 3.9).

$$T_c = T_f \rightarrow \eta = \frac{k}{\frac{n_2}{n_1} - 1} \tag{3.9}$$

Así pues, es fácil comprender que, tal y como indica la Ecuación 3.9, la viscosidad dinámica es inversamente proporcional a la diferencia de velocidad entre el tubo exterior (n_2) y el cilindro interior (n_1) dado que en función de la viscosidad del fluido la trasferencia de velocidad preestablecida del tubo exterior al rotor es diferente: fluidos viscosos transfieren más dicha velocidad al cilindro interior, por lo que provocan que su velocidad de giro sea mayor, mientras que si el fluido es poco viscoso, el cilindro interior girará mas lentamente debido a que el fluido no le comunica toda la velocidad del tubo. Teniendo esto claro, la medición de la velocidad y el par se realiza gracias a un sensor de efecto Hall que registra la frecuencia del campo magnético giratorio generado por el imán interno del cilindro interior, de modo que dicho registro se realiza sin contacto directo entre las partes móviles involucradas en la medición de la viscosidad dinámica (η) para luego, en conjunción con la densidad (ρ), obtener la viscosidad cinemática (υ).

Debido a la relevancia de la medición de la viscosidad en los aceites lubricantes, continuamente se están desarrollando nuevos equipos y nuevos sistemas (como por ejemplo, viscosímetros de fibra óptica, viscosímetros a base de resonadores piezoeléctricos, etc.) que permiten trabajar con cantidades de aceites lubricantes menores [106, 145], siendo sistema que no dañan la muestra (no destructivos) y/o poco invasivos. Además de poderse miniaturizar y construir sensores o dispositivos de medida on-line en lugar de interés donde la adquisición de datos es inmediata [2].

3.2.2 TAN y TBN

Un aceite lubricante, durante su vida útil, experimenta cambios físicos y químicos que alteran su composición original favoreciendo que aparezcan o se formen una serie de substancias con carácter ácido (más o menos marcado

en función del escenario que se tenga lugar). Este tipo de substancias tienen un efecto relevante sobre el comportamiento del aceite lubricante, por lo que su detección y cuantificación son de especial interés dado que brindan la posibilidad de conocer qué le sucede al aceite lubricante y, si la situación procede y lo permite, eliminar (en la medida de lo posible) esos ácidos (neutralizar) [95].

En el ámbito de los aceites lubricantes existen dos parámetros que permiten comprender este carácter ácido: el número ácido (TAN, de las siglas Total Acid Number) y el número básico (comúnmente llamado TBN por el nombre en inglés de Total Basic Number). Ambos parámetros son dos formas distintas de expresar una misma idea, por lo que se puede considerar como las dos caras en una moneda: el TAN es la forma de expresar la acidificación del aceite adquirida por su uso, mientras que el TBN es la pérdida de carácter básico (protector) que posee un aceite en su origen para contrarrestar los ácidos que pueden formarse en él a lo largo de su periodo de vida útil. Ellos son antagónicos, sus tendencias son opuestas tal y como se aprecia en la Figura 3.14:

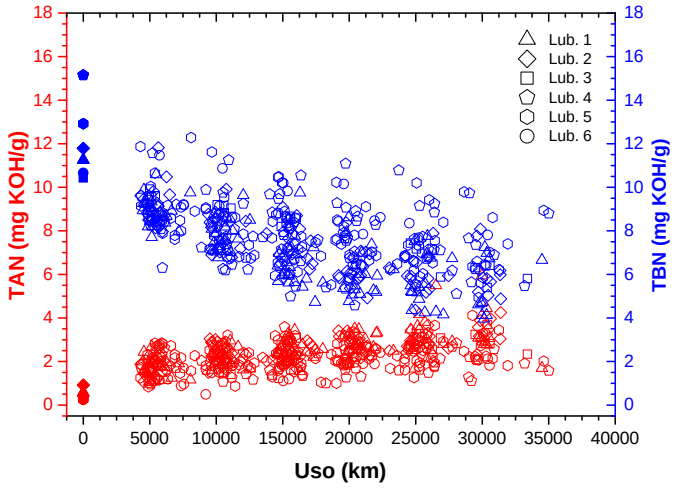

Figure 3.14. *Evolución del TAN y del TBN en 6 formulaciones de aceites lubricantes.*

Esta asociación TAN–TBN requiere controlarse de modo que nunca se dé el caso de que, llegados a un cierto punto, las curvas de ambos parámetros se inviertan. Si se da la situación de que la curva del TAN está por encima de la del TBN, significa que el aceite lubricante ya ha agotado todo aquel carácter básico (proporcionado por su formulación original) y no es capaz de hacer

frente a las especies o productos ácidos que pueda contener, principalmente compuestos de las familias de los ácidos de tipo sulfúrico y nítrico (procedentes de la combustión del combustible) así como ácidos orgánicos (derivados de la degradación–oxidación del lubricante). Llegado a este punto, el carácter de protección de las superficies frente al ataque ácido que posee el aceite lubricante queda comprometido o incluso anulado. Normalmente, los límites estipulados para determinar cuando se debe cambiar un aceite lubricante se pueden definir de dos formas:

- Cuando se observe una caída del valor de TBN correspondiente a la mitad de su valor en origen.
- O, por otra parte, ver la relación entre el TAN y el TBN. En este caso, se asume que es requerido un cambio de aceite cuando el valor del TAN es del orden del 80% del de TBN para un determinado momento.

Por todo ello, existen varias formas o alternativas para determinar estos dos parámetros: a nivel de laboratorio se puede escoger entre el uso de kits o set específicos para la determinación o bien se procede a una realizar una valoración ácido–base.

Para el primer caso, existen una serie de ensayos simples que permiten determinar, con una mayor o menor precisión, el TAN y el TBN. Haciendo referencia a este tipo de procedimientos, existe una gran variedad de sets de varios fabricantes: Mobil, Parker–Kittiwake, CMT, etc. que se emplean con tal propósito. En todos ellos, la característica principal es el uso de una serie de reactivos químicos que provocan un cambio medible en la muestra, cambio que a su vez está escalado y correlacionado con las respuesta que aporta el análisis de la misma muestra empleando alguna de las técnicas o metodologías estandarizadas.

No obstante, desde un enfoque más analítico, la valoración ácido–base es la opción más extendida gracias a su precisión y fiabilidad en los resultados que aporta. En cualquier caso, en una valoración (esquematizada en la Figura 3.15), la forma de proceder es mediante la adición (gradual y controlada) de un reactivo valorante (o titulador) que reacciona con el analito (especie que se requiere conocer su concentración en la muestra) de una forma predeterminada, generando una respuesta acorde con la concentración de dicho analito. La reacción entre el valorante, perfectamente conocida su concentración, y el analito llega a su fin (bajo unas situaciones dadas) en lo que se conoce como "punto de equivalencia": momento o punto teórico dónde la cantidad de valorante y de analito quedan igualadas, pudiéndose pues conocer

la cantidad del analito en función de la del valorante. Experimentalmente, determinar el punto de equivalencia es imposible, por lo que, en su lugar, se realiza una aproximación a esta situación mediante la observación de un cambio (físico o químico) relacionado con la condición de equivalencia conocido como "punto final" [118]. Experimentalmente, existen varias técnicas que permiten determinar cuándo se alcanza esta situación: si el punto se expresa mediante un cambio físico (como coloración, temperatura, conductividad, etc.) o químico (pH, aparición de precipitados, etc.) existen técnicas instrumentales capaces de detectarlas.

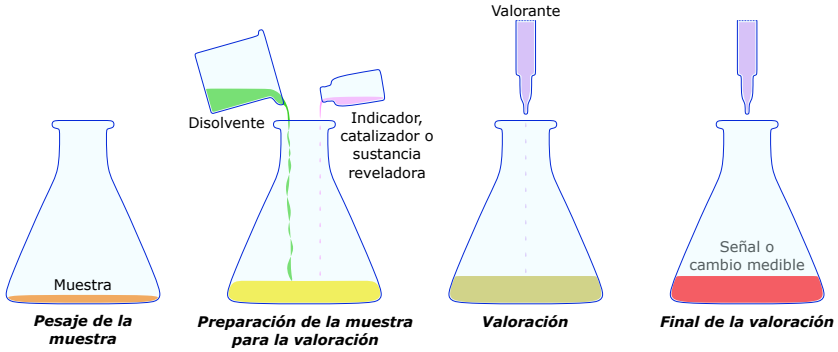

Figure 3.15. *Esquema del proceso de una valoración.*

Para el caso de los aceites lubricantes, las técnicas analíticas que se emplean son tres: valoración colorimétrica, valoración potenciométrica y la valoración termométrica. Las normas que rigen estos test son:

- La norma ASTM D974 [89] y la IP 139 [50] para la valoración colorimétrica de ambos, aunque existen de específicas: la ASTM D3339 [62] e IP 431 [49] para el TAN y la ASTM D5984 para el TBN [65].

- Por potenciometría, existe la norma ASTM D664 [68] y las IP 177 [52] e IP 449 [47] para le caso del TAN. Mientras que para el TBN existen: la ASTM D2896 [59] junto con la IP 276 [51] (ambas emplean como valorante el ácido perclórico) y al ASTM D4739 [64] e IP 417 [48] dónde el ácido valorante es el ácido clorhídrico.

- Para la valoración termométrica, actualmente solo se encuentra aprobada la norma ASTM D8045 [66] para el caso de la determinación del TAN. Más adelante se explicará con mayor detalle esta ruta analítica.

Tal es la variedad de formas y, por consiguiente, normas que rigen los diferentes ensayos que se pueden escoger a la hora de analizar el aceite lubricante para determinar su índice TAN y TBN que se han recogido en la siguiente tabla, Tabla 3.5, agrupándolas acorde con sus homólogos o equivalentes.

Table 3.5. *Equivalencias de las distintas valoraciones analíticas para la determinación del TAN y del TBN.*

Parámetro	**Técnica**	**Norma**					
		ASTM	*IP*	*ISO*	*DIN*	*JSA-JIS*	*AFNOR*
TAN	Potenciometría	D664	177	6619		K2501	
TAN/TBN	Colorimetría	D974	139	6618	51 558/T1	K2501	T60-112
TBN	Potenciometría	D2896	276	3771		K2501	
TAN	Colorimetría	D3339	431	7537			
TBN	Potenciometría	D4739	417	6619		K2501	
TBN	Colorimetría	D5894					

Actualmente, de entre estas tres: colorimetría, potenciometría y termometría, la más extendida es la valoración potenciométrica [33]. La obtención del TAN y del TBN a través de la ruta basada en la potenciometría emplea dicha técnica electroquímica para determinar, cuantitativamente, una especie electroactiva presente en la muestra que se requiere analizar. La valoración potenciométrica requiere de una serie de elementos (representados en la Figura 3.16) para poder llevarla a cabo:

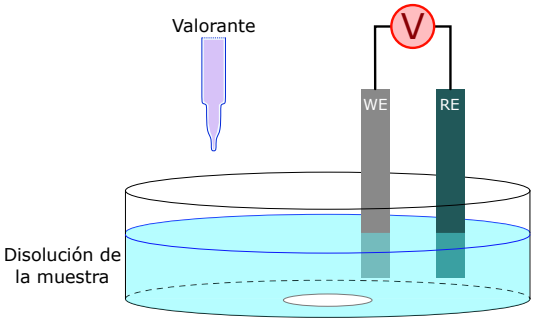

Figure 3.16. *Diagrama de un set experimental con los distintos elementos involucrados para la realización de un valoración potenciométrica.*

- En primer lugar se requiere la preparación de la celda electroquímica dónde se realizará la valoración. Para ello, son necesarios los siguientes elementos:
  - Un sistema de electrodos conformado por un electrodo de referencia (RE) y otro de trabajo (WE). Dónde el primero ayuda a fijar un potencial de referencia, mientras que el segundo se trata de un electrodo afín a la especie electroactiva que se sigue durante la valoración cuyo potencial se ve influenciado por la cantidad de especie electroactiva que se encuentra presente en un determinado momento.
  - Sistema de homogenización empleando un sistema mecánico o magnético, generalmente.
- Una disolución, de concentración perfectamente conocida, del reactivo valorante.
- Un medio de reacción que facilite el contacto entre todos los elementos involucrados en el proceso pero sin intervenir ni influenciar en la valoración en sí, salvo en el enfoque de actuar como vehículo o puente de contacto.

En estos casos, la sustancia electroactiva que se sigue en el proceso de valoración son los protones (H^+), por lo que los electrodos de trabajo que son usados en estas aplicaciones son electrodos de pH. Así pues, en este tipo de sistemas, para conocer que se ha alcanzado el punto de equivalencia en la valoración, se emplea un potenciómetro. Este potenciómetro es capaz de registrar el potencial, pH, que registra al mezcla de reacción en función de la cantidad de reactivo valorante incorporada, lo cual deriva en lo que se conoce como curva de titulación o valoración potenciométrica (ver Figura 3.17):

A partir de la curva de titulación potenciométrica, mediante la metodología de la primera derivada o mediante la segunda derivada, es posible estimar cuando se ha alcanzado el punto final y, de ese modo, calcular la acidez y alcalinidad de las muestra analizada. Esta forma de evaluación gráfica del final de la valoración es el más usado para esta aplicación, pero no se trata del único, dado que existen otras dos metodologías como, por ejemplo: el método de las tangentes y el método del círculo (según Tubbs) entre otros [118].

Escogiendo esta ruta, las normas que determinan cómo se debe proceder para realizar de forma correcta el ensayo son las normas ASTM D664 [68] y ASTM D2896 [59], siendo la primera redactada para la medición del TAN

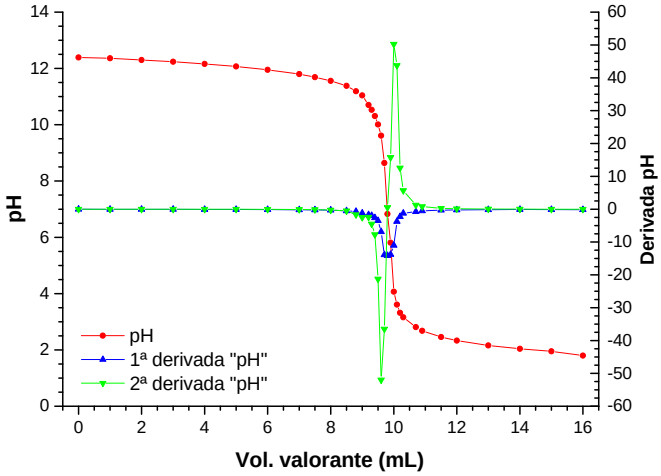

Figure 3.17. *Curva de titulación del pH (rojo) de una muestra dónde se observa el análisis de la primera y segunda derivada del pH (azul y verde, respectivamente) en función del volumen de valorante para la detección del punto final de la valoración.*

y la segunda para el TBN. Para este caso de valoraciones potenciométricas se emplean equipos preparados para tal propósito con una serie de elementos: bureta para dosificación automática, agitador, electrodo de referencia y el de trabajo tal y como se puede apreciar en la Figura 3.18.

Recientemente, la mejora de los reactivos y metodología que se han desarrollado en relación a la valoración termométrica, están provocando que cada vez esta técnica reúna una mayor presencia [7]. En este caso, la reacción química que se produce entre el analito y el reactivo titulante (o reactivo valorante) da lugar a procesos que liberan calor o bien absorben calor del entorno. Para el primer tipo, cuándo la reacción aporta al entorno calor se conoce como proceso o reacción exotérmica (3.19), mientras que si la misma reacción absorbe calor del entorno es llamada reacción endotérmica (3.20) [8, 16, 117].

Para poder seguir la evolución de la temperatura en las valoraciones termométricas, se trabaja buscando que la reacción entre el analito y el agente valorante sea lo más homogénea posible con el objetivo de que el calor (liberado o absorbido) se desarrolle a ritmo constante. Es por esa razón que, con el fin de buscar dicho propósito, la adición de la disolución del valorante sobre la disolución de la muestra que contiene el analito debe realizare de forma constante y estable. Gracias a ello, las condiciones que se generan durante

Figure 3.18. *Titulador Orion Star T940.*

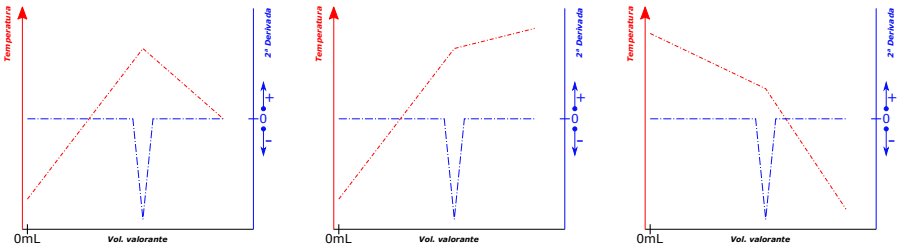

Figure 3.19. *Ejemplo de curvas de titulación para tres procesos exotérmicos, idealizados, dónde se registra la variación de la temperatura en función con el volumen de reactivo valorante incorporado.*

la valoración son propicias para que el comportamiento de la evolución de la temperatura sea constante dibujando un comportamiento lineal hasta alcanzar el "punto final" tal y como se extrae de la Figura (3.19) y Figura (3.20). Una vez se sobrepasa el "punto final" al incorporar a la mezcla más cantidad de valorante, la respuesta mostrada por la temperatura en esta situación de exceso de agente valorante también es lineal. En estos casos idealizados, la detección del fin de la valoración es muy clara: el "punto final" se localiza en la zona de inflexión o ruptura de las dos regiones de la curva de temperatura con

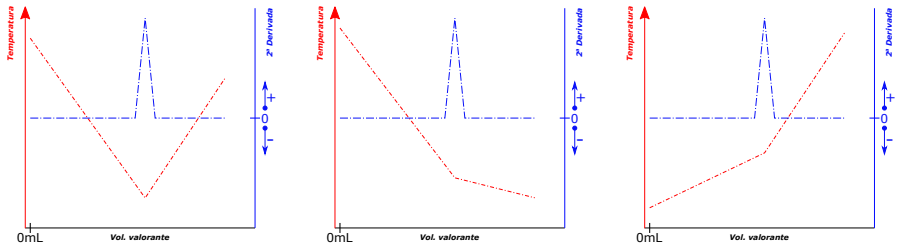

Figure 3.20. *Ejemplo de curvas de titulación para tres procesos endotérmicos, idealizados, dónde se registra la variación de la temperatura en función con el volumen de reactivo valorante incorporado.*

pendientes distintas, dicho de otra forma, en la intersección de las tangentes de los dos comportamientos lineales de la temperatura.

En estos casos, la detección del final de la valoración, "punto final", resulta sencilla gracias al análisis de la segunda derivada (linea azul) de la evolución de la temperatura con el volumen de valorante añadido. En estos casos, el pico queda muy nítido y es fácilmente detectable. No obstante, la forma de la curva que dibuja la evolución de la temperatura depende de varios factores: temperatura de la disolución del analito, temperatura de la disolución del valorante, temperatura del entorno dónde se realiza la valoración, dosado del valorante (tasa de adición), mezcla de las disoluciones, etc., pero lo más importante es tener siempre presente que si el proceso es exotérmico, la segunda derivada de dicha curva va a generar un pico negativo mientras que si, por lo contrario, la reacción es endotérmica, el pico tendrá el sentido opuesto. En ocasiones, no siempre se consiguen o se trabajan con sistemas dónde la reacción analito–valorante es estequiométrica. En estos casos, no ideales, lo que se observa ha sido representado en la Figura 3.21:

Esta curvatura en el "punto final" puede acarrearse a: falta de sensibilidad del sensor empleado y/o a lenta cinética en la reacción valorante–analito (la reacción no alcanza a completarse, estequiométricamente, lo suficientemente rápido) y/o por la dificultad de alcanzar el equilibrio térmico. Por lo que, la nitidez del "punto final" reside en un principio sencillo (ver Tabla 3.6):

Entonces:

- Si la reacción es favorable a producirse, desde el punto de vista de la energía libre ($\Delta G < 0$), ésta continuará su camino hasta completarse. En esta circunstancia, la forma del "punto final" está condicionada por la magnitud del cambio de entalpía (ΔH) de la reacción.

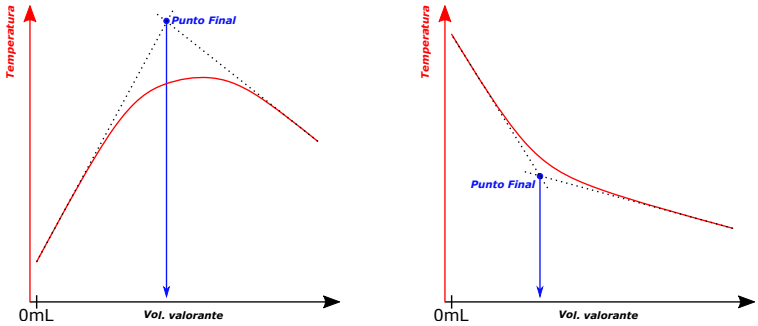

Figure 3.21. *Representación de curvas de titulación, bajo condiciones de reacción no estequiométricas, de un proceso exotérmico (izquierda) y de un proceso endotérmico (derecha).*

Table 3.6. *Predicción de la espontaneidad o no espontaneidad de una reacción a través del valor del cambio de la energía libre de Gibbs (ΔG).*

$\Delta G = \Delta H - T \cdot \Delta S$			
ΔH	ΔS	ΔG	*Condiciones*
+	+	-	Si $T \cdot \Delta S > \Delta H$
+	-	+	Siempre positivo
-	+	-	Siempre negativo
-	-	-	Si $\lvert T \cdot \Delta S \rvert < \lvert \Delta H \rvert$

- Por otro lado, si el proceso es desfavorable ($\Delta G > 0$) el "punto final" aparecerá de forma menos definida, por lo que ese punto de inflexión presentará una forma más redondeada independientemente de la magnitud del cambio de entalpía.

A pesar de ello, la valoración termométrica permite detectar con precisión el "punto final" dado que se basa en el análisis de la curva de temperatura y de su derivada, concretamente su segunda derivada. Para el primer caso, dónde sólo se analiza la curva de la evolución de la temperatura, se sigue un procedimiento a base de hallar la intersección de las dos tangentes de las secciones rectas (localizadas antes y después del punto final) de la curva de temperatura tal y como se indica en la Figura 3.21. Una vez se corrobora que se ha detectado el cambio de tendencia de la curva de evolución o gradiente de la temperatura de la disolución, se procede a comprobar que este punto es

el correcto gracias al análisis de la segunda derivada, dado que en unas curvas de este tipo un cambio de tendencia se plasma cómo un pico máximo (pico positivo, si la reacción es endotérmica) o un pico mínimo (pico negativo para procesos exotérmicos). De este modo, la ubicación precisa del punto de mayor cambio en el gradiente de la curva de temperatura queda garantizada y, por ende, el "punto final".

Con todo ello, el desarrollo de esta técnica de análisis se debe a varios aspectos muy específicos:

- En especial, la mejora del conocimiento focalizado a la mejor compresión del comportamiento térmico de las reacciones que involucran sistemas químicos que se catalogan como "idóneos" para su valoración termométrica en función de la cantidad mínima de analito presente y de la entalpía de la reacción de reacción de valoración analito–valorante.

- La aparición y evolución de sensores capaces de registrar, de forma rápida, cambios muy pequeños de temperatura (cambios muy bajos, incluso alcanzando niveles de $10^{-5}K$). Estos sensores son los termistores, los cuales se basan en un sistema de óxidos metálicos mixtos sinterizados. La virtud de estos sistemas es que presentan un comportamiento muy sensible a las variaciones de temperatura, concretamente los materiales de los termistores se caracterizan por mostrar cambios significativos del valor de su resistencia eléctrica para variaciones de temperatura muy pequeñas.

- El hallazgo de catalizadores útiles. Estas sustancias tiene como objetivo ayudar a la detección del fin de la valoración dado que son capaces de mejorar o magnificar el cambio de gradiente de temperatura, de modo que el contraste antes y después del "punto final" queda más acusado y la probabilidad de una detección satisfactoria del fin de la valoración aumenta.

- Como el sensor que se emplea no interactúa con la disolución (como lo harían los sensores eléctricos o electroquímicos, dónde se monitoriza la conductancia del medio), el medio de valoración deja de ser un parámetro relevante. En estos casos, la polaridad o no polaridad del medio y su limpieza (desde el punto de vista de turbidez, suspensiones o precipitados en el medio), deja de jugar un papel en la valoración.

- Por último, el aspecto instrumental y de software ha sido un factor crucial. Estas herramientas permiten englobar dentro de un factor

base (llamado ruido blanco o background), todos aquellos aspectos que pueden afectar al resultado de la valoración tales como: aspectos cinéticos de la reacción, la matriz de estudio y condicionantes térmicos (pérdidas o fluctuaciones de calor), que siempre están presentes e inducen a errores que son contantes. De este modo, este parámetro queda asilado y puede cuantificarse propiciando su eliminación o sustracción del resultado final de la valoración.

Con todo ello, la valoración termométrica es una técnica de aplicación diversa: valoraciones ácido–base, redox, gravimetrías, etc. [148] aunque su uso más exitoso radica en aquellas situaciones dónde la reacción analito–valorante reúna los siguientes aspectos: rápidas cinéticas y equilibrios estequiométricos o casi estequiométricos.

Ahora, aplicado al campo de los aceites lubricantes, la aplicación de la valoración termométrica resulta muy ventajosa para la determinación del TAN [18, 45] y del TBN [130]. En este caso, el protocolo a seguir queda definido, para cada una de los dos parámetros, por un determinado conjunto de aspectos: disolución del agente valorante, ratio de dosado de la disolución valorante, disolvente para valoración, cantidad de muestra requerida, catalizador (y su cantidad) y, por último, sistema y condiciones de homogenización de las distintas disoluciones. Todos estos puntos se realizan en unas condiciones y equipamiento diseñado para tal propósito, equipamiento que se muestra en la Figura 3.22.

Para un mayor detalle, se puede acudir a la documentación especializada proporcionada por el fabricante del sistema de valoración, Metrohm, para cada el TAN [21] y el TBN [22]. Empleando este sistema se es capaz de obtener lecturas de TAN y de TBN precisas, exactas, reproducibles y repetitivas a partir del estudio de las curvas de comportamiento de la temperatura, la cual es el parámetro que permite determinar el valor del TAN y del TBN.

El sistema de valoración tiene en cuenta la relación existente de la temperatura (T), la cual es función de volumen del valorante ($T = f(V)$). Por esa razón, cuando el software de tratamiento de la señal deriva la temperatura en función del volumen de valorante añadido a la mezcla, genera dos gráficos: uno para la primera derivada ($T' = f'(V)$) dónde se permite la detección del punto de inflexión (cambio de tendencia de evolución de la temperatura) alrededor del final de la valoración y otro para la segunda derivada ($T'' = f''(V)$) que corrobora que, al tratarse de un proceso exotérmico, ese cambio de pendiente en la curva de la temperatura da como resultado un pico negativo. Todo esto queda reflejado, tanto par el TAN como para el TBN en la Figura 3.23.

Figure 3.22. *Montaje experimental 859 Titrotherm para la realización de las valoraciones térmométricas de Metrohm compuesto por: software tiamo, bureta Dosino y termistor Thermoprobe 6.9011.020.*

Como consecuencia de estos buenos resultados, tal fue la relevancia adquirida por la técnica que recientemente se ha redactado una norma, legislada por la ASTM, para la valoración termométrica del TAN [66]. Tal ha sido la respuesta y el buen acogimiento de la sociedad especializada, que no es de extrañar que en breves ocurra lo mismo para que se prepare la correspondiente norma para el TBN.

3.2.3 Espectroscopia FT–IR

La espectroscopia infrarroja por transformada de Fourier, representadas por las siglas FT–IR, se trata de una técnica óptica de gran aplicabilidad al campo del análisis, cualitativo y cuantitativo, de los aceites lubricantes de motor. Básicamente, las espectroscopia FT–IR, emplea la radiación IR (gran región, desde el punto de vista energético: 800 nm - 1 mm, o lo que es equivalente 12500 cm^{-1} - 10 cm^{-1}) del espectro electromagnético para conocer la composición de una determinada muestra a partir de las vibraciones moleculares de la o las sustancias que la constituye. De las tres subdivisiones que componen esta sección: infrarrojo cercano (near–IR o NIR), infrarrojo medio (mid–IR o MIR) e infrarrojo lejano (far–IR o FIR) (ver Tabla 3.7), la que mayor información útil e interpretable aporta al analista acerca de la muestra de estudio es la región MIR [129, 133].

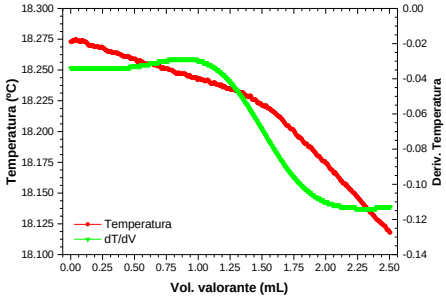

(a) Evolución de la T (rojo) y T' (verde) para la determinación del TAN

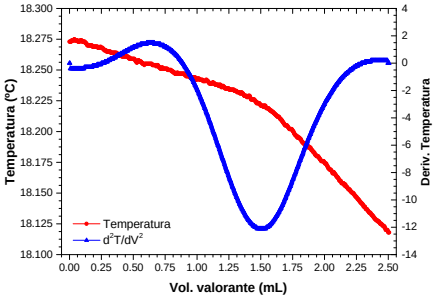

(b) Evolución de la T (rojo) y T" (azul) para la determinación del TAN

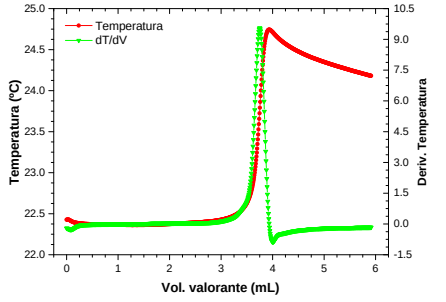

(c) Evolución de la T (rojo) y T' (verde) para la determinación del TBN

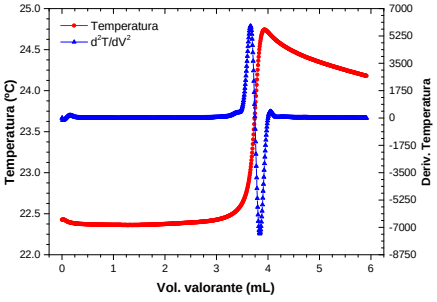

(d) Evolución de la T (rojo) y T" (azul) para la determinación del TBN

Figure 3.23. *Curvas registradas durante la valoración termométrica del TAN y del TBN de un aceite lubricante.*

Table 3.7. *Regiones IR del espectro electromagnético.*

Espectro IR		**Intérvalo**			
Símbolo	*Región*	λ *(m)*	$\bar{\nu}$ (cm^{-1})	ν *(Hz)*	*E (J)*
NIR	cercano	$3 \cdot 10^{-6} - 7.8 \cdot 10^{-7}$	$12820 - 3300$	$1 \cdot 10^{14} - 3.8 \cdot 10^{14}$	$6.6 \cdot 10^{-20} - 2.5 \cdot 10^{-19}$
MID	medio	$3 \cdot 10^{-5} - 3 \cdot 10^{-6}$	$330 - 3300$	$1 \cdot 10^{13} - 3.8 \cdot 10^{14}$	$6.6 \cdot 10^{-21} - 6.6 \cdot 10^{-20}$
FAR	lejano	$3 \cdot 10^{-4} - 3 \cdot 10^{-5}$	$33 - 330$	$1 \cdot 10^{12} - 3.8 \cdot 10^{13}$	$6.6 \cdot 10^{-22} - 6.6 \cdot 10^{-21}$

Longitud de onda (λ)
Número de onda ($\bar{\nu}$)
Frecuencia (ν)
Energía (E)

El principal fenómeno por el que se basa la espectroscopia IR es el hecho de la interacción entre la radiación electromagnética y aquellos compuestos (moléculas orgánicas) que absorben cierta cantidad de energía acorde con la energía de sus enlaces químicos. La forma de interacción de la radiación sobre las moléculas depende de la región considerada: si se acude a la región más energética, el NIR, lo que se observa son los procesos de excitación que derivan en la aparición de sobretonos y armónicos de las vibraciones naturales del esqueleto de las moléculas. Si se estudia el rango medio, MIR, los fenómenos que tienen lugar son dos: las vibraciones moleculares conocidas como vibraciones fundamentales y los procesos roto–vibracionales asociados a la propia estructura molecular. Por último, la región más alejada, el FIR, al ser una región pobre energéticamente solo se emplea para el estudio del espectro vibracional molecular. De entre todas ellas, la más empleada para el análisis de aceites lubricantes es el MIR, dado que en esa región es dónde se comprenden los fenómenos derivados de las frecuencias de vibración de la estructura molecular de las moléculas orgánicas (ver Figura 3.24) y es ahí dónde radica su interés [4].

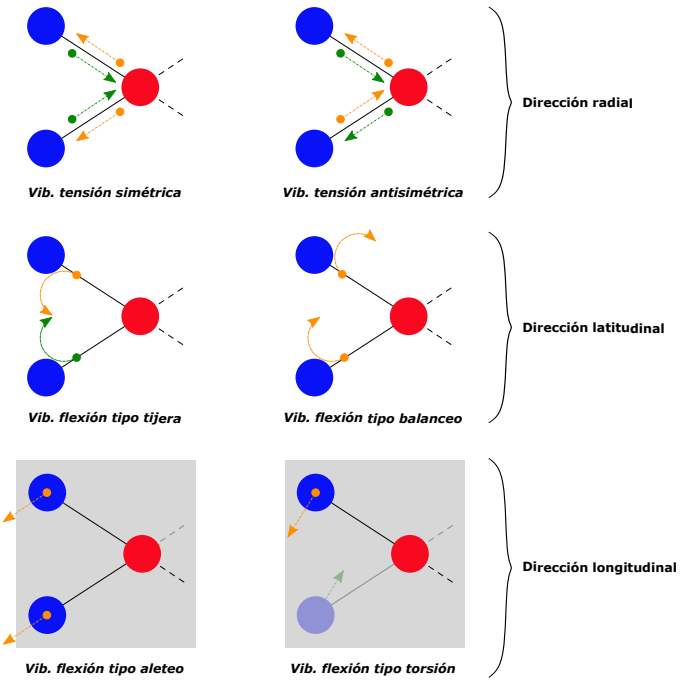

Figure 3.24. *Modos vibracionales: estiramiento simétrico (υ_s) y antisimétrico (υ_{as}), tijera (δ), balanceo (ρ), aleteo o meneo (ω) y torsión (τ).*

La radiación MIR provoca que, al irradiar una determinada muestra, sus moléculas experimentan una excitación al absorber dicha radiación, por lo que deriva en que ciertas partes de su estructura molecular (enlaces químicos) se deformen: modificando la distancia interatómica alargándose–acortándose a lo largo del eje del enlace (tensión) y/o modificando su ángulo (flexión). Esta vibración de los enlaces se produce para una determinada radiación que posea aquella energía acorde con la frecuencia de vibración del enlace químico concreto. De este modo, es posible relacionar directamente la frecuencia de radiación con la frecuencia de vibración de los enlaces. Desde un punto de vista más práctico, la espectroscopia MIR se emplea para la identificación de determinadas estructuras, los grupos funcionales. Los grupos funcionales son unas unidades químicas definidas por una serie de enlaces (simples, dobles o triples) entre diferentes átomos (principalmente carbono, nitrógeno, oxígeno, azufre, fósforo, hidrógeno y los halógenos) [96, 120].

La presencia de la vibración de estos grupos funcionales se puede distribuir en la ventana del MIR en dos zonas:

- La primera, comprendida entre 4000 cm^{-1} – $\leqslant$1500 cm^{-1}, es dónde se concentran las absorciones de la mayoría de los grupos funcionales, pero con ratios de canales por grupo funcional (bandas de absorción) relativamente bajos.
- La segunda es conocida como la "zona dactilar" (o fingerprint en inglés) y se localiza a partir de <1500 cm^{-1} y en adelante. En esta región los fenómenos de absorción son más numerosos, por lo que esta zona reúne una elevada densidad de bandas de absorción, por lo que el patrón que se genera es complejo.

La forma en la que se procede al estudio de los fenómenos de absorción de la radiación IR por los enlaces de los grupos funcionales es a través de la absorbancia ($Abs.$) y la transmitancia ($Trn.$). La primera se define como la cantidad de la energía radiante que ha sido absorbida por una sustancia, mientras que la segunda hace mención a la cantidad de energía que es capaz de atravesar una sustancia (I) (sin alterar la frecuencia de cada uno de los componentes monocromáticos que componen dicha radiación) [133]. Ambas magnitudes se encuentran relacionadas (Ecuación 3.10), dado que cuando se irradia una sustancia, esta energía incidente (I_0) experimenta ambos fenómenos (ver Figura 3.25):

$$Trn. = \log \frac{I}{I_0} \rightarrow Abs. = \log \frac{I_0}{I} = -\log Trn. \tag{3.10}$$

Table 3.8. *Absorciones en el IR de los distintos grupos funcionales.*

Enlace	Grupo funcional	Intervalo (cm^{-1})	Intensidad
C—H	*Alcano*	2970-2860	F
	Metilo	1460, 1375	M
	Metileno	1465	M
	Alqueno	3080-2975	M
		1680-650	F
	Aromático	3150-3000	F
		900-700	F
	Alquino	∼3300	F
	Aldehido	2900-2800	D
		2775-2695	D
C—C		No interpretable	
C=C	*Alqueno*	1680-1580	M-D
	Aromático	1600-1490	M-D
C≡C	*Alquino*	2250-2100	M-D
C=O	*Aldehido*	1740-1645	F
	Cetona	1765-1540	F
	Ac. carboxílico	1725-1700	F
	Éster	1750-1715	F
	Amida	1700-1640	F
	Anhídrido	∼1810, ∼1760	F
C—O	*Alcohol* *Éter* *Éster* *Ac. carboxílico*	1310-1020	F
O—H	*Alcohol*	3640-3610, 3400∼3200	M
	Fenol		M
	Ac. carboxílico	3300-2200	M
N—H	*Amina*	3500∼3300, 900∼650	M
C≡N	*Nitrilo*	2260∼2240	M
C—X	*Floruro*	1400-1000	F
	Cloruro	785-540	F
	Bromuro	650-510	F
	Ioduro	600-485	F

F – fuerte
M – media
D – débil

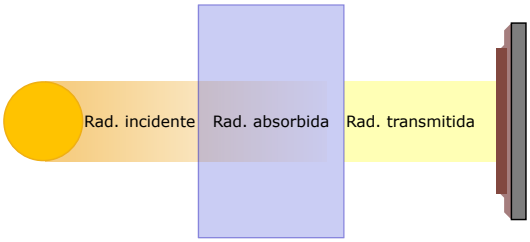

Figure 3.25. *Diagrama representativo de los fenómenos de absorción y transmisión de una radiación sobre una sustancia.*

Como resultado de ello, lo que se obtiene es lo que se conoce como espectro de IR, el cual se trata de una representación gráfica de la absorbancia/transmitancia registrada por una muestra concreta para cada una de los valores de frecuencias de la radiación incidente a la cual se expone o se le es sometida. En las figuras siguientes se plasman las dos posibilidades de expresar un espectro IR: según la absorbancia en la Figura 3.26 o bien transmitancia en la Figura 3.27.

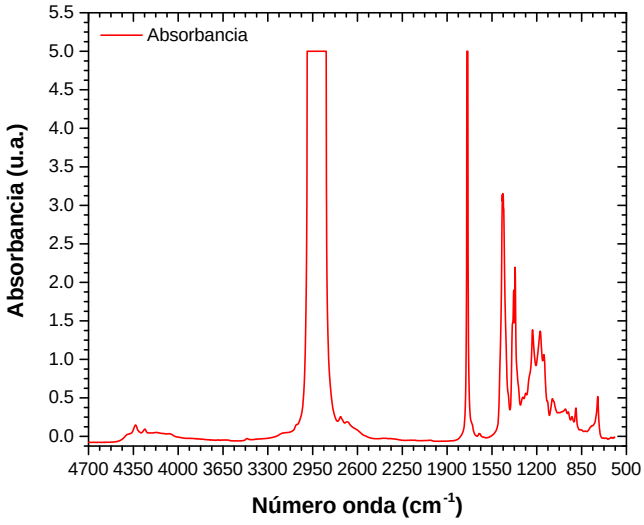

Figure 3.26. *Espectro IR de absorción.*

Aunque, de entre estos dos posibles magnitudes, la forma de expresar habitualmente el espectro de IR es mediante la absorbancia. Independientemente, de acuerdo a la vista de los espectros de la Figura 3.26 y de la Figura 3.27,

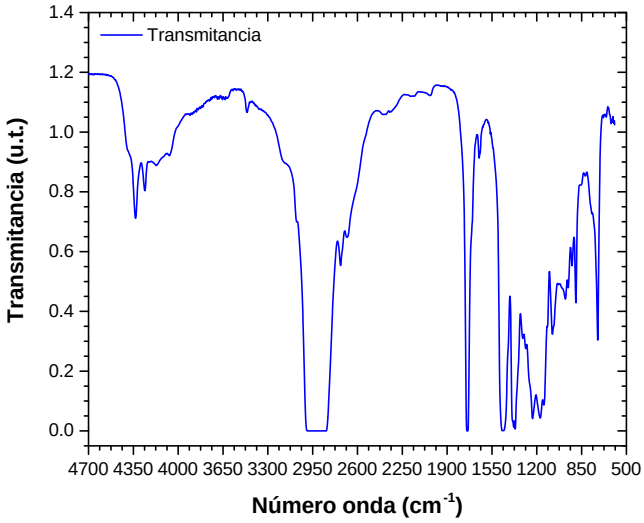

Figure 3.27. *Espectro IR de transmisión.*

un espectro de IR se caracteriza por poseer o construir un patrón propio e identificativo de la sustancia analizada [29]. Este patrón se compone por una serie de picos o bandas de absorción que aportan información, tras una interpretación adecuada, de la muestra atendiendo a los siguientes parámetros:

- Por lo que respecta a la posición de los picos, valor de frecuencia a la que aparecen, es indicativo de los diferentes grupos funcionales que pueda formar la estructura molecular de la sustancia analizada.
- La intensidad, entendida como la cantidad de energía que es absorbida a esa frecuencia. Aunque dependiente del grupo funcional, se puede correlacionar con la presencia (en mayor o menor grado) de un determinado tipo de estructura en una muestra.
- Por último, la forma del pico, la cual suele ser indicativo de un grupo o familia de grupos funcionales.

Teniendo estas tres premisas: posición, intensidad y forma de los picos, es posible obtener información cualitativa de la presencia de los ciertos grupos funcionales presentes en la muestra. No obstante, para extraer información cuantitativa a partir de estas señales, se requiere analizar más en detalle el pico fijando el foco sobre su altura (Peak Height en inglés) o bien por el área

que ocupa (Peak Area) siempre partiendo como referencia de un determinado punto o linea de interpolación. En la Figura 3.28 se han reunido las diferentes formas de determinar la altura y el área de un pico:

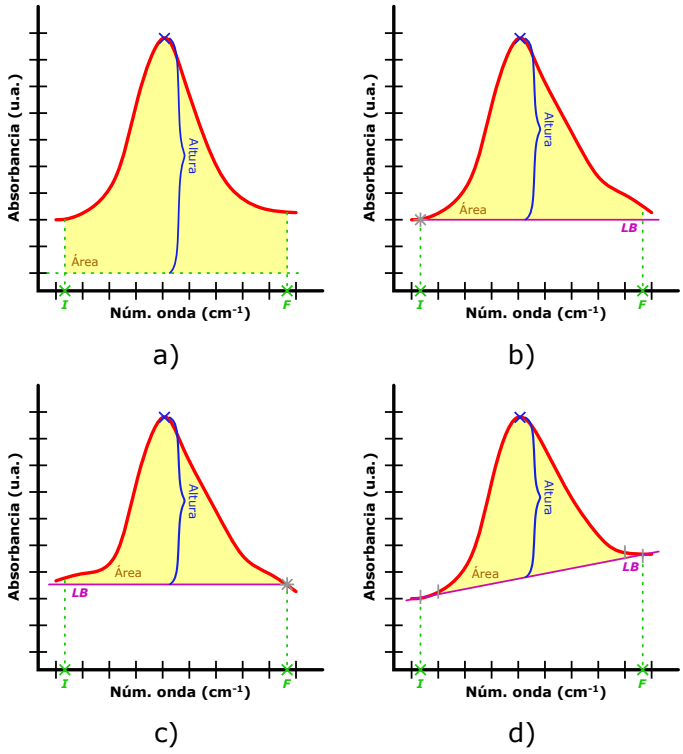

Figure 3.28. *Definiciones de altura y área de pico en función de distintas referencias: a) Línea base el eje de abscisas (en valor cero), b) Línea base, paralela al eje de abscisas, respecto al inicio (I) del pico c) Linea base, paralela al eje de abscisas, respecto al final (F) d) Dos líneas base.*

En función del parámetro que se desea considerar, altura (cuyas unidades son $u.a.$) o área ($u.a./cm$) de pico, la medición seleccionada para su estudio debe estar claramente definida acorde con la mayor afinidad o adecuación posible [61].

Para obtener y estudiar el espectro IR de una sustancia se emplea un dispositivo llamado espectrómetro IR. Este sistema puede presentarse en dos configuraciones: un espectrómetro IR dispersivo (EIR-D o DIR) o bien uno de Transformada de Fourier (EIR-FT o FT–IR), tal y como se muestra en la Figura 3.29.

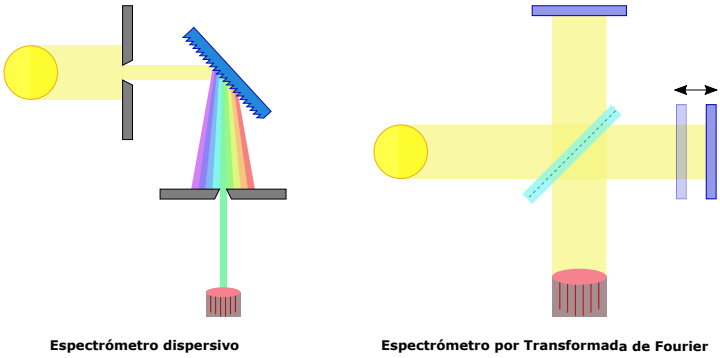

Figure 3.29. *Esquema de los sistemas ópticos empleados en cada una de las dos modalidades de espectrómetros infrarrojos existentes: la versión dispersiva (izquierda) y la por Transformada de Fourier (derecha).*

- Los espectrómetros dispersivos son construidos de modo que la radiación generada por la fuente es enviada a la muestra. A continuación, cierta cantidad de radiación es absorbida por la muestra y no es capaz de traspasarla pero otra si. La radiación transmitida incide en una rendija de entrada al monocromador que lo descompone en pequeños paquetes o haces de luz con un determinado grado de monocromaticidad. A continuación, estos haces son enfocados a una rendija de salida para aumentar aún más la monocromaticidad de la radiación transmitida de modo que la radiación que alcance el detector esté lo más cuantizada posible. Estos sistemas, requieren el análisis de la muestra junto a su referencia, ya sean espectrómetros de doble haz como de simple, dado que en estos equipos lo que se obtiene es el cociente de estas dos señales.

- Mientras, los espectrómetros por transformada de Fourier, son sistemas ópticos inspirados en el interferómetro de Michelson. Los espectrómetros FT–IR están constituidos básicamente por tres elementos: una fuente de radiación, un interferómetro y un detector. El principio de funcionamiento, de forma breve, de un equipo de estas características reside en el hecho de que la radiación policromática que genera la fuente es dirigida a un divisor de haz para que esta radiación sea reflejada en un conjunto de dos espejos: uno de ellos fijo estático y el otro móvil, ambos dispuestos en ángulo recto uno respecto del otro (de modo que el divisor del haz se encuentra a 45° de los espejos). Como consecuencia de ello, se produce un patrón de interferencias entre aquella radiación reflejada (50% de la radiación original de la fuente) que no ha pasado a través

de la muestra y por aquella porción (el otro 50% restante) que ha sido transmitida dado que existe una cierta cantidad que ha sido absorbida selectivamente por la muestra. De modo que este interferograma es lo que registra el detector, interferograma que a posterior debe ser tratado mediante el algoritmo de Transformada de Fourier.

De modo que las principales diferencias de un sistema u otro radican en el uso de un monocromador o un interferómetro, con sus consiguientes inconvenientes o peculiaridades a tener en cuenta a la hora de obtener la señal y de su tratamiento. Según lo expuesto, no es de extrañar que en los espectrómetros DIR, se produce una pérdida de información significativa debido a su propia filosofía de funcionamiento, lo cual deriva en que el ratio señal–ruido no es del todo favorable. Es por eso que los espectróemtros FT–IR han desplazado a los DIR debido a su mayor velocidad y sensibilidad.

En este estudio, el espectrómetro seleccionado ha sido el FT–IR de A2 Technologies con el sistema ThumbIR para la medición, por transmitancia, de muestras líquidas (Figura 3.30) dado que permite trabajar bajo la norma ASTM D7418 [84].

Figure 3.30. *Espectrómetro FT–IR 5500t de transmitancia para muestras líquidas de A2 Technologies.*

Este sistema se caracteriza por los siguientes elementos reunidos en la Tabla 3.9.

Ahora, mediante el uso de este tipo de espectrómetro infrarrojo medio mediante Transformada de Fourier (FT–IR), dentro del contexto del análisis de los aceites lubricantes, se puede aplicar esta técnica para extraer una gran cantidad de información acerca de la composición, degradación y

Table 3.9. *Principales características del espectrómetro FT–IR 5500t.*

Propiedad (unidades)	**Valor**
Rango espectral (cm^{-1})	4700 – 590
Resolución (cm^{-1})	4
Escaneo del fondo (-)	128
Escaneo de la muestra (-)	128
Longitud del paso óptico (mm)	0.1
Material de la ventana (-)	Seleniuro de cinc (ZnSe)
Interfaz de muestreo (-)	Liquid transmission – TumblIR
Apodización (-)	Triangular

contaminación del aceite lubricante que se desea estudiar [15]. Con esta técnica, resulta muy sencillo averiguar que le sucede al aceite lubricante durante su uso y conocer y seguir la evolución de su comportamiento. Las virtudes o ventajas que convierten a esta técnica en un procedimiento de análisis de lubricantes poderoso son: en primer lugar, como ya se ha introducido en las lineas anteriores, la versatilidad de respuesta e información (cualitativa y cuantitativa) que extrae, la rapidez con la que proporciona la información (facilitando el hecho de recopilar una cantidad de datos elevada), y por último la facilidad del manejo y operación instrumental y de preparación de muestra (abaratando los costes considerablemente) [137].

Para mantener un control y rigor a la hora de analizar, específicamente, aceites lubricantes con un espectrómetro FT–IR, existen una serie de normas y estándares que estipulan todo el procedimiento. Principalmente, la norma que rige la técnica de la espectroscopia FT–IR para el estudio de aceites lubricantes es la ASTM E2412: Standard Practice for Condition Monitoring of In–Service Lubricants by Trend Analysis Using Fourier Transform Infrared (FT–IR) Spectrometry [76]. No obstante, existen otra serie de estándares redactados por la ASTM con un ámbito de aplicación más concreto:

- Para el caso de analizar la oxidación de una aceite lubricante [1], se puede acudir a: la ASTM D7214 [82] o la ASTM D7414 [70].

- Otro aspecto de los lubricantes, su nitración, queda representada por la norma ASTM D7624 [73].

- La evolución de los aditivos antidesgaste, componentes muy relevantes en este campo, queda sometido bajo las pautas de la norma ASTM D7412 [69].
- Mientras que si se busca analizar los subproductos derivados de la sulfatación del aceite lubricante, se requiere acudir a la ASTM D7415 [71].
- Como último ejemplo de estas normas específicas es la norma ASTM D7844 [85], la cual permite determinar el contenido de hollín en el aceite lubricante.

Durante el desarrollo de esta investigación han sido empleadas las normas anteriormente citadas así como también se han realizado alguna serie de adaptaciones, inspiradas en éstas, con el objetivo de buscar la mejor señal de alguno de los parámetros que se requería para el estudio.

3.2.4 RULER

RULER es el acrónimo de la expresión en inglés: *Remaining Useful Life Evaluation Routine*, la cual da nombre a un tipo de equipo electroquímico comercializado por FLUITEC, ver Figura 3.31, focalizado en la determinación del estado de oxidación de un aceite lubricante a partir del estudio del paquete de aditivos antioxidantes empleados en las formulaciones consideradas [27].

Figure 3.31. *Equipo voltamperométrico RULERView de FLUITEC.*

El instrumento mostrado en la figura anterior (Figura 3.31) es un sistema electroquímico que realiza una voltamperometría lineal de barrido (LSV, siglas en inglés cuyo significado es Linear Sweep Voltammetry). El equipo,

básicamente, aplica un potencial el cual experimenta una variación con el tiempo de forma lineal por lo que al final lo que se está realizando es un barrido de potenciales (cuyas unidades serian voltios por unidad de tiempo) a una velocidad constante. Con ello, lo que se consigue es que aquellas especie químicas susceptibles a experimentar un proceso redox (oxidación o reducción en función del valor del potencial, positivo para oxidar y negativo para reducir). Al realizar este procedimiento, lo que se obtiene es un registro de la variación de la intensidad de corriente en función del potencial aplicado, es decir, un voltamperograma [95].

Haciendo hincapié en el aspecto de la técnica de la voltamperometría, el RULER funciona bajo unas condiciones de trabajo y configuración de la técnica analítica a emplear estrictas e independiente del tipo de aceite lubricante que se desea estudiar:

- Un primer aspecto es el que atañe a la celda electroquímica que se emplea. La celda está compuesta por un electrodo compuesto que aúna los tres distintos electrodos que se encuentran en una celda electroquímica común: el rol de electrodo de trabajo lo realiza un electrodo de carbón vitrificado, mientras que para el electrodo de referencia y el auxiliar unos electrodos de alambre de platino actúan como tal.

- El medio dónde se realiza el proceso electroquímico es específico para cada formulación de aceites lubricantes acorde con su aplicación en un campo de uso concreto. A pesar de ello, todos ellos presentan aspectos comunes: un disolvente polar para extraer los aditivos del aceite lubricante y un electrolito eléctricamente activo para cada caso. Además, en el vial que contiene dicho medio (5 mililitros), se acompaña de un medio adsorbente a base de arena purificada (1 gramo) que se encarga de retener aquellos componentes no electroactivos como las bases lubricantes, insolubles y compuestos apolares.

- El ensayo consiste en la oxidación de los aditivos antioxidantes mediante la aplicación controlada de un potencial creciente que inicia en 0.0 V y termina en 1.7 V a una ratio de 0.1 V/s.

- Para fijar un origen, se requiere analizar el aceite lubricante nuevo y la muestra degradada. De este modo es posible observar la diferencia entre el voltamperograma del aceite lubricante nuevo y el usado.

Con todo ello, en la Tabla 3.10 se muestran los diferentes tipos de análisis que son posibles ejecutar en este equipo teniendo en consideración la procedencia y aplicación del aceite lubricante:

Table 3.10. *Resumen de la metodología de análisis y reactivos a emplear, en función de la muestra de aceite a estudiar, según las recomendaciones para el correcto funcionamiento del RULER.*

Aplicación	Disolución	Vol. muestra	Análisis
Aceites de engranajes y de transmisión Aceites de turbinas de gas y de vapor Aceites hidráulicos Aceites de compresores Aceites de transformadores Aceites tipo o basados en fosfato-ésteres Aceites de circulación de ámbito industrial	Verde	200–400 μl	17 seg.
Grasas lubricantes		250 mg	
Aceites minerales para turbinas de gas y de vapor con antioxidantes fenólicos Aceites hidráulicos para bombas Aceites de transformadores	Amarillo	200–400 μl	11 seg.
Aceites lubricantes de motores diésel y gasolina Aceites lubricantes de motores de GNC y biogás	Azul	20–400 μl	17 seg.
Aceites lubricantes de motores de avión Aceites lubricantes de motores a reacción Aceites lubricantes para motores de helicóptero	Rojo	50–400 μl	11 seg.

Como resultado de estas pautas, la respuesta que devuelve el RULERView es un voltamperograma como el que se muestra a continuación en la Figura 3.32.

La forma de interpretar este tipo de gráficos es teniendo presente el hecho de que en este ensayo lo que realiza es una oxidación de los antioxidantes que pueda contener la muestra. Dicha oxidación se va a producir acorde con el potencial de oxidación propio de cada tipo de aditivos:

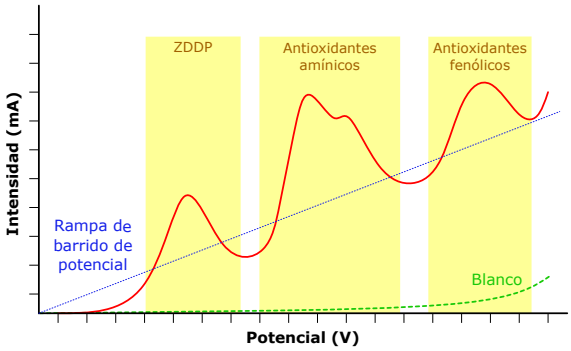

Figure 3.32. *Ejemplo de voltamperograma generado al analizar aceite lubricante mediante el dispositivo RULERView.*

- Para el caso de los aditivos amínicos, de todos las variedades que existen y se pueden englobar en esta familia, los potenciales de oxidación se localiza alrededor de 1.32 V.

- Si se analizan los aditivos fenólicos, el rango de potenciales dónde pueden aparecer queda limitado entre los 1.10 V a 1.35 V.

- Mientras que los aditivos a base de compuestos organometálicos a base de cinc (ZDDP), presentan los fenómenos de oxidación a valores de potencial comprendidos entre los 0.90 V y 1.10 V, aproximadamente.

Valores de potencial referenciados todos ellos respecto al electrodo de referencia de plata/cloruro de plata.

De modo que, para cada tipo de aditivos antioxidantes, se obtienen diferentes señales que son traducibles a la concentración de estos aditivos en la muestra de aceite lubricante analizada [110]. No obstante, la forma más habitual de trabajar con este sistema es mediante un voltamperograma cuyos ejes han sido modificados: para el eje de las abscisas, deja de representar el potencial y pasa a ser sustituido por una escala de tiempo (en unidades de segundos). Por lo que respecta al eje de ordenadas, el valor de la intensidad ahora se le nombra cómo índice RUL o RUL number (RN), el cual es una parámetro adimensional y arbitrario [92]. A pesar de ello, para el cálculo de la concentración de aditivos antioxidantes, este cambio de ejes no implica ningún inconveniente, dado que los aspectos que se emplean para el cálculo de la concentración reside en la relación existente de dos parámetros: el primero de todos es cuándo aparecen (indicativo del tipo de aditivo en cuestión) y

a continuación su intensidad (concentración del aditivo). Para extraer la información de los voltamperogramas, se pueden seguir dos rutas: medir el área del pico o bien su altura, lo cual deriva en el inconveniente de dónde referencia el punto de partida [93].

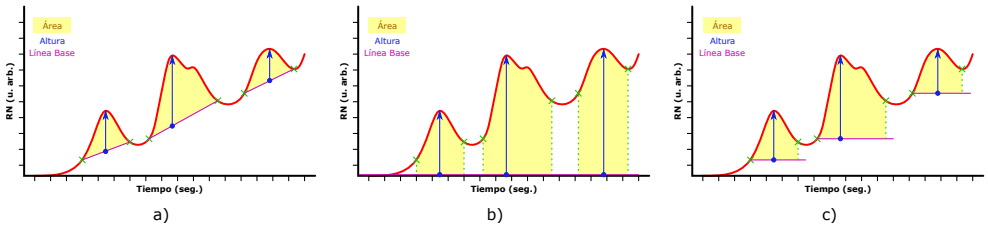

Figure 3.33. *Formas de calcular el área/pico de un voltamperograma: a) Construir una línea base dibujada en los puntos de inicio y final del pico b) La referencia está localizada sobre el 0 de las ordenadas c) Tomar un offset construido a partir del punto de inicio del pico que se prolonga paralelamente al eje de abscisas hasta alcanzar el punto final del pico.*

De entre estas tres posibilidades, la opción que mejor respuesta proporciona es la que determina el área del pico del antioxidante siguiendo el procedimiento de línea base.

El siguiente paso es expresar el grado de consumo o agotamiento de los aditivos, esta metodología requiere contrastar el aceite lubricante muestra con él mismo pero sin uso (llamado estándar) tal y como se observa en la Figura 3.34.

Esto es debido a que el ensayo ha sido diseñado como un ensayo comparativo, dónde lo que se realiza es una integración de la señal de la muestra en función de la señal de la referencia. En cada test se compara el índice RUL de la muestra de aceite lubricante usada frente a su correspondiente estándar, por esa razón, se pueden extraer dos tipos de datos: un valor que representa el contenido global de aditivos antioxidantes remanentes o una serie de valores para cada tipo de aditivo concreto. Para el primer caso, lo que se realiza es la integración de toda el área bajo la curva del voltamperograma, mientras que para el segundo se sigue lo mismo pero para cada pico de forma individual. Independientemente de la opción seleccionada, el resultado que se devuelve es un valor de índice RUL expresado en % y que puede tomar valores de entre 0 a 100 (ver Tabla 3.11).

Así pues, vistos los puntos clave de esta metodología que es capaz de analizar una gran variedad de tipos de aceites lubricantes, existe una cantidad

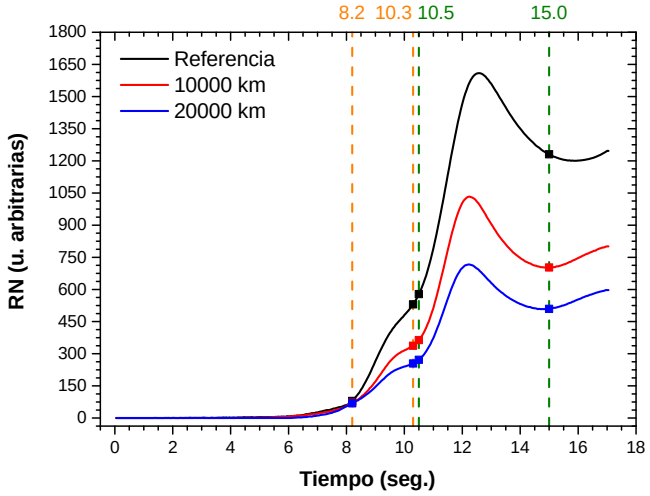

Figure 3.34. *Voltamperogramas de una misma formulación de aceite lubricante con dos tipos de aditivos AO diferentes presentes en su formulación a diferentes grados de uso.*

Table 3.11. *Resultados de la integración del voltamperograma para una serie de muestras de aceites lubricantes de motor de acuerdo con el protocolo pertinente para este tipo de muestras.*

Parámetro	**Estándar**	**Muestra A**	**Muestra B**
Uso (km)	0	10000	20000
Área RUL pico 1 (-)	814.0	616.9	512.1
Área RUL pico 2 (-)	42413.5	23953.9	15113.4
Área RUL total (-)	182420.9	113079.5	82479.1
RN pico 1 (%)	-	72.7	59.6
RN pico 2 (%)	-	56.6	35.7
RN Total (%)	100.0	62.0	45.2

acorde de normas que controlan y definen las pautas de ensayo para la aplicación de la voltamperometría lineal de barrido tales como:

- ASTM D4378: Standard Practice for In-Service Monitoring of Mineral Turbine Oils for Steam and Gas Turbine [80].

- ASTM D6224: Standard Practice for In-Service Monitoring of Lubricating Oils for Auxiliary Plant Equipment [60].
- ASTM D6810: Standard Test Method for Measurement of Hindered Phenolic Antioxidant Content in Non-Zinc Turbine Oils by Linear Sweep Voltammetry [54].
- ASTM D6971: Standard Test Method for Measurement of Hindered Phenolic and Aromatic Amine Antioxidant Content in Non-zinc Turbine Oils by Linear Sweep Voltammetry [55].
- ASTM D7527: Standard Test Method for Measurement of Antioxidant Content in Lubricating Greases by Linear Sweep Voltammetry [72].
- ASTM D7590: Standard Guide for Measurement of Remaining Primary Antioxidant Content in In-Service Industrial Lubricating Oils by Linear Sweep Voltammetry [56].

Para el caso de estudio al que hace mención este trabajo, los esfuerzos se centran en los aceites lubricantes de motor, por lo que las normas que más conciernen a este tipo de sistemas son la ASTM D7590, la ASTM D6971 y la ASTM D6810. Siguiendo las premisas que en estas normas definen, un ejemplo común de un estudio del comportamiento de una determinada formulación de aceite lubricante de motor sería el que se ha plasmado en la Figura 3.35.

Como se puede observar, la línea negra es la respuesta que genera el aceite lubricante nuevo, mientras que las de colores son las señales recogidas del aceite con diferente grado de uso. Al integrar el área de cada una de las señales de cada voltamperograma y contrastándolas frente al voltamperograma del aceite nuevo (se emplea como referencia, por lo que se le asigna el valor máximo 100%), el índice RUL para cada una de estas muestras queda plasmada en la Tabla 3.12.

De acuerdo con estos resultados, para este caso concreto, la muestra más usada aún presenta una concentración de aditivos antioxidantes activos suficientemente grande (dado que está por encima del umbral del ∼25–30%, para el caso de aceites lubricantes de motor) como para garantizar proseguir con el trabajo durante un cierto periodo más de tiempo con un nivel de fiabilidad aceptable. El límite entre lo que se considera suficiente o no el nivel remanente de aditivos está condicionado por: las exigencias que se ve sometido el motor como consecuencia de las demandas del motor en sus condiciones de trabajo. Por consiguiente, lo que se recomienda es alcanzar el fin del periodo de vida útil de uso del lubricante con cierto margen de aditivos antioxidante

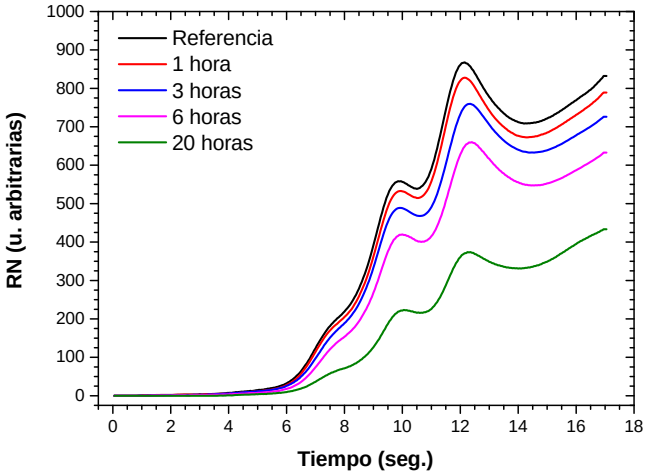

Figure 3.35. *Ejemplos de análisis, mediante RULERView, de la evolución del estado de unas muestras de aceite lubricante 0W40 con diferente grado de uso bajo condiciones de alta demanda.*

Table 3.12. *Estudio de la degradación del paquete de aditivos antioxidantes para la evaluación de la vida útil remanente de un aceite lubricante en condiciones de uso real.*

Muestra	**Índice RUL (%)**
Referencia	100.00
1 hora	98.38
3 horas	91.42
6 horas	77.59
20 horas	42.85

para que así los parámetros físico-químicos del aceite lubricante no alcanzan valores que impliquen problemas o perjudiquen el estado del motor.

Descrita la técnica, es necesario hacer un breve análisis acerca de la ventajas e inconvenientes que esta proporciona a la hora de diseñar un plan de análisis de aceite lubricante: las virtudes de este sistema radican en el hecho de que no le afecta el grado de degradación y contaminación de la muestra de aceite lubricante que se desea analizar. El sistema es inerte a la coloración y la cantidad de sustancias insolubles que pueda presentar la muestra, dado que gracias a su forma de preparar la muestra (vial que

contiene la disolución específica, el electrolito y la arena) aquellas sustancias no activas a la voltamperometría no intervienen en la medición. Además, todo el procedimiento de preparación de la muestra y análisis no se demora más de 3 minutos, por lo que se puede clasificar esta técnica como una técnica analítica rápida. Pero, esta técnica solamente aporta información acerca del contenido de aditivos antioxidantes (y en su defecto, se puede extrapolar a la oxidación del aceite). Como se monitorizan los aditivos antioxidantes, dejando a parte la formulación propia de un aceite determinado, cada tipo de aditivos: amínicos, fenólicos o los dialquilditiofosfatos de zinc (ZDDP), poseen su propio comportamiento y, por consiguiente, las velocidades de agotamiento de cada uno es diferente. Esto deriva en una mayor complejidad a la hora de interpretar los resultados. Otro aspecto negativo, desde un punto de vista instrumental, está relacionado con la preparación de la muestra bajo su protocolo. Este protocolo ha sido diseñado para conseguir la mayor repetibilidad posible en las medidas, pero en dicho protocolo existen factores que no son controlables, por lo que existen desviaciones en los valores de índice RUL para la misma muestra analizada. Además, el aspecto del costo de los viales y disoluciones son considerables, viéndose agravado por el hecho de que se requiere calibrar el equipo cada vez que se procede a su uso y del análisis del aceite lubricante nuevo (estándar, se trata de un ensayo comparativo), lo cual implica una pérdida de fungible inevitable.

3.2.5 Espectrometría ICP–OES

La Espectrometría de Emisión Óptica de Acoplamiento Inducido, ICP–OES (del inglés, Inductively Coupled Plasma Optical Emission Spectrometry), ha sido la técnica empleada en la Tesis para determinar la presencia de metales, tanto metales procedentes del paquete de aditivos de la formulación del aceite lubricante como aquellos cuyo origen se debe a fenómenos de desgaste del motor, en las muestras de aceites lubricantes de motor que han sido analizadas [122].

La espectrometría ICP–OES consiste en método atómico de emisión (ver Ecuación 3.11) dónde, mediante una fuente de energía, se excita una muestra (M^0) con una energía suficiente elevada como para provocar que alcance un estado electrónico excitado (M^*). Dicho estado excitado no es estable, por lo que la muestra tenderá a restaurar su estado original, estado fundamental, mediante la liberación de esa energía extra mediante la emisión de radiación electromagnética ($h\nu$) [13, 108].

$$M^* \leftrightharpoons M^0 + h\nu \tag{3.11}$$

Basándose en la interacción materia–radiación electromagnética cuando interviene el intercambio de energía mostrado en la Ecuación 3.11, es posible identificar cada uno de los elementos a partir del espectro electromagnético que se genera [44, 98, 116, 144]. Esto es posible gracias a que cada uno de estos espectros son propios de cada elemento, por lo que es un rasgo característico e identificativo (ver Figura 3.36).

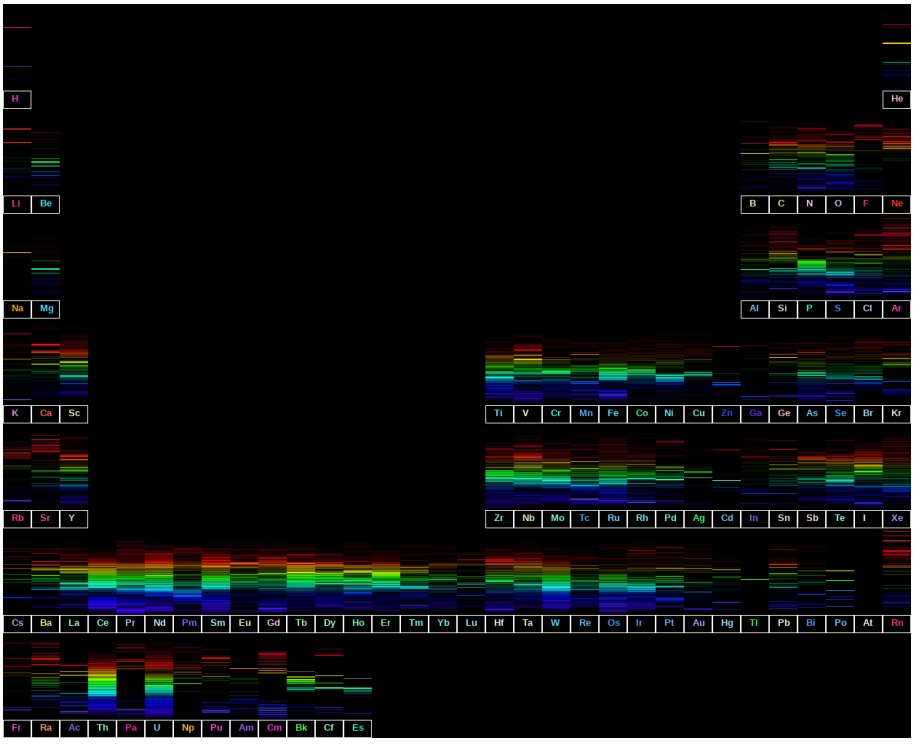

Figure 3.36. *Espectros de emisión atómica de los diferentes elementos de la tabla periódica, imagen basada en las tablas de longitudes de onda del MIT (1938) y de la base de datos de espectros atómicos del NIST.*

Para poder llevar a cabo este estudio se emplean los equipos conocidos como espectrómetros de emisión atómica, los cuales trabajan bajo condiciones que favorecen que el equilibro de la ecuación de Planck (Ecuación 3.11) se desplace hacia la derecha. Esto quiere decir que estos instrumentos son capaces de comunicar energía a los átomos para llevarlos a estados excitados de modo que, a continuación; cuando estos átomos regresan a su estado fundamental,

la energía que liberan en forma de espectro electromagnético la recogen e interpretan teniendo en cuenta la longitud de onda e intensidad para así determinar la concentración de los elementos que contiene la muestra que se ha analizado [123].

Espectrómetros de emisión atómica existen dos grandes tipos principales: los que emplean una llama como fuente de energía y los que no. Del primer tipo, sin aplicación al estudio de los aceites lubricantes, se encuentra la espectrometría de fluorescencia atómica y la fotometría de llama. Mientras que en el segundo caso, hay varios tipos de técnicas en función de la fuente de energía de excitación que emplean [10, 138, 146]. Por esa razón, se han reunido en la Tabla 3.13 las técnicas de espectrometría atómica más relevantes:

Table 3.13. *Compendio de las diferentes técnicas de espectrometría atómica.*

Fuente de excitación	Mecanismo de relajación	Técnica analítica
Radiación electromagnética	Calor	Esp. de Absorción Atómica (AAS)
	Radiación electromagnética	Esp. de Fluorescencia Atómica (AFS)
Térmica	Radiación electromagnética	Esp. de Emisión por Llama (FES)
Eléctrica	Radiación electromagnética	Esp. de Emisión Atómica por Electrodo de Disco Rotatorio (RDE–OES)
Plasma	Radiación electromagnética	Esp. de Emisión Atómica por Plasma Acoplado por Inducción (ICP–AES)
Rayos X	Radiación electromagnética	Esp. de Fluorescencia de Rayos X (XRF)

De entre ellas, la técnica mas empleada es la espectrometría ICP–AES (Inductively Coupled Plasma Atomic Emission Spectrometry) o, como también es conocida ICP–OES [36]. Por consiguiente, se desarrollará la explicación centrándose únicamente en esta variante [26, 147]. Para empezar, un espectrómetro de emisión atómica del tipo ICP–OES se trata de un sistema, como el que se muestra en la Figura 3.37, constituido por los siguientes elementos que se enuncian a continuación [14]:

- Un sistema de gases, el cual se debe encargar de suministrar argón. El argón es el gas de aplicación más extendida debido a que su potencial de ionización (el primero de ellos) se produce a energías de 15.7596 eV, energías a las cuales la mayor parte de los elementos químicos de la tabla periódica experimentan fenómenos de ionización (ver Figura 3.38).

  Las tareas que debe cumplir o realizar este gas para la técnica que se está describiendo se centran en tres objetivos:

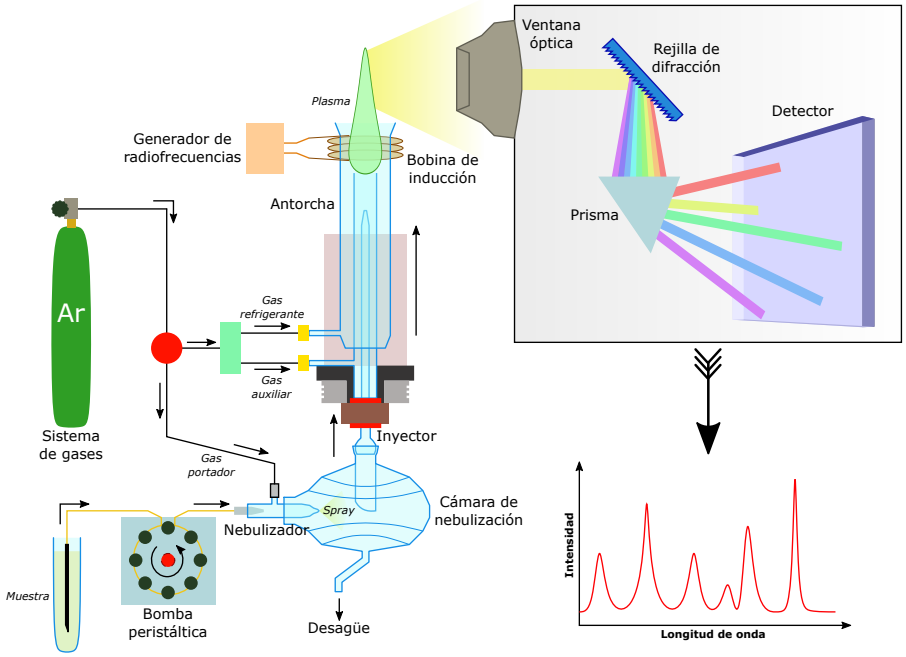

Figure 3.37. *Diagrama de un espectrómetro ICP–OES de configuración radial.*

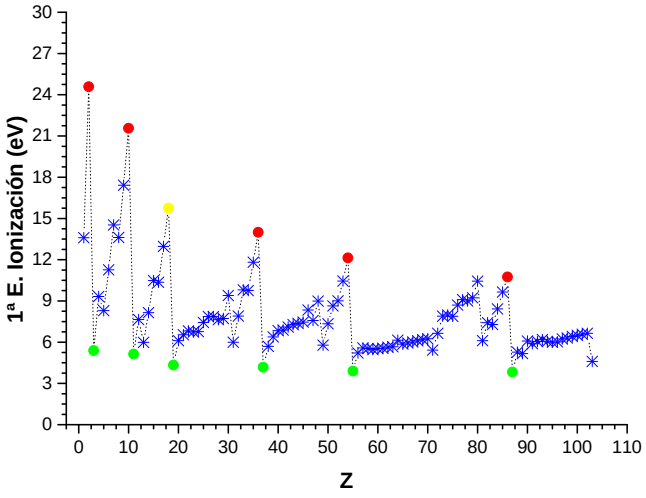

Figure 3.38. *Valores de la primera energía de ionización en función del número atómico (Z).*

  - En primer lugar, debe actuar como medio transporte o agente portador (carrier en inglés). Esto implica que el argón debe conducir la muestra hacia el nebulizador para que tenga lugar el proceso de nebulización (formación del spray o aerosol) requerido en esta técnica.
  - El siguiente cumplimiento es ser capaz de generar un plasma energético, es decir, de altas temperaturas. En estos equipos, se trabajan a temperaturas de entre 5000–10000 K.
  - Por último, debe ser capaz de refrigerar el calor generado por el plasma en aquellos componentes del espectrómetro más expuestos, siendo importante en el la región superior de la antorcha localizada dentro de la acción de la bobina.

- Un sistema de suministro de muestras al espectrómetro. Este conjunto abarca un gran número de componentes diversos: todos aquellos que existen desde dónde se toma la muestra hasta el momento de que ésta es conducida al plasma para su ionización [131]. Para el caso de muestras líquidas, lo más común es encontrar los siguientes elementos:

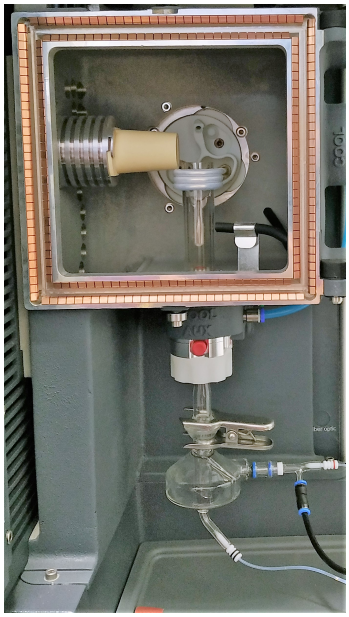

Figure 3.39. *Imagen del conjunto de elementos constituyentes del sistema de suministro de muestra: nebulizador, cámara de nebulización y antorcha del espectrómetro ICP–OES.*

- Una bomba peristáltica, dado que es capaz de proporcionar una alimentación de muestra al espectrómetro continua y con un control del flujo elevado. Básicamente, la bomba peristáltica impulsa la muestra hacia el nebulizador.
- El siguiente elemento es el nebulizador, cuya tarea reside en atomizar en forma de pequeñas gotas la muestra líquida que le ha proporcionado la bomba peristáltica. El diseño de este elemento es dependiente de la muestra, pero para este caso de estudio, los nebulizadores que se emplean son los nebulizadores neumáticos. Este tipo de nebulizadores hacen servir el argón (carrier) presurizado para conseguir pulverizar la solución líquida de la muestra. Con ello se busca que el aerosol húmedo, generado como consecuencia de la transferencia de la energía cinética del gas introducido a elevadas presiones a la corriente de la solución líquida, esté compuesto por pequeñas partículas líquidas, las cuales deben presentar una baja dispersión de diámetros (en la medida de lo posible) para facilitar el transporte de la muestra hacia las siguientes regiones del espectrómetro [17].
- A continuación le sigue la cámara de nebulización. Esta pieza se encarga de entregar a la antorcha, un aerosol más homogéneo y de tamaño de gotas no superiores a 10 μm, dado que el nebulizador (en general) es capaz de producir un aerosol con una distribución de tamaños de gotas amplio. Como consecuencia de la homogenización del aerosol por la cámara de nebulización, alrededor del 95% de éste es desechado y solo el porcentaje restante (oscila entre el 1% - 5%) es conducido a la antorcha. Diseños de cámaras de nebulización, hay varios: de paso simple, de paso doble o ciclónicos, pero de entre estas tres variedades, la que presenta mejores rendimiento de homogenización del aerosol son las cámaras de nebulización ciclónica.
- El último paso es la antorcha, región que contiene o contendrá el plasma (Figura 3.41). En ella, el flujo de gotas monodispersas y de diámetro pequeño que se ha producido en las fases anteriores se encuentra con el plasma. Este elemento, construido habitualmente en cuarzo para soportar las temperaturas extremas (de hasta 10000 K) a las que debe enfrentarse, está diseñado de modo que se distinguen tres regiones: segmento exterior, segmento intermedio y segmento interior. En cada una de ellas se busca un propósito diferentes, partiendo de la región más interna hasta el exterior de la antorcha: el segmento interno es por dónde viaja el aerosol

(gotas de muestra y gas portador), el intermedio se trata de otro tubo a través del cual se inyecta un aporte extra del gas portador con el propósito de apoyar la corriente del gas que fluye por el segmento más interno y para sustentar a la vez al plasma, mientras que mediante el más externo se hace circular una corriente de gas orientado a la refrigeración de la antorcha (aislamiento térmico) y permitir contener y estabilizar el plasma dentro de la región de acción de la bobina de inducción.

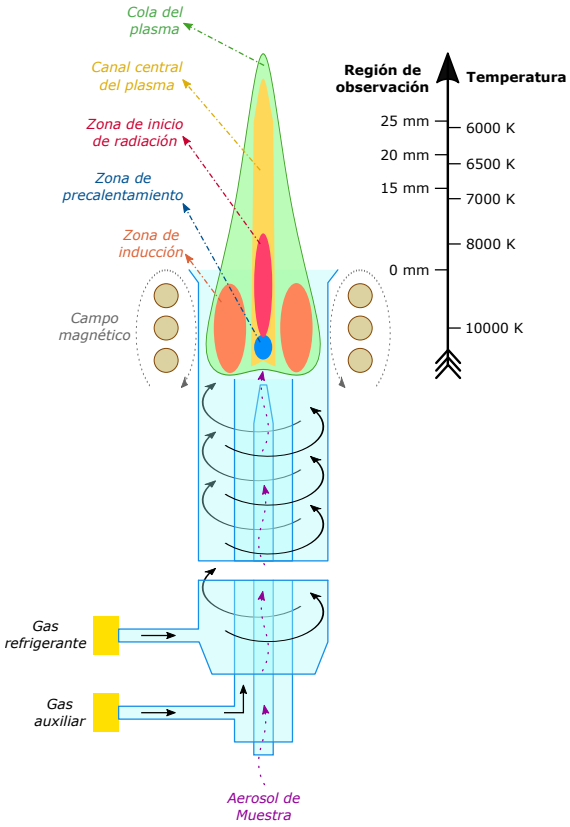

Figure 3.40. *Detalle de la antorcha y del plasma de argón que se emplea en un espectrómetro ICP–OES.*

- Un sistema de generación de radiofrecuencias (RF) que sea capar de suministrar la energía suficiente para generar y sustentar la descarga del plasma. De este modo, el sistema generador de RF permite confinar un plasma apto para el tipo de muestra que se requiere analizar. La forma

Figure 3.41. *Antorcha para matrices complejas, Enhanced Matrix Tolerance (EMT), en el espectrómetro ICP–OES.*

más habitual a la cual suelen trabajar la mayoría de los generadores de RF es con potencia que oscila entre los 700–1500 W y unas frecuencias superiores a 25 MHz (el estándar es entre 27.12 MHz y 40.68 MHz). Toda esta corriente de alta frecuencia es transferida al gas mediante la bobina de carga metálica (comúnmente construida en cobre, por 3 o 4 anillos, y refrigerada) que rodea el extremo superior de la antorcha. Gracias a esta descarga o aporte externo de energía radiomagnética, se favorece la ionización del gas (en este caso el argón) de acuerdo al equilibrio de la Ecuación 3.12, siendo capaz de sustentar esta condición o estado de plasma de forma estacionaria:

$$Ar \rightleftharpoons Ar^{+} + e^{-} \tag{3.12}$$

- La fuente de excitación, el plasma, se trata de una fuente de excitación altamente energética (ver Tabla 3.16 para comprender el rango de energía del que se hace referencia) que además, debido a su naturaleza (gas ionizado, ver Ecuación 3.12), se trata de un medio químicamente inerte y conductor de la electricidad como consecuencia de su elevada densidad electrónica (10^{13}–10^{16} e^{-}/cm^{3}). De acuerdo con la Figura 3.40, el plasma de argón que se emplea en este estudio se genera gracias a la excitación por la acción del campo magnético inducido por la corriente de alta frecuencia generada por el generador de RF. Este campo magnético oscilante que se genera en la llama, provoca que las especies con carga (iones y electrones) se muevan siguiendo las trayectorias anulares cerradas que dibujan las líneas del campo magnético (lineas del campo

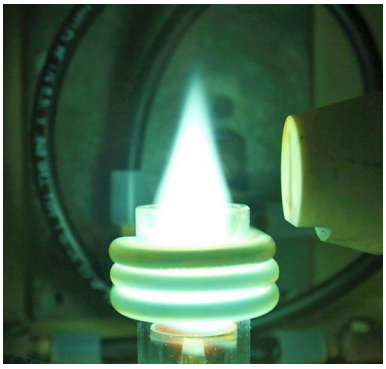

Figure 3.42. *Imagen del plasma de argón generado en un espectrómetro ICP–OES.*

orientadas axialmente respecto a la antorcha). Así pues, estas especies experimentan un aceleración de su movimiento debido a la alternancia del campo magnético al cual están sujetas. Como resultado de la resistencia al movimiento que sufren las especies con carga por acción el campo magnético, se consigue una llama toroidal (Figura 3.42) de alta temperatura (oscilando entre los 6000 K y 10000 K) como consecuencia de la energía térmica liberada por el efecto Joule que se está produciendo en esa región de la antorcha.

Table 3.14. *Diferentes sistemas de atomización para espectrometría y temperatura de atomización que consiguen generar.*

Tipo de atomizador	**Temperatura (K)**
Llama	1700–3150
Vaporizador electrotérmico (ETV)	1200–3000
Plasma por Acoplamiento Inductivo (ICP)	4000–6000
Plasma por Corriente Continua (DCP)	4000–6000
Plasma Inducido por Microondas (MIP)	2000–3000
Plasma por descarga luminiscente (GDS)	No térmico
Arco eléctrico	4000–5000
Chispa eléctrica	40000*

De este modo, el plasma tiene la finalidad de aportar una serie de ítems a la espectrometría ICP tales como:

- En primer lugar, generar de un entorno estable para garantizar la máxima homogeneidad del proceso de emisión. El primer punto conlleva a que la fuente de emisión, el plasma, sea capaz de disociar de forma completa la muestra y, además, ser lo suficientemente intensa enérgicamente como para atomizarla.
- En segundo lugar, la señales del plasma (sus líneas de emisión) no deben afectar o interferir a la hora de la detección y/o cuantificación del espectrómetro de modo que no altere la precisión del resultado que se reporte.
- Por último, se debe tratar de un sistema que se retroalimente a sí mismo con el objetivo de evitar comunicar continuamente cualquier energía u acción innecesaria para mantener un plasma funcional.

Por todo ello, las características que se buscan en el plasma de argón, plasma con el que se trabaja en el espetrómetro ICP–OES empleado en esta Tesis, son:

- Para cumplir el primer punto, el plasma de argón es capaz de alcanzar temperaturas lo suficientemente elevadas (oscilando entre los 6000 K y 10000 K) como para permitir que la muestra introducida en forma de aerosol pase por todos los procesos de desestructuración-disociación de los compuestos presentes en la muestra (desolvatación, vaporaización y atomización) con una elevada eficiencia y reproducibilidad independientemente de la matriz que contenga la sustancia a cuantificar, para así dar paso a la excitación e ionización final con garantías de éxito.
- El siguiente aspecto es la configuración del plasma, es decir: qué forma se le confiere y las regiones térmicas que se vislumbran. Para el caso de la forma, se intenta lograr la forma de toroide, dado que se ha observado que esta geometría de la llama permite una mejor incorporación del aerosol de la muestra en su seno (región de alta temperatura). Por lo que respecta a las diferentes regiones térmicas, se distinguen cuatro: zona de precalentamiento, la zona de inducción, la zona de inicio de radiación y la zona de observación o de análisis. Dónde en cada una de ellas tiene lugar una serie concreta de fenómenos ligados a su temperatura (ver Figura 3.40).

Así pues, en el plasma, los efectos o fenómenos que suceden son diferentes según se avance en su interior (Figura 3.44): la muestra alcanza la zona inferior del plasma, región de precalentamiento, en forma de un aerosol de gotas finas. Una vez entra dentro del plasma, esas gotas primeramente

se libran del disolvente (proceso de desolvatación) de modo que se quedan en forma de un aerosol seco (gas portador y partículas microscópicas sólidas). A continuación, ese aerosol seco sufre un evaporación de modo que sus componentes cambian de estado sólido a gaseoso. Llegado este punto, los compuestos en fase gas son disociados en sus respectivos elementos (atomización). Los átomos generados, al pasar a una zona de mayor energía del plasma, se ven excitados y sufren una ionización para, a posteriori, emitir la radiación pertinente (fotones de una longitud de onda específica para cada elemento en función del salto electrónico producido) cuando salen de la región de máxima energía del plasma para regresar a sus estado electrónico fundamental.

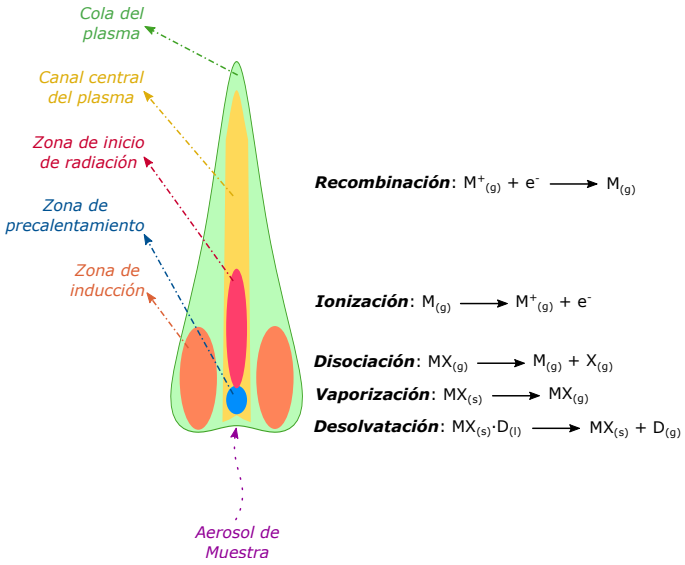

Figure 3.43. *Procesos y fenómenos que se producen en el interior del plasma.*

- Un sistema óptico capaz de recoger la información procedente de los fenómenos que tienen lugar y se desarrollan en el plasma. En el plasma, debido sus altas temperaturas, los átomos constituyentes de las muestras son llevados a estados electrónicos excitados. Estos estados no son estables, por lo que una vez las condiciones de excitación son modificadas (descenso de la temperatura), rápidamente el átomo regresará a su estado fundamental liberando ese excedente de energía mediante la emisión de un fotón de una determinada longitud de onda comprendida dentro de la región del espectro localizada entre 190 nm y 900 nm. Debido a la riqueza de señales (radiación luminosa policromática) que

es emitida por la variedad de diferentes átomos que puede contener una muestra, el sistema óptico debe ser capaz de discernir entre toda esa variedad. Para ello, lo más común es diseñar un sistema óptico capaz de disgregar ese haz de radiación policromática en sus diferentes paquetes individuales monocromáticos que la constituyen para luego enfocar aquellas deseadas sobre el detector. El sistema óptico disponible para esta técnica puede ser muy variado, pero siempre aparecen (en general) los siguientes componentes fundamentales: rendija de entrada y de salida para controlar el flujo de radiación que entra y sale del sistema óptico, respectivamente, y un dispositivo de dispersión (que puede ser un monocromador o un policromador). En el equipo empleado en este trabajo, la configuración del sistema óptico para el estudio multielemental sigue el diseño de un sistema tipo Echelle (Figura 3.44) debido a la eficiencia y resolución que consigue esta configuración para situaciones con múltiples órdenes espectrales [53].

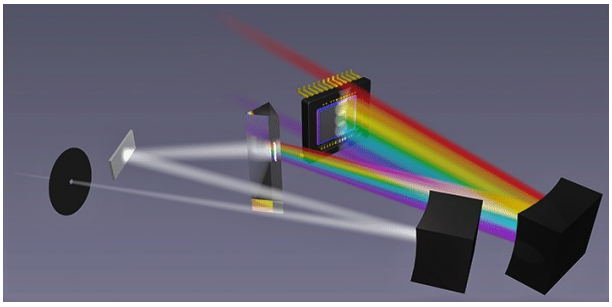

Figure 3.44. *Montaje óptico tipo Echelle.*

- El último componente que debe formar parte de un espectrómetro ICP–OES se trata de un sistema de detección y de tratamiento de señal que permita su interpretación analítica. Como la espectrometría de emisión permite conocer aspectos tanto cualitativos como cualitativos de las muestra analizadas, es necesario que el sistema de detección sea capaz de trabajar en esos dos niveles: primeramente el de identificar, en función de las longitudes de onda de los espectros de emisión característico de cada elemento, la presencia o no de un elemento concreto en la muestra y, el siguiente nivel, tratar de cuantificar dicho elemento haciendo uso de la intensidad de las lineas espectrales registradas. Por consiguiente, en un espectrómetro ICP–OES, se requiere de un sistema que sea capaz de recoger toda esa información procedente de la radiación emitida por la muestra y transformarla de una señal óptica a una eléctrica más

fácilmente manipulable mediante herramientas computacionales. Por esa razón, las alternativas que existen son dos: optar por un sistema basado en fotomultiplicadores (poco a poco entrando en desuso) o bien emplear detectores de estado sólido. Actualmente, los nuevos equipos están provistos de detectores de estado sólido y, en concreto, en este caso se emplea una variante de detector sólido conocida bajo las siglas de CID (Charge Injection Device), el cual se trata de un chip de estado sólido a base de silicio que es capaz de determinar la cantidad de fotones que ha recibido durante el tiempo al cual ha sido expuesto a la luz.

Así pues, el procedimiento de uso de un espectrómetro ICP–OES está condicionado a una serie de pasos necesarios para poder proceder de forma correcta y obtener la información deseada: preparación de la muestra acorde con la naturaleza de la misma y de las especificaciones del espectrómetro, seleccionar las líneas analíticas a as cuales se desea detectar el conjunto de los elementos presentes en la muestra (teniendo en cuenta minimizar las posibles interferencias de las señales seleccionadas), realizar una calibración del equipo con patrones estandarizados y, por último, ejecutar la medida en sí.

Para el caso que concierne a esta Tesis, el espectrómetro requiere una calibración con una serie de patrones específicos que contengan aquellos elementos metálicos que pueden encontrarse en una muestra de aceite lubricante. Así pues, los contenidos metálicos que pueden encontrarse en un aceite lubricante usado, según su procedencia o foco de generación, se pueden catalogar en 3 grupos: metales de desgaste, metales de contaminación y metales de aditivación. Para el primer tipo, es dependiente de la composición de los elementos constructivos de los motores, el segundo hace referencia a aquellos agentes extraños a la formulación original del aceite lubricante que son capaces de llegar a combinarse a él y, por último, esos metales pertenecen a los aditivos que forman parte de la formulación final del aceite lubricante en cuestión. Ejemplos, típicos, de estos metales son los que se muestran listados a continuación:

- **Metales de desgaste**: Al, Cd, Cr, Cu, Fe, Pb, Mn, Mo, Ni, Ag, Sn, Ti, V.
- **Metales de contaminación**: B, K, Na, Si.
- **Metales de aditivación**: Ba, Ca, Mg, P, S, Zn.

De este modo que, gracias a la calibración con patrones de concentración conocida, es capaz de correlacionar la energía que llega al detector del

espectrómetro con la concentración de cada metal concreto. De este modo, es posible realizar la cuantificación de la concentración de los metales presentes en una muestra de aceite lubricante a partir de la comparación de la intensidad registrada por el espectrómetro (a la longitud de onda correspondiente de cada elemento, Tabla 3.15).

Table 3.15. *Líneas espectrales de los diferentes elementos químicos empleadas en un análisis de aceites lubricantes de motor.*

Elemento	**Símbolo**	**λ de emisión (nm)**	**λ seleccionada (nm)**
Plata	Ag	328.07	328.07
Aluminio	Al	308.22, 309.27, 396.15	308.22
Boro	B	208.96, 249.77	208.96
Bario	Ba	233.53, 455.40, 493.41	233.53
Calcio	Ca	184.01, 315.89, 317.93, 364.44, 422.67	184.01
Cadmio	Cd	214.44, 224.85, 226.50, 228.80	228.80
Cromo	Cr	205.55, 267.72	205.55
Cobre	Cu	324.75, 327.40	327.40
Hierro	Fe	238.20, 259.94	259.94
Magnesio	Mg	279.08, 279.55, 285.21	279.08
Manganeso	Mn	257.61, 260.57, 293.31, 293.93	257.61
Molibdeno	Mo	202.03, 281.62	202.03
Sodio	Na	589.59	589.59
Níquel	Ni	221.65, 231.60	231.60
Fósforo	P	177.51, 178.29, 213.62, 221.65, 227.02	178.29
Plomo	Pb	178.29, 213.62, 214.91, 220.35, 253.40	220.35
Azufre	S	180.73	180.73
Silicio	Si	182.04, 182.62, 212.41, 251.61, 288.16	251.61
Estaño	Sn	189.99, 251.61, 284.00	189.99
Titanio	Ti	295.40, 334.94, 337.28, 350.50	334.94
Vanadio	V	292.40, 310.23, 334.94	292.40
Zinc	Zn	202.55, 213.86, 309.31, 310.23, 311.07, 481.05	481.05

En la presente Tesis, la configuración empleados para el análisis de las muestras de aceites lubricantes por espectrometría ICP–OES es la compuesta por: el espectrómetro ICP–OES empleado ha sido el equipo de Thermo Scientific llamado iCAP 7400 en su configuración radial junto con el sistema de automostreador Autosampler ASX-520 de CETAC (ver Figura 3.45).

Las características principales del espectrómetro que se empleó en este estudio quedan recogidas en la Tabla 3.16 [9]:

Este equipo permite trabajar bajo las siguientes normas ASTM:

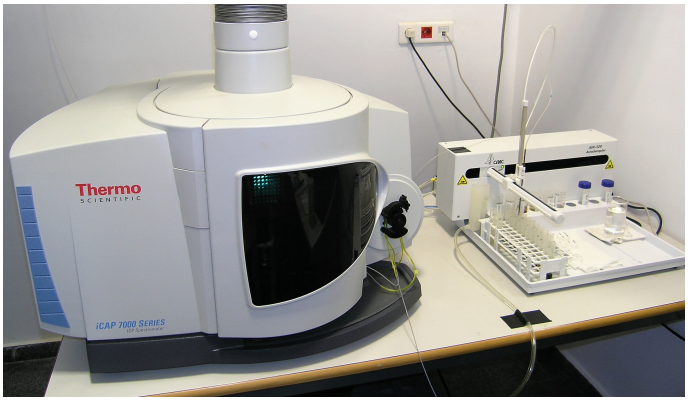

Figure 3.45. *Fotografía del sistema de análisis compuesto por el espectrómetro ICP–OES y el sistema anexo de introducción de muestras (autosampler).*

Table 3.16. *Aspectos principales del espectrómetro modelo iCAP 7400 ICP–OES Radial de Thermo Scientific.*

Parámetro	**Valor**
Gas	Argón
Flujo de plasma (l/min)	12
Flujo auxiliar (l/min)	0.0, 0.5, 1.0, 1.5
Flujo portador (l/min)	0.0–1.5
Sistema de suministro de muestra	Bomba persitáltica de 4 canales
Velocidad de bombeo (rpm)	40
Nebulizador	V-groove
Cámara de nebulización	Baffled cyclonic
Antorcha	EMT Radial Plasma Torch
Generador de RF	Free-running solid-state RF generator
Frecuencia de trabajo del RF (MHz)	27.12
Potencia de trabajo del generador de RF (W)	750–1500
Sistema óptico	Tipo Echelle
Altura de visión radial (mm)	12
Rango de longitudes de onda (nm)	166–847
Detector	Estado sólido, Chip CID86

- ASTM D4951: Standard Test Method for Determination of Additive Elements in Lubricating Oils by Inductively Coupled Plasma Atomic Emission Spectrometry [77].
- ASTM D5185: Standard Test Method for Multielement Determination of Used and Unused Lubricating Oils and Base Oils by Inductively Coupled Plasma Atomic Emission Spectrometry (ICP–AES) [67].

Para concluir, la espectrometría ICP–OES se trata de una técnica de análisis multielemental que, como el resto de técnicas, tiene sus puntos fuertes pero también sus limitaciones [19]. Por lo que respecta a las ventajas que proporciona, se pueden resaltar las siguientes:

- Dentro de las virtudes de la técnica, básicamente radica en el hecho de poder seguir una gran variedad de metales a la vez, no importando la concentración de dichos gracias a la linealidad que presenta la técnica dentro de un amplio rango de concentraciones (dependiente de la calibración realizada previamente, llegando a abarcar hasta 4 o 5 órdenes de magnitud) pudiendo abarcar concentraciones muy bajas del orden de ppb hasta miles de ppm [6].
- Otro punto a su favor, frente al resto de técnicas de emisión (como por llama, arco o chispa), es debido a las buenos rendimientos de atomización y excitación del plasma gracias a: sus elevadas temperaturas y al mayor tiempo de residencia del analito en el plasma. Todo ello conlleva a que un mayor tiempo de retención bajo unas temperaturas elevadas, la posibilidad de aparición de interferencias químicas sea menor.
- La facilidad de automatización del todo el conjunto, permite agilizar mucho el proceso de análisis sin la intervención del operario una vez puesto en marcha el análisis, hecho que lo vuelve muy atractivo a la hora de realizar análisis rutinarios o para requerimientos de análisis de un gran volumen de muestras.

Mientras que, por otra parte, hay algunos inconvenientes a tener presente a la hora de trabajar con la espectrometría ICP–OES:

- Para empezar, se requieren de patrones estandarizados, los cuales deben ser específicos para el caso de elementos que se desean detectar/cuantificar y estar preparados con una matriz lo más similar posible a la muestra que se analizará. Este aspecto provoca que se trate de un costo inherente al análisis, por lo que siempre deberá considerarse.

- Debido a la naturaleza viscosas de los aceites lubricantes, sin olvidar el efecto también de la densidad y de la tensión superficial, provoca que las muestras requieran una preparación con un disolvente afín que permita reducir su viscosidad. Esto es un factor muy importante, dado que afecta directamente al proceso de nebulización (para la nebulización de tipo neumática).Normalmente se opta por xileno o por queroseno, realizando diluciones 1 a 10 (al peso) para conseguir un viscosidad más amable para el sistema de toma de muestras e inyección al espectrómetro. Por consiguiente, este mismo proceso de dilución se le deberá aplicar a los patrones que se vayan a emplear en la determinación.

- Otra limitación, que no se puede controlar en una primera aproximación, es la influencia que tiene el diámetro de las partículas metálicas (en especial, las de desgaste) que pueda contener la muestra. Si el diámetro excede el límite de 5–8 μm, el espectrómetro no es capaz de detectarlas.

- Y por último lugar, la complejidad de la instalación de un espectrómetro funcional debido a los sistemas auxiliares que éste requiere para poder funcionar debidamente: sistema de extracción de gases, sistema de refrigeración, sistema de gases y sistema de introductorio de muestras. Lo cual lo convierte en un paquete bastante complejo y delicado de operar con él por la variedad de equipamiento que entran en juego.

3.3 Detection and quantification of contaminants in engine oils

Contamination in a lubricating engine oil is understood as the presence of any foreign element or elements to the engine oil itself. These foreign materials that may appear in the engine oil have different sources and/or causes; therefore, there is a classification of contamination into two main groups: external contamination and internal contamination.

- The first type, external contamination, refers to the entry of contaminants from outside the engine. This type includes all those substances that are not expected to be found in any of the different elements that make up the engine and that can ultimately reach the lubricating oil. An example of this type would be atmospheric dust.

- The next group, internal contamination, originates in the engine. This means that these types of pollutants can come from various systems:

mechanical components as a result of wear and tear, internal leaks (from the cooling system or fuel system) and from the lubricating oil itself as it degrades.

- In addition to these two divisions, a third one could be considered. This type of pollution would come from the processes derived from the manufacture of the engine, as well as from the maintenance tasks that may be carried out on it. This group would include those products or wastes that are used or produced in these two activities.

According to this, the different pollutants that a lubricating oil may contain are: impurities and atmospheric dust, metallic particles, by-products derived from the combustion process (carbonaceous products, unburned fuel, etc.), products derived from the degradation of the lubricating oil, cooling fluids and fuel [135].

3.3.1 Soot

In the case of soot, a specific chapter of this Thesis has been devoted to its study: 6 *Soot in oil*. Therefore, in this section, we will proceed to show the procedure chosen for its quantification in relation to the analysis of lubricating oil according to the OCM tasks. In this study, soot dissolved in lubricating oil is monitored using FT–IR spectroscopy following the guidelines of the standard ASTM D7844: "Standard Test Method for Condition Monitoring of Soot in In–Service Lubricants by Trend Analysis using Fourier Transform Infrared (FT–IR) Spectrometry" [85], which takes as reference the already mentioned ASTM E2412 [76].

In line with this standard, the quantification of soot is based on the phenomenon of radiation scattering when it encounters an obstacle (particles in this case) in its path. As a consequence, soot does not present an specific absorption band in the IR, instead a different phenomenon occurs: light scattering. This phenomenon, in an IR spectrum, was detected by an elevation of the baseline spectrum, as a consequence of the reduced radiation reaching the sensor due to losses caused by the particle-radiation interaction. In accordance with this, the section of the IR spectrum useful for observing the baseline will be the section (wavenumbers) where no absorption peaks or bands appear.

Focusing on the premise of finding a band-free region, there is a large area in the IR spectrum of lubricating oils that meets this requirement: the area between approximately 2200 cm^{-1} and 1800 cm^{-1}. Figure 3.46 shows

a common case example of the monitoring of a lubricating oil used in a diesel vehicle. A preliminary comment on Figure 3.46 is appropriate as it will serve as a precedent for the rest of the FT–IR spectra of lubricating oils: FT–IR spectroscopy works in the mid–IR region between 4000 to 400 cm^{-1} (wavelengths from 2.5 to 25 μm), it is most commonly used to delimit this region up to 550 cm^{-1}, this being the lowest point which is used as a reference for baselines.

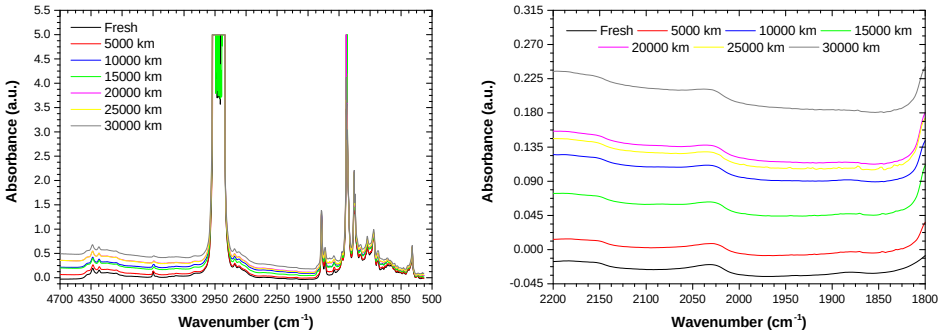

(a) IR spectrum of a lubricating oil throughout the ODI

(b) Selected measurement domain

Figure 3.46. *IR spectrum oriented to SiO quantification.*

As shown in Figure 3.46, this window of about 400 cm^{-1} is a good candidate for observing the baseline IR spectrum. However, determining the area where the measurement is to take place is only the first step. The next phase, aimed at monitoring the soot in oil (SiO) content, requires the selection between two different calculation options or methods: either a directional trending or a more precise protocol based on the elimination of the contribution of the new lubricating oil to the reading of the sample of the same oil but already used (differential trending). Figure 3.47 shows an example of how one would work with one alternative or the other, taking into account the modification of the IR spectrum of the lubricating oil depending on one protocol or the other.

In both cases, the way to operate is to determine the intensity of the absorbance at 2000 cm^{-1} (although, in some cases, there may be a change in the choice of where to measure) without the need to define any kind of baseline to reference it. As a result, the value of the soot content in the lube oil expressed in % (by weight) can be obtained from the IR spectrum.

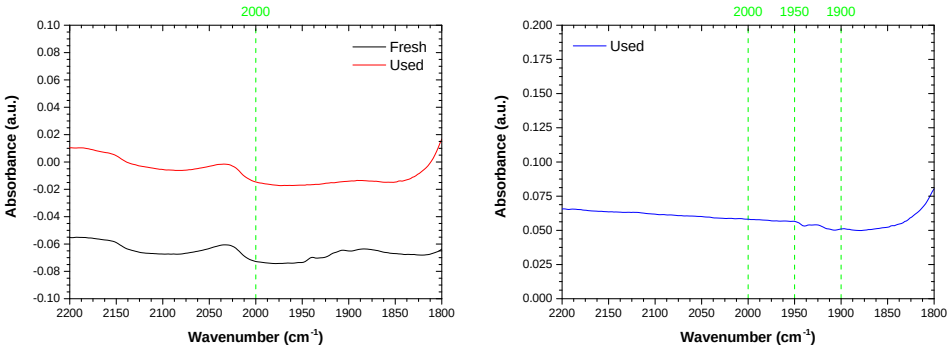

(a) IR SiO analysis by direct trending (b) IR SiO analysis by spectral subtraction

Figure 3.47. *IR SiO analysis according to ASTM D7844.*

FTIR spectroscopy applied to the quantification of SiO has a number of drawbacks: one is that it is based on the measurement of the baseline of the spectrum and the other is related to the dispersion principle that it uses. For the first case, with the objective to read correctly the spectral baseline tilt, in the major part is necessary to do some spectra correction to remove any undesirable contribution that affects the baseline. Finally, it should be taken into account that if the SiO content is very high, the amount of radiation reaching the detector will be very small and therefore a dilution treatment would be necessary to analyze the sample. Usually, the limit of applicability of an FT–IR spectroscopy is around a carbonaceous concentration of 3%; if this threshold is exceeded, the system will most likely be blinded and will not be able to measure.

To conclude, this option for measuring the SiO content is very attractive for oil condition monitoring. For that reason, according to the research carried out in this thesis, the use of FT–IR spectroscopy as a technique for soot quantification was advantageous, useful and easy to implement in the OCM analysis protocol that was designed.

3.3.2 Fuel

The presence of fuel or unburned hydrocarbon (UHC) is a problem in the engine oil as it primarily causes a reduction of its viscosity, which is a serious effect since it significantly affects the lubricity (it provokes a disruption in oil film causing asperity contact between the surfaces inducing engine wear).

It does not only affect or compromise the viscosity (although this is the most crucial effect), but also other properties such as: volatility, dispersancy and detergency (causing its decrease, so the varnish formation is promoted), chemical stability against the oxidation degradation and other degradation processes.

In the ICE, the source of high fuel levels in engine oil is, in most cases, due to problems in the combustion condition or mechanical problems. In the first case the fuel-to-air ratio can be the reason, either because the engine performs this dosing incorrectly or as a consequence of emission aftertreatment systems altering or modifying the injection schedule in order to perform longer and more delayed injections for its own benefit (e.g. DPF regeneration); therefore, under these assumptions, incomplete combustion takes place. On the other hand, on the mechanical side in includes damages to the engine parts such as: piston rings, injector malfunction, excessive blow-by, and also working conditions such as excessive idling or low temperatures that allow the contamination of the engine oil by fuel.

For the case of fuel dilution in the engine oil, there are two options: either to detect the presence or not of diluted fuel (indirect measurement), or to be able to quantify it (in a more or less precise way, depending on the requirements of the situation). From a practical operational point of view in a lubricating oil analysis laboratory, according to the system under study (application and engine operating conditions), levels of up to 2% dilution are acceptable as they do not cause relevant variation in the engine oil viscosity. However, if the levels are between 2.5–5.0%, it is necessary to study the case more closely.

The reference technique or the absolute method for the quantification of fuel dilution in engine oil is Gas Chromatography (GC) [42], according to the standards:

- ASTM D3524: Standard Test Method for Diesel Fuel Diluent in Used Diesel Engine Oils by Gas Chromatography [78].
- ASTM D3525: Standard Test Method for Gasoline Fuel Dilution in Used Gasoline Engine Oils by Wide-Bore Capillary Gas Chromatography [79].

For the case study proposed in this Thesis, the recommended standard to be followed is the ASTM D7593: "Standard Test Method for Determination of Fuel Dilution for In-Service Engine Oils by Gas Chromatography" [57]. In Figure 3.48 an example of a GC capable of working with hydrocarbons is shown:

Figure 3.48. *GC Reformulyzer M4: Hydrocarbon Group Type Analysis.*

The chromatograph evaporates an injected oil sample in liquid phase and passes it through a chromatographic capillary column (Figure 3.49) thanks to a carrier inert gas (He, N_2, H_2).

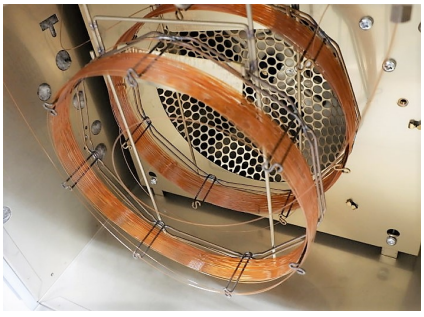

Figure 3.49. *Capillary column inside the GC oven.*

The phenomenon of physical separation takes place inside the column, which basically consists of a retention of the hydrocarbon molecules consisting of the injected sample. The column retains, in decreasing order according to the weight of the constituent molecules of the sample, the heavier ones (which have a higher boiling point). This implies that the retention time in the column of the heavier molecules (having a higher boiling point) will be longer than that of the lighter molecules (lower boiling point) [5]. Table 3.17 lists the

most common petroleum compounds or petroleum derivatives with their basic characteristics for GC [34].

Table 3.17. *Boiling points of the main petroleum products according to the number of carbons.*

Product	Carbon atoms number range	Boiling range (°C)
Gasoline	4–10	30–125
Jet Fuel	9–16	150–250
Diesel	9–24	163–370
Lubricating Oil	20–40	300–570

As far as the physical process of separating the different hydrocarbons (according to their boiling points) that make up the sample is concerned, the next step is the quantification of the dissolved fuel [11]. The quantification stage is done using a Flame Ionisation Detector (FID), after a previous calibration with standards (or sometimes, with the sample injection, an internal standard is injected also). Regardless of the calibration mode selected, what is obtained is a chromatogram like the one shown in Figure 3.50. However, there is an increasing trend to couple the chromatograph to a Mass Spectrometer (MS) or, it is often also coupled with FT–IR spectrophotometer in order to identify the compounds present in the sample.

During quantification, the procedure to follow is to integrate the area of the peaks obtained in the chromatograph and then, thanks to the calibration of the chromatograph with the standard (internal or external), to correlate or associate this area with the area of the standards in order to translate the value obtained into mass percentage (% (m/m)) of fuel dissolved in the engine oil.

To conclude, the GC is the most reliable and accurate (its detection limit is as low as 0.1%) technique or methodology to quantify the fuel dilution in engine oil. Despite its precise results, GC has a number of disadvantages or drawbacks that make it a technique that is not accessible to all laboratories:

- The technique is a purely laboratory technique that requires an expesnive experimental setup. This is a major drawback, although portable GC equipment such as that marketed by Energy Support GmbH (Figure 3.51) has already been designed.
- With complex samples, such as used engine oil, more analysis time is required to obtain good results (∼30 min approximately). In samples,

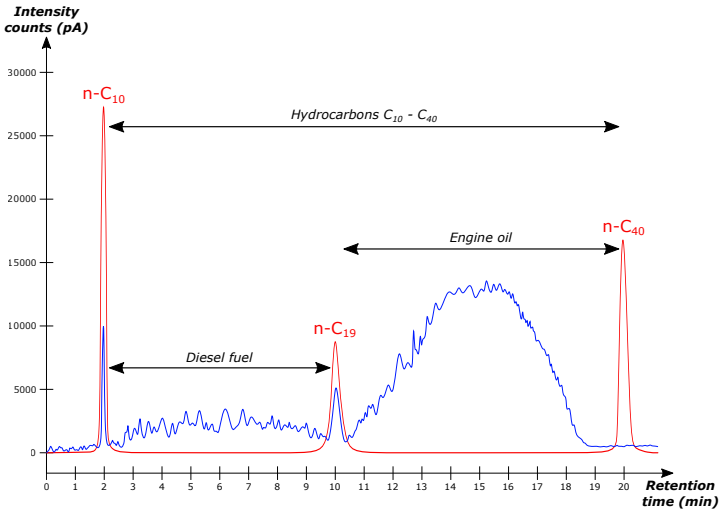

Figure 3.50. *Chromatogram of standard (red line) and engine oil sample (blue line) with fuel dilution problems.*

which may be considered dirty, GC may not be recommended for determining the fuel oil content (especially if OCM maintenance work is being carried out).

- In order to be able to operate and assess the results generated by a GC, as both fuel and lubricant share certain hydrocarbons, there is an overlap of boiling points in those compounds common to both substances. Therefore, qualified and experienced technicians are required [35].

Currently, as already mentioned, new equipment, configurations, detectors and procedures are being developed (e.g. "backflushing", which allows to reduce the measurement time to 5 minutes) [28, 100, 101]. However, according to the Thesis approach, GC would not be the most suitable technique and therefore, alternatives are needed.

A simple way to know whether or not there is fuel dilution in lubricating oil (at certain levels) is employing alternatives such as kinematic viscosity measurement and flash point. These two alternatives, although more qualitative in approach, can provide useful information at a low cost and without requiring long analysis periods (for both cases, working according to the relevant standards, the time is in the order of less than 10 minutes). For the first alternative, the measurement of kinematic viscosity, the presence of

Figure 3.51. *MOBILE GC Portable Gas Chromatograph.*

dissolved fuel levels in the engine oil can be clearly observed as a KV drop (see Figure 3.52).

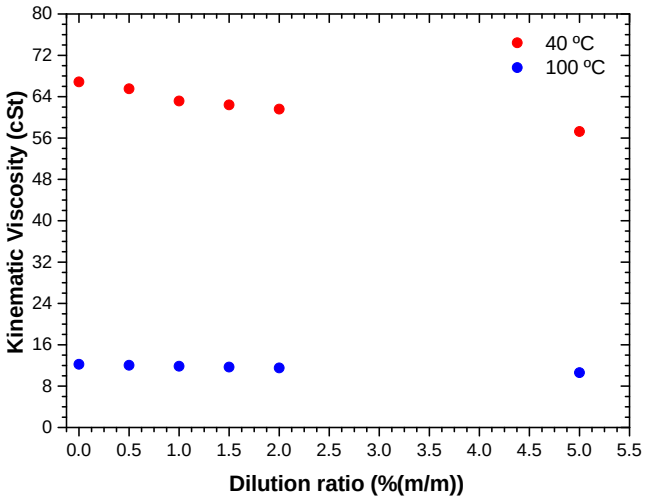

Figure 3.52. *KV evolution according to the fuel amount diluted in the engine oil.*

This form of detecting dilution in the lubricating oil is an indirect procedure, because it is necessary to compare the viscosity value of the sample with the value of fresh oil (unused, uncontaminated). Unfortunately, a change in kinematic viscosity is not exclusively caused by the presence of fuel, several other potential causes can produce the same effect. However, since kinematic

viscosity is an analysis that is routinely performed in a laboratory lubricant analysis, it may be useful to use it as a screening test.

If there are indications of fuel contamination, after analyzing the kinematic viscosity, the next step is to measure the flash point. The Flash Point test, similar to the kinematic viscosity, requires the original value of fresh engine oil to compare the flash point temperature [112]. Fuel has lighter hydrocarbon components, so if the engine oil sample is contaminated by fuel, its flash point temperature will decrease as consequence of the presence of lighter hydrocarbon fuel components. Most commonly, lubricating oils have flash point temperatures in the order of 200–250 °C, while diesel is in the order of 60 degrees. Due to this difference in temperature between both substances, a study could initially be carried out to see how many degrees the flash point of the lubricating oil is reduced depending on the amount of fuel it contains, in order to try to get a more quantitative estimation of the fuel content in a sample. However, due to possible agents that also interfere with the ignition temperature of a lubricant, this option is not commonly used. Rather, the flash point measurement is used as a pass/fail test [37].

The equipment for determining the flash point is basically based on two options: the Cleveland open cup method (ASTM D92 [75]) or the Pensky-Martens closed cup method (ASTM D93 [86]). Depending on the selected method of flash point measurement, the results obtained will be different. Nowadays, the Pensky-Martens closed cup method is the most employed due to its more significant reduction magnitude of the flash point temperature if both working methods are normalised. This means that the variation per unit agent (for this case it would be °C per %fuel) using the closed-cup methodology offers a higher resolution. Figure 3.53 shows an example of equipment for measuring the flash point according to ASTM D93 standard.

Usually, the option of determining fuel dilution through viscosity and/or with flash point analysis is rather predictive since, as stated above, it is not a reliable way to diagnose this problem. For this reason, based on the values of the sample (values obtained by either one or both of these two options), a dilution analysis protocol can be designed or planned with more specific techniques.

One of the most widely used alternatives in the analysis of lubricating oil is Fourier-Transform Infrared (FT–IR) Spectroscopy. Applied in the case of the quantification of fuel dissolved in the lubricating oil, this alternative makes it possible to obtain (in a simple and fast way) the fuel content. For this purpose, the equipment is pre-calibrated with lubricating oil standards with different fuel proportions. These standards are then analysed in terms of

Figure 3.53. *Petrotest PM5 Pensky-Martens Closed Cup Flash Point tester.*

their spectra (standard curves in Figure 3.54) and the absorption bands are correlated with the parameter being monitored, the fuel content dissolved in the lubricant [134].

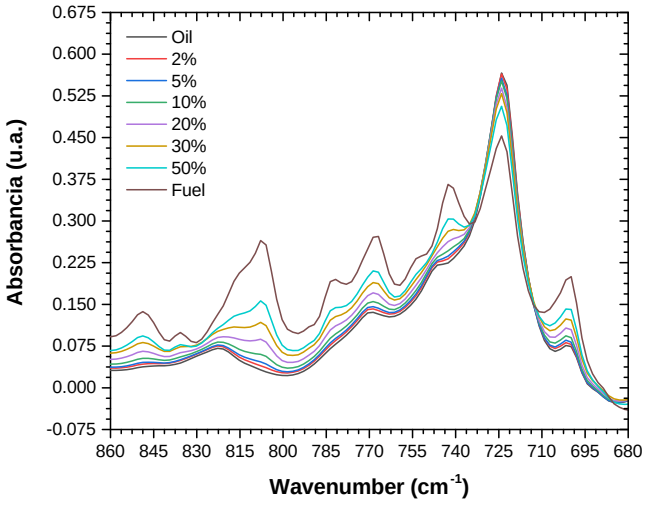

Figure 3.54. *FT–IR spectrum of samples with different dilution ratio.*

Thus, when analysing the sample, the fuel content of the sample can be extracted from the selected absorbance bands or registers and, by means of

the previously performed calibration, these absorbance units (a.u.) can be translated into %fuel.

Firstly, the use of FT–IR spectroscopy is very interesting, but it is not as straightforward as it has seen in the course of this Thesis. An FT–IR spectrum provides a lot of information, so you need to know what you are analysing in order to know how it will show up in the spectrum and in what form. For this reason, a good understanding of what you are analysing is crucial to get accurate results. Initially, the way to work with this technique was by monitoring the sulphur content (Aromatic Sulphur peak) since it exhibited absorbances at different wavenumbers: 3050, 1605, 874, 811, 748 cm^{-1} approximately, because this form of monitoring was very much conditioned by the type of fuel one was trying to quantify, so there could be fluctuations in the sulphur levels and in the bands that were accessible (not surprisingly, the method had some problems of accuracy in quantifying the fuel entering the lubricating oil). Nowadays, fuels have very low levels of sulphur (between <10–500 ppm), so an improvement of the fuel quantification methodology by FT–IR spectroscopy was required [3]. Nowadays, the fuels used have a decreasing concentration of aromatic compounds, in other words, they are increasingly free of aromatic compounds. Therefore, the lower concentration of aromatic compounds means that FT–IR fuel dilution monitoring is becoming more and more complex. This is why, to date, this analysis is not used to determine the fuel dilution in lubricating oil.

To try to improve the accuracy of this methodology, taking into account current fuels, better calibrations are being developed. The first option, whenever possible and working conditions permit, is to use a tracer or marker. This substance, which is incorporated into the fuel, allows a better tracking of the presence of the fuel in the lubricating oil by means of its distinctive absorption band (see Figure 3.55).

Nonetheless, in most cases, this option is difficult to implement. For this reason, we have opted for a specific case study. This implies that the study system is narrowed down: the specific lubricating oil (required to determine the baseline) and fuel to be analysed are selected, as it is difficult to distinguish the origin of the hydrocarbons (from the fuel or from the engine oil). Once both agents are clear, a calibration is performed using a spectra/data collection and then, by means of a series of algorithms, the relevant absorbance–fuel correlation is extracted [141]. This is a complex way of working, so FT–IR spectroscopy is used more for the purpose of extracting performance trends. For the purposes of this investigation, according to the ASTM E2412 standard [76], FT–IR spectroscopy is applied in condition monitoring in–service engine

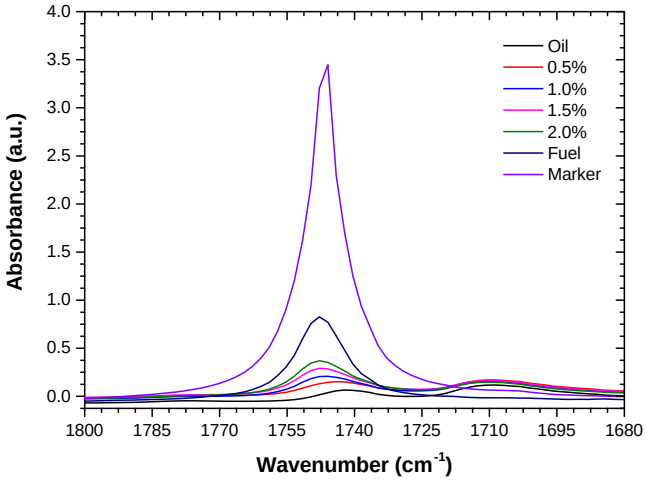

Figure 3.55. *FTIR fuel dilution standard curves employing a marker.*

oils with regard to diesel dilution. Monitoring was therefore carried out according to a number of premises:

- It is required to know the diesel and lubricating oil being used, in order to generate a specific calibration of the equipment.
- Second, it was decided to perform an analysis procedure of the signal, selected between 817–804 cm^{-1}, in two different ways: measuring the area with one or with two baselines.
- To further secure the analysis, it was chosen to track also the rest of the diesel peaks with the aim of not losing any useful information.

According to these three points, it was chosen to measure the area of the diesel peak between 817–804 cm^{-1} with two baselines, the first at 835–825 cm^{-1} and the second at 795–785 cm^{-1} to follow the trend.

In summary, the choice of one technique or another [124] will depend on the needs and requirements that exist in certain situations. The tendency is to choose, for quantification, the alternative of FT–IR spectroscopy due to its versatility and speed in providing information. In this Thesis, FT–IR spectroscopy was the technique chosen to determine the amount of fuel dissolved in the engine oil samples as it was the method currently available for this purpose.

3.3.3 Cooling system fluid

As a consequence of the ongoing development of the ICE to increase its efficiency, higher working temperatures are also encountered inside the engine, for which the cooling fluids have evolved to be able to cope with these more stringent performance requirements. Cooling system fluids, in the vast majority of cases applied to ICEs, are binary mixtures of ethylene glycol (ETG) or propylene glycol (PG) with water in a 1:1 volume ratio (excluding all the additives that are incorporated to improve freeze protection, heat transfer, corrosion protection and others) [25]. As a consequence of the composition of these fluids, there are two main elements that need to be analysed separately: water on the one hand, and glycol (either ETG or PG) on the other.

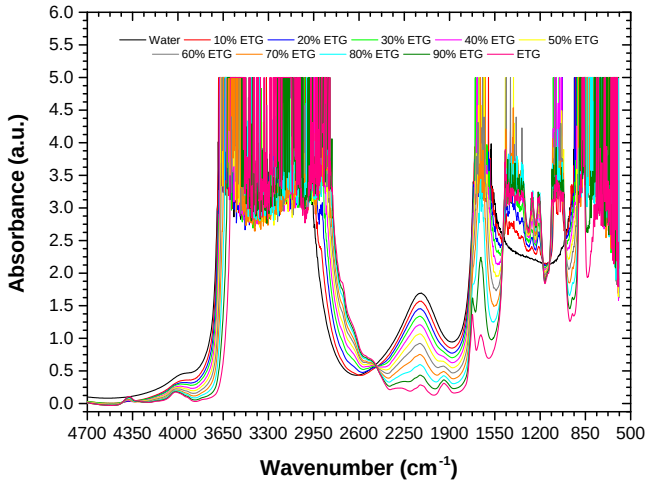

Figure 3.56. *Example of different coolant ETG–Water mixtures analysed by FT–IR.*

Water aside, as far as glycol is concerned, the most commonly used component is ethylene glycol (ETG, CAS: 107-21-1, CH_2OHCH_2OH) due to its advantages over propylene glycol (PG, CAS: 57-55-6, $CH_3CHOHCH_2OH$). To summarise, the reasons for the increased use of the ETG can be found in Table 3.18.

According to the data in Table 3.18, ETG allows to reach lower temperatures than PG for the same amount added to water. This freeze point depression allows to work in a wider temperature range. Furthermore, conditioned by the viscosity (correlated to the head loss in the cooling system), the ETG is able to capture and transfer heat more efficiently, but more fluid is necessary to be circulated to transfer the same amount of energy since

Table 3.18. *Properties of binary mixtures Glycol–Water.*

Properties	**ETG–Water**	**PG–Water**
Kinematic Viscosity (cSt)	0.63	0.71
Dynamic Viscosity (cP)	0.65	0.70
Density (kg/m^3)	1030	980
Vapor pressure (kPa)	84.4	90.4
Surface Tension (dyne/cm)	47	36
Specific Heat (kJ/kg·K)	3.642	3.851
Thermal conductivity (W/m·K)	0.385	0.390
Minimal working temperature (° C)	-37 – -34	-33 – -28

At 100°C

Propylene glycol has higher specific heat (this is no more inconvenient than regulating the flow of coolant to the engine) [38, 40, 94]. Consequently, the ETG option is the most commonly used.

The use of the ETG–Water coolant mixture (see Figure 3.57) allows the engine to be cooled efficiently [46]. In consequence, detecting ETG or water levels in the lubricant is a very important issue. Commonly, control levels for this pair of elements are variable, since they are highly dependent on the application for which they are used, but canonical values can be taken:

- For water, if water levels are $\geqslant$0.10% that is indicative of a problem, whereas if the levels exceed the 0.25–0.30% limit, the problem could be classified as critical.
- For glycol, the most common way of expressing its concentration is by parts per million (ppm). So, if the glycol is found at a concentration of 200 ppm, this is not a problem, although monitoring is recommended. But, when glycol exceeds 400 ppm, its presence is already considered important, whereas it is a critical case if the concentration found exceeds 1000 ppm.

Therefore, specific protocols and methodologies have been developed for each of these two elements.

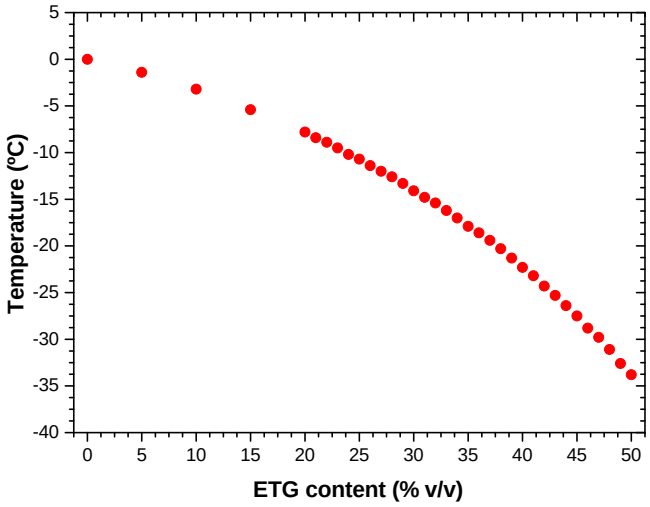

Figure 3.57. *Freezing Point of different ETG–Water mixtures.*

3.3.3.1 Water

Firstly, to obtain the value of water content of a sample of lubricating oil (bearing in mind the working temperatures at which the engine oil is subjected, part of the water evaporates as seen in Figure 3.58), there are several ways to go about it, dependeing on water levels and requirements: crackle test, test kits based on hydride reagent, Karl Fisher titration, capacitative relative humidity sensors and FT–IR spectroscopy [125].

This is because, depending on the amount of water in the lubricant and how tightly bound the water with the lubricant, water can appear in three states or forms: dissolved, free or emulsified (see Figure 3.59). These different phases of the water could be found both individually and coexisting at the same time; therefore, sometimes it can be difficult to obtain a representative sample of the state of the lubricating oil. For engine oils, in a lubricating systems, the most problematic and harmful situation is when the waters appears in an emulsion or free because this means that the level of moisture depends on the lubricant's ability to hold a certain amount of dissolved water [132].

The first state, dissolved water, is when the water is dispersed (molecule-by-molecule) and its presence cannot be visually perceived. However, the fresh lubricating oils have additives that favour the immiscibility of water, so that, gradually, the water molecules group together to form small droplets or bubbles and separate from the rest of the oil, giving rise to two phases:

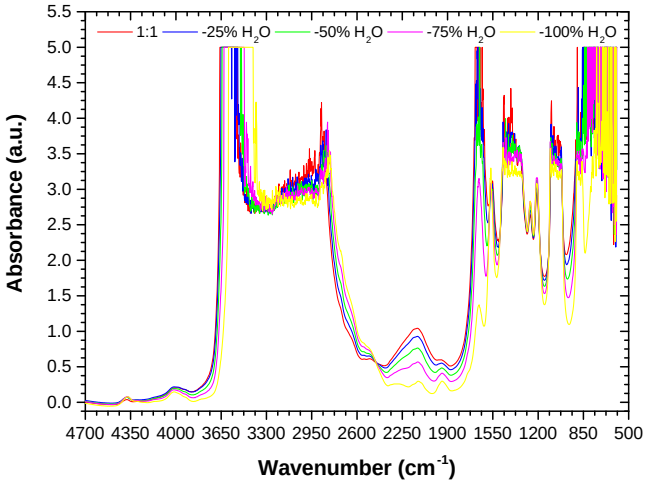

Figure 3.58. *Coolant water losses in commercial coolant fluid 1:1 ratio ETG and water analysed by FT–IR.*

Figure 3.59. *Water in oil phases: dissolved (minor level), free (overloaded level) and emulsified (major level).*

the major part is oil and the other consisting only of water (and other by-products). So now, depending on temperature and age of the engine oil, it is possible to determine the water presence. Dissolved water, approximately, is encountered when its concentration in the lubricant oscillates between 0.05% (or 500 ppm) to 0.10% (or 1000 ppm). If the water concentration increases, the lubricating oil is not able to keep it dissolved because it becomes saturated. At this point the water will start to form microscopic discrete droplets forming an emulsion. Under these conditions, the lubricating oil shows a detectable change, as the emulsion gives the oil a milky or hazy appearance. If the amount of water in the lubricant is further increased, the emulsified oil–water mixture becomes unstable. In that moment, the engine oil is oversaturated

and the water separates from the lubricating oil in an independent phase or layer (depending of the specific gravity of the engine oil, this water free layer could appear over or under the engine oil).

Water is an undesirable contaminant in lubricants because of all the problems it causes such as rust, hydrolysis process and thus, it is an important contaminant to control [132]. The first technique available to detect the presence of water in oil is the Crackle or Bubble Test. This tests is a simple way to detect the presence of water because it is based on the difference between water–oil boiling points. Figure 3.60 shows the four possible events that can occur when testing a used lubricating oil sample:

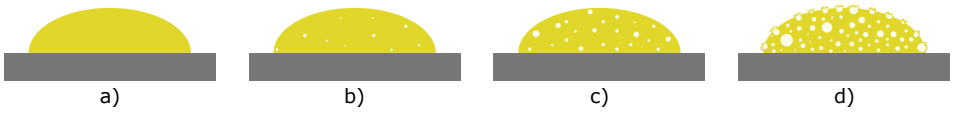

Figure 3.60. *Crackle Test situations in engine oil samples: a) Lubricant without water, b) Lubricant with 0.02%–0.10% of water, c) Lubricant with 0.10%–0.20% of water and d) Lubricant with ⩾0.20% of water.*

From a more analytical point of view, the Crackle Test is used as a screening test where the parameter that is judged is the presence or absence of water. As this is a purely qualitative test, although a range of concentrations can be estimated on the basis of the test result, no complex system is required to perform the test. The working procedure is as follows:

- Homogenise the oil sample, by means of efficient agitation, so as to obtain a representative sample of the water suspension.
- Next, on a hot surface (approximately 110–130°C, above the boiling temperature of water) a couple of drops of the sample are deposited. It is important to try to perform the test at the same temperature and with the same amount of sample in order to obtain more repeatable results.
- Finally, look at what happens in the aliquot of the sample. Analyse the water content in terms of the bubbles that appear as a result of evaporation.

Although it is a simple test that does not require complex instrumentation, its disadvantages or drawbacks consist on that it is not used for water quantification. While some quantitative judgements can be made here,

interference from other contaminants that the lubricant may contain (e.g. fuel, among others) means that this test is only used to assess the presence of water. In addition, in order to detect water, it must be present in concentrations of 0.05% (approximately) to obtain an observable result as this test is sensitive only to emulsified and free water. Nonetheless, depending on the situation, this level is already sufficient to cause severe engine problems [31].

Therefore, the use of a more sensitive and specific methodology to monitor this element is required. The first option is to make use of what are known as hydride analytical kits for water quantification. In these kits, the main chemical reagent is Calcium hydride (CaH_2), which reacts with water according to the exothermic reaction 3.13:

$$CaH_2 + 2H_2O \rightarrow Ca(OH)_2 + 2H_2 \tag{3.13}$$

According to the reaction 3.13, two products will be generated: a solid ($Ca(OH)_2$) and a gas (H_2). As the reaction is stoichiometric, for each mole of water one mole of hydrogen is generated (both are directly proportional), the measurement of the pressure difference between reactants and products is used to determine the amount of water present in a sample. For this purpose, the reaction is carried out in an airtight environment (inside a sealed container) to measure the pressure of the gas resulting from the process and thus determine the amount of water (in this case, free and emulsified water).

Figure 3.61. *Reaction vessel for hydride reaction from Parker Hannifin.*

This way of working allows quick results to be obtained, in a couple of minutes, with a really small sample amount (between 20 and 30 mL, generally). This alternative only requires a few elements:

- The reaction vessel consisting of a barrel to which a cap with a seal is screwed. A system for registering the pressure inside the vessel is located in this container.
- The properly amount of sample, according to the specifications of the test kit.
- The calcium hydride as the chemical substance reactive with the water.
- A diluent agent to facilitate contact between the water and the hydride.

Thus, reaction 3.13 is carried out under controlled conditions, which makes it possible to determine the amount of water present in the sample (in %) from the pressure recorded inside the vessel (depending upon the relative mix of oil and diluent, to ensure that the reaction takes place within the range of application of the test).

The hydride reagent test kits are an interesting procedure because, if working properly, it is possible to detect low water levels (in the order of 50 ppm) with high accuracy quantitative results. However, the optimal conditions for its use are not always met. For this reason, when the precise amount of water in a sample of lubricating oil is required, the Karl Fischer (KF) titration is used, which is a specific technique for water quantification. KF titration is the most accepted and reliable method for detecting and determining the presence of water in any state: dissolved, emulsified or free. That is possible because this selective technique can measure a wide range of water content: from low as 10 ppm (near zero) to 100%, with accuracy and repeatability.

The Karl Fischer Titration is based on an iodine (I_2)/iodide (I^-) reaction with water [97]. This 1:1 stoichiometric reaction (of iodine with water) requires to be performed in the presence of Sulphur Dioxide (SO_2) and a base; the detection of endpoint (EP) is done by the voltametric detection of the excess of iodine (all water is consumed) by an Indicator electrode (double platinum pin electrode). In this way, the quantification of water is based on the concentration of iodine in the KF titriating reagent and the amount of this consumed during the titration. Accordingly, in KF titration, the amount of iodine consumed in the titration is equivalent to the water content in the sample so it is possible to determine precisely the water content of the oil from the iodine quantity.

The KF titration is supported by a 2–step mechanism based on two reactions: the first reaction (reaction 3.14) is where the reaction intermediate (alkylsulfite salt) is generated, while the second reaction (reaction 3.15) is an

oxidative process of the alkylsulfite salt intermediate by the iodine (I_2), and in this oxidation reaction the water is consumed [139].

$$ROH + SO_2 + R'N \rightleftarrows [R'NH]SO_3R \tag{3.14}$$

$$H_2O + I_2 + [R'NH]SO_3R + 2R'N \rightleftarrows [R'NH]SO_4R + 2[R'NH]I \tag{3.15}$$

In essence, the reaction is the next reaction 3.16):

$$H_2O + I_2 + SO_2 + 3R'N + ROH \rightleftarrows [R'NH]SO_4R + 2[R'NH]I \tag{3.16}$$

According to the reaction 3.16, the KF titration requires these basic reagents: iodine, sulphur dioxide, base (buffering agent) and solvent [128]. In the KF titration, the measuring or Indicator electrode allows to detect if the EP of the titration is reached. This polarisable electrode determines whether or not iodine needs to be added in the sample solution to react with the water present in that mixture thanks to a change in the electrical properties of the solution (closer to the double platinum polarisable electrode): potential (bivoltameric indication process, constant current) or current (biamperometric indication process, constant potential). So the EP is detected by the Indicator electrode according to the relationship between voltage and/or current and the concentration of iodine.

But, in KF titration procedure the selection of the methodology for doing the titration is an important decision. There are two main alternatives for carrying out a KF titration: either the titrant reagent with iodine is incorporated into the sample or the iodine is generated in situ during the titration. In the first case, is a volumetric titration, while the second case is coulometric [97]. Figure 3.62 shows the different alternatives that can be chosen to perform the KF titration.

Each of these two alternatives has been specifically designed for a certain application (see Figure 3.63): normally, if high amounts of water (of the order of %, high level moisture) are expected, a volumetric titration is chosen, whereas if the levels to be detected are low (a few ppm, low level moisture), the coulometric option is the best.

These two methods, each one based on iodine providing principles, are characterised by distinctive features. In general terms, these two versions of KF titration have the following aspects:

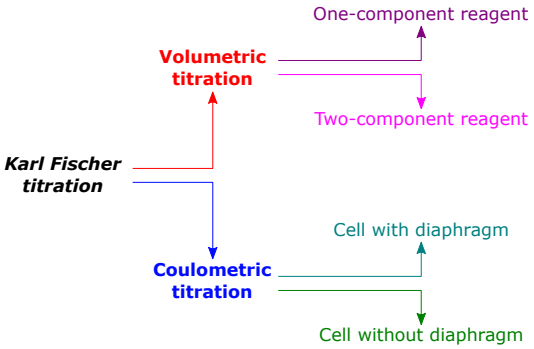

Figure 3.62. *Different pathways to do Karl Fischer titration.*

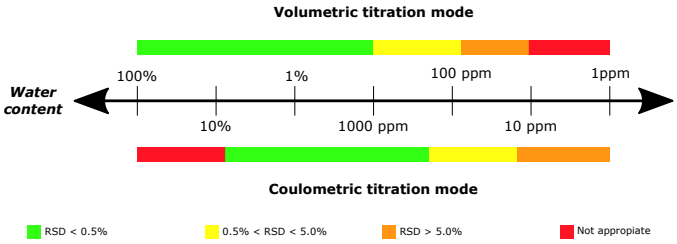

Figure 3.63. *Range of applicability of each of the two ways of realisation of the water titration by KF.*

- In **volumetric KF titration**, the KF titrating reagent that contains iodine (I_2) is added mechanically (using a burette) over the solvent solution where the sample is dissolved (all of which takes place in a reaction cell or vessel under controlled conditions). According to the I_2–solution volume dispensed/consumed it is possible to determine the amount of water (in a range from 100 ppm to 100%). There are two versions of volumetric KF reagent: with one-component or with two-component KF titrating reagent.

  - The first type all the reactants (iodine, sulphur dioxide and base) are dissolved in a suitable solvent (alcohol) which acts as a working medium.
  - But, the second option uses separately the solvent (which contains sulphur dioxide, base and solvent) and the titrant solution (it consists of iodine dissolved in the solvent).

- For **coulometric KF titration** method, the I_2 is produced electrochemically in situ during the titration inside the reaction cell thanks to a generator electrode. In this version of KF titration, the water quantification is done by the relationship iodine–water–current (according to Faraday's law 3.17) allowing to work in a water range between 1 ppm to 5%. The most important component of this system is the Generator electrode, an electrode consisting of an anode and a cathode (both of which are usually platinum) which conduct current through the cell: the anode is responsible for the generation of iodine (by oxidation of the iodide), while the cathode is responsible for the generation of hydrogen (gas) as a consequence of the reduction of H^+ ions. Recalling reaction 3.16, two electrons ($n_e = 2$) are involved in this electrochemical process. As the electrochemical process involved in this titration is well known, by means of Faraday's law it is possible to know the amount of water contained in a sample as a function of the charge (Q, $Q(C) = i(A) \cdot t(s)$) needed to generate the iodine necessary to react with the water.

$$m = \frac{M_r \cdot Q}{n_e \cdot F} \xrightarrow[F=96487C/mol]{M_r=18g/mol,n=2} m = \frac{9}{96487} \cdot Q \tag{3.17}$$

Based on the relationship between coulombs (C) and iodine, the exact amount of iodine generated is determined, and since it subsequently reacts 1:1 with the water in the sample, the amount of water can be quantified. However, for coulometric titration there are two options or versions depending on the morphology of the generator electrode: fritted–cell (with diaphgram) or fritless–cell (without diaphragm).

  - The fritted-cell delimits two regions in the reaction vessel that form the electrolytic cell: catholyte and anolyte department. In each of these regions there is a solution composed of: iodine, sulphur dioxide, base and solvent (the most common is that in both compartments the solution formulation is the same, although sometimes some adaptations of some of them are required to improve the evaluation). This alternative is the conventional selection to do a KF titration.
  - However, an innovative cell design removes the diaphragm and defines an unique compartment. In this option, the one reagent used contains all the elements involved in the KF reaction.

Figure 3.64 presents the composition of the measuring cell for the KF titration for the two versions of this titration [23].

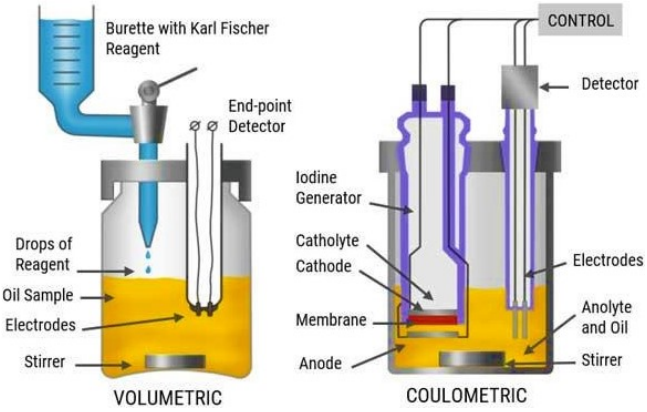

Figure 3.64. *Karl Fischer titration experimental setup: volumetric and coulometric, image from Noria Corporation "Practicing Oil Analysis" - March 2004 [24].*

In this Thesis, the KF water titration option chosen was coulometric, which follows the ASTM D6304 standard [81]. Initially, the research tasks started working with the configuration of the diaphragm coulombimetric KF titration, but due to the nature of the samples, the porous frit (that acts as a membrane) would be contaminated and its channels were constantly sealed or clogged by the presence of solids (mainly soot and other insoluble material that is dissolved in the engine oil). For this reason, it was decided to select the diaphragm-free version, which avoids the separation of the anolyte and the catholyte, since the iodine is generated in situ in the titration cell [20, 113]. Figure 3.65 shows a schematic diagram of the two configurations used, showing the electrochemical processes that occur in each of them.

According to Figure 3.65, the main difference between the two configurations is the possibility that the iodine reach the cathode of the generator electrode and it is reduced to iodide. The generator electrode with diaphragm, this fritt acts as a physical barrier, so that iodine is only in the anolyte compartment and reacts with water. Whereas, in the version without diaphragm, it is possible that the iodine can go to the cathode and convert to iodide. However, there are protocols to prevent this iodine reduction process from occurring: the cathode surface should be as small as possible to achieve the smallest possible iodine–cathode contact area, efficient titration cell agitation system to facilitate contact between the iodine and the sample

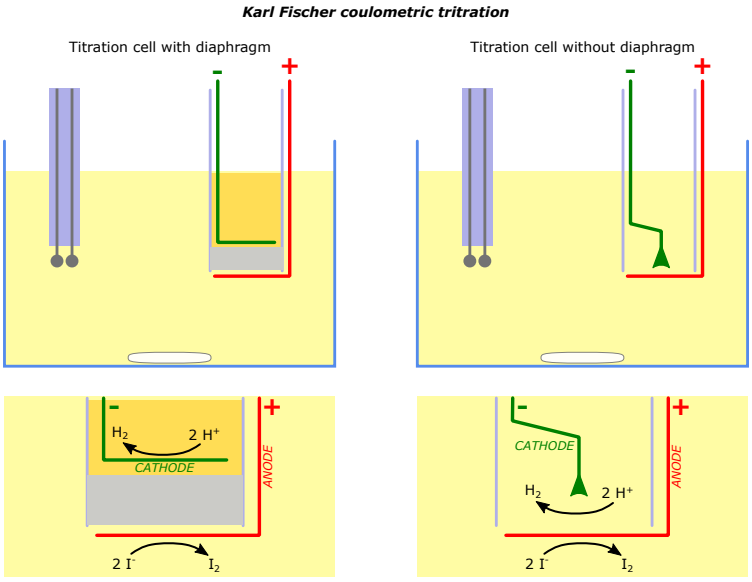

Figure 3.65. *Electrode generator of coulometric Karl Fischer titration: with diaphragm and without diaphragm.*

water and to produce iododine at high rates, as the hydrogen that is generated is isolated from the cathode [99].

Despite this apparent drawback, there were several reasons for the selection of the diaphragm–free configuration: the main one is that only a single reagent is required and that the titration cell is easier to clean (considerably lowering the cost of analysis and equipment maintenance). This option has been developed recently (both in terms of design and reagents) that it has become a standard set-up for hydrocarbon samples (long/short chain hydrocarbons, halogenated hydrocarbons, alcohols, esters, ethers, acetamides, mineral oils, edible oils, ethereal oils, etc.) [90].

Next, Figure 3.66 shows the results of the KF titrations using the new coulometric diaphragm–free electrode system.

According to Figure 3.66, the absolute water values that the system registers during the titration (solid line) can be observed. The tritation is complete when the Indicator electrode determines that the EP has been reached (note the curves drawn with dash lines) when the evolution of the potential recorded presents an L-type shape. So, Table 3.19 compiles the results for these five titration.

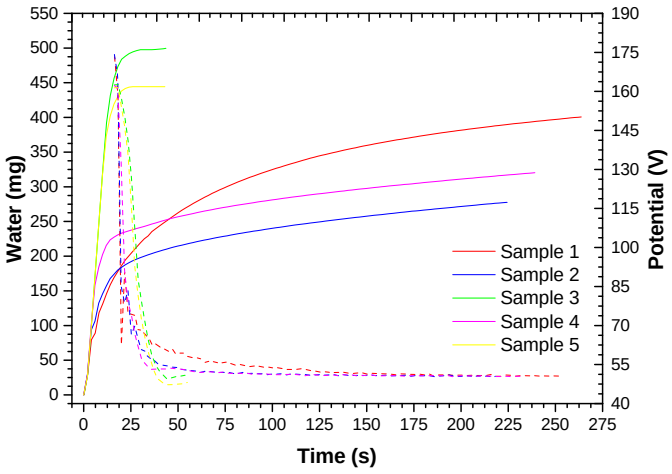

Figure 3.66. *Examples of coulometric KF titrations of 5 samples of used engine oils.*

Table 3.19. *Results of coulometric KF titrations.*

Sample	Mass (g)	Potential EP (mV)	Absolute water (mg)	Water content (ppm)
Sample 1	0.374	50.7	348.4	931.7
Sample 2	0.263	50.6	235.3	894.8
Sample 3	0.143	50.7	489.8	3425.4
Sample 4	0.283	50.5	281.9	996.2
Sample 5	0.149	48.1	433.7	2911.0

To conclude, Karl Fischer titration is the most reliable laboratory method (although portable systems already exist, so it is no longer restricted to a laboratory environment) for testing samples in order to quantify the water contamination, and the coulometric KF titration is the best option when the amount of water in the samples is low. Nevertheless, the alternative of using FT–IR spectroscopy for the quantification of water in used lubricating oil samples has attracted much interest.

FT–IR spectroscopy is a chemical-free measurement method for screening samples (in laboratory and on–site) of engine oils that contain water. Liquid water, in IR region, has three main vibration modes: symmetric stretch (3280 cm^{-1}), asymmetric stretch (3490 cm^{-1}) and bending (1644 cm^{-1}) of its covalent bonds. According to that, FT–IR spectroscopy uses the absorption band of the hydrogen–bonded hydroxyl group (−OH) of water (stretching

vibration band), located near 3300 cm^{-1} (in the case of pure water), as a reference for the quantification of water when it is mixed with the lube oil. When water is contained in lubricating oil environment, this band might be shifted or moved (a few wavenumber values around the reference value) as a consequence of the environment surrounding the water molecules [114].

In accordance with the guidelines laid down by ASTM standard practice E2412 [76], for the case study of the Thesis focusing on engine lubricating oils, the IR region of interest lies between 3500 cm^{-1} and 3150 cm^{-1} as shown in Figure 3.67.

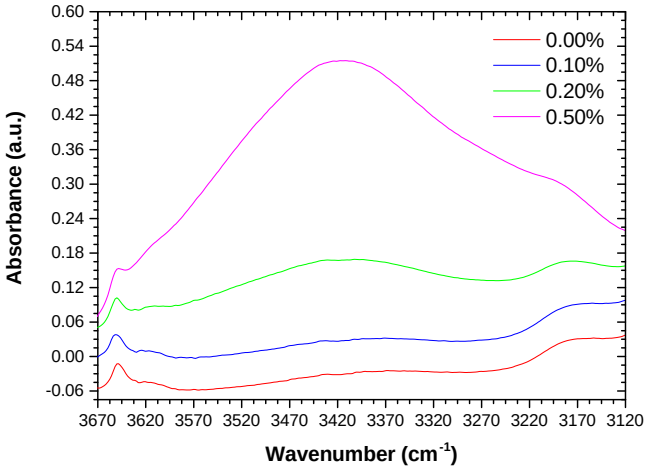

Figure 3.67. *IR water band absorption at 3500–3150 cm^{-1} of 4 engine oil samples with different moisture levels.*

Now that the study region is located, it is useful to state how it will be used and interpreted. Basically, there are two ways: either a direct trending monitoring or a signal processing based on the subtraction of the new engine oil spectrum. The choice of one way or the other will depend on the situation, but the choice of either of them involves different work:

- If an indicative value is required, direct trending is the most appropriate option. With this option, the evolution of the water content in the lubricating oil can be observed by measuring the area between 3500 and 3150 cm^{-1} (taking as baselines: 4000–3680 cm^{-1} and 2200–1900 cm^{-1}).
- However, if a higher accuracy is required to provide a value, it is necessary to use methods of IR signal calibration, the most common

way of working being the so-called spectral subtraction. According to ASTM E2412, two options are available:

- The first one consists of measuring the height of the peak at 3428 cm^{-1} by taking a single point baseline at 3700 cm^{-1}.
- The second one is based on finding the maximum of absorption around the –OH absorption (340–3350 cm^{-1}), measuring the height taking as a starting point a baseline drawn from 3740 cm^{-1} to 3120 cm^{-1}.

In theory, the quantification of water contained in lubricating oil by FT–IR spectroscopy does not involve any major complexity [136]. However, it presents a number of problems that must be taken into consideration: interferences, incompatibility of materials, etc. The main problem lies in the amount of water in the sample to be analysed. This is because, depending on the water concentration, water can be found in one or more of its three different phases (dissolved, free or emulsified). Although engine oils are formulated with specific additives to keep the water in the dissolved phase, it may be the case that conditions are favourable to reach the saturation limit conditions, and the other two phases to occur. If this is the case, FTIR spectroscopy presents problems as it is a technique that is strongly influenced by free and emulsified water, because these small clusters of water cause the IR beam to scatter (elastic light scattering) as it travels through the sample. This effect or impact on the measurement can be corrected or even avoided if specific water stabilising reagents and an efficient homogenising process are used. Of these two options, the easier to implement is the homogenisation of the sample prior to analysis.

Following these guidelines, a properly sample preparation prior to analysis with the FT–IR spectrometer is required and to avoid samples with highly concentrated water–in–oil moistures. In this Thesis, a methodology based on spectra subtraction has been developed . In particular, based on experience, it was found that the best responses were those obtained by measuring the peak area between 3574–3261 cm^{-1}, using two baselines to correctly define the peak: the first one located at 3979–3975 cm^{-1} and the second one at 2819–2815 cm^{-1}. In addition, scaling treatment was used to change the value reported by this methodology with the goal to obtain an appropriate scale. In this way, it was possible to define a methodology that allowed results to be obtained quickly and easily with a high degree of accuracy and reliability.

3.3.3.2 Glycol

Having closed the section on water, the other component of the coolant fluid that needs to be described is the glycol component and in particular the ETG. In that case, there are several direct and indirect analysis for glycol detection in engine oil, thus the most representative and currently most widely used ones will be explained: Gas Chromatography, Atomic Emission Spectroscopy and FT–IR spectroscopy [30].

The first option, the Gas Chromatography (GC), is the most accurate way to detect and quantify the presence of glycol that contains an engine oil sample. This technique, regulated by the ASTM D4291 [63], involves an exhaustive and delicate experimental procedure in order to carry out the glycol measurement: an extraction of the glycol from the sample using water (polar phase to which the glycol migrates due to its relative solubility) and a subsequent centrifugation process to separate the organic phase (lubricant) from the aqueous phase (that contains the glycol), the aqueous extract is removed and injected into the chromatograph (with a calibrated gas chromatography column) for analysis (see Figure 3.68). The result of that is a chromatogram where the polar compounds are separated and detected (commonly by FID, Flame Ionisation Detector), including glycol.

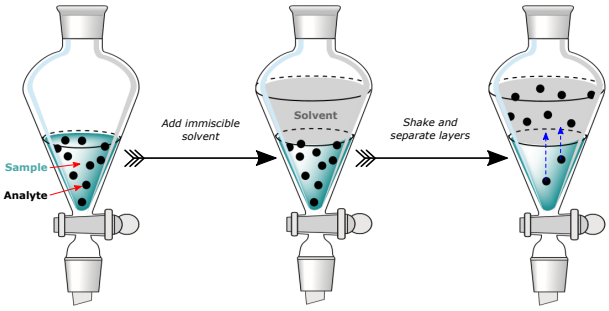

Figure 3.68. *Scheme of liquid–liquid extraction.*

Although this route of analysis has low detection limits, making it useful for determining glycol levels from 5 ppm to 200 ppm, and is specific for glycol, it is not always easy to work with this option. The most relevant problems encountered by GC in determining the glycol content of lubricating oil are the following:

- As in any chromatography test, a prior process of calibration of the system with standards is required to generate the appropriate calibration

curve to convert the glycol peak area of the chromatogram into he corresponding units (ppm or %, mainly). It is advisable and helpful to analyse the new lubricating oil to obtain a base value in case the lubricant originally contained traces of glycol or glycol derivatives.

- Due to the properties of the ETG molecule: low molecular weight (62.068 g/mol), low volatility and high polarity, its chormatographic peak is complicated to detect and quantify.
- In addition, during the test, glycol is susceptible to decomposition into other by-products or derivatives (such as esters, aldehydes and acids) leading to errors in detection and false negatives resulting in a misreading of the true glycol concentration.
- Finally, GC is an expesnive technique due to several aspects: the time of analysis cost (around 30–45 minutes per test), qualified personnel to perform the test and the cost of the device.

However, some of these problems have been mitigated by the development of alternative sample preparation and testing methods [39, 102, 121]. One such methodology is the determination of ETG in engine oil (fresh and used) by Headspace-Gas Chromatography which is collected under ASTM D7922 [58].

If a GC is not available, the next option is to use gas chromatographic techniques based on Atomic Emission Spectroscopy. Of the different Atomic Emission techniques, the ICP (Inductively Coupled Plasma) emission spectroscopy and the arc-spark RDE (Rotating Disc Electrode) emission spectroscopy are the most widely used. In this Thesis, according to the elemental analysis technique available in the laboratory, ICP–OES spectroscopy was chosen (according to ASTM D5185 [67]).

ICP–OES could be the best option to verify the contamination of glycol or any of its derivatives (such as ETG or PG) used in the coolant fluids in samples of lubricating oil. The detection of this contaminant is carried out by monitoring those organo-metallic additives which are used in the composition of coolant (see Table 3.20).

These metals are reliable clues to verify coolant contamination levels are getting into the engine oil. Consequently, if the analysis of lubricating oil samples, under standard practice ASTM D5185 [67], shows levels of these metals (act as markers/indicator since the glycol molecule cannot be measured in this technique), it confirms the fact that the lubricant has received a certain amount of coolant.

Table 3.20. *Common metallic additives in coolant formulations.*

Element	Chemical symbol	Application
Potassium	K	pH buffer Corrosion inhibitor for Fe and Al
Silicon	Si	Defoamant or antifoam Corrosion inhibitor for Al
Boron	B	pH buffer Corrosion inhibitor for Fe and ferrous metals
Sodium	Na	Corrosion inhibitor
Molybdenum	Mo	Anticavitation Corrosion inhibitor for Fe
Phosphorous	P	pH buffer Corrosion inhibitor for Fe and ferrous metals

Therefore, the presence of some of these elements is associated with glycol contamination, potassium and sodium being the main ones (because both are among the most stable elements within the glycol). Besides being one of the primary additives, potassium and sodium are practically only used in coolant fluids, so that if these two metals are detected in lubricating oil samples, they are almost certainly due to coolant contamination problems (the other metal elements may have originated from other sources, these are not exclusive to the formulation of the coolant).

At first glance, the option of quantifying the presence of glycol in the lubricant oil by ICP–OES is interesting, but requires some prior knowledge or information to be able to provide a correct interpretation:

- The first data is about the composition of the coolant fluid in order to know which specific additives are present in their formulation and in what proportion.

- The next consideration has to do with finding out which of these elements are unique to the coolant in order to use them as indicators. This is because, depending on the application, there may be different sources of the same elements to be used as indicators: additives in lubricating oils, contamination/degradation of the oil, mixtures of unknown agents, etc.

- Finally, it is advisable to monitor the coolant to see how it performs. This, considering that certain compounds may change during the use of the coolant.

For the study topic developed in this Thesis, the alternative of monitoring the glycol contamination by ICP–OES proved to be a viable way due to several factors: the first one is that information was available on the lubricating oil formulations to be tested, as well as that of the coolant and, the second and most useful, is that the coolant formulation contained a sodium based compound with no sodium in the composition of the lubricating oils. The additive in question is the sodium salt of 2-ethylhexanoic acid ($CH_3(CH_2)_3CH(C_2H_5)CO_2Na$) in almost 14000 ppm. Therefore, if an accurate quantification of the glycol contamination in the lubricant is desired or required, it would simply be necessary to calibrate the spectrophotometer with standards with coolant-oil mixtures at different concentrations.

However, if working with an ICP–OES spectrophotometer is not possible, taking into account its requirements for determining the presence of glycol, FT–IR spectroscopy may be the most suitable alternative. FT–IR spectroscopy is a widespread technique for analysing lubricating oils, so it is not surprising that there are also guidelines and standards (ASTM E2412) for how glycol can and should be determined in a lubricating oil sample.

ETG (or Ethane–1,2–diol IUPAC name) molecule is a divalent primary alcohol (also known as glycols): primary alcohol means that it is an alcohol where the hydroxyl group ($-OH$) is on a terminal carbon (at the end of the chain, $-CH_2-$) and divalent means that it has two hydroxyl groups. According to its molecular structure, ETG has two different IR active alcohol groups: $O-H$ and $C-O$. Both groups generate absorption bands in different regions of IR spectrum:

- The first, related to the hydroxyl functional group, absorption band is a strong band located in a broad region around 3500–3200 cm^{-1} (and also ∼3640–3610 cm^{-1}, but more difficult to work with, which is why it is not often used).
- The second absorption region correponding to $C-O$ bonds (in a primary alcohol). It is usually found between 1075 cm^{-1} and 1025 cm^{-1}.

Despite knowing in which region of the IR spectrum the glycol will give a response, it is complex to determine which region to select and how to interpret it. This is due to interferences (overlapping bands because it shares

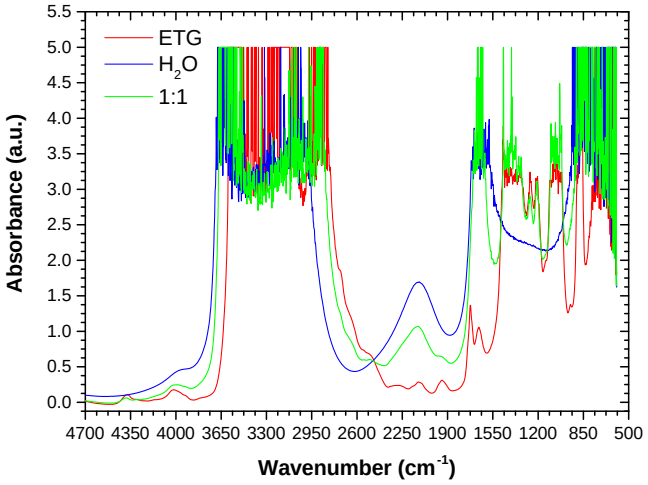

Figure 3.69. *FT–IR spectrum of: Etilene glycol (red), Water (blue) and Coolant (50% ETG - 50% Water) (green).*

common spectral absorption regions) from a variety of agents: water (because of its –OH absorption band), engine oil additives (specially oxygenated compounds), contaminants and degradation by-products of the engine oil. Any presence of any of these compounds in the sample to be analysed will lead to errors in the measurement of glycol. In addition, the low stability of the ETG molecule (it degrades chemically and thermally easily) adds to the complexity of analysing and interpreting the IR spectrum.

As a first approximation, the simplest option is to eliminate any possible interference that can be avoided in advance. This is the case of O–H absorption, there is the interference generated by water (since the coolant fluids are practically binary mixtures ETG:water), so that both signals cohabit and it is impossible to distinguish between the ETG contribution and the water contribution. Therefore, the candidate band for ETG monitoring in lubricating oil is the C–O band. Focusing on this group, the ASTM E2412 describes the standard practice for measuring the glycol content in engine oil. According to this ASTM E2412, two main analysis can be done in order to quantify the presence of glycol in engine oil samples: by direct trending or by spectral subtraction. In both cases, bands or peaks that are characteristic only of the glycol and have no interference or contribution from water have been selected.

- The first methodology is focused on the measurement of peak area at 1100–1030 cm^{-1}, with two double baseline points: one at 1131–1099 cm^{-1} and the other one at 1031–1009 cm^{-1}. This alternative is good to obtain trends.

- But, if a more comprehensive quantification is desired, it is necessary to carry out a study using standards. In this situation, a calibrated method for the detection of glycol in lubricating oil is constructed based on analysing the height of the absorption peak located at 880 cm^{-1} (referenced to a single–point baseline at 917 cm^{-1}). Sometimes, this peak is a doublet because two maximum absorptions appear: 883 and 867 cm^{-1}. Therefore, depending on the situation, an adjustment must be made to select the maximum absorption within an admissible wavenumber range.

Depending on the performance of each of these two pathways, differences were observed in their viability or functionality for the case study developed in this Thesis:

- In the first case, basically focused on the absorption bands generated by the C–O bond (1260 cm^{-1} and 1000 cm^{-1}), overlapping and interference from oil degradation by–products were noted. As a consequence, despite being bands with a good intensity, such is the degree of interference they suffer, that it is not possible to extract robust and reliable results about the glycol content in the sample.

- Whereas, in the other area of analysis, the effect of the interferences that may appear as a consequence of the use of the lubricant are not that relevant. However, the absorption at 880 cm^{-1} does not give very precise values either; this is due to the nature of the samples, the maximum of the absorbance is subject to shifts. Therefore, in order to determine the real maximum of the band, it is advisable to apply an extra treatment to the IR spectrum (e.g. to determine the second derivative).

Due to these limitations of the method, it was decided to develop our own method that better suits the needs and requirements of the samples to be studied in this Thesis. Thus, a similar philosophy to the one described above was followed: firstly, a methodology would be prepared to monitor the presence of glycol, to analyse its trend. On the other hand, a calibrated procedure was prepared in order to provide more accurate results for those situations where such degree of appreciation was required.

- For the first case, the best response for the control of the trend evolution was collected when working on the C−O band. Specifically, the area under the peak between 1104 cm^{-1} and 1022 cm^{-1} was analysed by taking two baselines: the first at 1338–1309 cm^{-1} and the second at 920–892 cm^{-1}.

- For the second case, where more precise quantifications are required, it was decided to analyse the two glycol doublets peaks recorded in the FT–IR spectrum. After considering several alternatives, the option that provided the best response was the one that involved the measurement of the area under the peaks post-subtraction of the spectrum of the fresh oil. This calibrated method is built on the 1089–1037 cm^{-1} and 886–862 cm^{-1} regions of the IR spectrum.

Figure 3.70 shows the results derived from the analysis using the calibrated method, being this option the one chosen as definitive for the case of the glycol study by FT–IR spectroscopy.

In order to analyse the response of the proposed procedure for the detection and quantification of glycol in oil, a test was carried out where a set of six samples of used engine oil from a vehicle were analysed during the whole ODI period. Table 3.21 shows the results for each of the samples when applying the proposed protocol.

Table 3.21. *5W30 engine oil samples from vehicle with coolant leakages.*

Sample	**Area integration (Abs·cm^{-1}/0.1mm)**	**Glycol (%)**
Sample 1	6.89064	1.3(4)
Sample 2	9.18067	1.7(8)
Sample 3	12.26192	2.3(8)
Sample 4	13.55167	2.6(3)
Sample 5	20.07002	3.8(9)
Sample 6	56.94008	11.0(4)

The following Figure 3.71 shows the performance of the six different samples (represented by solid lines) in contrast to the calibration standards used (represented by dashed lines).

In view of the results, the selection of the spectral range, in which to carry out the analysis and the signal treatment protocol, allow quality results to be obtained, always taking into account the fact that influences and interference

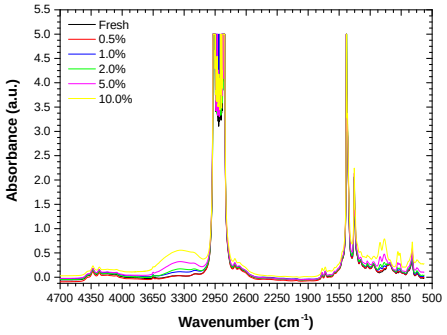

(a) FT–IR spectrum of the coolant–oil calibration standards

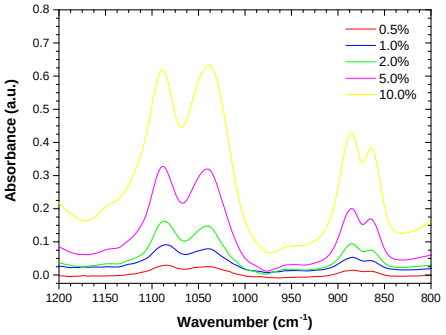

(b) Result of spectra subtraction of Fresh Oil (0% coolant content) in the calibration standards

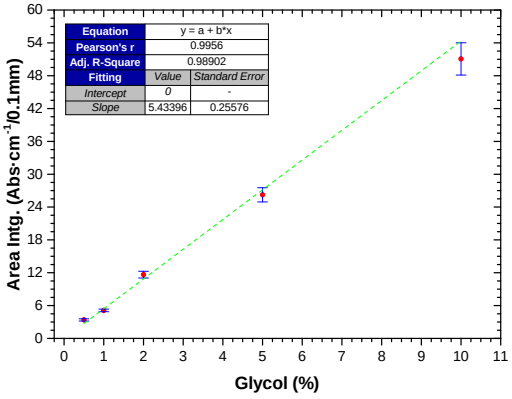

(c) Glycol integration signal

Figure 3.70. *Protocol for the study of Glycol content in lubricant oil by FT–IR spectroscopy.*

from external agents (contaminants, degradation by–products, etc.) are always present. In view of the above, FT–IR spectroscopy can be used for the monitoring (by trending analysis) of the presence of glycol in used oil samples, as is the majority of the subject and object of study in this Thesis.

However, the level of judgement required in this study for the quantification of Glycol, developed during the course of the thesis, had to be more severe. FT–IR spectroscopy, under these conditions, where a higher level of appreciation (below 0.1%) is required, leads to the need for extensive signal processing to try to achieve reliable and consistent results to obtain the true value of ETG content of the coolant dissolved in the oil. It is for this reason

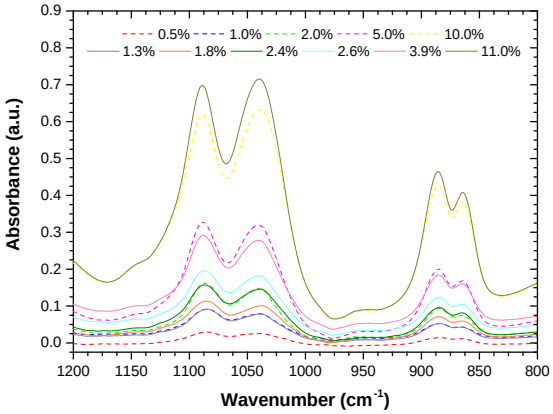

Figure 3.71. *IR response of Glycol in selected spectra region: signal from calibration standards represented by dashed lines and signal from the samples represented by solid lines.*

that, as explained above, the way to determine the ETG in the oil is more reliable and efficient when it is carried out by monitoring the sodium by means of ICP–OES spectroscopy. Nevertheless, during the research work, the ETG result obtained by ICP–OES has always been accompanied by the results' analysis of the collected IR spectrum. In this way it has a double point or control bias that guarantees the viability of the values reported for this very important parameter of contamination.

3.3.4 Wear metals

Wear is a phenomenon that involves the erosion of a solid surface, causing loss of mass [91]. For the case of study, ICEs, this process takes place in those systems composed of movable mechanical elements that have relative movement between them: tribological pairs (or commonly know as tribo–pairs). The interaction of the surfaces of such engine assemblies is minimised by the action of the lubricant, which interposes itself between them (forming a protective film) and prevents (as far as possible according to the lubrication regime, Figure 3.72) the direct contact of the surfaces [143]. As a result, the lubricant helps to reduce wear of these elements and also favours other aspects, such as improving the efficiency of the engines, by reducing mechanical losses

due to friction, and extending the useful life of the engines and their internal components.

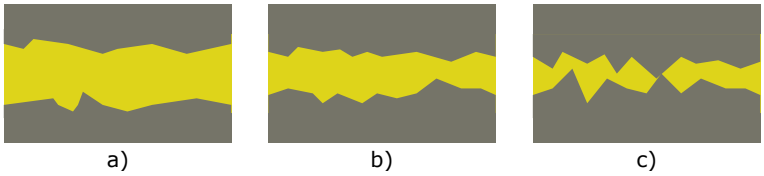

Figure 3.72. *Lubrication regimes: a) Hydrodynamic lubrication, b) Mixed film lubrication and c) Boundary lubrication.*

In this way, the involvement of the lubricant means that in the end it is the one that receives the particles from the surfaces it lubricates. Therefore, the analysis of the presence of these particles in the lubricant oil is a vital parameter to be carried out under the OCM tasks [142]. A study of the wear particle content of a lubricating oil can be carried out in two ways: a qualitative option based on determining the nature and composition of the constituent elements of the particles or, knowing the quantity of these particles. The possibility of knowing one or even both of these aspects will depend on the needs and requirements to be fulfilled, as not all applications require the same information.

In the case of study in this research, there are several choices in determining the wear particle content of a sample of lubricating oil (see Figure 3.73) [107]. Within this field, the main techniques are listed below [150]:

- Atomic spectrometry, either in the form of absorption, emissivity or fluorescence spectrometry.
- Ferrography: analytical or by direct reading.
- Particle counting analyser systems: optical (by light scattering [12]), by pore blockage or by image analysis [115].
- Magnet collectors [43, 109, 149].
- Microscopy: optical or electron microscopy (SEM, scanning electron microscopy)
- Energy Dispersive X–ray (EDX) microanalysis.

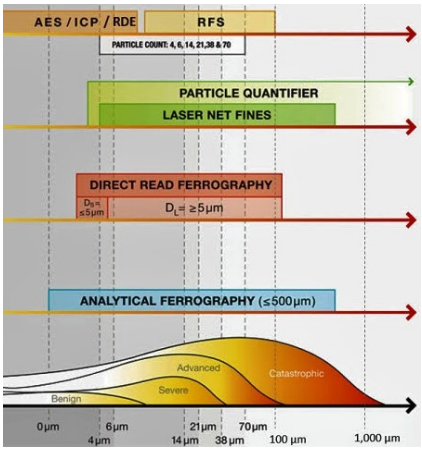

Figure 3.73. *Range of application of the different techniques for the determination of wear particle content according to the particle size and its impact in the engine damage.*

Determining engine wear by analysing the particles contained in the lubricating oil can be done in several ways. Nevertheless, two procedures have been used in this Thesis: optical particle counting analyser and ICP–OES. Generally speaking, the first option is oriented towards quantifying the number of particles by size classification [119], while the second option determines particle concentration according to its composition.

For the first option three different devices, capable of providing wear particle content according to the ASTM D7647 [74] methodology and to give the information according to ISO 4406 cleanliness code [32], have been used in this research work. Three devices involved are shown in Figure 3.74: Spectro 5200 Trivector Analyzer, PAMAS GmbH S–40 and OilWear S100 from Atten2.

All three are inspired by optical systems and provide information according to the cleanliness code set out in ISO 4406: a system of three digits representing the number of particles (per millilitre) of a certain diameter, in this case 4, 6 and 14 microns in diameter. Accordingly, the data collection form is coded $R_4/R_6/R_{14}$. Table 3.22 shows the translation of particle number to ISO code:

These three devices, starting from the same principle (see Figure 3.75), present a series of distinctive characteristics that make them particular and individual cases:

(a) Spectro 5200 Trivector Analyzer

(b) PAMAS GmbH S–40

(c) OilWear S100

Figure 3.74. *Particle counting analyser devices to obtain ISO codes of wear metals in lubricants.*

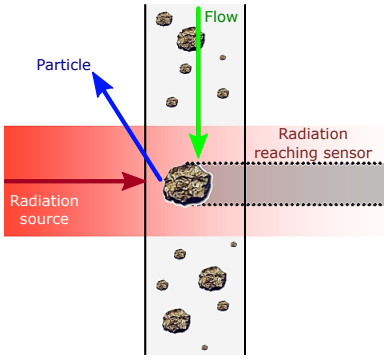

Figure 3.75. *Particle counting analyser operating principle.*

Table 3.22. *ISO 4406 table showing the number of particles per millilitre to generate a given output value according to ISO code.*

Scale number	More than	Up to / Including	Scale number	More than	Up to / Including
>28	2500000	-	*14*	80	160
28	1300000	25000000	*13*	40	80
27	640000	1300000	*12*	20	40
26	320000	640000	*11*	10	20
25	160000	320000	*10*	5	10
24	80000	160000	*9*	2.5	5.0
23	40000	80000	*8*	1.3	2.5
22	20000	40000	*7*	0.64	1.30
21	10000	20000	*6*	0.32	0.64
20	5000	10000	*5*	0.16	0.32
19	2500	5000	*4*	0.08	0.16
18	1300	2500	*3*	0.04	0.08
17	640	1300	*2*	0.02	0.04
16	320	640	*1*	0.01	0.02
15	160	320	*0*	0.00	0.01

- Spectro 5200 Trivector Analyzer employs a laser to count and classify particles simultaneously. To obtain the ISO code, the device needs to feed the sensor with 30 millilitres of sample at a constant flow rate (thanks to a forced mechanical injection system). The main disadvantages of this system lie in the fact of sample preparation: degassing to remove air bubbles, removal of water (by chemical processes) if necessary and dilution of the sample (from 1:1 to 1:99, sample:solvent ratios) with a solvent according to the lubricant base. This makes the test complex to perform and facilitates the occurrence of operational faults leading to discrepancies between measurements.

- The next equipment, PAMAS GmbH S–40, is provided with a pressurised optical measuring cell (PAMAS volumetric sensor HCB-LD-50/50) and a sample supply system to the sensor which injects pressurised sample at a controlled constant flow rate and volume by means of a ceramic piston pump. The main advantage over the previous system lies in the construction of the sensor itself, since it is pressurised, if the sample contains dissolved air, this will not interfere with the measurements as the sample will not degas. However, any other external contribution to the oil: water and/or coolant, can cause interference as these small droplets of fluid, if not removed, will cause erroneous ISO codes. Given that this is a system where the operator's participation is reduced, control over the sample and the measurement process is lost and, if

the situation requires it, it would be appropriate to correct the ISO code values reported by the equipment.

- The latest device, the OilWear S100, is a sensor for online monitoring of wear in oils. This sensor has been adapted to a laboratory system for use at the CMT–Motores Térmicos Institute. This option is selected because the OilWear S100 sensor provides a real–time view of the sample passing through the measuring cell (see Figure 3.76). This makes it possible to observe any anomalies in the sample, in particular the ingress of air bubbles as well as water or coolant bubbles or any pre–treatment of the sample (basically dilution) is required to ensure the correct functioning of the sensor.

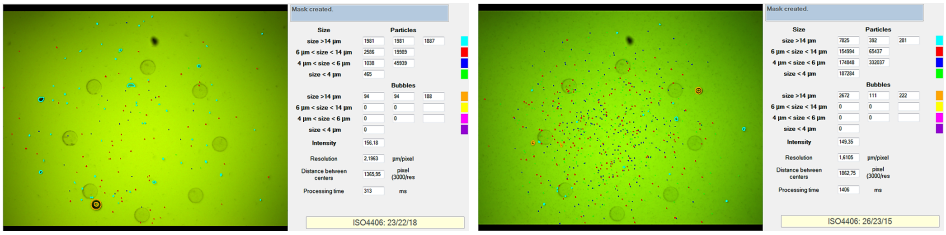

(a) Example of diesel lubricant oil (b) Example of CNG lubricant oil

Figure 3.76. *Measurement samples with the OilWear S100 sensor: of a diesel engine lubricating oil (with dilution) and of a CNG (without dilution).*

Although all three devices give relatively equal results, see Table 3.23, the best option is the OilWear S100 sensor.

Table 3.23. *ISO codes obtained by the three particle counting analyser devices of used engine oil in GNC engine.*

Device	**ISO 4406 code**
Spectro 5200 Trivector Analyzer	23/22/11
PAMAS GmbH S–40	23/21/14
OilWear S100	23/21/15

Focusing on the OilWear S100 sensor, its adaptation to bench-top equipment required the following elements: a stand to accommodate the sensor as well as all the auxiliary systems: electrical system, mechanical stirrer and sample feed system. Figure 3.77 shows the different elements involved.

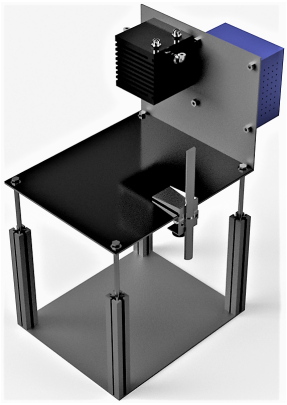

(a) Structure designed to accommodate the different systems involved in the configuration of the equipment

(b) Sample supply system to the sensor based on peristaltic system

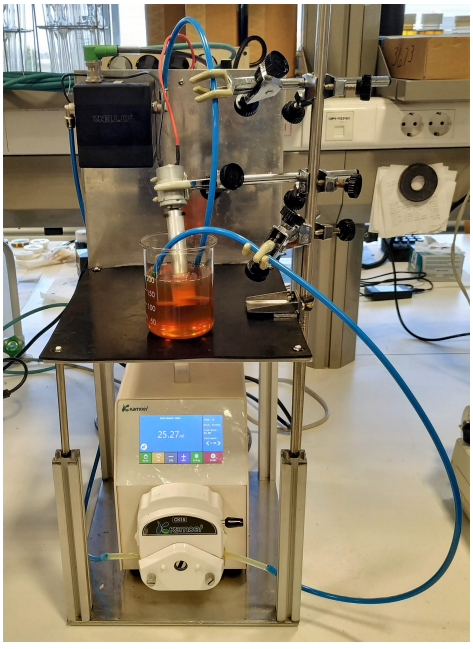

(c) System in action during an analysis

Figure 3.77. *Design for the adaptation of the OilWear S100 sensor to a laboratory oil analysis equipment.*

By means of the designed configuration, it has been possible to obtain a functional device for the desired purpose. Figure 3.78 shows how the system works to obtain the ISO code of a given sample as a function of the number of particles of a given diameter.

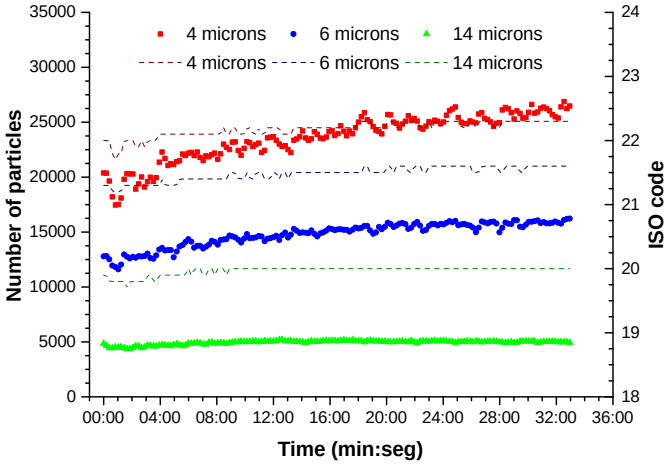

Figure 3.78. *Recording of particle number and ISO code during the analysis of a used lubricating oil sample in the OilWear S100 sensor based system.*

Despite the potential of this technology, taking into account the approach for this Thesis, the wear control of ICEs is investigated from another perspective. Thus, the OilWear S100 is relegated to a backup system in case the final alternative presents any issues or problems in determining the degree of presence of wear metals. Specifically in this Thesis, ICP–OES spectrometry has been used to monitor wear rates in a lubricating oil, taking advantage of the fact that it was already used for other purposes.

In this research work, given that the ICP–OES spectrophotometer from the Fuel and Lubricants Laboratory of CMT–Motores Térmicos department, the quantification of wear metals in the engine lubricating oil samples was performed according to ASTM D5185: "Standard Test Method for Multi-element Determination of Used and Unused Lubricating Oils and Base Oils by Inductively Coupled Plasma Atomic Emission Spectrometry (ICP–AES)" [67]. As this technique has already been the subject of a separate section: 3.2.5 *Espectrometría ICP–OES*, it is not convenient to return to a discussion or analysis of the technique, since everything that needs to be explained has already been described.

Bibliography

[1] A. M. Abdul-Munaim, T. Holland, P. Sivakumar, and D. G. Watson. Absorption wavebands for discriminating oxidation time of engine oil as detected by FT-IR spectroscopy. *Lubricants*, 7(3):24, 2019.

[2] A. Agoston, C. Ötsch, and B. Jakoby. Viscosity sensors for engine oil condition monitoring: application and interpretation of results. *Sensors and Actuators A: Physical*, 121(2):327–332, 2005.

[3] E. Akochi-Koble, M. Pelchat, D. Pinchuk, J. Pinchuk, and S. Dwight. *Validation of a FTIR spectroscopy method for measuring and monitoring fuel dilution in lubricating oils*, 1998.

[4] N. L. Alpert, W. E. Keiser, and H. A. Szymanski. *IR: theory and practice of infrared spectroscopy*. Springer Science & Business Media, 2012.

[5] A. Amirav and D. Muller. Arson analysis by GC-MS with cold EI–Fuel fingerprinting by isomer distribution analysis. `http://blog.avivanalytical.com/2012/11/arson-analysis-by-gc-ms-with-cold-ei.html`, nov 2012.

[6] R. Q Aucélio, R. M. de Souza, R. C. de Campos, N. Miekeley, and C. L. P. da Silveira. The determination of trace metals in lubricating oils by atomic spectrometry. *Spectrochimica Acta Part B: Atomic Spectroscopy*, 62(9):952–961, 2007.

[7] L. S. Bark and S. M. Bark. *Thermometric titrimetry: International series of monographs in analytical chemistry*, volume 33. Elsevier, 2016.

[8] J. Barthel and R. Wachter. Thermometric titrations. *Journal of Chemical Education*, 55(1):A48, 1978.

[9] N. Bartsch. *Lubricating oil analysis according to ASTM D5185 using the Thermo Scientific iCAP 7400 ICP-OES*, 2017. Application Note AN43158-EN 0617.

[10] N. H. Bings, A. Bogaerts, and J. A. C. Broekaert. Atomic spectroscopy: a review. *Analytical chemistry*, 82(12):4653–4681, 2010.

[11] J. Blomberg, P. J. Schoenmakers, and U. A. T. Brinkman. Gas chromatographic methods for oil analysis. *Journal of Chromatography A*, 972(2):137–173, 2002.

[12] C. F. Bohren and D. R. Huffman. *Absorption and scattering of light by small particles*. John Wiley & Sons, 2008.

[13] P. W. J. M. Boumans. Inductively coupled plasma-atomic emission spectroscopy: its present and future position in analytical chemistry. *Fresenius' Zeitschrift für Analytische Chemie*, 299(5):337–361, 1979.

[14] J. A. C. Broekaert. Atomic emission spectroscopy instrumentation. *Spectrochimica Acta*, 37:727, 1982.

[15] J. M. Brown. *Infrared spectroscopic analysis of petroleum, petroleum products, and lubricants*. ASTM International, 2011.

[16] M. W. Brown, K. Issa, and A. G. Sinclair. Precise manual enthalpimetric titrations. *Analyst*, 94(1116):234–235, 1969.

[17] R. F. Browner and A. W. Boorn. Sample introduction techniques for atomic spectroscopy. *Analytical Chemistry*, 56(7):875A–888A, 1984.

[18] M. J. D. Carneiro, M. A. Feres Júnior, and O. E.S. Godinho. Determination of the acidity of oils using paraformaldehyde as a thermometric end-point indicator. *Journal of the Brazilian Chemical Society*, 13(5):692–694, 2002.

[19] M. Cassap. The analysis of used lubrication oils by inductively coupled plasma spectrometry for predictive maintenance. *Spectroscopy Europe*, 20(1):17–20, 2008.

[20] A. Cedergren and S. Jonsson. Progress in Karl-Fischer coulometry using diaphragm-free cells. *Analytical chemistry*, 73(22):5611–5615, 2001.

[21] Metrohm Competence Center Titration. *Acidity in crude oils and petroleum products by thermometric titration according to ASTM D8045*, 2016. Application Bulletin 427/2 e.

[22] Metrohm Competence Center Titration. *Determination of the total base number in petroleum products*, 2016. Application Bulletin 405/2 e.

[23] Noria Corporation. How to measure water in oil. `https://www.machinerylubrication.com/Read/327/water-oil-analysis`, may 2002.

[24] Noria Corporation. Karl Fischer coulometric titration explained and illustrated. `https://www.machinerylubrication.com/Read/594/karl-fischer-coulometric-titration`, mar 2004.

[25] CWG. Properties of mixture water/glycol - Extract from VDI-Warmeatlas Dd 17- VDI-Verlag GmbH. `https://detector-cooling.web.cern.ch/data/Table%208-3-1.htm`, aug 1991.

[26] V. A. Fassel and R. N. Kniseley. Inductively coupled plasma. Optical emission spectroscopy. *Analytical Chemistry*, 46(13):1110A–1120a, 1974.

[27] A. Fentress, J. Sander, and J. Ameye. The use of linear sweep voltammetry in condition monitoring of diesel engine oil. *Journal of ASTM International*, 8(7):1–10, 2011.

[28] A. B. Fialkov, A. Gordin, and A. Amirav. Hydrocarbons and fuels analyses with the supersonic gas chromatography mass spectrometry–The novel concept of isomer abundance analysis. *Journal of Chromatography A*, 1195(1-2):127–135, 2008.

[29] L. D. Field, H. L. Li, and A. M. Magill. *Organic structures from spectra*. John Wiley & Sons, 2020.

[30] J. Fitch. Glycol in lubricating oil - Detection, analysis and removal. `https://www.machinerylubrication.com/Read/193/oil-glycol`, jul 2001.

[31] J. C. Fitch. *Oil analysis for maintenance professional*. Noria Corporation, 1998.

[32] International Organization for Standarization. *ISO 4406:2021 Hydraulic fluid power–Fluids–method for coding the level of contamination by solid particles*, 2021. https://www.iso.org/standard/79716.html.

[33] M. F. Fox, Z. Pawlak, and D. J. Picken. Acid-base determination of lubricating oils. *Tribology international*, 24(6):335–340, 1991.

[34] K. Galer-Tatarowicz, G. Pazikowska-Sapota, G. Dembska, and K. Stasiek. Determination of petroleum compounds in bottom sediments. *Bulletin of the Maritime Institute in Gdansk*, 30:174–179, 01 2015. `doi:10.5604/12307424.1186448`.

[35] Torkelson Geochemistry. Examples of chromatograms: regular gasoline, aviation gasoline, aviation spirits, jet fuel, diesel fuel, 10w30 motor oil, crude oil. `https://torkelsongeochemistry.com/chromatogramexamples.html`, may 2007.

[36] S. Ghosh, V. L. Prasanna, B. Sowjanya, P. Srivani, M. Alagaraja, and et al. Inductively coupled plasma–optical emission spectroscopy: a review. *Asian Journal of Pharmaceutical Analysis*, 3(1):24–33, 2013.

[37] Grabner Instruments Messteckhnik GmbH. *Shipboard flashpoint testing of fuels and lube oils*, 2011. Application Note.

[38] M. Gollin and D. Bjork. Comparative performance of ethylene glycol/water and propylene glycol/water coolants in automobile radiators. In *International Congress & Exposition*. SAE International, mar 1996. doi:10.4271/960372.

[39] K. Gras, J. Luong, M. Lin, R. Gras, and R. A. Shellie. Determination of ethylene glycol in lubricants by derivatization static headspace gas chromatography. *Analytical Methods*, 7(13):5545–5550, 2015.

[40] J. P. Greaney and G. E. Cozzone. Comparative performance of aqueous propylene glycol and aqueous ethylene glycol coolants. In *International Congress & Exposition*. SAE International, mar 1999. doi:10.4271/1999-01-0134.

[41] S. V. Gupta. *Viscometry for Liquids*. Springer, 2016.

[42] G. Hall and E. Lightle. Determining fuel diluents in lubrication oils. *Practicing Oil Analysis*, 10:3–4, 2008.

[43] L. Han, W. Hong, and S. Wang. The key points of inductive wear debris sensor. In *Proceedings of 2011 International Conference on Fluid Power and Mechatronics*, pages 809–815. IEEE, 2011.

[44] G. R. Harrison. *Massachusetts Institute of Technology wavelength tables: Wavelengths by element*, volume 1. Mit Press, 1969.

[45] J. Hu, S. Yang, J. Zhang, L. Guo, and Y. Xin. The determination of lower acidity in several coloured oils by catalyzed thermometric titration. *Petroleum Chemistry*, 57(12), 2017.

[46] W. C. Hull, C. Robertson, J. Mullen, J. Stradling, and B. Sidwell. Analysis of ethylene glycol-based engine coolant as a vehicle fire fuel. In *Proceedings of the International Symposium on Fire Investigation Science and Technology, National Association of Fire Investigators, Sarasota, FL*, pages 1–12, 2008.

[47] Energy Institute. *IP 449: Petroleum products and lubricants - Determination of acid number - Non-aqueous potentiometric titration method*, 2000. ISBN:IP449-2934869.

[48] Energy Institute. *IP 417: Determination of base number - Potentiometric titration method*, 2004. ISBN:IP417-2938621.

[49] Energy Institute. *IP 431: Petroleum products - Determination of acid number - Semi-micro colour-indicator titration method*, 2004. ISBN:IP431-2934869.

[50] Energy Institute. *IP 139: Petroleum products and lubricants - Determination of acid or base number - Colour-indicator titration method*, 2017. ISBN:IP139-2938621.

[51] Energy Institute. *IP 276: Petroleum products - Determination of base number - Perchloric acid potentiometric titration method*, 2018. ISBN:IP276-7250659.

[52] Energy Institute. *IP 177: Determination of weak and strong acid number - Potentiometric titration method*, 2019. –.

[53] SPECTRO Analytical Instruments. *Which spectrometer optical technology offers superior performance? Echelle vs. ORCA*, 2020. White Paper.

[54] ASTM International. *ASTM D6810-13 Standard test method for measurement of hindered phenolic antioxidant content in non-zinc turbine oils by linear sweep voltammetry*, 2013. doi:10.1520/D6810-13.

[55] ASTM International. *ASTM D6971-09(2014) Standard test method for measurement of hindered phenolic and aromatic amine antioxidant content in non-zinc turbine oils by linear sweep voltammetry*, 2014. doi:10.1520/D6971-09R14.

[56] ASTM International. *ASTM D7590-09(2014) Standard guide for measurement of remaining primary antioxidant content In in-service Industrial lubricating oils by linear sweep voltammetry*, 2014. doi:10.1520/D7590-09R14.

[57] ASTM International. *ASTM D7593-14 Standard test method for determination of fuel dilution for in-service engine oils by gas chromatography*, 2014. doi:10.1520/D7593-14.

[58] ASTM International. *ASTM D7922-14 Standard test method for determination of glycol for in-service engine oils by gas chromatography*, 2014. doi:10.1520/D7922-14.

[59] ASTM International. *ASTM D2896-15 Standard test method for base number of petroleum products by potentiometric perchloric acid titration*, 2015. doi:10.1520/D2896-15.

[60] ASTM International. *ASTM D6224-16 Standard practice for in-service monitoring of lubricating oil for auxiliary power plant equipment*, 2016. doi:10.1520/D6224-16.

[61] ASTM International. *ASTM E168-16 Standard practices for general techniques of infrared quantitative analysis*, 2016. doi:10.1520/E0168-16.

[62] ASTM International. *ASTM D3339-12(2017) Standard test method for acid number of petroleum products by semi-micro color indicator titration*, 2017. doi:10.1520/D3339-12R17.

[63] ASTM International. *ASTM D4291-04 Standard test method for trace ethylene glycol in used engine oil*, 2017. doi:10.1520/D4291-04R17.

[64] ASTM International. *ASTM D4739-17 Standard test method for base number determination by potentiometric hydrochloric acid titration*, 2017. doi:10.1520/D4739-17.

[65] ASTM International. *ASTM D5984-11(2017) Standard test method for semi-quantitative field test method for base number in new and used lubricants by color-indicator titration*, 2017. doi:10.1520/D5984-11R17.

[66] ASTM International. *ASTM D8045-17e1 Standard test method for acid number of crude oils and petroleum products by catalytic thermometric titration*, 2017. doi:10.1520/D8045-17E01.

[67] ASTM International. *ASTM D5185-18 Standard test method for multielement determination of used and unused lubricating oils and base oils by Inductively Coupled Plasma Atomic Emission Spectrometry (ICP-AES)*, 2018. doi:10.1520/D5185-18.

[68] ASTM International. *ASTM D664-18e2 Standard test method for acid number of petroleum products by potentiometric titration*, 2018. doi:10.1520/D0664-18E02.

[69] ASTM International. *ASTM D7412-18 Standard test method for condition monitoring of phosphate antiwear additives in in-service petroleum and hydrocarbon based lubricants by trend analysis using Fourier Transform Infrared (FT-IR) spectrometry*, 2018. doi:10.1520/D7412-18.

[70] ASTM International. *ASTM D7414-18 Standard test method for condition monitoring of oxidation in in-service petroleum and hydrocarbon based lubricants by trend analysis using Fourier Transform Infrared (FT-IR) spectrometry*, 2018. doi:10.1520/D7414-18.

[71] ASTM International. *ASTM D7415-18 Standard test method for condition monitoring of sulfate by-products in in-service petroleum and hydrocarbon based lubricants by trend analysis using Fourier Transform Infrared (FT-IR) spectrometry*, 2018. doi:10.1520/D7415-18.

[72] ASTM International. *ASTM D7527-10(2018) Standard test method for measurement of antioxidant content in lubricating greases by linear sweep voltammetry*, 2018. doi:10.1520/D7527-10R18.

[73] ASTM International. *ASTM D7624-18 Standard test method for condition monitoring of nitration in in-service petroleum and hydrocarbon-based lubricants by trend analysis using Fourier Transform Infrared (FT-IR) spectrometry*, 2018. doi:10.1520/D7624-18.

[74] ASTM International. Astm d7647-10(2018) standard test method for automatic particle counting of lubricating and hydraulic fluids using dilution techniques to eliminate the contribution of water and interfering soft particles by light extinction. 2018. doi:10.1520/D7647-10R18.

[75] ASTM International. *ASTM D92-18 Standard test method for flash and fire points by Cleveland open cup tester*, 2018. doi:10.1520/D0092-18.

[76] ASTM International. *ASTM E2412-10(2018) Standard practice for condition monitoring of in-service lubricants by trend analysis using Fourier Transform Infrared (FT-IR) spectrometry*, 2018. doi:10.1520/E2412-10R18.

[77] ASTM International. *ASTM D4951-14(2019) Standard test method for determination of additive elements in lubricating oils by Inductively Coupled Plasma Atomic Emission Spectrometry*, 2019. doi:10.1520/D4951-14R19.

[78] ASTM International. *ASTM D3524-14(2020) Standard test method for diesel fuel diluent in used diesel engine oils by gas chromatography*, 2020. doi:10.1520/D3524-14R20.

[79] ASTM International. *ASTM D3525-20 Standard test method for gasoline fuel dilution in used gasoline engine oils by wide-bore capillary gas chromatography*, 2020. doi:10.1520/D3525-20.

[80] ASTM International. *ASTM D4378-20 Standard practice for in-service monitoring of mineral turbine oils for steam, gas, and combined cycle turbines*, 2020. doi:10.1520/D4378-20.

[81] ASTM International. *ASTM D6304-20 Standard test method for determination of water in petroleum products, lubricating oils, and additives by coulometric Karl Fischer titration*, 2020. doi:10.1520/D6304-20.

[82] ASTM International. *ASTM D7214-20 Standard test method for determination of the oxidation of used lubricants by FT-IR using peak area increase calculation*, 2020. doi:10.1520/D7214-20.

[83] ASTM International. *ASTM D7279-20 Standard test method for kinematic viscosity of transparent and opaque liquids by automated Houillon viscometer*, 2020. doi:10.1520/D7279-20.

[84] ASTM International. *ASTM D7418-20 Standard practice for set-up and operation of Fourier Transform Infrared (FT-IR) spectrometers for in-service oil condition monitoring*, 2020. doi:10.1520/D7418-20.

[85] ASTM International. *ASTM D7844-20 Standard test method for condition monitoring of soot in in-service lubricants by trend analysis using Fourier Transform Infrared (FT-IR) Spectrometry*, 2020. doi:10.1520/D7844-20.

[86] ASTM International. *ASTM D93-20 Standard test methods for flash point by Pensky-Martens closed cup tester*, 2020. doi:10.1520/D0093-20.

[87] ASTM International. *ASTM D445-21 Standard test method for kinematic viscosity of transparent and opaque liquids (and calculation of dynamic viscosity)*, 2021. doi:10.1520/D0445-21.

[88] ASTM International. *ASTM D7042-21 Standard test method for dynamic viscosity and density of liquids by Stabinger viscometer (and the calculation of kinematic viscosity)*, 2021. doi:10.1520/D7042-21.

[89] ASTM International. *ASTM D974-21 Standard Test Method for Acid and Base Number by Color-Indicator Titration*, 2021. doi:10.1520/D0974-21.

[90] P. G. Ivanova and Z. V. Aneva. Assessment and assurance of quality in water measurement by coulometric Karl-Fischer titration of petroleum products. *Accreditation and quality assurance*, 10(10):543–549, 2006.

[91] Y. Iwai, T. Honda, T. Miyajima, S. Yoshinaga, M. Higashi, and Y. Fuwa. Quantitative estimation of wear amounts by real time measurement of wear debris in lubricating oil. *Tribology International*, 43(1-2):388–394, 2010.

[92] A. Jefferies and J. Ameye. RULER and used engine oil analysis programs. *Tribology & Lubrication Technology*, 54(5):29, 1998.

[93] D. W. Johnson. *Lubrication - Tribology, lubricants and additives*. BoD–Books on Demand, 2018.

[94] J. J. JuGer and R. F. Crook. Heat transfer performance of propylene glycol versus ethylene glycol coolant solutions in laboratory testing. In *International Congress & Exposition*. SAE International, feb 1999. doi:10.4271/1999-01-0129.

[95] R. E. Kauffman. Rapid, portable voltammetric techniques for performing antioxidant, total acid number (TAN) and total base number (TBN) measurements. *Tribology & Lubrication Technology*, 54(1):39, 1998.

[96] W. Kemp. *Organic spectroscopy*. Macmillan International Higher Education, 2017.

[97] M. Koch, S. Tenbohlen, I. Hoehlein, and J. Blennow. Reliability and improvements of water titration by the karl fischer technique. In *Proceedings of the XVth International Symposium on High Voltage Engineering, ISH, Ljubljana, Slovenia*, volume 1, page 2, 2007.

[98] A. Kramida, Y. Ralchenko, J. Reader, and NIST ASD Team. *Atomic spectra database - NIST standard reference database 78, Version 5.8*, 2020. doi:10.18434/T4W30F.

[99] M. Lanz, C. A. De Caro, K. Rüegg, and A. De Agostini. Coulometric Karl-Fischer titration with a diaphragm-free cell: cell design and applications. *Food chemistry*, 96(3):431–435, 2006.

[100] D. M. Levermore, M. Josowicz, W. S. Rees, and J. Janata. Headspace analysis of engine oil by gas chromatography/mass spectrometry. *Analytical chemistry*, 73(6):1361–1365, 2001.

[101] Z. Liang, L. Chen, M. S. Alam, S. Z. Rezaei, C. Stark, H. Xu, and R. M. Harrison. Comprehensive chemical characterization of lubricating oils used in modern vehicular engines utilizing GC× GC-TOFMS. *Fuel*, 220:792–799, 2018.

[102] J. Luong, R. Gras, H. J. Cortes, and R. A. Shellie. Determination of trace ethylene glycol in industrial solvents and lubricants using phenyl boronic acid derivatization and multidimensional gas chromatography. *Analytica Chimica Acta*, 805:101–106, 2013.

[103] C. W. Mackosko. *Rheology: principles, measurements and applications*. Wiley-VCH, 1994.

[104] A. Y. Malkin and A. I. Isayev. *Rheology: concepts, methods, and applications*. Elsevier, 2017.

[105] T. Mang and W. Dresel. *Lubricants and lubrication*. John Wiley & Sons, 2007.

[106] M. Marzban, M. Packirisamy, and J. Dargahi. 3D suspended polymeric microfluidics (SPMF3) with flow orthogonal to bending (FOB) for fluid analysis through kinematic viscosity. *Applied Sciences*, 7(10):1048, 2017.

[107] G. Miró Mezquita, B. Tormos, H. Allmaier, and C. Knauder. Current trends in ICE wear detection technologies: from lab to field. *ASRO Journal of Applied Mechanics*, 2(1):32–41, 2017.

[108] G. L. Moore. *Introduction to inductively coupled plasma atomic emission spectrometry*. Elsevier, 2012.

[109] P. Muthuvel, B. George, and G. A. Ramadass. Magnetic-capacitive wear debris sensor plug for condition monitoring of hydraulic systems. *IEEE Sensors Journal*, 18(22):9120–9127, 2018.

[110] B. Myle and R. Kauffman. The use of cyclic voltammetric antioxidant analysis for proactive engine oil condition monitoring program. In *Spring Fuels & Lubricants Meeting & Exposition*. SAE International, jan 2000. doi:10.4271/2000-01-1810.

[111] R. A. K. Nadkarni and J. L. Lane. Determination of kinematic viscosity of used lubricating oils using houillon viscometer. *Journal of ASTM International*, 8(7):1–11, 2011.

[112] R. Niculescu, V. Iorga-Simăn, A. Trică, and A. Clenci. Study on the engine oil's wear based on the flash point. *IOP Conference Series: Materials Science and Engineering*, 147(1):012124, aug 2016.

[113] U. Nordmark and A. Cedergren. Conditions for accurate Karl-Fischer coulometry using diaphragm-free cells. *Analytical chemistry*, 72(1):172–179, 2000.

[114] National Insitute of Standards and Technology. NIST Chemistry WebBook, SRD 69: Water. https://webbook.nist.gov/cgi/cbook.cgi?ID=C7732185&Type=IR-SPEC&Index=1, oct 2021.

[115] Y. Peng, T. Wu, S. Wang, and Z. Peng. Wear state identification using dynamic features of wear debris for on-line purpose. *Wear*, 376:1885–1891, 2017.

[116] F. M. Phelps III. MIT wavelength tables. Second Edition, Volume 2: Wavelengths by element. *Cambridge: Massachusetts Institute of Technology (MIT) Press*, 1982.

[117] G. O. Piloyan and Y. V. Dolinina. On the theory of thermometric titration. *Talanta*, 21(9):975–978, 1974.

[118] W. Richter and U. Tinner. *Practical aspects of modern titration*, 2004.

[119] J. Rinkinen and L. Elo. Clean components of fluid power system reduce maintenance costs. In *International conference on maintenance, condition monitoring and diagnostics, and maintenance performance measurement and management*, pages 81–88, 2015.

[120] K. A. Rubinson and J. F. Rubinson. *Análisis instrumental*. Pearson Publications Company, 2001.

[121] T. D. Ruppel and G. Hall. Determination of ethylene glycol in used engine oil by headspace-gas chromatography. *PerkinElmer Life and Analytical Sciences*, 2005.

[122] R.l Sánchez, J. L. Todolí, C. Lienemann, and J. Mermet. Determination of trace elements in petroleum products by inductively coupled plasma techniques: a critical review. *Spectrochimica Acta Part B: Atomic Spectroscopy*, 88:104–126, 2013.

[123] G. Schlemmer, L. Balcaen, J. L. Todolí, and M. W. Hinds. *Elemental analysis: An introduction to modern spectrometric techniques*. Walter de Gruyter GmbH & Co KG, 2019.

[124] Spectro Scientific. *Guide to measuring fuel dilution in lubricating oil*, 2017. White Paper.

[125] Spectro Scientific. *Guide to measuring water in oil*, 2017. White Paper.

[126] L. Severa, M. Havlíček, and V. Kumbár. Temperature dependent kinematic viscosity of different types of engine oil. *Acta Universitatis Agriculturae et Silviculturae Mendelianae Brunensis*, 57(4):95–102, 2009.

[127] B. Sharma and O. P. Gandhi. Reliability analysis of engine oil using "polygraph approach". *Industrial Lubrication and Tribology*, 2008.

[128] F. B. Sherman. Determination of water with a modified Karl-Fischer reagent–Stability and the mechanism of reaction with water. *Talanta*, 27(12):1067–1072, 1980.

[129] B. C. Smith. *Fundamentals of Fourier Transform Infrared Spectroscopy*. CRC press, 2011.

[130] T. Smith. *Practical thermometric titrimetry*, 2006.

[131] J. Sneddon. *Sample introduction in atomic spectroscopy*. Elsevier, 2012.

[132] D. M. Stehouwer and R. D. Hudgens. Coolant contamination of diesel engine oils. In *International Congress & Exposition*. SAE International, jan 1987. doi:10.4271/1870645.

[133] B. H. Stuart. *Infrared spectroscopy: fundamentals and applications*. John Wiley & Sons, 2004.

[134] A. M. Toms, J. R. Powell, and J. Dixon. *The utilization of FT-IR for Army oil condition monitoring*, 1998.

[135] B. Tormos. *Diagnóstico de motores diesel mediante el análisis del aceite usado*. Reverté, 2005.

[136] F. R. van de Voort, J. Sedman, R. Cocciardi, and S. Juneau. An automated FTIR method for the routine quantitative determination of moisture in lubricants: An alternative to Karl-Fischer titration. *Talanta*, 72(1):289–295, 2007.

[137] F. R. Van De Voort, J. Sedman, R. A. Cocciardi, and D. Pinchuk. FTIR condition monitoring of in-service lubricants: ongoing developments and future perspectives. *Tribology Transactions*, 49(3):410–418, 2006.

[138] J. C. Van Loon. *Analytical atomic absorption spectroscopy: selected methods*. Elsevier, 2012.

[139] J. C. Verhoef and E. Barendrecht. Mechanism and reaction rate of the Karl-Fischer titration reaction: Part I. Potentiometric measurements. *Journal of Electroanalytical Chemistry and Interfacial Electrochemistry*, 71(3):305–315, 1976.

[140] D. S. Viswanath, T. K. Ghosh, D. H. L. Prasad, N. V. K. Dutt, and K. Y. Rani. *Viscosity of liquids: theory, estimation, experiment, and data*. Springer Science & Business Media, 2007.

[141] J. Wakiru, L. Pintelon, P. Chemweno, and P. Muchiri. Analysis of lubrication oil contamination by fuel dilution with application of cluster analysis. In *Proceedings of the XVII International Scientific Conference on Industrial Systems, University of Novi Sad, Novi Sad, Serbia*, pages 4–6, 2017.

[142] J. M. Wakiru, L. Pintelon, P. N. Muchiri, and P. K. Chemweno. A review on lubricant condition monitoring information analysis for maintenance decision support. *Mechanical Systems and Signal Processing*, 118:108–132, 2019.

[143] H. Wei, C. Wenjian, W. Shaoping, and M. M. Tomovic. Mechanical wear debris feature, detection, and diagnosis: A review. *Chinese Journal of Aeronautics*, 31(5):867–882, 2018.

[144] R. K. Winge, V. J. Peterson, and V. A. Fassel. Inductively coupled plasma-atomic emission spectroscopy: prominent lines. *Applied Spectroscopy*, 33(3):206–219, 1979.

[145] A. Wolak, G. Zajac, and T. Slowik. Measuring kinematic kiscosity of engine oils: a comparison of data obtained from four different devices. *Sensors*, 21(7):2530, 2021.

[146] C. Xinkun. Atomic emission spectroscopy. *Chinese Journal of Analysis Laboratory*, 4, 1991.

[147] V. Yeung, D. D. Miller, and M. A. Rutzke. Atomic absorption spectroscopy, atomic emission spectroscopy, and inductively coupled plasma-mass spectrometry. In *Food Analysis*, pages 129–150. Springer, 2017.

[148] S. T. Zenchelsky. Thermometric titration. *Analytical Chemistry*, 32(5):289–292, 1960.

[149] H. Zhan, Y. Song, H. Zhao, J. Gu, H. Yang, and S. Li. Study of the sensor for on-line lubricating oil debris monitoring. *Sensors & Transducers*, 175(7):214, 2014.

[150] X. Zhu, C. Zhong, and J. Zhe. Lubricating oil conditioning sensors for online machine health monitoring–a review. *Tribology International*, 109:473–484, 2017.

Chapter 4

Evaluation of lubricating engine oils under real-working conditions

Contents

4.1 Introduction

In this chapter, the results of a real fleet test, lasting 2 years, where the performance of several formulations of Low Viscosity Engine Oils (LVEO) were studied [1], are presented. The study of the performance of this type of engine oil is based on the interest in fuel savings due to the reduction of mechanical losses resulting from the use of engine oils with a lower viscosity. However, viscosity reduction (outside the range recommended by the OEMs) always carries the risk of engine problems due to the use of engine oils that do not comply with the engine manufacturers' recommendations. It is in this aspect that this study is being carried out, as the aim is to find out whether these new engine oils do not have negative repercussions on engines in order to benefit from their potential in terms of fuel economy.

4.2 Definition of field tests on vehicle fleet

With the objective to achieve the most reliable study possible, a series of prior aspects were defined that had to be fulfilled in order to neutralise possible external influences that could disturb or alter the results that would be obtained. The assumptions made in this study were as follows:

- As it is required to contrast the performance of the LVEOs with those recommended by the OEM, the recommended engine oil (Lube A) was selected as the reference oil to compare the performance of the other formulations: Lube B, Lube C, Lube D and Lube E.
- In order to obtain a representative sample of the current automotive population, it was decided to take several vehicle models with different engine technologies. In this way a certain validation of the results derived from the study is given.
- Another aspect is to design a long-term research project, at least on an annual basis, so that the vehicles involved are under the conditions they would experience in a year of regular use. Thanks to this, fluctuations due to external environmental factors (temperature, humidity, pressure, etc.) are minimised, so that at the end of the trial all participants would be exposed to the same weather of each season.
- The amount of data required for such an investigation must be large in order to give statistical significance to the data obtained. For that

reason, the field test required a large number of vehicles involved that were accessible to be monitored to ensure that the maximum amount of data could be collected in the selected annual period.

- The last assumption is correlated with the precision. In order to achieve accurate results, a sampling plan was designed following defined guidelines according to how the engine oil sample had to be collected and the sampling interval (mileage) for the entire test.

In accordance with these premises, a two-stage test was carried out covering a total of more than 500 samples collected (260 in the first stage and 255 in the second stage), totalling around 7250000 kilometres between them.

This chapter will present the results obtained from the study of 5 different engine oil formulations tested. The main characteristics of the 5 formulations studied, A, B, C, D, and E, are listed in the Table 4.1.

Table 4.1. *Main properties of the different engine oils studied.*

Parameter	Lub. A	Lub. B	Lub. C	Lub. D	Lub. E
SAE grade	5W30	5W30	5W30	10W30	10W30
Base Oil	G III + IV	G III	G III	G III	G III
SAPS level	Mid	Mid	Mid	Mid	Mid
API category	CJ–4	CK–4	FA–4	CK–4	FA–4
HTHS @ 150° C (cP)	3.5	3.5	3.0	3.5	3.0
KV @ 40° C (cSt)	71.45	68.22	54.97	76.80	57.06
KV @ 100° C (cSt)	12.04	12.61	10.47	12.23	9.66
TBN (mg KOH/g)	10.66	11.26	11.79	15.15	12.92

Each of the formulations has been selected to analyse and evaluate their performance in real conditions of use, taking into account their difference in viscosity and additivation (Figure 4.1), on vehicles having distinct engine technologies and using two different fuels: diesel and Compressed Natural Gas (CNG).

In order to assess the different aspects that are capable of providing the tasks of OCM (Oil Condition Monitoring) through the analysis of engine oil, it is required:

- First, to investigate the degradation of the different engine oil formulations that were chosen.

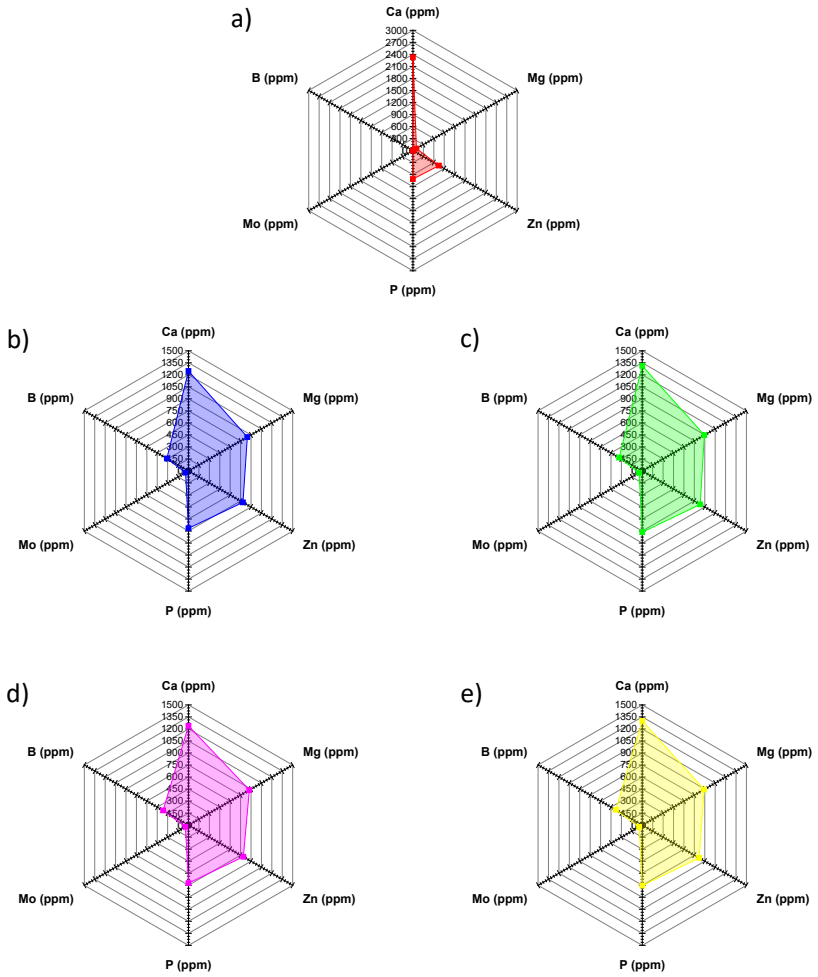

Figure 4.1. *Additive package of the different engine oil formulations tested: a) Lubricant A, b) Lubricant B, c) Lubricant C, d) Lubricant D and e) Lubricant E.*

- The second point is to analyse the possible effects on the engine wear rate and its potential consequences on the engine lifetime.
- The final objective is to corroborate that the lubricant formulations fulfil their purpose satisfactorily, in relation to the lubricant Oil Drain Interval (ODI), without having negative effects on the vehicles used in the test.

A total of 46 vehicles will take part in the test, distributed in several categories according to the characteristics listed in the Table 4.2.

Table 4.2. *Main features of the vehicles selected for testing.*

Parameter	Type I	Type II	Type III	Type IV
Year	2008	2010	2007	2010
Cert. emissions	Euro IV	Euro V	EEV	EEV
Fuel type	Diesel	Diesel	CNG	Diesel
Length, Width, Height (m)	17.94, 2.53, 3.00	11.95, 2.53, 3.00	12.00, 2.50, 3.30	12.00, 2.50, 3.10
Weigth (tons)	17.50	12.70	12.10	12.41
Eng. Volum. Displacement (c.c.)	11967	7200	11967	9300
Cylinders	6	6	6	5
Max. power (kW)	220 @ 2200 rpm	210 @ 2200 rpm	180 @ 2200 rpm	170 @ 1900 rpm
Max. torque (N·m)	1600 @ 1100 rpm	1100 @ 1100 rpm	880 @ 1000 rpm	1050 @ 1500 rpm
BMEP (bar)	16.80 @ 1100 rpm	19.50 @ 1100 rpm	9.24 @ 1000 rpm	14.20 @ 1500 rpm
Thermal load (W/mm^2)	2.85	3.97	2.33	2.56
Crankcase volume (L)	31	29	33	31
Turbocharging	Turbo+Intercooler	Turbo+Intercooler	Turbo+Intercooler	Turbo+Intercooler
EGR	No	No	No	Yes
Number of vehicles	9	10	19	10

In addition to the characteristics of the vehicles, information has also been collected related about the metals present in the internal elements of the different types of engines (metallographic study) participating in the test. All the information that could be collected has been compiled and organised in Table 4.3.

Table 4.3. *Metallography of the engines of the different types of vehicles participating in the study.*

Components	Type I	Type II	Type III	Type IV
Piston-Cylinder Interface	Hardened steel sleeve	Liner	Hardened steel sleeve	-
Piston rings	Ceramic Cr (3.0 mm) Cr (3.0 mm) Ceramic Cr (4.0 mm)	Ceramic Cr (3.5 mm) Cr (2.5 mm) Cr (4.0 mm)	Ceramic Cr (3.5 mm) P (3.0 mm) Cr (4.0 mm)	-
Coonecting rod bearings	-	Steel + Al coating Steel + Bronze/Pb + Cu 6% coating	Steel + Bronze/Pb + Cu 6% coating	Steel + Bronze + Cu 3% coating
Main shaft bearings	Steel + Bronze/Pb + Cu 3% coating Steel + Bronze/Pb + Cu sputter	Steel + Al coating Steel + Bronze/Pb + Cu 6% coating	Steel + Bronze/Pb + Cu 3% coating	Steel + Bronze + Cu 3% coating
Valve control system	OHV Roller follower (hardened steel)	OHV Cam follower (steel)	OHV Cam follower (steel)	OHV
Camshaft bearings	Bronze/Pb	Steel + Bronze/Pb coating	Steel + Al coating Steel + Bronze/Pb coating	-

For reasons of organisational efficiency, the study of engine oil formulations performance was planned in two stages; in each stage, a different pair of oil formulations and a reference oil (formulation A) were studied. The distribution of the different engine oils in each vehicles followed the next pattern (Table 4.4):

Table 4.4. *Engine oil distribution in the two stages test.*

Vehicle	Total	Lub. A	Lub. B	Lub. C	Lub. D	Lub. E
Type I	9	-	4^{a}	5^{a}	4^{b}	5^{b}
Type II	10	$5^{a,b}$	5^{a}	-	5^{b}	-
Type III	19	-	9^{a}	10^{a}	9^{b}	10^{b}
Type IV	10	-	6^{a}	4^{a}	6^{b}	4^{b}

a) First iteration: Lubes A (ref.), B, C

b) Second iteration: Lubes A (ref.), D, E

According to Table 4.4, in addition to follow the distribution of engine oils, the vehicles employed in the two stages were the same. This means that, for a given vehicle, the change of oil between stages would follow the pattern: Lube A–Lube A, Lube B–Lube D and Lube C–Lube E. In this way, the aim is to achieve a better monitoring of the condition of the vehicles and to keep the API grade of the investigated formulations constant.

For each of these two stages, a sampling campaign was required in order to analyse the samples at the CMT–Motores Térmicos Fuels and Lubricants laboratory (Figure 4.2).

Figure 4.2. *Fuels and Lubricants laboratory of CMT–Motores Térmicos.*

The sampling plan was organised according to the mileage accumulated by the engine oil starting from its initial stage (new or fresh engine oil, 0 km) until the ODI at 30000 kilometres was reached. Within this range, samples were taken every 5000 kilometres (see Figure 4.3), so that for each case, a total

of 7 samples were available: 0, 5000, 10000, 15000, 20000, 25000 and 30000 kilometres.

Figure 4.3. *Sampling of engine oil directly into the crankcase.*

For each of these collected samples an analysis protocol was carried out, comprising a wide variety of parameters, see Table 4.5, which were monitored with the final purpose of being able to observe the trend of the performance for each formulation studied.

Table 4.5. *Analytical techniques applied to the study of engine oils.*

Topic	Parameter	Analytical technique	Standard
Degradation	Kinematic viscosity	Capillarity viscometer	ASTM D455
Degradation	TAN	Thermometric titration	ASTM D8045
Degradation	TBN	Thermometric titration	Metrohm App. Bulletin AB–405/2
Degradation	Oxidation	FT–IR spectroscopy	ASTM D7414
Degradation	Nitration	FT–IR spectroscopy	ASTM D7624
Degradation	Aminic additives	FT–IR spectroscopy	ASTM E2412
Degradation	Antiwear additives	FT–IR spectroscopy	ASTM D7412
Degradation	Antoixidant additives	Linnear Sweep Votammetry	ASTM D7590
Contamination	Soot	FT–IR spectroscopy	ASTM D7844
Contamination	Fuel dilution	FT–IR spectroscpy	ASTM E2412
Contamination	Coolant	FT–IR spectroscpy	ASTM E2412
Contamination	Water	Karl–Fischer coulometric titration	ASTM D6304
Wear	Metallic additive package	ICP–OES spectrometry	ASTM D4951
Wear	Wear metals	ICP–OES spectrometry	ASTM D5185

Accordingly, at the end of this study, a library of data was built pertaining to each vehicle and engine oil formulation with which to analyse the performance trends of the specific engine oil as well as their impact on

the vehicle in which they were used. An example of the document with the collected data is shown in the Figure 4.4.

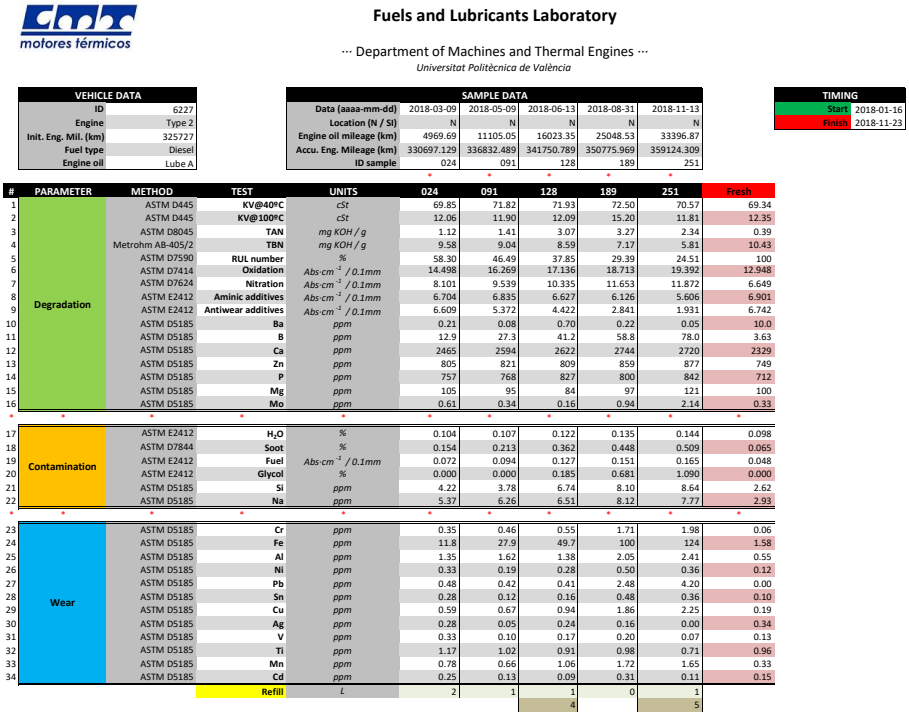

motores térmicos

Fuels and Lubricants Laboratory

··· Department of Machines and Thermal Engines ···

Universitat Politècnica de València

VEHICLE DATA	
ID	6227
Engine	Type 2
Init. Eng. Mil. (km)	325727
Fuel type	Diesel
Engine oil	Lube A

SAMPLE DATA					
Data (aaaa-mm-dd)	2018-03-09	2018-05-09	2018-06-13	2018-08-31	2018-11-13
Location (N / SI)	N	N	N	N	N
Engine oil mileage (km)	4969.69	11105.05	16023.35	25048.53	33396.87
Accu. Eng. Mileage (km)	330697.129	336832.489	341750.789	350775.969	359124.309
ID sample	024	091	128	189	251

TIMING	
Start	2018-01-16
Finish	2018-11-23

#	PARAMETER	METHOD	TEST	UNITS	024	091	128	189	251	Fresh
1	Degradation	ASTM D445	KV@40ºC	cSt	69.85	71.82	71.93	72.50	70.57	69.34
2		ASTM D445	KV@100ºC	cSt	12.06	11.90	12.09	15.20	11.81	12.35
3		ASTM D8045	TAN	mg KOH / g	1.12	1.41	3.07	3.27	2.34	0.39
4		Metrohm AB-405/2	TBN	mg KOH / g	9.58	9.04	8.59	7.17	5.81	10.43
5		ASTM D7590	RUL number	%	58.30	46.49	37.85	29.39	24.51	100
6		ASTM D7414	Oxidation	$Abs{\cdot}cm^{-1}$ /0.1mm	14.498	16.269	17.136	18.713	19.392	12.948
7		ASTM D7624	Nitration	$Abs{\cdot}cm^{-1}$ /0.1mm	8.101	9.539	10.335	11.653	11.872	6.649
8		ASTM E2412	Aminic additives	$Abs{\cdot}cm^{-1}$ /0.1mm	6.704	6.835	6.627	6.126	5.606	6.901
9		ASTM E2412	Antiwear additives	$Abs{\cdot}cm^{-1}$ /0.1mm	6.609	5.372	4.422	2.841	1.931	6.742
10		ASTM D5185	Ba	ppm	0.21	0.08	0.70	0.22	0.05	10.0
11		ASTM D5185	B	ppm	12.9	27.3	41.2	58.8	78.0	3.63
12		ASTM D5185	Ca	ppm	2465	2594	2622	2744	2720	2329
13		ASTM D5185	Zn	ppm	805	821	809	859	877	749
14		ASTM D5185	P	ppm	757	768	827	800	842	712
15		ASTM D5185	Mg	ppm	105	95	84	97	121	100
16		ASTM D5185	Mo	ppm	0.61	0.34	0.16	0.94	2.14	0.33
17	Contamination	ASTM E2412	H_2O	%	0.104	0.107	0.122	0.135	0.144	0.098
18		ASTM D7844	Soot	%	0.154	0.213	0.362	0.448	0.509	0.065
19		ASTM E2412	Fuel	$Abs{\cdot}cm^{-1}$ /0.1mm	0.072	0.094	0.127	0.151	0.165	0.048
20		ASTM E2412	Glycol	%	0.000	0.000	0.185	0.681	1.090	0.000
21		ASTM D5185	Si	ppm	4.22	3.78	6.74	8.10	8.64	2.62
22		ASTM D5185	Na	ppm	5.37	6.26	6.51	8.12	7.77	2.93
23	Wear	ASTM D5185	Cr	ppm	0.35	0.46	0.55	1.71	1.98	0.06
24		ASTM D5185	Fe	ppm	11.8	27.9	49.7	100	124	1.58
25		ASTM D5185	Al	ppm	1.35	1.62	1.38	2.05	2.41	0.55
26		ASTM D5185	Ni	ppm	0.33	0.19	0.28	0.50	0.36	0.12
27		ASTM D5185	Pb	ppm	0.48	0.42	0.41	2.48	4.20	0.00
28		ASTM D5185	Sn	ppm	0.28	0.12	0.16	0.48	0.36	0.10
29		ASTM D5185	Cu	ppm	0.59	0.67	0.94	1.86	2.25	0.19
30		ASTM D5185	Ag	ppm	0.28	0.05	0.24	0.16	0.00	0.34
31		ASTM D5185	V	ppm	0.33	0.10	0.17	0.20	0.07	0.13
32		ASTM D5185	Ti	ppm	1.17	1.02	0.91	0.98	0.71	0.96
33		ASTM D5185	Mn	ppm	0.78	0.66	1.06	1.72	1.65	0.33
34		ASTM D5185	Cd	ppm	0.25	0.13	0.09	0.31	0.11	0.15
			Refill	L	2	1	1	0	1	
							4		5	

Figure 4.4. *Example of report colleted along the study.*

In accordance with the parameters listed in the report shown in Figure 4.4, the aspects to be considered for the research study that concerns this Thesis are listed below:

- The first point is the kinematic viscosity values at both test temperatures, 40 and 100 degrees Celsius, measured by glass capillarity viscometers.

- TAN and TBN indexes, determined by thermometric titration procedure, are also discussed in more depth below.

- By using FT–IR spectroscopy, oxidation and nitration values are obtained, as well as the evolution of the amine and anti-wear additives.

- To monitor the degradation of the antioxidant additive (AO) package, the RUL number is used to understand its evolution during the whole test.

- With regard to the contamination that may be present in a sample of engine oil, efforts are focused on determining the content of: soot, silicon (atmospheric dust) and sodium (additive in the coolant). At this point, the representation of the percentage of fuel present in the lubricating oil was discarded (for those engine oil formulations used in diesel vehicles) since in none of the samples the diesel content was higher than 2%. Similarly, the water content collected was not of interest for monitoring purposes. However, as a preview of what will be shown later, problems of coolant leakage could be monitored by ICP–OES by monitoring the sodium content in a satisfactory way (leaving aside the FT–IR study).

- Finally, the analysis of metallic content in the oil samples, both from the additive package and from the engine wear, carried out by ICP–OES spectrometry focused particularly on:

  - As far as metals from engine wear are concerned, the selection of elements was based on their relevance; therefore, the elements chosen were: iron, copper, aluminium and lead.
  - Whereas for metals whose origin lies in the additive package of the engine oil formulation, only those elements that are present will be shown: calcium, magnesium, molybdenum, zinc, phosphorus and boron.

These parameters mentioned above are the ones that will be used, due to their interest during the whole test in order to study the performance of the five engine oil formulations. The proposed study procedure consists of analysing the trends of each of the selected parameters. Therefore, a series of graphs have been prepared for each parameter where each individual data analysed has been plotted. Therefore, a total of 22 plots will be prepared in this section.

Due to the large number of different graphics, a more generalised representation of the data was chosen because, despite having each participating vehicle identified, the complexity of the symbols in the graphs made them difficult to understand. So, in view of this event, graphs have been generated only by vehicle type (type I, type II, type III and type IV) and by lubricating oil (Lube A, Lube B, Lube C and Lube D).

In the following graphs, each engine oil formulation has been identified with an individual colour:

- **Lube A** will be red.
- **Lube B**, its identifying colour shall be blue.
- **Lube C** will be coloured by green.
- **Lube D** shall be identified by the colour pink.
- **Lube E** will finally be represented by the colour yellow.

And the initial values (at 0 km) of each of these five formulations shall be symbolised by a ■ coloured with its corresponding colour. From this point onwards, the results will be displayed according to the vehicle where they were tested.

4.3 Engine oil analysis results

The results obtained from the analysis of the different engine lubricating oil samples collected during the two stages of the study are shown below, organised according to the type of engine where tested: type I, type II, type III and type IV. In this way, it is easier to understand the performance of the different lubricating oil formulations between the two stages, given that the vehicles involved are the same so that any differences that may be reported are a direct consequence of the lubricating oil used in each case and situation (leaving aside problems or failures that were not foreseen).

4.3.1 Engine oil performance in type I vehicles

In this type of vehicles, the engine oils tested are the following: B, C, D and E. So each of the graphs will show the evolution of the performance of these four different formulations.

Firstly, as the most important parameter, the results obtained by analysing the kinematic viscosity (KV) at 40 and 100 degrees are shown in Figure 4.5.

When analysing the first pair, Lube B and Lube C, the evolution of their kinematic viscosity is very similar. Looking at the viscosity at 40 degrees, the value remains practically stable throughout the period of use, while at 100

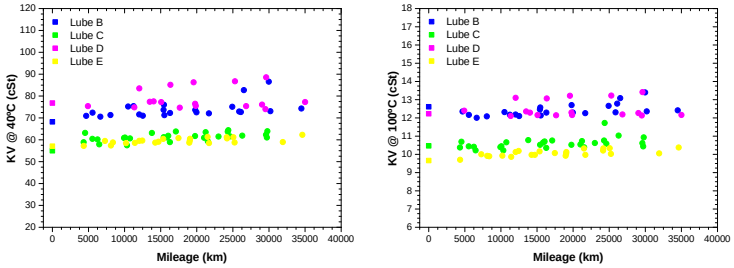

(a) Kinematic viscosity at 40°C (b) Kinematic viscosity at 100°C

Figure 4.5. *Evolution of KV of the engine oils used in vehicles type I.*

degrees, a slight increase is observed. Furthermore, in the case of Lube B, according to its API CK–4 lubricant classification, the values at 100°C (for fresh oil) are slightly outside the range stipulated by the SAE J300 standard. For the next couple, Lube D and Lube E, both at 40°C and 100°C, in all cases it can be detected that the value remains stable during the whole test.

The following Figure 4.6 shows the results obtained when analysing the oxidation and nitration of the 4 engine oil formulations by FT–IR spectroscopy according to the corresponding ASTM standards.

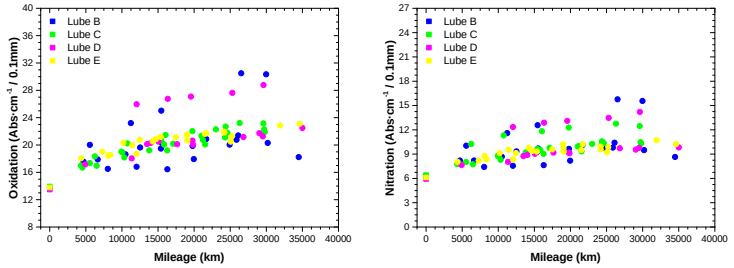

(a) Oxidation, by FT–IR, of the tested engine oils (b) Nitration, by FT–IR, of the tested engine oils

Figure 4.6. *Evolution of oxidation and nitration of the engine oils used in vehicles type I.*

In general terms, given that sometimes the influences of different vehicles can alter the correct interpretation of results, oxidation and nitration values for each pair (Lube B–Lube C and Lube D–Lube E) show a very similar upward trend between them as the engine oil accumulates mileage.

So, if we now move on to analyse the additives that are present in the formulations, it is here where we begin to see divergences between one type of engine oil and another. The casuistry that takes place during this study is reflected in Figure 4.7.

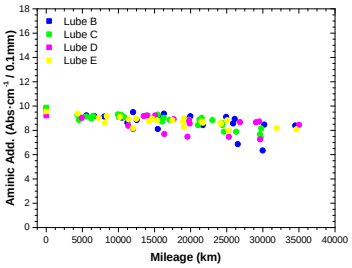

(a) Aminic additives by FT–IR spectroscopy

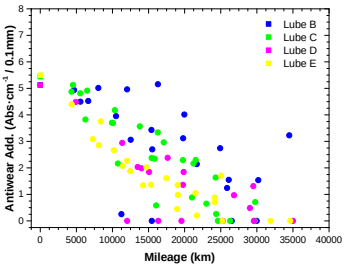

(b) Antiwear additives by FT–IR spectroscopy

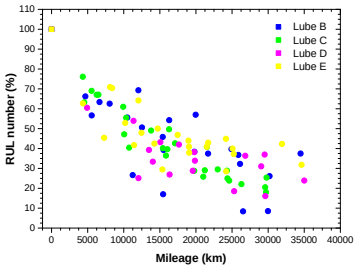

(c) RUL number

Figure 4.7. *Depletion of antioxidant additives of the engine oils used in vehicles type I.*

For the four engine oils, the performance reflected by the aminic and antiwear additives (according to the data obtained by FT–IR spectroscopy) are different: the variation experienced by the aminic additives is stable and of small magnitude, the drop in the value is not very pronounced. However, the antiwear additives suffer a more pronounced depletion. Their depletion rate is such that in most of the data obtained, it can be seen that by the middle of the period (around 15000 km) they have practically been consumed. As a consequence, when analysing the RUL index, its drop is not linear. This is due to the influence of the evolution of the depletion of antiwear additives. In this case, such additives are mainly ZDDP, which have the dual function of protecting against wear and counteracting oil oxidation. Thus, while the amine additives (antioxidant additives) maintain a fairly stable performance,

the counteracting effect of the antiwear additives on the evolution of the RUL number accentuates its reduction.

Concerning the TBN and TAN, according to the above lines, the trends that have been collected are shown in Figure 4.8.

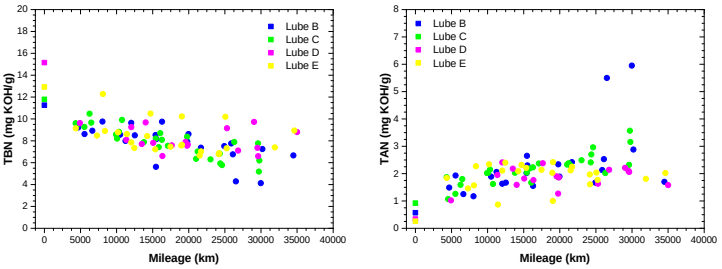

(a) TBN index by thermometric titration

(b) TAN index by thermometric titration

Figure 4.8. *Performance of TBN/TAN index of the engine oils used in vehicles type I.*

These parameters are antagonistic: while the TBN is consumed, the TAN increases. In general terms, it can be observed that there is a rapid variation in both parameters during a short period of use, which then tends to stabilise as the engine oil accumulates mileage. However, focusing on the performance shown by the TBN in the four lubricating oils, it suffers a drop of 4–5 units (approximately) but then remains stabilised during the whole test, experiencing a smooth drop that allows it to reach the end of the ODI with a value close to or higher than 50% of its original value. While, in contrast, the TAN gradually increases to values of 2.5–3.0 mg KOH/g at 30000 km.

Concerning the content of metallic additives present in the samples taken from the different engine oil formulations and analysed by means of ICP–OES spectrometry, the results are shown in Figure 4.9.

In these cases, the levels of the metals remain stable, taking into account the possible refill of the volume of engine oil in the vehicles which could have a cumulative effect during the whole test and, consequently, cause a slight increase. This is because, although the corresponding action of the additive property is consumed, the metallic part of the molecule remains in the total volume of engine oil in the vehicle. However, as can be seen, there is a discordance in the case of boron, which shows a significant decrease in concentration in the oil formulations. This apparently unusual behaviour will be explained in the section 4.4 *General engine oil performance discussion.*

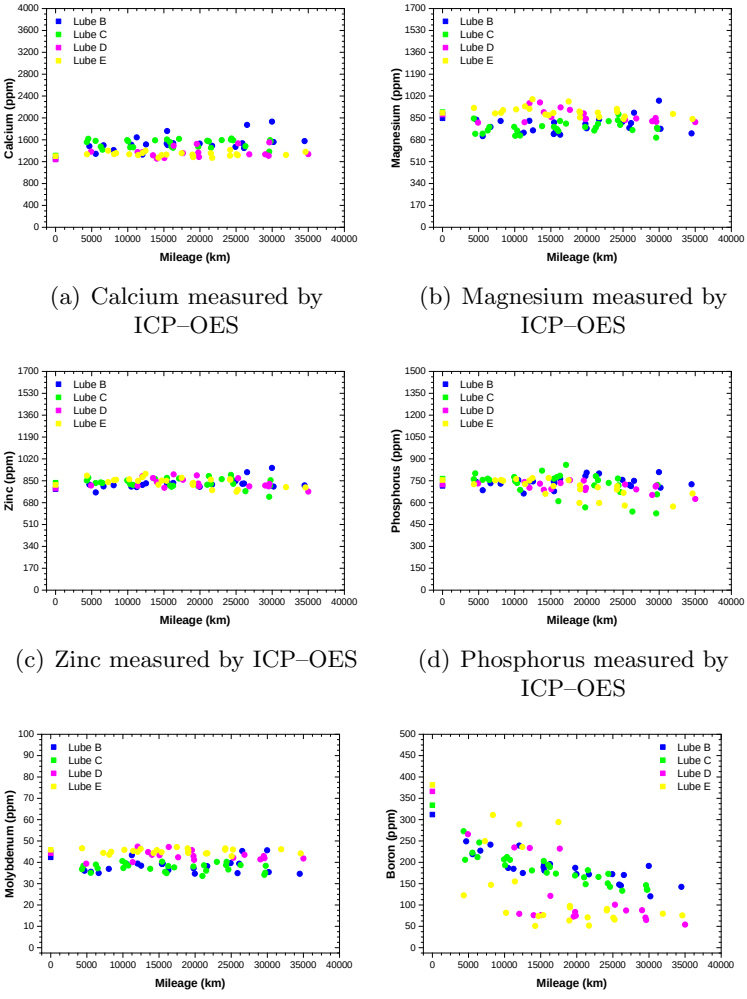

(a) Calcium measured by ICP–OES

(b) Magnesium measured by ICP–OES

(c) Zinc measured by ICP–OES

(d) Phosphorus measured by ICP–OES

(e) Molybdenum measured by ICP–OES

(f) Boron measured by ICP–OES

Figure 4.9. *Additive package of the engine oils used in vehicles type I.*

The contamination of engine oils has focused on the control of three parameters: soot, silicon and sodium. Each of them is of interest depending on the characteristics of the test (vehicle, engine oil, auxiliary fluids, working conditions, etc.), so that in the Figure 4.10 their evolution has been represented.

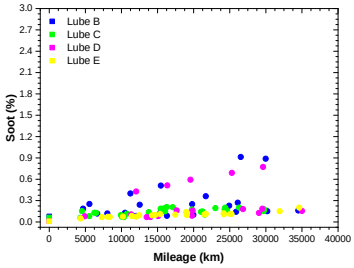

(a) Soot quantified by FT–IR

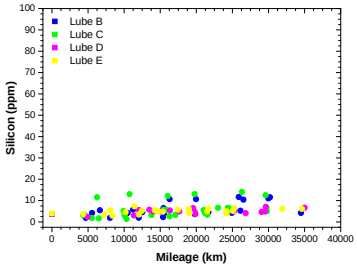

(b) Silicon quantified by ICP–OES

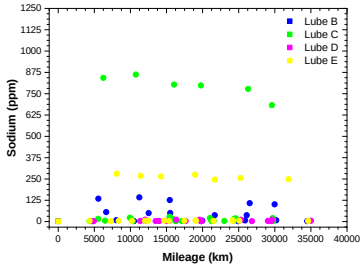

(c) Sodium quantified by ICP–OES

Figure 4.10. *Presence of contaminants in engine oils used in vehicles type I.*

In view of the results, it appears that there are some problems with the sodium, these problems are not to be justified by the used engine oil, but are rather caused by some issues in the engine. For this, please refer to the 4.A Appendix to observe the vehicle in question with such a problem.

In order to analyse the wear of the internal lubricated engine parts of the participating vehicles, the following wear metals were monitored: iron, aluminium, copper and lead which are shown in Figure 4.11.

According to the results, none of the engine internal parts have suffered wear/damage as shown by the collected metal values. None of them showed values that would cause an alarm of engine damage.

In the following Table 4.6, the values at 0 km and at 30000 km of the parameters represented in the previous graphs are gathered in order to observe their increase/decrease.

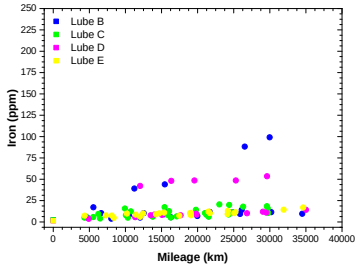

(a) Iron measured by ICP–OES

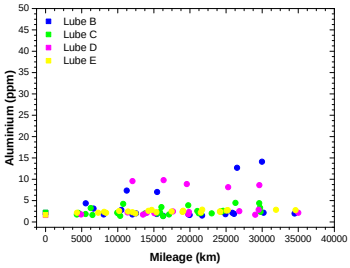

(b) Aluminium measured by ICP–OES

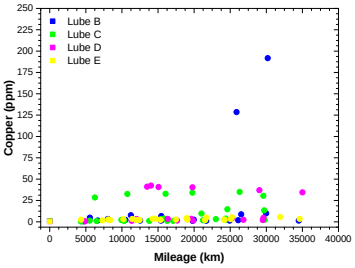

(c) Copper measured by ICP–OES

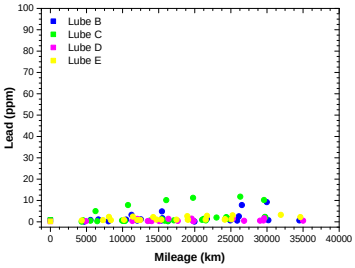

(d) Lead measured by ICP–OES

Figure 4.11. *Wear metals found in the engine oils used in vehicles type I.*

Table 4.6. *Summary of variations in the formulations used in type I vehicles.*

		Lube B		Lube C		Lube D		Lube E	
Parameter	**Units**	*Fresh*	*End*	*Fresh*	*End*	*Fresh*	*End*	*Fresh*	*End*
KV@40°C	cSt	68.22	76.77	54.97	62.69	76.80	79.30	57.06	62.70
KV@100°C	cSt	12.61	12.71	10.47	10.87	12.23	12.61	9.66	10.57
Oxidation	Abs·cm^{-1}/0.1 mm	13.670	23.083	13.929	22.306	13.480	22.777	13.781	20.702
Nitration	Abs·cm^{-1}/0.1 mm	6.253	11.339	6.411	11.019	5.919	10.520	6.119	9.753
Aminic Ad.	Abs·cm^{-1}/0.1 mm	9.712	8.098	9.881	8.016	9.214	8.417	9.553	7.994
Antiwear Ad.	Abs·cm^{-1}/0.1 mm	5.129	1.471	5.440	0.373	5.121	1.164	5.496	1.354
RUL number	%	100.0	27.0	100.0	23.4	100.0	33.4	100.0	40.1
TBN	mg KOH/g	11.26	6.34	11.79	6.51	15.15	8.51	12.92	8.90
TAN	mg KOH/g	0.57	3.19	0.92	2.73	0.34	1.90	0.26	1.97
Calcium	ppm	1248	1628	1312	1548	1239	1392	1300	1552
Magnesium	ppm	847	825	895	785	876	842	889	698
Zinc	ppm	784	856	835	821	790	822	818	788
Phosphorous	ppm	715	740	765	657	724	693	755	656
Molybdenum	ppm	42	39	45	37	44	43	46	35
Boron	ppm	312	156	334	145	366	86	381	62
Iron	ppm	2.16	11.48	2.29	14.72	1.36	22.05	1.41	11.09
Aluminium	ppm	2.18	5.25	2.22	3.15	1.55	3.98	1.66	2.43
Copper	ppm	1.01	4.66	1.12	14.56	0.41	12.23	0.40	3.69
Lead	ppm	0.79	3.18	0.90	4.54	0.17	0.77	0.20	1.84
Soot	% weight	0.08	0.39	0.09	0.18	0.01	0.31	0.01	0.14

In order to better understand some of the data contained in the case of vehicle type I, the 4.A Appendix shows a distinction of the individual vehicles using this engine technology.

4.3.2 Engine oil performance in type II vehicles

In type II vehicles, only three type of oils were studied: Lube A, Lube B and Lube D. The reason for this is that in the two iterations of the study, it was necessary to reference the comparison between formulations with an engine oil which performance was well known, and was recommended for the different engine technologies involved in the test. This oil is Lube A, which is why it appears twice: in the first iteration (Lube A–B–C) and in the second one (Lube A–D–E).

As for type I vehicles, the results will be presented in the same way for type II vehicles.

The evolution of the kinematic viscosity is shown in Figure 4.12.

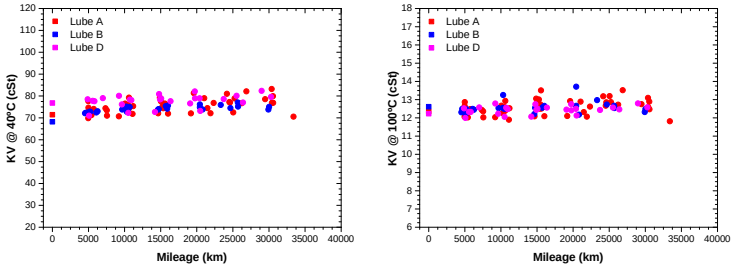

(a) Kinematic viscosity at 40°C (b) Kinematic viscosity at 100°C

Figure 4.12. *Evolution of KV of the engine oils used in vehicles type II.*

In this case, formulations with different SAE grades are studied, two SAE 5W30 (red and blue) and one SAE 10W30 (pink). According to the results shown for the kinematic viscosities, the performance of the three oils, in spite of their differences: Lube A (5W30 CJ–4), Lube B (5W30 CK–4) and Lube D (10W30 CK–4), is very similar. For all of them, the shown trends are comparable, although in the case of Lube A, the viscosity variation (relative to its original value) is slightly higher than for the other two engine oils.

In order to explain the performance observed in type II vehicles, regarding the oxidation and nitration suffered by the engine oils, the results of the study have been shown in the following Figure 4.13.

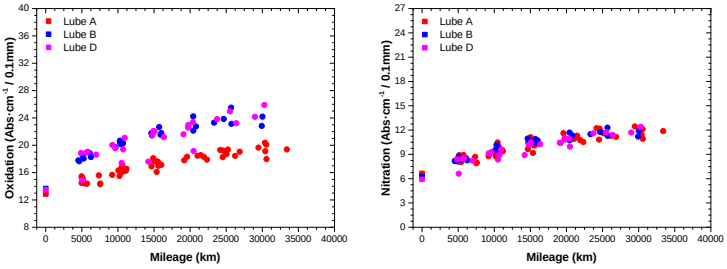

(a) Oxidation, by FT–IR, of the tested engine oils

(b) Nitration, by FT–IR, of the tested engine oils

Figure 4.13. *Evolution of oxidation and nitration of the engine oils used in vehicles type II.*

Differences are observed, which may be subjected to the different degrees of additivation of the engine oils. When comparing Lube A–Lube B and Lube A–Lube D, the differences are remarkable. The oxidative performance is quite different since the oxidation ratio of Lube B and Lube D is higher than that of Lube A. This could be justified as a result of its different additive package: despite having a lower amount of aminic additives, they degrade at a slower rate, almost coinciding at the end of the ODI with the levels of aminic additives in Lube B and Lube D. However, in the case of antiwear, the situation is different, Lube A has a higher amount (almost two points difference) and it does not degrade as quickly. Therefore, this seems to be the main factor causing this discrepancy when analysing oxidation. Nonetheless, when analysing nitration, the variation of the three engine oils shows trends with a comparable correspondence.

As already mentioned, the additive package plays a very important role in the performance of the engine oils; the Figure 4.14 shows this situation.

As mentioned in the previous lines, the balance between aminic additives and antiwear additives is different between the reference oil (Lube A) and Lube B and Lube D, as well as showing remarkable differences in performance. Much of these differences are due to the different levels of these additives, which in turn leads to these different performances. Going into detail, in the case of aminic additives, there are two different starting points, that of Lube A centred around 7.0 Abs·cm^{-1}/0.1 mm and that of Lube B and Lube D around 9.5 Abs·cm^{-1}/0.1 mm (approximately). Despite starting from different values, when analysing the evolution of the degradation of these additives, the drop is small and quite similar. Nevertheless, when looking at antiwear additives the

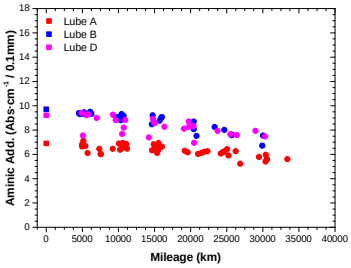

(a) Aminic additives by FT–IR spectroscopy

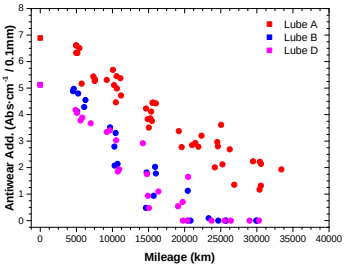

(b) Antiwear additives by FT–IR spectroscopy

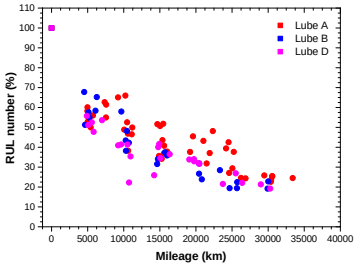

(c) RUL number

Figure 4.14. *Depletion of antioxidant additives of the engine oils used in vehicles type II.*

most striking differences are found, worthy of further analysis. To start with, the starting levels are also different: around 7 Abs·cm^{-1}/0.1 mm for Lube A and around 5 Abs·cm^{-1}/0.1 mm for Lube B and Lube D, but the depletion ratio (extracted by looking at the slope of the collected data evolution) is similar. Therefore, the problem lies in the quantity of additives present in these three formulations, those starting with lower proportions experience total additive exhaustion halfway through the test (15000–20000 km), while Lube A still retains sufficient quantity of antiwear additives to finish the test with a certain margin. So, when we look at the RUL number, we see that the Lub B and Lube D formulations are below Lube A. For the first two, the amount of additives remaining at the end of the test can be estimated at around 20%, while for Lube A it is 30%.

The next aspect to be considered is to study the TBN and TAN indexes, shown in Figure 4.15.

Both parameters are also influenced by the described aminic and antiwear additives. To begin with, if the acidification of the oils is observed, in all three

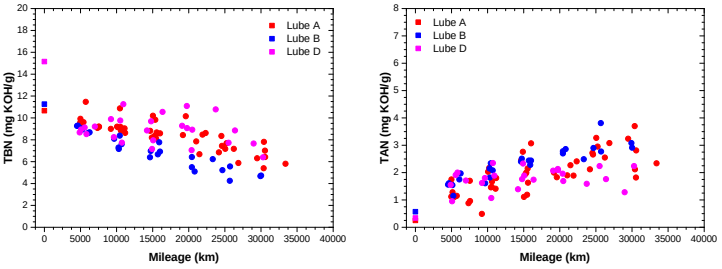

(a) TBN index by thermometric titration

(b) TAN index by thermometric titration

Figure 4.15. *Performance of TBN/TAN index in the engine oils used in vehicles type II.*

cases signs of abnormal acidification are shown. In all of them, the process is gradual and steady, reaching values of 3 mg KOH/g at the end of the test. For TBN, however, differences are found between the formulations: the two SAE 5W30 engine oils (Lube A and Lube B) show a lower degree of variation than the more viscous Lube D (which is a SAE 10W30). Lube D experiences a sharp drop in its initial TBN value in the early stages of the test (with a low degree of use, 5000 km), but once this phase is overcome, the evolution is more uniform and becomes comparable to that of Lube A and Lube B oils. Nevertheless, the reduction of TBN is different at the end of the test: Lube A and Lube B show levels of 50%, while for Lube D its value has been reduced by about 60%.

In relation to the content of metallic additives (Figure 4.16) in the three formulations used in this type of vehicle, there appear to be no changes that would indicate any possible problems with the engine oil performance.

At first glance, there are differences in the concentrations of certain metals (as can be seen in Figure 4.1), but the general performance of all metals is similar, with no differences worth mentioning. However, boron again shows a special pattern, taking into account the differences in the formulation of the three engine oils. Leaving aside Lube A, which does not contain notable amounts of boron in its formulation, the other two engine oils have a number of distinctive characteristics: Lube B continues to show the boron depletion already described, but what stands out at this point is that Lube D (of higher concentration than Lube B) shows very marked boron depletion, resulting in the near disappearance of boron at the end of the test (a loss of 85% is estimated).

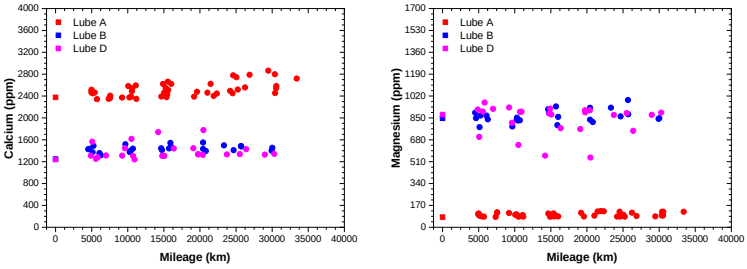

(a) Calcium measured by ICP–OES

(b) Magnesium measured by ICP–OES

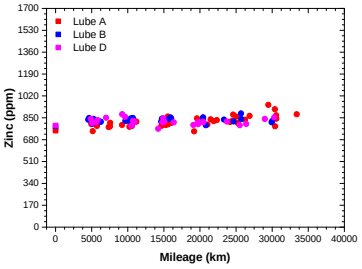

(c) Zinc measured by ICP–OES

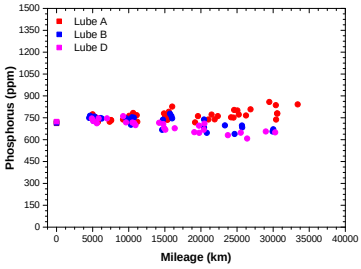

(d) Phosphorus measured by ICP–OES

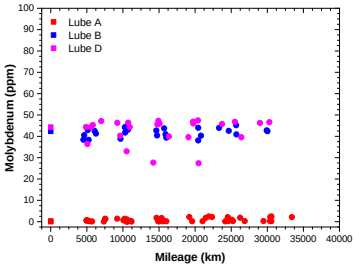

(e) Molybdenum measured by ICP–OES

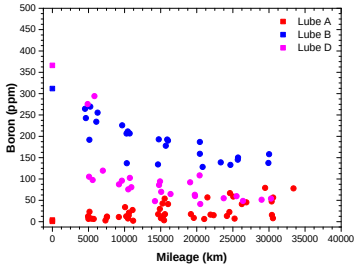

(f) Boron measured by ICP–OES

Figure 4.16. *Additive package evolution of the engine oils used in vehicles type II.*

Following the results of the analysis of contaminants present in engine oils, Figure 4.17 has been prepared.

In the case of soot, the levels are not high, although there are differences. Among type II vehicles, those using the Lube A formulation tend to accumulate more soot in oil, but still at acceptable levels for the ODI at 30000 kilometres. The levels of silicon collected are not at all inconvenient or

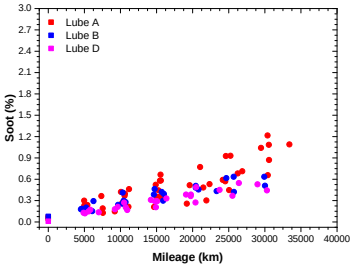

(a) Soot quantified by FT–IR

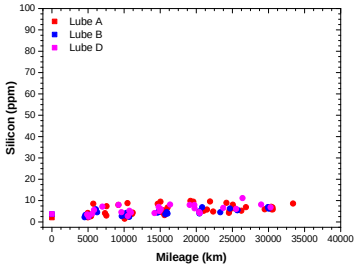

(b) Silicon quantified by ICP–OES

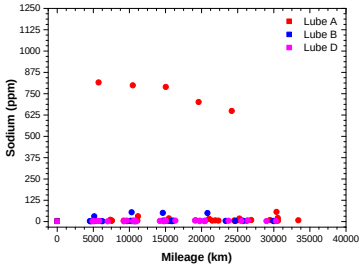

(c) Sodium quantified by ICP–OES

Figure 4.17. *Presence of contaminants in engine oils used in vehicles type II.*

anomalous for the type of vehicles under consideration, since the barrier that seems to have formed is located at around 10 ppm. But, moving on to sodium, there are a number of points in the case of Lube A whose levels are higher than the rest from the beginning of the test, although from the evolution shown, it seems that the problem that caused those sodium levels in the engine oil were being amended. For special cases such as the one described above, further information can be found in the 4.A Appendix at the end of the chapter.

In order to discuss the engine oils used in type II vehicles, results derived from the analysis of wear metals are shown in Figure 4.18.

From the point of view of engine wear, the performance obtained is within the range of this type of vehicle. In all formulations the behaviour is similar except for two aspects:

- In those vehicles using the reference engine oil, Lube A, the iron levels obtained by analysing their oil samples were higher than that of the other two formulations. However, in this case, the iron levels obtained

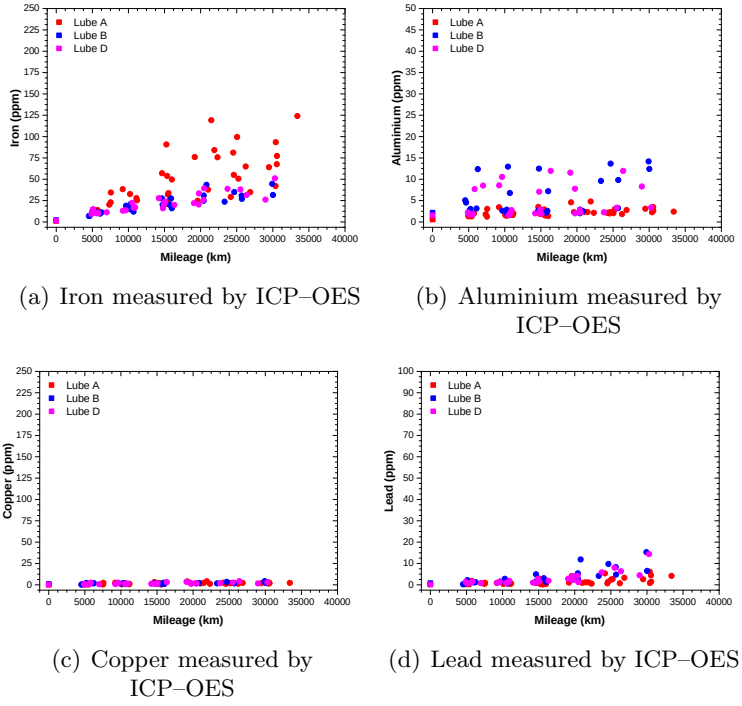

(a) Iron measured by ICP–OES

(b) Aluminium measured by ICP–OES

(c) Copper measured by ICP–OES

(d) Lead measured by ICP–OES

Figure 4.18. *Wear metals found in the engine oils used in vehicles type II.*

do not indicate any type of problem in the engine as a direct consequence of using formulation A.

- The other detail, which is difficult to see in Figure 4.18, but can be seen more easily in the 4.A Appendix, is that formulas B and D, as a consequence of their depletion of antiwear additives, give indications of a higher wear rate in soft metals such as copper and lead.

A summary of the parameters monitored when the engine oils were fresh (unused), and how they arrived at the end of the test has been prepared in Table 4.7.

Table 4.7. *Summary of variations in the formulations used in type II vehicles.*

		Lube A		Lube B		Lube D	
Parameter	**Units**	*Fresh*	*End*	*Fresh*	*End*	*Fresh*	*End*
KV@40°C	cSt	71.45	78.04	68.22	75.09	76.80	80.34
KV@100°C	cSt	12.04	12.69	12.61	12.55	12.23	12.68
Oxidation	Abs·cm^{-1}/0.1 mm	12.948	19.291	13.670	23.896	13.480	24.415
Nitration	Abs·cm^{-1}/0.1 mm	6.649	11.735	6.253	11.688	5.919	11.593
Aminic Ad.	Abs·cm^{-1}/0.1 mm	6.901	5.773	9.712	7.495	9.214	7.767
Antiwear Ad.	Abs·cm^{-1}/0.1 mm	6.742	1.999	5.129	0.000	5.121	0.000
RUL number	%	100.0	29.2	100.0	20.7	100.0	22.8
TBN	mg KOH/g	10.66	6.76	11.26	4.89	15.15	7.93
TAN	mg KOH/g	0.25	2.68	0.57	3.09	0.34	1.80
Calcium	ppm	2376	2617	1248	1446	1239	1364
Magnesium	ppm	79	102	847	884	876	864
Zinc	ppm	761	859	784	838	790	821
Phosphorous	ppm	722	794	715	669	724	649
Molybdenum	ppm	0.33	2.45	42	43	44	45
Boron	ppm	3.63	39	312	145	366	61
Iron	ppm	1.15	70.67	2.16	33.80	1.36	37.30
Aluminium	ppm	0.67	2.71	2.18	10.66	1.55	5.16
Copper	ppm	0.18	2.05	1.01	2.72	0.41	3.08
Lead	ppm	0.13	3.19	0.79	8.93	0.17	6.98
Soot	% weight	0.07	0.77	0.08	0.56	0.01	0.45

4.3.3 Engine oil performance in type III vehicles

Type III vehicles are the only vehicles that do not use diesel fuel, but instead use CNG. As a consequence, the combustion conditions and engine types are different from the others, as the thermal demand on the engine is higher in this type of vehicle. As a consequence, the conditions to which engine oil formulations B, C, D and E are subjected in these vehicles are different.

To begin with, by looking at Figure 4.19 where the kinematic viscosity data at 40 and 100 Celsius degrees are plotted, it can be seen that the increase per use is higher than their diesel counterparts. This higher variation is due to the fact that in this type of vehicle the thermal stress on the engine oil is higher.

Another consequence of the higher thermal demand of CNG engines is shown in Figure 4.20. In these situations where higher combustion temperatures are reached, the engine oil undergoes more intense oxidation, so that the oxidative degradation rates in these vehicles are more pronounced. Equivalently, the performance reflected by nitration follows the same pattern as oxidation, all of them conditioned by the new combustion conditions of this type of engines used in type III vehicles.

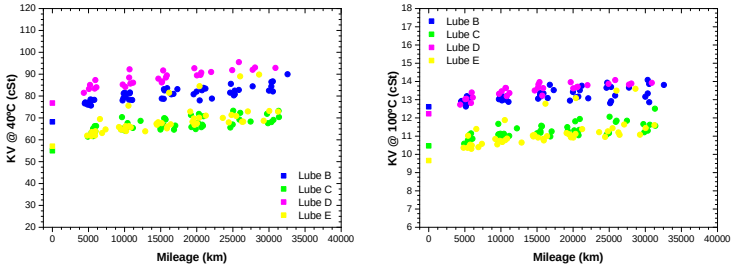

(a) Kinematic viscosity at 40°C (b) Kinematic viscosity at 100°C

Figure 4.19. *Evolution of KV of the engine oils used in vehicles type III.*

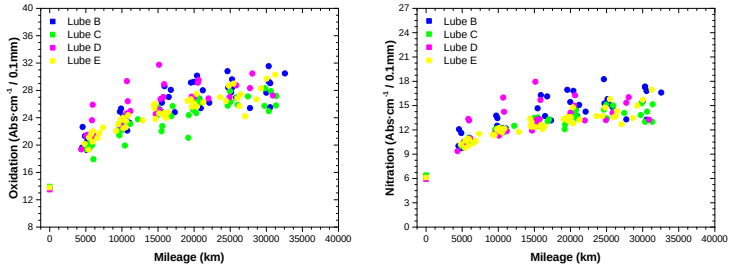

(a) Oxidation, by FT–IR, of the tested engine oils (b) Nitration, by FT–IR, of the tested engine oils

Figure 4.20. *Evolution of oxidation and nitration of the engine oils used in vehicles type III.*

Having described the effects of oxidation and nitration on engine oils by this type of vehicle, it is necessary to look at how the additives have been affected. Figure 4.21 has been prepared for this purpose.

With regard to the evolution of the additive content measured by FT–IR spectroscopy, it is clear that there are two clearly different situations:

- On the one hand, the aminic additives for the four engine oils behave in a homologous way. In all of them, a gradual drop has been registered, which has caused that, starting from an average value of 9.5 Abs·cm^{-1}/0.1 mm at the beginning, a value of 6.5 Abs·cm^{-1}/0.1 mm is reached at the end of the test (a reduction of 32%).
- On the other hand, the depletion of antiwear additives is very important. And, between the two different CK–4 and FA–4 formulations, the

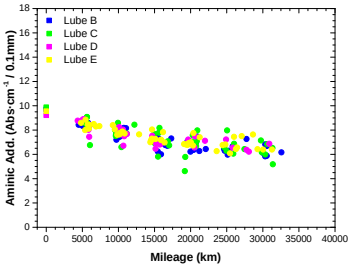

(a) Aminic additives by FT–IR spectroscopy

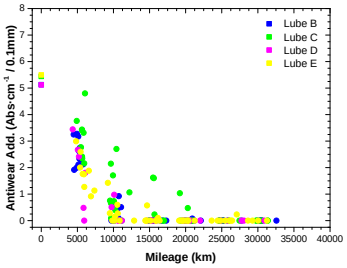

(b) Antiwear additives by FT–IR spectroscopy

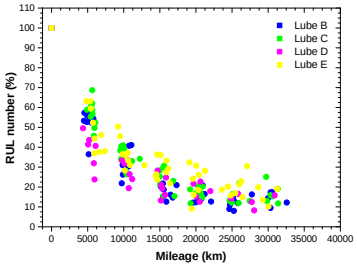

(c) RUL number

Figure 4.21. *Depletion of antioxidant additives of the engine oils used in vehicles type III.*

depletion in the case of CK–4 is higher than that in FA–4. Now, in general terms, at 10000 kilometres, the antiwear additives have almost all been used up.

Switching to the RUL number, the results obtained are consistent with those described for the additive pair described above: as in the CK–4 formulations the depletion of the additives is higher, consequently the RUL number also follows the same pattern. Instead, for the FA–4, the additives drop is not as pronounced. From a more generic point of view, the RUL number of engine oils used in CNG engines is lower than in diesel engines. Such is the demand of CNG engines on oils that, even at an average value, at the end of the ODI the RUL number is about 10% of the original additive content of the oil (against the 20% in diesel engines).

Moving on to explain the TBN and TAN in these four engine oils, the results are shown in Figure 4.22.

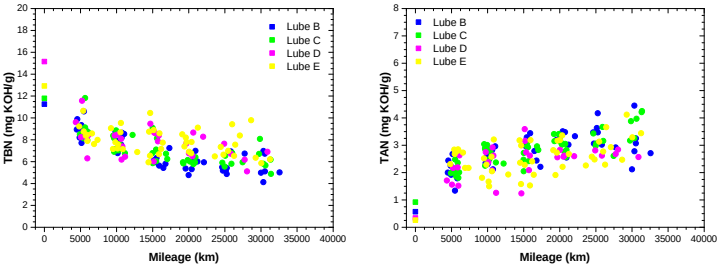

(a) TBN index by thermometric titration

(b) TAN index by thermometric titration

Figure 4.22. *Performance of TBN/TAN index of the engine oils used in vehicles type III.*

For CNG-powered vehicles, the TBN and TAN results are also slightly different from those obtained for diesel vehicles: the basic reserve (TBN) is consumed more quickly and, on the other hand, the acidification of the engine oil (TAN) is accelerated. This being said, there is a significant decrease of more than 50% of the original TBN value at the end of the test and TAN values of 3.5–4.0 mg KOH/g have been reached. However, looking closely, differences in the CK–4 and FA–4 formulations become apparent again. Focusing on TBN, CK–4 oils show a drop of about 50% in the first sampling phase (5000 km), while FA–4 oils show a relatively more gradual drop. But, from the second sampling cycle at 10000 km, the response collected in both categories is the same. Finally, with TAN there is a difference of 0.5 and 1.0 mg KOH/g between CK–4 (Lube B and D) and FA–4 (Lube C and E) engine oils.

Thanks to ICP–OES spectrometry (Figure 4.23), the performance of the metallic additives package was recorded as follows: the levels (in ppm) remained stable throughout the test, with the exception of boron, which declined. Any possible discrepancies about these behaviours or general trends can be found in the 4.A Appendix at the end of this chapter.

In this type of vehicle, only silicon and sodium will be studied for the contaminants, since according to the combustion properties of CNG, soot is an irrelevant parameter. Therefore, Figure 4.24 shows the results for silicon and sodium only.

When analysing silicon, some high values were found for vehicles using the Lube B engine oil formulation. Some of them do seem to show signs of considerable problems with silicon contamination (which is, after all, from atmospheric dust), but it does not seem to indicate that this is a consequence

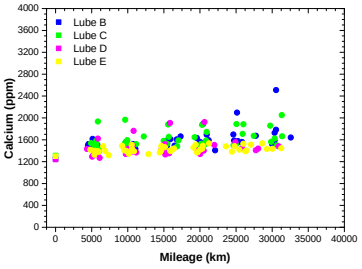

(a) Calcium measured by ICP–OES

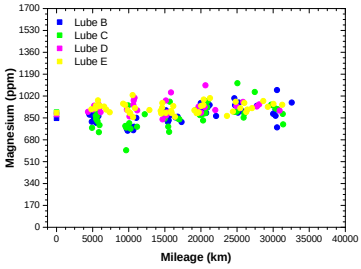

(b) Magnesium measured by ICP–OES

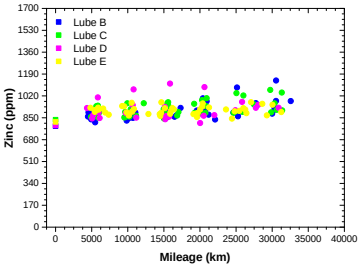

(c) Zinc measured by ICP–OES

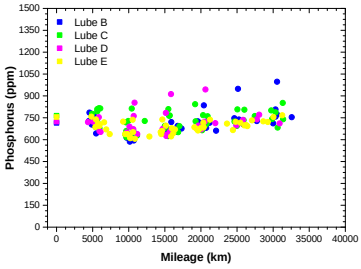

(d) Phosphorus measured by ICP–OES

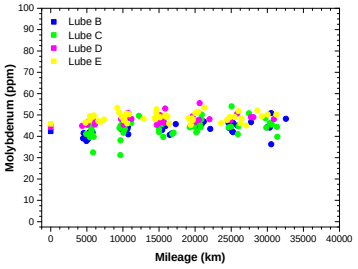

(e) Molybdenum measured by ICP–OES

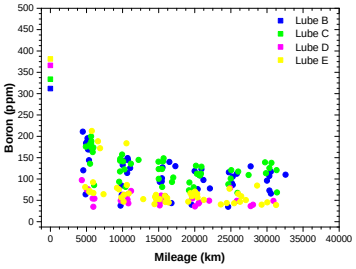

(f) Boron measured by ICP–OES

Figure 4.23. *Additive package evolution of the engine oils used in vehicles type III.*

of the oil used, since if it were, the rest of them would also show the same signs of increasing silicon concentrations as the test progresses. Accordingly, the results give reason to believe that this is an isolated case, which will be described in the final 4.A Appendix to this chapter. Furthermore, when looking at sodium, the pattern shown in the graph is homologous to that of silicon, so it is not surprising that we are looking at some vehicle or vehicles that suffer from a series of specific problems in some of the vehicle's systems

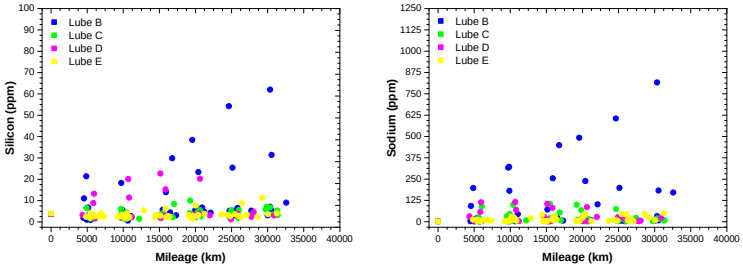

(a) Silicon quantified by ICP–OES

(b) Sodium quantified by ICP–OES

Figure 4.24. *Presence of contaminants in engine oils used in vehicles type III.*

that cause these anomalous values. As with silicon, a specific explanation will be given for each vehicle in question in the relevant 4.A Appendix.

With the indications of increased demands placed on the oil by engine operating conditions and the presence of significant levels of contaminants, it is important to consider how this has affected internal engine wear. To this end, the information collected from all the engine oil samples analysed has been compiled in Figure 4.25.

Conditioned by the contamination of the lubricating oil, it is difficult to determine a general pattern for this type of vehicle, as several sources can cause fluctuations in the trends recorded for the four metals analysed:

- In the case of iron, there are some high values in the data from the Lube B and Lube D formulation, values which may be due to the vehicles involved with the silicon and sodium probes (to be discussed later in the 4.A Appendix). Leaving this aspect aside, overall, the iron wear rates are within the levels considered normal for a 30000 km test, since in the end, the presence of iron does not even reach 30 ppm.

- When moving to aluminium, something similar happens as with iron, certain values for Lube B and Lube D diverge from the general trend. Similarly, these are not alarming levels of wear either, since in the worst cases, the 25 ppm is not even reached.

- With copper there are no apparent problems, although there are with lead. The increased acidification of the engine oil and the presence of contaminants at considerable levels create favourable conditions for the degradation of lead-based engine internal components. This accelerated

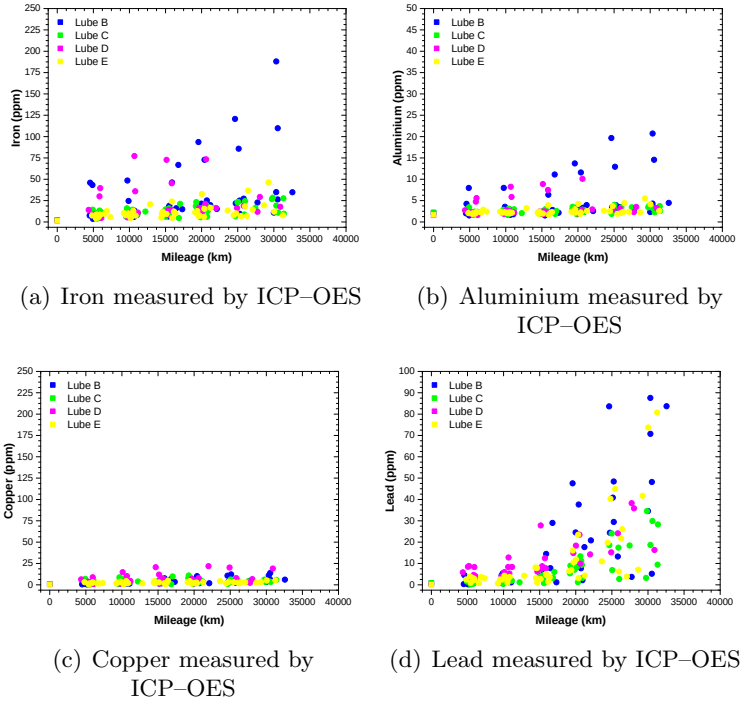

(a) Iron measured by ICP–OES

(b) Aluminium measured by ICP–OES

(c) Copper measured by ICP–OES

(d) Lead measured by ICP–OES

Figure 4.25. *Wear metals found in the engine oils used in vehicle types III.*

wear leads to a trend that loses the linearity observed for diesel vehicles and shows a rather exponential behaviour.

Table 4.8. *Summary of variations in the formulations used in type III vehicles.*

		Lube B		Lube C		Lube D		Lube E	
Parameter	**Units**	*Fresh*	*End*	*Fresh*	*End*	*Fresh*	*End*	*Fresh*	*End*
KV@40°C	cSt	68.22	85.22	54.97	70.01	76.80	90.98	57.06	72.19
KV@100°C	cSt	12.61	13.54	10.47	11.70	12.23	13.73	9.66	11.51
Oxidation	Abs·cm^{-1}/0.1 mm	13.670	28.423	13.929	26.808	13.480	27.249	13.781	27.449
Nitration	Abs·cm^{-1}/0.1 mm	6.253	15.724	6.411	14.298	5.919	14.036	6.119	14.541
Aminic Ad.	Abs·cm^{-1}/0.1 mm	9.712	6.398	9.881	6.374	9.214	6.747	9.553	6.717
Antiwear Ad.	Abs·cm^{-1}/0.1 mm	5.129	0.000	5.440	0.000	5.121	0.077	5.496	0.041
RUL number	%	100.0	14.7	100.0	15.2	100.0	16.4	100.0	19.3
TBN	mg KOH/g	11.26	5.67	11.79	6.21	15.15	7.50	12.92	7.26
TAN	mg KOH/g	0.57	3.04	0.92	3.58	0.34	2.56	0.26	3.14
Calcium	ppm	1248	1777	1312	1725	1239	1606	1300	1567
Magnesium	ppm	847	917	895	912	876	863	889	907
Zinc	ppm	784	970	835	962	790	929	818	930
Phosphorous	ppm	715	790	765	767	724	732	755	748
Molybdenum	ppm	42	45	45	45	44	45	46	47
Boron	ppm	312	100	334	111	366	60	381	50
Iron	ppm	2.16	25.95	2.29	19.12	1.36	19.97	1.41	21.27
Aluminium	ppm	2.18	7.47	2.22	3.15	1.55	2.80	1.66	3.62
Copper	ppm	1.01	7.10	1.12	4.85	0.41	5.57	0.40	3.55
Lead	ppm	0.79	22.90	0.90	18.07	0.17	17.32	0.20	34.09

4.3.4 Engine oil performance in type IV vehicles

Type IV vehicles are the remaining participant group in the study of the performance of the different formulations of engine oil. In this section, the formulations that have been tested are: Lube B, Lube C, Lube D and Lube E. A distinctive feature of this type of vehicle is the presence of an EGR and DPF system, so that some differences in the performance of the engine oil formulations are expected as a result of the action of these pollutant emission aftertreatment systems on the way the engines of the type IV vehicles operate.

First of all, the evolution of the kinematic viscosity during the whole test shall be observed, as shown in Figure 4.26 below.

The evolution of both viscosities analysed is comparable. Both have experienced an increase compared to their original values, but some interesting details can be noted: when analysing the percentage increase in viscosities, formulations with API CK–4 grades have seen their value increase by over 25%, while for FA–4 the increase is around 18%.

In this type of vehicle, as they have EGR and DPF, they have a series of particularities that differentiate them from the other diesel vehicles used in the test (type I and type II). These differences are clearly highlighted when analysing the oxidation and nitration that these engines cause on the oil, see Figure 4.27.

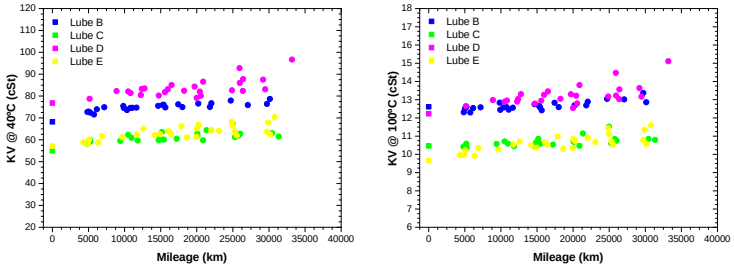

(a) Kinematic viscosity at 40°C (b) Kinematic viscosity at 100°C

Figure 4.26. *Evolution of KV of the engine oils used in vehicles type IV.*

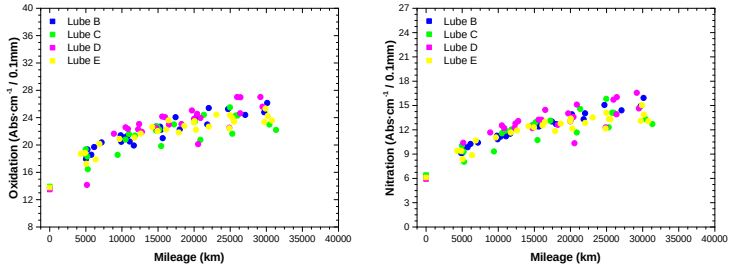

(a) Oxidation, by FT–IR, of the tested engine oils (b) Nitration, by FT–IR, of the tested engine oils

Figure 4.27. *Evolution of oxidation and nitration of the engine oils used in vehicles type IV.*

To begin with, the recorded evolution of oxidation and nitration in these vehicles, compared to type I and type II, means that the final levels in both parameters are greater. For oxidation the increase is 70% and for nitration 125% (of the values obtained by FT–IR spectroscopy, the units of which are Abs·cm^{-1}/0.1 mm), always taking approximate average values. These values however, do not indicate that the engine oil is fully oxidised or nitrated, as the percentages are calculated from absorbance units and are therefore not absolute units. So these percentages should be understood as a degree of variation (with respect to the origin) and not as an absolute status.

By analysing the results provided by FT–IR spectroscopy and linear sweep voltammetry for the study of the evolution of the antioxidant additives (aminic and antiwear), it is possible to obtain the data shown in Figure 4.28.

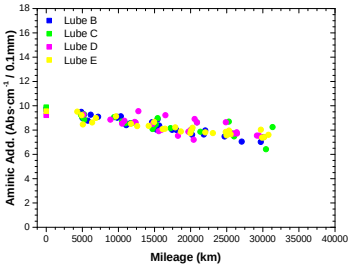

(a) Aminic additives by FT–IR spectroscopy

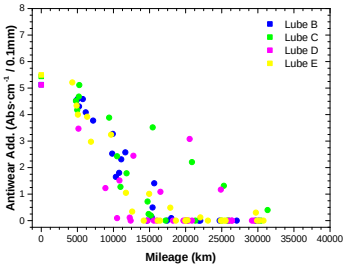

(b) Antiwear additives by FT–IR spectroscopy

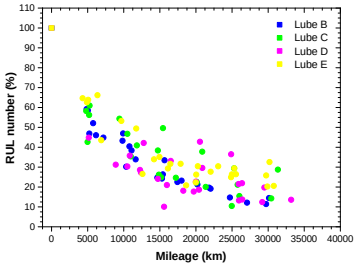

(c) RUL number

Figure 4.28. *Depletion of antioxidant additives of the engine oils used in vehicles type IV.*

The amininc additives show a drop of 2 Abs·cm^{-1}/0.1 mm during the whole test, showing a higher retention (as will be seen later) than the antiwear additives. In the case of antiwear additives, the evolution shown is particularly interesting. For this type of additives, there are differences in performance between the pair of lubricating oils of different API grades: CK–4 and FA–4. In the case of API CK–4 oils (Lube B and Lube D), the antiwear additives are almost completely exhausted after 10000 km, while for FA–4 oils (Lube C and Lube E) this exhaustion is prolonged, occuring 5000 km later. This dissimilar performance is due to the difference between the oxidation and nitration ratios shown in Figure 4.27. Finally, the RUL number combines the rapid depletion of the antioxidant additives in these formulations: both aminic and antiwear additives (which in this case are mainly ZDDP and its zinc and phosphorous derivatives). In this case, as the consumption of additives is high, this leads to a further drop in the RUL number and consequently, the engine oil is not able to counteract the degradation to which it is subjected, causing oxidation and nitration levels to be considerable.

The evolution of the TBN and TAN of the engine oils is analysed using the patterns plotted in Figure 4.29.

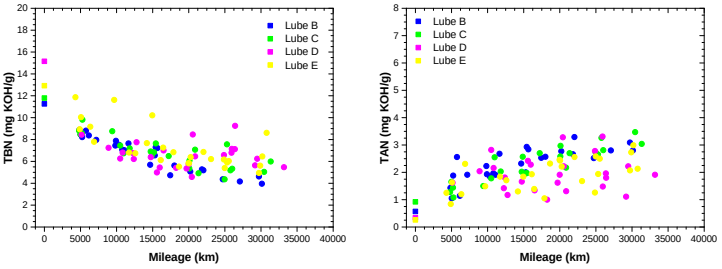

(a) TBN index by thermometric titration

(b) TAN index by thermometric titration

Figure 4.29. *Performance of TBN/TAN index of the engine oils used in vehicles type IV.*

According to the described parameters of degradation and loss of additives by the lubricants as a consequence of the varying boundary conditions introduced by the aftertreatment pollutant emission systems, it is not surprising that both TBN and TAN in these vehicles behave differently from their diesel counterparts. Now, both the reduction of TBN and the increase of TAN are more intense. Beginning with the TBN, all four engine oils show a significant drop in the first 5000–10000 km, with the most significant drops in the case of Lube D and E, in that order (Lube D suffers a reduction of 6–7 mg KOH/g in the first 5000 km). At the completion of the ODI, the TBN levels shown by the formulations are estimated to be in the order of 40% (in the worst case) and 50% (in the most favourable conditions) of their starting values. The other parameter, TAN index, shows differences between the least and most viscous oils. The 5W30 SAE grade engine oils, Lube B and C, present results that are not very dispersed; in other words, with sufficient traceability to observe without complication that the final acidification of these formulations is located above 3.0–3.5 mg KOH/g. However, when switching to SAE 10W30 (Lube D and Lube E), the variability of results increases and it is therefore difficult to observe a clear trend. However, its evolution indicates that the TAN value is below the SAE 5W30 threshold.

The results gathered on the quantification of the metallic additives package by means of ICP–OES spectrometry available at the Fuels and Lubricants Laboratory of the department are shown in Figure 4.30.

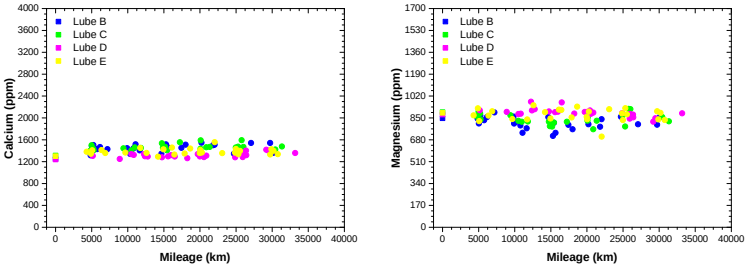

(a) Calcium measured by ICP–OES

(b) Magnesium measured by ICP–OES

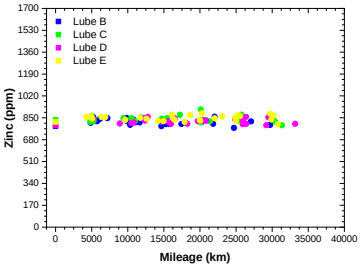

(c) Zinc measured by ICP–OES

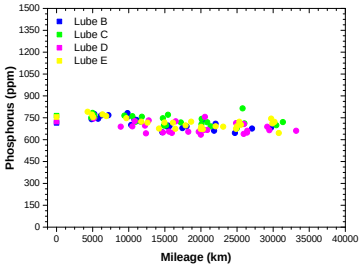

(d) Phosphorus measured by ICP–OES

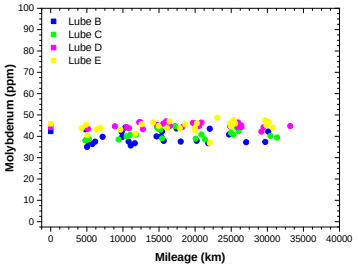

(e) Molybdenum measured by ICP–OES

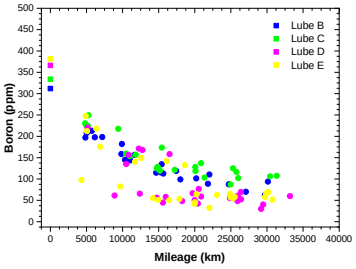

(f) Boron measured by ICP–OES

Figure 4.30. *Additive package evolution of the engine oils used in vehicles type IV.*

From the point of view of the metallic additive package performance: calcium, magnesium, zinc, phosphorus, molybdenum and boron, only the latter is the only one that shows a noticeable tendency. All formulations show that boron is consumed relatively quickly. The reason for this phenomenon will be explained later in section 4.4 *General engine oil performance discussion*:

The next group of data is made up of the contaminants: soot, silicon and sodium, all of which are collected in Figure 4.31.

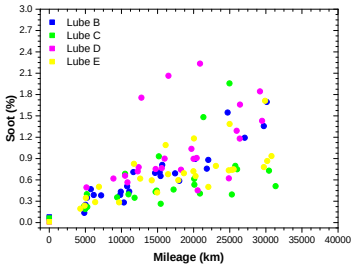

(a) Soot quantified by FT–IR

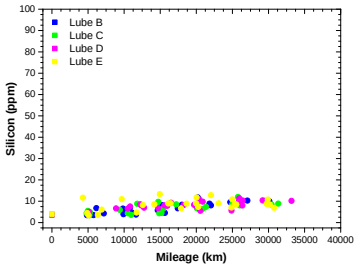

(b) Silicon quantified by ICP–OES

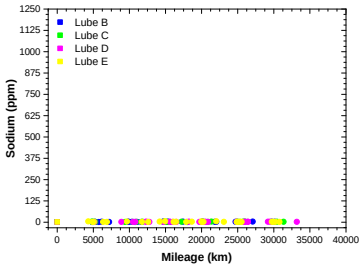

(c) Sodium quantified by ICP–OES

Figure 4.31. *Presence of contaminants in engine oils used in vehicles type IV.*

The three engine oil contaminants, the only one worthy of study is soot, as neither silicon nor sodium are of any interest. The interest in the soot lies precisely in the EGR and DPF that the vehicles of this group have. These technologies encourage more soot formation, so that some of the soot becomes mixed with the lubricant oil. This is precisely what is observed in these vehicles. Normally, the stipulated maximum limit for soot contamination of lubricating oil is 3% (by weight) and, according to the values collected at the end of the test, they were quite close to this limit.

In order to conclude the study of the engine oils for type IV vehicles regarding wear, the data collected during the whole process of sampling and laboratory analysis will be presented in the different plots of Figure 4.32.

At first instance, the higher concentration of soot in the lubricating oil (an abrasive material) should lead to higher levels of wear metals in these vehicles, but this is not the case. From the point of view of wear metals, it

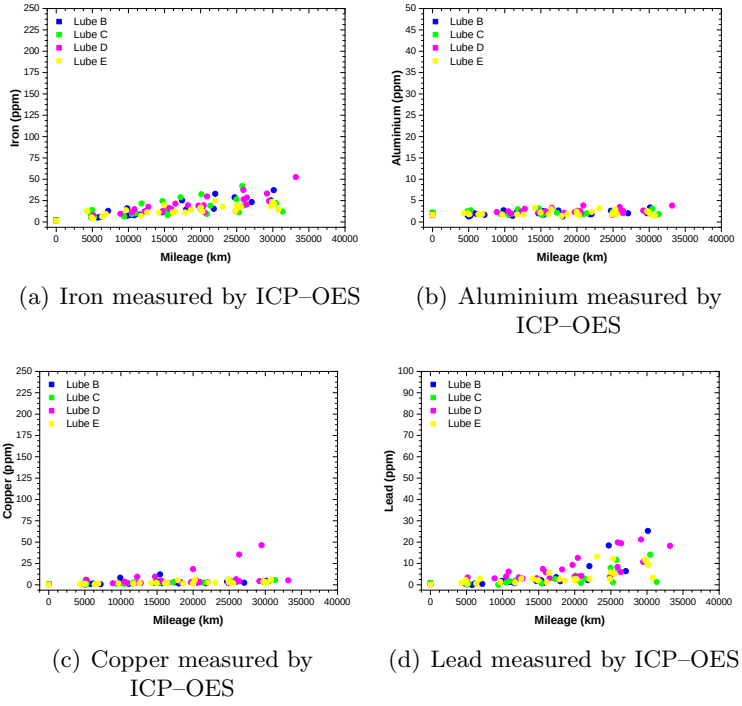

(a) Iron measured by ICP–OES

(b) Aluminium measured by ICP–OES

(c) Copper measured by ICP–OES

(d) Lead measured by ICP–OES

Figure 4.32. *Wear metals found in the engine oils used in vehicles type IV.*

can be seen that their presence is very limited and only the evolution of lead requires special mention. It can be seen that the lead level rises in the middle of the period of use (15000 km), which is to be expected with the pre-mature exhaustion of the additives. Such is the consistency of this observation that there is a coincidence between the depletion of the antiwear additives and the sharp increase in lead in the same section of the test, in the middle.

In order to understand how the engine oils have been affected in this type of vehicle, in Table 4.9 the values of the parameters have been plotted against each other when the engine oils are fresh and when they have accumulated 30000 km.

Table 4.9. *Summary of variations in the formulations used in type IV vehicles.*

		Lube B		Lube C		Lube D		Lube E	
Parameter	**Units**	*Fresh*	*End*	*Fresh*	*End*	*Fresh*	*End*	*Fresh*	*End*
KV@40°C	cSt	68.22	77.21	54.97	63.03	76.80	85.83	57.06	64.30
KV@100°C	cSt	12.61	13.07	10.47	10.92	12.23	13.47	9.66	10.85
Oxidation	Abs·cm^{-1}/0.1 mm	13.670	25.149	13.929	23.330	13.480	25.804	13.781	24.109
Nitration	Abs·cm^{-1}/0.1 mm	6.253	15.084	6.411	13.651	5.919	14.989	6.119	13.791
Aminic Ad.	Abs·cm^{-1}/0.1 mm	9.712	7.242	9.881	7.751	9.214	7.657	9.553	7.666
Antiwear Ad.	Abs·cm^{-1}/0.1 mm	5.129	0.000	5.440	0.343	5.121	0.000	5.496	0.051
RUL number	%	100.0	13.2	100.0	20.8	100.0	17.1	100.0	26.8
TBN	mg KOH/g	11.26	4.28	11.79	5.63	15.15	7.03	12.92	5.72
TAN	mg KOH/g	0.57	2.80	0.92	3.03	0.34	1.99	0.26	2.47
Calcium	ppm	1248	1447	1312	1485	1239	1358	1300	1387
Magnesium	ppm	847	829	895	851	876	855	889	878
Zinc	ppm	784	804	835	830	790	817	818	858
Phosphorous	ppm	715	678	765	723	724	664	755	716
Molybdenum	ppm	42	39	45	41	44	44	46	46
Boron	ppm	312	78	334	109	366	52	381	61
Iron	ppm	2.16	28.63	2.29	22.80	1.36	29.69	1.41	19.61
Aluminium	ppm	2.18	2.51	2.22	2.35	1.55	2.65	1.66	2.22
Copper	ppm	1.01	3.63	1.12	4.09	0.41	14.00	0.40	2.72
Lead	ppm	0.79	15.42	0.90	7.25	0.17	13.40	0.20	9.19
Soot	% weight	0.08	1.45	0.09	0.88	0.01	1.39	0.01	1.04

4.4 General engine oil performance discussion

Taking an overall view of the test, the following facts can be drawn about the performance of the four formulations under study (leaving aside the Lube A, which was considered as reference): 5W30 API CK–4 (Lube B), 5W30 API FA–4 (Lube C), 10W30 API CK–4 (Lube D) and 10W30 API FA–4 (Lube E). The most relevant results have been summarised in the list below:

- The first, and therefore the most important aspect, is that all the engine oil formulations have shown a suitable response (as expected) for a period of use of 30000 km under the different conditions and demands of the vehicles involved in the study. However, it is also necessary to state that in none of them is advisable to extend the ODI. The useful life of the engine oils is clearly justified at 30000 km in view of the obtained performance, and it is not possible to extend it any further, especially for CNG vehicles.

- As far as the degradation of the engine oils is concerned, the following patterns have been extracted:

  – The degradation of the additive package is quite significant, being more noticeable in the case of the antiwear additives (always when

compared to the Lube A lubricating oil, taken as reference). This has to be put into context, as the four engine oils do not start from the same initial additive values. Taking this into account, it is understandable that with similar depletion ratios in the Lube B, Lube C, Lube D and Lube E formulations (with lower ZDDP contents), total additive depletion occurs in the middle of the oil drain interval (approximately 15000–20000 km). On this basis, of the variety of antiwear additives available, ZDDPs are the most widely represented family. Assuming that this type of compound is used for this purpose, it is known that in addition to this property of protection against wear, they also have an antioxidant action. It is because of this additional characteristic that their consumption can influence the wear effects and also the effects of excessive oxidation of the engine oil: increased acidification, attack on soft metals, etc.

- The loss or drop of the initial TBN value during the test is quite significant, especially the drop at low mileage (at the first sampling, 5000 km). Apart from the relationship between anti-wear additives and TBN evolution, this effect does not imply a major significance. The effect of TBN reduction on the possible damage to the engines is minimised because the fuels used in this test have a high degree of cleanliness (so the amount of sulphur content is practically null).
- The acidification levels (TAN) are, from the experience gained in the Maintenance Engineering group of CMT–Motores Térmicos, relatively high in the four engine oils. This can be a disadvantage, as it can cause the soft metals (mainly lead, but also copper) in the engines to experience wear problems. This is a further problem to be considered due to the performance reflected by the antiwear additives in the studied formulations. However, TAN levels are conditioned or sensitive to several factors to be taken into consideration: firstly, the composition of the engine oil (base oil and additives package) and also the characteristics of the engine where it is used. Taking this into account, it is not surprising that in some cases, the variability of results obtained was considerable.

Thus, combining the effects of antiwear additive depletion and oil acidification, it is not surprising that when these factors go out of control, wear levels, especially of soft metals (such as lead), reach significant values.

- Another point to be explained in detail is the case of the boron-based additive. A satisfactory explanation could be found for the repeated

behaviour of boron in the Lube B, Lube C, Lube D and Lube E formulations. Typically, the additive packages used in engine oils are polymeric compounds or molecules involving metal atoms. With use, additives degrade (destroy/decompose), but it has been observed that the metal content is, within certain levels, stable. But in the case of boron, this rule was broken. After a careful study of the problem to find a potential and academic explanation as to why the boron content decreases during the use of engine oil, the most plausible hypothesis lies on boron chemistry. Organic boron compounds are water (humidity) and air sensitive substances, so when they are exposed to conditions that combine one or both of these factors, these compounds begin to undergo changes. Under these wet and oxidising conditions, boron compounds often decompose and transform into boric acid (H_3BO_3). These unfavourable conditions for boron are found in ICEs. As a result of combustion in ICEs, water (in the form of vapour), carbon dioxide and heat are mainly generated. Therefore, the boron when combined with these elements will give rise to the formation of boric acid. This acid is a non-soluble substance in the lubricating oils, and it is therefore a precursor of deposits, which are ultimately removed or retained by the oil filter or sedimented at the bottom of the crankcase. To conclude, in accordance with the reasons set out in this point, it is confirmed that the evolution shown by boron throughout the test was not entirely abnormal, since it has a satisfactory and logical explanation.

- The presence of sodium in the oils is most likely due to the type of coolant used in the vehicles involved in the test. The coolant used is an antifreeze based on ETG (ethylene glycol, CAS: 107-21-1) (about 30–40% vol), which also contains an additive based on sodium, the sodium salt of 2-ethylhexanoic acid ($CH_3(CH_2)_3CH(C_2H_5)CO_2Na$, CAS: 19766-89-3). The most commonly used long-life coolants, whose formulation is based on EG and corrosion inhibitors (mostly copper and bronze), use as additives inhibitors derived from carboxylates, thiazoles and/or triazoles. This is due to the enhanced corrosion protection provided by these compounds, which covers all internal metal engine parts (including aluminium). So it is not surprising that these types of coolants are the most widespread choice due to their wide applicability irrespective of the engine technology under consideration. In the case of the carboxylate salt mentioned above, it is known that carboxylates are corrosion inhibitors which have a slow depletion rate and are also compounds with a high chemical stability (when compared to other traditional inhibitors such as silicate-based inhibitors). The levels of

sodium detected in some engine oil samples may therefore, as described above, be due to some incidence in the cooling system of certain vehicles, as this is the only feasible source of sodium that can reach the engine oil. Therefore, if the cooling system leaks, the leaking coolant reaches the engine oil and contaminates it. However, due to the temperatures at which the engine oil works, the major component of the coolant, water, is susceptible to evaporation (disappears), while the rest (EG and additives) becomes more and more concentrated. However, the control and monitoring of coolant contamination, commonly performed by FT–IR spectroscopy according to ASTM E2412, seems to be invalid for the engine oil formulations studied in this research. The trend reflected by the glycol signal by FT–IR does not present a coherent pattern, so its use to determine problems with the coolant system was abandoned in favour of the analysis of sodium by ICP–OES, which has allowed a correct analysis and detection of this type of contamination problems with the coolant fluid.

- Finally and to conclude, the problems (external to the oils) that have been detected in the vehicles during the evolution of the test have been basically two: problems with the cooling system (described in the previous point) and with the intake and/or air filtration system. In the latter, the most logical reason is that there has been a problem with the intake system, as high levels of dust (measured by ICP–OES spectrometry following the evolution of silicon levels) have been collected in some cases.

4.A Appendix: In-depth study of the performance of engine oils

The purpose of this appendix is to provide a better explanation of certain registered data that are far from logical in relation to the global trends of the different formulations. Basically, in these cases, those anomalies are justified by a problem with a vehicle (of whatever type, I, II, III or IV) which, at the time of the study, was not in optimal conditions or had previous failures or problems.

This appendix shows the results of the study of the lubricating oils performance, but with an extra aspect that has not been considered before as it was not the main objective of the study. Now, the data of each participating vehicle will be shown individually. Thanks to this, it will be possible to discern any differences in the performance of the different formulations (Lube A, Lube B, Lube C, Lube D and Lube E), which were caused either by the condition of the vehicles at the time of the test or by the occurrence of some specific problems along the test. The aim of this appendix is therefore to provide a better understanding of the actual performance of the engine oil formulations by eliminating, as far as possible, the contribution of the vehicle.

Because the study was conducted in two parts, given that it was a time-consuming study (about two years, from 2017 until almost entering 2020), the results will also be shown in two groups:

- One, for the first iteration with the engine oils: Lube A, Lube B and Lube C.
- And the second for the iteration corresponding to the oils: Lube A, Lube D and Lube E.

Accordingly, each vehicle within each typology (type I, type II, type III or type IV) has been tracked individually and represented by a unique and identifying symbol.

4.A.1 Type I vehicles

Type I vehicles were the vehicles selected to test the performance of four engine oil formulations: Lube B and Lube C in the first stage and Lube D and E for the second stage.

4.A.1.1 First iteration

In this stage of the test, studying the Lube B and Lube C engine oil formulations, the results for each vehicle are shown below.

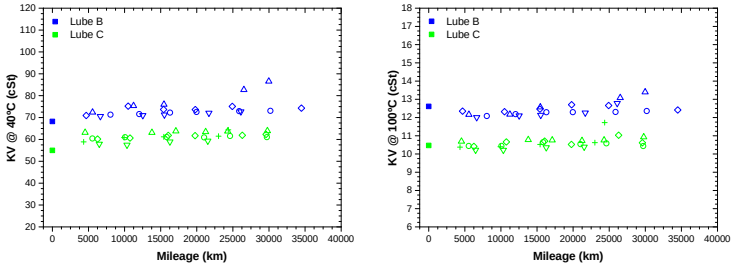

(a) Kinematic viscosity at 40°C (b) Kinematic viscosity at 100°C

Figure 4.33. *Evolution of KV of Lube B and Lube C used in vehicles type I.*

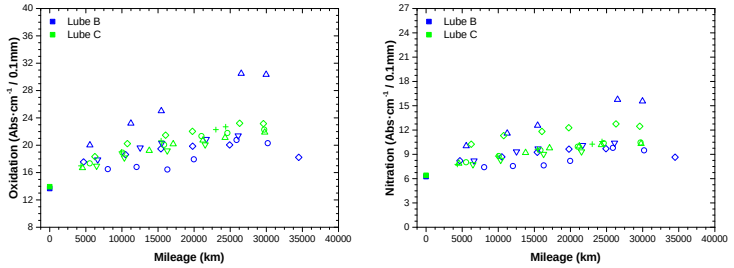

(a) Oxidation, by FT–IR, of the tested engine oils (b) Nitration, by FT–IR, of the tested engine oils

Figure 4.34. *Evolution of oxidation and nitration of Lube B and Lube C used in vehicles type I.*

Among the 9 type I vehicles involved, problems have been detected in:

- The vehicle symbolised by △ in blue edges shows problems resulting from a poor general condition of the vehicle before the test. As a result, its oil is observed to undergo more oxidation and nitration than its homologues (Figure 4.34), which, in turn, leads to a higher TBN depletion and consequently to a noticeable increase in the acidity of the lubricating oil, as shown in Figure 4.36. The poor condition of the engine and the marked degradation of the oil used in this vehicle, together

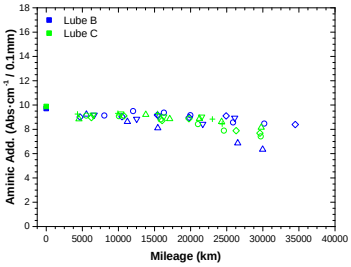

(a) Aminic additives by FT–IR spectroscopy

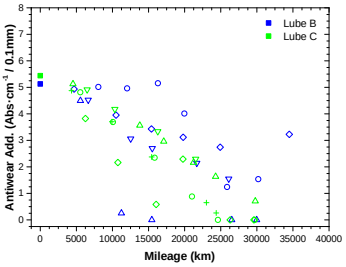

(b) Antiwear additives by FT–IR spectroscopy

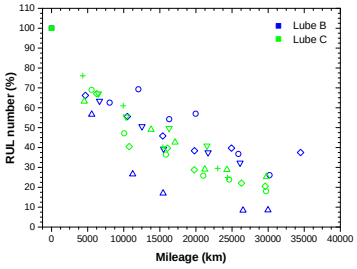

(c) RUL number

Figure 4.35. *Depletion of antioxidant additives of Lube B and Lube C used in vehicles type I.*

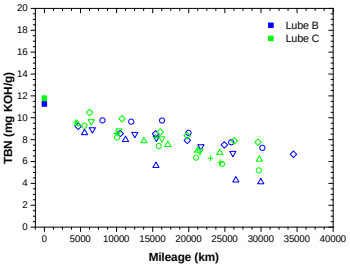

(a) TBN index by thermometric titration

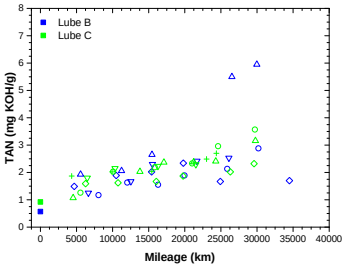

(b) TAN index by thermometric titration

Figure 4.36. *Performance of TBN/TAN index of Lube B and Lube C used in vehicles type I.*

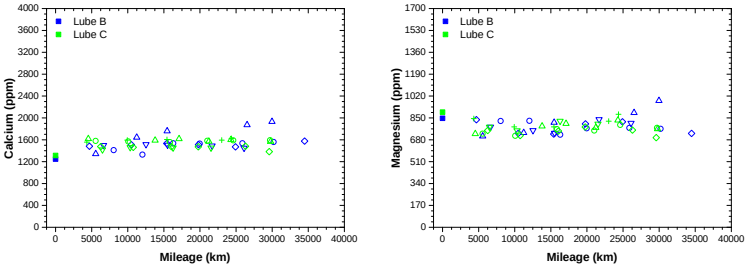

(a) Calcium measured by ICP–OES

(b) Magnesium measured by ICP–OES

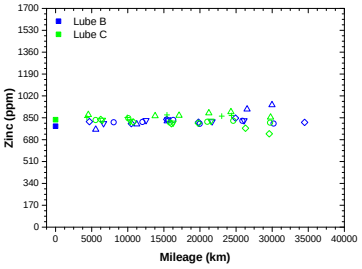

(c) Zinc measured by ICP–OES

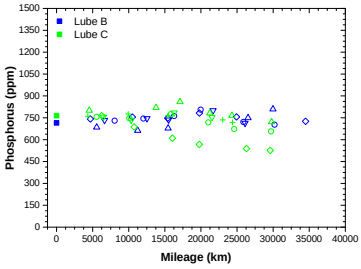

(d) Phosphorus measured by ICP–OES

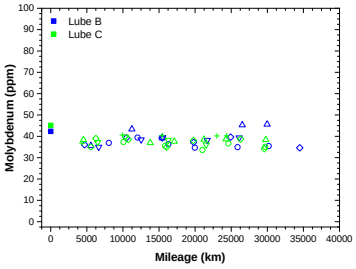

(e) Molybdenum measured by ICP–OES

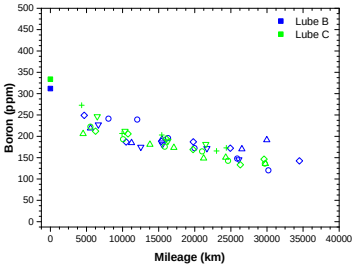

(f) Boron measured by ICP–OES

Figure 4.37. *Additive package of Lube B and Lube C used in vehicles type I.*

with problems with soot and the cooling system (Figure 4.38). Soot, an abrasive agent, will cause metal levels to increase (see the evolution of iron and aluminium in Figure 4.39). Leaks from the cooling system, followed by the sodium content present in the lubricating oil samples (Figrua 4.38), is another problem blamed on the poor maintenance of this vehicle. Water contamination is an undesirable problem in engines because of all the issues it entails (increased corrosion of lubricated

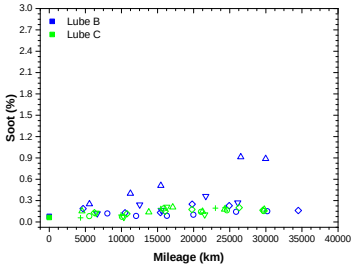

(a) Soot quantified by FT–IR

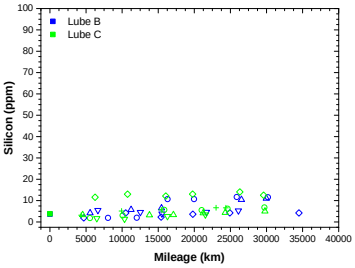

(b) Silicon quantified by ICP–OES

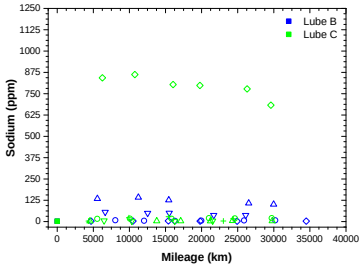

(c) Sodium quantified by ICP–OES

Figure 4.38. *Presence of contaminants in Lube B and Lube C used in vehicles type I.*

elements, loss of efficiency of the lubricant film, etc.), so this type of problem has been detected with this monitoring and requires prompt action to solve it. In addition, the higher acidity shown throughout the test results in copper and lead levels close to 10 ppm although, for the ODI, these are not very alarming levels (taking into consideration all the previous problems described).

- The copper levels shown in the last two samples of engine oil (Lube B) by the vehicle represented by blue ○, seem to have no apparent justification to explain this situation. As this was a very interesting case, the problem was investigated further and information was obtained about interventions on main shaft and camshaft bearings, which are either made of copper alloys or directly finished with copper. As problems were reported on these two systems, it is not surprising that any tampering or replacement of elements affecting them could cause the copper levels collected.

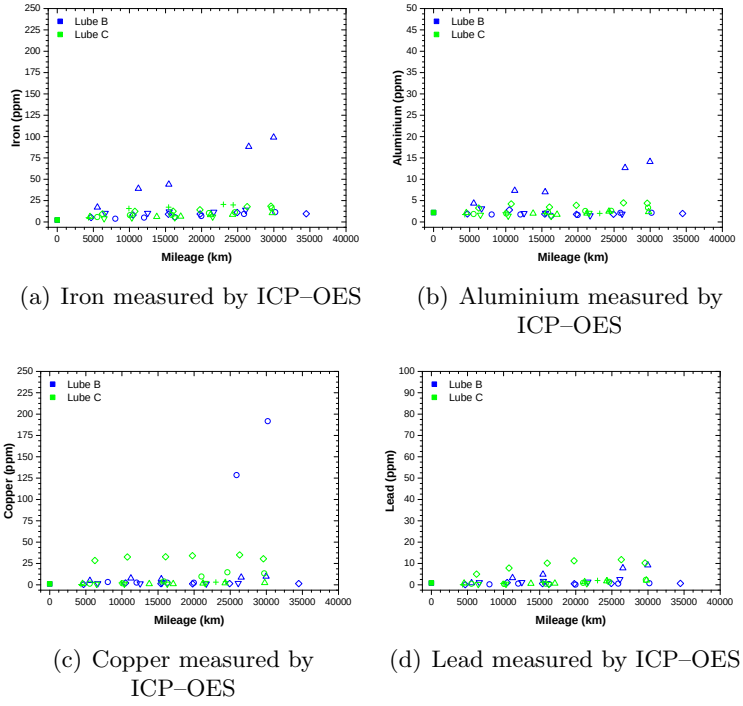

(a) Iron measured by ICP–OES

(b) Aluminium measured by ICP–OES

(c) Copper measured by ICP–OES

(d) Lead measured by ICP–OES

Figure 4.39. *Wear metals found in Lube B and Lube C used in vehicle types I.*

- For the formulation of Lube C engine oil, the vehicle symbolised by ◇ in green shows signs of meeting a set of problems. Most alarming is the more than 800 ppm of sodium over the entire duration of the test that each of the 6 samples showed in Figure 4.38. The cooling system is composed of a set of pipes and heat exchangers based on copper and lead alloys, so detecting levels of these metals gives indication of some kind of leakage problem in the system. Due to the intercommunication between the lubrication and cooling system, the levels of sodium are so high. Another aspect to be taken into account is the presence of silicon, indicative of oil contamination by atmospheric dust, in the oil. However, these levels do not cause abrasive wear on any of the typical metals (iron and aluminium), except for the soft metals (copper and lead) already explained. The last aspect to consider is that this vehicle causes a slight nitration of the engine oil compared to the others using Lube C engine oil formulation, but this was not of major significance.

4.A.1.2 Second iteration

In the next phase of the research, the engine oils were changed to the other two formulations: Lube D and Lube E. The following is a compilation of the results of this particular stage.

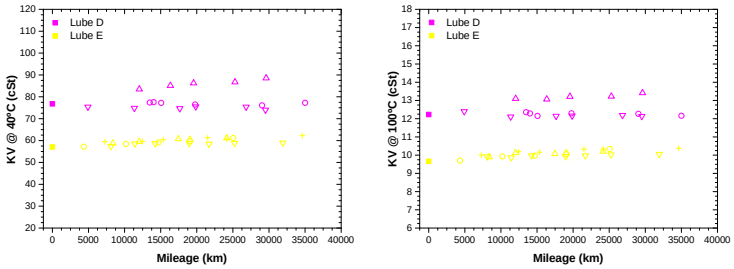

(a) Kinematic viscosity at 40°C (b) Kinematic viscosity at 100°C

Figure 4.40. *Evolution of KV of Lube D and Lube E used in vehicles type I.*

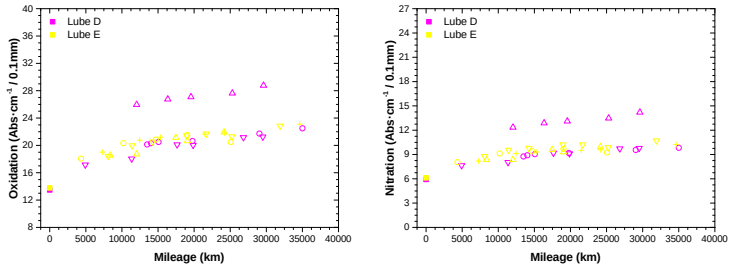

(a) Oxidation, by FT–IR, of the tested engine oils (b) Nitration, by FT–IR, of the tested engine oils

Figure 4.41. *Evolution of oxidation and nitration of Lube D and Lube E used in vehicles type I.*

According to the philosophy behind the research, in the second phase it is possible to determine whether certain problems with the vehicles have been solved or, for whatever reason, new ones have appeared. With this in mind, observations in the second iteration are described in the following lines:

- Again, the vehicle symbolised by a △, but now in pink color indicating the Lube D formulation, is still showing problems. The features that make the behaviour displayed by this vehicle distinctive are varied:

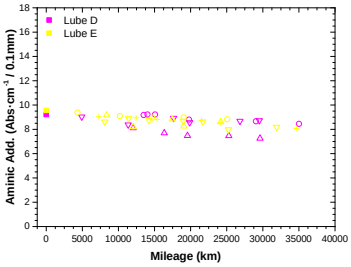

(a) Aminic additives by FT–IR spectroscopy

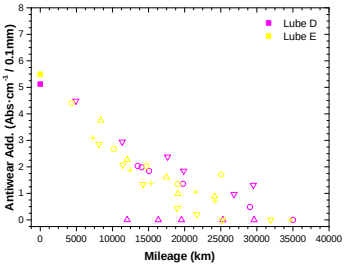

(b) Antiwear additives by FT–IR spectroscopy

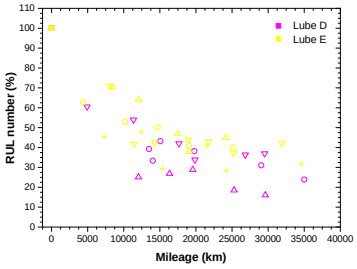

(c) RUL number

Figure 4.42. *Depletion of antioxidant additives of Lube D and Lube E used in vehicles type I.*

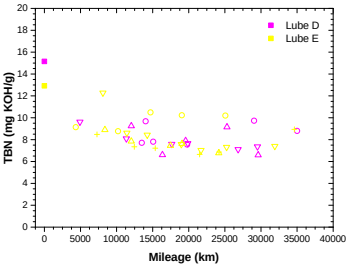

(a) TBN index by thermometric titration

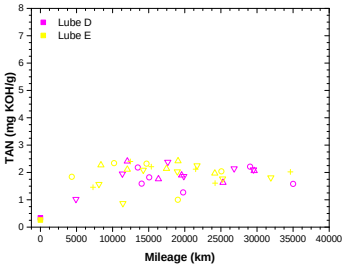

(b) TAN index by thermometric titration

Figure 4.43. *Performance of TBN/TAN index of Lube D and Lube E used in vehicles type I.*

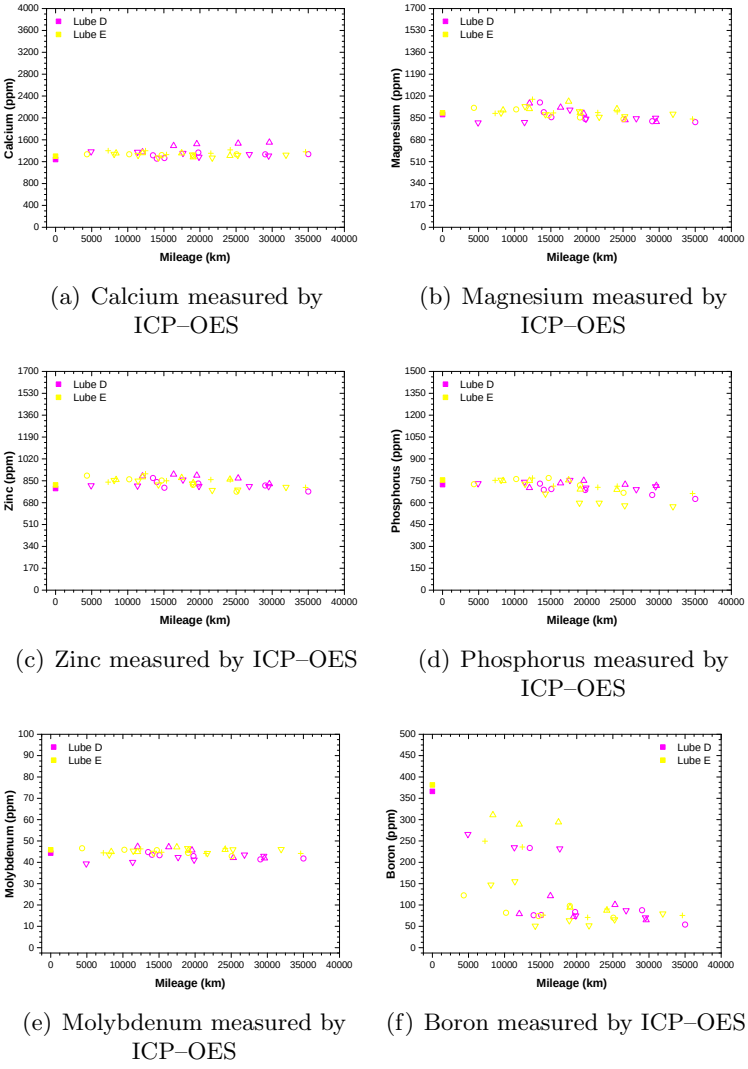

(a) Calcium measured by ICP–OES

(b) Magnesium measured by ICP–OES

(c) Zinc measured by ICP–OES

(d) Phosphorus measured by ICP–OES

(e) Molybdenum measured by ICP–OES

(f) Boron measured by ICP–OES

Figure 4.44. *Additive package of Lube D and Lube E used in vehicles type I.*

firstly, it shows significantly higher kinematic viscosity values (Figure 4.40) than the rest, both at 40 and 100 degrees Celsius together with the oxidation and nitration parameters of Figure 4.41. In terms of the aminic and antiwear additive package, in both, the levels of this vehicle are below the trend set by the rest (a fact highlighted by looking at the RUL number graph in Figure 4.42). As these additives, and especially the antiwear, are compromised, it is not surprising that iron and aluminium

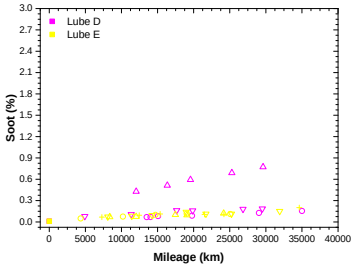

(a) Soot quantified by FT–IR

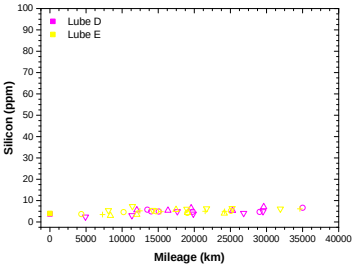

(b) Silicon quantified by ICP–OES

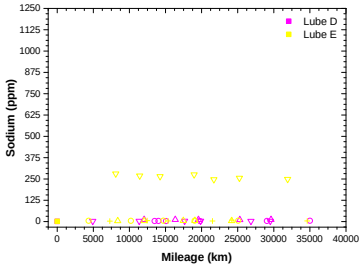

(c) Sodium quantified by ICP–OES

Figure 4.45. *Presence of contaminants in Lube D and Lube E used in vehicles type I.*

levels are significant, as this property loss is compounded by soot concentrations (Figure 4.45) which enhance metallic wear. However, the good aspect of this study is that the problem with the cooling system has been solved, as no sodium has been detected again in the oil samples of this vehicle.

- Another case, inherited from the first stage, is the vehicle symbolised by a pink–○. As in the results reported in the first iteration, it seems that there is no logical reason to justify these copper values (around 40 ppm). According to the other parameters that have been monitored, none of them stands out and, moreover, affect copper. Therefore, given that the copper levels remain constant throughout the test, this suggests that the vehicle in question is undergoing some kind of intervention beyond the control of the study, since if it were due to wear and tear of any kind, this copper concentration would be increasing over time (which is not the case).

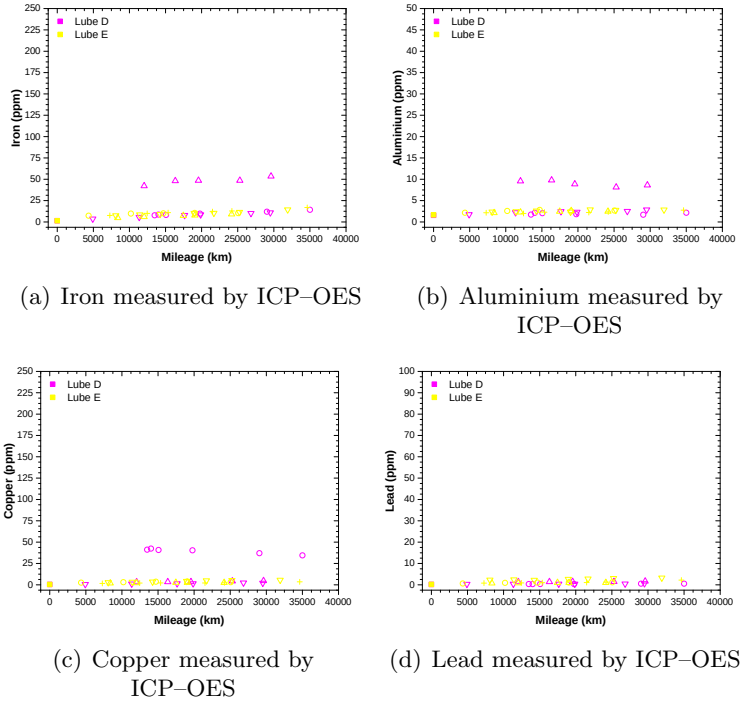

(a) Iron measured by ICP–OES

(b) Aluminium measured by ICP–OES

(c) Copper measured by ICP–OES

(d) Lead measured by ICP–OES

Figure 4.46. *Wear metals found in Lube D and Lube E used in vehicle types I.*

- Finally, a case related to sodium contamination in engine oil samples of Lube E formulation (Figure 4.45) in the vehicle was shown by a yellow inverted triangle (▽). The levels obtained (∼250 ppm) indicates cooling system problems/leaks reaching the engine oil.

4.A.2 Type II vehicles

This section will show the results of the two phases of the research involving Type II vehicles. Here it should be noted that, in both phases, the reference engine oil (Lube A) was used. This reference engine oil, recommended for the type of fleet to which all the vehicles belonged (from type I to IV), is the one used as a point of comparison for the analysis of the performance of the new formulations: Lube B, Lube C, Lube D and Lube E. Specifically, for type II vehicles, the engine oils to be studied were Lube B and Lube D, in the first and second iteration, respectively.

4.A.2.1 First iteration

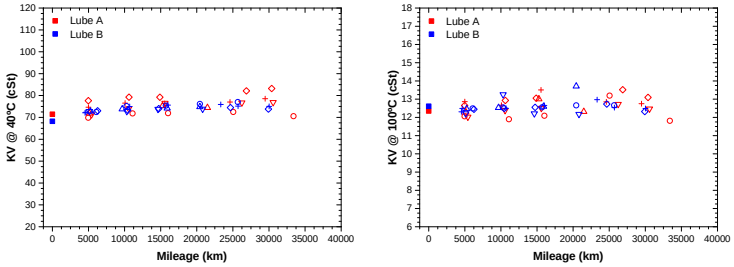

(a) Kinematic viscosity at 40°C (b) Kinematic viscosity at 100°C

Figure 4.47. *Evolution of KV of Lube A and Lube B used in vehicles type II.*

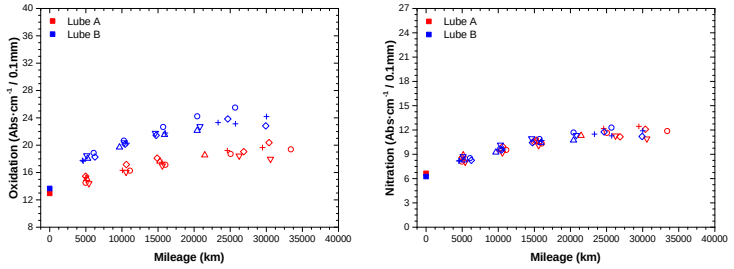

(a) Oxidation, by FT–IR, of the tested engine oils (b) Nitration, by FT–IR, of the tested engine oils

Figure 4.48. *Evolution of oxidation and nitration of Lube A and Lube B used in vehicles type II.*

From the analysis of all the graphs generated, a number of aspects should be noted:

- In general, for the case of the vehicles studied with the Lube A formulation (colored by red), all the parameters measured (for each individual vehicle) fall within the expected range. However, some signs of iron wear have been detected in the vehicles symbolised by ∘ and △ which, it is expected that in the second iteration, they will no continue to occur and will be a one-off case.

- In the case of the vehicle represented by the blue ▽ (according to the Lube B formulation used by the vehicle), some levels of sodium have been

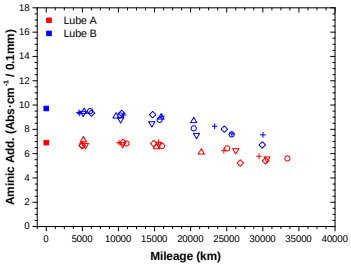

(a) Aminic additives by FT–IR spectroscopy

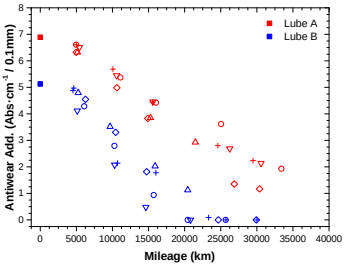

(b) Antiwear additives by FT–IR spectroscopy

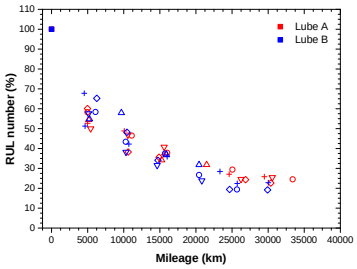

(c) RUL number

Figure 4.49. *Depletion of antioxidant additives of Lube A and Lube B in vehicles type II.*

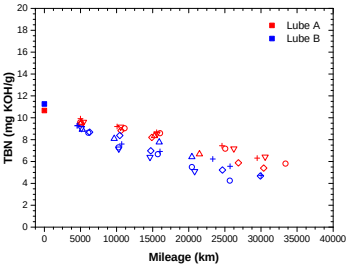

(a) TBN index by thermometric titration

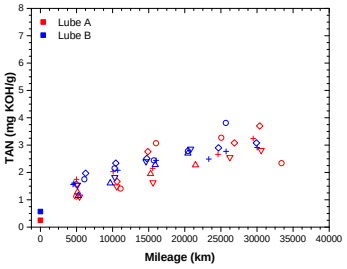

(b) TAN index by thermometric titration

Figure 4.50. *Performance of TBN/TAN index of Lube A and Lube B used in vehicles type II.*

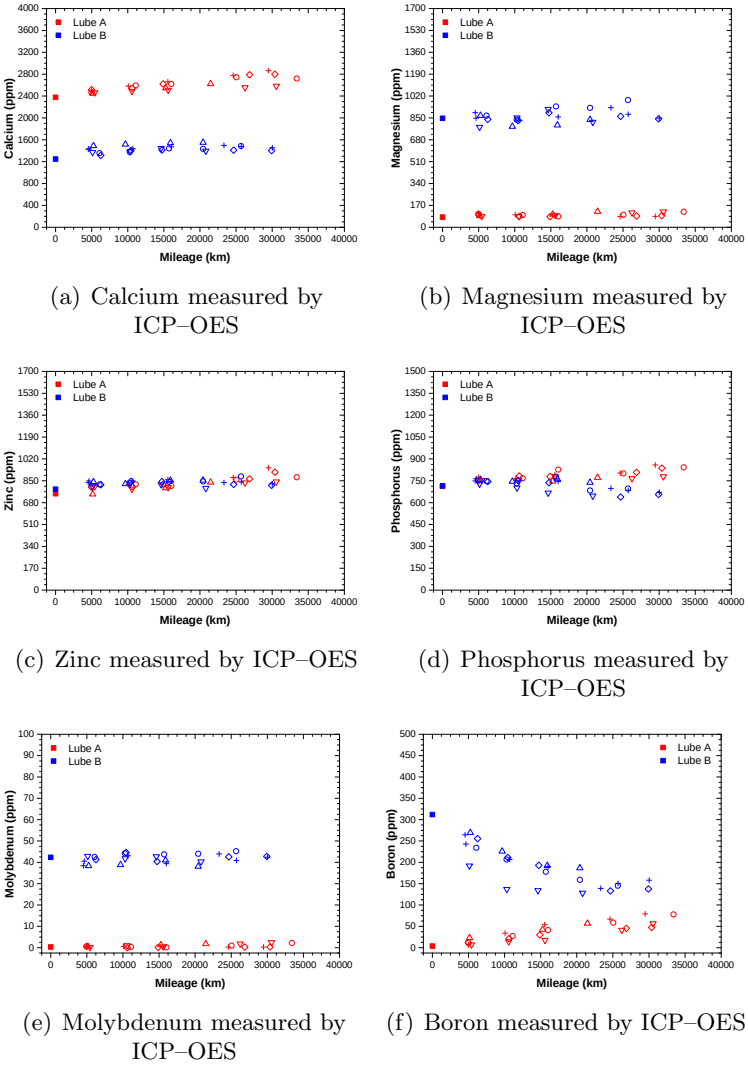

(a) Calcium measured by ICP–OES

(b) Magnesium measured by ICP–OES

(c) Zinc measured by ICP–OES

(d) Phosphorus measured by ICP–OES

(e) Molybdenum measured by ICP–OES

(f) Boron measured by ICP–OES

Figure 4.51. *Additive package of Lube A and Lube B used in vehicles type II.*

detected (Figure 4.52), so it can be indicative that it has some small leaks in the cooling system, but not to the extent of being a serious problem. Another aspect that must be controlled so that it does not become a major issue is the case of lead, at the end of the test a total of 10 ppm has been accumulated but, according to the problems in the cooling system that have been detected, it can be a vector of major problems if it is not monitored.

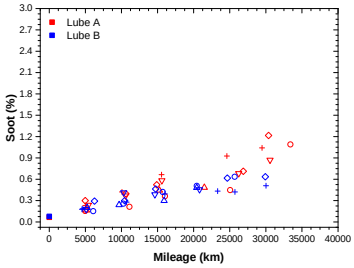

(a) Soot quantified by FT–IR

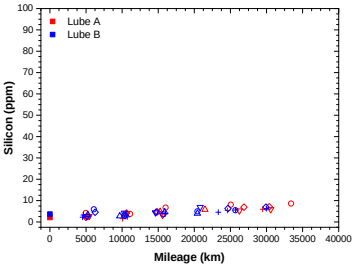

(b) Silicon quantified by ICP–OES

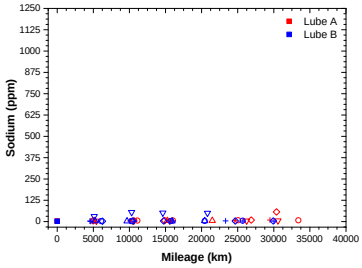

(c) Sodium quantified by ICP–OES

Figure 4.52. *Presence of contaminants in Lube A and Lube B used in vehicles type II.*

- For the vehicle using Lube B engine oil formulation and being symbolised by ◇, it shows aluminium wear problems (see Figure 4.53). As with the previous vehicle (represented by blue ▽), there are indications of some lead wear at the end of the test. The levels collected are not high, but according to the characteristics and age of the vehicles, a follow-up is desirable.

- Vehicle blue–+ simply has a higher aluminium wear rate than the other participating vehicles using the same engine oil formulation. These levels of aluminium, after studying the rest of the parameters, are not easy to deduce since it is difficult to find a source or focus of these levels of aluminium in the oil. The most likely candidate is that the connecting rod bearings have some problems or damage, so they experience wear and tear. For this reason, special attention should be paid to this issue in the future (second stage) in case it is still occurring and/or aggravating.

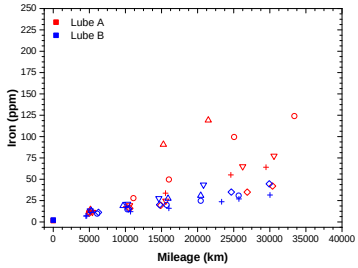

(a) Iron measured by ICP–OES

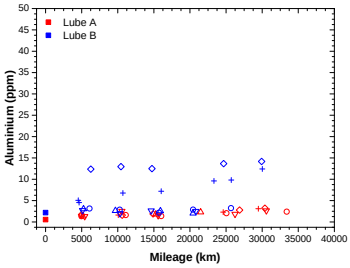

(b) Aluminium measured by ICP–OES

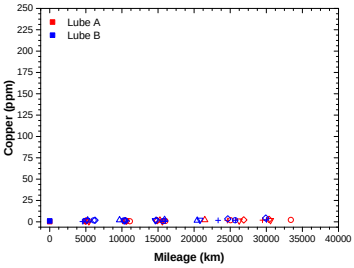

(c) Copper measured by ICP–OES

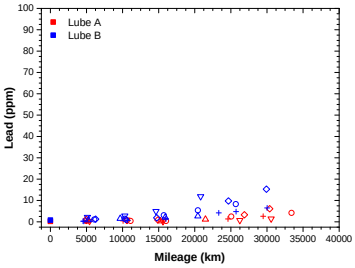

(d) Lead measured by ICP–OES

Figure 4.53. *Wear metals found in Lube A and Lube B used in vehicle types II.*

4.A.2.2 Second iteration

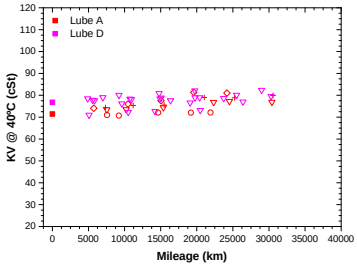

(a) Kinematic viscosity at 40°C

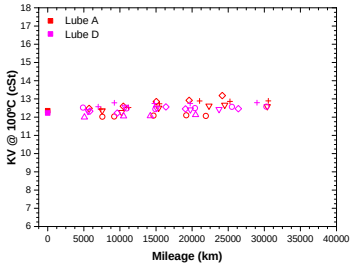

(b) Kinematic viscosity at 100°C

Figure 4.54. *Evolution of KV of Lube A and Lube D used in vehicles type II.*

Now, in the second iteration of engine oil formulations: Lube A to Lube A (is constant due to its role like reference) and Lube B to Lube C, the test

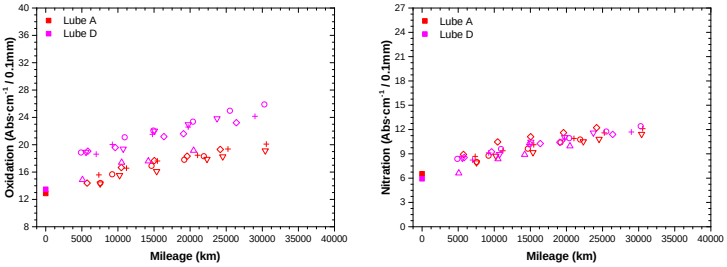

(a) Oxidation, by FT–IR, of the tested engine oils

(b) Nitration, by FT–IR, of the tested engine oils

Figure 4.55. *Evolution of oxidation and nitration of Lube A and Lube D used in vehicles type II.*

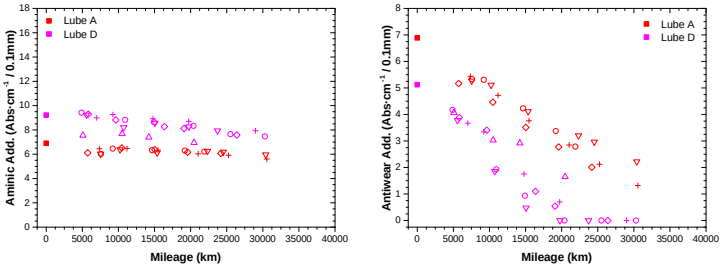

(a) Aminic additives by FT–IR spectroscopy

(b) Antiwear additives by FT–IR spectroscopy

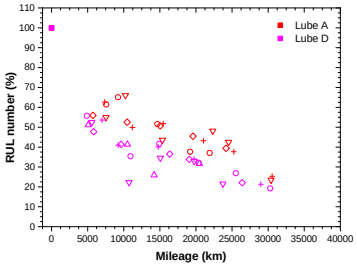

(c) RUL number

Figure 4.56. *Depletion of antioxidant additives of Lube A and Lube D used in vehicles type II.*

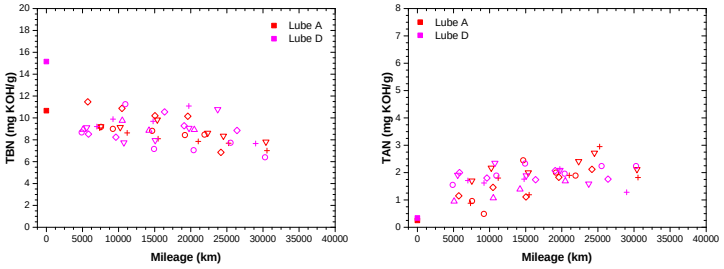

(a) TBN index by thermometric titration

(b) TAN index by thermometric titration

Figure 4.57. *Performance of TBN/TAN index of Lube A and Lube D used in vehicles type II.*

will check whether the problems (detected in the first stage) of maintenance or condition of certain vehicles have been solved, or whether the increase in viscosity of the engine oil (from SAE 5W30 to 10W30) has a beneficial effect, or the opposite is true. Accordingly, the conclusions drawn for each vehicle are listed below:

- There are two vehicles, ○ and ▽ both in red (Lube A), which show signs of iron wear during the whole test. These are values to be taken into account, but due to the age of the vehicles, it is not surprising that they are already starting to experience some wear problems (in particular, according to its characteristics set out in Table 4.3, all those systems where bearings are involved). Of these two, ○ was already indicated in the previous stage as having iron wear problems, thus being a historical problem that drags behind this particular vehicle. In addition, throughout the test, the vehicle red–○ has had levels of silicon detected in its oil samples, silicon from atmospheric dust which can enter the oil due to intake system or air filtration failures. So, if it already had iron wear problems, but in addition to the presence of this abrasive element, the wear phenomena are magnified, justifying the concentration of iron that has been recorded.

- Switching to a different case, vehicle red–◇ shows problems with the cooling system at this stage (no such problems were detected at the first stage). The sodium levels detected (Figure 4.59), although decreasing, are not easily justifiable by comparison with the other monitored parameters. For this particular case, in the first stage there were no

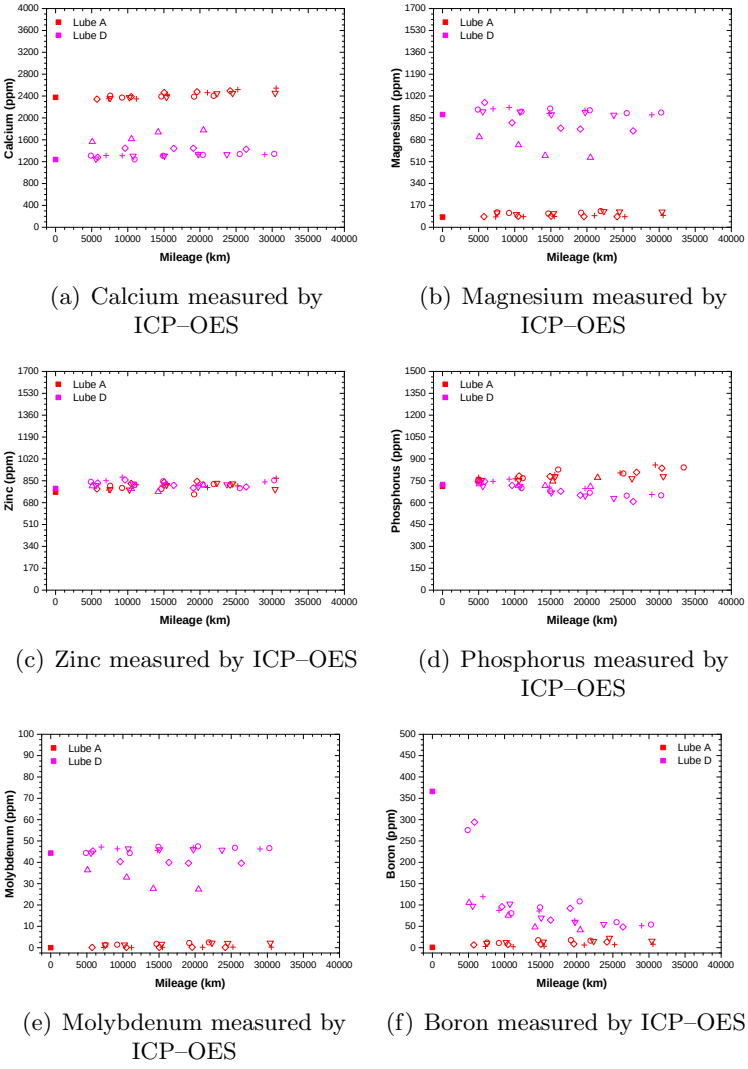

(a) Calcium measured by ICP–OES

(b) Magnesium measured by ICP–OES

(c) Zinc measured by ICP–OES

(d) Phosphorus measured by ICP–OES

(e) Molybdenum measured by ICP–OES

(f) Boron measured by ICP–OES

Figure 4.58. *Additive package of Lube A and Lube D used in vehicles type II.*

problems with the cooling system, so according to the very high levels reported, it seems to clearly indicate some incidence during the inter-stage period where the engine oil and other consumable engine fluids, including the coolant, were replaced. It is possible that some kind of failure or negligence, external to the control capabilities in this test, occurred at that time.

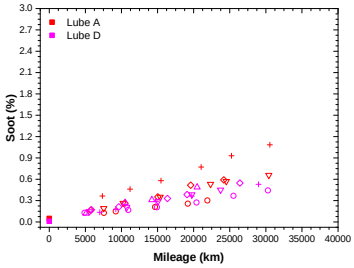

(a) Soot quantified by FT–IR

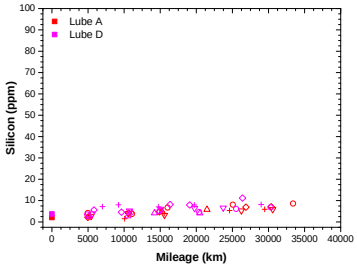

(b) Silicon quantified by ICP–OES

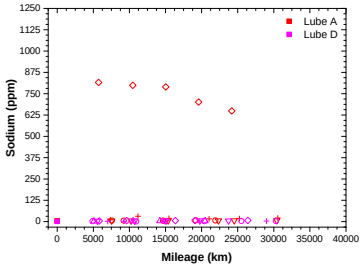

(c) Sodium quantified by ICP–OES

Figure 4.59. *Presence of contaminants in Lube A and Lube D used in vehicles type II.*

- The last vehicle to be mentioned, which uses Lube A, is red–+. It appears that the soot generation ratio is slightly higher than the other participating vehicles using the reference engine oil. This performance has not led to any problems related to an increase in engine oil viscosity or wear of the internal lubricated elements of the engine. Therefore, it seems that the combustion in this vehicle is not entirely efficient, and it would be recommended that the injection system and the oil filtration system be checked to rule out possible future failures.

- By changing the formulation, Lube E (pink), certain wear effects or phenomena have been detected in some vehicles. Specially, ◇ and + vehicles show signs of aluminium wear as shown in Figure 4.60. In perceiving this degradation process, it was noted that it already existed in the first iteration. It seems that in these two particular vehicles, elements manufactured with this metal: connecting rod bearings and main shaft bearings (mainly), are subjected to more

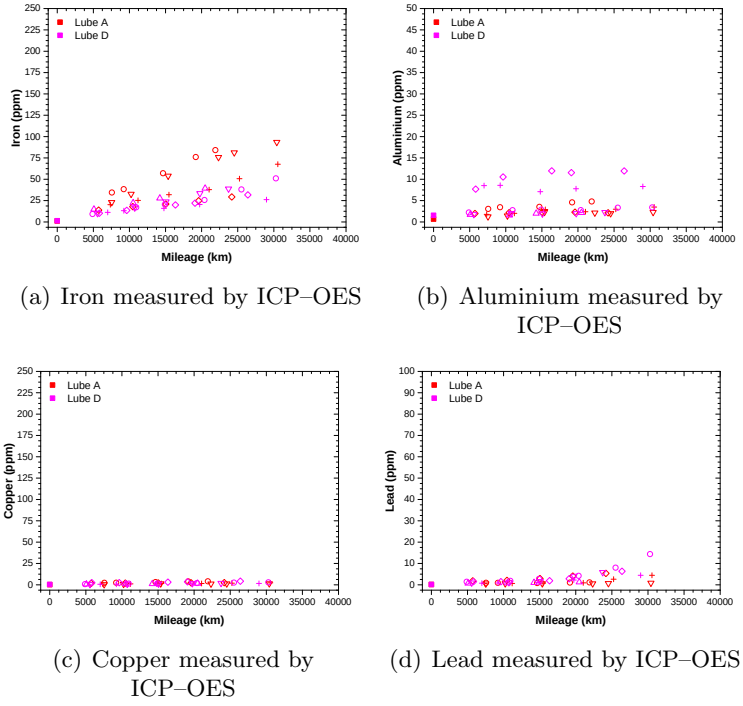

(a) Iron measured by ICP–OES

(b) Aluminium measured by ICP–OES

(c) Copper measured by ICP–OES

(d) Lead measured by ICP–OES

Figure 4.60. *Wear metals found in V used in vehicle types II.*

demanding conditions. One reason for this increased wear may be the contamination of their engine oil by dust, as the silicon levels in their samples ranged from 10 ppm, making it a significant abrasive wear vector. These two cases could be categorised as historical problems for these particular vehicles, since they are occurring in both stages of the study.

- The vehicle, symbolised by a circle (○) with a pink outline, was found to have an increased concentration of lead in its engine oil samples taken close to the end of the test. This break in the general trend justifies the general idea that the ODI cannot be extended, since it appears that the acidification of the engine oil would be increased to considerable levels.

- Finally, a special case is the pink–△. There is a certain abnormal performance in this vehicle. This performance is evident if the whole set of monitored parameters is analysed, as it is not surprising that incorrect engine oil refills have occurred. Indeed, when looking in detail at the distinguishing features between the Lube A and Lube D formulations,

this is noticeable. Looking at the additive package, Figure 4.58, it can be seen that the levels of calcium, magnesium and molybdenum (the most dissimilar parameters between the two formulations) are midway between the two lubricating oils. So, in conclusion, Lube D engine oil has been contaminated by a certain volume of Lube A as a result of an error in refilling the volume of engine oil. However, despite this, the mixing of engine oils has not led to any problems, apart from the slight discrepancies observed when monitoring the parameters of the lubricating oil.

4.A.3 Type III vehicles

In Type III vehicles, powered by Compressed Natural Gas (CNG), the engine oil formulations Lube B and Lube C were studied in the first stage of the research, while in the second phase they were replaced by its higher SAE grade equivalents, Lube D and Lube E, respectively. In this way, when moving on to the second stage, the API grade was kept constant but the effect of engine oils with a higher SAE viscosity was studied: from 5W30 API CK–4 (Lube B) to 10W30 API CK–A4 (Lube D) and from 5W30 API FA–4 (Lube C) to 10W30 API FA–A4 (Lube E).

4.A.3.1 First iteration

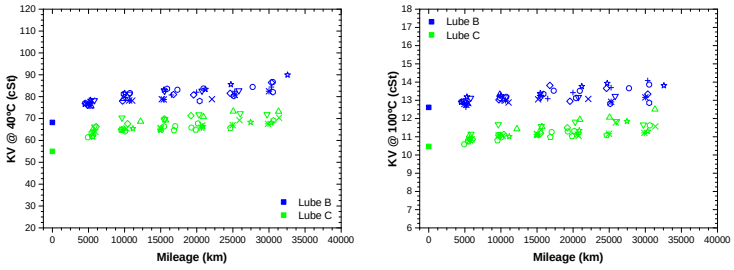

(a) Kinematic viscosity at 40°C (b) Kinematic viscosity at 100°C

Figure 4.61. *Evolution of KV of Lube B and Lube C used in vehicles type III.*

According to the results collected from the sampling of engine oils and its subsequent chemical-physical analysis in the institute's laboratory, the following facts can be extracted:

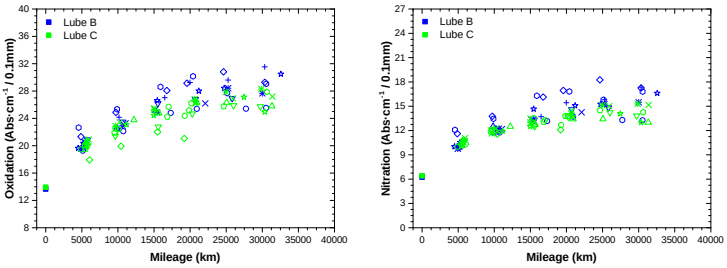

(a) Oxidation, by FT–IR, of the tested engine oils

(b) Nitration, by FT–IR, of the tested engine oils

Figure 4.62. *Evolution of oxidation and nitration of Lube B and Lube C used in vehicles type III.*

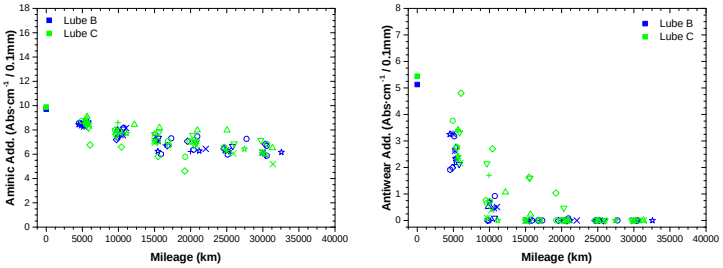

(a) Aminic additives by FT–IR spectroscopy

(b) Antiwear additives by FT–IR spectroscopy

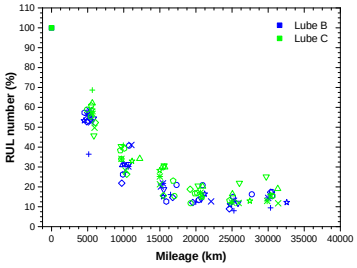

(c) RUL number

Figure 4.63. *Depletion of antioxidant additives of Lube B and Lube C used in vehicles type III.*

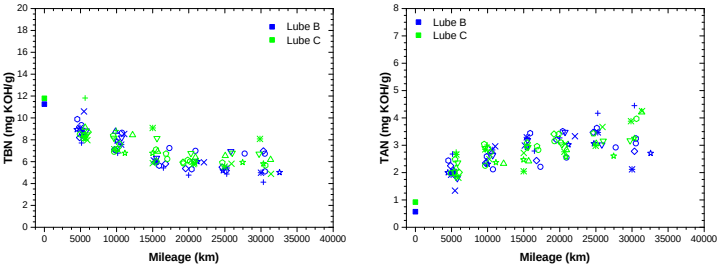

(a) TBN index by thermometric titration

(b) TAN index by thermometric titration

Figure 4.64. *Performance of TBN/TAN index of Lube B and Lube C used in vehicles type III.*

- In the case of Lube B (coloured in blue), the following vehicles present a number of problems:
  - The first to be discussed is the vehicle symbolised by a ◇. This vehicle in question is in an overall bad state for several reasons: it suffers from higher levels of oxidation and nitration than the rest (Figure 4.62), but also contamination by silicon and sodium at high levels (Figure 4.66). Consequently, the engine oil is not in an optimal state and is therefore an engine oil with a certain acidic (copper and lead levels are visible) and abrasive character, as reported by the levels of iron and aluminium (Figure 4.67).
  - Vehicle + is the one that has the highest TAN value (with a corresponding decrease in the TBN). This fact justifies that metals susceptible to acid attack, such as lead and copper, are present in the engine oil samples of this vehicle. They are more pronounced in the first of them, given that it experiences an exponential increase from 15000 kilometres onwards (see Figure 4.67).
  - The next participant, represented by ⬭, is also a vehicle with a variety of problems. More importantly, similarly to the previous case (vehicle +), it presents contamination problems. This is due to the ingress of dust (monitored by the silicon) and by the coolant flowing into the engine oil due to high sodium levels (250 ppm), as shown in Figure 4.66. As a result, the oil is in poor condition and lubrication is inadequate, leading to wear phenomena. To corroborate this impression, it is sufficient to observe the levels of iron and aluminium. However, not only does this contamination

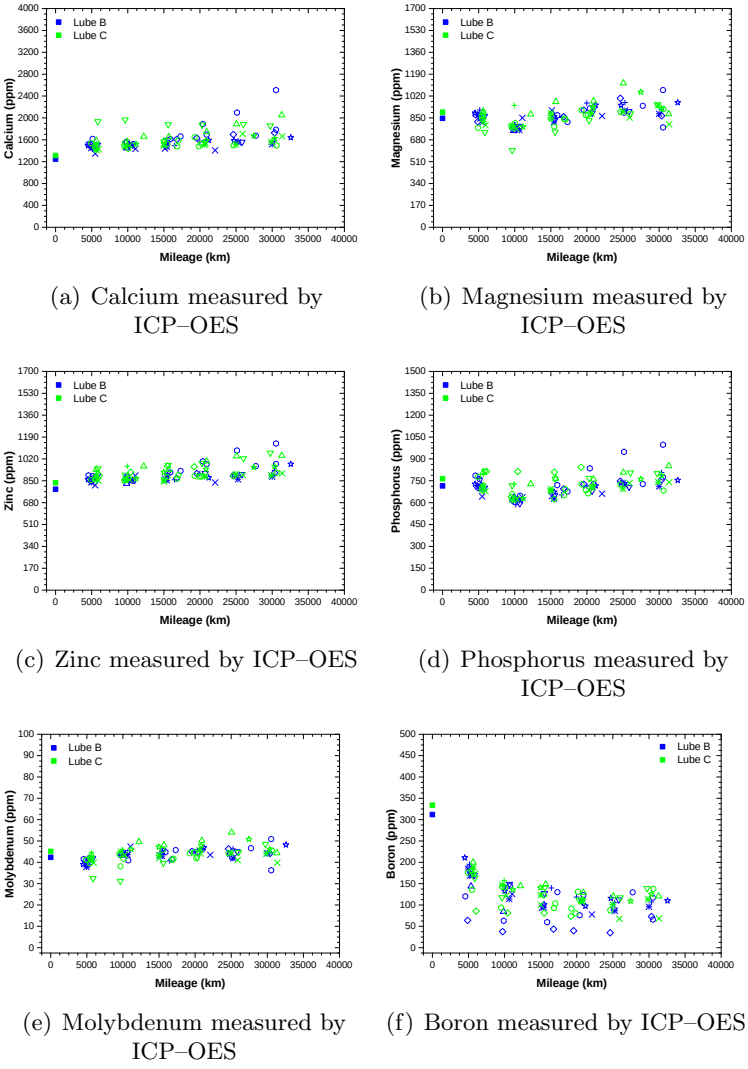

(a) Calcium measured by ICP–OES

(b) Magnesium measured by ICP–OES

(c) Zinc measured by ICP–OES

(d) Phosphorus measured by ICP–OES

(e) Molybdenum measured by ICP–OES

(f) Boron measured by ICP–OES

Figure 4.65. *Additive package of Lube B and Lube C used in vehicles type III.*

modify the physical aspects of the engine oil, it also alters/modifies its chemical properties: enhances its degradation and depletion of additives, leading to wear problems due to corrosive attack on the lead (mostly). In view of the results, it would be advisable to intervene extensively on the vehicle in order to try to solve the different systems involved and, in addition, to detect the cause of

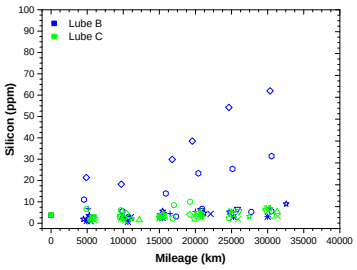

(a) Silicon quantified by ICP–OES

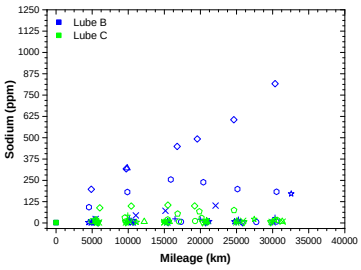

(b) Sodium quantified by ICP–OES

Figure 4.66. *Presence of contaminants in Lube B and Lube C used in vehicles type III.*

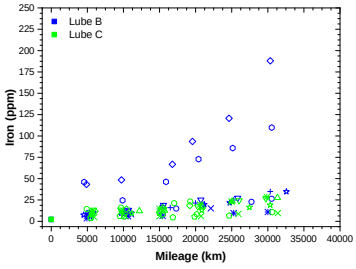

(a) Iron measured by ICP–OES

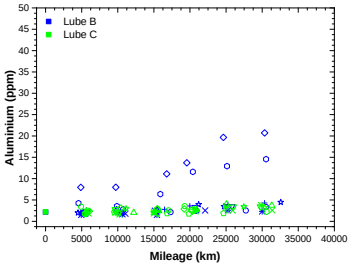

(b) Aluminium measured by ICP–OES

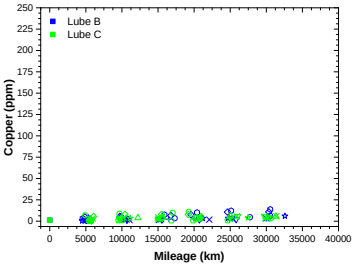

(c) Copper measured by ICP–OES

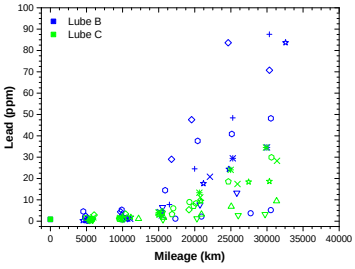

(d) Lead measured by ICP–OES

Figure 4.67. *Wear metals found in Lube B and Lube C used in vehicle types III.*

the high consumption of engine oil (as indicated by increasing levels of metallic additives).

- The last vehicle to be discussed, which uses Lube B oil, is the vehicle symbolised by ⋆. For this case, problems with the cooling system have also been detected, although not as serious as its predecessors at the end of the test (sodium levels of 125 ppm are observed). But, the most worrying fact is the sharp drop in lead levels (see Figure 4.67). Initially, this jump has occurred beyond the defined threshold of 30000 kilometres, which serves as a compelling reason to state that these formulations are not designed for periods of use longer than the one being tested.

- Switching to the Lube C formulation, coloured by green, the cases to be discussed are as follows:

  - Another case of erroneous engine oil refill is the one involving vehicle ▽. The first indicator is the slight increase in kinematic viscosity (Figure 4.61) without any apparent reason. Only if one looks at the metallic additive package in Figure 4.65, where the recorded calcium values corroborate this suspicion.
  - The next case is that of the vehicle represented by ◇, which shows a more pronounced depletion of the aminic and antiwear additives in the engine oil (Figure 4.63). It appears that the coolant contamination (∼100 ppm) which also occurs may act as an accelerator of this marked additive depletion in this particular vehicle.
  - The vehicle represented by ⬠ shows signs of problems with the refrigeration system, since there is coolant contamination in the engine oil, as indicated by the 70 ppm of sodium that has been recorded. The last reason is that, in the absence of the last sample of 30000 mileage, indications of lead wear were already occurring and should be taken into consideration for the future.
  - The latter are a set of four vehicles: ×, ∗, ⬡ and ⋆, which all have lead wear problems. For this set, the reason for this wear is due to the acidification of the engine oil in accordance with the TAN levels (see Figure 4.64) measured in their samples.

According to the cases reported, it seems that in this type of engines, the problems are more numerous, but basically they are centred on two sources: the cooling system and the higher thermal demand of the oil by the engines.

Now, in the second iteration of the test, it is hoped that the problems have been solved or at least have not worsened.

4.A.3.2 Second iteration

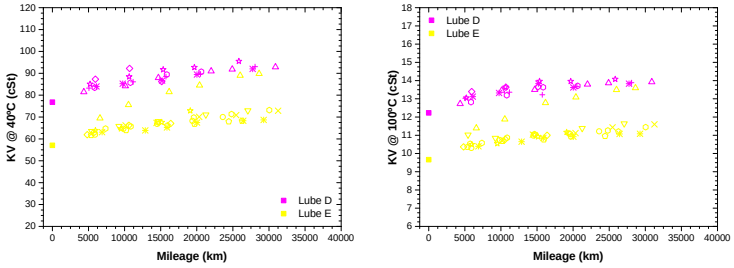

(a) Kinematic viscosity at 40°C (b) Kinematic viscosity at 100°C

Figure 4.68. *Evolution of KV of Lube D and Lube E used in vehicles type III.*

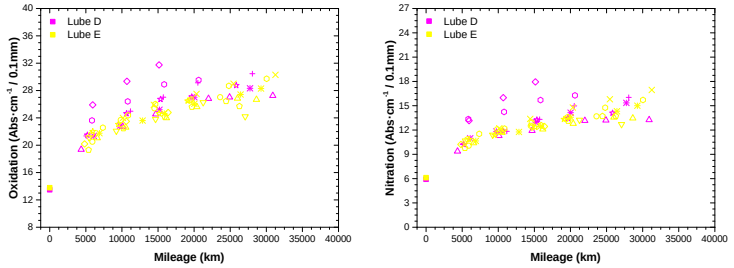

(a) Oxidation, by FT–IR, of the tested engine oils (b) Nitration, by FT–IR, of the tested engine oils

Figure 4.69. *Evolution of oxidation and nitration of Lube D and Lube E used in vehicles type III.*

The results for each vehicle involved in this research on the performance of these two new more viscous formulations, Lube D and Lube E (both SAE 10W30) than those used in the first one (SAE 5W30), are listed below:

- For vehicles lubricated with Lube D engine oil, there are three cases to be considered:
  - There are two vehicles with serious maintenance problems, one of them is represented by a ◇ and the other by an ⬡, even though

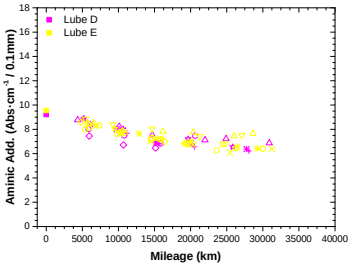

(a) Aminic additives by FT–IR spectroscopy

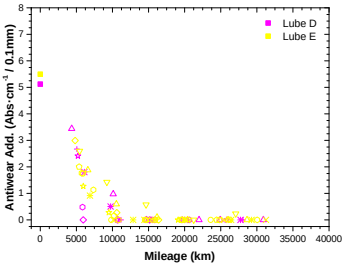

(b) Antiwear additives by FT–IR spectroscopy

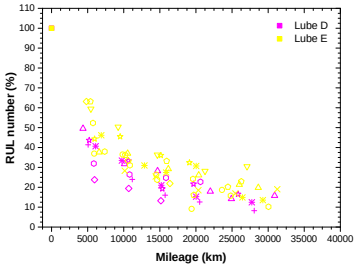

(c) RUL number

Figure 4.70. *Depletion of antioxidant additives of Lube D and Lube E used in vehicles type III.*

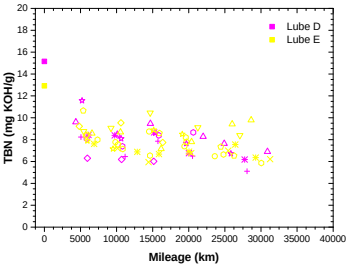

(a) TBN index by thermometric titration

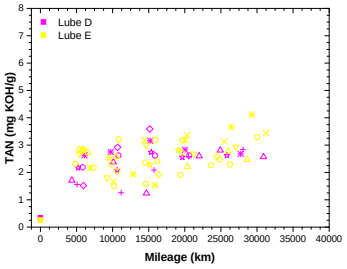

(b) TAN index by thermometric titration

Figure 4.71. *Performance of TBN/TAN index of Lube D and Lube E used in vehicles type III.*

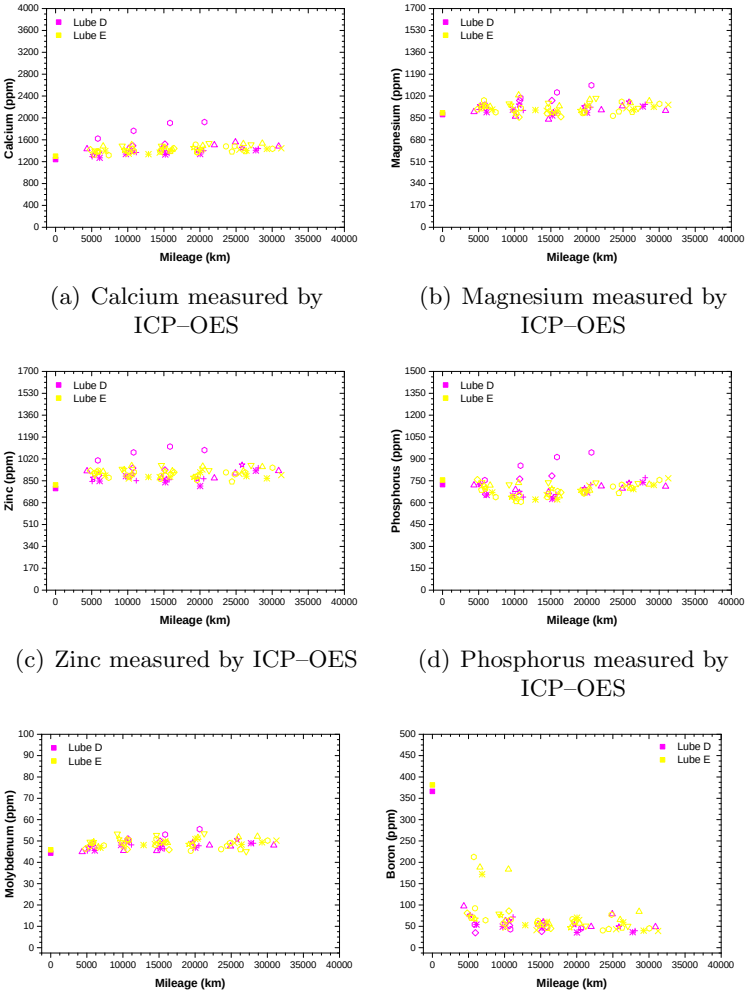

(a) Calcium measured by ICP–OES

(b) Magnesium measured by ICP–OES

(c) Zinc measured by ICP–OES

(d) Phosphorus measured by ICP–OES

(e) Molybdenum measured by ICP–OES

(f) Boron measured by ICP–OES

Figure 4.72. *Additive package of Lube D and Lube E used in vehicles type III.*

these vehicles have similar results, the first being the more worrying. Both present problems on several fronts: the oxidative degradation and nitration of the engine oil is very high, and so its additives (see Figure 4.70) are used up more quickly, with the antiwear additives having been completely used up by 5000 kilometres. Thus, as a consequence, TBN levels decline to low levels (◇ in the first sample already undergoes a 50% reduction) and TAN increases following a

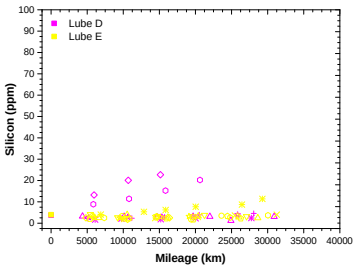

(a) Silicon quantified by ICP–OES

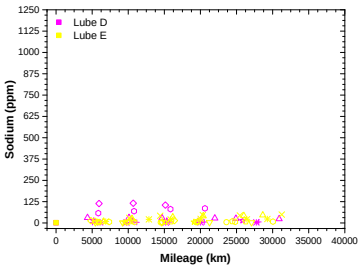

(b) Sodium quantified by ICP–OES

Figure 4.73. *Presence of contaminants in Lube D and Lube E used in vehicles type III.*

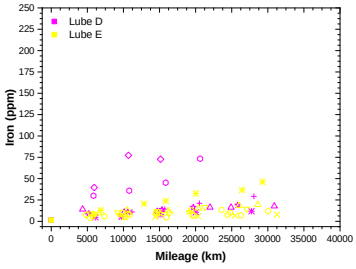

(a) Iron measured by ICP–OES

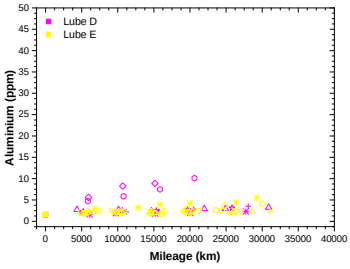

(b) Aluminium measured by ICP–OES

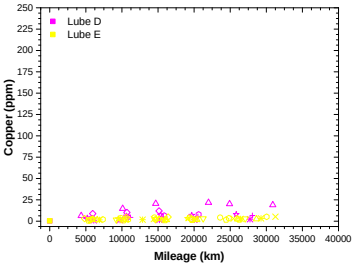

(c) Copper measured by ICP–OES

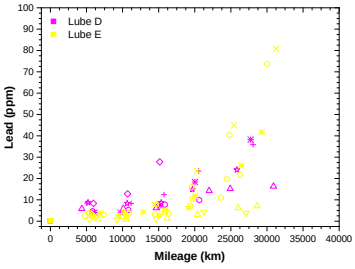

(d) Lead measured by ICP–OES

Figure 4.74. *Wear metals found in Lube D and Lube E used in vehicle types III.*

higher ratio. In addition, there are problems of silicon and sodium contamination (Figure 4.73), so that the conditions of the oil are not the most suitable. Working under these circumstances, it is not uncommon to collect wear levels of metals, both abrasive (iron and aluminium) and corrosive (mainly lead). Furthermore, it was noted that on this pair of vehicles, different engine oil refills were done throughout the test, being very pronounced in the case of the ⬡, as can be seen by the increasing levels of the metallic additive package (Figure 4.72).

- Moving on, vehicle △ has been found to have copper engine oil wear problems with the levels observed in Figure 4.74 (around 25 ppm). It appears that this is not a critical problem, but should be kept under control to prevent the problem from continuing and worsening.
- To conclude with the vehicles lubricated with the Lube D formulation, there is the pair represented by ∗ and +, both of which present problems with the lead levels detected in this study (see Figure 4.74).

- Switching to Lube E, what is found when analysing the performance of the engine oil for each vehicle comes together in the following points:

  - The first case is represented by a triangle (△). This vehicle in particular has a more pronounced increase in kinematic viscosity than the others as shown in Figure 4.68. Despite this phenomenon, no other divergence in performance has been detected in the other monitored parameters, so it does not raise any further concerns. However, taking a more global view of the parameters, it is not surprising that this vehicle experienced engine oil refills (necessary during the test) with the other 10W30 CK–4 formula.
  - The next case is the one involving the ×-vehicle. First of all, the problems with the cooling system (as pointed out by the sodium levels in their engine oil samples) have to be mentioned. Leaving aside the contamination issue described above, the other aspect is that this vehicle places higher demands on the engine oil, so the oxidation and nitration monitored (see Figure 4.69) during the test is higher than the others. Thus, a derivation of this event is that the TAN recorded for this vehicle is as high as 3 mg KOH/g, which favours an increase in lead content at the end of the test, see Figure 4.74.

– The vehicle with Lube E symbolised by ∗, as a consequence of the levels of silicon (Figure 4.73) carried in its engine oil during the test, has caused the iron and aluminium constituent elements of the engine to suffer wear as shown in Figure 4.74. In addition, it is also important to note how the acidity shown by the engine oil, indicated by the level of TAN in the Figure 4.71 over 4 mg KOH/g, has led to the presence of significant lead levels (increasing further towards the end of the test).
– Finally, the vehicle represented by ⎔ shows lead values in the samples collected during the sampling phase. As can be seen in Figure 4.74, lead starts to appear in significant concentrations from 15000 – 20000 kilometres, at this point the ratio increases markedly.

4.A.4 Type IV vehicles

In the last type of vehicles, the engine oils assigned to the study were: Lube B, Lube C, Lube D and Lube E. It should be taken into account that these diesel-powered vehicles have an EGR exhaust gas recirculation system and, in addition, do not necessarily experience high mechanical requirements (see Table 4.2). So, in this case, the performance that can be obtained will be different from the rest of the vehicles in the test that also used diesel fuel (type I and type II).

4.A.4.1 First iteration

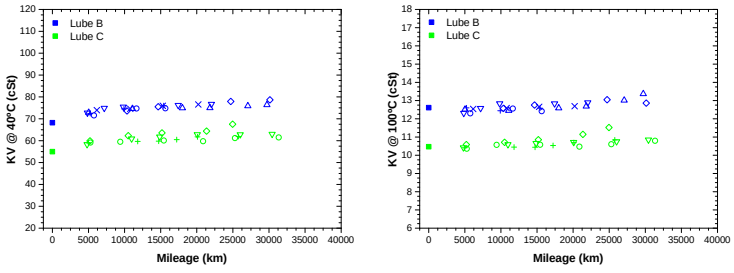

(a) Kinematic viscosity at 40°C (b) Kinematic viscosity at 100°C

Figure 4.75. *Evolution of KV of Lube B and Lube C used in vehicles type IV.*

For the description and discussion of the results obtained, these will be organised into two groups: the first group will discuss the results obtained

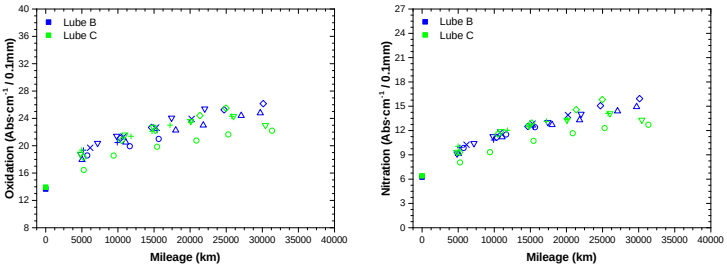

(a) Oxidation, by FT–IR, of the tested engine oils

(b) Nitration, by FT–IR, of the tested engine oils

Figure 4.76. *Evolution of oxidation and nitration of Lube B and Lube C used in vehicles type IV.*

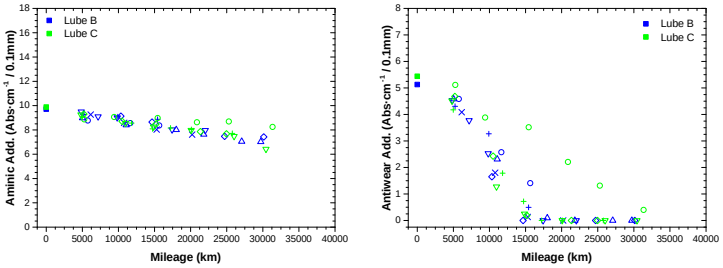

(a) Aminic additives by FT–IR spectroscopy

(b) Antiwear additives by FT–IR spectroscopy

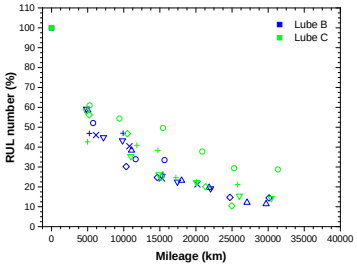

(c) RUL number

Figure 4.77. *Depletion of antioxidant additives of Lube B and Lube C used in vehicles type IV.*

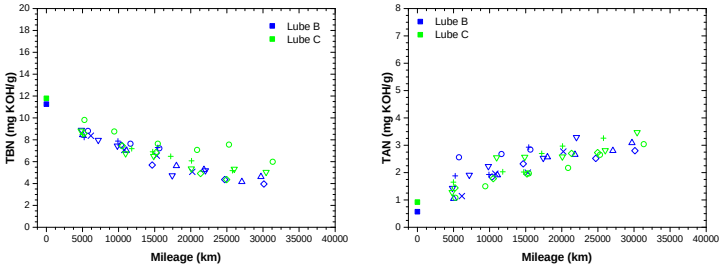

(a) TBN index by thermometric titration

(b) TAN index by thermometric titration

Figure 4.78. *Performance of TBN/TAN index of Lube B and Lube C used in vehicles type IV.*

for vehicles using Lube B engine oil (coloured by blue) and the second group will discuss the results obtained for vehicles using Lube C engine oil (green). Thus, for the first case, the results are shown in the following list:

- The first interesting vehicle is the one symbolised by a blue circle (○). The most relevant fact is that this vehicle did not complete the test for reasons beyond the control of this investigation. However, this does not prevent valuable information from being extracted simply by obtaining three samples of engine oil taken from this vehicle: 5000, 10000 and 15000 kilometres. With all three of them, it could be seen that the degradation and wear parameters of this vehicle were higher than the rest, being the case of the TAN the most remarkable, as shown in Figure 4.78.

- The vehicle with the blue–△ symbol has a considerable concentration of soot, ∼1.5%, not surprisingly due to the EGR on the engine of these vehicles and the beginnings of lead wear.

- Vehicle ▽ on the other hand, shows considerable levels of acidification of the engine oil, as can be seen in Figure 4.78, but in addition, the iron wear rates should not be neglected due to the ppm contained in the samples.

- For the ◇ vehicle, the levels of almost 2% of soot in oil (see Figure 4.80) cause its engine oil to acquire an abrasive character, so that wherever this contaminated oil runs, it causes erosion on the surfaces involved. This is particularly noticeable when 50 ppm of iron and almost 30 ppm

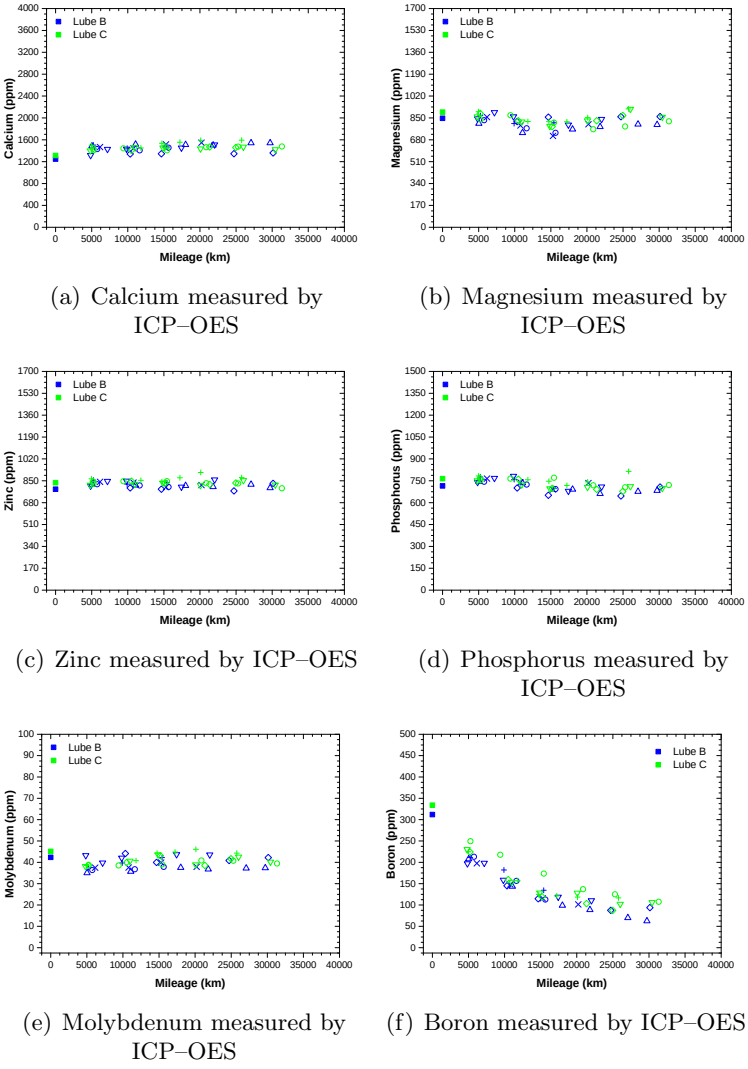

(a) Calcium measured by ICP–OES

(b) Magnesium measured by ICP–OES

(c) Zinc measured by ICP–OES

(d) Phosphorus measured by ICP–OES

(e) Molybdenum measured by ICP–OES

(f) Boron measured by ICP–OES

Figure 4.79. *Additive package of Lube B and Lube C used in vehicles type IV.*

of lead are found, which confirms the idea that the engine oil needs to be replaced or the oil filter in order to minimise the concentration of this problematic soot.

- Finally, vehicle + shows light levels of copper (Figure 4.81), which are within the levels established as normal, but as it stands out from the

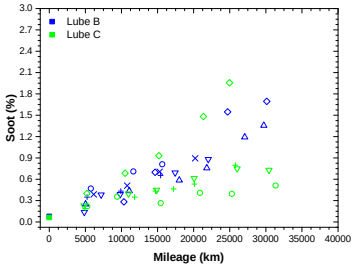

(a) Soot quantified by FT–IR

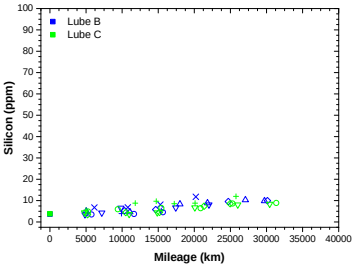

(b) Silicon quantified by ICP–OES

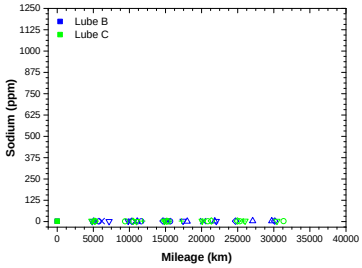

(c) Sodium quantified by ICP–OES

Figure 4.80. *Presence of contaminants in Lube B and Lube C used in vehicles type IV.*

rest, it is convenient to take it into consideration for the second iteration of the test.

Now, for Type IV vehicles using Lube C engine oil, the most relevant data are listed below:

- The green-*circle* vehicle is a special case; the engine oil retains its properties better than the others: as far as oxidation and nitration are concerned, this vehicle shows the lowest values (check by looking at Figure 4.76), so that the additives (aminic and antiwear) reach the end of the test (which is exceptional in the case of antiwear as corroborated in Figure 4.77) and consequently, the TBN level of the engine oil is high and does not allow the TAN to shoot up.

- Vehicle ▽ has been found to have lead values of around 10 ppm at the end of the test, approximately. Given that this occurred at the end of

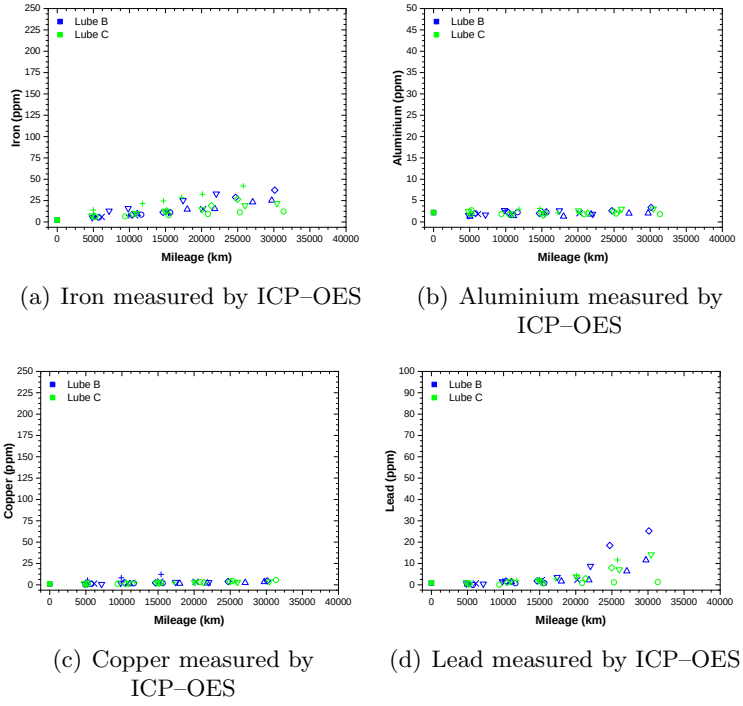

(a) Iron measured by ICP–OES

(b) Aluminium measured by ICP–OES

(c) Copper measured by ICP–OES

(d) Lead measured by ICP–OES

Figure 4.81. *Wear metals found in Lube B and Lube C used in vehicle types IV.*

the test and does not present any other problem, it can be left under observation to see if in the second stage this problem will reappear.

- A more complex case is that of the vehicle represented by ◇. In this module, first of all, the engine oil is more viscous than the rest as shown in Figure 4.75, which can be seen by the oxidation and nitration levels, together with the soot levels of almost 2%. The combination of these three parameters conditions this increase in viscosity. Additionally, lead has also been detected in the oil samples, so the vehicle must be kept under observation in order to avoid unwanted problems in the second stage.

- Finally, vehicle + has problems with silicon contamination, which leads to the appearance of wear metal levels in the engine oil. The most noticeable is iron with about 50 ppm and lead with more than 10 ppm.

4.A.4.2 Second iteration

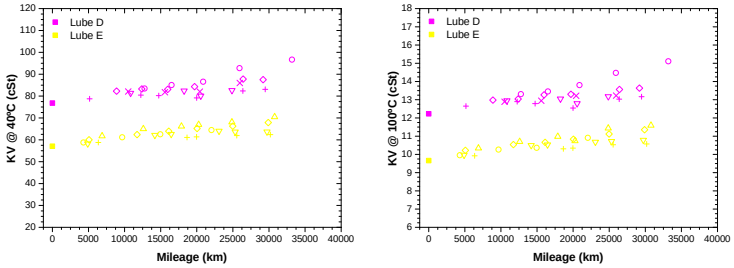

(a) Kinematic viscosity at 40°C (b) Kinematic viscosity at 100°C

Figure 4.82. *Evolution of KV of Lube D and Lube E used in vehicles type IV.*

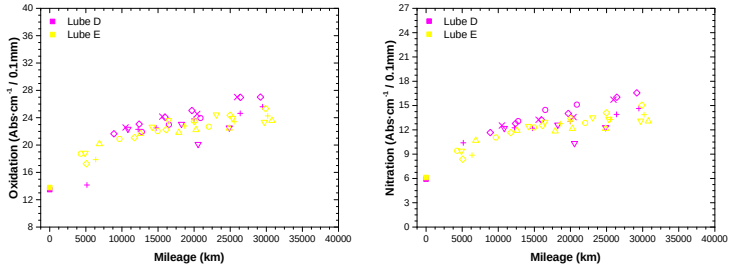

(a) Oxidation, by FT–IR, of the tested engine oils (b) Nitration, by FT–IR, of the tested engine oils

Figure 4.83. *Evolution of oxidation and nitration of Lube D and Lube E used in vehicles type IV.*

As in the previous interation, the results will be organised into two groups: one for Lube D and one for Lube E. For the first formulation, the cases that have been selected for explanation are listed below:

- There is a group of vehicles that experience signs of early stages of wear, with lead being particularly prevalent as the test progresses to full performance (30000 km). These vehicles are represented by: ○, ◇, + and ×. It appears that the TAN levels (Figure 4.85) shown in these groups are sufficiently high to be able to attack the lead material. It is necessary to underline the fact that we are working on the early stages of lead wear, as the recorded levels do not exceed 30 ppm.

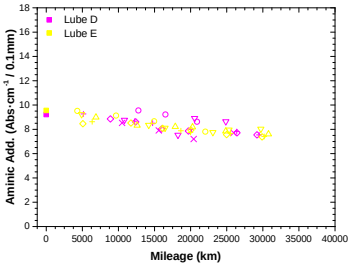

(a) Aminic additives by FT–IR spectroscopy

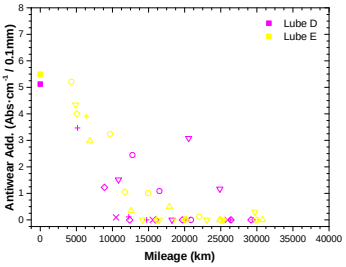

(b) Antiwear additives by FT–IR spectroscopy

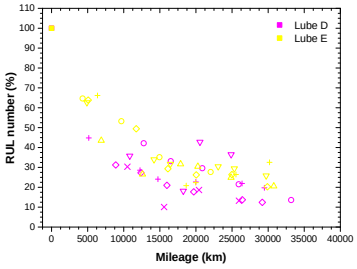

(c) RUL number

Figure 4.84. *Depletion of antioxidant additives of Lube D and Lube E used in vehicles type IV.*

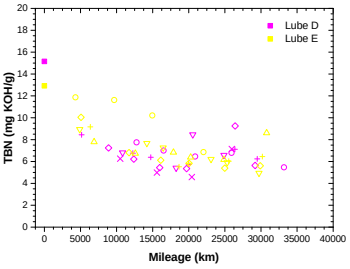

(a) TBN index by thermometric titration

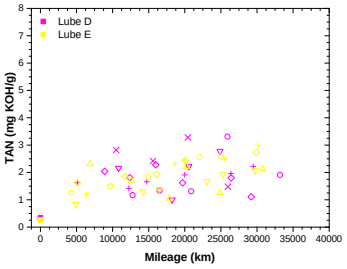

(b) TAN index by thermometric titration

Figure 4.85. *Performance of TBN/TAN index of Lube D and Lube E used in vehicles type IV.*

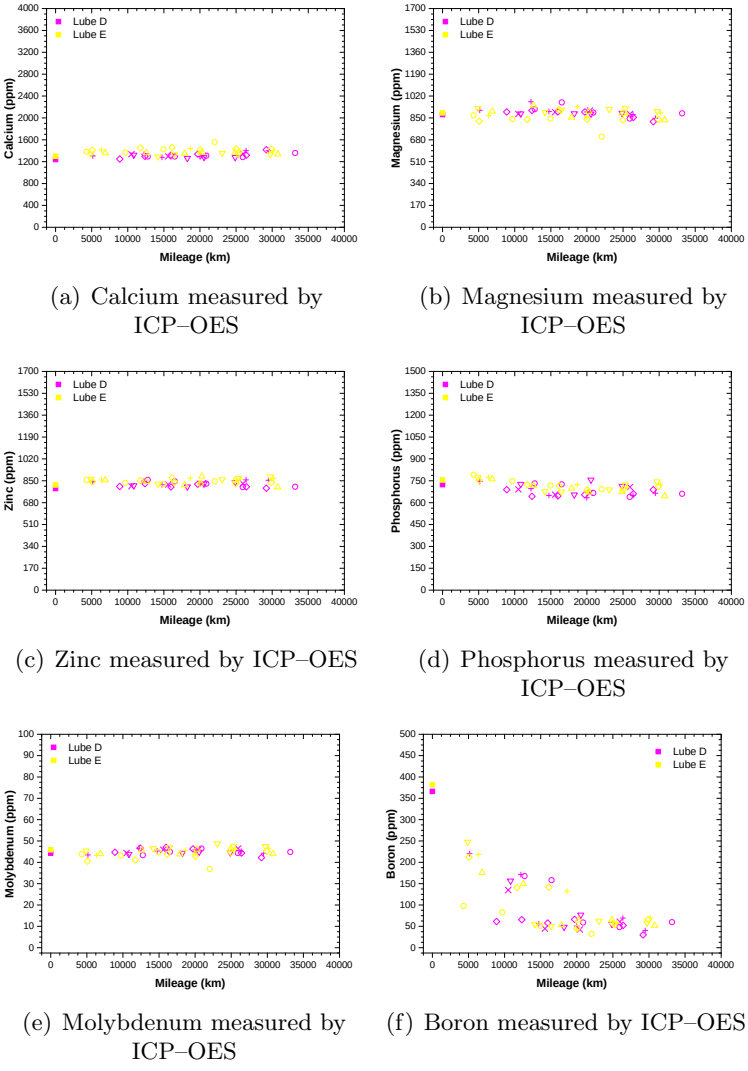

(a) Calcium measured by ICP–OES

(b) Magnesium measured by ICP–OES

(c) Zinc measured by ICP–OES

(d) Phosphorus measured by ICP–OES

(e) Molybdenum measured by ICP–OES

(f) Boron measured by ICP–OES

Figure 4.86. *Additive package of Lube D and Lube E used in vehicles type IV.*

- For the vehicle represented by ○, it already showed some problems in the first iteration. In this case, the vehicle shows significant levels of soot so that, in addition to the lead problem, it also presents problems of wear of other metals such as iron (see Figure 4.88). The same phenomenon is repeated for vehicle ◇, in a very similar way.

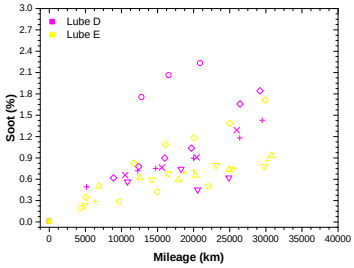

(a) Soot quantified by FT–IR

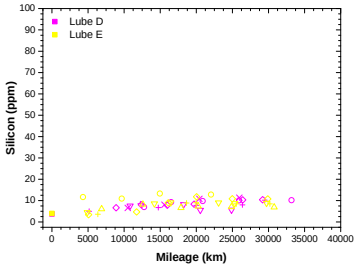

(b) Silicon quantified by ICP–OES

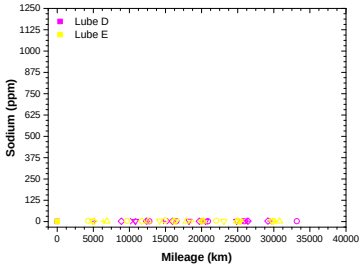

(c) Sodium quantified by ICP–OES

Figure 4.87. *Presence of contaminants in Lube D and Lube E used in vehicles type IV.*

- Equivalently to what happens with the previous vehicle (○), in the case of the +, it can be seen how the soot also favours the wear and tear of other metals, in this case affecting copper (check Figure 4.88).

Having completed the explanation with the Lube D formulation, it is time to move on to Lube E:

- The vehicle represented by a ○ shows signs of iron wear problems possibly caused by the presence of dust (see silicon levels in Figure 4.87) in the lubricating oil.
- Vehicle ◇ is in a similar situation. It has high soot levels compared to other vehicles using the Lube E formulation. However, it appears that this has not resulted in metal wear rates, as can be seen in Figure 4.88, where the evolution of iron, aluminium, copper and lead show normal behaviour. The only noteworthy fact is that, due to this increased soot concentration, viscosity has increased (Figure 4.82).

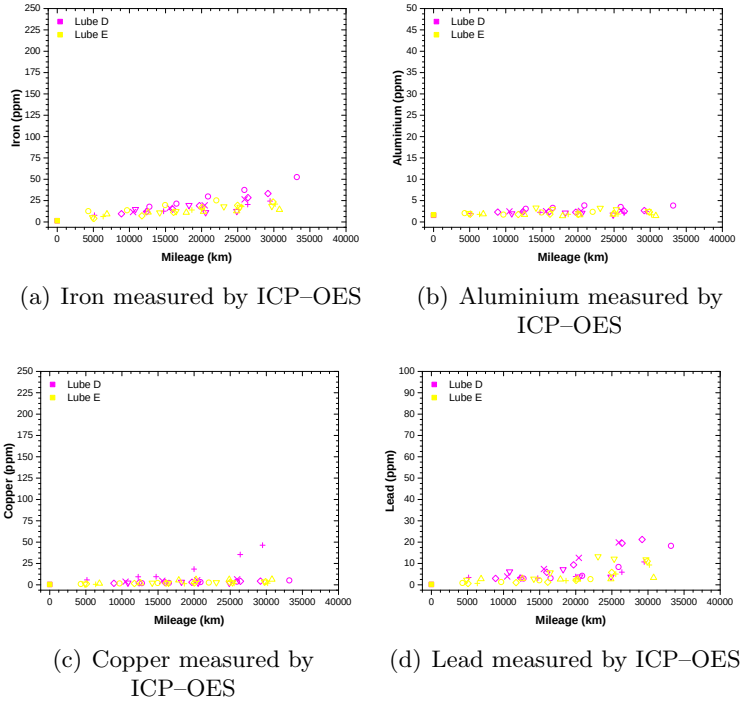

(a) Iron measured by ICP–OES

(b) Aluminium measured by ICP–OES

(c) Copper measured by ICP–OES

(d) Lead measured by ICP–OES

Figure 4.88. *Wear metals found in Lube D and Lube E used in vehicle types IV.*

- Therefore, there is a pair of vehicles that share similar traits: one represented by ▽ and the other by +. Specifically, both show signs of the onset of lead wear as they approach the end of the test, 30000 km. This phenomenon can be explained by the acidification of the lubricating oil in these vehicles since, according to the TAN values in Figure 4.85, the engine oil acidification levels are significant. However, the reported levels are below 15 ppm, so this is not a problem that requires action, but simply monitoring to keep it under control.

Bibliography

[1] J. A. Spearot. *High-temperature, high-shear (HTHS) oil viscosity: measurement and relationship to engine operation*, volume 1068. ASTM International, 1989.

Chapter 5

Chemometric analysis applied to lubricating oils

Contents

5.1 Introduction

This chapter is motivated by the description and use of chemometric methods and procedures applied to the subject of study: engine lubricating oils. As will be shown in the following lines, the combination of spectroscopic techniques and chemometrics offers the opportunity to obtain a very powerful and versatile tool for the analysis and diagnosis of lubricating oils which, in the near future, can take over a large part of the classical analyses used in today's lubricant analysis laboratories. This chapter is designed as a space where to show the results obtained in this new field of study, so it is focused on showing the potential of these tools.

5.2 Chemometrics

In a very concise way, chemometrics can be defined as the application of mathematical and statistical methods in the field of chemistry, specifically in chemistry from a more analytical point of view, for the final purpose of extracting information of interest [10, 14]. Finally, the application of chemometrics on chemical data allows the following achievements or goals to be reached [18]:

- Perform what is known as an **exploratory analysis** to detect outliers and pattern trends in the data set being analysed.
- Next, the application of chemometrics makes it possible to predict a series of properties from a given signal thanks to the data-signal correspondence previously studied. This is known as **regression analysis**.
- Finally, the **classification of data** allows the grouping or ranking of unknown samples according to the response or signal collected from an analysis.

However, the way of obtaining the data to be analysed can come from various origins, most commonly: from spectroscopic measurements, chromatographic measurements or physical measurements. However, not all the information obtained is the same or has the same properties. That is why, data can be classified into two main groups: univariate or multivariate data. The first type, univariate data, is a data type that involves a single variable to measure and a single variable to predict (e.g., tracking the

characteristic absorption band of a compound through a chemical process), whereas multivariate data refers to multiple variables and, consequently, multiple predictions [3].

Knowing the type of data or results required to carry out an analysis of this type, it is necessary to define a procedure that is extensible to any situation and conditions that may arise in a study of this type. For this purpose, the general steps that define a chemometric process [18] are:

- First of all, the generation of the required database, from which this whole procedure is to be built. For this purpose, it is necessary to carry out the measurements and to collect the data for the generation of the database library.
- The next stage consists of the mathematical and statistical processing of these data in order to be able to extract information of interest for the study.
- Once the data has been transformed into information, the next step is to analyse how this information is linked to the phenomenon under study. This approach leads to being able to gain useful knowledge of the phenomenon related to the study topic.
- Finally, with the knowledge gained, it is possible to reach a better understanding of the phenomenon under study, which has a direct practical implication for making judgements and decisions.

According to these steps of the chemometric process (shown in Figure 5.1, in the case of the analysis of lubricating oils), it is possible to obtain information not only from the sample, but also going back in the process, in order to know the engine condition and its evolution.

As already mentioned, chemometrics offers the possibility to improve the impact of instrumental analytical techniques, being of particular interest in spectroscopic techniques, thanks to its potential for analysis and information gathering [1]. This is why, in this Thesis, a first incursion into this field of science was made.

5.3 Multivariate Calibration

Multivariate calibration refers to the processing and analysis of multivariate data, i.e. data with a dimensionality of higher order than zero (scalar

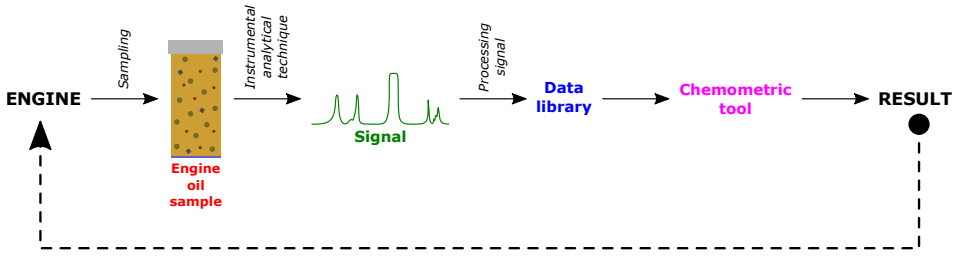

Figure 5.1. *Chemometric process applied to engine lubricating oil analysis.*

data): vector data (order 1), matrix data (order 2) and higher order data. In this Thesis, the data that have been dealt with are multivariate data, so from this point onwards the discourse and the development of the content will focus solely on multivariate calibration (although several alternatives exist) [9].

Within the multivariate calibration, there is a set of chemometric tools that allows to work with a large number of measurements to find relationships between them, that would otherwise be very difficult to find [16, 20]. Regardless of the chosen route, any multivariate calibration requires a number of specific steps to ensure that the value of the studied property they predict is reliable. A robust multivariate calibration is one that combines the following elements:

- A set of samples (whose property is known) to build or train the model. This set of samples must be representative of the total study set in order to be able to transfer the model to a new set of samples to predict the same property.

- The next aspect is that all the information from the instrumental analysis of the sample, that is likely to be used in the construction of the calibration model, must be collected.

- Next is the calibration model. In this section is where, first of all, the data is pre–processed in order to obtain a database free of anomalous or erroneous values that could affect the process. In addition, in this preliminary step, an attempt will be made to adapt the database in such a way that it is suitable for the processing that will be done afterwards. Once this preliminary stage has been carried out, the next step is to find the model with the best response [17].

- Then, with the model that best describes the most reliable relationship between the property and the analytical signal, a verification with another set of samples (whose study property is characterised) is carried out to validate the model.

By following these steps, it is possible to obtain a valid model capable of predicting a particular property. All that is required is to provide the selected model with the relevant data (from the analysis system) and run the model.

In addition to the predictive power of multivariate calibration, it has a number of advantages that make it particularly attractive, especially in the case (as will be seen in section 5.4 *Application of Multivariate Analysis*) where spectroscopic techniques are used [4]. These advantages are listed below:

- Multivariate calibration allows to work in systems where selectivity between the instrumental set of analysis and the property (chemical or physical) to be studied is not achieved. This implies that if the measurement equipment is not capable of monitoring or recording specifically that property, it is not an impediment.
- Another aspect is the ability to discriminate variables that are not of significant relevance to the model. If during model generation, one or several variables have no implication on the property prediction, they can be ignored. This virtue implies that the robustness of the model can be improved in a relatively simple way.
- In a similar way multivariate calibration allows discriminating between profitable and nonprofitable variables, it is capable of detecting anomalous values resulting from errors that may have occurred at any stage of the process (experimental errors, instrumental errors, etc.).
- Finally, the other advantageous aspect of multivariate calibration is the amount of statistical information it reports for a given variable in relation to the property under study.

Nonetheless, any multivariate calibration requires validation to determine its predictive ability. This step is required for two main reasons: the first is to know whether the proposed model will be able to perform (predict values) when applied to a new dataset, while the second reason is to determine the optimal dimensionality (in terms of the number of components and the number of variables of the system under study) [15]. There are several methods available to perform this validation, but among the most commonly used

are: prediction test set validation, cross-validation (within this type, K-fold cross-validation and "leave-one-out" cross-validation are the most common), laverage correlation and bootstrapping [13].

Therefore, the statistical parameters that explain or indicate the predictive capacity of the model are the following: Coefficient of determination (R^2), Correlation coefficiente (r), Root Mean Square Error (RMSE), Standard Error of Performance (SEP), Bias and Ratio of Predictive Deviation (RPD). Where, the ones that have been taken as evaluators of the predictive capacity of the models in this Thesis have been the R^2, r and the RMSE; more information on these statistics is provided below.

- Coefficient of determination (R^2) is a statistical parameter that measures, in a regression model, the proportion of variance in the observed data that is explained by the model. In other words, the coefficient of determination tells the goodness of fit of the model. It normally ranges from 0 to 1, where 1 means that the model predictions perfectly fit the data (the explained variance is 100% of the total).

$$R^2 = 1 - \frac{\sum_{i=1}^{n} (\hat{y}_i - y_i)^2}{\sum_{i=1}^{n} (y_i - \bar{y})^2} \tag{5.1}$$

  Where: $\hat{y}_i$ is the predicted value and y_i is the measured value (for both calibration and validation of the model), and $\bar{y}$ is the average value.

- Correlation coefficient (r) is a useful statistics for picking up on the lineal realtionship between variables. In other words, the correlation coefficient is the specific measure that quantifies the strength of the linear association between two variables in a correlation analysis. Its formula is defined as the covariance of the variables ($cov(X, Y)$) divided by the product of their standard deviations ($s_x{}^2$ and $s_y{}^2$):

$$r = \frac{cov(X, Y)}{\sqrt{s_x{}^2 \cdot s_y{}^2}} \tag{5.2}$$

  In addition to quantifying the level of the association, r also allows to know its direction: positive or negative. For this purpose, this coefficient takes values between -1 and +1. The information that can be extracted is twofold: the more extreme the values (close to -1 and +1) the greater the relationship between the variables considered, while the sign of the coefficient indicates whether the relationship is direct (if one variable

increases, so does the other) or inverse (the variables evolve in opposite directions). It is necessary to take into account the fact that a significant correlation between two variables means that changes in one variable are associated (positively or negatively) with changes in the other variable. However, a significant correlation does not indicate that changes in one variable cause changes in the other variable, it is only an significant association.

- Root Mean Square Error (RMSE) is a metric that explains the average distance between the predicted values from the model and the actual values in the dataset. Formally it is defined as follows:

$$RMSE = \sqrt{\frac{\sum_{i=1}^{n} (\hat{y}_i - y_i)^2}{n}} \tag{5.3}$$

Now, in this mathematical expression: $\hat{y}_i$ represents the predicted values, while y_i is the observed values and n is the number of samples in the set. RMSE is a positive numeric value, never negative, that indicates how good the model prediction is. To do this, one should look at the value of the RMSE: small values indicate a good match, while large values indicate a poor fit.

Although there are more statistics to measure the model's performance, for the case studies on which statistical analysis has been carried out, the three mentioned above were sufficient.

5.4 Application of Multivariate Analysis

The fields to which calibration can be applied are very diverse [5], but in this Thesis the effort has been focused on those analytical techniques that are acquiring relevance (such as FT–IR spectroscopy and NIR spectroscopy) in the analysis of lubricant; this in order to have a first contact with this subject.

5.4.1 Engine oil parameters relationship

To start with the treatment of the data extracted from the analysis of the lubricating oils, it is interesting to study the relationship between the different parameters monitored and described in Chapter 4. Among all the parameters that were studied, those that can be interconnected and which are

the most representative have been selected. With this in mind, the following parameters were selected: kinematic viscosity at 100°C, TAN and TBN, RUL number, oxidation and nitration degradation, aminic and antiwear additives depletion, soot and silicon contamination and engine wear (iron, alumminium, lead and copper).

The purpose of this section is to find and test the pairwise relationship between the above mentioned variables. To achieve this, a so-called "Scatter Plot Matrix" is prepared, which is a graphical representation that gathers all the pairwise scatter plots of the variable set into a single set in matrix format. There are several alternatives for making a graph of this type but, according to the subject of study, the most suitable of them is the one with the following characteristics:

- Given a specific number of variables (n) the scatter plot matrices will be formed by n rows and n columns. Each row and column defines a single scatter plot.
- In the main diagonal, where the relationship between a variable and itself (X_i-X_i) is located, it is preferable to use this space to plot a univariate histogram of the specific variable for that position in the matrix.
- For each scatterplot, a linear fit was applied in order to exploit and obtain the degree of fit between the pair of variables under study.

In order to be able to observe this possible relationship between parameters, the scatter matrix plot is an elegant way to get an answer to:

- The existence or non-existence of relationships between the pairs of variables.
- If there is a relationship, identify what is and how.
- The detection of outliers and clusters in the data.

Given that the study of the performance of new lubricating oil formulations took into account not only the lubricating oil, but also the type of vehicle in which the oil was used, the graphs generated followed the same principle. In this way, there are four groups of graphs (one for each vehicle: type I, type II, type III and type IV) composed in turn, by four other graphs (one for each lubricant under study).

5.4.1.1 Type I vehicles

In the case of type I vehicles, the oils used were: B, C, D and E, so in the next figures the results for each of these formulations have been grouped together. The interpretation of the results will be made globally, for the four lubricating oil formulations, at the end of the section.

The first case involves the use of lubricating oil B.

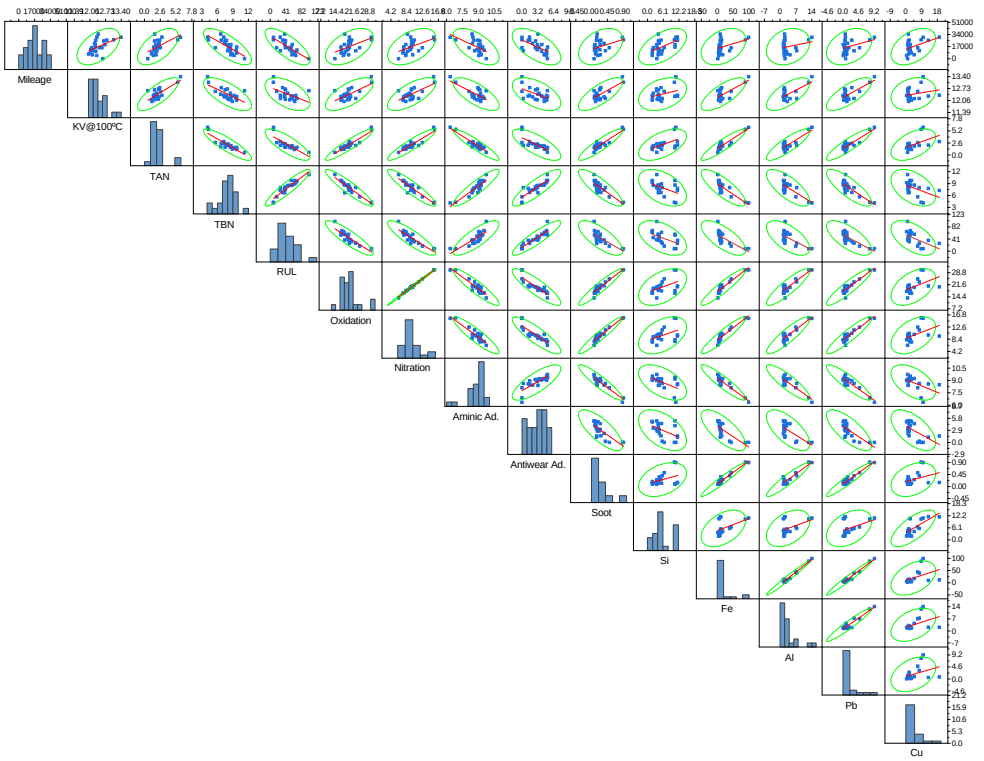

Figure 5.2. *Relationship between lube B parameters in vehicles type I.*

In the following Table 5.7, the r's for each of the parameters' combinations are gathered, allowing to better observe the correlation between those pairs.

The next study group is the one where lube C is involved. Both the plot matrix (Figure 5.3) and the linearity of the correlations (see Table 5.2) are shown below.

The next group is the one where the lubricating oil D is monitored. For this case, following the same methodology as shown above, the results are shown in two formats: Figure 5.4 and Table 5.8.

Table 5.1. *Parameter of adjustment for lube B in vehicle type I.*

r	*Mileage*	*KV@100°C*	*TAN*	*TBN*	*RUL*	*Oxidation*	*Nitration*	*Aminic Ad.*	*Antiwear Ad.*	*Soot*	*Si*	*Fe*	*Al*	*Pb*	*Cu*
Mileage	–	0.50755	0.58449	-0.73629	-0.74159	0.51394	0.48925	-0.59647	-0.61164	0.38206	0.55172	0.36614	0.24014	0.34778	0.44179
KV@100° C	0.50755	–	0.76648	-0.68799	-0.52205	0.67808	0.69017	-0.71001	-0.54214	0.74086	0.34816	0.73566	0.67275	0.74560	0.22165
TAN	0.58449	0.76648	–	-0.87857	-0.79998	0.93248	0.92342	-0.93038	-0.74214	0.90639	0.54898	0.91541	0.85206	0.89401	0.51061
TBN	-0.73629	-0.68799	-0.87857	–	0.92679	-0.92450	-0.91567	0.90764	0.86165	-0.84616	-0.46988	-0.81227	-0.73293	-0.81066	-0.45388
RUL	-0.74159	-0.52205	-0.79998	0.92679 –	-0.88242	-0.86892	0.80635	0.90398	-0.73980	-0.50019	-0.70851	-0.62472	-0.69500	-0.54216	
Oxidation	0.51394	0.67808	0.93248	-0.92450	-0.88242	–	0.99725	-0.91781	-0.87410	0.94717	0.47125	0.93156	0.88384	0.91822	0.48748
Nitration	0.48925	0.69017	0.92342	-0.91567	-0.86892	0.99725	–	-0.90886	-0.86458	0.95706	0.44879	0.93641	0.89295	0.92237	0.46215
Aminic Ad.	-0.59647	-0.71001	-0.93038	0.90764	0.80635	-0.91781	-0.90886	–	0.78260	-0.91944	-0.53174	-0.91814	-0.86698	-0.89473	-0.51894
Antiwear Ad.	-0.61164	-0.54214	-0.74214	0.86165	0.90398	-0.87410	-0.86458	0.78260	–	-0.75490	-0.49915	-0.72535	-0.66690	-0.74476	-0.60116
Soot	0.38206	0.74086	0.90639	-0.84616	-0.73980	0.94717	0.95706	-0.91944	-0.75490	–	0.37988	0.96727	0.93288	0.95594	0.35053
Si	0.55172	0.34816	0.54898	-0.46988	-0.50019	0.47125	0.44879	-0.53174	-0.49915	0.37988	–	0.46239	0.42565	0.41866	0.71021
Fe	0.36614	0.73566	0.91541	-0.81227	-0.70851	0.93156	0.93641	-0.91814	-0.72535	0.96727	0.46239	–	0.98476	0.98012	0.42782
Al	0.24014	0.67275	0.85206	-0.73293	-0.62472	0.88384	0.89295	-0.86698	-0.66690	0.93288	0.42565	0.98476	–	0.95801	0.42814
Pb	0.34778	0.74560	0.89401	-0.81066	-0.69500	0.91822	0.92237	-0.89473	-0.74476	0.95594	0.41866	0.98012	0.95801	–	0.37732
Cu	0.44179	0.22165	0.51061	-0.45388	-0.54216	0.48748	0.46215	-0.51894	-0.60116	0.35053	0.71021	0.42782	0.42814	0.37732	–

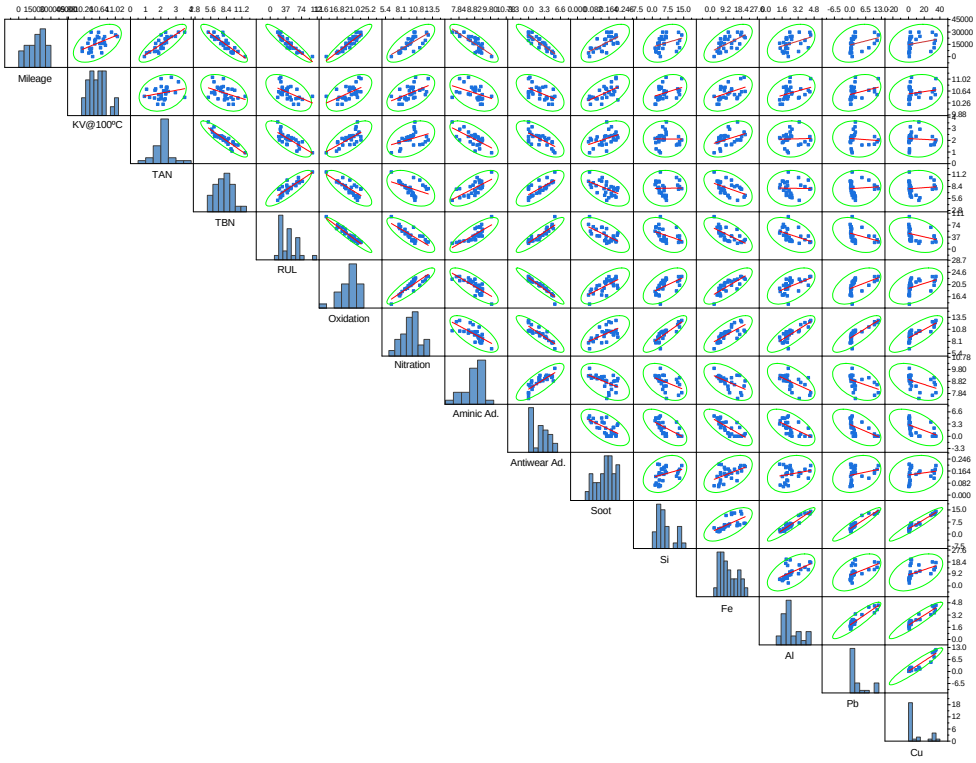

Figure 5.3. *Relationship between lube C parameters in vehicles type I.*

Table 5.2. *Parameter of adjustment for lube C in vehicle type I.*

r	*Mileage*	*KV@100° C*	*TAN*	*TBN*	*RUL*	*Oxidation*	*Nitration*	*Aminic Ad.*	*Antiwear Ad.*	*Soot*	*Si*	*Fe*	*Al*	*Pb*	*Cu*
Mileage	–	0.51607	0.83051	-0.87079	-0.93316	0.92106	0.72975	-0.83029	-0.90807	0.65637	0.34834	0.61954	0.39379	0.32532	0.25787
KV@100° C	0.51607	–	0.23952	-0.40037	-0.52745	0.55451	0.53195	-0.42404	-0.53037	0.60209	0.37022	0.43883	0.36658	0.34352	0.21201
TAN	0.83051	0.23952	–	-0.90052	-0.75627	0.70420	0.39173	-0.68052	-0.67194	0.45047	-0.00886	0.42011	0.03036	-0.09628	-0.07745
TBN	-0.87079	-0.40037	-0.90052	–	0.85227	-0.78027	-0.43662	0.69062	0.73701	-0.55829	0.01804	-0.47372	-0.01972	0.08721	0.10643
RUL	-0.93316	-0.52745	-0.75627	0.85227	–	-0.96237	-0.80491	0.80043	0.91772	-0.67282	-0.42557	-0.66186	-0.44648	-0.38001	-0.34774
Oxidation	0.92106	0.55451	0.70420	-0.78027	-0.96237	–	0.88906	-0.78529	-0.95702	0.68249	0.56549	0.78666	0.53952	0.51297	0.46634
Nitration	0.72975	0.53195	0.39173	-0.43662	-0.80491	0.88906	–	-0.70764	-0.87541	0.59020	0.84906	0.72327	0.81025	0.82423	0.79630
Aminic Ad.	-0.83029	-0.42404	-0.68052	0.69062	0.80043	-0.78529	-0.70764	–	0.81336	-0.52670	-0.47199	-0.56565	-0.58401	-0.44448	-0.46241
Antiwear Ad.	-0.90807	-0.53037	-0.67194	0.73701	0.91772	-0.95702	-0.87541	0.81336	–	-0.62905	-0.62514	-0.76128	-0.61705	-0.56634	-0.53865
Soot	0.65637	0.60209	0.45047	-0.55829	-0.67282	0.68249	0.59020	-0.52670	-0.62905	–	0.32546	0.50628	0.22610	0.27065	0.19741
Si	0.34834	0.37022	-0.00886	0.01804	-0.42557	0.56549	0.84906	-0.47199	-0.62514	0.32546	–	0.64374	0.94270	0.93427	0.95557
Fe	0.61954	0.43883	0.42011	-0.47372	-0.66186	0.78666	0.72327	-0.56565	-0.76128	0.50628	0.64374	–	0.56759	0.52423	0.47532
Al	0.39379	0.36658	0.03036	-0.01972	-0.44648	0.53952	0.81025	-0.58401	-0.61705	0.22610	0.94270	0.56759	–	0.91068	0.93266
Pb	0.32532	0.34352	-0.09628	0.08721	-0.38001	0.51297	0.82423	-0.44448	-0.56634	0.27065	0.93427	0.52423	0.91068	–	0.94302
Cu	0.25787	0.21201	-0.07745	0.10643	-0.34774	0.46634	0.79630	-0.46241	-0.53865	0.19741	0.95557	0.47532	0.93266	0.94302	–

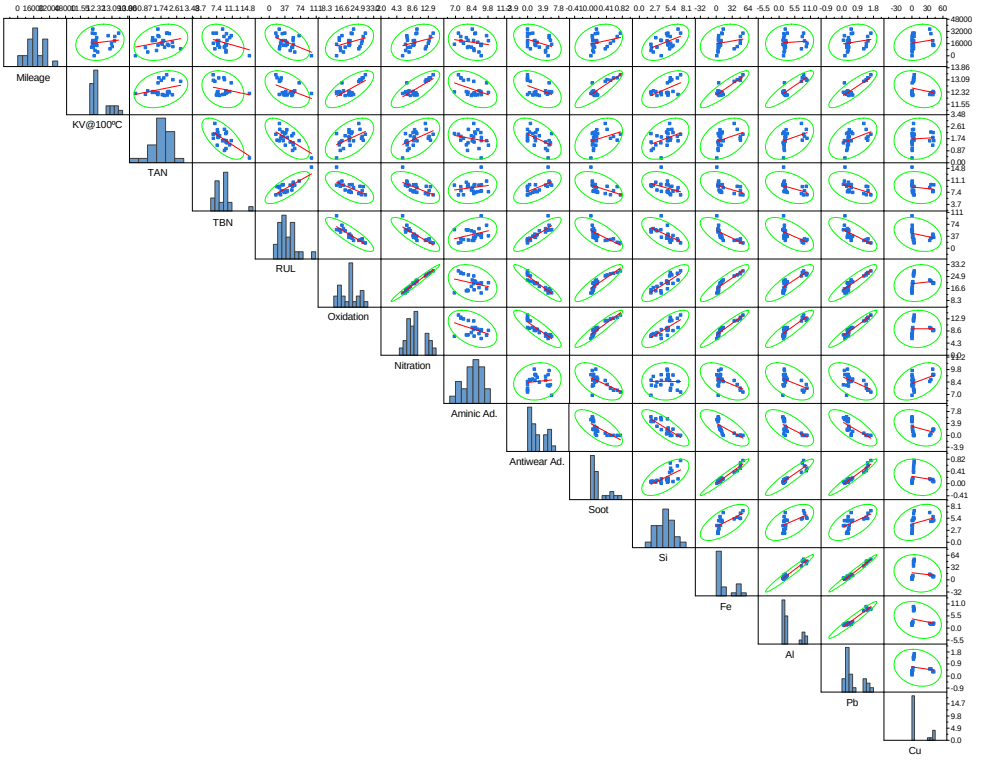

Figure 5.4. *Relationship between lube D parameters in vehicles type I.*

Table 5.3. *Parameter of adjustment for lube D in vehicle type I.*

r	*Mileage*	*KV@100°C*	*TAN*	*TBN*	*RUL*	*Oxidation*	*Nitration*	*Aminic Ad.*	*Antiwear Ad.*	*Soot*	*Si*	*Fe*	*Al*	*Pb*	*Cu*
Mileage	–	0.15715	0.27421	-0.32788	-0.4969	0.37111	0.35442	-0.1950	-0.38894	0.29010	0.51591	0.23568	0.08482	0.21185	0.21247
KV@100°C	0.15715	–	0.29343	-0.23585	-0.45772	0.72161	0.78399	-0.45913	-0.46649	0.86996	0.54594	0.89992	0.89144	0.86316	-0.27431
TAN	0.27421	0.29343	–	-0.66357	-0.65521	0.53583	0.53180	-0.20964	-0.53424	0.36455	0.43277	0.40382	0.41011	0.45420	0.07622
TBN	-0.32788	-0.23585	-0.66357	–	0.77962	-0.62178	-0.60355	0.19804	0.60403	-0.46734	-0.40951	-0.44551	-0.41194	-0.46831	-0.15340
RUL	-0.49690	-0.45772	-0.65521	0.77962	–	-0.86327	-0.83925	0.33302	0.86224	-0.69054	-0.64273	-0.69875	-0.62198	-0.71229	-0.28973
Oxidation	0.37111	0.72161	0.53583	-0.62178	-0.86327	–	0.98466	-0.29590	-0.93838	0.89107	0.81439	0.90851	0.85522	0.90623	0.14390
Nitration	0.35442	0.78399	0.53180	-0.60355	-0.83925	0.98466	–	-0.43218	-0.87937	0.94406	0.76470	0.95531	0.90879	0.95378	0.01459
Aminic Ad.	-0.19500	-0.45913	-0.20964	0.19804	0.33302	-0.29590	-0.43218	–	0.12892	-0.57488	-0.00826	-0.54805	-0.51765	-0.56634	0.47056
Antiwear Ad.	-0.38894	-0.46649	-0.53424	0.60403	0.86224	-0.93838	-0.87937	0.12892	–	-0.71324	-0.80955	-0.74111	-0.67935	-0.75448	-0.35072
Soot	0.29010	0.86996	0.36455	-0.46734	-0.69054	0.89107	0.94406	-0.57488	-0.71324	–	0.63408	0.97504	0.92710	0.96784	-0.20778
Si	0.51591	0.54594	0.43277	-0.40951	-0.64273	0.81439	0.76470	-0.00826	-0.80955	0.63408	–	0.66546	0.58077	0.62358	0.37213
Fe	0.23568	0.89992	0.40382	-0.44551	-0.69875	0.90851	0.95531	-0.54805	-0.74111	0.97504	0.66546	–	0.97487	0.98618	-0.15080
Al	0.08482	0.89144	0.41011	-0.41194	-0.62198	0.85522	0.90879	-0.51765	-0.67935	0.92710	0.58077	0.97487	–	0.97000	-0.26012
Pb	0.21185	0.86316	0.45420	-0.46831	-0.71229	0.90623	0.95378	-0.56634	-0.75448	0.96784	0.62358	0.98618	0.97000	–	-0.19175
Cu	0.21247	-0.27431	0.07622	-0.15340	-0.28973	0.14390	0.01459	0.47056	-0.35072	-0.20778	0.37213	-0.15080	-0.26012	-0.19175	–

And finally, the case of the lubricant E with this particular type of vehicle is discussed. Figure 5.5 and Table 5.4 present the results obtained.

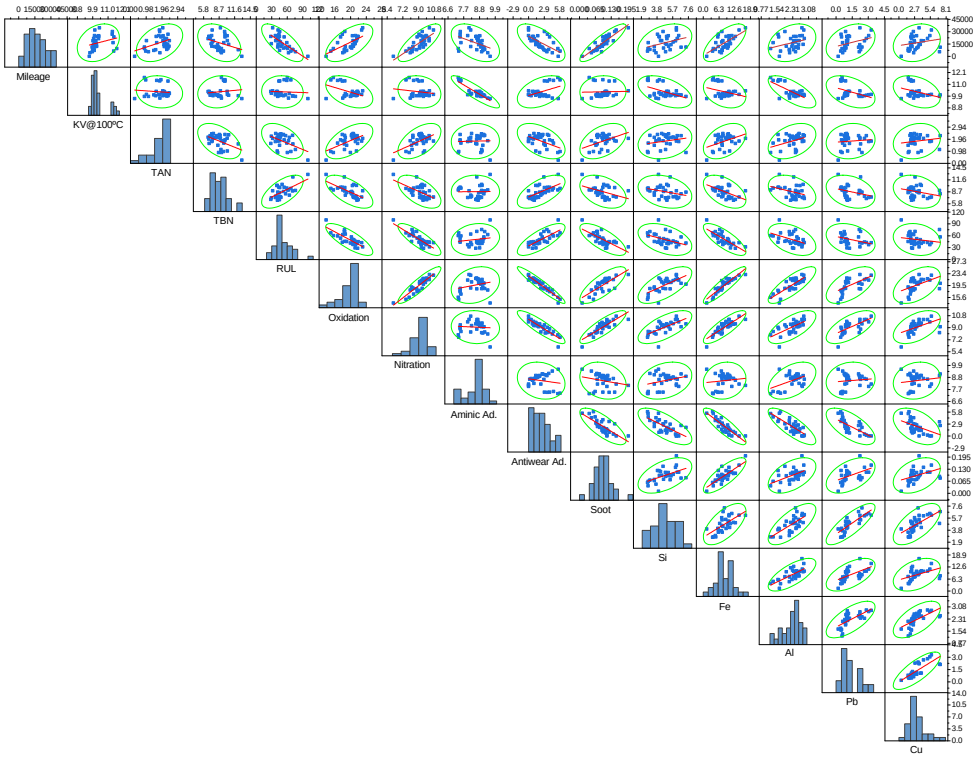

Figure 5.5. *Relationship between lube E parameters in vehicles type I.*

The conclusions that can be drawn from the analysis of the results presented above are set out below. From Figure 5.2, Figure 5.3, Figure 5.4 and

Table 5.4. *Parameter of adjustment for lube E in vehicle type I.*

r	*Mileage*	*KV@100°C*	*TAN*	*TBN*	*RUL*	*Oxidation*	*Nitration*	*Aminic Ad.*	*Antiwear Ad.*	*Soot*	*Si*	*Fe*	*Al*	*Pb*	*Cu*
Mileage	–	0.28708	0.40314	-0.34993	-0.72494	0.60810	0.76245	-0.46205	-0.64891	0.87630	0.35119	0.66368	0.29988	0.32058	0.19747
KV@100°C	0.28708	–	-0.10158	0.12583	-0.04656	-0.43703	-0.15448	-0.89012	0.44014	0.02673	-0.48592	-0.30192	-0.70387	-0.42579	-0.34888
TAN	0.40314	-0.10158	–	-0.48433	-0.48242	0.56317	0.54489	0.03122	-0.49441	0.44867	0.21307	0.41109	0.38524	0.09822	0.16341
TBN	-0.34993	0.12583	-0.48433	–	0.62541	-0.63943	-0.58201	0.00972	0.61194	-0.38633	-0.29065	-0.49849	-0.34970	-0.30995	-0.26129
RUL	-0.72494	-0.04656	-0.48242	0.62541	–	-0.78736	-0.82405	0.16449	0.75815	-0.72478	-0.43360	-0.77600	-0.44840	-0.31655	-0.17355
Oxidation	0.60810	-0.43703	0.56317	-0.63943	-0.78736	–	0.90792	0.25425	-0.95389	0.76270	0.66479	0.90994	0.80762	0.58110	0.47693
Nitration	0.76245	-0.15448	0.54489	-0.58201	-0.82405	0.90792	–	-0.06492	-0.89169	0.84343	0.66813	0.83204	0.66856	0.65001	0.49912
Aminic Ad.	-0.46205	-0.89012	0.03122	0.00972	0.16449	0.25425	-0.06492	–	-0.17849	-0.22437	0.29075	0.12238	0.46200	0.10429	0.15581
Antiwear Ad.	-0.64891	0.44014	-0.49441	0.61194	0.75815	-0.95389	-0.89169	-0.17849	–	-0.76142	-0.7111	-0.86956	-0.80525	-0.66154	-0.46024
Soot	0.87630	0.02673	0.44867	-0.38633	-0.72478	0.76270	0.84343	-0.22437	-0.76142	–	0.51022	0.79587	0.50905	0.49000	0.38758
Si	0.35119	-0.48592	0.21307	-0.29065	-0.43360	0.66479	0.66813	0.29075	-0.71110	0.51022	–	0.63289	0.70286	0.81216	0.64452
Fe	0.66368	-0.30192	0.41109	-0.49849	-0.77600	0.90994	0.83204	0.12238	-0.86956	0.79587	0.63289	–	0.71039	0.58358	0.41445
Al	0.29988	-0.70387	0.38524	-0.34970	-0.44840	0.80762	0.66856	0.46200	-0.80525	0.50905	0.70286	0.71039	–	0.68200	0.62638
Pb	0.32058	-0.42579	0.09822	-0.30995	-0.31655	0.58110	0.65001	0.10429	-0.66154	0.49000	0.81216	0.58358	0.68200	–	0.77644
Cu	0.19747	-0.34888	0.16341	-0.26129	-0.17355	0.47693	0.49912	0.15581	-0.46024	0.38758	0.64452	0.41445	0.62638	0.77644	–

Figure 5.5, focusing on those linear relationships (with a value of r equal to or greater than 0.8000) shown in the scatterplots, the following performances can be noted:

- The formulation of lubricating oil B shows a higher degree of linearity between the various variables compared to the other three formulations (see Table 5.7). This is due to the fact that the situations in which the study was carried out were sufficiently favourable to allow a constant and homogeneous evolution of the parameters throughout the test.

- It can be seen that there are a number of samples within the users of the B lube, for example in copper, where the evolution (depending on the mileage) is higher than the rest (see Table 5.7). This must indicate that there are some vehicles that show some kind of incidence.

- Moving on to formulation C, Table 5.2, it can also appreciate the relationships between variables that are logical (taking the OCM perspective). But, within this family, there is a relationship between TAN-Pb-Cu where it is clearly observed how in some of the vehicles there are wear problems of these metals as a consequence of the acidification of the lubricant.

- For the users of lubricating oil D (Table 5.8) and lubricating oil E (Table 5.4), already in the first Mileage-KV@100°C plot, two groups of data are clearly visible. This division of the data into two parts already indicates the difference in behaviour. This fact causes that in most cases, the interpretation of the linearity of the pairwise relationship needs to be done separately.

These insights are confirmed by all those values of the correlation coefficiente (r) given in the aboe medionetd tables according to the following graduation of the different values adopted by r:

- **+1.0**, exactly: a perfect uphill (positive) linear relationship.
- **+0.8 − +1.0**: a very strong positive linear relationship.
- **+0.6 − +0.8**: a strong positive linear relationship.
- **+0.4 − +0.6**: a moderate positive linear relationship.
- **+0.2 − +0.4**: a weak positive linear relationship.
- **0.0 − 0.2**: a very weak positive linear relationship.
- **0.0**, exactly: no linear relationship.
- **0.0 − -0.2**: a very weak negative linear relationship.
- **-0.2 − -0.4**: a weak negative linear relationship.
- **-0.4 − -0.6**: a moderate negative linear relationship.
- **-0.6 − -0.8**: a strong negative linear relationship.
- **-0.8 − -1.0**: a very strong negative linear relationship.
- **-1.0**, exactly: a perfect downhill (negative) linear relationship.

5.4.1.2 Type II vehicles

In this type of vehicles, the engine oils tested are the following: A (differentiated between: A_1 and A_2), B, and D. So each of the graphs will show the evolution of the performance of these four different formulations. Under these conditions, the results derived from the statistical analysis of the experimental data have been grouped in several figures and tables.

First, information was collected on formulation A. This lubricant formulation, as used in the LVEO study, was used in both stages. That is why it was differentiated in two: A_1 and A_2. Thus, the results of the first iteration, involving lube A_1, are shown first: see Figure 5.6 and Table 5.5.

And, once the results A_1 have been exposed, the next step is to proceed with lube A_2. Accordingly, their respective Figure 5.7 and Table 5.6 were prepared.

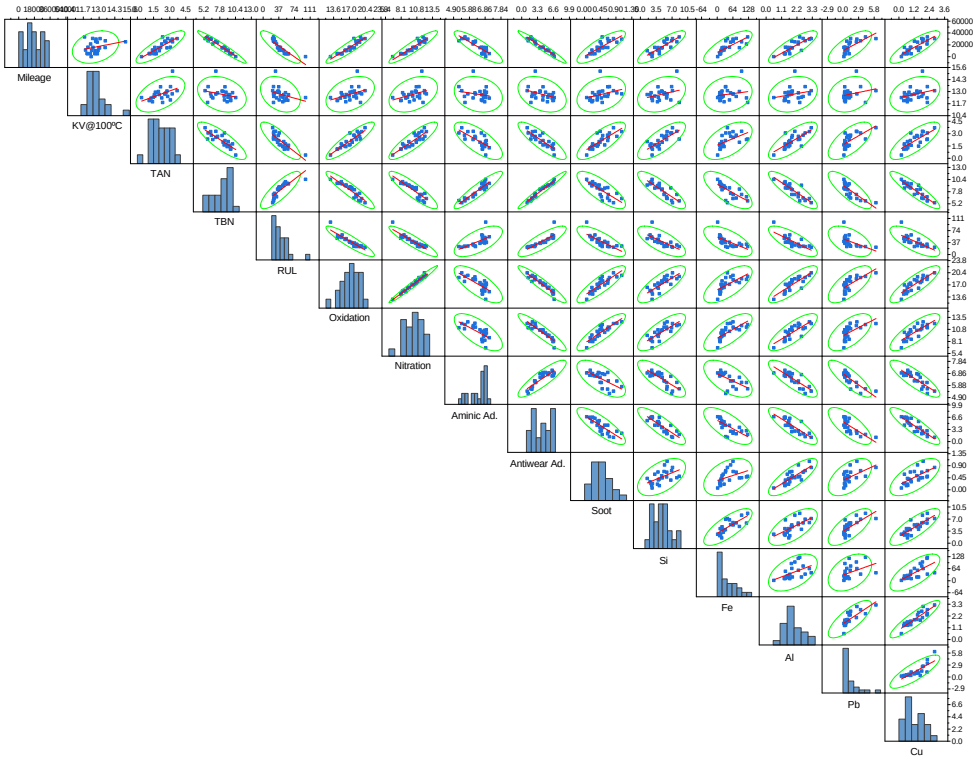

Figure 5.6. *Relationship between lube A_1 parameters in vehicles type II.*

Table 5.5. *Parameter of adjustment for lube A_1 in vehicle type II.*

r	*Mileage*	*KV@100°C*	*TAN*	*TBN*	*RUL*	*Oxidation*	*Nitration*	*Aminic Ad.*	*Antiwear Ad.*	*Soot*	*Si*	*Fe*	*Al*	*Pb*	*Cu*
Mileage	–	0.28084	0.84342	-0.96905	-0.86165	0.93085	0.92779	-0.86680	-0.97364	0.82263	0.84935	0.75209	0.82568	0.71709	0.83936
KV@100°C	0.28084	–	0.49525	-0.27004	-0.31049	0.39199	0.37982	-0.20688	-0.34923	0.32688	0.30846	0.17976	0.24358	0.25517	0.31573
TAN	0.84342	0.49525	–	-0.83173	-0.82837	0.89463	0.87185	-0.71746	-0.85907	0.78015	0.75859	0.53536	0.75868	0.66125	0.77022
TBN	-0.96905	-0.27004	-0.83173	–	0.82932	-0.92209	-0.89199	0.92233	0.97798	-0.78573	-0.84574	-0.71704	-0.86767	-0.80614	-0.90900
RUL	-0.86165	-0.31049	-0.82837	0.82932	–	-0.91331	-0.91850	0.64893	0.84274	-0.77008	-0.70543	-0.63628	-0.77222	-0.52496	-0.73180
Oxidation	0.93085	0.39199	0.89463	-0.92209	-0.91331	–	0.98470	-0.74091	-0.94669	0.86247	0.78703	0.67827	0.83279	0.69345	0.84933
Nitration	0.92779	0.37982	0.87185	-0.89199	-0.91850	0.98470	–	-0.69242	-0.92353	0.86619	0.77770	0.72315	0.79450	0.61259	0.80370
Aminic Ad.	-0.86680	-0.20688	-0.71746	0.92233	0.64893	-0.74091	-0.69242	–	0.87337	-0.65793	-0.78539	-0.60539	-0.82059	-0.82999	-0.85019
Antiwear Ad.	-0.97364	-0.34923	-0.85907	0.97798	0.84274	-0.94669	-0.92353	0.87337	–	-0.82677	-0.84812	-0.70829	-0.82952	-0.73503	-0.88130
Soot	0.82263	0.32688	0.78015	-0.78573	-0.77008	0.86247	0.86619	-0.65793	-0.82677	–	0.52652	0.41928	0.79253	0.53832	0.65189
Si	0.84935	0.30846	0.75859	-0.84574	-0.70543	0.78703	0.77770	-0.78539	-0.84812	0.52652	–	0.76073	0.64956	0.71121	0.80915
Fe	0.75209	0.17976	0.53536	-0.71704	-0.63628	0.67827	0.72315	-0.60539	-0.70829	0.41928	0.76073	–	0.49871	0.41360	0.70055
Al	0.82568	0.24358	0.75868	-0.86767	-0.77222	0.83279	0.79450	-0.82059	-0.82952	0.79253	0.64956	0.49871	–	0.77204	0.89804
Pb	0.71709	0.25517	0.66125	-0.80614	-0.52496	0.69345	0.61259	-0.82999	-0.73503	0.53832	0.71121	0.41360	0.77204	–	0.82388
Cu	0.83936	0.31573	0.77022	-0.90900	-0.73180	0.84933	0.80370	-0.85019	-0.88130	0.65189	0.80915	0.70055	0.89804	0.82388	–

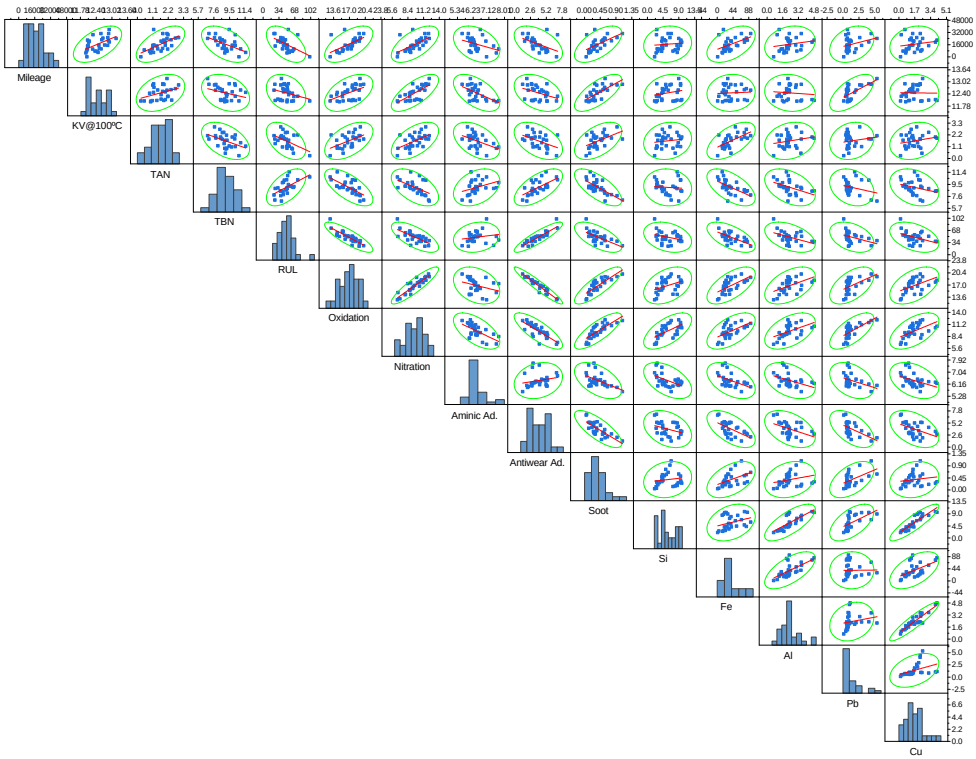

Figure 5.7. *Relationship between lube A_2 parameters in vehicles type II.*

Table 5.6. *Parameter of adjustment for lube A_2 in vehicle type II.*

r	*Mileage*	*KV@100°C*	*TAN*	*TBN*	*RUL*	*Oxidation*	*Nitration*	*Aminic Ad.*	*Antiwear Ad.*	*Soot*	*Si*	*Fe*	*Al*	*Pb*	*Cu*
Mileage	–	0.55123	0.59860	-0.50215	-0.53343	0.60118	0.61190	-0.35669	-0.49198	0.59640	0.09763	0.49269	0.19435	0.31030	0.17656
KV@100°C	0.55123	–	0.35501	-0.30148	-0.28260	0.49542	0.70435	-0.55438	-0.38235	0.69534	0.21971	0.05681	-0.09633	0.62593	-0.01492
TAN	0.59860	0.35501	–	-0.45871	-0.48256	0.51330	0.54360	-0.45660	-0.46633	0.51184	0.14086	0.59293	0.22036	0.17911	0.22148
TBN	-0.50215	-0.30148	-0.45871	–	0.56780	-0.67179	-0.53433	0.35468	0.63311	-0.69938	-0.07327	-0.58647	-0.42684	-0.26787	-0.29179
RUL	-0.53343	-0.28260	-0.48256	0.56780	–	-0.84399	-0.68535	0.18983	0.89262	-0.63479	-0.29842	-0.60954	-0.45478	-0.37854	-0.41841
Oxidation	0.60118	0.49542	0.51330	-0.67179	-0.84399	–	0.89875	-0.31015	-0.95266	0.82488	0.40413	0.62573	0.48956	0.54162	0.49226
Nitration	0.61190	0.70435	0.54360	-0.53433	-0.68535	0.89875	–	-0.60713	-0.79522	0.79527	0.62149	0.58082	0.49243	0.67210	0.56404
Aminic Ad.	-0.35669	-0.55438	-0.45660	0.35468	0.18983	-0.31015	-0.60713	–	0.21491	-0.51741	-0.50257	-0.48056	-0.40722	-0.38337	-0.39579
Antiwear Ad.	-0.49198	-0.38235	-0.46633	0.63311	0.89262	-0.95266	-0.79522	0.21491	–	-0.76615	-0.34574	-0.59397	-0.44503	-0.54529	-0.45185
Soot	0.59640	0.69534	0.51184	-0.69938	-0.63479	0.82488	0.79527	-0.51741	-0.76615	–	0.15129	0.47730	0.25332	0.51820	0.15889
Si	0.09763	0.21971	0.14086	-0.07327	-0.29842	0.40413	0.62149	-0.50257	-0.34574	0.15129	–	0.32373	0.72825	0.58597	0.88473
Fe	0.49269	0.05681	0.59293	-0.58647	-0.60954	0.62573	0.58082	-0.48056	-0.59397	0.47730	0.32373	–	0.64884	0.01278	0.54216
Al	0.19435	-0.09633	0.22036	-0.42684	-0.45478	0.48956	0.49243	-0.40722	-0.44503	0.25332	0.72825	0.64884	–	0.21718	0.92299
Pb	0.31030	0.62593	0.17911	-0.26787	-0.37854	0.54162	0.67210	-0.38337	-0.54529	0.51820	0.58597	0.01278	0.21718	–	0.40681
Cu	0.17656	-0.01492	0.22148	-0.29179	-0.41841	0.49226	0.56404	-0.39579	-0.45185	0.15889	0.88473	0.54216	0.92299	0.40681	–

Having shown formulations A_1 and A_2, the same procedure will be carried out for the case of lubricant formulation B, generating Figure 5.8 and Table 5.7.

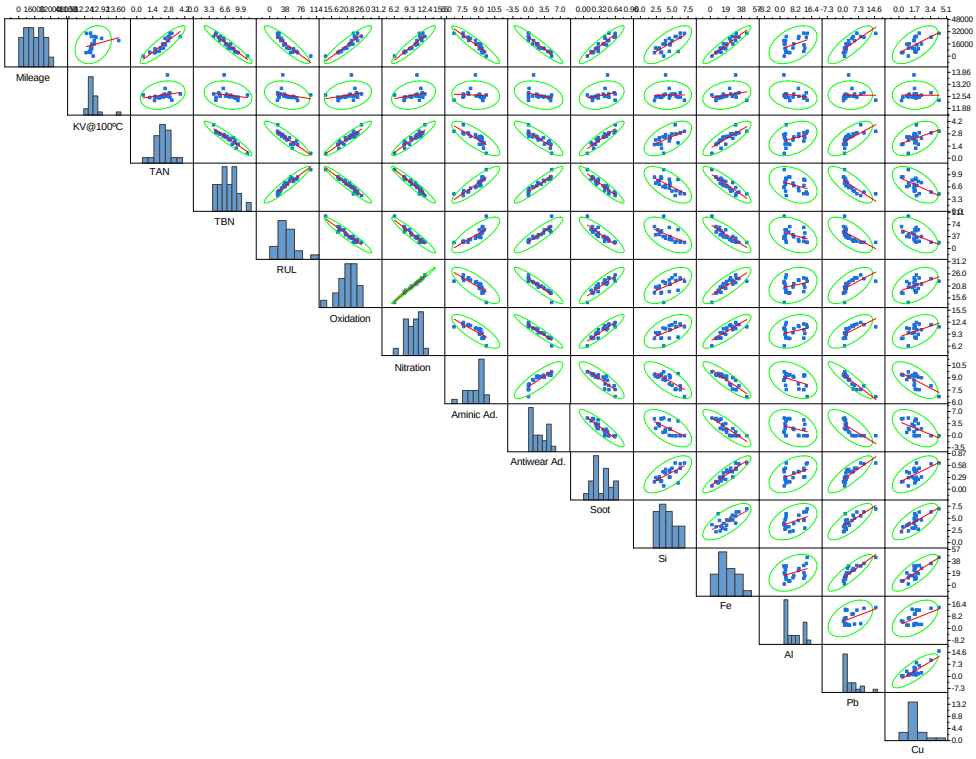

Figure 5.8. *Relationship between lube B parameters in vehicles type II.*

Table 5.7. *Parameter of adjustment for lube B in vehicle type II.*

r	*Mileage*	*KV@100°C*	*TAN*	*TBN*	*RUL*	*Oxidation*	*Nitration*	*Aminic Ad.*	*Antiwear Ad.*	*Soot*	*Si*	*Fe*	*Al*	*Pb*	*Cu*
Mileage	–	0.26446	0.89172	-0.95861	-0.90500	0.91503	0.93563	-0.93286	-0.95565	0.92097	0.71182	0.93057	0.43110	0.81473	0.61306
KV@100°C	0.26446	–	0.23784	-0.21584	-0.24049	0.26740	0.28863	-0.06802	-0.31965	0.27953	0.02270	0.28057	-0.22816	-0.00811	-0.01269
TAN	0.89172	0.23784	–	-0.94349	-0.91247	0.94282	0.93459	-0.80365	-0.88337	0.92611	0.59819	0.82517	0.38038	0.70180	0.47431
TBN	-0.95861	-0.21584	-0.94349	–	0.94297	-0.96617	-0.96508	0.89507	0.94530	-0.94216	-0.65381	-0.88795	-0.35988	-0.78250	-0.56513
RUL	-0.90500	-0.24049	-0.91247	0.94297	–	-0.95383	-0.95737	0.79180	0.90084	-0.88054	-0.56208	-0.84765	-0.36418	-0.66563	-0.50763
Oxidation	0.91503	0.26740	0.94282	-0.96617	-0.95383	–	0.99439	-0.79189	-0.94061	0.89808	0.55516	0.83114	0.27910	0.64956	0.45532
Nitration	0.93563	0.28863	0.93459	-0.96508	-0.95737	0.99439	–	-0.80383	-0.96113	0.91050	0.56016	0.84759	0.31047	0.66404	0.46689
Aminic Ad.	-0.93286	-0.06802	-0.80365	0.89507	0.79180	-0.79189	-0.80383	–	0.85184	-0.85630	-0.73607	-0.88939	-0.40930	-0.91880	-0.64923
Antiwear Ad.	-0.95565	-0.31965	-0.88337	0.94530	0.90084	-0.94061	-0.96113	0.85184	–	-0.90766	-0.60784	-0.85999	-0.32424	-0.72525	-0.50251
Soot	0.92097	0.27953	0.92611	-0.94216	-0.88054	0.89808	0.91050	-0.85630	-0.90766	–	0.66170	0.89894	0.45090	0.82710	0.61150
Si	0.71182	0.02270	0.59819	-0.65381	-0.56208	0.55516	0.56016	-0.73607	-0.60784	0.66170	–	0.70807	0.45654	0.77885	0.73565
Fe	0.93057	0.28057	0.82517	-0.88795	-0.84765	0.83114	0.84759	-0.88939	-0.85999	0.89894	0.70807	–	0.38031	0.86747	0.79153
Al	0.43110	-0.22816	0.38038	-0.35988	-0.36418	0.27910	0.31047	-0.40930	-0.32424	0.45090	0.45654	0.38031	–	0.45954	0.49728
Pb	0.81473	-0.00811	0.70180	-0.78250	-0.66563	0.64956	0.66404	-0.91880	-0.72525	0.82710	0.77885	0.86747	0.45954	–	0.80468
Cu	0.61306	-0.01269	0.47431	-0.56513	-0.50763	0.45532	0.46689	-0.64923	-0.50251	0.61150	0.73565	0.79153	0.49728	0.80468	–

Finally, we continue with the results of the oil formulation D: Figure 5.9 and Table 5.8.

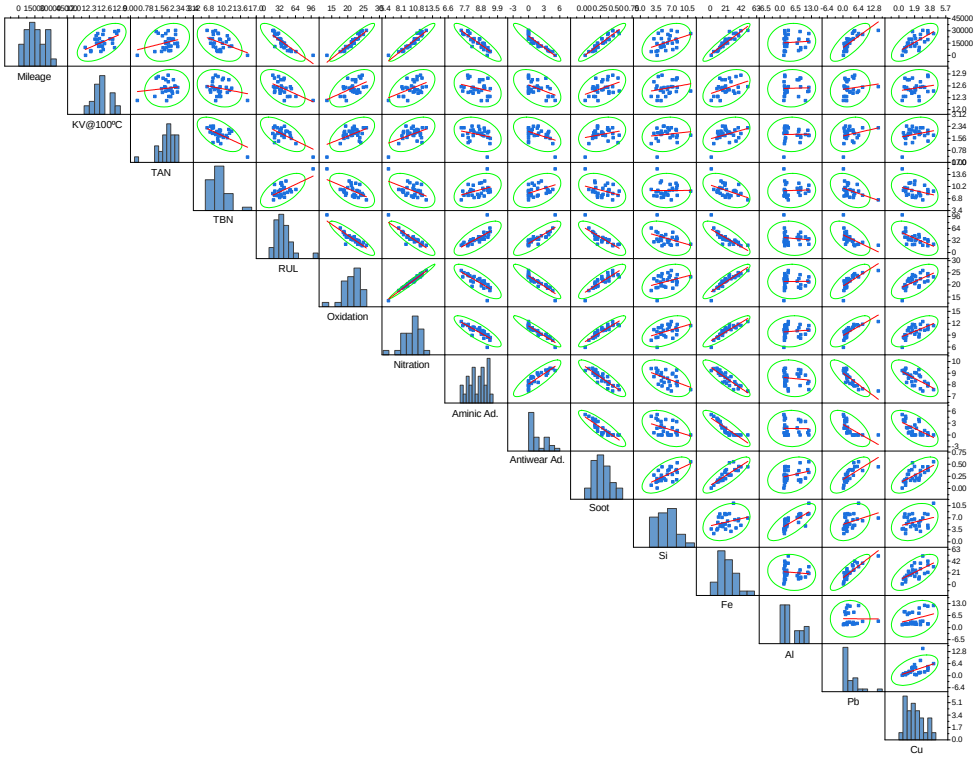

Figure 5.9. *Relationship between lube D parameters in vehicles type II.*

Table 5.8. *Parameter of adjustment for lube D in vehicle type II.*

r	*Mileage*	*KV@100°C*	*TAN*	*TBN*	*RUL*	*Oxidation*	*Nitration*	*Aminic Ad.*	*Antiwear Ad.*	*Soot*	*Si*	*Fe*	*Al*	*Pb*	*Cu*
Mileage	–	0.55866	0.29602	-0.44135	-0.82420	0.93764	0.94760	-0.89669	-0.92773	0.93279	0.42065	0.93087	0.07565	0.75816	0.69225
KV@100°C	0.55866	–	0.13624	-0.23368	-0.53383	0.54348	0.49442	-0.29811	-0.48294	0.44980	0.23763	0.41971	0.03204	0.15957	0.19727
TAN	0.29602	0.13624	–	-0.59927	-0.63508	0.52279	0.49219	-0.28008	-0.44465	0.25637	0.15529	0.37755	0.01453	0.26557	0.26213
TBN	-0.44135	-0.23368	-0.59927	–	0.61791	-0.57247	-0.52103	0.36748	0.43144	-0.35632	0.00246	-0.46146	0.04154	-0.40480	-0.31918
RUL	-0.82420	-0.53383	-0.63508	0.61791	–	-0.89680	-0.89553	0.74791	0.84373	-0.80792	-0.40700	-0.79331	-0.12494	-0.56072	-0.57812
Oxidation	0.93764	0.54348	0.52279	-0.57247	-0.89680	–	0.98694	-0.79447	-0.92105	0.85835	0.36745	0.91323	0.01976	0.73309	0.60524
Nitration	0.94760	0.49442	0.49219	-0.52103	-0.89553	0.98694	–	-0.83663	-0.94231	0.91180	0.46465	0.90871	0.11155	0.73973	0.62144
Aminic Ad.	-0.89669	-0.29811	-0.28008	0.36748	0.74791	-0.79447	-0.83663	–	0.85780	-0.87792	-0.49613	-0.87945	-0.13417	-0.80590	-0.67663
Antiwear Ad.	-0.92773	-0.48294	-0.44465	0.43144	0.84373	-0.92105	-0.94231	0.85780	–	-0.87279	-0.41176	-0.87438	-0.02182	-0.62499	-0.61321
Soot	0.93279	0.44980	0.25637	-0.35632	-0.80792	0.85835	0.91180	-0.87792	-0.87279	–	0.63695	0.83488	0.30128	0.69147	0.66839
Si	0.42065	0.23763	0.15529	0.00246	-0.40700	0.36745	0.46465	-0.49613	-0.41176	0.63695	–	0.29502	0.75390	0.34979	0.30870
Fe	0.93087	0.41971	0.37755	-0.46146	-0.79331	0.91323	0.90871	-0.87945	-0.87438	0.83488	0.29502	–	-0.10861	0.85101	0.64504
Al	0.07565	0.03204	0.01453	0.04154	-0.12494	0.01976	0.11155	-0.13417	-0.02182	0.30128	0.75390	-0.10861	–	-0.00611	0.32819
Pb	0.75816	0.15957	0.26557	-0.40480	-0.56072	0.73309	0.73973	-0.80590	-0.62499	0.69147	0.34979	0.85101	-0.00611	–	0.51355
Cu	0.69225	0.19727	0.26213	-0.31918	-0.57812	0.60524	0.62144	-0.67663	-0.61321	0.66839	0.30870	0.64504	0.32819	0.51355	–

In view of all the gathered information, both in figures and tables, the most interesting aspects raised by the analysis of this information have been organised in the following list:

- Firstly, when comparing the response between the same lubricating oil formulation A, there are clear indications of a difference in performance between formulation A_1 and A_2. For the first case, the recorded response can be classified as expected according to the evolution of each variable of the lubricating oil, with no discordance of the reported values. But, for the A_2 case, this behaviour is not the same and the linearity is lost. A justification for this phenomenon could be attributed to errors in lubricating oil allocation or wrong fillings, which cause that the oil in use is not the A_2, solely. These problems are beyond the control of the study. But, thanks to this tool, it is possible to detect this type of behaviour and to find an explanation for it.

- Another remarkable fact with the lubricating oil pair A_1 and A_2 is the detection of anomalous cases, both of them for high mileage values, namely at the end of the ODI.

- Switching to lubricating oil B, there are several details to be taken into account: firstly, an anomalous value is observed in the middle of the study, so it would be convenient to carry out a follow-up or control to corroborate that this anomalous value is a one-off event or the beginning of a problem that is occurring. And the other phenomenon is the appearance of two wear trends of aluminium and lead in type II vehicles; apparently there are some vehicles that show signs of wear that should be checked.

- The same behaviour observed in formulation D appears in the case of formulation D. This is logical given that the user vehicles of formulation B and formulation D are the same but in different iterations of the study.

5.4.1.3 Type III vehicles

For these vehicles, which are powered by CNG fuel, the soot parameter has been discarded from this analysis. So the number of variables considered at this point has been reduced from 15 to 14. In these vehicles, the used formulations were: lube B, lube C, lube D and lube E. Therefore, the following lines will show the results according to this alphabetical order.

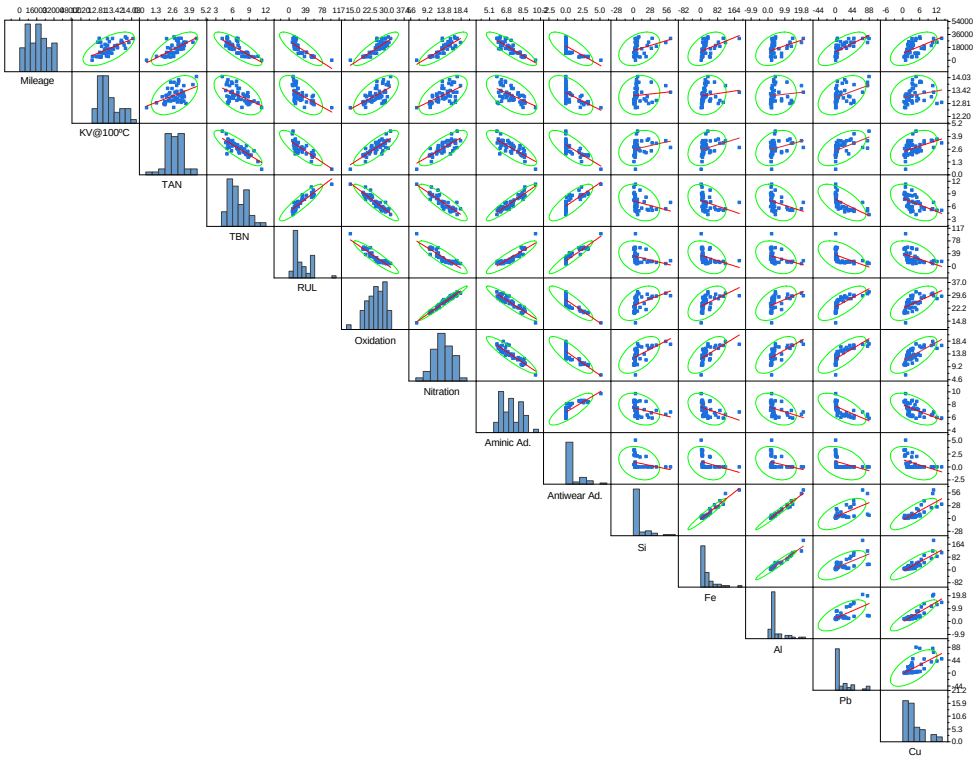

Figure 5.10. *Relationship between lube B parameters in vehicles type III.*

Table 5.9. *Parameter of adjustment for lube B in vehicle type III.*

r	*Mileage*	*KV@100º C*	*TAN*	*TBN*	*RUL*	*Oxidation*	*Nitration*	*Aminic Ad.*	*Antiwear Ad.*	*Si*	*Fe*	*Al*	*Pb*	*Cu*
Mileage	–	0.63133	0.69113	-0.81537	-0.82596	0.86276	0.84513	-0.87333	-0.74197	0.36828	0.46740	0.41136	0.71529	0.57222
KV@100º C	0.63133	–	0.45947	-0.54616	-0.59917	0.62119	0.58224	-0.58050	-0.56247	0.11371	0.14874	0.11571	0.45566	0.21973
TAN	0.69113	0.45947	–	-0.82981	-0.81991	0.82745	0.78677	-0.79712	-0.75057	0.25767	0.33428	0.31108	0.54996	0.42616
TBN	-0.81537	-0.54616	-0.82981	–	0.90815	-0.92110	-0.88282	0.93897	0.80919	-0.30361	-0.35390	-0.35827	-0.63741	-0.49558
RUL	-0.82596	-0.59917	-0.81991	0.90815	–	-0.92836	-0.89482	0.91213	0.93959	-0.30519	-0.36776	-0.34442	-0.52959	-0.46730
Oxidation	0.86276	0.62119	0.82745	-0.92110	-0.92836	–	0.98240	-0.93588	-0.86281	0.46530	0.53616	0.51284	0.74129	0.61325
Nitration	0.84513	0.58224	0.78677	-0.88282	-0.89482	0.98240	–	-0.91531	-0.82993	0.58058	0.63947	0.62594	0.77367	0.70298
Aminic Ad.	-0.87333	-0.58050	-0.79712	0.93897	0.91213	-0.93588	-0.91531	–	0.81647	-0.32261	-0.40984	-0.39489	-0.64960	-0.56545
Antiwear Ad.	-0.74197	-0.56247	-0.75057	0.80919	0.93959	-0.86281	-0.82993	0.81647	–	-0.25792	-0.32741	-0.29249	-0.40166	-0.43291
Si	0.36828	0.11371	0.25767	-0.30361	-0.30519	0.46530	0.58058	-0.32261	-0.25792	–	0.96925	0.98290	0.64226	0.81053
Fe	0.46740	0.14874	0.33428	-0.35390	-0.36776	0.53616	0.63947	-0.40984	-0.32741	0.96925	–	0.97250	0.67679	0.86332
Al	0.41136	0.11571	0.31108	-0.35827	-0.34442	0.51284	0.62594	-0.39489	-0.29249	0.98290	0.97250	–	0.67318	0.87906
Pb	0.71529	0.45566	0.54996	-0.63741	-0.52959	0.74129	0.77367	-0.64960	-0.40166	0.64226	0.67679	0.67318	–	0.66067
Cu	0.57222	0.21973	0.42616	-0.49558	-0.46730	0.61325	0.70298	-0.56545	-0.43291	0.81053	0.86332	0.87906	0.66067	–

The first results, see Figure 5.10 and Table 5.9, are the result of the analysis of the parameters related to lubricant B.

The second results are for the lubricating oil C: Figure 5.11 and Table 5.10.

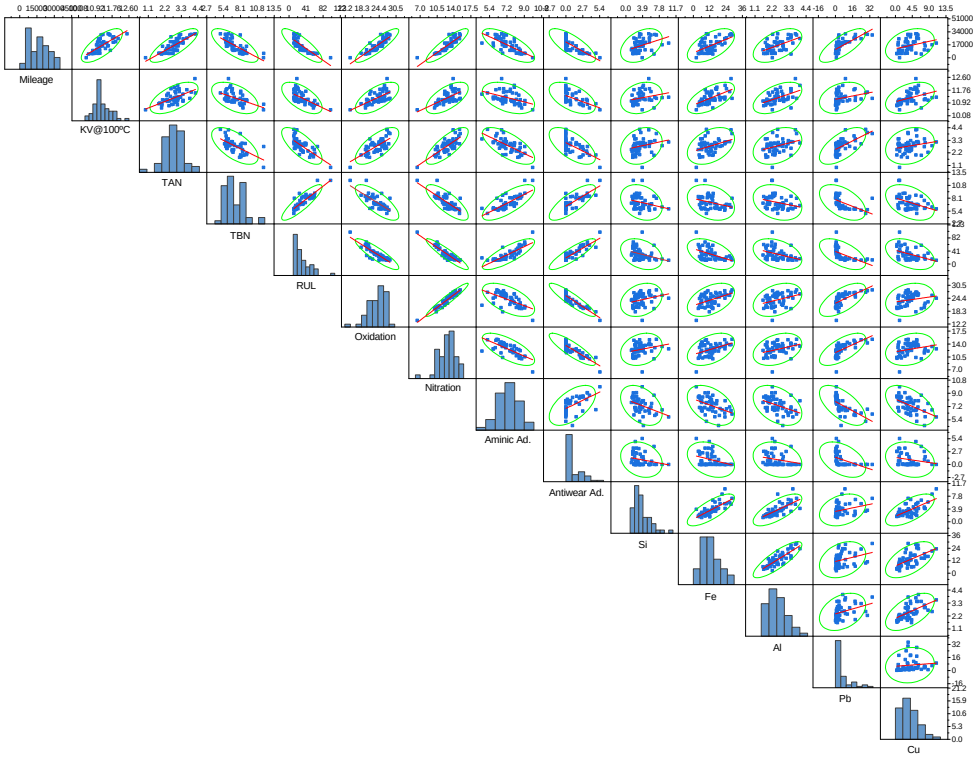

Figure 5.11. *Relationship between lube C parameters in vehicles type III.*

Table 5.10. *Parameter of adjustment for lube C in vehicle type III.*

r	*Mileage*	*KV@100º C*	*TAN*	*TBN*	*RUL*	*Oxidation*	*Nitration*	*Aminic Ad.*	*Antiwear Ad.*	*Si*	*Fe*	*Al*	*Pb*	*Cu*
Mileage	–	0.72182	0.79510	-0.73287	-0.83622	0.87947	0.87765	-0.72201	-0.75835	0.40115	0.57322	0.52656	0.75276	0.31308
KV@100º C	0.72182	–	0.59855	-0.50398	-0.61135	0.63974	0.62512	-0.42103	-0.53610	0.24780	0.60740	0.52310	0.28553	0.39701
TAN	0.79510	0.59855	–	-0.61892	-0.72739	0.69701	0.77119	-0.68378	-0.62604	0.24642	0.39308	0.34046	0.62798	0.22068
TBN	-0.73287	-0.50398	-0.61892	–	0.87184	-0.75861	-0.77826	0.74868	0.78448	-0.26923	-0.29919	-0.27692	-0.50476	-0.41934
RUL	-0.83622	-0.61135	-0.72739	0.87184	–	-0.88395	-0.92684	0.80956	0.87154	-0.33716	-0.47094	-0.37526	-0.57200	-0.42542
Oxidation	0.87947	0.63974	0.69701	-0.75861	-0.88395	–	0.95841	-0.58289	-0.90869	0.27652	0.45501	0.35660	0.65179	0.21121
Nitration	0.87765	0.62512	0.77119	-0.77826	-0.92684	0.95841	–	-0.70066	-0.86324	0.24635	0.43553	0.34405	0.65779	0.25332
Aminic Ad.	-0.72201	-0.42103	-0.68378	0.74868	0.80956	-0.58289	-0.70066	–	0.56482	-0.40118	-0.42885	-0.41276	-0.62240	-0.52276
Antiwear Ad.	-0.75835	-0.53610	-0.62604	0.78448	0.87154	-0.90869	-0.86324	0.56482	–	-0.22264	-0.33241	-0.23193	-0.44356	-0.20416
Si	0.40115	0.24780	0.24642	-0.26923	-0.33716	0.27652	0.24635	-0.40118	-0.22264	–	0.76625	0.71830	0.30086	0.66402
Fe	0.57322	0.60740	0.39308	-0.29919	-0.47094	0.45501	0.43553	-0.42885	-0.33241	0.76625	–	0.83574	0.31580	0.57432
Al	0.52656	0.52310	0.34046	-0.27692	-0.37526	0.35660	0.34405	-0.41276	-0.23193	0.71830	0.83574	–	0.35776	0.58278
Pb	0.75276	0.28553	0.62798	-0.50476	-0.57200	0.65179	0.65779	-0.62240	-0.44356	0.30086	0.31580	0.35776	–	0.10536
Cu	0.31308	0.39701	0.22068	-0.41934	-0.42542	0.21121	0.25332	-0.52276	-0.20416	0.66402	0.57432	0.58278	0.10536	–

For the lubricating oil D, the Figure-Table set is composed by the Figure 5.12 and Table 5.11, which show and compile the results for this lubricant formulation.

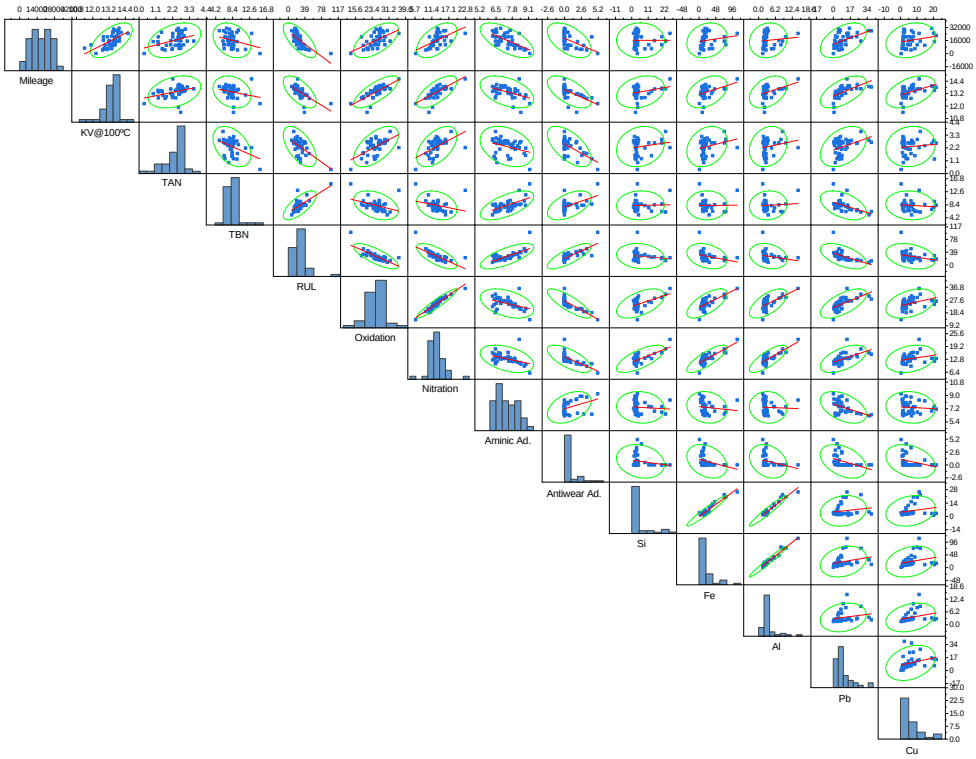

Figure 5.12. *Relationship between lube D parameters in vehicles type III.*

Table 5.11. *Parameter of adjustment for lube D in vehicle type III.*

r	*Mileage*	*KV@100° C*	*TAN*	*TBN*	*RUL*	*Oxidation*	*Nitration*	*Aminic Ad.*	*Antiwear Ad.*	*Si*	*Fe*	*Al*	*Pb*	*Cu*
Mileage	–	0.61148	0.38818	-0.28850	-0.70203	0.59465	0.54409	-0.65110	-0.52559	-0.00198	0.17893	0.11118	0.48368	0.22884
KV@100° C	0.61148	–	0.33839	-0.23474	-0.63323	0.74826	0.68140	-0.45513	-0.60440	0.27258	0.40350	0.38544	0.57901	0.45852
TAN	0.38818	0.33839	–	-0.41062	-0.58315	0.58955	0.52864	-0.33248	-0.60539	0.17463	0.25302	0.19987	0.40154	0.11051
TBN	-0.28850	-0.23474	-0.41062	–	0.71778	-0.38365	-0.27740	0.62577	0.52462	0.03099	0.00615	0.07725	-0.47603	-0.09981
RUL	-0.70203	-0.63323	-0.58315	0.71778	–	-0.77841	-0.70219	0.71828	0.78307	-0.15866	-0.29911	-0.22667	-0.55314	-0.30594
Oxidation	0.59465	0.74826	0.58955	-0.38365	-0.77841	–	0.94313	-0.42261	-0.82386	0.54315	0.67676	0.63564	0.64734	0.39762
Nitration	0.54409	0.68140	0.52864	-0.27740	-0.70219	0.94313	–	-0.42611	-0.68329	0.69786	0.81387	0.77955	0.55579	0.28600
Aminic Ad.	-0.65110	-0.45513	-0.33248	0.62577	0.71828	-0.42261	-0.42611	–	0.41046	-0.08582	-0.13761	-0.04912	-0.45491	-0.08737
Antiwear Ad.	-0.52559	-0.60440	-0.60539	0.52462	0.78307	-0.82386	-0.68329	0.41046	–	-0.19890	-0.31296	-0.27242	-0.40287	-0.31956
Si	-0.00198	0.27258	0.17463	0.03099	-0.15866	0.54315	0.69786	-0.08582	-0.19890	–	0.96307	0.96449	0.16075	0.21481
Fe	0.17893	0.40350	0.25302	0.00615	-0.29911	0.67676	0.81387	-0.13761	-0.31296	0.96307	–	0.97956	0.24867	0.27496
Al	0.11118	0.38544	0.19987	0.07725	-0.22667	0.63564	0.77955	-0.04912	-0.27242	0.96449	0.97956	–	0.20651	0.30411
Pb	0.48368	0.57901	0.40154	-0.47603	-0.55314	0.64734	0.55579	-0.45491	-0.40287	0.16075	0.24867	0.20651	–	0.30637
Cu	0.22884	0.45852	0.11051	-0.09981	-0.30594	0.39762	0.28600	-0.08737	-0.31956	0.21481	0.27496	0.30411	0.30637	–

The following and last pair, Figure 5.13 and Table 5.12, are relative to the formulation E used in the vehicles fueled by CNG.

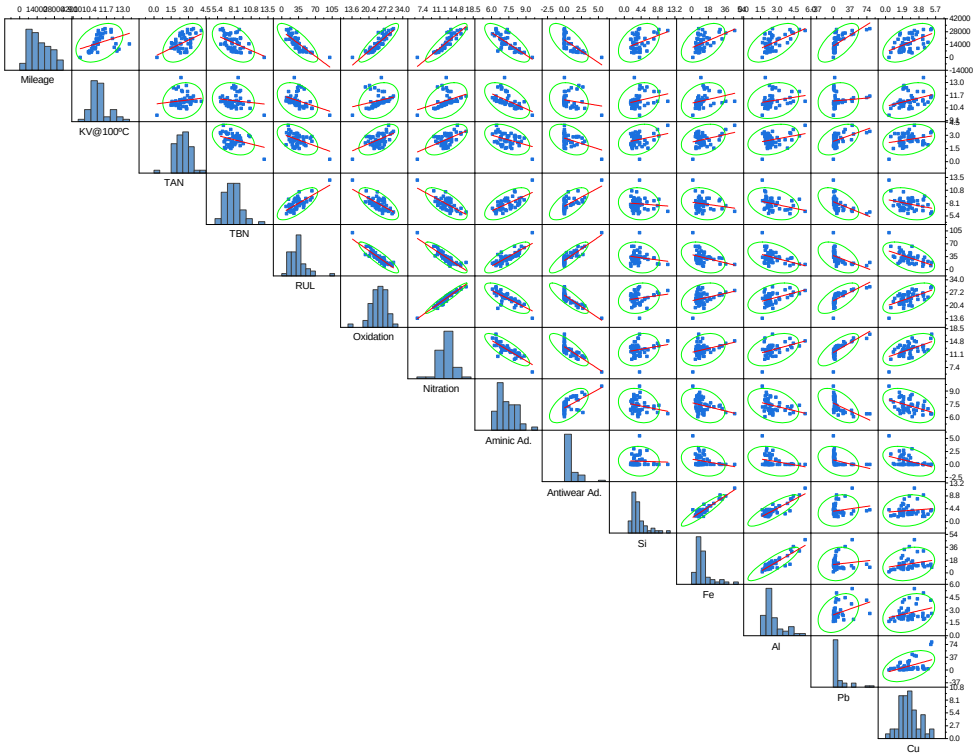

Figure 5.13. *Relationship between lube E parameters in vehicles type III.*

Table 5.12. *Parameter of adjustment for lube E in vehicle type III.*

r	*Mileage*	*KV@100º C*	*TAN*	*TBN*	*RUL*	*Oxidation*	*Nitration*	*Aminic Ad.*	*Antiwear Ad.*	*Si*	*Fe*	*Al*	*Pb*	*Cu*
Mileage	–	0.38022	0.49570	-0.47162	-0.78577	0.87001	0.87896	-0.75661	-0.67113	0.40555	0.48813	0.58235	0.66209	0.53138
KV@100º C	0.38022	–	0.13914	-0.13057	-0.37207	0.26094	0.37043	-0.54791	-0.18127	0.26974	0.28041	0.22485	0.09859	0.36526
TAN	0.49570	0.13914	–	-0.34489	-0.47576	0.55103	0.58335	-0.40961	-0.40220	0.27722	0.32436	0.30537	0.47758	0.25765
TBN	-0.47162	-0.13057	-0.34489	–	0.72514	-0.68151	-0.69722	0.62825	0.65096	-0.09859	-0.18859	-0.33222	-0.51274	-0.31425
RUL	-0.78577	-0.37207	-0.47576	0.72514	–	-0.89521	-0.88355	0.81570	0.86391	-0.17559	-0.34425	-0.42519	-0.49784	-0.54771
Oxidation	0.87001	0.26094	0.55103	-0.68151	-0.89521	–	0.96706	-0.74616	-0.85449	0.18878	0.31733	0.43460	0.67890	0.59487
Nitration	0.87896	0.37043	0.58335	-0.69722	-0.88355	0.96706	–	-0.82455	-0.78870	0.22328	0.32074	0.42602	0.73535	0.55729
Aminic Ad.	-0.75661	-0.54791	-0.40961	0.62825	0.81570	-0.74616	-0.82455	–	0.61868	-0.23832	-0.31244	-0.35965	-0.55037	-0.43070
Antiwear Ad.	-0.67113	-0.18127	-0.40220	0.65096	0.86391	-0.85449	-0.78870	0.61868	–	-0.04483	-0.25664	-0.29951	-0.31839	-0.42785
Si	0.40555	0.26974	0.27722	-0.09859	-0.17559	0.18878	0.22328	-0.23832	-0.04483	–	0.92265	0.85167	0.18712	0.12531
Fe	0.48813	0.28041	0.32436	-0.18859	-0.34425	0.31733	0.32074	-0.31244	-0.25664	0.92265	–	0.88303	0.13362	0.23427
Al	0.58235	0.22485	0.30537	-0.33222	-0.42519	0.43460	0.42602	-0.35965	-0.29951	0.85167	0.88303	–	0.36698	0.30186
Pb	0.66209	0.09859	0.47758	-0.51274	-0.49784	0.67890	0.73535	-0.55037	-0.31839	0.18712	0.13362	0.36698	–	0.46296
Cu	0.53138	0.36526	0.25765	-0.31425	-0.54771	0.59487	0.55729	-0.43070	-0.42785	0.12531	0.23427	0.30186	0.46296	–

Grouping all the information derived from the four lubricating oil formulations tested in these vehicles, the following performance aspects could be observed:

- First of all, as a general feature for this type of vehicles using CNG as fuel, two elements should be highlighted: one, is that this type of vehicles exert a greater demand on the tested oils, specially in the case of the antiwear additives, which are exhausted at the middle of the ODI (15000 km). And the other aspect is that, in most of the parameters that are being tested, several trends appear or are observed.
- According to the study plan of the LVEOs, the analysis can be developed in pairs: formulation B with formulation D, and formulation C with formulation E. So the analysis will be carried out in this way:
  - In this first B-D couple, the consumption of antiwear additives seems to be very high. As a consequence, when passing from one iteration to another, metallic wear problems (very clearly observable in the case of lead) are aggravated. In addition, it appears that, when lubricating oil B was used, there were problems with dust entering the engine (as indicated by the silicon values), but these were solved when the second iteration of the study was carried out.
  - This consistent approach or deduction developed for the B-D couple is transferable to the C-E couple. It is simply necessary to clarify two aspects: one is that in both stages, there are problems of attack on soft metals copper and lead, and the other is the appearance of certain cases that show values that differ from the rest of the family (apparently there is a specific vehicle that is not in the correct state of maintenance and has a series of problems that need to be corrected).

5.4.1.4 Type IV vehicles

The last type of vehicles studied are those classified as type IV. In this category, the oils tested were: lube B, lube C, lube D and lube E. For all these formulations, a graph and a table have been compiled where the relationships between the oil parameters and the linear goodness of fit (indicated by the r parameter), respectively, are included.

To begin with, formulation B generates the following matrix (Figure 5.14) whose linear behaviour (if it exists) is gathered in Table 5.13.

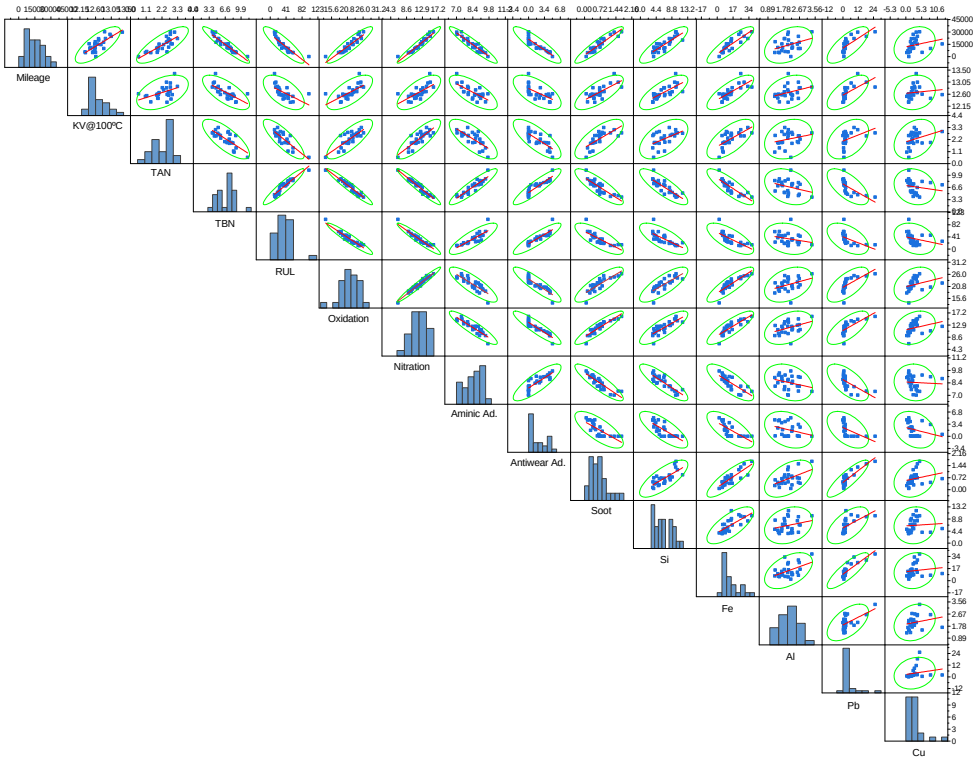

Figure 5.14. *Relationship between lube B parameters in vehicles type IV.*

Table 5.13. *Parameter of adjustment for lube B in vehicle type IV.*

r	*Mileage*	*KV@100°C*	*TAN*	*TBN*	*RUL*	*Oxidation*	*Nitration*	*Aminic Ad.*	*Antiwear Ad.*	*Soot*	*Si*	*Fe*	*Al*	*Pb*	*Cu*
Mileage	–	0.75690	0.79250	-0.94194	-0.88053	0.91751	0.96243	-0.94562	-0.88610	0.92741	0.83888	0.86362	0.37467	0.74114	0.23835
KV@100°C	0.75690	–	0.47076	-0.70754	-0.58768	0.68001	0.68299	-0.71160	-0.62985	0.72705	0.72354	0.76592	0.34395	0.65253	0.11916
TAN	0.79250	0.47076	–	-0.75930	-0.82644	0.79859	0.82854	-0.74075	-0.76283	0.71353	0.51565	0.66169	0.24074	0.41571	0.32432
TBN	-0.94194	-0.70754	-0.75930	–	0.93339	-0.96300	-0.96415	0.91491	0.90678	-0.84814	-0.83366	-0.84715	-0.31551	-0.64935	-0.16767
RUL	-0.88053	-0.58768	-0.82644	0.93339	–	-0.95017	-0.95281	0.83229	0.89391	-0.77532	-0.72179	-0.71541	-0.24472	-0.51193	-0.27435
Oxidation	0.91751	0.68001	0.79859	-0.96300	-0.95017	–	0.97660	-0.84074	-0.89528	0.83310	0.79151	0.85957	0.37193	0.66289	0.29418
Nitration	0.96243	0.68299	0.82854	-0.96415	-0.95281	0.97660	–	-0.90513	-0.90883	0.90605	0.81422	0.84051	0.39416	0.69681	0.27937
Aminic Ad.	-0.94562	-0.71160	-0.74075	0.91491	0.83229	-0.84074	-0.90513	–	0.82894	-0.88032	-0.85441	-0.78200	-0.28009	-0.63284	-0.05815
Antiwear Ad.	-0.88610	-0.62985	-0.76283	0.90678	0.89391	-0.89528	-0.90883	0.82894	–	-0.74040	-0.77224	-0.71346	-0.30943	-0.49643	-0.28385
Soot	0.92741	0.72705	0.71353	-0.84814	-0.77532	0.83310	0.90605	-0.88032	-0.74040	–	0.75288	0.84566	0.50285	0.86207	0.23401
Si	0.83888	0.72354	0.51565	-0.83366	-0.72179	0.79151	0.81422	-0.85441	-0.77224	0.75288	–	0.71836	0.26257	0.59813	0.07217
Fe	0.86362	0.76592	0.66169	-0.84715	-0.71541	0.85957	0.84051	-0.78200	-0.71346	0.84566	0.71836	–	0.48146	0.84549	0.12487
Al	0.37467	0.34395	0.24074	-0.31551	-0.24472	0.37193	0.39416	-0.28009	-0.30943	0.50285	0.26257	0.48146	–	0.56873	0.22042
Pb	0.74114	0.65253	0.41571	-0.64935	-0.51193	0.66289	0.69681	-0.63284	-0.49643	0.86207	0.59813	0.84549	0.56873	–	0.19398
Cu	0.23835	0.11916	0.32432	-0.16767	-0.27435	0.29418	0.27937	-0.05815	-0.28385	0.23401	0.07217	0.12487	0.22042	0.19398	–

For lubricant C, its respective Figure 5.15 and Table 5.14 are attached below.

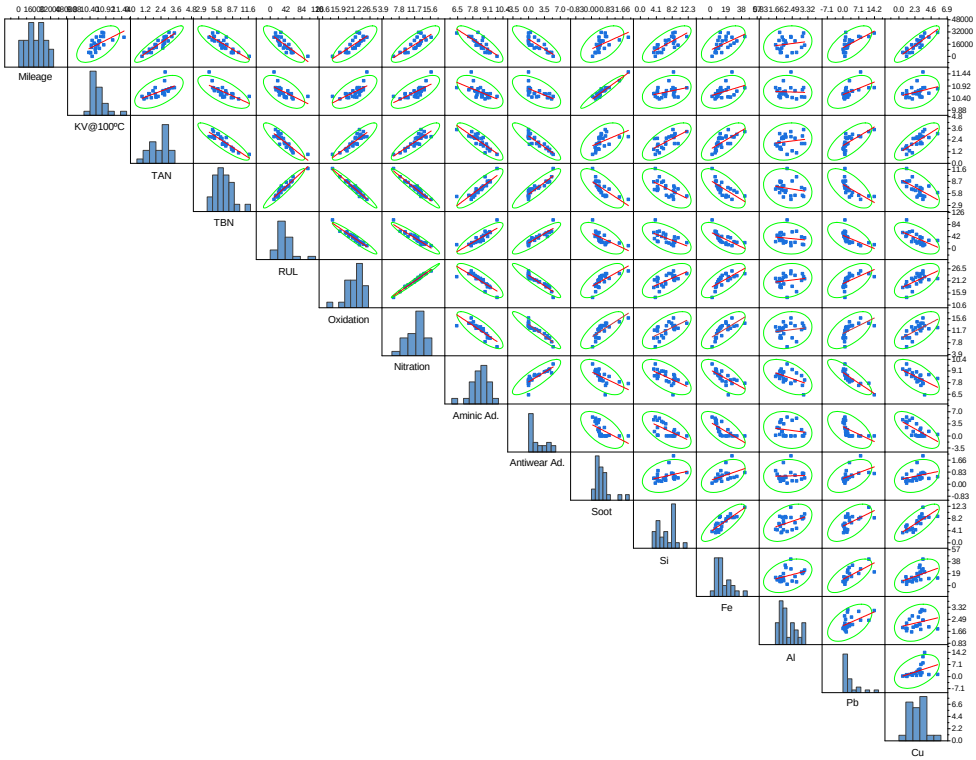

Figure 5.15. *Relationship between lube C parameters in vehicles type IV.*

Table 5.14. *Parameter of adjustment for lube C in vehicle type IV.*

r	*Mileage*	*KV@100°C*	*TAN*	*TBN*	*RUL*	*Oxidation*	*Nitration*	*Aminic Ad.*	*Antiwear Ad.*	*Soot*	*Si*	*Fe*	*Al*	*Pb*	*Cu*
Mileage		0.59491	0.91020	-0.83980	-0.82235	0.80219	0.82211	-0.81897	-0.81807	0.53463	0.73181	0.55336	0.17238	0.63873	0.87378
KV@100°C	0.59491	–	0.55877	-0.70613	-0.61882	0.67111	0.72175	-0.57588	-0.59381	0.95713	0.31145	0.40493	-0.04267	0.53606	0.33834
TAN	0.91020	0.55877	–	-0.89245	-0.87576	0.87278	0.86785	-0.86200	-0.89550	0.49147	0.68836	0.69858	0.16422	0.70246	0.76140
TBN	-0.83980	-0.70613	-0.89245	–	0.95502	-0.97706	-0.97236	0.87678	0.91158	-0.71991	-0.60783	-0.68359	-0.19959	-0.64560	-0.62261
RUL	-0.82235	-0.61882	-0.87576	0.95502	–	-0.96234	-0.95122	0.85599	0.90402	-0.64671	-0.57988	-0.66235	-0.14665	-0.58477	-0.61206
Oxidation	0.80219	0.67111	0.87278	-0.97706	-0.96234	–	0.99197	-0.82783	-0.94118	0.70310	0.62761	0.72888	0.17387	0.58316	0.60767
Nitration	0.82211	0.72175	0.86785	-0.97236	-0.95122	0.99197	–	-0.82869	-0.94249	0.75455	0.63945	0.72271	0.16245	0.58988	0.63404
Aminic Ad.	-0.81897	-0.57588	-0.86200	0.87678	0.85599	-0.82783	-0.82869	–	0.83559	-0.58661	-0.63114	-0.68192	-0.47485	-0.83864	-0.62072
Antiwear Ad.	-0.81807	-0.59381	-0.89550	0.91158	0.90402	-0.94118	-0.94249	0.83559	–	-0.60060	-0.61753	-0.69974	-0.17441	-0.56709	-0.67789
Soot	0.53463	0.95713	0.49147	-0.71991	-0.64671	0.70310	0.75455	-0.58661	-0.60060	–	0.32638	0.45316	0.03654	0.49419	0.28439
Si	0.73181	0.31145	0.68836	-0.60783	-0.57988	0.62761	0.63945	-0.63114	-0.61753	0.32638	–	0.82008	0.43573	0.58656	0.77492
Fe	0.55336	0.40493	0.69858	-0.68359	-0.66235	0.72888	0.72271	-0.68192	-0.69974	0.45316	0.82008	–	0.36828	0.69116	0.47740
Al	0.17238	-0.04267	0.16422	-0.19959	-0.14665	0.17387	0.16245	-0.47485	-0.17441	0.03654	0.43573	0.36828	–	0.52645	0.28021
Pb	0.63873	0.53606	0.70246	-0.64560	-0.58477	0.58316	0.58988	-0.83864	-0.56709	0.49419	0.58656	0.69116	0.52645	–	0.42813
Cu	0.87378	0.33834	0.76140	-0.62261	-0.61206	0.60767	0.63404	-0.62072	-0.67789	0.28439	0.77492	0.47740	0.28021	0.42813	–

For the case of lubricating oil D, by performing a statistical analysis of its parameters, Figure 5.16 and Table 5.15 were obtained.

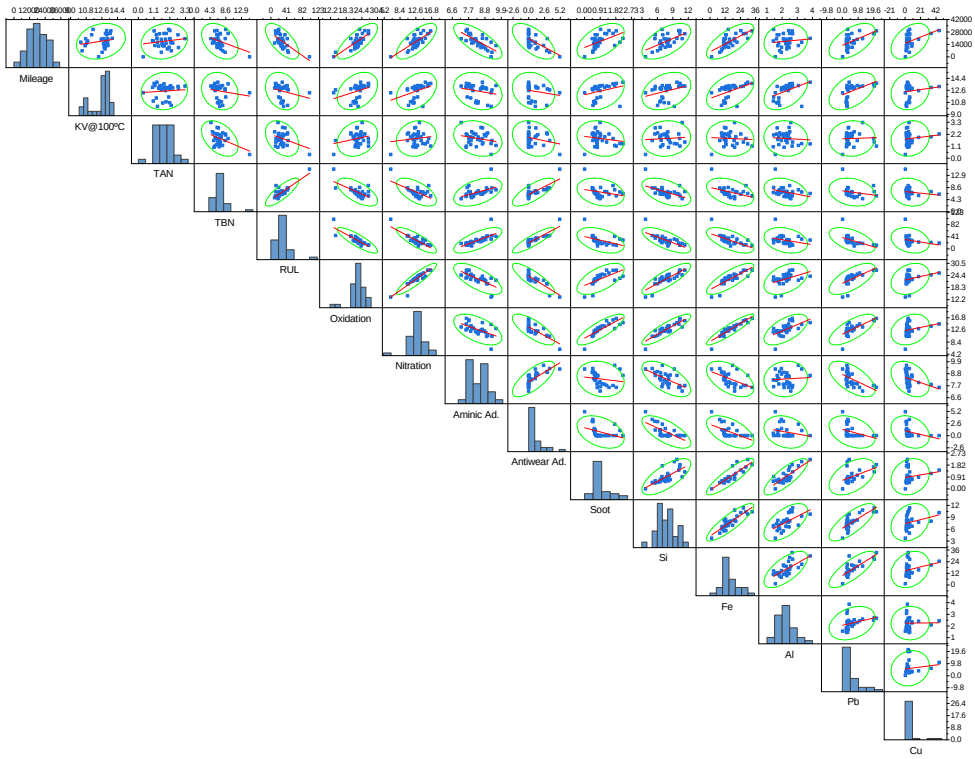

Figure 5.16. *Relationship between lube D parameters in vehicles type IV.*

Table 5.15. *Parameter of adjustment for lube D in vehicle type IV.*

r	*Mileage*	*KV@100°C*	*TAN*	*TBN*	*RUL*	*Oxidation*	*Nitration*	*Aminic Ad.*	*Antiwear Ad.*	*Soot*	*Si*	*Fe*	*Al*	*Pb*	*Cu*
Mileage	–	0.21050	0.15973	-0.37694	-0.65790	0.75984	0.71815	-0.72564	-0.63255	0.51411	0.58107	0.69535	0.11762	0.55374	0.43109
KV@100°C	0.21050	–	0.08106	-0.16480	-0.23305	0.34625	0.38110	-0.22043	-0.18785	0.28789	0.32442	0.45906	0.45519	0.49269	0.14813
TAN	0.15973	0.08106	–	-0.43687	-0.34614	0.24964	0.13986	-0.22888	-0.24883	-0.17568	0.07716	-0.05866	-0.07189	0.04560	0.12995
TBN	-0.37694	-0.16480	-0.43687	–	0.82082	-0.63979	-0.60980	0.46879	0.75719	-0.26481	-0.51482	-0.39575	-0.29571	-0.22196	-0.14137
RUL	-0.65790	-0.23305	-0.34614	0.82082	–	-0.85314	-0.82908	0.70702	0.88221	-0.42730	-0.71148	-0.63072	-0.27659	-0.54040	-0.24320
Oxidation	0.75984	0.34625	0.24964	-0.63979	-0.85314	–	0.91087	-0.69655	-0.83913	0.61749	0.83326	0.80164	0.42080	0.67305	0.27883
Nitration	0.71815	0.38110	0.13986	-0.60980	-0.82908	0.91087	–	-0.55196	-0.74946	0.81676	0.87500	0.91721	0.60341	0.71555	0.25490
Aminic Ad.	-0.72564	-0.22043	-0.22888	0.46879	0.70702	-0.69655	-0.55196	–	0.73102	-0.16155	-0.61500	-0.51583	0.07011	-0.61354	-0.37507
Antiwear Ad.	-0.63255	-0.18785	-0.24883	0.75719	0.88221	-0.83913	-0.74946	0.73102	–	-0.38726	-0.68591	-0.54856	-0.23543	-0.37647	-0.27916
Soot	0.51411	0.28789	-0.17568	-0.26481	-0.42730	0.61749	0.81676	-0.16155	-0.38726	–	0.70980	0.87425	0.81076	0.48412	0.18402
Si	0.58107	0.32442	0.07716	-0.51482	-0.71148	0.83326	0.87500	-0.61500	-0.68591	0.70980	–	0.86695	0.60015	0.76035	0.26154
Fe	0.69535	0.45906	-0.05866	-0.39575	-0.63072	0.80164	0.91721	-0.51583	-0.54856	0.87425	0.86695	–	0.67026	0.78525	0.25943
Al	0.11762	0.45519	-0.07189	-0.29571	-0.27659	0.42080	0.60341	0.07011	-0.23543	0.81076	0.60015	0.67026	–	0.32963	0.01454
Pb	0.55374	0.49269	0.04560	-0.22196	-0.54040	0.67305	0.71555	-0.61354	-0.37647	0.48412	0.76035	0.78525	0.32963	–	0.13597
Cu	0.43109	0.14813	0.12995	-0.14137	-0.24320	0.27883	0.25490	-0.37507	-0.27916	0.18402	0.26154	0.25943	0.01454	0.13597	–

And to conclude the study, for the oil formulation E used in the type IV vehicles, the results treated from a statistical approach led to the generation of Figure 5.17, which is completed with Table 5.16 where the goodness of fit is shown.

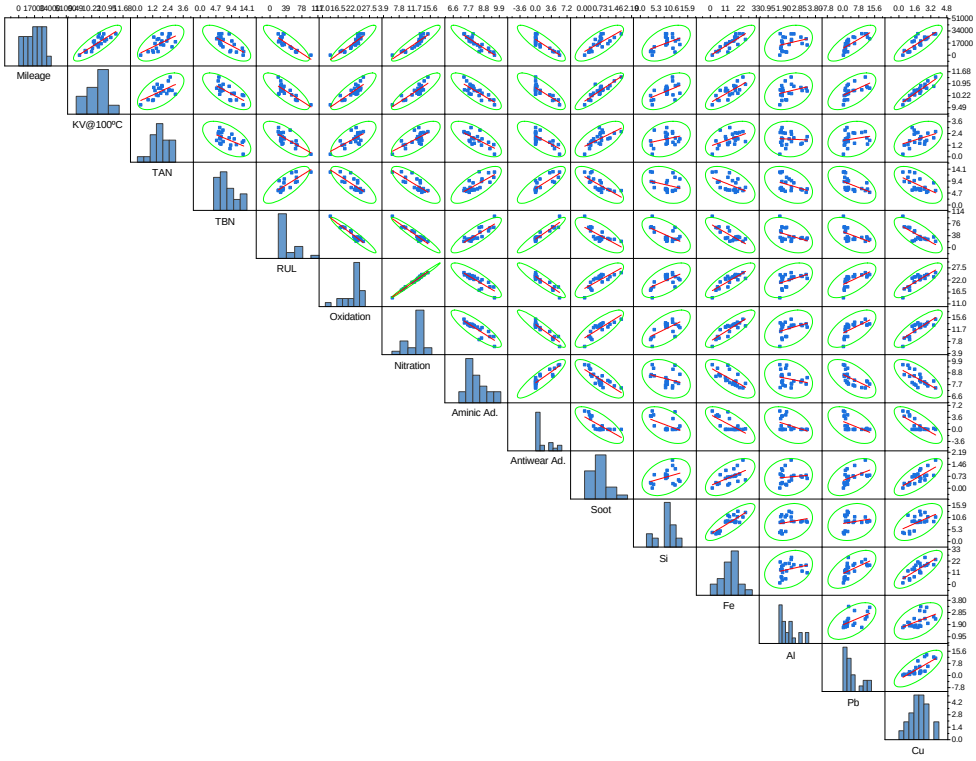

Figure 5.17. *Relationship between lube E parameters in vehicles type IV.*

Table 5.16. *Parameter of adjustment for lube E in vehicle type IV.*

r	*Mileage*	*KV@100°C*	*TAN*	*TBN*	*RUL*	*Oxidation*	*Nitration*	*Aminic Ad.*	*Antiwear Ad.*	*Soot*	*Si*	*Fe*	*Al*	*Pb*	*Cu*
Mileage	–	0.84071	0.63031	-0.70869	-0.84324	0.90360	0.91613	-0.90006	-0.86253	0.75667	0.49851	0.85484	0.30955	0.77496	0.83257
KV@100°C	0.84071	–	0.58546	-0.70830	-0.79795	0.84466	0.87186	-0.81192	-0.80380	0.88900	0.54475	0.76940	0.31034	0.60115	0.91935
TAN	0.63031	0.58546	–	-0.55321	-0.72694	0.68178	0.71494	-0.70870	-0.70189	0.67222	0.28881	0.49202	-0.06353	0.20797	0.41892
TBN	-0.70869	-0.70830	-0.55321	–	0.77727	-0.79338	-0.79682	0.75797	0.81810	-0.73461	-0.30424	-0.52822	-0.38529	-0.51158	-0.60040
RUL	-0.84324	-0.79795	-0.72694	0.77727	–	-0.95923	-0.95930	0.85816	0.94221	-0.73164	-0.61527	-0.78304	-0.40951	-0.50059	-0.73843
Oxidation	0.90360	0.84466	0.68178	-0.79338	-0.95923	–	0.99447	-0.84316	-0.92274	0.77123	0.62361	0.82737	0.44250	0.65289	0.81620
Nitration	0.91613	0.87186	0.71494	-0.79682	-0.95930	0.99447	–	-0.85972	-0.93371	0.80920	0.63404	0.84200	0.38382	0.62481	0.82485
Aminic Ad.	-0.90006	-0.81192	-0.70870	0.75797	0.85816	-0.84316	-0.85972	–	0.88317	-0.79383	-0.32467	-0.70759	-0.25160	-0.59838	-0.68668
Antiwear Ad.	-0.86253	-0.80380	-0.70189	0.81810	0.94221	-0.92274	-0.93371	0.88317	–	-0.74017	-0.49133	-0.70960	-0.41581	-0.52722	-0.74315
Soot	0.75667	0.88900	0.67222	-0.73461	-0.73164	0.77123	0.80920	-0.79383	-0.74017	–	0.37166	0.57879	0.11303	0.50439	0.74683
Si	0.49851	0.54475	0.28881	-0.30424	-0.61527	0.62361	0.63404	-0.32467	-0.49133	0.37166	–	0.81845	0.23879	0.21515	0.57314
Fe	0.85484	0.76940	0.49202	-0.52822	-0.78304	0.82737	0.84200	-0.70759	-0.70960	0.57879	0.81845	–	0.27975	0.58495	0.77320
Al	0.30955	0.31034	-0.06353	-0.38529	-0.40951	0.44250	0.38382	-0.25160	-0.41581	0.11303	0.23879	0.27975	–	0.55612	0.51496
Pb	0.77496	0.60115	0.20797	-0.51158	-0.50059	0.65289	0.62481	-0.59838	-0.52722	0.50439	0.21515	0.58495	0.55612	–	0.75219
Cu	0.83257	0.91935	0.41892	-0.60040	-0.73843	0.81620	0.82485	-0.68668	-0.74315	0.74683	0.57314	0.77320	0.51496	0.75219	–

With the four formulations used in Type IV vehicles already analysed and their results treated, it is possible to discern a number of features that need to be explained. These aspects are listed in the following lines:

- In these vehicles, the correlation records between the different variables are generally satisfactory, always taking into account the nature of the study from which the data have been extracted.
- Also in a paired observation (according to the SAE viscosity grade), the results for each pair are shown below:
  - For the 5W30 B-C couple, the response shown for the two oils is practically the same, except for the fact that there is an improvement in metal wear rates in those vehicles using a more viscous formulation, as it seems to indicate that this formulation protects the internal lubricated parts better.
  - For the D-E couple (both SAE 10W30 lubricating oils), there are common features; however, for the users of the lubricating oil D there is a wrong refill of the oil, since in the Mileage-KV@100°C plot there are clearly two groups or families, which have an effect on the correspondence between the 15 variables.
- But if one now compares the vehicles, i.e. the passage from one iteration of the study to the other, the conclusions reached are different:
  - When comparing the formulations B and D, given that the vehicles employing the two oils are the same, it can be observed that for certain cases, the problems on vehicle's condition are the same.
  - The phenomenon mentioned for the couple B-D is also observed for the other pair of oils: C-E.

5.4.1.5 General remarks

According to the data analysed above, there are a series of general lines that are common to all of them and are continuously repeated. In order to facilitate their understanding, the main conclusions, result of analysing the data and information in these scatter matrix graphs, have been organised in the following list:

- Given that the data come from a study designed in such a way that all the parameters analysed are referenced to the accumulated oil mileage,

it is not surprising that parameters related to the degradation and contamination of the lubricating oil, as well as the engine, show upward trends with the use of the lubricant. While parameters related to properties that are consumed or depleted over the ODI show downward trends.

- For the oxidation-nitration couple, it has been observed that, in all the tested formulations there exists a great correlation. This is reflected in the linear association that, for all the cases, it presents an r value higher than 0.9.

- The pair of variables oxidation and nitration are one of the main causes of the additives depletion (both antiwear and aminic additives), which is manifested in the decreasing trend shown by both the oxidation-additive and nitration-additive bonds, as well as the RUL number. In these, the relationship is inverse: the higher the oxidation or nitration, the lower the variable facing it (RUL or additives).

- Another influential pair is the one formed by soot and silicon, which are always directly proportional to the wear metals: iron (Fe), aluminium (Al), lead (Pb) and copper (Cu).

- If the TAN-TBN pair is now analysed, it can be understood that both factors are antagonistic and opposing. TAN and TBN share their influence or effect on several variables of the set, although their individual relationship with each other is in different directions.

- Finally, thanks to this type of work, it is possible to clearly appreciate groups of values that escape from the majority set of data, that follow a logical evolution, breaking that trend. Focusing on the field of OCM, this usually indicates problems in the vast majority of cases.

In view of all of this, it is demonstrated that the deductions drawn are consistent with the observations of the lubricating oils' performance explained in Chapter 4. However, these conclusions, especially those concerning the linearity of the correlation response between each pair of parameters, need to be qualified by the nature of the study. The study on which this statistical treatment has been carried out is a research work where the sources of variability are several and beyond our control. In order to be able to carry out a study with a higher resolution and quality, it would have been necessary to study only one vehicle with a single lubricating oil thus and under the working conditions of the same driving cycle. This type of approach was not possible

in this Thesis and, in spite of the good results and conclusions obtained, if we wish to carry out a statistical analysis of this type in the future, it would be advisable to simplify the study system.

5.4.2 FT–IR spectroscopy

Regarding to the procedures applied to the FT–IR spectra of a lubricating oil, a study was carried out with the aim of correlating the mean IR spectrum (MIR) of lubricating oils with the TAN and TBN parameters obtained through a new analytical protocol, analytical thermometry. The most interesting aspects of the study were the way in which it was approached and, taking into account the conditions and situations (both in terms of equipment and its requirements/limitations, samples, etc.), it was possible to generate a chemometric protocol that was adjusted to the conditions in which it was, and could be, carried out.

In this study, a considerable battery of real-service engine lubricating oil samples was available, which was perfectly characterised beforehand, which facilitated the whole process that was carried out later on. This set of samples presented different origins and states, being attractive to corroborate that the final work is able to be applied to real samples and not samples generated or adulterated in the laboratory. In detail, these samples were basically three different lubricating oil formulations: A, B and C (see Table 5.17), which came from different vehicles (both in terms of fuel used and engine technology).

From the whole set it is necessary to perform a first sampling stage to choose which samples will be used for model generation and which are reserved for validation, according to an external validation approach (given that the number of samples allows it) (see Figure 5.18). Therefore, a first approximation was made to match the values extracted from the thermometric titration (TAN and TBN values) with the spectra recorded for each sample with the FT–IR spectrophotometer available in the Fuels and Lubricants laboratory of the institute.

For this purpose, all analytical measurements were performed in triplicate to make the future model more robust and to avoid large effects of outliers or experimental errors. However, according to the technical characteristics of the spectrophotometer used in the study, not all spectral data pretreatment procedures were feasible. As a consequence, after an exploration of what was useful for further study, two viable alternatives were chosen:

Table 5.17. *Main characteristics of the three engine oils tested.*

Parameters	Lub. A	Lub. B	Lub. C
SAE grade	5W30	5W30	5W30
API category	CJ-4	CK-4	FA-4
API base oil	G-III+IV	G-III+IV	G-III+IV
KV@40° C (cSt)	68	68	55
KV@100° C (cSt)	11.7	12.6	10.5
HTHS@150° C (cP)	3.58	3.57	3.10
VI (-)	<169	168	165
TBN (mg KOH/g)	10	11	12
SAPS level	Mid	Mid	Mid
Barium (ppm)	10	n.d.	n.d.
Boron (ppm)	<5	312	334
Calcium (ppm)	2329	1248	1312
Zinc (ppm)	749	784	835
Phosphorous (ppm)	712	715	764
Magnesium (ppm)	100	847	895
Molybdenum (ppm)	n.d.	42	45

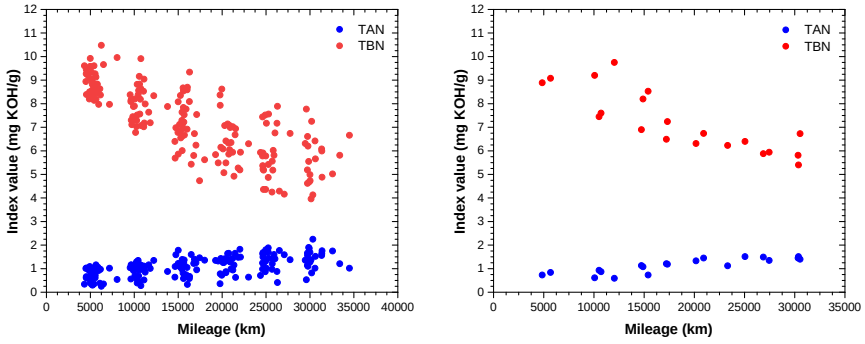

(a) Samples for the model calibration (b) Samples for the model validation

Figure 5.18. *Set of samples used in the calibration and validation of the TAN-TBN by FT–IR chemometric model.*

- For each of the oil formulations studied, a reference signal was assigned to construct or develop the calculations. It is quite clear that choosing fresh (unused) lubricating oil as the starting point is the ideal choice in this approach (see Figure 5.19).

- It was decided to make a selection of regions of the spectrum which, from a chemical point of view, do correlate with the acidification of the lubricating oil. The selected MIR regions are the next: 4500–4000 cm^{-1}, 3800–3100 cm^{-1} and 1900–590 cm^{-1}. This considerably reduces the number of variables, in this case wavenumbers, to be introduced for the calibration of the model and adjusts their number to the number of available experimental data.

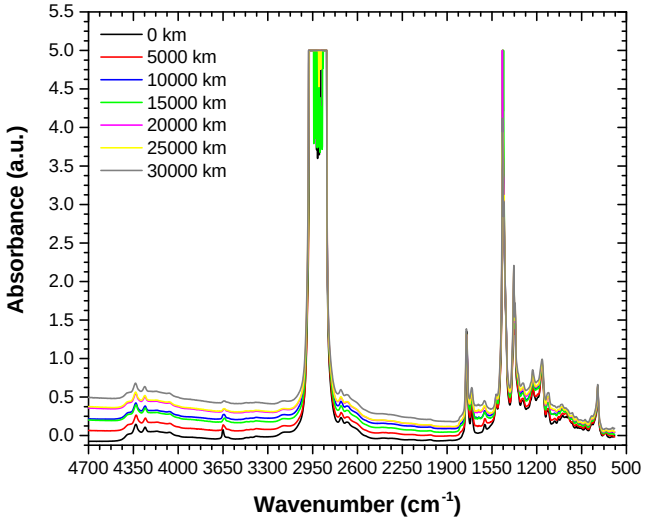

Figure 5.19. *Example of evolution of FT–IR spectrum in used engine oil.*

With these two aspects in mind, it is time to implement them. As a large number of spectral data will be analysed and then correlated with the TAN and TBN indices, the most intelligent option is to perform a dimensionality reduction of these data by means of a Principal Component Analysis (PCA) [8] before doing a Multivariate calibration method. PCA is a statistical method that assumes that data with large variation is important. PCA tries to find a unit vector (first principal component) that minimises the average squared distance from the points to the line. Other components are lines perpendicular to this line. Thanks to that, it ensures that no information is lost and checks

if the data has a high standard deviation. At the end, PCA reduces the dimensionality to select just the top few features that satisfactorily represent the variation in data.

By performing this data treatment (see the results in Figure 5.20), a set of components (PCi) was chosen that was able to explain more than 99.5% of all the variance. Table 5.18 shows the PCi that allow this level to be reached.

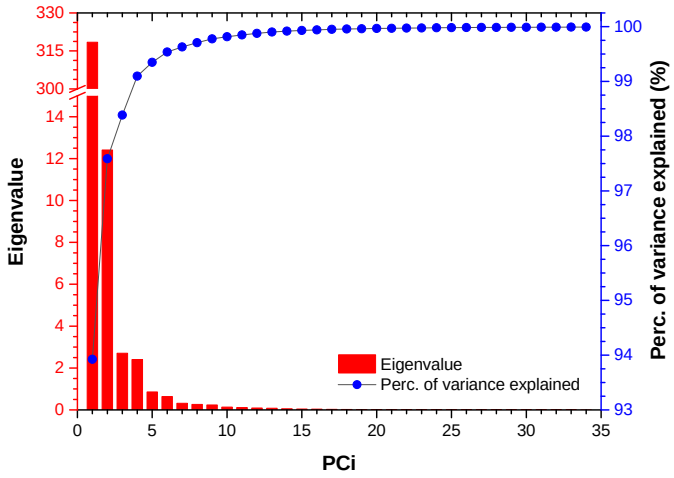

Figure 5.20. *Percentage of variance explained per each PCi for MIR spectrum.*

Table 5.18. *PCA analysis and the main characteristics of the four selected PCs.*

PCi	Eigenvalue	Perc. of variance (%)	Perc. var. accumulated (%)
1	318.406	93.925	93.925
2	12.414	3.662	97.587
3	2.707	0.799	98.385
4	2.406	0.710	99.095
5	0.860	0.254	99.349
6	0.635	0.187	99.536
7	0.314	0.093	99.629
8	0.260	0.077	99.706
9	0.237	0.070	99.776
10	0.135	0.040	99.815

From this point on, it is possible to continue the chemometric process in a simpler way, since the calculation has been simplified. The next step is therefore to calibrate a multivariate model capable of providing a tool for extracting the TAN and TBN indices from the FT–IR spectrum of a lubricating oil sample.

The analyses applied on the sample set for the qualification of a valid model were several: Once the PCA is completed, different analysis can be performed: PLS (Partial Least Squares), Linear Regressions (LR), Support Vector Machine (SVM) and Gaussian Process Regression (GPR), in Table 5.19 we have compiled the parameters indicative of the descriptive power of each of the models tested.

Table 5.19. *Regression models for TAN and TBN prediction by FT–IR spectra.*

Regression model	Parameter	R^2 cal.	RMSE cal.	R^2 val.	RMSE val.
PLS	TAN	0.88169	0.10629	0.73764	0.16235
PLS	TBN	0.84601	0.52074	0.83215	0.61004
Linear	TAN	0.99143	0.11132	0.97898	0.16326
Linear	TBN	0.99515	0.51716	0.99357	0.59544
Linear SVM	TAN	0.99109	0.11233	0.97708	0.16707
Linear SVM	TBN	0.99501	0.52101	0.99329	0.60964
Quadratic SVM	TAN	0.98879	0.12494	0.39800	1.19896
Quadratic SVM	TBN	0.99659	0.42904	0.87487	2.95411
Cubic SVM	TAN	0.96691	0.21847	0.56330	0.84993
Cubic SVM	TBN	0.99432	0.56046	0.55425	7.71572
Fine Gaussian SVM	TAN	0.98842	0.12678	0.94267	0.26041
Fine Gaussian SVM	TBN	0.99286	0.62583	0.98079	1.03102
Medium Gaussian SVM	TAN	0.98968	0.12038	0.96444	0.20753
Medium Gaussian SVM	TBN	0.99492	0.52297	0.99269	0.63405
Coarse Gaussian SVM	TAN	0.97821	0.16897	0.93733	0.28245
Coarse Gaussian SVM	TBN	0.98974	0.75465	0.98699	0.84822
Squared Exponential GPR	TAN	0.99129	0.11295	0.94956	0.24803
Squared Exponential GPR	TBN	0.99620	0.45272	0.99568	0.49450
Matern 5/2 GPR	TAN	0.99054	0.11554	0.94801	0.25181
Matern 5/2 GPR	TBN	0.99656	0.43094	0.99564	0.49689
Exponential GPR	TAN	0.99046	0.11779	0.96243	0.21658
Exponential GPR	TBN	0.99718	0.38956	0.99422	0.56370
Rotational Quadratic GPR	TAN	0.99237	0.10498	0.95829	0.22791
Rotational Quadratic GPR	TBN	0.99637	0.44259	0.99499	0.52925

Now, the selection of the model that best fits this case is the one whose Determination Coefficient (R^2) and Root Mean Square Error (RMSE) are close to 1 and less than 1, respectively. According to these two parameters, the best options are:

- For the TAN, as prepared in Figure 5.21, Linear Regression is the best fitting.
- While for the TBN, the Squared Exponential GPR describes better this parameter (see Figure 5.22).

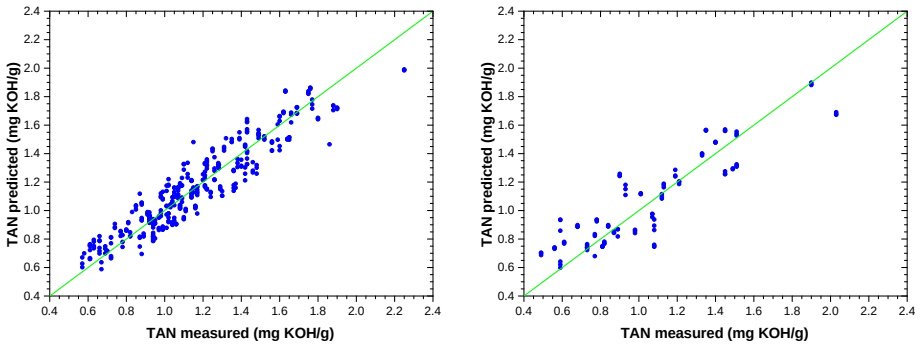

(a) TAN model calibration (b) TAN model validation

Figure 5.21. *Linear Regression model for TAN prediction.*

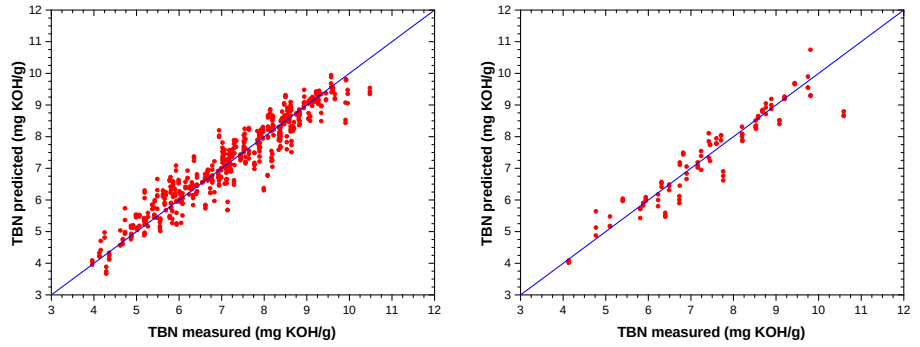

(a) TBN model calibration (b) TBN model validation

Figure 5.22. *Squared Exponential GPR model for TBN prediction.*

These results obtained from this research work were published in an impact journal, *Chemometrics and Intelligent Laboratory Systems*, with the title: "Applying chemometric procedures for correlation the FTIR spectroscopy with the new thermometric evaluation of Total Acid Number and Total Basic Number in engine oils" [12]. So, in view of all this, we have managed to leave a useful and advantageous tool in the Fuels and Lubricants laboratory of CMT-Motores Térmicos , which can even be improved or adapted to new scenarios and situations to come.

5.4.3 NIR spectroscopy

NIR spectroscopy is a type of spectroscopy where, due to the range of the electromagnetic spectrum in which it works, between 14000 and 4000 cm^{-1}, it does not present a high degree of specificity. This is due to the fact that in NIR spectroscopy, what is recorded is a spectrum of overtones of the MIR spectrum but in the near-range (NIR) of the IR region [11]. Thus, in the bands obtained in the NIR spectrum (see Figure 5.23), what is really being observed is an overtone or overlapping of bands [6].

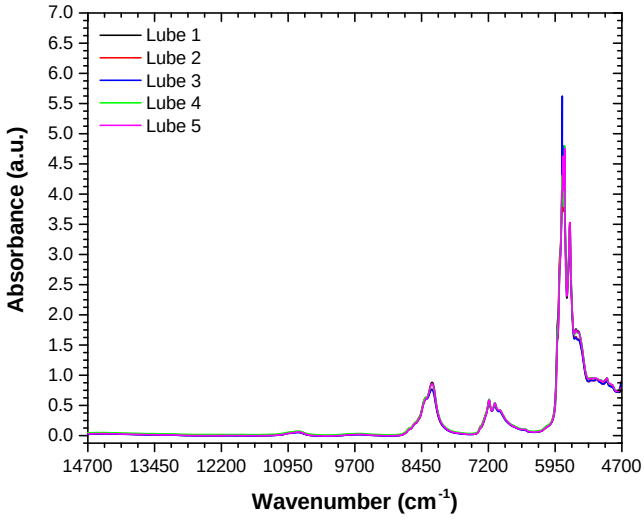

Figure 5.23. *NIR spectrums of 6 different lubes.*

Consequently, in this situation, in order to be able to detect changes in the NIR spectrum, a considerable chemical change must take place. This low sensitivity leads to the need to apply multivariate methods in order to find

these associations between the analysed parameters and the NIR spectrum [2].

In this study, the equipment used was the PerkinElmer Spectrum Two FT-IR (see Figure 5.24), which is capable of working with lubricating oils. Table 5.20 shows the main characteristics of this system.

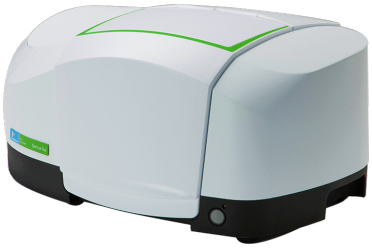

Figure 5.24. *PerkinElmer Spectrum Two FT-IR spectrometer.*

Table 5.20. *Main characteristics of the Spectrum Two FT-IR spectrometer.*

Feature (units)	**Value or property**
Spectral range / Resolution (cm^{-1})	8300 - 350 / 0.5 max.
Peak-peak signal-to-noise ratio	9300:1
Time per scan (seg.)	5
Path length (mm)	10.0
Window material (-)	Potassium bromide (KBr)
Detector material (-)	Lithium tantalate ($LiTaO_3$)
Sampling interface (-)	Cuvette and baseplate holder
Working temperature (-)	Room-temperature (5-45°C)

In order to study the potential application of NIR spectroscopy for the prediction of lubricating oil parameters [7, 19], a first study was carried out with the aim of determining its viability in the future. For this purpose, following the same philosophy as shown for the FT–IR spectroscopy, in section 5.4.2 *FT–IR spectroscopy*, it was decided to study the case of four lubricating oil formulations (Lube A, Lube B, Lube C and Lube D) that were used in CNG engines; this in order to determine, by analysing their NIR spectra, their kinematic viscosity, TAN and TBN, degree of oxidation and nitration and finally, the content of aminic and antiwear additives. This selection has not been random, since all of them are properties of the oil that have already

been proven to be possible to determine from chemometric studies applied to spectroscopic techniques [21].

Each of these oils are different but, as a consequence of the characteristics of the NIR technique, their spectra are practically coincident (see Figure 5.25). This means that in order to monitor any change in the spectrum as a consequence of a chemical change in the lubricant, a multivariate chemometric analysis is necessary.

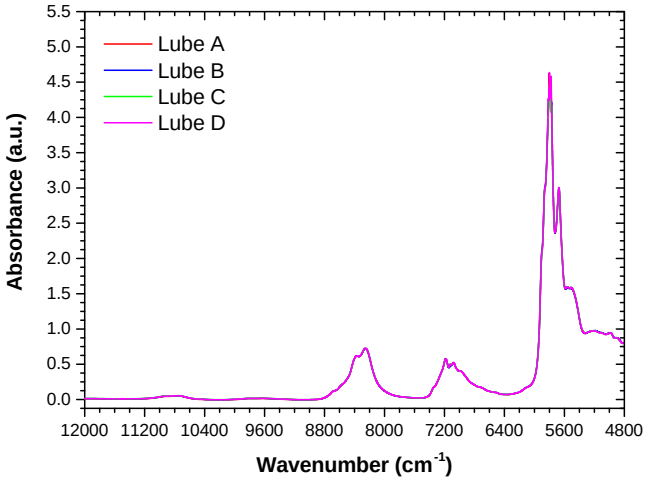

Figure 5.25. *NIR spectrums of the four formulations studied with chemometrics: Lube A (red), Lube B (blue), Lube C (green) and Lube D (pink).*

So, for the whole NIR spectrum: from 12000 cm^{-1} to 4800 cm^{-1}, the study was carried out where a total of 131 lubricating oil samples were selected for model calibration and 60 samples for further validation. As the study is extensive due to the number of properties to be determined, Figure 5.26 and Figure 5.27 have been prepared to help show the values of each of these properties for both the calibration sample set and the validation sample set, respectively.

Despite the large number of available data that can be used to build the model, each of these parameters was analysed in triplicate, these are far from the number of variables provided by the NIR spectrum: 7201 wavenumbers. To try to compensate for this difference between the two parts, a PCA treatment was performed on the NIR spectra of the lubricating oil samples. Here, the criterion for selecting the number of individual components (PCi) needed for this study was decided by the number of components capable of describing

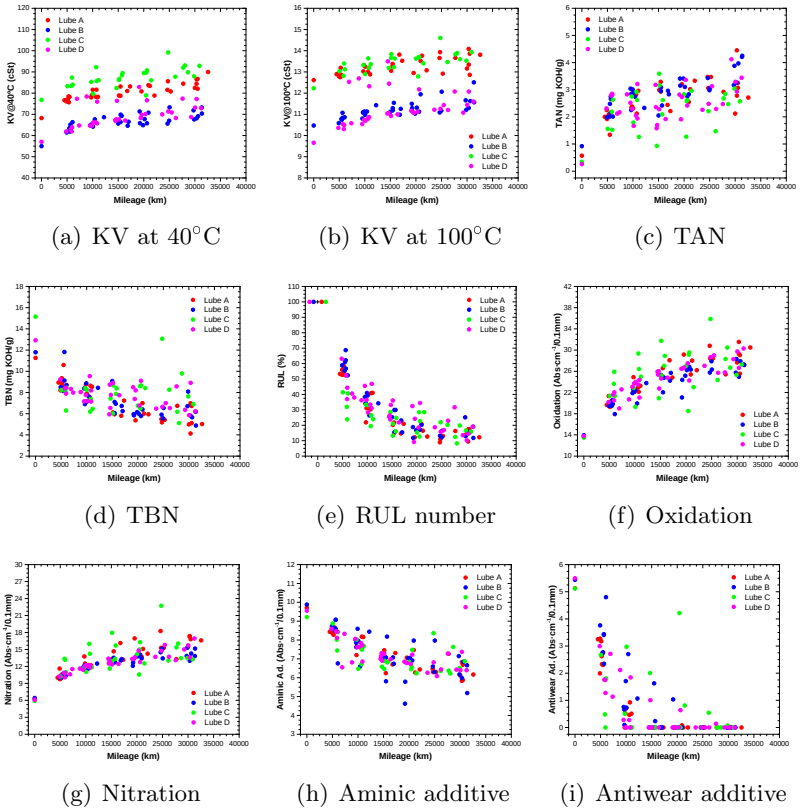

(a) KV at 40°C (b) KV at 100°C (c) TAN

(d) TBN (e) RUL number (f) Oxidation

(g) Nitration (h) Aminic additive (i) Antiwear additive

Figure 5.26. *Calibration samples organised by those parameters to be extracted from the NIR study of a lubricant.*

more than 99.9% of the total variance. Accordingly, as shown in Figure 5.28, the number of components to be selected is 15.

If we now analyse the numerical value of both the eigenvalue of each individual component and its percentage of variance, see Table 5.21, we can clearly see that the relevance of the components declines very quickly: with the first three (PC1, PC2 and PC3), it is already possible to describe more than 99.0% of the total variance. However, the most demanding criterion of 99.9% was maintained.

Thereafter, a selection of different multivariate calibration models were applied for each of the parameters to be described: LR (Linear Regression), PLS (Partial Least Squares), SVM (Support Vector Machine) and GPR (Gaussian Process Regression). Not all protocols are valid or suitable for

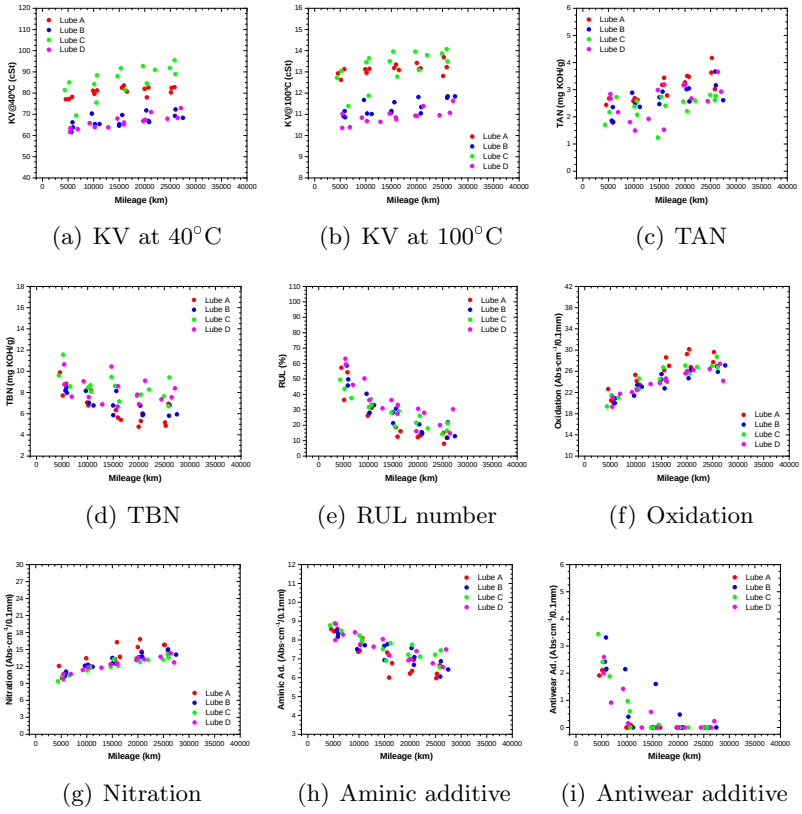

(a) KV at 40°C (b) KV at 100°C (c) TAN

(d) TBN (e) RUL number (f) Oxidation

(g) Nitration (h) Aminic additive (i) Antiwear additive

Figure 5.27. *Validation samples organised by those parameters to be extracted from the NIR study of a lubricant.*

every parameter, as there are some that achieve a more accurate description, as indicated by the R^2 and RMSE parameters. Table 5.22 lists the best fitting regression models for each parameter.

Graphically, the goodness of fit between the measured data fed into the model (either during calibration or validation) and those predicted by the model is best understood when they are plotted against each other. It is for this reason that, in the following figures, these comparisons are shown: in red are the calibration data and in blue the validation data. The first couple, Figure 5.29, is the kinematic viscosity at 40°C.

As can be seen in Figure 5.29, there are about two sectors of data: some with higher viscosity values and some with lower viscosity values. This leads to a detrimental effect on the quality parameters of the model, but this was to be

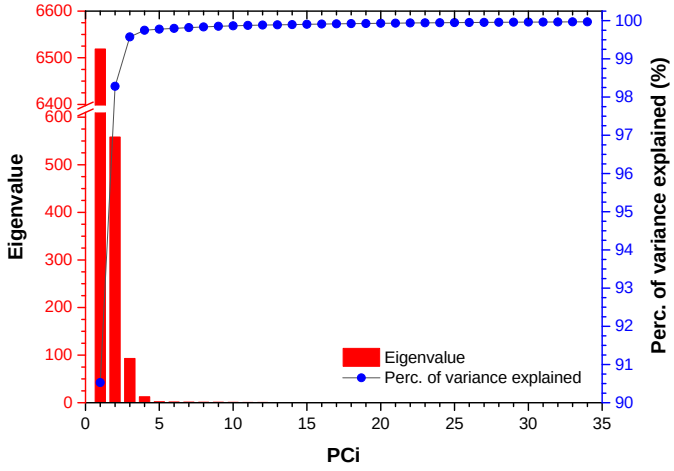

Figure 5.28. *Percentage of variance explained per each PCi for NIR spectrum.*

Table 5.21. *PCA analysis and the main characteristics of the fifteen selected PCs.*

PCi	Eigenvalue	Perc. of variance (%)	Perc. var. accumulated (%)
1	6518.874	90.527	90.527
2	538.373	7.527	98.281
3	93.126	1.293	99.575
4	12.533	0.174	99.749
5	2.018	0.028	99.777
6	1.605	0.022	99.799
7	1.420	0.020	99.819
8	1.242	0.017	99.836
9	1.174	0.016	99.852
10	0.978	0.014	99.866
11	0.686	0.010	99.875
12	0.618	0.009	99.884
13	0.528	0.007	99.891
14	0.467	0.006	99.898
15	0.465	0.006	99.904

Table 5.22. *Best-fit regression models for the prediction of each of the investigated lubricant parameters by NIR spectroscopy.*

Parameter	Regression model	R^2 cal.	RMSE cal.	R^2 val.	RMSE val.
KV@40° C	Rational Quadratic GPR	0.99500	5.32290	0.98766	8.40103
KV@100° C	Rational Quadratic GPR	0.99686	0.68830	0.99220	1.08392
TAN	Rational Quadratic GPR	0.98670	0.30440	0.96108	0.51592
TBN	Exponential GPR	0.99209	0.68093	0.98429	0.95718
RUL	Exponential GPR	0.98850	3.78885	0.96270	6.21386
Oxidation	Exponential GPR	0.99757	1.21205	0.99818	1.04472
Nitration	Exponential GPR	0.99490	0.92957	0.99625	0.79566
Aminic Ad.	Rational Quadratic GPR	0.99888	0.24586	0.99406	0.56322
Antiwear Ad.	Exponential GPR	0.97019	0.27098	0.87815	0.45438

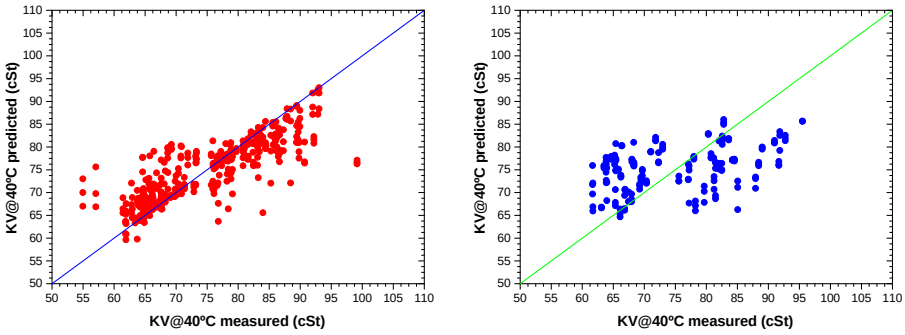

(a) Model calibration (b) Model validation

Figure 5.29. *Regression model for KV@40° C prediction by NIR.*

expected due to the nature of the samples: Lube A and Lube B formulations are SAE 5W30 oils, while the other two are SAE 10W30. Under these circumstances, it would be advisable to have carried out the chemometric study separately in view of the results obtained, although this was not the original objective of the study.

When switching to the kinematic viscosity but now at 100°C, the pattern shown in Figure 5.30 corresponds to that in Figure 5.29.

Figure 5.31 and Figure 5.32 below show the results obtained for the prediction of the TAN and TBN, respectively, according to the regression model shown in Table 5.22.

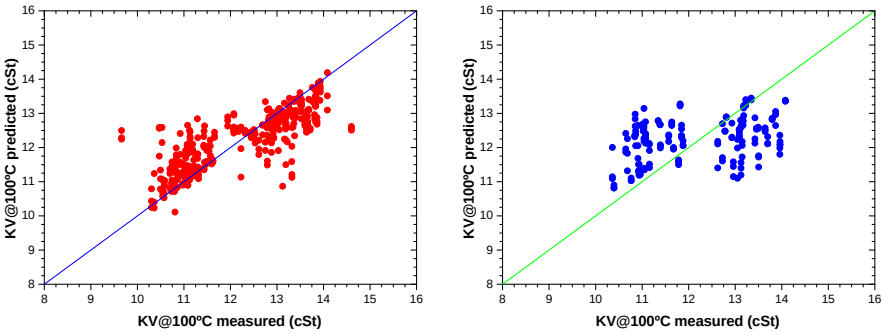

(a) Model calibration (b) Model validation

Figure 5.30. *Regression model for KV@100° C prediction by NIR.*

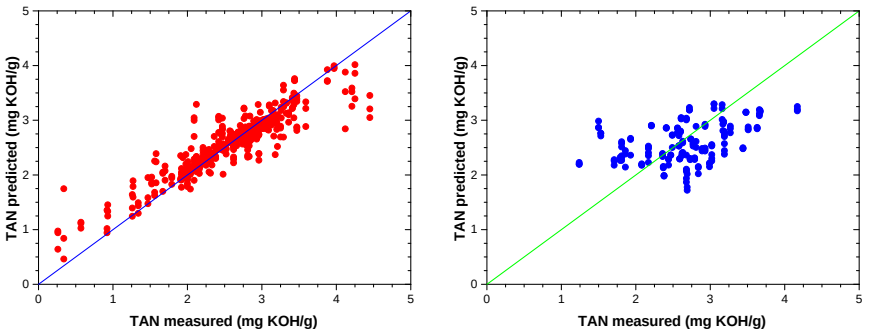

(a) Model calibration (b) Model validation

Figure 5.31. *Regression model for TAN prediction by NIR.*

In both cases, the prediction during calibration of the two models generates a more than satisfactory response (as indicated by the reported values of R^2 and RMSE in Table 5.22). However, in the validation, the fit is somewhat impaired as a consequence, depending on the validation data set, of a lack of dispersion between the values. As can be seen in Figure 5.31 and Figure 5.32, there is a very dense focus of values, leaving regions with very low or no density of experimental values. However, a simple way around this would be to incorporate more experimental data whose values are centred in these sparsely populated regions.

Analysing now the response of the model to the predicted RUL number, see Figure 5.33, the results are very satisfactory.

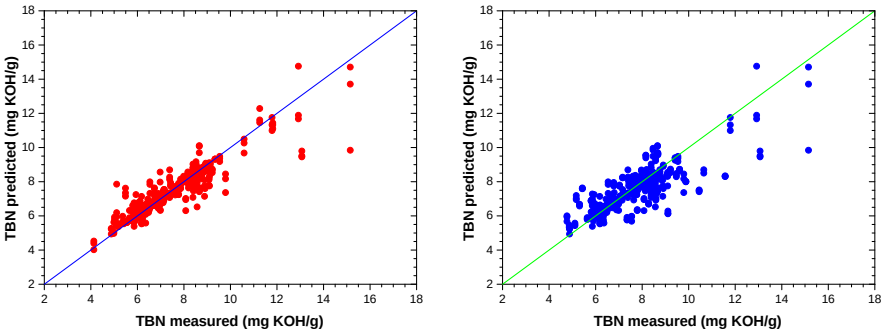

(a) Model calibration (b) Model validation

Figure 5.32. *Regression model for TBN prediction by NIR.*

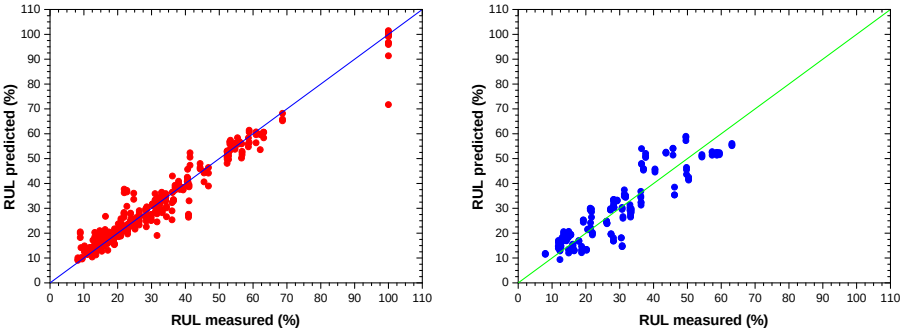

(a) Model calibration (b) Model validation

Figure 5.33. *Regression model for RUL prediction by NIR.*

This may be due to the parameter itself, which is a percentage value of the depletion of the antioxidant additive package in the lubricants. Accordingly, this parameter is indifferent to the starting point, since a value of 100% is always assigned, so that the relevant sample will show a remaining AO content, relative to that starting value. As with the NIR, by having the spectra of the new oils (whose RUL is 100%) and then samples of these oils with different degrees of use, it is possible to generate a very useful data library (from the point of view of the chemometric analysis procedure). In view of the reflected behaviour, both during calibration and validation, the prediction of the RUL number by NIR seems to be a viable alternative in the future.

The next group, Oxidation (Figure 5.34) and Nitration (Figure 5.35), are two properties that are intimately linked, so they can be analysed together.

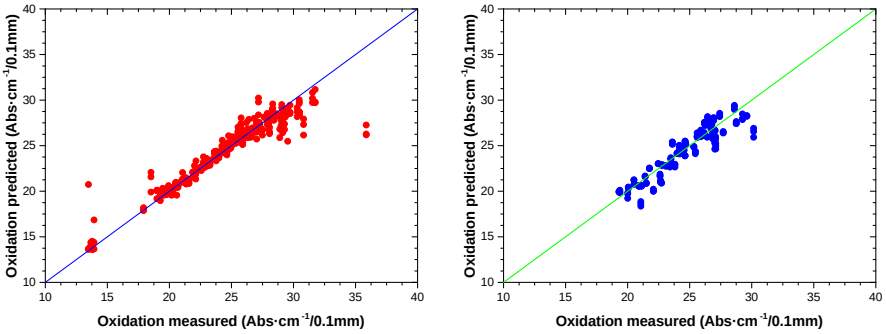

(a) Model calibration (b) Model validation

Figure 5.34. *Regression model for Oxidation prediction by NIR.*

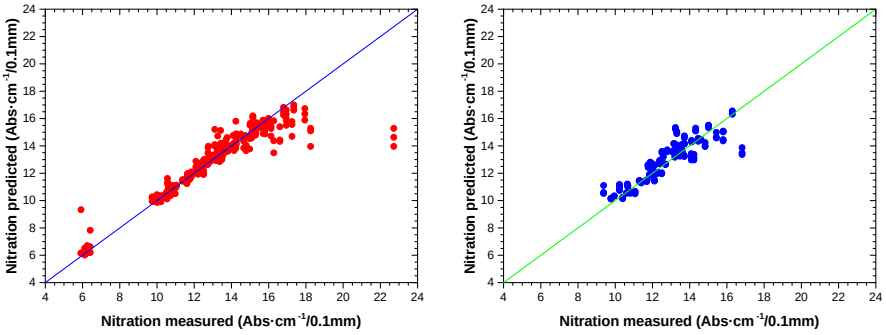

(a) Model calibration (b) Model validation

Figure 5.35. *Regression model for Nitration prediction by NIR.*

Considering the results, the goodness of prediction for both parameters is among the highest achieved (see Table 5.22). Oxidation and nitration values are obtained by FT–IR spectroscopy according to ASTM E2412, so it is not surprising that if the measurement is made in the MIR range, the same (or at least equivalent) behaviour should be achieved in the NIR. Although the way to treat a NIR spectrum is different from that of a MIR spectrum, these results justify the possibility of obtaining the oxidation and nitration values by means of this first option.

Finally, the remaining couple of parameters: aminic additives and antiwear additives, have also been evaluated for their predictive capability using NIR. As with the oxidation-nitration couple, these two parameters are obtained according to the guidelines established by the ASTM E2412 standard. Thus, Figure 5.36 and Figure 5.37 show the NIR prediction results for aminic additives and antiwear additives, respectively.

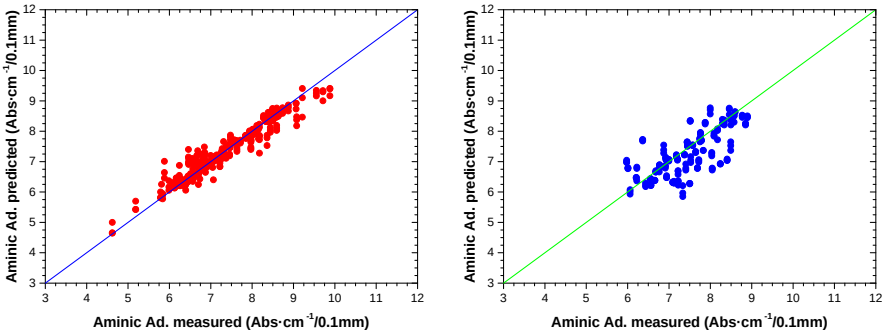

(a) Model calibration (b) Model validation

Figure 5.36. *Regression model for Aminic additives prediction by NIR.*

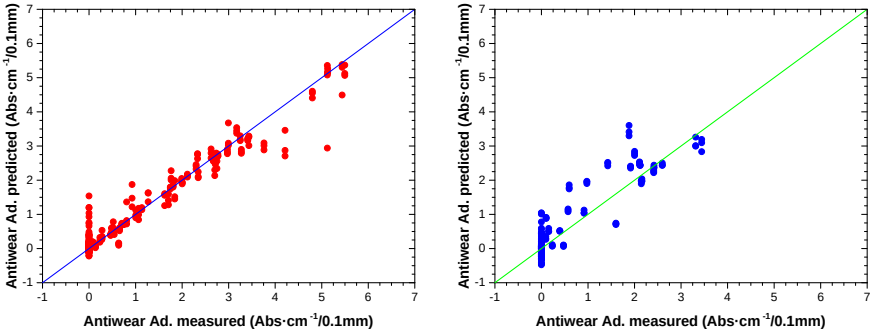

(a) Model calibration (b) Model validation

Figure 5.37. *Regression model for Antiwear additives prediction by NIR.*

The difficulty in the case of using NIR spectroscopy for the determination of these two additives is different and, consequently, their predictive performance is also different. Therefore, each of the additives will be analysed separately.

- When analysing the response of the model for the aminic additives, a very good correspondence between the experimental value and the predicted value is observed, both during the calibration stage of the model and in its subsequent validation, according to the fit parameters reflected in Table 5.22.

- In the antiwear additives, in all four lubricating oils, the situation was reached where the additives were completely depleted. This implies that during the calibration of the model there are a large number of different spectra (since in this spectrum, in principle, contributions from several factors appear as it is not exclusive to a single factor) which are assigned a value of zero for the antiwear additives parameter. One consequence of this is that the degree of fit between the measured and predicted response is reduced, but nevertheless, the level of prediction is significant enough to be reliable.

In conclusion, the use of NIR spectroscopy to predict certain aspects of lubricants has shown signs of being an effective and rapid way of achieving this. However, it has been observed that its performance is conditioned by the parameter to be described, so that, in this situation, it would be advisable to carry out a more in-depth study. The next step would be to analyse the effects that cause the divergences between the response or prediction returned by the model in contrast to the real value (measured experimentally), so as to classify those parameters in degrees of goodness: starting from those where the parameter and the NIR spectrum are closely related, to the opposite extreme, where the relationship is not that direct and is influenced by other factors.

5.5 Discussion

The prediction of TAN and TBN by FT–IR spectroscopy, a technique widely used in lube oil analysis laboratories, adds extra value to this technique. Therefore, implementing this model into a routine analysis can be very advantageous, as it can make it easier to decide to opt in or out of further analysis of the samples. This can be an interesting and useful aspect when performing control tasks within a maintenance plan based on OCM.

Switching techniques, a similar situation occurs with NIR. NIR spectroscopy is just starting to be implemented in lubricant analysis laboratories, so it is an avenue that still needs to be developed further to become widespread. For that reason, this study aims to show the predictive potential of NIR

spectroscopy when combined with chemometric procedures, prediction capable of being applied to both physical and chemical engine oil parameters.

Bibliography

[1] M. J. Adams. *Chemometrics in analytical spectroscopy*. Royal Society of Chemistry, 2004.

[2] M. Blanco and I. Villarroya. NIR spectroscopy: a rapid-response analytical tool. *TrAC Trends in Analytical Chemistry*, 21(4):240–250, 2002.

[3] K. S. Booksh and B. R. Kowalski. Theory of analytical chemistry. *Analytical Chemistry*, 66(15):782A–791A, 1994.

[4] R. Bro. Multivariate calibration: what is in chemometrics for the analytical chemist? *Analytica Chimica Acta*, 500(1-2):185–194, 2003.

[5] S. D. Brown, R. Tauler, and B. Walczak. *Comprehensive chemometrics: chemical and biochemical data analysis*. Elsevier, 2020.

[6] A. M. C. Davies. An introduction to near infrared (NIR) spectroscopy. *J. Near Infrared Spectrosc*, 2014.

[7] Metrohm International Headquarters. *Quality control of lubricants–Fast and chemical-free determination of the acid number, viscosity, moisture content, and color number of lubricants with NIRS*, 2020. AN-NIR-041, Version 2.

[8] I. T. Jolliffe and J. Cadima. Principal component analysis: a review and recent developments. *Philosophical Transactions of the Royal Society A: Mathematical, Physical and Engineering Sciences*, 374(2065):20150202, 2016.

[9] S. Kokot, M. Grigg, H. Panayiotou, and T. D. Phuong. Data interpretation by some common chemometrics methods. *Electroanalysis: An International Journal Devoted to Fundamental and Practical Aspects of Electroanalysis*, 10(16):1081–1088, 1998.

[10] B. Lavine and J. Workman. Chemometrics. *Analytical chemistry*, 80(12):4519–4531, 2008.

[11] J. C. Lindon, G. E. Tranter, and D. Koppenaal. *Encyclopedia of spectroscopy and spectrometry*. Academic Press, 2016.

[12] V. Macián, B. Tormos, A. García-Barberá, and A. Tsolakis. Applying chemometric procedures for correlation the FTIR spectroscopy with the new thermometric evaluation of Total Acid Number and Total Basic Number in engine oils. *Chemometrics and Intelligent Laboratory Systems*, 208:104215, 2021.

[13] H. Mark and J. Workman. *Chemometrics in spectroscopy*. Elsevier, 2010.

[14] J. Miller and J. C. Miller. *Statistics and chemometrics for analytical chemistry*. Pearson Education, 2018.

[15] F. Murtagh and A. Heck. *Multivariate data analysis*, volume 131. Springer Science & Business Media, 2012.

[16] T. Næs, T. Isaksson, T. Fearn, and T. Davies. *A user-friendly guide to multivariate calibration and classification*, volume 6. NIR Chichester, 2002.

[17] T. O'Haver. A pragmatic introduction to signal processing. *University of Maryland at College Park*, 2021.

[18] M. Otto. *Chemometrics: statistics and computer application in analytical chemistry*. John Wiley & Sons, 2016.

[19] D. Timm, C. Kurowski, U. Grummisch, U. Meyhack, and H. Grunewald. Applications of near infrared spectroscopy for qualification of lubricants and other mineral oil products. *Journal of Near Infrared Spectroscopy*, 6(A):A243–A246, 1998.

[20] K. Varmuza and P. Filzmoser. *Introduction to multivariate statistical analysis in chemometrics*. CRC press, 2016.

[21] D. Zamora, M. Blanco, M. Bautista, R. Mulero, and M. Mir. An analytical method for lubricant quality control by NIR spectroscopy. *Talanta*, 89:478–483, 2012.

Chapter 6

Soot in oil

Contents

6.1 Introduction

Soot is a by-product of the fuel combustion in ICEs. In a first approximation, soot has a direct effect on colouring the lubricant, in particular it is responsible for changing the original colour of the lubricating oil to a darker, blacker colour. This change in colour, which is the indisputable sign of the presence of dissolved soot in oil, is a very simple judgement to indicate the presence of this pollutant.

However, this type of analysis is not useful to quantify, in more detail, the soot in the lubricating oil. In order to meet the relevant requirements (depending on the application and under certain circumstances), there are several analytical techniques and procedures that could be used.

Accordingly, it is possible to study soot using a variety of techniques: from existing techniques for lubricant analysis that are capable of providing information about soot to techniques specifically developed. As the case may be, it appears that the levels of appreciation that can be applied to the study of soot in oil (SiO, for short) are as follows:

- One can choose to select a level that provides data on the presence or absence of soot in lubricating oil. Techniques that provide information of this type are known as "qualitative analysis techniques", since they provide a non-numerical result.

- On the other hand, if the selected technique allows information to be obtained about how much soot is in a sample of oil, this technique is said to be a "quantitative analysis technique". Within these techniques, which indicate the concentration of a certain analyte in a sample, the differences in the level of appreciation of the parameter during quantification can be very variable.

- Finally, there are those techniques that provide other types of information. This group includes "structural analysis techniques" among others.

In this chapter, focus is put on the quantification of soot in engine lubricating oil samples. Therefore, existing techniques will be studied with the aim of improving or adapting them better to the specific application (in this case, engine oils) and, in addition, new techniques and methodologies will be studied to asses the applicability to the field of soot quantification.

6.2 Contextualising the soot problem

Currently, the situation in the automotive world attending new legislation and regulations on pollutant emissions control, fuels (market, availability, new alternatives [39, 91], etc.), the development of new engine designs and technologies, etc., it is a somewhat delicate situation [93]. For the case that involves this chapter, soot in oil, the factors that come into play or are influential vectors are the following:

- The first of all are those emission control regulations, in particular the Euro 6 regulation (and its post-revision Euro 7, which will be applied in 2025), which obliges to reduce the levels of nitrogen oxides (NOx), hydrocarbons (HC), carbon monoxide (CO) and particulate matter (PM). Figure 6.1 shows the evolution (from Euro I to Euro VI) of the permitted exhaust emissions.
- As a direct consequence of these emission limits imposed on OEMs, they have been forced to develop and apply new technologies aimed at reducing pollutant emissions from their engines.

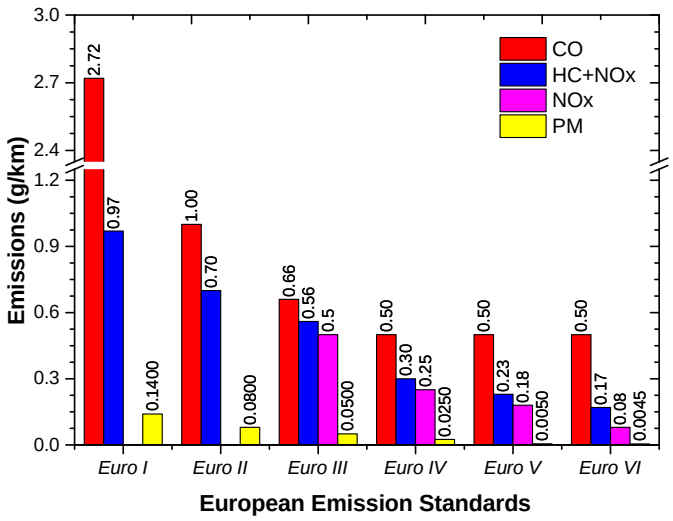

Figure 6.1. *Evolution of European emission standards for diesel engines.*

For soot in diesel engine oils, there are a number of mechanisms and tools for achieving the necessary emission reduction in diesel engines will affect

higher o lower presence of soot in oil [90]. Diesel engines have several possibilities/technologies to reach the permitted pollutant emission limits. In summary, the main solutions have been developed in different ways: injection systems, gas exchange processes and aftertreatment devices [3]. It is in the latter that the impact on soot in the ICEs is greatest. Therefore, based on this relevance, it was decided to investigate how aftertreatment and the exhaust gas recirculation systems influence soot generation [94]. Basically, the principal or primary systems incorporated in diesel engines are three: the Selective Catalytic Reduction (SCR), the Exhaust Gas Recirculation (EGR) system and the Particulate Filter (DPF for diesel engines). Figure 6.2 is a representation of the configuration of the above mentioned systems in a diesel engine.

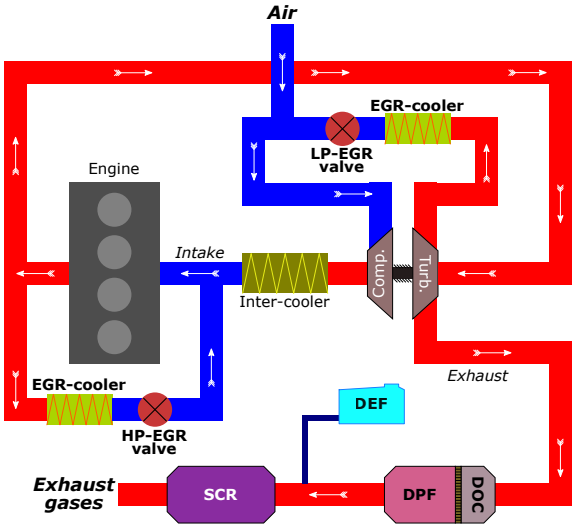

Figure 6.2. *Primary components of aftertreatment systems and the two versions of EGR system, low pressure (LP–EGR) and high pressure (HP–EGR) configuration, of a diesel engine.*

All of these are the result of a response to an increasing push for clean diesel emissions and reducing environmental impact, so diesel engines have been forced to adapt complex exhaust and emission aftertreatment systems in the new engine designs.

Finally, as a consequence of these two aspects: the regulations and technologies implemented in the engines create an ideal scenario for soot in oil [56, 78].

6.2.1 Soot generation in ICE

ICEs, all of them, produce soot as a result of incomplete fuel combustion. CI engines are the biggest soot generators as a consequence of the injection and ignition process of the fuel. In this Thesis, the research has been carried out on ICEs fueled by diesel, therefore the development of soot research work is focused on this type of engines and with this particular fuel.

Soot is one of the by–products generated in the combustion of diesel: Unburnt Hydrocarbons (UHC), CO, NOx and Particulate Matter (PM). In particular, soot is embedded in the PM, as this is clearly visible from the diagram in Figure 6.3 [59]. This diagram distinguishes, within the PM, two main families: volatile or soluble organic compounds (generally known as Soluble Organic Fraction, SOF) and the Insoluble Fraction (ISF).

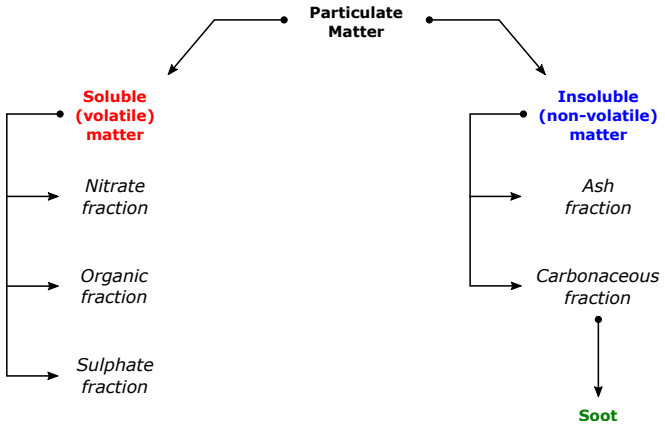

Figure 6.3. *Composite fraction of Particulate Matter.*

Focused on soot, it is formed as small particles, whose major composition is carbon, although the appearance of other substances and/or elements that are retained during the genesis of the particles also occurs [74]. In accordance with the combustion reaction 6.1, the complexity of the combustion process can be understood [11].

$$C_xH_y + B \cdot (O_2 + a \cdot N_2 + b \cdot CO_2 + c \cdot Ar) \rightarrow$$
$$\rightarrow (x + B \cdot b) \cdot CO_2 + (y/2 + B \cdot d) \cdot H_2O + (B - x - y/2) \cdot O_2 + B \cdot a \cdot N_2 + B \cdot c \cdot Ar \quad (6.1)$$

However, the combustion reaction does not occur through the reaction 6.1 above since, depending on the conditions under which it takes place, the combustion of the fuel is completed to different rates. When diesel is combusted, some fraction of the injected diesel mass cannot combine with oxygen and that leaves behind small unburned particles of carbon. This particles are progressively accumulated in each engine cycle and they can migrate into the lubricating oil or it can be removed together with the exhaust gases [22].

In diesel engines, soot is dependent on the different phases that occur during the combustion of diesel [27]. In Figure 6.4 the temporal comparison between the fuel injection rate and the heat release rates from its combustion has been depicted.

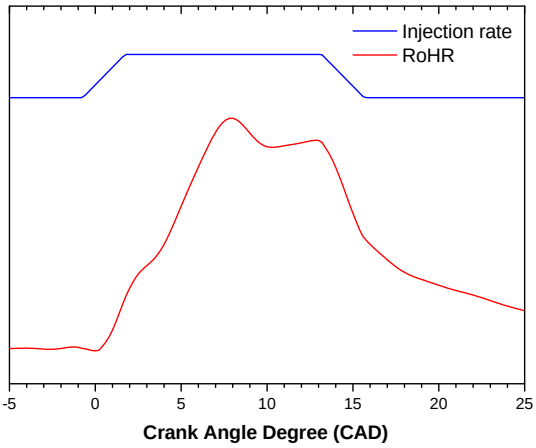

Figure 6.4. *Conventional diesel combustion.*

Each of these five elements are due to the different elements that come into play during combustion in an ICE: diesel, air, lubricant and engine internal parts. Consequently, each of these four elements are generating sources for each of the elements that make up the PM. In order to better appreciate this phenomenon, Figure 6.5 has been prepared as an illustration of the relative importance of each of them on the PM constituents (leaving aside those pollutants or extraneous elements that may appear).

According to the previous diagram, the transformation of fuel into soot implies that during combustion a series of stages occur that make it possible form the carbon from the hydrocarbons in the fuel (in liquid or gaseous phase) to evolve into solid soot condensed particles [116]. This process is normally

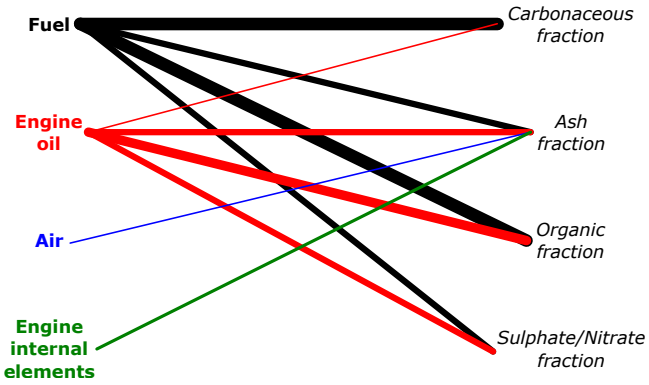

Figure 6.5. *Sources of the different fractions of PM.*

described as a set of 5 steps: pyrolisis, nucleation, coalescence, surface growth and agglomeration, and an extra step called oxidation where the HC residues are oxidised to CO, CO_2 or water [54, 103]. The development of a model describing the soot generation process is a work in progress for many years [9, 28, 29, 40, 107] and is continuously being adapted and improved according to the needs or conditions that arise. However, in the case of liquid fuels, this modelling is more complex because it requires to take into account several agents: physical parameters (temperature, pressure, etc.), aspects related to fuel combustion and injection (spray structure, atomisation and spray combustion), engine among others [67, 77, 80, 111]. Figure 6.6 below shows one of the suitable soot–forming mechanisms currently in use [57].

In view of the model presented in Figure 6.6, it is not surprising that efforts are being made to improve it in order to achieve a better understanding of the phenomenon applied to diesel combustion [86]. While the mechanism of soot generation is not yet a settled issue, it is possible to find a series of stages that have been accepted by a large part of the scientific community studying this process [61]. The stages being referred to are those mentioned above and will be briefly developed below:

- **Pyrolisis**: The burning of diesel causes a variety of substances to be formed. Some of these gas–phase substances are soot precursor chemicals, so–called building blocks, from which the whole process of soot particle formation starts. The most representative chemical species are: unsaturated hydrocarbons, polycyclic aromatic hydrocarbons (PAH), acetylene (C_2H_2) and polyacetylenes.

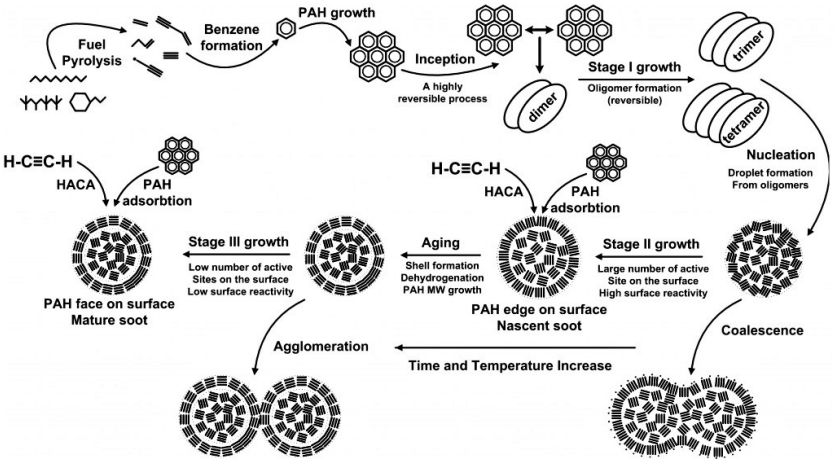

Figure 6.6. *Model of soot generation from liquid fuels.*

- **Nucleation**: This is the next stage after pyrolysis. This is where gaseous compounds (building blocks) are converted into solid nucleated structures. During this stage, the particles acquire mass through surface deposition processes that take place in the growth regions of these primeval or primary particles, which have a large specific area.

- **Surface growth**: These nucleated soot particles then accumulate more of these gaseous precursors (mainly PAHs and acetylenes) on their surface via additional condensation and heterogeneous surface reactions.

- **Colescence**: Coalescence or coagulation is a process where several of these initial particles collide with each other and as a result of the collision form a single unit. This is due to the fact that these particles start to become large enough that attractive forces appear between them, which leads to the generation of particle–particle collision processes that cause them to coagulate in a single spherically shaped particle. As a consequence, the number of particles decreases, but the soot mass remains constant (the masses of the particles involved in the collision add up).

- **Agglomeration**: Occurs when two or more particles come into contact with each other and stick together while maintaining their structural identity (no alteration of morphology). The agglomeration produces a large chain-like particle (in most cases, although cluster particles may

also be produced) where each of its links are the individual particles mentioned above.

Figure 6.7. *Example of the final aggregates of carbon particles [102].*

Regardless of the specific reactions that may lead to the generation of soot [10], they could all be arranged in one of the stages described above. The first three stages take place in the engine cylinder, while the last is observed in the exhaust system.

6.2.2 Physico–chemical properties and characteristics

Soot from diesel combustion in ICEs presents a variety of physical and chemical properties that make it a substance of interest for study due to the great impact it generates in fields as diverse as human health, environment, engineering, among others. It is therefore important to characterise these particles as well as possible, since knowing what they are like allows to know or determine how they will behave or affect the particular field of study. However, the objective of this chapter of the Thesis is not to characterise soot particles but rather to quantify their presence, which is why this sub–section has been prepared to provide an overview of what soot particles look like in order to better understand why a series of analytical techniques (to be discussed in 6.3.2 *Soot in oil quantification*) have been selected in accordance with the properties of soot particles.

Soot is a complicated substance to study as a consequence of its variability according to several factors: fuel origin source, combustion process, fuel injection, chemical reaction mechanisms, kinetic process, etc. so it exhibits a diverse morphology (chemical structure) and composition [26]. This means that soot can behave in a wide variety of manners: electrical

conductivity, hydrophobicity, photon absorption, thermochemical reactivity, photon emission, among others, and consequently, its characterisation is complex. Table 6.1 lists different relevant aspects of the soot as well as the analytical technique(s) needed to obtain this information [84].

Table 6.1. *Soot characterisation.*

Information	**Method or Technique**
Morphology, microstructure and nanostructure	HRTEM and Raman spectroscopy
Biological reactivity	Langendorff hear
Hydrophobic behaviour	Supersaturation in multisept condensation–nuclei counter
Electrical conductivity	Sensor chip with interdigital electrode structure
Soot volume fraction	Incravity laser light absorption
Soot particle mass concentration	Single–particle soot photometer (SP2)
Particle number concentration	Photoacoustic spectroscopy
Particle mass concentration	Laser–induced incandescence
Radical centres	Electron paramagnetic resonance (EPR)
Photophoretic velocity	Photophoresis
Oxidation reactivity	Temperature–programmed oxidation (TPO)
Elemental composition	ICP-MS
Elemental species composition	Photoelectron spectroscopy (PES)

With the objective to better understand this solid material, soot must be described according to its physical and chemical aspects. In accordance with this idea, Figure 6.8 below shows physical aspects such as the organisation and structures of the soot particles as well as the constituent components.

The soot will therefore be described in these two ways.

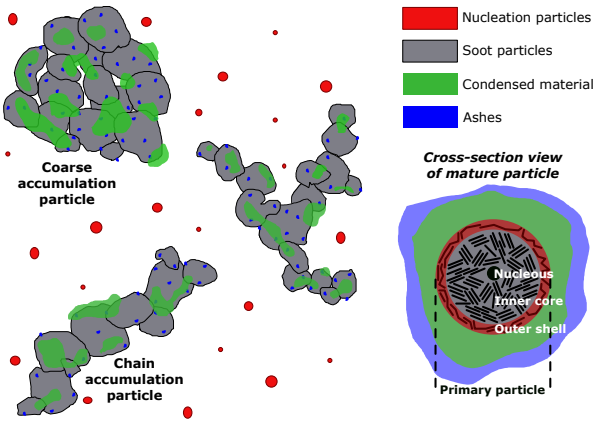

Figure 6.8. *Scheme of soot particles aggregation and cross-section view of a single soot particle.*

6.2.2.1 Physical characterisation

The most relevant physical aspects of PM are aimed at describing how the different constituent structures are structurally organised (at different degrees of complexity) as well as physical metrics that can be associated with the structure and organisation of these particles. For this reason, the parameters to be described are as follows: structure and morphology, density, surface area and electrical charge.

- **Structure**: soot consists of a complex network of small interconnected particles forming an agglomerated structure of a higher order (in the order of micrometers). Starting with the most basic elements, each individual particle (nanoparticle, with diameters ranging from 5 to 30 nm) in the agglomerate is characterised by its own nanostructure: these nanoparticles are composed by layers of carbon arrangement in face–centred planar hexagonal conformation (six–membered rings) arrays called "platelets" [98], which in turn are arranged or organised to form an ordered laminar domain called "crystallites" [116]. From these simple structures, through the union of several of them, it is possible to reach a higher grade called "spherule", a turbostratic particle (a particle where the building blocks are concentrated in a random orientation around the centre of the particle) [26]. Figure 6.9 represents the different substructures of soot particles: from carbon atoms array to, step–by–step, the final spherule.

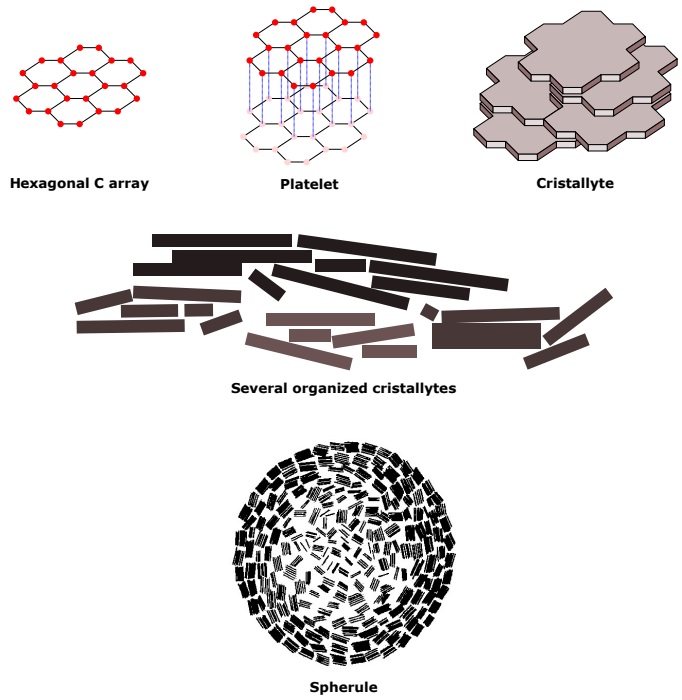

Figure 6.9. *Substructures of soot particle.*

Once these spherical structures, spherules, are formed, they can increase their dimensionality by the inclusion or stacking of other particles (agglomeration processes). Within these particles, what is interesting is to observe how their components are structured, since it is possible to observe ordered and less ordered regions. The more ordered ones are known as graphenic domains or regions, while the disordered or chaotic ones are called graphitic. This different degree of crystallinity within the same particle is due to various factors (fuel and lubricant composition, agglomerate lability, temperature, time [52], engine operating conditions [65], etc.). In any case, for all spherules, a characteristic pattern is fulfilled or followed: in all cases, as can be seen in the TEM images (Figure 6.10), the microstructural order increases as the radius of the particle increases.

As can be seen in Figure 6.10, the central regions (core) present a short–range order as the crystallite orientations do not follow a systematic pattern (they are governed by chance) but, as the particle grows, the crystallites organise themselves into a series of domains with defined

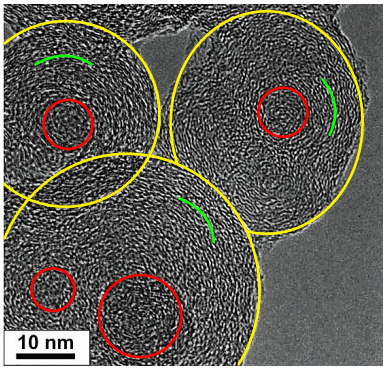

Figure 6.10. *TEM image of soot particle (adapted from M. Pawlyta and H. Hercman [88]): the nuclei or cores of the particles are highlighted in red, while their envelopes are highlighted in yellow. Between core–shell region are the tightly ordered fringes (green lines).*

crystallite orientations. As a result of this constant tangential (with respect to the surface) orientation of the crystallites, the particle shows a quasi–concentric high–density lamellar pattern.

- **Morphology**: particles generated by diesel combustion in an ICE have a spherule-like morphology, which is the general trend observed. However, each of the different spherules are often found in aggregates, which increases the complexity of studying their morphology [60]. In Figure 6.11, the population of particles has been plotted according to their number, area and mass.

  From the information provided in Figure 6.11, it can be deduced that the morphology is a parameter depending on the situation and conditions in which the particle generation process is taking place [66, 76, 82, 113], since the final morphology of the particles can be very variable: from very small particles (in the order of nanometers) to large aggregates (around 10 microns in diameter) according to Figure 6.12. However, if it is desired to characterise the morphology of these particles in a rigorous way, fractality studies are carried out on the electron microscopy images of the particles [70].

  In Figure 6.12 in the SEM image it is possible to see the small spherical soot particles ($D_p > 1\mu$m) and, when the soot particles are analysed by TEM (extracted from [15]), the result allows to distinguish each of the parts that form the agglomerates.

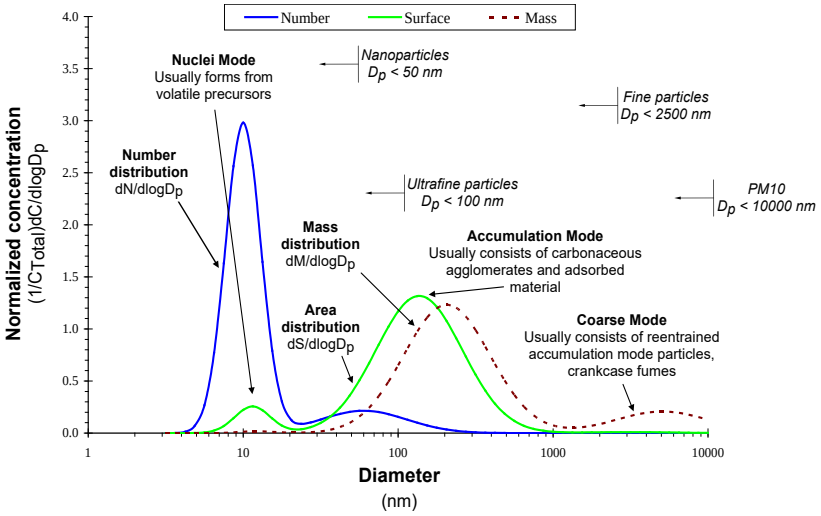

Figure 6.11. *Size distributions for particles emitted by ICEs by number (N), surface area (S) and mass (M) [58].*

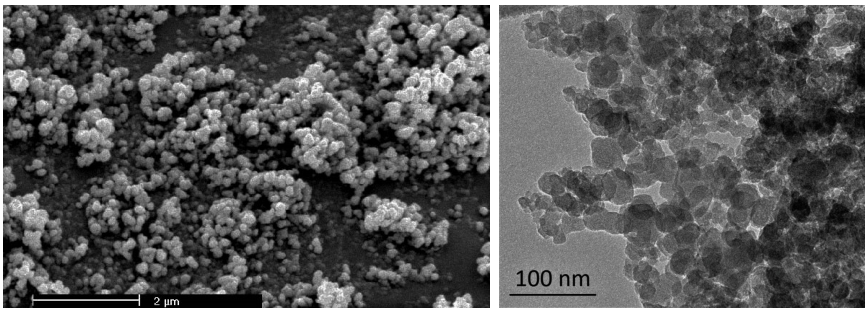

(a) SEM image (b) TEM iamge

Figure 6.12. *Diesel soot electron microscopy images obtained by Scanning Electron Microscope (SEM) and Transmission Electron Microscope TEM, respectively.*

- **Density**: Because of the complex structure of the particles, it is difficult to determine the precise density of the particles, since voids (pores, crevices, etc.) and attached (condensed and adsorbed) layers and other agents that constitute the mature particle have to be taken into account. This is why it is necessary to distinguish between the bulk density and the effective density, in this case the bulk density is the selected one because, according to the growth process of the particles, it is the density

that seems to govern the process. Thus, some studies give different density values ranging from 0.8 to 2.4 g/cm^3, e.g. M. Y. Choi et al. reports density values of 1.7-1.8 g/cm^3 [17]. The density values is conditioned by how the particles are generated, which leads to the fact that it is a parameter dependent on how the engine operates: it has been observed that for high load situations, the density decreases as a consequence of the particle structure having more discontinuity (voids, openings, etc.) and a lower ratio of adhered material [95]. This observation is justified by the fact that at high loadings the carbonaceous fraction is the predominant fraction in the particle, while at low loadings the dominant fraction is the organic fraction. As these fractions have different bulk densities (the bulk density of the carbonaceous fraction is higher than that of the organic fraction), it is obvious that the final bulk density of the particle is determined by the ratio of these two fractions. Furthermore, this density is also conditioned by the particle size, since the larger the particle size, the larger the defects and discontinuities in the particle structure, which favours the entry of volatile substances into these spaces to fill the space (not contributing to the bulk density of the particle) [85].

- **Surface area**: this parameter defined as the total area that the surface of the object or body occupies, is dependent on the particle structure and is sometimes very difficult to measure accurately due to the variety of structures that the particles can adopt. One way of estimating an approximate value is to idealise the structure of the isolated particle by providing or suggesting surface areas of 100-150 m^2/g (although much depends on how this parameter is measured) [95]. The surface area is a relevant parameter to understand the chemical kinetics of various processes, being in this case the interaction between the gas phase and the solid phase, during the nucleation process, the one that determines the diffusion rate into the particle of these adsorbed gaseous substances.

- **Electrical charge**: as a consequence of the structure of soot and its composition, these particles may be in the situation of being electrically charged as a consequence of the presence of charged elements, bipolar and radical species. It is not yet clear how these charges can be formed since they can be generated in several ways (chemiionisation, thermionic emission, diffusion charging by flame ions, contact electrification or thermoelectric effect), but this charge is not entirely stable since, according to the nature of the particles, it presents a wide variety of alternatives to neutralise it.

6.2.2.2 Chemical characterisation

Soot is a material composed by carbon and hydrogen in ratios 8/1 or 9/1, but it may also be accompanied by a number of other substances that make its composition not fully defined [75]. For example, in heavy–duty diesel engines, the PM chemical composition [114] is: 75% (but can fluctuate between a 33% and a 90%) elemental carbon, 19% (7–49%) of organic carbon (whose origin can be either unburned fuel or lubricant), metals and other (non-metallic) elements of the periodic table account for 2% (1–5%) of the total, around 1% (at most 4%) are sulphate and nitrate compounds and the remaining 3% (although levels range from 1% to as high as 10%) are other substances. But, among all the variability of compositions that can be produced, the constituent elements are the same (see Figure 6.3), so it is now time to elaborate on each of them.

These five fractions may be well defined or, in occasions, there may be a situation where the distinction between them is not entirely clear (diffuse boundaries). And there may even be conditions where some of these five layers may not appear at all (most commonly the nitrate fraction) [79]. Regardless, all five will be described below:

- **Carbonaceous fraction**: in this portion of the particle, the predominant element is carbon, but not exclusively because other elements appear to a minor extent: hydrogen (H), oxygen (O), nitrogen (N) and sulphur (S), ordered from highest to lowest concentration. In fact, the C/H ratio is $\sim$9, while for the rest of the elements the difference is such that their presence is neglected (they are found in trace form).

- **Ash fraction**: contains a mixture of elements where the primarily of them are a metallic elements (Cr, Ca, Cu, Fe, Zn and Na) and the minority are some or few non–metals (P, S and Cl). This is an incombustible fraction of the particles composed mainly by oxides and sulphates (although outside this majority pair, other compounds are possible: phosphates, carbonates, silicates and chlorides).

- **Sulphate fraction**: this fraction is directly related to the sulphur contents of the diesel fuel. This fraction concerns water–soluble sulphates ($SO_4{}^{-2}$) and nonvolatile or water–nonsoluble sulphates (i.e. $CaSO_4$, which is soluble in water at rates ranging from 0.20 to 0.88 grams per 100 millilitres of water, depending on its anhydrous or hydrated form). Of the two types of sulphate, soluble sulphates are the most problematic as they are precursors of sulphuric acid (H_2SO_4). Sulphuric

acid tends to be found in association with water ($H_2SO_4 \cdot nH_2O$), so in this fraction of the PM it is common to find water [96].

- **Nitrate fraction**: similarly to the sulphate fraction, in this small part of the PM the primary or main element is the water–soluble nitrates based on NO_3^-. Like the sulphate ion, the nitrate ion (connected to the NOx chemistry) is also a precursor of its corresponding acid: nitric acid (HNO_3). However, because the boiling point of nitric acid is low (considerably lower than sulphuric acid), once formed it is not fully transferred to the particle as a result of its high volatility. It is for this reason that this fraction is the smallest of the PM constituent fractions.

- **Organic fraction**: this fraction presents a wide variety of organic compounds based on the following elements: C, H, O, N and S. As the constituent elements are purchased with the carbonaceous fraction, the distinction between the one or the other is made when the C/H ratio is less than 8. This complex fraction consists of all substances derived from the incomplete combustion of fuel and their oxidation by–products such as: alkenes, alkanes, alcohols, esters, ketones, acids, esters and aromatics. As these are chemical species that tend to condense on a solid body, they are usually compounds with a certain number of carbons. This amount is 23–24 carbons and is the delimiting factor that favours these substances to become part of the final particle. However, as a consequence of the strong surface interactions, in this fraction it is possible to find some volatile substances composed by 4 to 8 carbon atoms (which, theoretically, should be in the gaseous phase).

6.2.3 Soot in exhaust and soot in lube oil

Both the soot generated by the combustion of the fuel and the soot (the main source) also coming from emission aftertreatment processes, once in the combustion chamber can choose to follow two different paths: either it is expelled together with the exhaust gases or it is combined with the oil. Considering these two options, the vast majority of the soot is eliminated together with the exhaust gases, with a small portion going on to combine with the lubricant located in the engine crankcase (around 3% of the soot that is generated by the combustion of the fuel [25], without considering that which may be introduced into the combustion chamber [108]). As a consequence of these two routes available for the soot, the soot undergoes changes and concrete processes that cause differences when comparing their compositions (see Table 6.2) [19] and its structural characteristics [101]. Independently,

each of these two situations has its own set of characteristics and, therefore, peculiarities and disadvantages.

Table 6.2. *Main constituent composition of the two different soot.*

Constituent	Carbon (%)	Oxygen (%)	Volatile substances (%)
Soot in oil	90	4	6
Soot in exhaust	>50	<30	20

In the case of soot entering the exhaust system (called Soot–in–Exhaust or, more abbreviated, SiE), the aim is to continue its growth process (agglomeration and absorption of volatile and non–volatile substances travelling in the exhaust gases) until it forms what is known as particulate matter (PM), which at the end of the process must be retained by the DPF in the exhaust system of diesel engines. So, in this case, the main problems that these particles can cause are two: firstly, an excessive generation of smoke in the exhaust gases (already in its emission to the atmosphere) and, secondly, they can cause premature clogging of the channels that make up the DPF [26].

In this Thesis, the soot of most interest is the one that is combined with the lubricant, SiO (Soot–in–Oil). Although it is a small portion of the total soot that is susceptible to mixing with the lubricating oil, its presence in the oil proves to be a major problem due to its effect on the tribological properties of the host lubricant and the magnification of wear phenomena in the engine. Furthermore, it is a cumulative problem because soot that has already mixed with the oil cannot be completely removed by the oil filter or "trapped" by the additives in the lubricant. This is why it is very important to monitor soot levels in the lubricant.

There are two situations that allow the soot and the oil to come into contact: either by blow–by, in which the combustion chamber gases (a portion of them) pass towards the crankcase, or by the oil film exposed on the cylinder walls [63, 108]. Below is explained how the soot is mixed with the oil by these two mechanisms:

- **Blow–by**: it refers to the gas leakage (composed of unburnt fuel, air and combustion by-products) that always occurs between the piston rings and the cylinder liner into the crankcase (see Figure 6.13). Normal blow–by values should be below 1% (typically 0.4–0.6% of the total gas flow, in litres per minute, for an engine in good mechanical condition)

[81]. Blow-by occurs because the sealing between the cylinder walls and the rings is not perfect. Although the tangential load pressing the piston rings against the cylinder wall creates a good seal, there are always leakage areas and gaps (see Figure 6.14) through which gases are able to pass into the crankcase [69, 109]. In addition, two factors occur due to wear and tear, which considerably accentuate the blow-by phenomenon: firstly, the piston, the piston rings and cylinder liners experience wear and tear, which leads them to be less able to maintain a tight seal. On the other hand, the accumulation of soot and other deposits (such as lacquers) on the piston rings causes them to work inefficiently, resulting in inhibited sealing.

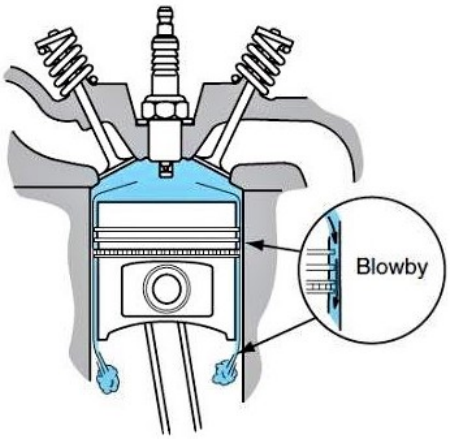

Figure 6.13. *Blow-by process in ICE.*

- **Thermophoresis**: At this point, this route means that the soot reaches the film of lubricating oil that is exposed in the combustion chamber and then combines with it and thus (see Figure 6.15), during the piston stroke towards the BDC, the contaminated oil film can be renewed and removed thanks to the scrapping effect of the piston rings (specifically of the oil control ring and the scraper ring) [105]. This process occurs as a result of the temperature difference between the combustion chamber walls (cold) and the combustion gases (hot). As a consequence of the gradient that is generated, the particles (in this case soot) in the fluid (the combustion gases) experience a net force that causes them to move from the hot to the cold source.

  This physic process is the dominating particle transport mechanism in the lubricating oil film on the combustion chamber walls and thus

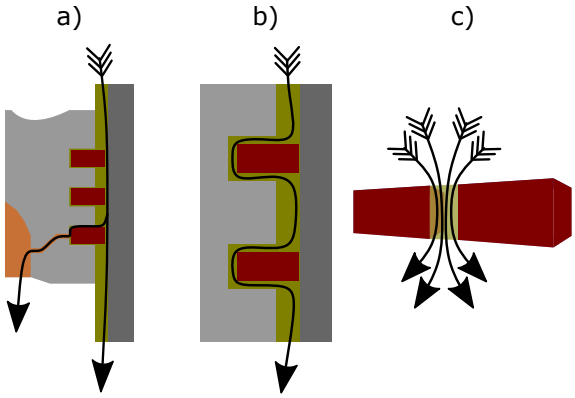

Figure 6.14. *Blow-by flow paths: a)Between piston ring and cylinder, b)Between piston ring and groove side and c)Through ring gap.*

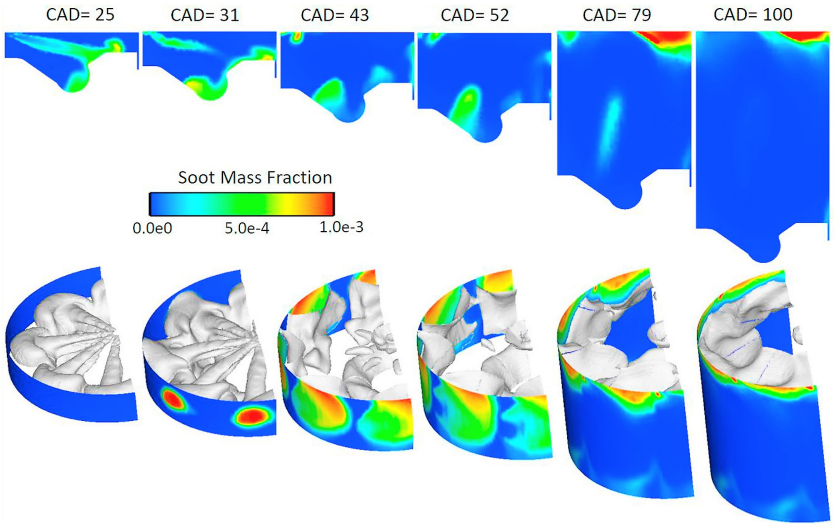

Figure 6.15. *In-cylinder contours and soot iso-surface evolution in the combustion chamber (on a vertical plane along the spray axis, above) and on the walls (on the boundary cells near the liner, below) at different crank angles [25].*

governs the rate of deposition of soot particles on this lubricant film. This process is complex, so it has been studied in detail in order to better understand its mechanism and to determine which are the predominant conditioning parameters [24, 51]. Basically, the parameters that determine how much soot is deposited by thermophoresis are those that affect the particles themselves and condition their characteristics and behaviour such as: size, trajectory, etc. All the features involved can be grouped into parameters of injection, nozzle and the geometry of the chamber (in particular the piston bowl).

Nonetheless, determining SiE is not the same as determining SiO. Each of these two types of soot uses specific sampling and analysis techniques. The case of SiE has been extensively studied and satisfactory results have been achieved for the detection limits and quantification levels required for this particular case of soot [33]. However, for SiO, several techniques exist, but new equipment, sensors and analytical procedures are currently being developed to improve the levels of soot detection and to obtain measurements in a shorter period of time. This last aspect is further discussed in section 6.3.2 *Soot in oil quantification*.

6.3 Soot in engine oil

This section will show the effects of soot in the lubricant oil in terms of alterations or changes in its physical, chemical and tribological properties [1] and, having gained an insight into the importance of knowing the amount of soot present in the lubricant, show the different possible analytical techniques that can be used to quantify its content, covering several orders of magnitude: from high levels (in the order of about 10%) to very low levels.

6.3.1 Effects of soot in lubricating oil

By combining the two processes: blow–by and thermophoresis, that facilitate the process of soot contamination of engine lube oil, it is logical to consider how it will be affected. When soot is added to the lubricating oil, as it is a foreign agent to its composition, this will cause the oil to diverge from its original performance as its properties will be modified, affecting its functionality as far as the engine is concerned [6, 35, 42].

The following is a list of the most relevant changes induced in the lubricating oil by the soot contant:

- **Colour**: the change in the colour of the lubricant is the simplest and easiest change to detect. A darkening of the oil is already indicative of the presence of dissolved soot in it, as soot is a black particle. Thus, as a result, depending on the amount of dissolved soot, the lubricant will show a certain degree of opacity and a colour change towards darker shades. This appreciation turns out to be subjective, although there are processes that provide a certain gradation; nonetheless, this is not a change exclusively caused by soot, as there are other agents or processes that cause the same effect on the lubricant (e.g. oxidation).

- **Thermal capacity**: the alteration of the thermal capacity of the lubricating oil is due to the fact that soot absorbs thermal radiation, because it acts as a black body. So when the lubricating oil is contaminated by soot, there is an extra contribution to the thermal capacity of the lubricant which leads to an apparent improvement in the cooling performance of the oil (in contrast to clean oil). However, this effect is dependent on three aspects (leaving aside the contribution of the lubricating oil formulation): the first is the concentration of soot, then how it is distributed in the oil (the dispersivity of its particles in the bulk) and finally the morphology and size of the particles [71].

- **Viscosity**: another effect of soot in the lubricant is the viscosity increase [7, 8, 32]. Soot loading, in excessive levels, leads to lubricant thickening which can interfere with the normal flow of oil in the engine and reduce lubrication protection. In addition, an increase in viscosity will lead to a higher consumption of lubricant by the engine as the lubricant tends to stick to the cylinder walls more intensively, which results in more oil being exposed or available in the combustion process [73].

- **Dispersing/detergent capacity**: the presence of soot in the lubricant causes a mobilisation of the lubricant's dispersant additives in order to prevent soot particles from forming deposits (sludge). For this purpose, these additives combine with the soot particles and cause them to remain in suspension in the lubricant. In addition to these additives, there are also detergent additives, which remove soot adhering to the surfaces in order to prevent unwanted deposits in the engine. It is clear that both additives are consumed as a result of the progressive overloading of the soot on the additive package of the lubricant [106]. Therefore, if the amount of soot is high, it may happen that these additives are not able to cope with the demands of this situation, causing problems.

- **Electrical properties**: soot, due to its nature, has electrically conductive properties. This property is conferred by the possible adsorbed spices on its surface (e.g. metallic particles) as well as by molecules which are involved in its structure, but which in the outermost layers may present a series of charges, dipoles or free radicals. Therefore, if the oil contains dissolved soot, it is not surprising that the electrical conductivity of the oil increases (and hence the value of its dielectric constant) because the soot particles act as bridges across which, the current flow is facilitated [18, 55].

- **Wear**: soot, due to its structure, is a material that exhibits abrasive behaviour [36, 37, 50]. Consequently, when the lubricating oil contains soot, the anti-wear additives act to prevent (depending on the environmental and working conditions) excessive wear or erosion [30, 31], which is always susceptible to surface wear generated by the surface-to-surface friction of the lubricated internal parts of the engine [16, 34]. Thus, the presence of soot will mean that these protective additives will be consumed more quickly. Moreover, this extra contribution to engine wear is accentuated directly proportional to the soot concentration (under certain conditions, the soot may reduce the coefficient of friction [68]), as the amount of soot dissolved in the oil increases, it tends to form larger particle sizes which in turn are even more abrasive [20].

- **Additives depletion**: with regard to soot particles, it has been shown that they have an affinity to absorb certain types of additives in lubricating oils: mainly anti-wear and detergent/dispersant additives [2]. This effect causes the actual amount available in the oil to be less than expected, which can lead to premature degradation processes in the lubricated internal parts of an engine.

The soot accumulates in the lubricating oil until it reaches a point where the soot levels are too high. At this point, the lubricating oil is no longer able to keep the soot particles dispersed and the soot follows its natural tendency to coalesce and clump together, further magnifying its effects. Because of this, it is important to know in detail how much soot is present in the lubricating oil in order to avoid further problems and damage to the engine.

6.3.2 Soot in oil quantification

There are different analytical procedures and techniques that are able to report information about SiO content. However, not all alternatives provide the same information and appreciation. Therefore, this section will show the analytical techniques employed in this Thesis, already used and developed in the department, with the purpose of providing an exhaustive view of the variety of possibilities for SiO quantification depending on the given conditions (sample amount, detection levels, etc.).

6.3.2.1 Analytical thermogravimetry

Thermogravimetric analysis (TGA) is the reference analytical technique for the quantification of the soot content in a sample of engine lubricating oil. TGA provides an accurate and highly repeatable measurement of soot content, which is expressed in units of mass percentage. In order to be able to work with lubricating oil samples, the analysis procedure is described in the standard ASTM D5967-17: "Standard Test Method for Evaluation of Diesel Engine Oils in T-8 Diesel Engine" [44]. Figure 6.16 shows the experimental set–up used in this Thesis during the research stay at the Mechanical Engineering Department of the University of Birmingham. The figure shows the Pyris 1 TGA thermobalance from PerkinElmer together with the control system and software installed on the attached computer.

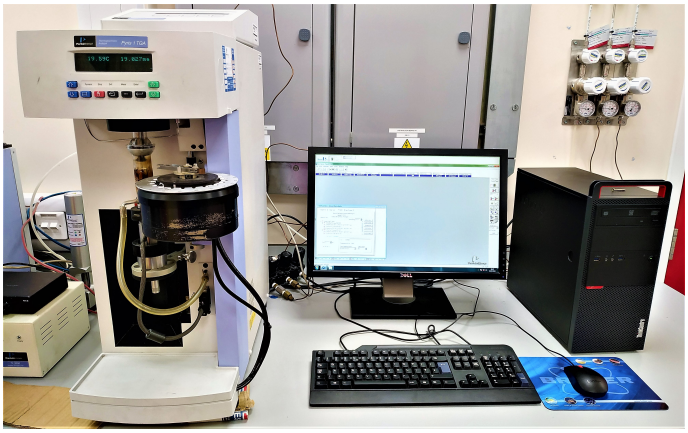

Figure 6.16. *Thermogravimetric Analyzer - Pyris 1 TGA of PerkinElemer from the Department of Mechanical Engineering of the University of Birmingham.*

Analytical thermogravimetry is mainly based on monitoring the evolution of the mass of a given substance under certain environmental conditions: atmosphere (mainly inert or oxidising), temperature rate and time. For the case of SiO quantification, these three aspects are specified and defined in Annex 4 of ASTM D5967-17: "Enhanced Thermal Gravimetric Analysis (TGA) Procedure". In accordance with the indications set out in the annex, the test consists of the following steps:

- First of all, the recommended mass for the test is 20 mg which should be homogenised to obtain a representative fraction of the bulk of the sample.
- The next step is to remove any volatile substances that the sample may contain. This stage is carried out under a high purity nitrogen atmosphere (N_2>99.99%), avoiding any oxidation process (combustion).
  - To begin with, the system needs to be tempered to 50°C. To do this, the system is heated and a 1-minute isotherm is performed to stabilise the measurement of the mass that has been introduced into the equipment.
  - After this time, a heating ramp of 100°C/min is programmed to increase the temperature from 50°C to 550°C.
  - Again, a 1-minute isotherm is performed when reaching 550°C.
  - Finally, the sample is heated again at a rate of 20°C/min to bring the temperature up to 650°C.
- The other step is to change the atmosphere from an inert or non-oxidising one to an oxidising one, specifically pure oxygen (O_2>99.99%). Now, what is done, is the total oxidation of the sample to cause all those substances susceptible to oxidation to oxidise so that the non-combustible (non-oxygen reactive) portion of the sample is reached or remains at the end.
  - Once in an oxidising atmosphere, the sample is heated again to 750°C at a rate of 20°C/min.
  - When 750°C are reached, the heating is stopped and the temperature is kept constant (isotherm). This period is prolonged as long as necessary (preferably more than 5 minutes) until no further loss of mass from the sample occurs. In other words, the stability of the residual mass value on the microbalance is indicative of the overall performance of the test.

- At the end of the test, what remains on the microbalance of the thermobalance is residue, basically ash and pyrolysis by–products.

Following these steps, the system generates a graph of the evolution of the mass loss jumps, normally expressed in %. Figure 6.17 shows an actual analysis of a sample of used engine lubricating oil with the thermobalance used in this research.

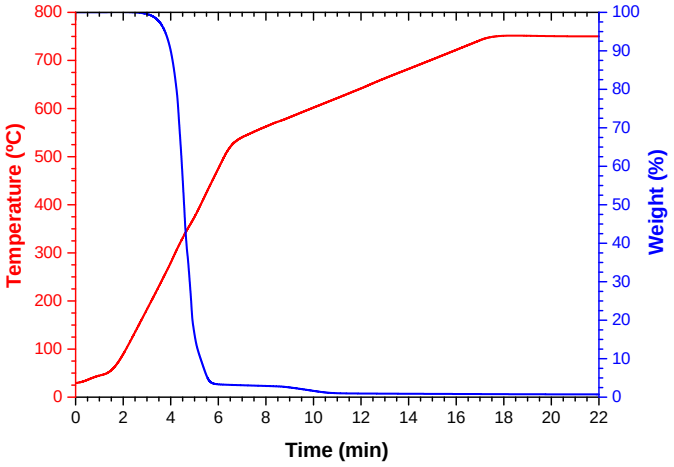

Figure 6.17. *Thermogravimetric analysis of a used engine lubricating oil sample: the red line represents the evolution of the temperature during the test and the blue line the mass loss of the analysed sample.*

According to Figure 6.17 it can be seen that, with the progressive heating of the sample, a loss of mass is registered. During this process, two different mass changes occur: the first mass change is the most noticeable and corresponds to the loss of the volatile fraction of the sample which usually occurs between 550–600°C and can imply a mass reduction of ∼90% with respect to the origin. The second mass jump that occurs, over 600°C, is where the calculation of the soot content takes place [12, 99]. Normally, the second mass loss occurs within the temperature range of 625–700°C, which is the region of interest for the determination of SiO content. Figure 6.18 shows the region of the graph obtained by TGA to better observe the procedure for the extraction of the soot content in the lubricating oil.

In Figure 6.18, two aspects have been brought together: the first is the mass loss rate, which is represented in the upper part of the figure by a red line. While the second one is the variation (percentage) of mass as a function

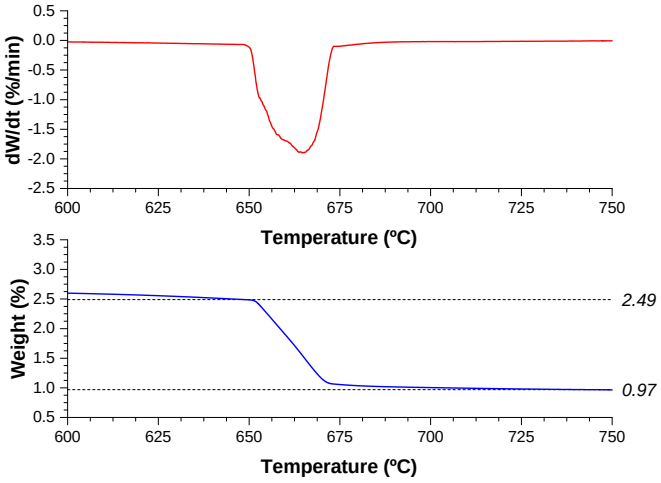

Figure 6.18. *Soot in oil quantity by thermogravimetric analysis: red line is the rate of weight loss of the sample and the blue line is the plot of this mass.*

of temperature. The first part allows us to detect those areas where mass variations are taking place. As in this type of test the mass decreases as the test progresses, we can observe the valleys indicative of mass loss. Moving on to the second part, this is where the amount of soot contained in the sample is determined. For the example analysed, the amount of soot that is quantified with this TGA test is 1.52%.

Following this procedure, a series of certified SiO standards from LGC Standards were analysed: 1.2%, 3.1%, 5.1%, 7.6% and 10.7%, all of them composed of a matrix of a SAE 15W40 engine oil for diesel engines to which, particulate carbon has been incorporated as an analyte in their respective proportions to obtain these five standards. The results of the TGA analysis of these five standards are shown in Figure 6.19.

This Figure 6.19 shows very clearly how the % weight jump caused by the combustion of the lubricant matrix (given that the volatile components have been removed in the previous phase) is directly proportional to the amount of soot contained in these standards. Thus, 3 repetitions of this test were carried out to corroborate the robustness of the SiO analysis procedure, and the accuracy of the reported values can be seen (see Figure 6.20).

However, the use of TGA for soot quantification has a number of drawbacks that should not be overlooked:

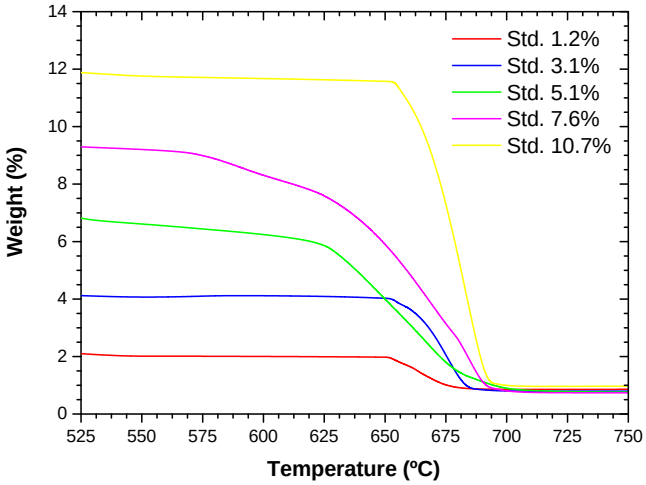

Figure 6.19. *Soot in oil standards analysed by TGA, detail of the soot quantification region.*

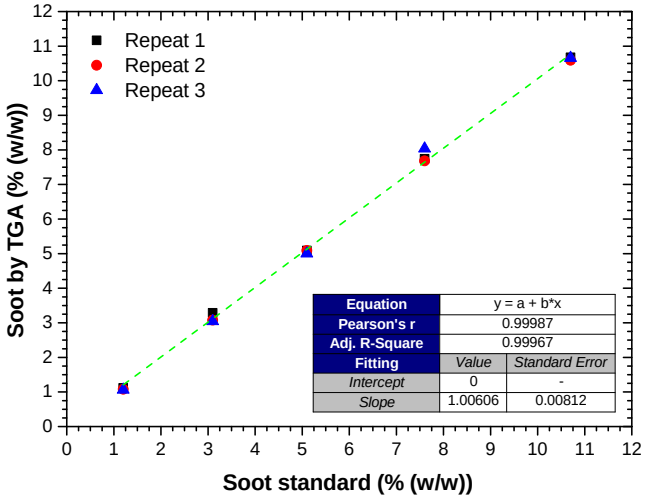

Figure 6.20. *Accuracy of the 3 different TGA measurements of each SiO standards.*

- Firstly, the results reported (in different studies and works) by this technique justify the fact that it is considered as the reference technique for the determination of SiO. However, in spite of the good results it provides, the cost of the equipment, the installation and the performance of the tests must be taken into account. TGA is an expensive equipment and requires skilled technical personnel to operate it, which makes it difficult to expand its applicability outside the field of research.

- Another aspect that is detrimental, is the analysis time and the use of consumables (pure gases). Normally each measurement takes more than 20 minutes, so if repetitions of the same sample are required, a new test has to be prepared (this is a destructive test and as such, the sample cannot be recovered). As far as consumables are concerned, their consumption is considerable, which has an impact on the final analysis price per sample.

- Another aspect of interest is the influence of the sample on the test. It has been observed that parameters such as: engine oil formulation (base oil and additives) and the presence of degradation by–products (both oxidation and sulphation) affect the test's accuracy. Bredin et al. [12] were already aware of this problem and therefore stated the need to be able to improve the quantification method. In fact, during this work, another aspect that was not considered was the relevance of new lubricant formulations. During the study, samples of low ash engine oils were analysed, which showed divergences in behaviour compared to the classical formulations (where ash levels were higher) (see Table 6.3 to obtain an idea of ash content of new engine oil formulations). Figure 6.21 shows the comparison of the results obtained by analysing three sets of 4 used engine lubricating oil samples with different degrees of use and contamination. The plots highlight the importance of getting a better methodology to be able to correctly determine where to reference the mass loss points for soot quantification. This observation could be a possible problem in the close future and will need to be studied further.

In conclusion, despite the good results it provides, there are several compelling reasons to choose alternative techniques capable of quantifying SiO. As the focus in this thesis is on quantifying small increments of soot in the lubricating oil, TGA is not the best option.

Table 6.3. *SAPS levels for ACEA 2016 categories, where Sulphated Ash (ASTM D874), Phosphorous (ASTM D5185) and Sulphur (ASTM D5185) are expressed in % by mass.*

ACEA Category	Sulphated Ash (%)	Phosphorous (%)	Sulphur (%)
A3/B3	H (⩾0.90, ⩽1.50)	Report	Report
A3/B4	H (⩾1.00, ⩽1.60)	Report	Report
A5/B5	H (⩽1.60)	Report	Report
C1	L (⩽0.50)	L (⩽0.05)	L (⩽0.2)
C2	M (⩽0.80)	M (⩾0.07, ⩽0.09)	M (⩽0.30)
C3	M (⩽0.80)	M (⩾0.07, ⩽0.09)	M (⩽0.30)
C4	L (⩽0.50)	M (⩽0.05)	L (⩽0.20)
C5	M (⩽0.80)	M (⩽0.20)	M (⩽0.30)
E4	H (⩽2.00)	-	-
E6	M (⩽1.00)	L (⩽0.08)	L (⩽0.30)
E7	H (⩽2.00)	-	-
E9	M (⩽1.00)	M (⩽0.12)	M (⩽0.40)

L: Low
M: Medium
H: High

6.3.2.2 Blotter Spot Method

This test is included in the standard ASTM D7899-19: Standard Test Method for Measuring the Merit of Dispersancy of In-Service Engine Oils Blotter Spot Method [47]. It is a simple procedure to determine the dispersant properties of the engine oil, although an assessment of the contaminants (particles, soot, sludge, deposits, etc.) present in the lubricating oil analysed can also be extracted or estimated.

The way to perform this test is not complex, it simply consists of following a series of simple indications (see Figure 6.22 to observe the scheme process):

- With a dipstick of about 5 mm diameter, having previously dipped one end in the lubricating oil, place a drop (or two) on absorbent paper (not glossy) or standard chromatography paper.
- The sample is then allowed to spread freely on the paper (until self–dried). It is for this reason that the paper should not be coated (satin

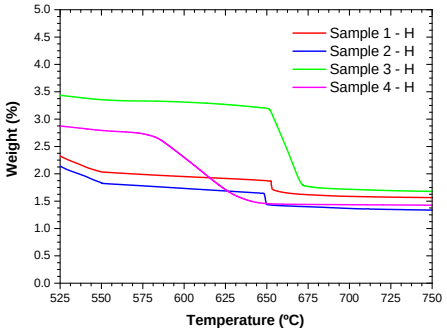

(a) High SAPS used engine oil samples

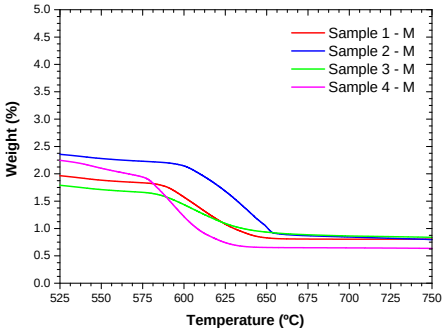

(b) Medium SAPS used engine oil samples

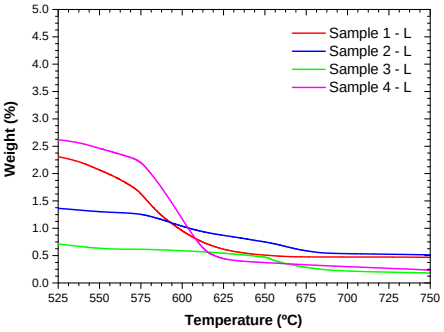

(c) Low SAPS used engine oil samples

Figure 6.21. *Compilation of a set of 4 used engine oil samples with the three different SAPS levels: high (H), medium (M) and low (L).*

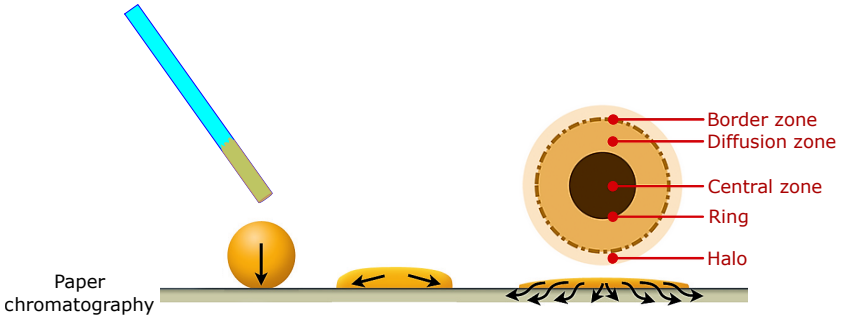

Figure 6.22. *Scheme process of Blotter Spot Method.*

paper), as the sample is intended to travel through the fibres that make up the paper by capillary processes.

- When the spot diffusion is complete, a characteristic pattern will be visible on the paper (see Figure 6.23). This pattern has been found to be related to the condition of the lubricating oil.

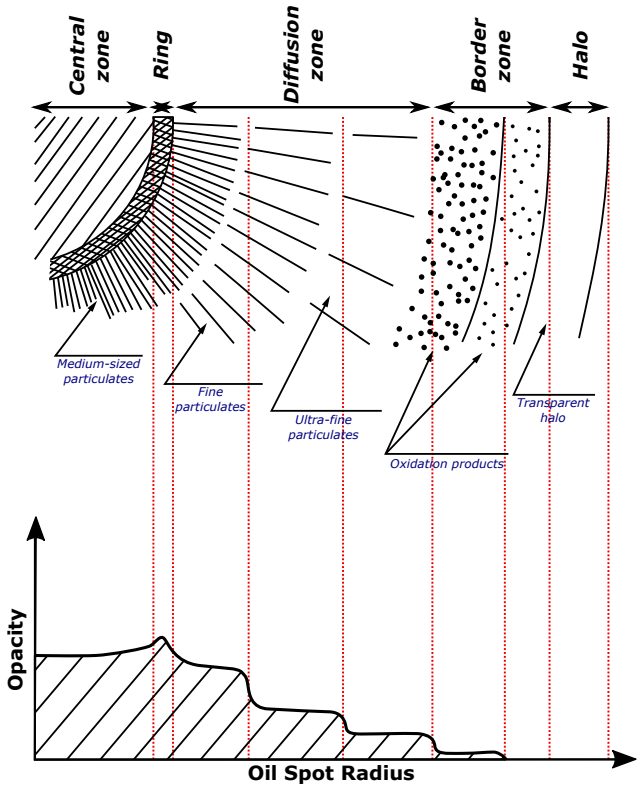

Figure 6.23. *Composition of the different zones that build the spot pattern (1 hour for a sample heated at 80° C), adapted from ASTM D7899-19.*

When interpreting the results, an assessment must be made on the basis of the information provided by each of the zones, as the different substances that contains the engine oil are located in the proper zones of the spot according to the engine oil dispersancy performance. Consequently:

- **Central zone**: its appearance, uniform (more or less dark) colour, is related to the quantity of insoluble deposits, dirt/dust, abrasion particles and carbonaceous matter contained in the oil.

- **Ring**: this boundary layer of the first circle provides information according to its diameter and colour. Both parameters allow estimating the content of particles of considerable size, both of carbonaceous origin and of other contaminants.

- **Diffusion zone**: this is characteristic of the way in which the oil disperses the soot. It can be grey to black in colour, depending on the level of deposits in the oil.

- **Border zone**: the morphology of the edges of this separation layer indicates the presence or not of water/coolant in the lubricant.

- **Halo**: this is not usually coloured, as it does not contain soot that would darken it. This is usually fuel dissolved in the oil and is related to the degree of oxidation of the oil.

According to the way in which the information was obtained, it is clear that the diagnosis of soot concentration is done by qualitative interpretation (trained eye) of the laboratory operator or technician. This estimate does not quantify the soot concentration with certainty as it is not a result that is free from suspicion or doubt [99].

In attempts to improve the performance of this technique, various procedures have been tested and specific equipment has been developed to achieve more rigorous reporting of values (free from the subjectivity of operator assessment). One of the first options is the so-called "Lantos Method" adaptation [64], which uses solvents to improve the resolution of different areas of the spot pattern. In that case, the insoluble materials dissolved in the engine oil are separated from the oil matrix thanks to the use of different solvents. Now, what is sought is the affinity between each of the families or kind of insolubles that the lubricant may contain with one of the solvents used in this separation. As a result of this solvent-insoluble material affinity, it is more easy to do the identification of the different insolubles presents in the sample, including soot. The other option is the use of photometer (see Figure 6.24) that allows to analyse the oil spot digitally and thus, to make a more accurate and precise determination.

Despite the attempt to standardise and automate the process of evaluating the stain pattern, this test proves to be deficient in providing a reliable value for the soot content since, according to its procedure, several elements can interfere and falsify the measurement (oxidation by–products, sludge, varnish, etc.). This test does not guarantee that the signal used to quantify soot

Figure 6.24. *DT100DL equipment of Analysis and Diagnosis Systems to measures soot and dispersancy, operating according to ASTM D7899 standard.*

is specifically produced by soot, which makes the Blotter Spot Method a qualitative test.

6.3.2.3 Determination of insoluble content

Insolubility test is one of the older test employed to measure SiO. This test is based on a procedure of successive extractions using a series of solvents which induce the precipitation-dissolution of certain elements present in the lubricating oil, under controlled conditions. This makes it possible to separate the different insolubles (solid products, both organic and inorganic) according to their affinity for the solvent in the particular stage of the extraction process.

Nominally, as depicted in Figure 6.25, this extraction follows a chemical sequence of cycles of dissolution and precipitation in various solvents (most commonly, but not exclusively, toluene and pentane). This process causes an alteration in the lubricating oil which allows the removal of the insoluble substances by a final filtration or centrifugation step (depending on the system available) for subsequent mass determination. Once the mass is known, the values are presented as mass percentages (% weight).

As already mentioned above, the most common solvents are toluene and pentane, so the procedure is regulated by the standard ASTM D893-14 Standard Test Method for Insolubles in Used Lubricating Oils [45]. This standard includes the use or non-use of a number of substances called "coagulating agents". The purpose of these agents is to facilitate the separation of the dissolved material in the oil by causing its deposition.

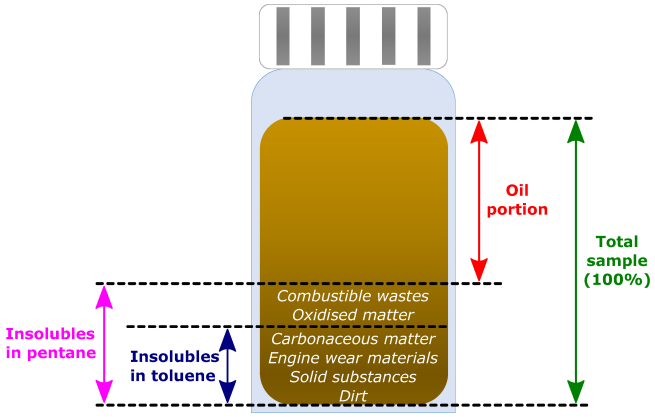

Figure 6.25. *Distribution diagram of the different insoluble compounds in the oil according to the solvent, toluene or pentane, selected for their precipitation.*

Regardless of the analytical route selected, the protocol to be followed is common: pentane is used first (with or without the coagulant) and then toluene. For each reagent, a solvent-oil homogenisation step is performed first, followed by separation (centrifugation or filtration, as appropriate). Centrifugation is the most common method, since it improves the separation yield, so once the centrifugation is complete, the excess of the supernatant solution is decanted. Finally, the solid is washed with the relevant solvent, dried and weighed.

According to Figure 6.25, soot is extracted by toluene, but not selectively as it is found together with other elements. This is a problem for the quantification of SiO. However, there are adaptations and improvements of the process. One of these alternatives is the soot precipitation shown in Figure 6.26, where toluene and a mixture in equal proportions of toluene and ethanol are used to achieve a more selective separation of soot. However, the procedure is highly time consuming (especially the centrifugation steps, ∼15 min/cycle).

As a consequence of the time needed to obtain a value and the possibility of making mistakes due to the high number of steps to follow and the meticulousness required in the way of operating, it has been decided to develop equipment that allows to approach this process by providing values that are greater than or equivalent to the real ones with a lower time cost. In this Thesis, the system developed by Kittiwake (part of the Parker Hannifin Corporation S.L. group) shown in Figure 6.27 has been used.

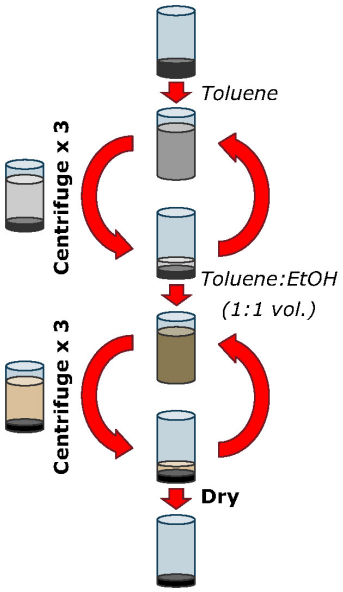

Figure 6.26. *Soot precipitation process.*

Figure 6.27. *Experimental setup to analyse the insoluble content in engine oils.*

This equipment is capable of expressing the insoluble content on two different scales, see Figure 6.28, in a very simple way: the system simply employs a special cell fitted with a red diode which focuses its beam into the vail containing the sample dissolved in the specific reagent. So the equipment collects the light that escapes through the sample, which is inversely proportional to the content of insolubles that opacify the sample, and can

report a value that (depending on the selected protocol) is checked against the internal calibrations of the equipment and can be translated into the desired units of insoluble concentration.

(a) Result according to IP 316 (b) Result according to Mobil Soot Index

Figure 6.28. *Insoluble result values obtained for the same sample using the two calibrations: IP 316 and Mobil Soot Index.*

- **Protocol IP316**: determination of n-heptane insolubles in engine lubricating oils. As with pentane, heptane precipitates all carbonaceous matter and its derivatives (including soot) as well as wear particles and other insoluble elements in this medium. Therefore, the value reported is the result of the combination of these three sources. Consequently, the levels of insolubles that it is able to quantify are between 0.0% and 3.5%.
- **Mobil Soot Index**: determines the amount of insolubles, under identical conditions to the previous point. But now it makes an estimation in order to only try to capture the value due to the action of the soot that the oil may contain. For this reason, the range of values that can be obtained in this way is from 0.00% to 1.75%.

However, the equipment was subjected to a series of SiO standards from very low concentrations (0.05%) to values close to 3%. According to the way of working of the equipment, whose tests last between 2–3 minutes, it could be observed that this system does not have sufficient resolution to be able to discern between small variations of soot. This is clear from Figure 6.29, where a staircase pattern can be seen when comparing the response provided by the system with the real value of the soot content.

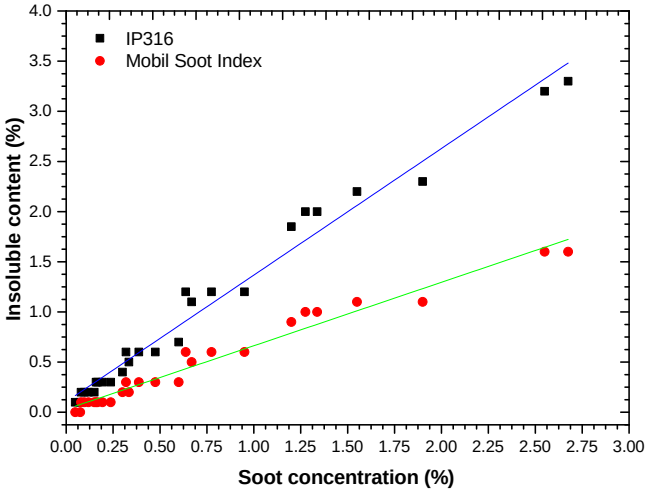

Figure 6.29. *Correlation between the IP316 and Mobil Soot Index protocols results against the soot content of the SiO standards.*

Despite the limitations of this technique, for lubricant condition monitoring (encompassed within the OCM tasks) this alternative provides a quick response and does not require difficult equipment or protocols, which makes it attractive from an applicability point of view.

6.3.2.4 IR Spectroscopy

When mentioning infrared spectroscopy applied to the field of analysis of engine lubricating oils, it only referes to Fourier Transform Infrared (FT–IR) spectroscopy focused on the MIR spectrum region. FT–IR spectroscopy has been one of the most widely used techniques in the field of lubricating oil analysis. However, in this section we will discuss its ability to quantify dissolved soot in an engine lubricating oil matrix.

FT-IR spectroscopy is a widely used analytical tool for the quantification of soot concentration in oil as its response is easily contrasted with the reference analysis technique, TGA. Basically, the way FT–IR spectroscopy works for soot quantification is by monitoring the broadband change in absorption; essentially, when soot absorbs infrared light it has an effect on the whole IR spectrum, namely a baseline shift. Consequently, by analysing this phenomenon, it is possible to know the amount of soot present in a given

sample of used lubricating oil. Candidate regions for the quantification of soot in lubricating oil must meet a number of conditions:

- First of all, they must not have strong absorption bands, so it looks for the flatter regions of the IR spectrum where absorption is not as strong.
- Secondly, it must be checked that no signals (absorptions) appear in these regions, neither from elements of the lubricating oil itself nor from elements derived from the degradation/contamination of the lubricating oil.

Following these guidelines, the areas of greatest interest for study are the ones between the next regions: 4500–4000 cm^{-1}, 3250–2500 cm^{-1} and 1800–650 cm^{-1} (see Figure 6.30).

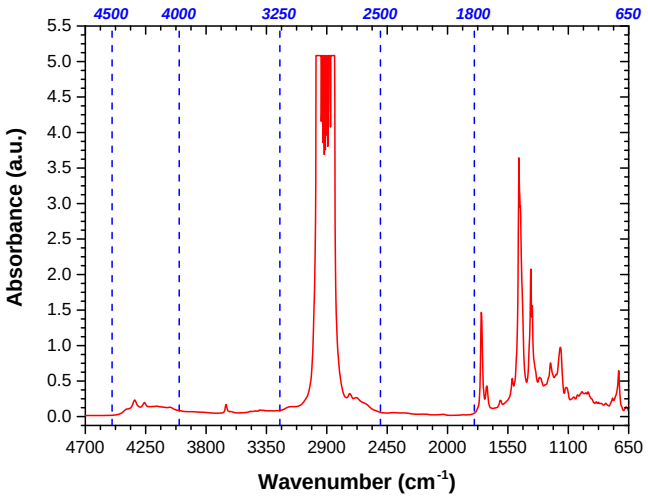

Figure 6.30. *IR regions that do not satisfy the two requirements: no strong absorption and no regions where absorption bands of lubricant degradation/contamination elements appear.*

Thus, outside these regions, contributions that could mask or mislead the measurement of the soot concentration do not usually occur. With a clear understanding of the conditions required for IR spectroscopy for the quantification of soot content in lubricating oil, a set of standardised soot in oil samples were analysed (see Figure 6.31).

Figure 6.31 shows only 13 of the 20 standards analysed by FT–IR in order to illustrate how this increase in the baseline absorbance spectrum is produced

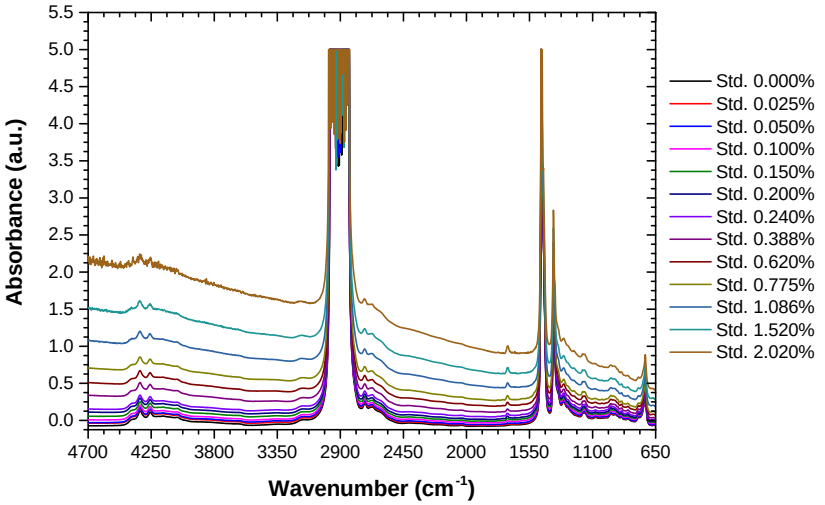

Figure 6.31. *IR spectra of soot in oil standarised samples, not including the whole set of samples to simplify the graph.*

as function of the soot content. This figure also confirms the suitable and unsuitable areas for the determination of the soot content.

According to the standards and bilbiographic resources [48, 97], the selection of the wavenumber for the quantification of soot in the MIR region is localised to 6 specific values: 3800, 3600, 2250, 2000, 1980 and 1870 cm^{-1}. Figure 4.76 in the appendix 4.A.1 shows the results of the evolution of the absorption value as a function of the soot count of the analysed standard.

As can be seen in Figure 6.32, the error induced by the 0.000% standard absorbance itself is relatively small. Nevertheless, it is advisable to make this correction in order to better follow the trend of the evolution of the soot content in a real used lubricating oil sample in the future.

If the linearity of the response is analysed for the case where the signal is extracted from the 0.000% SiO standard, it is possible to extract a correlation of the type $Abs. = k_{wavenumber} \cdot [Soot]$ which can be used to determine the soot content of an used oil sample by simple extrapolation (knowing that it would be advisable to have the clean oil in the sample to obtain better results). In Table 6.4 the different values of $k_{wavenumber}$ have been collected.

Based on this idea, it is possible to quantify the soot content in any of the valid regions, as long as the selected region is indicated. In this Thesis, for reasons of compliance with the ASTM D7844 standard and for

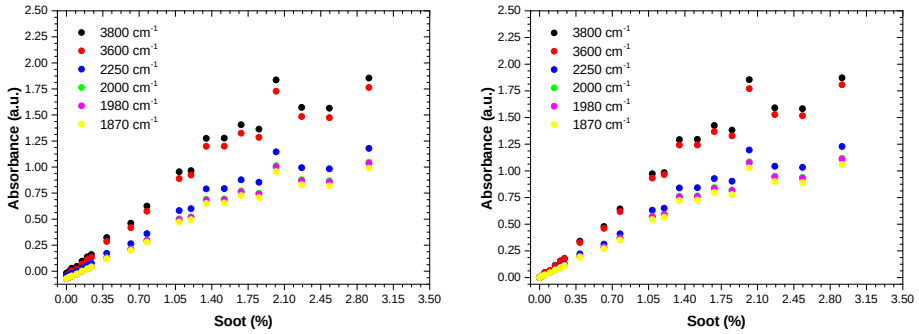

(a) Without subtraction of 0.000% SiO standard signal

(b) With subtraction of 0.000% SiO standard signal

Figure 6.32. *Linear trend of absorbance, for a given wavenumber value, with soot content.*

Table 6.4. *Soot in oil extrapolation constants (k) for each wavenumber.*

Wavenumber (cm^{-1})	$k_{wavenumber}$	**Standard error**
3800	0.74858	0.02607
3600	0.71945	0.02484
2250	0.48832	0.01649
2000	0.44393	0.01491
1980	0.44026	0.01480
1870	0.42062	0.01410

practicality (since this region is free of interference from other signals), the 2000 wavenumber was chosen as the area where the analysis will be carried out. For the case study of this Thesis, this wavenumber (2000 cm^{-1}) was the most suitable selection for the research. In Figure 6.33, the three measurements applied to each of the SiO standards have been gathered and the linear assumption of the response has been attached in the table in the same figure.

In Figure 6.33, it can be noted how the results of the analysis are repetitive, since in the three repetitions the reported values are practically coincident, but they do show divergences in the linearity between the nominal concentration of soot in the standard (X axis) and the value of soot reported by the extrapolation (Y axis) from the empirical law obtained for the concerned wavenumber. So, in order to better understand this response deviation, a

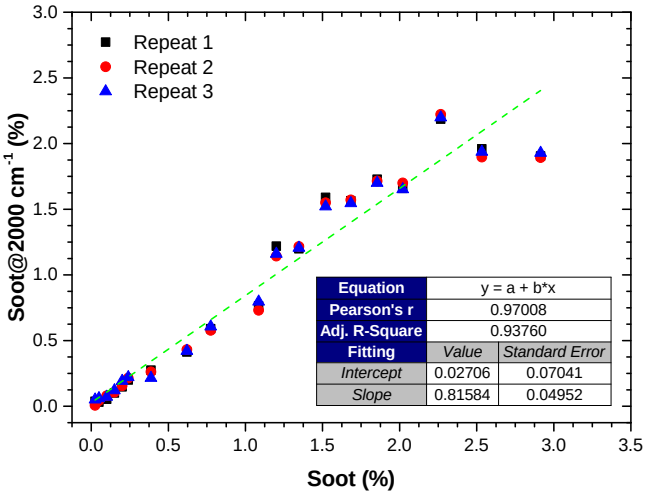

Figure 6.33. *Relationship of the empirical law response extracted for 2000 cm^{-1} versus the nominal soot value of the calibration standard.*

study of the optimal application range of FT–IR spectroscopy was carried out. For this purpose, Table 6.5 was prepared in which, for the 2000 cm^{-1} case, the three different soot values (calculated as a function of $Abs._{2000}$ and k_{2000}) were collected and their dispersion analysed.

Looking at the values reported by FT–IR at 2000 cm^{-1}, it can be seen that the technique has a number of limitations when trying to accurately quantify small soot levels (below 0.050%) and levels above 2.000%. It is for this reason that, according to this study, the optimal working range for FT–IR is within the limits of 0.050% to 2.000%. Although it is prescribed that this technique is suitable for samples with up to 3.000% dissolved soot, it has been found that the error that would be made in analysing such a sample would be considerable.

As far as FT–IR spectroscopy is concerned, there is a technique that allows quantifications of soot in oil when the sample has high levels (generally above 3.000%). When a common FT–IR spectrophotometer is not able to analyse a highly contaminated sample, two options are possible: either the optical path of the cell or measurement region is reduced, so that the thickness of the sample is reduced, or the sample needs to be treated to dilute the high soot content. Both alternatives will affect the analysis, so in these situations the safest and most comfortable option is to use FT–IR equipment with an ATR (Attenuated Total Reflection) probe [62]. This probe has the virtue that the

Table 6.5. *Soot in oil standards analysed by FT–IR.*

Standard soot in oil	**Nominal soot concentration (% weight)**	**FT–IR calculation@2000 cm^{-1}**				**Abs. diff. in percentage (%)**
		Rep. 1	Rep. 2	*Rep. 3*	*Average*	
Std. 0.000%	0.000(0)	0.031	0.038	0.027	0.032	–
Std. 0.025%	0.025(0)	0.051	0.042	0.061	0.051	105
Std. 0.050%	0.050(0)	0.053	0.080	0.072	0.068	37
Std. 0.100%	0.100(0)	0.101	0.106	0.121	0.109	9
Std. 0.150%	0.150(0)	0.148	0.156	0.192	0.165	10
Std. 0.200%	0.200(0)	0.200	0.214	0.221	0.212	6
Std. 0.240%	0.240(0)	0.275	0.262	0.215	0.251	4
Std. 0.388%	0.387(5)	0.413	0.431	0.421	0.422	9
Std. 0.620%	0.620(0)	0.590	0.578	0.607	0.592	5
Std. 0.775%	0.775(0)	0.764	0.730	0.796	0.763	2
Std. 1.086%	1.085(7)	1.219	1.143	1.160	1.174	8
Std. 1.200%	1.200(0)	1.199	1.216	1.206	1.207	1
Std. 1.347%	1.346(7)	1.590	1.549	1.521	1.553	15
Std. 1.520%	1.520(0)	1.565	1.571	1.545	1.560	3
Std. 1.683%	1.683(3)	1.728	1.715	1.700	1.714	2
Std. 1.855%	1.854(5)	1.659	1.700	1.652	1.670	10
Std. 2.020%	2.020(0)	2.186	2.222	2.199	2.202	9
Std. 2.267%	2.266(6)	1.960	1.897	1.937	2.034	15
Std. 2.533%	2.533(3)	1.905	1.893	1.929	2.125	25
Std. 2.914%	2.914(2)	2.250	2.281	2.277	2.491	22

thickness of the oil sample to be analysed is very small (in the micron range) compared to 0.1 mm in typical optical path of common liquid cell of FT–IR spectrophotometer equipment. As a consequence of the advantages and capabilities of this technique, it has already been implemented in the analysis of used lubricating oil in the same way as in the case of FT–IR [83, 100].

The procedure with this new equipment does not differ much from that of a liquid FT–IR spectrophotometer. In these cases, it is the inherent absorption of the ATR probe (which depends on its material of construction), which can overlap with the absorbance of the sample, that has to be taken into account. What happens now, applied to the case of soot quantification, is that in the region around 2000 cm^{-1} there is an apparent discontinuity in the spectrum. In the region between 2400 cm^{-1} and 1900 cm^{-1} the IR spectrum shows a behaviour which apparently breaks the continuity of the spectrum. Figure 6.34 shows the IR spectra of high soot content lubricating oil patterns analysed by ATR.

This is because, due to the sample thickness, the soot in these samples is high enough causing a deposit to form on the probe. This deposit is therefore

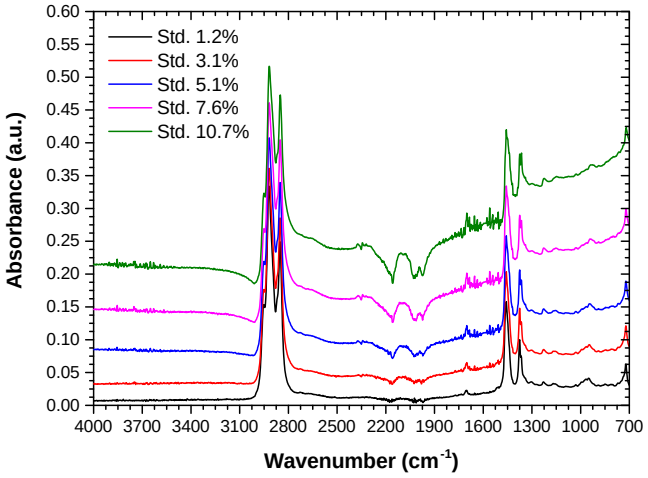

Figure 6.34. *IR spectra of SiO standards with high soot content by ATR.*

the cause of this phenomenon. Therefore, in view of the behaviour shown by these SiO standards (see Figure 6.34), applying the same requirements or conditions to determine the suitable regions or zones of the IR spectrum, the situation is almost identical to the FT–IR. Specifically, for the selected wavenumber values: 3800, 3600, 2250, 2000, 1980 and 1870 cm^{-1}, which are illustrated in Figure 6.35.

According to the trend shown for each of the soot patterns for each of the six selected wavenumbers, it is possible to obtain the same empirical law of the type $Abs. = k_{wavenumber} \cdot [Soot]$ as that obtained for the FT–IR case but, with the advantage that it is possible to analyse more samples of lubricating oil with higher soot levels.

This study of SiO by means of Thermo Nicolet Nexus FTIR spectrophotometer was carried out thanks to the collaboration with the Institut de Ciència dels Materials de la Universitat de València (ICMUV), which kindly lent us their equipment to carry out the tests.

6.3.2.5 UV–Vis Spectroscopy

Ultraviolet-Visible Spectroscopy (UV–Vis) is an optical technique that works in the range of the electromagnetic spectrum from 190 nm to 800 nm, thus comprising the ultraviolet region (N–UV and M–UV) to the visible (all visible spectral window, 380-800 nm), even making a small incursion into the

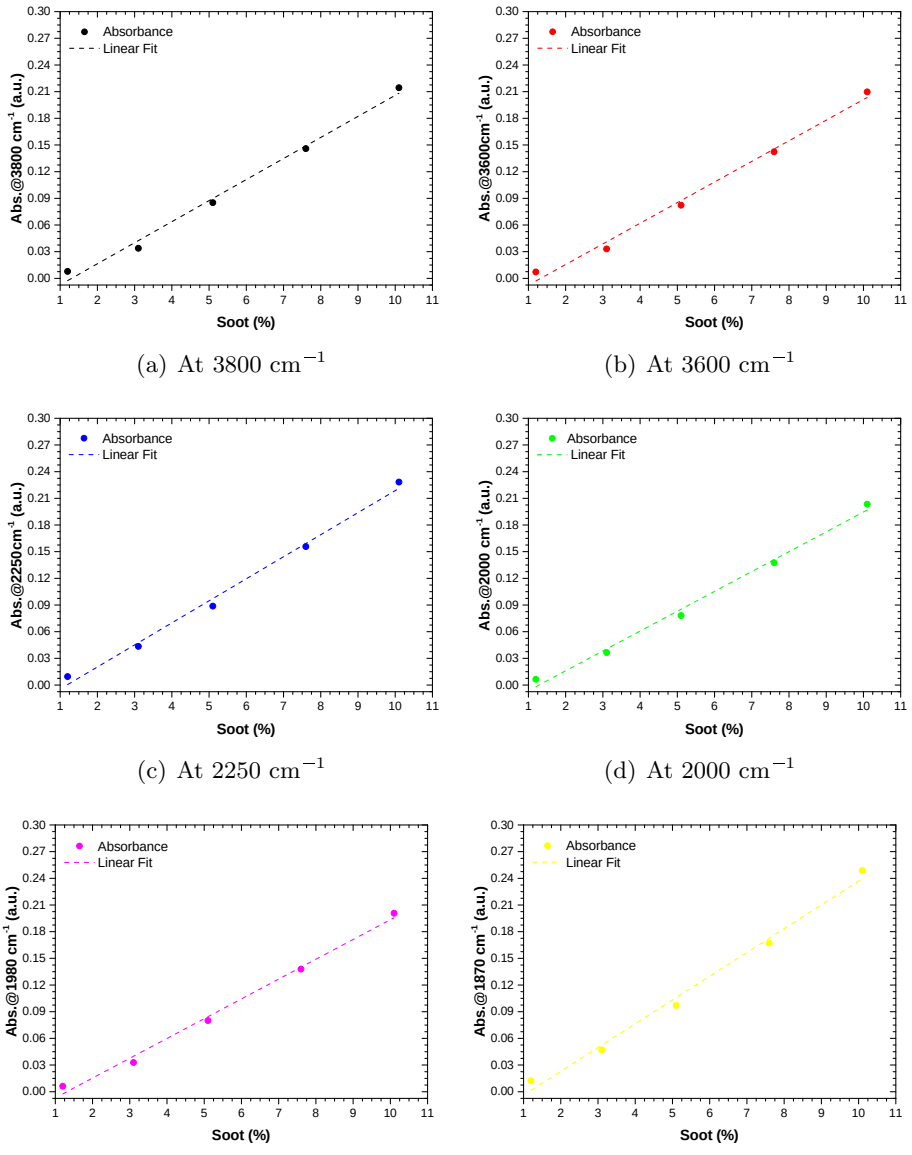

(a) At 3800 cm^{-1} (b) At 3600 cm^{-1}

(c) At 2250 cm^{-1} (d) At 2000 cm^{-1}

(e) At 1980 cm^{-1} (f) At 1870 cm^{-1}

Figure 6.35. *Evolution of absorbance as a function of soot concentration for a given wavenumber.*

NIR. Figure 6.36 summarises the relationship between the parameters that define the electromagnetic spectrum: radiation energy and wavelength; which in turn, define the different regions in which the electromagnetic spectrum is divided.

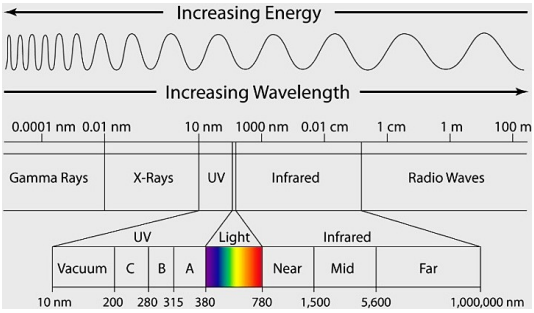

Figure 6.36. *UV–Vis range in the electromagnetic spectrum.*

Normally this technique is used to observe electronic phenomena or processes in those molecules susceptible to interact with this type of radiation. As shown in Figure 6.37, the UV–Vis radiation is energetic enough to cause an electronic promotion between the last occupied molecular orbital (called HOMO, Highest Occupied Molecular Orbital) to the first empty orbital (LUMO, Lowest Unoccupied Molecular Orbital) of the fundamental electronic state of the molecule, overcoming the existing energy jump (gap). This energetic jump made by the electron from the HOMO to the LUMO results in an alteration of the electronic structure, more specifically in the valence layer (outermost layer of the electronic structure), which is characteristic of each molecule or chemical compound.

Thus, according to the range of the electromagnetic spectrum that we are going to work with, the electronic phenomena that are capable of occurring are those that have or involve electronic transitions of more than 6 eV of energy. This implies that only in those substances where the HOMO and LUMO (between which transitions can occur) are sufficiently close it will be possible for these electronic jumps to occur: compounds with conjugated systems with π-bonds (double and/or triple bonds) and in complexes of transition metals are the most common cases [89].

However, in this research, the focus of the study is not on these substances. Now, the substance to be quantified is soot, which can be described as a black particle in solution in a matrix (in this case, lubricating oil). For this purpose, given that with soot it is not expected that such electronic processes will be

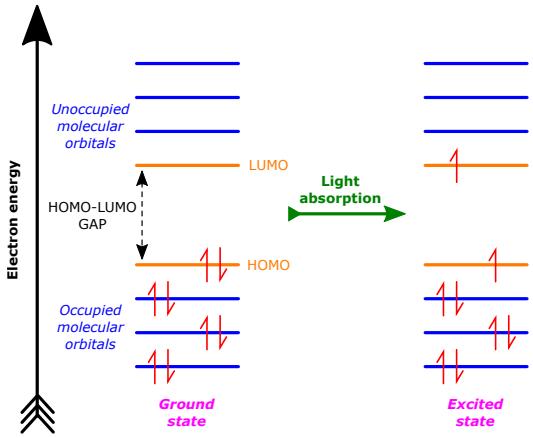

Figure 6.37. *Scheme of valence electronic levels of chemical molecule.*

observed, the phenomenon that is useful here is the fact that the sensitivity of the UV–Vis radiation is determined by the concentration and opacity of the sample being analysed. Soot is a non-UV-absorbing solid compound that scatters the radiation so that, due to this scattering, the amount of energy reaching the detector is less than that emitted by the source.

Scattering is caused by particles suspended in a solution which cause a background absorbance effect, an apparent absorbance, which affects or interferes with the absorption processes. In a brief description (see Figure 6.38), what happens is that the light, on its way from the emitting source to the detector (passing through the solution), is scattered at an angle [87]. So, although no absorption occurs, the amount of light reaching the detector is smaller, which causes an apparent absorption ($A_{scattering}$) to appear [112] (see Equation 6.2). In the UV–Vis region of the spectrum, two types or possibilities of scattering process occur according to the particle size: Rayleigh scattering and Mie scattering.

$$A_{scattering} \propto 1/\lambda^n \tag{6.2}$$

- Rayleigh scattering (RS): it appears when the particles are small relative to the wavelength of the incident light. So, the scattered irradiance is inversely proportional to the fourth power ($n = 4$) of the wavelength and increases by the order of the radius of the particle raised to the sixth power. As a result, the angular distribution of the scattered light is isotropic.

- Mie scattering (MS): it is like RS but it occurs when the particles are larger relative to the wavelength of light and is inversely proportional to the square ($n = 2$) of the wavelength.

Figure 6.38 shows a simple schematic of the light scattering event described above, where as a results of the light scattering (generated by the solid particles, soot) and the absorption of the sample, UV–Vis radiation undergoes extinction (although they differ drastically in their causes and effects). This implies that the reduction in intensity from the source emitting the radiation to the detector can be a useful parameter that can be quantified in a UV–Vis spectrophotometer. Thus, taking this phenomenon into account, in the case of UV–Vis spectroscopy, it is possible to quantify the soot content in oil if the Beer-Bouguer-Lambert law is taken into account.

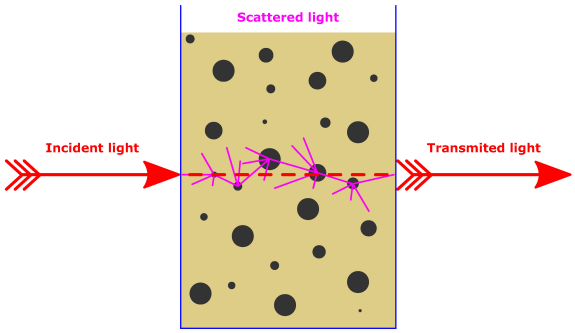

Figure 6.38. *Interaction light–particles and the scattering process.*

Beer-Bouguer-Lambert law is an empirical relation that allows to correlate the properties of a medium (chemical nature, concentration and thickness) with the changes in radiation before and after passing through the medium. Thus, the principle that governs the Beer-Bouguer-Lambert law is the analysis of the attenuation experienced by a light beam when passing through a medium of a given thickness (L), containing a given concentration (C) of an absorbing chemical species (which has a characteristic Molar Absorption Coefficient (ϵ)). Therefore, the intensity that is collected (I) undergoes a deviation (is attenuated, loses intensity) from that which could be obtained at the exit of the light source (I_0). Consequently, the fraction of that radiation that is able to pass through the sample is known as Transmittance ($Trn.$), while that which is retained by the sample is called Absorbance ($Abs.$). Absorbance is the most widespread concept for understanding the

concentration of the analyte in a sample. One way to understand what is described is to look at Figure 6.39.

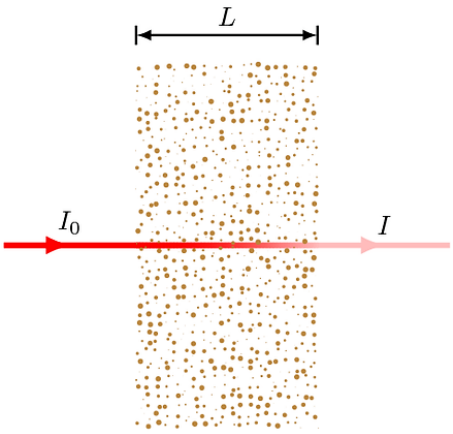

Figure 6.39. *Beer-Bouguer-Lambert law.*

As shown in Figure 6.39, when the light beam crosses the medium, a part of it is absorbed, an the other is transmitted. So, mathematically the ratio between the original intensity of the light and its residual intensity allows to define the Transmittance and the Absorbance (see Equation 6.3).

$$Abs. = -\log Trn. == -\log I/I_0 = \log I_0/I = \epsilon \cdot L \cdot C \tag{6.3}$$

Where: the units of ϵ is $dm^3/mol{\cdot}cm$, L is a length expressed in centimetres (cm) and C units are molar concentration (moles per volume of the mixture, in SI units is mol/m^3, although it is most common to work with mol/dm^3).

Following the Beer-Bouguer-Lambert law and applying it to the type of study to be carried out: quantifying the amount of soot in a lubricating oil matrix, it is possible to achieve an effective protocol using UV–Vis spectroscopy, capable of obtaining satisfactory quantifications of this substance. Therefore, in order to be able to work under the guidelines that allow compliance with this law, it is necessary to take into account its limitations, as they are determining factors when carrying out the extrapolations or calculations necessary to obtain the concentration of the substance we wish to know. Basically, the deviations that the Beer-Bouguer-Lambert law can undergo are as follows:

- The first type are those requirements necessary to comply with the law:

  - The relationship between absorbance and concentration is linear (as shown in Equation 6.3) as long as one is working under dilute concentration conditions.
  - Interaction processes between the rest of the constituent components of the samples. If the molecules interact with each other, they can falsify the measurements since the behaviour of the solution when irradiated would be different from the expected response.
  - The value of the molar absorption coefficient of the analyte is refractive index dependent.

- The next type is the one that brings together deviations caused by chemical factors.
  - This has to do with the preparation of the sample to be analysed in a UV–Vis spectrophotometer. As you are working in solution, you have to check that the solvent does not alter the sample to avoid changes in the collected signal as it may not be generated by the analyte, but by other substances resulting from the solvent-sample reaction.
  - Other aspects are those related to the pH or the presence of chemical reactions, etc.
  - Last but not least, chemical changes induced by UV–Vis radiation itself, such as molecular dissociation processes, should not be neglected.

- The last aspect is related to the instrumental limitations of the technique. This is of vital importance because linearity of response is sought in this technique. To achieve this linearity performance, it is required that the method would be applied in the region of the spectrum where the maximum absorbance is produced and monochromatic radiation is used. Consequently, that is a technique instrument-dependent.

The PerkinElmer LAMBDA 365 UV/Vis Spectrophotometer (see Figure 6.40) was used in this Thesis to describe the conditions that must be fulfilled in order to use UV–Vis spectroscopy for the quantification of soot in oil.

LAMBDA 365 UV/Vis Spectrophotometer is a double-beam spectrophotometer that works with solutions. This design of spectrophotometer allows to analyse simultaneously the reference (solvent) and the sample which results in optimised accuracy and sensitivity and a reduction stray light. The most

Figure 6.40. *LAMBDA 365 UV/Vis Spectrophotometer.*

relevant parameters of the spectrophotometer used are listed in Table 6.6 below.

Table 6.6. *Main features of the spectrophotometer and the cuvettes.*

Feature type	Value or property
Lamp	Deuterium (D) and Tungsten halogen (WI)
Beam	Double-beam
Spectral range (nm)	1050-250
Scan (nm/min)	400
Cuvette material	Quartz
Cuvette's path length (mm)	10
Useful cuvette's spectral range (nm)	2700-170

With this equipment, it is initially necessary to perform an analysis of soot patterns in oil to see how it responds. For this purpose, a series of oil soot standards ranging from 0.000% to 3.100% were used (see Table 6.7).

Sample preparation to measure in this equipment is explained in the research work by Macián et al. [72]. In accordance with the guidelines set out in this work, the results of analysing the patterns are shown in Figure 6.41.

However, it can be seen that not all patterns are valid for the study. There are a small number of candidate standards that do meet the requirements of Beer-Bouguer-Lambert law (see Figure 6.42).

According to this Figure 6.42, in order to work in Beer-Bouguer-Lambert conditions, it would be convenient to select those standards whose absorbance does not exceed the value of 1 a.u., so the standards that do fulfil this condition are the soot content standards: 0.000%, 0.025%, 0.050%, 0.100%, 0.150% and

Table 6.7. *Soot in oil standards employed to calibrate the spectrophotometer.*

SiO standard	Soot concentration (% weight)
Std. Blank	0.000
Std. 0.025	0.025
Std. 0.050	0.050
Std. 0.100	0.100
Std. 0.150	0.150
Std. 0.200	0.200
Std. 0.240	0.240
Std. 0.388	0.388
Std. 0.564	0.564
Std. 0.775	0.775
Std. 1.086	1.086
Std. 1.200	1.200
Std. 1.347	1.347
Std. 1.520	1.520
Std. 1.683	1.683
Std. 1.855	1.855
Std. 2.020	2.020
Std. 2.267	2.267
Std. 2.533	2.533
Std. 2.914	2.914
Std. 3.100	3.100

0.200%. For the quantification of soot, the option chosen was to analyse the absorbance at 800 nm, since this is a region of the spectrum where there is no contribution from the base, additives, dyes or other excipients that a lubricating oil usually contains in its formulation. Therefore, if the absorbance of each of the patterns is measured at a given wavelength, a linear trend is observed (see Figure 6.44).

In view of the results shown in Figure 6.44, it is very clear that for those patterns that do not exceed the 1 a.u. threshold (coloured in red), the linearity as a function of soot concentration adjusts more closely than those that do surpass the 1 a.u. threshold. Once the selection of those standards that do meet the requirements of the Beer-Bouguer-Lambert law has been corroborated, it is possible to extract a relationship between the absorption at

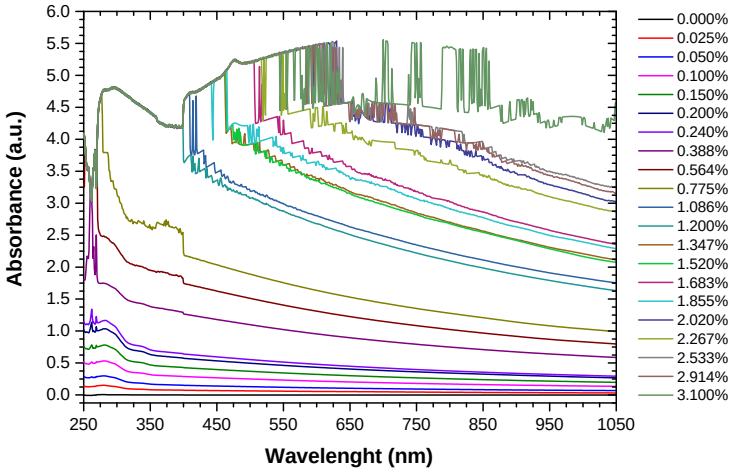

Figure 6.41. *UV–Vis spectra of soot in lubricating oil standards.*

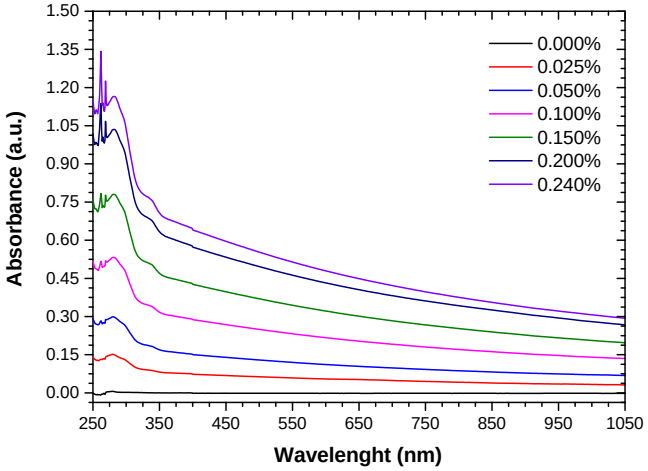

Figure 6.42. *UV–Vis spectra of soot in lubricating oil standards.*

800 nm and the soot concentration useful for subsequent application to real samples in order to know their soot content. Figure 6.44 shows the correlation mentioned previously:

According to the correlation, there is a small error in centring the initial value at the point (0;0). When analysing the value of the intercept, $9.84737 \cdot 10^{-4}$, and its error, it can be seen that the error is higher. This leads us to

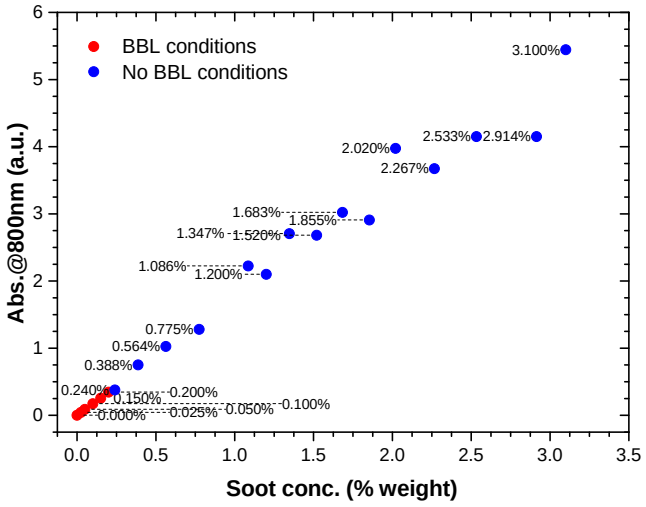

Figure 6.43. *Absorption of soot in oil standards at 800 nm: the red circles symbolise those standards whose UV–Vis spectra do not exceed 1 a.u., while the blue circles are those that do.*

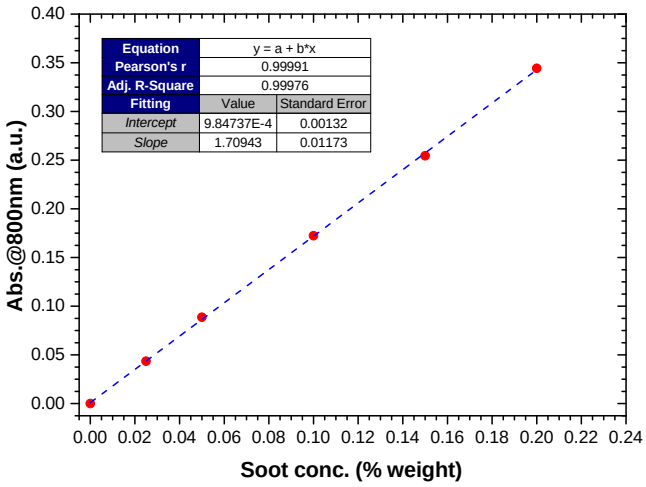

Figure 6.44. *Absorption of soot in oil standards at 800 nm.*

think that this variability is a consequence of inherent errors in the equipment. That is why, taking into account that this type of fluctuations will always be present, it is convenient to force the correlation to pass through the point (0;0). Performing this process, the correlation is now as follows, see Table 6.8:

Table 6.8. *Correlation of soot content obtained from UV–Vis analysis of the soot in oil standards.*

Parameter	**Value**
Equation	y = 0 + b·x
Pearson's r	0.99996
Adj. R-Square	0.99990
Slope	1.71627
Std. error of the slope	0.00702

From the correlation obtained, by extrapolation, it is possible to determine the soot content in a sample of used lubricating oil. However, it is necessary to choose the right target samples that are valid for analysis by this technique.

In this Thesis, the quantification of soot in lubricating oil has been focused on rapid analyses, which do not use many consumables (low impact on waste generation), which do not involve sample loss (non-destructive testing) and which are capable of appreciating small increases in concentration. With this in mind, an engine lubricating oil sampling campaign was carried out for very short periods of time (low-mileage of use): 0 (new oil), 5, 15, 30, 45, 60 and 240 minutes (see Figure 6.45).

Figure 6.45. *Picture of a set of low-mileage samples, where it can be see the evolution of the oil colouring to blacker tones as the oil accumulates use: 0, 15, 30, 45, 60 and 240 minutes (from left to right).*

Thus, when analysing each of these seven samples (Sample 1 to Sample 7) collected at different times, the changes in the UV–Vis spectra are practically

negligible. Figure 6.46 shows the UV–Vis spectra of a set of samples where this phenomenon is observed.

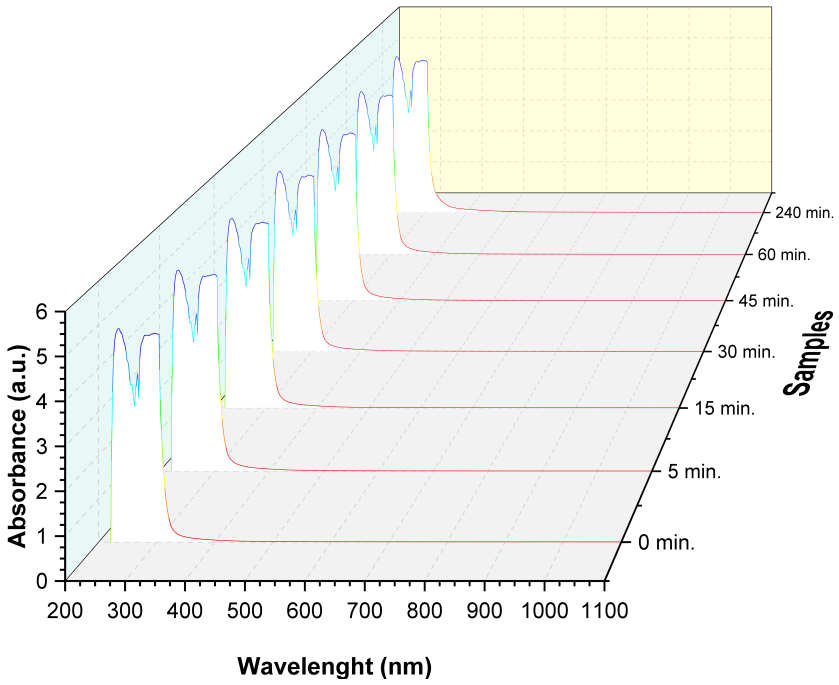

Figure 6.46. *Set of UV–Vis spectrums: 0 min. (fresh oil), 5 min., 15 min., 30 min., 45 min., 60 min. and 240 min..*

In this Figure 6.46, the colour patterns indicate that there is no substantial difference in the absorbance values over the wavelength sweep at which the test has been performed. It can be seen that there is the same colour (indicative of the absorbance value) for the same wavelength range for the different samples. However, if we analyse in detail a certain wavelength value (in this case 800nm was chosen), substantial changes are observed.

In the following Figure 6.47, we have superimposed the same set of spectra as in Figure 6.46, zooming in on the region of interest. As explained in the work by Macián et al. [72]. and following the same steps and procedures as those applied to the spectra of the soot in oil standards, changes in background absorbance are observed at 800 nm, in accordance with the mileage of the samples.

According to Figure 6.47, as the oil accumulates usage time, the amount of soot contaminating the oil also increases. Thus, under stationary engine

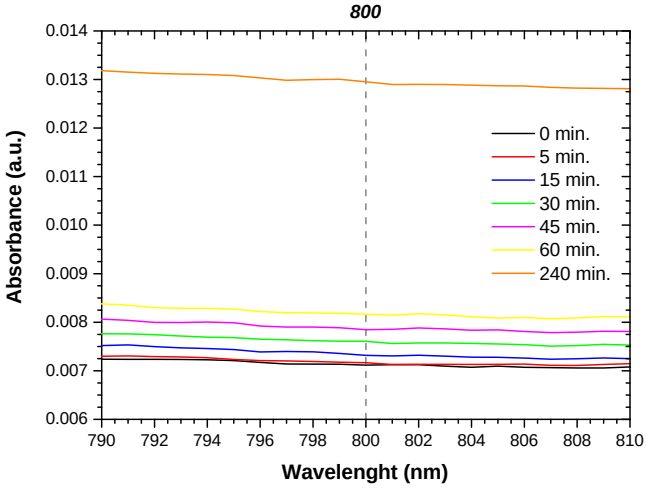

Figure 6.47. *Detail of a set UV–Vis spectrums centred at the wavelength selected for the quantification of soot in oil, 800 nm.*

operating conditions, the evolution of soot content is expected to be linear with mileage. In this sense, Figure 6.48 has been prepared, where all the collected samples have been represented (already calculated the soot concentrations by extrapolating their absorbance at 800nm): in the figure on the left are shown the values without subtraction of the new spectrum (0 min.), and in the figure on the right, once the contribution of this oil has been eliminated.

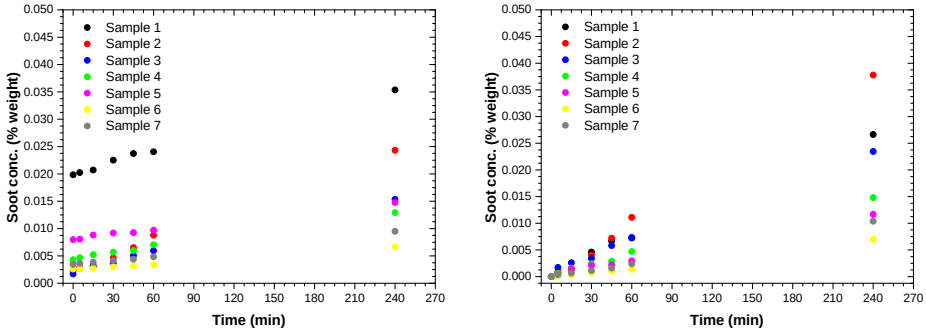

(a) Without removing the contribution of new oil

(b) Removing the contribution of new oil

Figure 6.48. *Comparison between the effect of removing or not the signal of the fresh oil (0 min.) for calculating the SiO.*

Analysing this Figure 6.48, several observations are worth noting:

- Firstly, the evolution of the soot content in all of them is linear with the accumulated time of the samples. This was to be expected given the stationary nature of the test, where samples were taken from an engine arranged on an engine bench and tested for 4 hours at a given operating point. In appendix 4.A.2 the trends of the evolution of the soot content in the lubricant are grouped for each of the 7 cases mentioned.
- The next aspect is that, depending on the test that was being carried out at the time, the evolution of this soot contamination is different. Accordingly, it can be seen that at those points of the engine operation where the oil was most contaminated with soot, the slope of the line drawn by the different samples (0, 5, 15, 30, 45, 60 and 240 min) is greater. This dependence is directly proportional, i.e. the points where the oil contamination is highest have the steepest slopes and vice versa.
- To conclude, the planned application of this technique for cases low usage lubricating oil samples (even very good correlations have been observed in increments of 15 minutes) proves to be valid for monitoring the evolution of the soot content and can extract not only discrete values but also generation ratios. Moreover, its consistency (according to the designed analysis protocol) is guaranteed within the range of concentrations that occurs in these short periods of time, avoiding that the linearity between absorbance and concentration is affected by chemical-physical phenomena.

In conclusion, UV–Vis spectroscopy is a technique that is able to provide soot content values in a quick and easy way. It simply requires knowledge of sample preparation (solvent selection and dissolution rate) to obtain satisfactory results. Moreover, due to the way of working of this technique, the range of applicability can be very wide depending on the absorption of the sample (without forgetting that this technique was chosen for cases where the oil is not very degraded, i.e. in short periods of time where the predominant factor is its contamination), a parameter that can be modulated depending on two factors: the optical pathlength and the dilution ratio. For the first case, there are cells with different optical pitches, in this study we used cells of 1 cm optical thickness (so there is a lot of room for improvement). While for the case of the dilution ratio, it is limited by instrumental aspects (micropipettes, sample viscosity, etc.). Thus, all in all, UV–Vis spectroscopy is a candidate technique for the quantification of soot in oil and can be improved in the future as materials and technology improve.

6.3.2.6 Specific techniques and methodologies

Specific equipment has been designed for the quantification of the amount of soot in engine lubricating oils. But among the existing equipment, one of them stands out: the InfraCal 2 - Soot Meter (see Figure 6.49).

Figure 6.49. *InfraCal 2 - Soot Meter of Spectro Scientific.*

The InfraCal 2 - Soot Meter is a bench-top device based on an IR spectrophotometer that follows the ASTM D7686-19: Standard Test Method for Field-Based Condition Monitoring of Soot in In-Service Lubricants Using a Fixed-Filter Infrared (IR) Instrument [46] standard to quantify the soot in oil content. For the quantification of soot, this system is based on the phenomenon of Horizontal Attenuated Total Reflectance (HATR) at a fixed wavelength of 3.9 microns (equivalent to a wavenumber of 2464 cm^{-1}). For this purpose, the sample is located over a horizontally arranged ATR sample plate made of zinc selenide (ZnSe) crystal (parallel to the surface) and irradiated with this infrared light, see Figure 6.50.

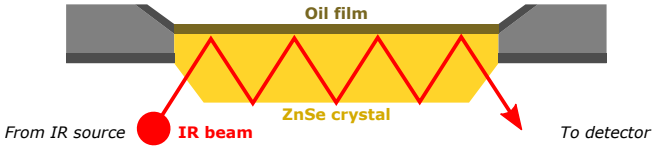

Figure 6.50. *Principle of operation of InfraCal 2 - Soot Meter.*

Thanks to this design, the infrared light bounces several times between the top and bottom surfaces of the ZnSe crystal as it travels horizontally across it. During this process, the radiation is absorbed by the sample in all those situations where it bounces off the top face of the crystal. As a consequence, the original IR radiation experiences losses of its intensity (at

certain wavelengths) due to absorption by the oil sample on the top plate. Thus, as the IR radiation leaves the glass and reaches the detector, its intensity is different, which is used for the calculation of the soot percentage (based on a previous calibration with standards). InfraCal 2 - Soot Meter is therefore, a comparative test where, in order to obtain the value of the soot concentration, the contaminated sample has to be compared with a sample of the same clean oil.

Nonetheless, this system has a number of aspects or features that give it a high potential for application both as a bench-top system in a laboratory and as a field device. The most relevant aspects are described below:

- The most applicable aspect is that the system does not require any pre-treatment of the sample, which makes it very easy to use.
- In addition, the equipment develops the analysis in a very short time: less than 30 seconds per sample.
- The range of analytical applicability of the equipment is for lubricating oil samples containing soot levels from 0.0% (new oil) to 12.0% (rising to 15.0%), under conditions of no sample dilution. Inside this range, the instrument repeatability is ± 0.2 % (by weight) soot in engine oil.

Figure 6.51 shows a comparison between the response provided by the InfraCal 2 - Soot Meter and the commonly used techniques for the determination of the amount of soot in lubricating oil: TGA and FT–IR spectroscopy.

It is observed that the response is satisfactorily in line with that of the two techniques. However, for the purpose of soot quantification in this thesis, the system does not provide sufficient resolution to detect small variations of soot in the lubricant (given that the level of quantification of the system allows to discern only up to the first decimal place). Thus, in order to find a system capable of low LODs (Limit Of Detection), InfraCal 2 - Soot Meter is not the best choice.

This section will also present a system specially designed for online quantification of soot in lubricating oil, which can be coupled to an engine test bench in order to monitor the soot content in the oil in real time, as well as the contamination rate of the oil. This section has been promoted by the fact that it has been possible to carry out studies of soot contamination in engine lubricating oil using this device.

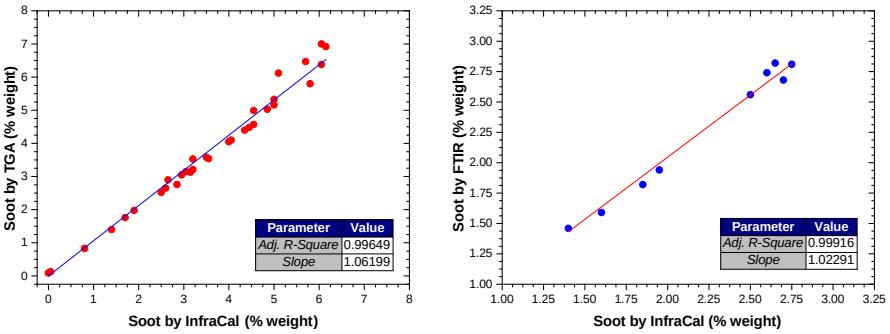

(a) InfraCal 2 vs. TGA (b) InfraCal 2 vs. FT–IR

Figure 6.51. *Comparison of the response of the InfraCal 2 - Soot Meter versus classical quantification techniques: TGA and FT–IR.*

The system is known as BTSA (see Figure 6.52), an acronym of Bench Top Soot Analyser, of Analytical Engineering Inc. (AEI). The BTSA is an spectroscopic system capable of providing real–time data on the concentration of soot in a lubricating oil used in a running engine [4].

Figure 6.52. *BTSA 7.0 of AEI.*

This equipment is made up of a series of systems that allow the online quantification of soot without any chemical or physical changes in the engine oil. Principally, the systems being referred to are the following:

- An optical system based on a spectroscopic setup that works in a range of electromagnetic spectrum compressed between FIR region(>20.0 μm) and the visible region (0.5 μm).
- A direct unobtrusive sampling system from the engine crankcase based on a special pump that recirculates oil without affecting engine operation. The system works continuously avoiding interruptions in the oil flow BTSA–engine.
- A system for the automatic control of the internal temperature of the equipment to ensure a constant temperature in the optical system in order to guarantee the highest possible accuracy and to avoid the effect of thermal fluctuations on the measurement of the concentration of soot.

The operation of the BTSA is very simple, the pumping system itself is able to extract a sample of lube oil from the engine and then, drive a fraction of that lube oil flow to its optical system or soot measurement module and then, reintroduce it back into the main flow and return it to the engine. Figure 6.53 shows a schematic of the connections and oil flow rates that illustrate, in a more schematic way, the direct sampling of the BTSA.

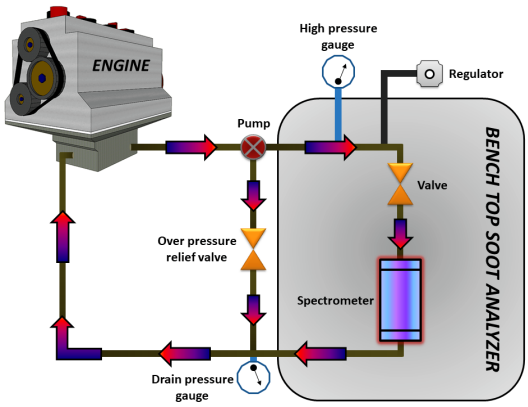

Figure 6.53. *BTSA and crankcase connection diagram.*

Focusing on the quantification of soot, the optical system produces an irradiation of the oil flow by the FIR-Vis light source. As a consequence of the light-particle interaction, the radiation reaching the sensor is different from that emitted by the light source. Thus, the sensor, depending on the amount of light reaching it, is able to correlate it with the amount of soot in the oil (this concentration is accurately measured with precision approaching 0.0001%

by weight). This sensor is extremely sensitive and has a fast response, which means that soot concentration values can be obtained in a very short time, 6 seconds to be precise, and with high accuracy (with a deviation of 0.2%).

An interesting aspect of this equipment is that, due to its own way of working, it allows rapid SiO ratios (%/hour) to be obtained by analysing the trends of successive measurements of soot concentration (see Figure 6.54). This is an advantage over traditional ways of obtaining these ratios (either by TGA or FT–IR) which require more time-consuming engine testing and sampling. Figure 6.54 shows an image of the controller software of the equipment where it can be seen how, in the upper section, the evolution of the soot content is represented in real time, while in the lower section, it shows the ratio at 100 hours.

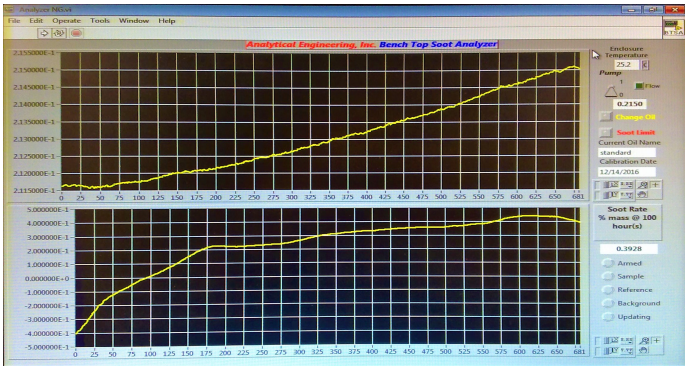

Figure 6.54. *Screen of the BTSA control system where you can see how the software works to obtain the concentration of soot in oil and its ratio.*

Accordingly, the BTSA is able to monitor the soot content in the lubricating oil during stationary bench tests (dynamometer testing) on a continuous basis as depicted in Figure 6.55. This is because under these operating conditions, soot generation is linear, so that the soot production rate of the engine, at that particular point, can be calculated through a linear regression of the individual values of soot concentration within the given sampling time.

Figure 6.55 shows that in the transition from session 1 to session 2, the soot content ends and starts at the same levels (at 0.27% weight). This implies that with this equipment it is possible to characterise very quickly the soot content and its ratio for the whole engine map, and these entire soot maps can be obtained in a few hours. Normally, the characterisation of an operating point requires about 15 minutes of testing to obtain satisfactory results (although

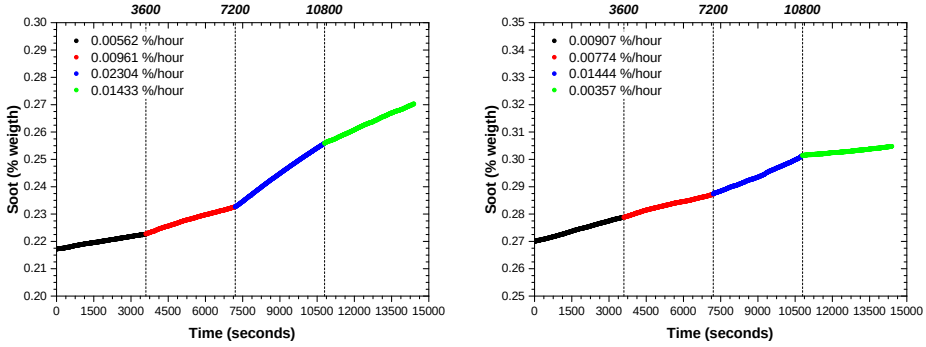

(a) Session 1 with 4 stationary points of 1 hour each

(b) Session 2 with 4 stationary points of 1 hour each

Figure 6.55. *Examples of two successive test sessions on the engine bench with the BTSA attached to it.*

if a longer test duration, e.g. 1 hour, is used, the results obtained are much more accurate) of the soot rate since enough individual values of soot content have already been accumulated (15 minutes is equivalent to 150 values of instantaneous soot concentration). In addition, within each of the sessions, it can be observed how each test point presents a different accumulation trend as a result of each of them adding soot to the oil at different rates during the engine operation. Those engine operating points, which are more contaminating to the lubricant, show a steeper slope in the evolution of the soot concentration (during the 1 hour test) and vice versa.

Despite the capability to work quickly, the BTSA is consistent with the results it delivers in stationary dynamometer tests. Figure 6.56 shows how the same point: point 1 and point 2, analysed at different times and with a lubricating oil in different conditions (given that the soot content between repetition a (red) and repetition b (blue) is different) gives the same soot rate values.

In Figure 6.56, the starting values of soot concentration (refer to the "Intercept" field in the table contained in the graph) and the rate (as a "Slope" expressed in %/second) of each of the repetitions have been incorporated. Analysing these values, it can be seen that the ratio of the measurements (a vs b) show homologous values despite the fact that the oil is in a different condition, in this case due to the soot content.

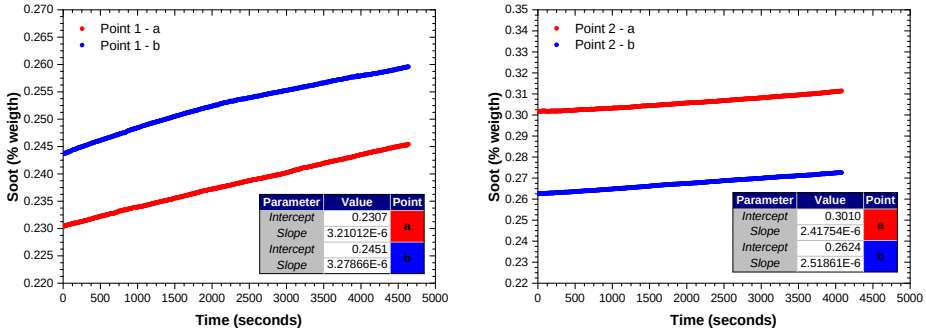

(a) Point 1: 3400 rpm and 305 Nm (b) Point 2: 1200 rpm and 140 Nm

Figure 6.56. *Examples of repetition of the same operating point at different test times on the engine bench.*

Despite the undeniable virtues of the BTSA equipment, as a result of its sensitivity and speed in analysing soot in the lubricating oil, it has a number of drawbacks that limit its application. These are described below:

- The first problem encountered by the BTSA is the need for calibration. This equipment requires an internal calibration with perfectly characterised oil samples (preferably by TGA) so that the system's software can correlate the signal picked up by its optical system and translate it into the desired units.

- The next aspect is the range of applicability of the equipment. According to the manufacturer's recommendations, this system may experience irreversible damage when attempting to analyse lubricating oils with a soot content of more than 1.0%. It is therefore advisable to work with oils with a concentration of less than 0.8% in order to have a safety margin.

- Another problem is that obtaining a soot rate will always require at least 15 minutes of analysis; during that time, it is estimated that the soot accumulation in the oil is sufficient to induce a smooth effect between the fluctuations of the individual soot count values. In addition, remembering that it is necessary to circulate the lubricating oil through the whole system (engine-connections-BTSA) to ensure that the lubricating oil is homogeneous. In this way, there is no dead oil volume which could lead to incorrect soot values.

- Finally, the problem that can generate the most interest is related to the way the optical system works. This system is based on determining the concentration of soot in the lubricating oil according to the degree of darkening of the oil: the blacker the oil, the more soot it contains. This is true as long as no other substance alters the oil. Considering the speed at which the results are reported, the contribution of oxidation of the oil (which also causes the oil to turn darker) can be ignored but, the presence of fuel is a significant source of error. The BTSA is not able to discriminate fuel dilution problems, so that, if they exist, the soot concentration is affected. Note in Figure 6.57, how the soot content pattern no longer follows the linear evolution shown above.

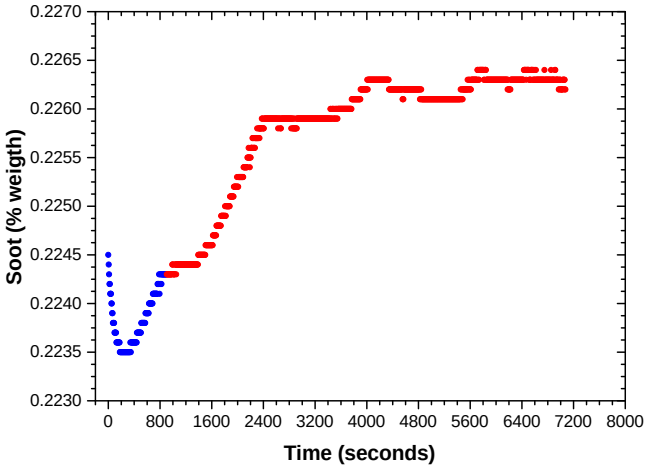

Figure 6.57. *BTSA soot quantification problems: the blue circles are the soot content values obtained during the stabilisation time of 15 minutes, while the circles coloured in red are the soot content values when the oil is homogenised and in suitable conditions for the test.*

6.4 Case of study on engine bench testing

The main objective of this study, reported in the publication by B. Tormos et al. [110], is the characterisation of the engine oil by the soot generated in the combustion chamber of a DI diesel engine, specially to asses the effects of the operating settings in terms of soot content but also fuel dilution. According to that, a CIDI (Compression Ignition Direct Injection) medium–duty diesel

engine was tested in two operating settings: in conventional combustion mode and during the DPF regeneration mode in order to determine how these specific conditions affect both engine oil parameters: soot and fuel dilution.

With this objective in mind, it was decided to study the problem from two perspectives: the first by means of experimental tests on the engine bench in order to obtain empirical values of the two parameters to be studied, while the other perspective focuses on a CFD (Computational Fluid Dynamics) study to obtain a model that describes the phenomena involved and, if possible, to make satisfactory predictions of the problem.

In summary, in this research, theoretical analyses (CFD simulation) have been combined with experimental tests in order to find synergies when dealing with this problem and thus, provide greater rigour to the study. In order to achieve this merging of the two perspectives on soot in lubricating oil, a procedure was defined:

- Firstly, engine tests were carried out in order to evaluate the lubricant contamination, as follows:
  - Collect experimental data (instantaneous cylinder pressure, torque, engine speed, throttle position, EGR value, smoke in the exhaust, content of soot in oil, etc.) from the most interesting engine operating points to study the phenomenon.
  - Next, focus the experimental tests on the most promising engine operating conditions for soot generation.
  - Analyse the sensitivity about the effect of various engine parameters: operating conditions (nominal or regenerative), EGR, injection pressure (IP), injection timing and injection mapping.
- Computational Fluid Dynamics (CFD) model development of soot contamination in engine oil, and its validation using engine test results in order to correlate the soot levels measured experimentally in the engine oil. This campaign, employing the experimental database, will be carried out for finding out some correlation between the predicted soot levels in the combustion chamber close to the cylinder walls and the soot contamination in the oil.
- CFD model predictions of soot in oil according to the previous parameters

6.4.1 Experimental tools: engine test cell and laboratory lube analysis

Once the research development plan had been decided, the problem was first approached from an experimental point of view. The diesel engine employed was a 4–cylinder 4–stroke Compression–Ignition (CI) medium-duty Direct Injection (DI) engine equipped with a common–rail injection and a turbocharger/intercooler air loop system (for more information, see Table 6.9).

Table 6.9. *Main specifications of the engine.*

Engine type	**CIDI engine**
Combustion chamber	Re–entrant
Cylinders	4 in line
Unitary displacement (cm^3)	738.3
Engine capacity (cm^3)	2953
Bore x Stroke (mm)	96.0 x 102.0
Bowl width (mm)	62.4
Valves (valves/cylinder)	4
Connecting rod length (mm)	154.5
Geometric compression ratio (-)	15.5
Maximum effective power @ 3600 rpm (kW)	111.3
Maximum effective torque @ 2000 rpm (Nm)	350.0

This engine was accommodated on a test bench provided with all the necessary facilities and auxiliary instrumentation systems to monitor and control the engine operation and, finally, for the recording of data required for the study (Figure 6.58).

With this configuration for soot measurements, two specific measurement systems were coupled:

- The first device is coupled in order to obtain the soot content in the exhaust emissions. This device is a Smokemeter AVL 451S, with an operating principle based on passing the exhaust gases through a filter and, depending on the footprint of the gases left in the filter, being able to determine the amount of soot that these gasses contain.
- The last is the Bench Top Soot Analyser (BTSA), a system for on–line measurement of soot content in oil. Thanks to this device it is possible to

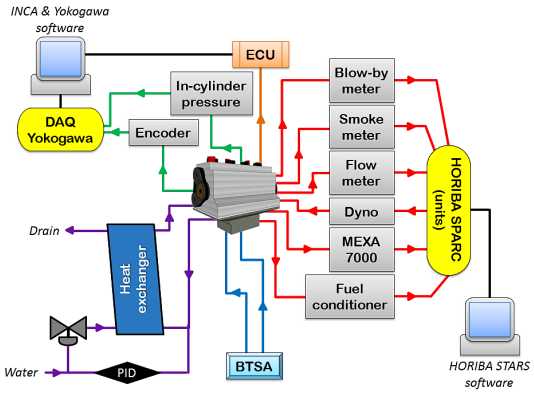

Figure 6.58. *Engine test bench sketch.*

determine the soot concentration (by weight) in real time in the engine oil.

Figure 6.59 shows a picture of the engine test cell where the two systems mentioned above are highlighted: in green the tailpipe smoke measurement system and in blue the BTSA.

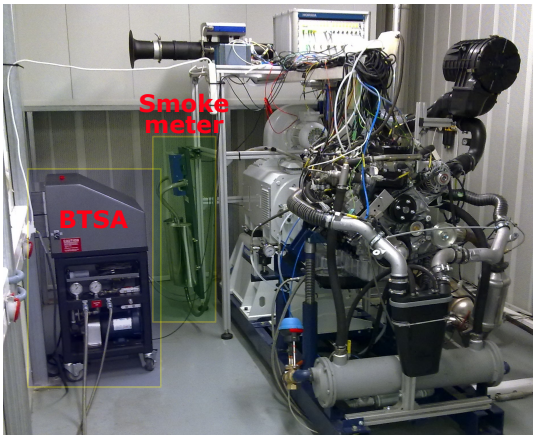

Figure 6.59. *Engine test bench during test with the two specific systems for soot measuring.*

For engine oil–fuel dilution, the measurements were carried out as follows: for the case of fuel in the exhaust, namely unburned hydrocarbons (UHC), a

state–of–the–art exhaust gas analyser was employed (MEXA 7000 in Figure 6.58).

To provide assurance of soot in oil content and fuel dilution, for each test performed, a plan was made to collect samples of lubricating oil directly from the engine crankcase at the start and end of the test. These samples can then be analysed in the laboratory by kinematic viscosity and FT–IR spectroscopy in order to check the value of both of them.

6.4.2 Numerical model

Having completed the section on experimental tools, the numerical model applied to the subject of study will be described. In this way, the items considered in this modelling were developed as follows:

- First, a numerical model of a single cylinder engine was implemented in the commercial code StarCD version 4.22 [104]. The constructed mesh, which size was obtained after a complete grid convergence study, took into account the most relevant combustion parameters; it is a 1/9–sector mesh with periodic boundary conditions containing 131360 cells at Bottom Dead Center (BDC). The simulations were performed during the closed cycle [13, 14] that is, from the closure of the intake valves to the opening of the exhaust ones (from -113.2° to 103.0° with the Top Dead Center (TDC) at 0.0°).
- Next, turbulent flow properties were modelled by the RNG $k-\epsilon$ model [117], coupled with the wall–functions model proposed by Angelberger [5] to simulate the wall heat transfer. The time discretisation was implicit, while the divergence terms used the second order Monotone Advection and Reconstruction Scheme (MARS) [104]. Pressure–velocity coupling was achieved by the Pressure Implicit with Splitting of Operators (PISO) method [49].
- In terms of combustion, several models were required. For combustion modelling, the ECFM–3z model from IFPEN [21] was employed and completed by another series of sub–models focused on the injection process:
  - DF1 fuel provides the physical properties of diesel in this model [38].
  - To calculate the diesel spray features, standard Droplet Discrete Model (available in StarCD) was used.

  - Huh-Gosman [43] and Reitz–Diwakar [92] models simulate the spray atomisation and break–up.

- For pollutants, NOx and soot have been studied. For the first one, employing the extended Zeldovich (thermal) mechanism (source terms acquired from a flamelet library) [53] while for soot, two models were required: its formation and oxidation were calculated from a two–step Hiroyasu–like model [41] and to estimate the amount of soot mixed with the lubricant, a thermophoretic deposition model was applied [23, 115].

6.4.3 Methodology of the study

Next, due to the variety of systems involved in this study, it was necessary to define a specific methodology to ensure that the data and information collected throughout the study would be accurate and reliable. Therefore, the experimental methodology was as follows: firstly, an extensive mapping of points (defined by engine speed and Brake Mean Effective Pressure (BMEP)) along the entire engine operating map was carried out in order to know under which circumstances the study was to take place. This engine mapping, Figure 6.60, shows the different test points: seven of them under conventional combustion conditions and the other four under DPF regeneration conditions, in order to obtain information of total soot generated and how much of this soot is ultimately expelled with the exhaust gases and how much is combined with the lubricant.

According to Figure 6.60, each of these selected points, 10 for conventional combustion and 4 for the DPF regeneration case, presents a number of specific parameters or characteristics (see Table 6.10) from which they can be modified or adjusted according to the desired effect or response.

Table 6.10. *Main running settings of the operation points studied for SiO analysis.*

	1200@2.5	**1200@5**	**1200@8**	**1200@13**	**2400@2.5**	**2400@8**	**2400@13**	**3400@2.5**	**3400@8**	**3400@13**	**1200@6**	**2000@2**	**2000@10**	**3400@6**
Engine speed (rpm)	1200	1200	1200	1200	2400	2400	2400	3400	3400	3400	1200	2000	2000	3400
BMEP (kPa)	250	500	800	1300	250	800	1300	250	800	1300	600	200	1000	600
EGR (%)	31.0	18.0	13.1	0.2	37.4	21.8	11.7	16.0	17.1	17.6	0.3	0.2	0.1	0.2
Combustion mode (-)	C	C	C	C	C	C	C	C	C	C	R	R	R	R
Injection pressure (bar)	536	672	733	750	1042	1397	1268	1008	1574	1799	693	456	794	1073
SoI Pilot 1 (CAD)	-16.0	-19.8	-25.2	-	-27.4	-	-	-	-	-	-	-	-	-
SoI Pilot 2 (CAD)	-7.6	-2.0	-8.2	-20.4	-6.8	-23.6	-11.8	-17.2	-20.6	-10.8	-19.6	-13.0	-25.2	-21.4
SoI Main (CAD)	7.2	7.2	5.0	-3.2	3.6	4.4	1.0	1.2	-2.4	-10.8	7.4	5.6	1.4	-4.8
SoI Post (CAD)	-	-	-	-	-	-	-	-	-	-	54.6	39.9	48.2	52.0
MoI Pilot 1 (mg/str)	1.5	2.3	2.8	-	3.0	-	-	-	-	-	-	-	-	-
MoI Pilot 2 (mg/str)	0.7	1.0	1.3	1.4	2.3	1.7	1.7	2.6	1.7	2.7	2.5	5.1	2.9	4.9
MoI Main (mg/str)	11.6	22.5	34.5	57.7	11.5	39.3	61.4	18.2	43.7	61.2	26.0	10.7	44.6	26.4
MoI Post (mg/str)	-	-	-	-	-	-	-	-	-	-	9.4	7.6	6.8	4.4

C: Conventional
R: Regeneration

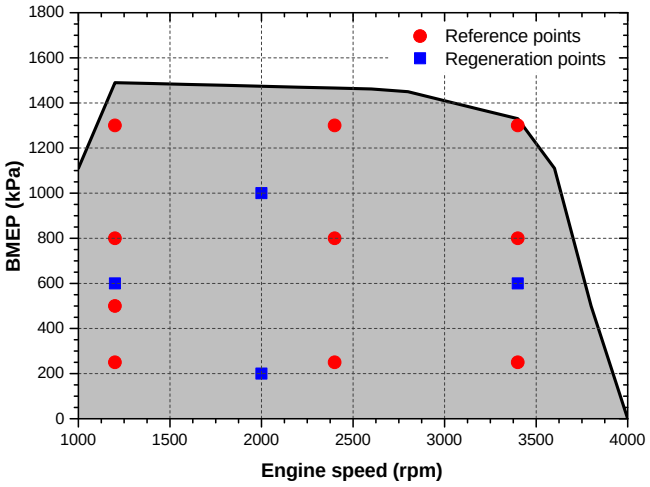

Figure 6.60. *Engine operating points: reference (conventional combustion) and regeneration mode, for the SiO analysis.*

So, once it has been defined in which regions and engine operating conditions the study is to be carried out, it is necessary to determine the most appropriate way to collect the information: the tests were conducted over a period of 1 hour for each engine operating point. This hour included a 15–minute stabilisation period for the engine and all the test cell equipment, and the next 45 minutes were used for sampling or data collection. These data cover a wide range of information relevant to the study: engine operating parameters, opacimeter measurements for soot in exhaust, soot in oil values (values from BTSA equipment and laboratory KV and FT–IR analysis), fuel dilution in oil (by KV and FT–IR laboratory analysis) and exhausts tailpipe HC emissions.

6.4.4 Results

The results of the soot study are shown below. These results are organised into those obtained from the reference tests and the results derived from the parametric tests.

6.4.4.1 Reference points

Accordingly, the results of analysing these reference points are shown in Figure 6.61, where the soot values in oil are shown in red and in blue for soot in the exhaust.

To better understand how both soot in the oil (SiO) and soot in the exhaust (SiE) are related, further studies are required, as will be seen below.

- There are a number of interesting situations for conventional combustion (see Figure 6.61) where soot values are significant: 2400@13, 3400@8 and 3400@13 (leaving aside point 3400@2.5, since the soot values at both locations are lower than the previous ones considered). All of them are points with high load and high speed conditions, but each of them show noticeable differences in terms of how much soot is in the oil and how much is expelled together with the exhaust gases: for point 2400@13, the ratio is 38%. This value, the maximum obtained, differs from 21% of 3400@8 and 6% of 3400@13. The other side of this situation is shown in point 1200@2.5, where the soot values obtained are the minimum values.

- The same approach can be applied in the case of regeneration points (see Figure 6.63), where the most important aspect is the delayed post injection that is done to clean the DPF. Compared to the values reported for conventional (reference) combustion conditions, certain performance stand out. Under the circumstances that this mode of combustion implies, where the local equivalence ratio at the reaction regions tend to increase, while the incomplete combustion during the expansion stroke favours the generation of soot particles, the soot values observed (whether in the lubricant or in the exhaust gases) are systematically higher than in the reference conditions. Even the values reported for these points are far from being the highest that could be compared to conventional combustion points (leaving aside the high load/speed condition points, which have recorded soot levels well above the global trend). However, within these four points, two different behaviours appear: the first one is represented by points 1200@6 and 2000@10, which show high levels of soot in oil, almost reaching 60% (59% and 48%, respectively) of the value of the soot contained in the exhaust gases. On the other hand, the other two remaining points, 2000@2 and 3400@6, do not show high levels of soot in the oil. In addition, it has been found that 2000@2 shows no signs of noticeable soot generation in the exhaust while 3400@6 shows the highest values of the four regeneration points.

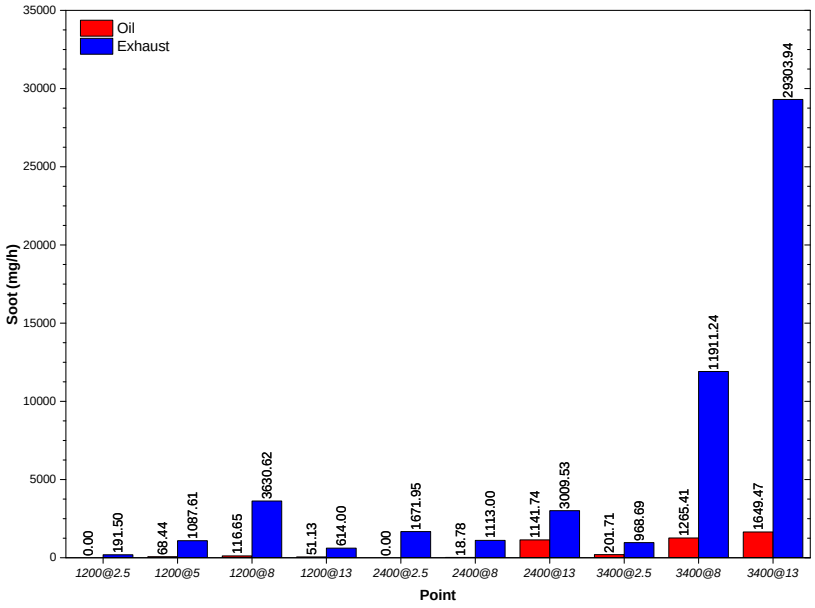

(a) Conventional combustion mode

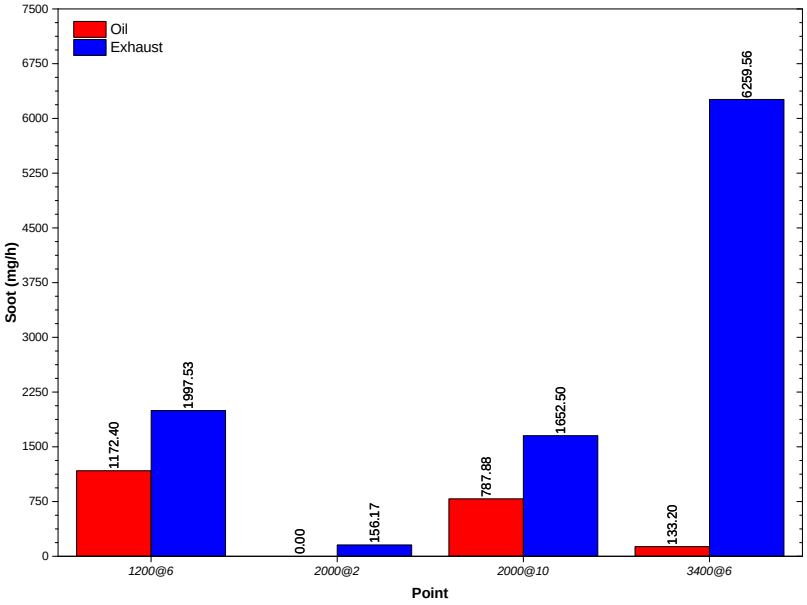

(b) DPF regeneration mode

Figure 6.61. *Soot in oil and soot in exhaust for conventional (a) and DPF regeneration (b) operating conditions.*

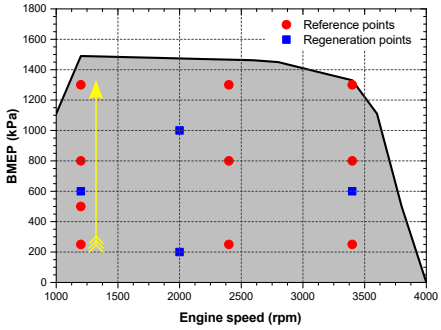

(a) BMEP evolution at constant engine speed at 1200 rpm

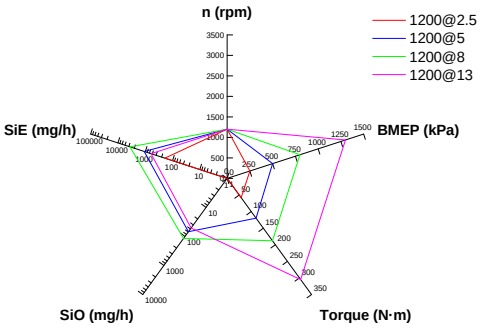

(b) Parameters at 1200 rpm

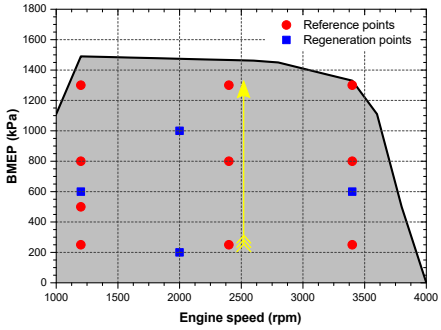

(c) BMEP evolution at constant engine speed at 2400 rpm

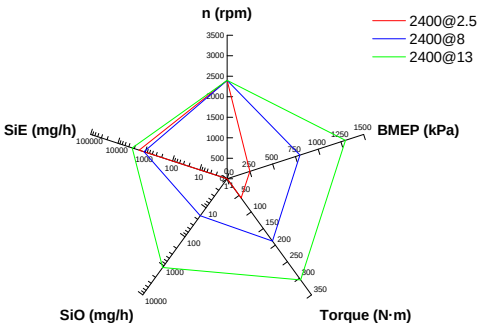

(d) Parameters at 2400 rpm

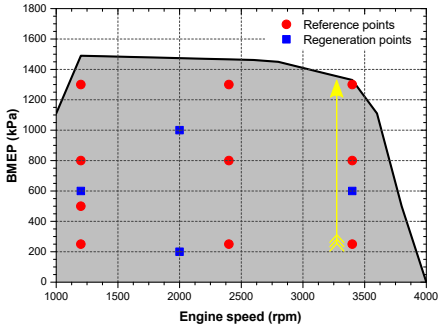

(e) BMEP evolution at constant engine speed at 3400 rpm

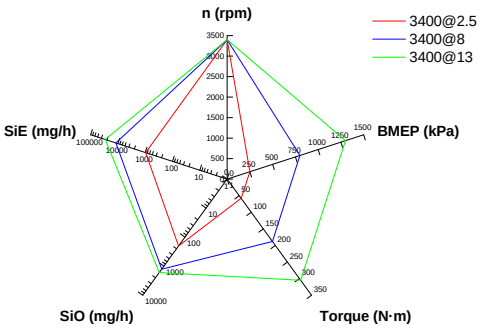

(f) Parameters at 3400 rpm

Figure 6.62. *Regular combustion mode parameter evolution at different engine speed value.*

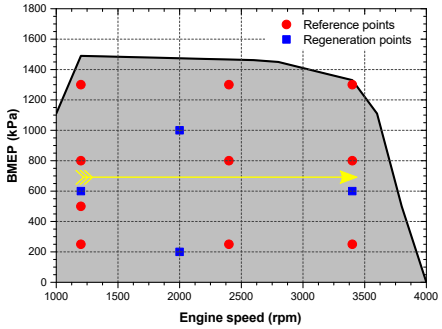

(a) Engine speed evolution at constant BMEP at 600 kPa

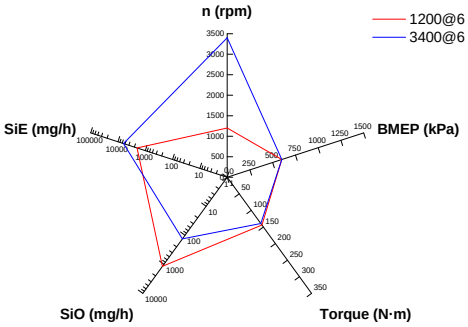

(b) Parameters at 600 kPa

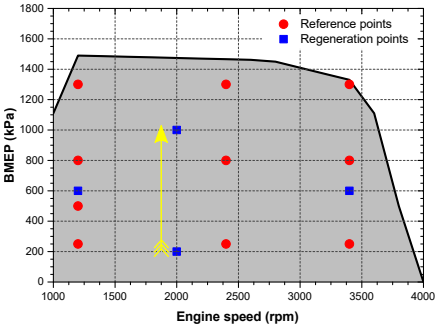

(c) BMEP evolution at constant engine speed at 2000 rpm

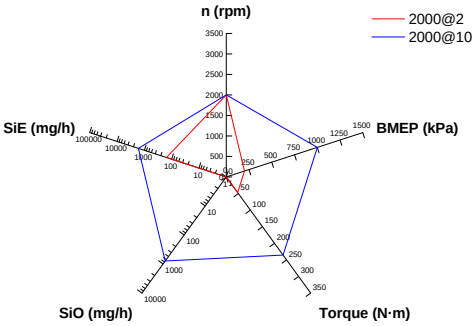

(d) Parameters at 2000 rpm

Figure 6.63. *Regeneration combustion mode parameter evolution at different situations: at constant BMEP and at constant engine speed value.*

However, in order to corroborate that the results reported in the test cell are valid, laboratory analyses were carried out on the lubricating oil samples taken during the measurement of each of the points. This off–line analysis focused on kinematic viscosity (at 40 °C) and FT–IR spectral analysis of the oil at the beginning and end of each point measurement. In this way, the aim is to determine the variation that occurs in the oil when it is exposed to the working conditions of each of the 14 points studied (10 reference points and 4 DPF regeneration points).

The first way to deal with the problem is by measuring the KV, which acts as an indicator or tracer of the lubricating oil condition: if its value is high (in relation to the original value of the lubricating oil), it is suggested that there is a considerable level of soot dissolved in the oil; whereas if it drops, then it

is the presence of fuel in the oil that is the main problem. With this principle clear, it is possible to create the Figure 6.64 and to discern between soot or fuel problems.

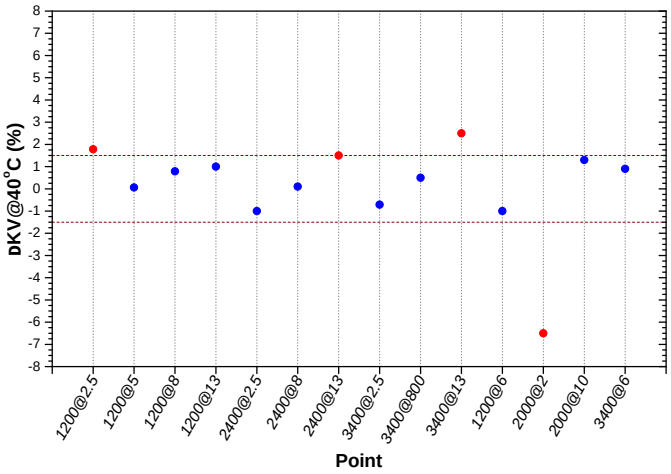

Figure 6.64. *Variation of KV at 40 degrees Celsius of engine oil from testing the reference points.*

In accordance with the test procedure proposed in this research, it was agreed to take as control limits a variation of ±1.5% of the original KV value. Four operating points are outside this confidence interval: 1200@2.5, 2400@13, 3400@13 and 2000@2. The first, 1200@2.5, it is a low speed–load test point which is an interesting example. Point 1200@2.5 has a ΔKV@40°C value that exceeds the threshold of the confidence interval, namely 1.78%. This value suggests that in this case there is a considerable presence of dissolved soot in the oil, but the values reported by BTSA and FT–IR are inconsistent. As a consequence, point 1200@2.5 should be considered as a special case requiring further study, which is beyond the scope of this research and will not be taken into consideration. The other two points with a KV increase of more than 1.5% are 2400@13 and 3400@13 (1.5% and 2.5%, respectively). In both cases, the BTSA and FT–IR measurements are consistent with the reported viscosity, given that for point 2400@13, the soot variation (ΔSoot (%) between the start of the point measurement and its end was 4.0% and for 3400@13 it was 7.7%. Finally, point 2000@2 (regeneration point) is the only point that shows a significant drop in KV. This drop is due to the fact that in this specific case, the lubricating oil contains an amount of 6.1% dissolved fuel (obtained by FT–IR). Also, note the direct relationship between HC levels registered in

the oil and exhaust (454.876 g/h HC). Furthermore, as can be seen in Figure 6.61, it is interesting the relationship between the soot obtained in the exhaust and the soot contained in the oil. In both regions, if compared with the other points, the soot values are not relevant.

6.4.4.2 Parametric points

Now, according to the results obtained in the first part of the study, it is necessary to go more deeply into the soot problem. To this end, a parametric study is carried out with the aim of obtaining a better understanding of the physical mechanisms and parameters involved in the problem under investigation. For this purpose, Table 6.11 shows the various tests where the original operating parameters (both regular combustion modes and DPF regeneration modes) were altered to identify the best scenario for reducing oil contamination by soot. Table 6.11 shows the case studies in which the influence of various agents has been studied: EGR, injection pressure (IP), injection timings (SoI for the Main and Post injection) and injected fuel mass (MoI).

This study now contrasts the response of the original point with the parametric one following the same protocol as described for the 14 original points. Figure 6.65 brings together the SiO and SiE results from each of these parametric tests.

The first parametric study is focused on the influence of EGR on the soot content in two extreme situations: one where the amount of soot, both in the oil and in the exhaust gases, is minimal (not zero) and the other where it is maximal. For this reason, the points meeting these conditions are 1200@13 and 3400@13, respectively. At these points, the EGR rate has been modified, increasing it from 0% to 8% in the case of point 1200@13, and from 17.6% to 19.8% in the case of point 3400@13. As a result, as can be seen in Figure 6.66, an increase in soot has been experienced at both locations. The presence of residual gases within the combustion chamber promotes the soot generation, specially the one registered at the exhaust.

The following parametric study is related to the effect of the injection pressure. For this purpose, the work continues with the 1200@13 and 3400@13 points, to which IP has been reduced by 200 bar: from 750 bar to 550 bar in point 1200@13 (represented as 1200@13_IP), and from 1800 bar to 1600 in point 3400@13 (represented as 3400@13_IP). Figure 6.67 shows the SiO and SiE values of this test.

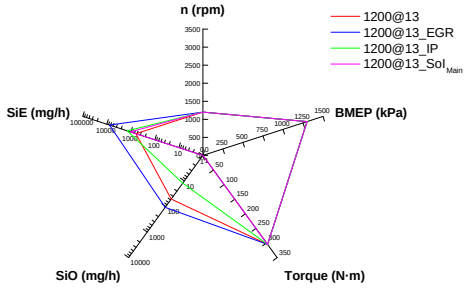

(a) 1200@13 conventional point

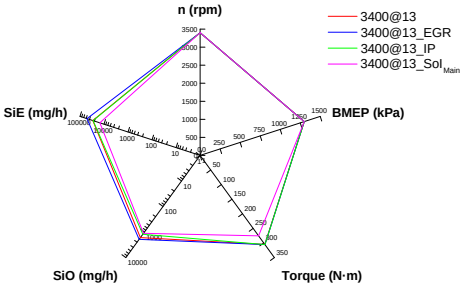

(b) 3400@13 conventional point

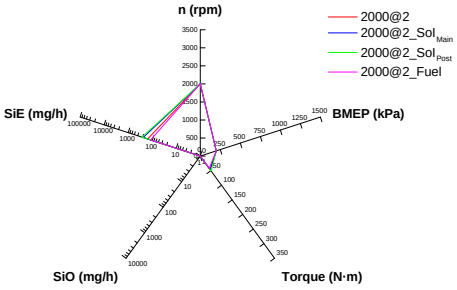

(c) 2000@2 regeneration point

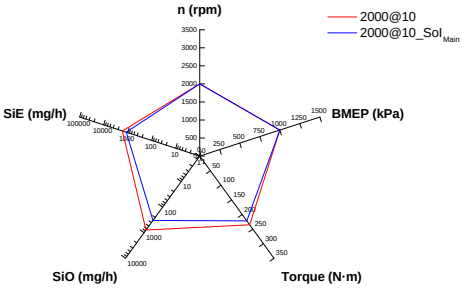

(d) 2000@10 regeneration point

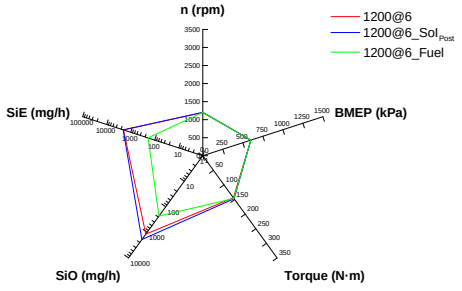

(e) 1200@6 regeneration point

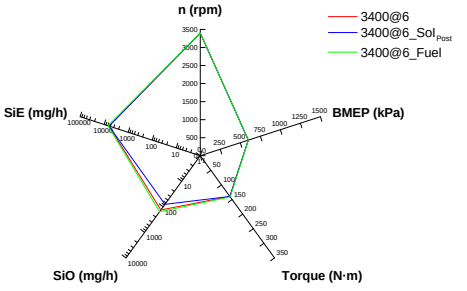

(f) 3400@6 regeneration point

Figure 6.65. *Parametric test results grouped according to the original canonical point to which they are referenced.*

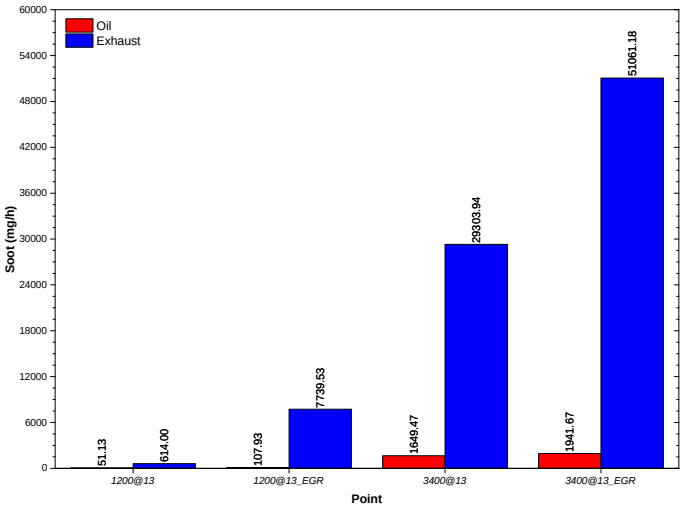

Figure 6.66. *Effect of EGR increment on the soot content.*

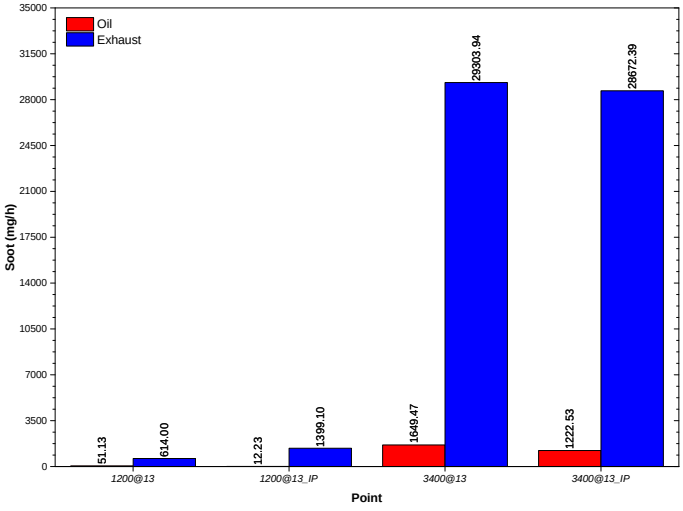

Figure 6.67. *Impact of injection pressure reduction on the soot content.*

Table 6.11. *Engine settings for the five sets of parametric studies done in the SiO study.*

Study	**ID**	**EGR** (%)	**IP** (bar)	**SoI$_{Main}$** (CAD)	**SoI$_{Post}$** (CAD)	**MoI$_{Post}$** (mg/str)
EGR	*1200@13*	0.0	750	-3.1	-	59.0
	1200@13_EGR	8.0	752	-3.2	-	59.0
	3400@13	17.6	1800	-10.8	-	60.4
	3400@13_EGR	19.8	1800	-10.8	-	60.3
IP	*1200@13*	0.0	750	-3.1	-	59.0
	1200@13_IP	0.0	550	-3.2	-	59.8
	3400@13	17.6	1800	-10.8	-	60.4
	3400@13_IP	16.8	1600	-10.8	-	60.2
SoI$_{Main}$	*1200@13*	0.0	750	-3.1	-	59.0
	1200@13_SoI$_{Main}$	0.0	752	0.8	-	59.0
	3400@13	17.6	1800	-10.8	-	60.4
	3400@13_SoI$_{Main}$	15.8	1800	-6.8	-	60.4
	2000@2	0.0	456	5.6	39.9	23.3
	2000@2_SoI$_{Main}$	0.0	440	9.4	39.8	22.7
	2000@10	0.0	794	1.4	48.2	49.5
	2000@10_SoI$_{Main}$	0.0	789	4.4	48.2	49.4
SoI$_{Post}$	*1200@6*	0.0	693	7.4	54.6	37.7
	1200@6_SoI$_{Post}$	0.0	693	7.4	50.6	37.7
	3400@6	0.0	1073	-4.8	52.0	36.2
	3400@6_SoI$_{Post}$	0.0	1075	-4.8	47.8	36.3
	2000@2	0.0	456	5.6	39.9	23.3
	2000@2_SoI$_{Post}$	0.0	456	5.6	35.8	23.4
MoI$_{Post}$	*1200@6*	0.0	693	7.4	54.6	37.7
	1200@6_Fuel	0.0	691	7.2	54.6	35.6
	3400@6	0.0	1073	-4.8	52.0	36.2
	3400@6_Fuel	0.0	1075	-4.8	52.2	34.1
	2000@2	0.0	456	5.6	39.9	23.3
	2000@2_Fuel	0.0	456	5.6	-	16.2

As far as SiO is concerned, the drop in injection pressure results in a reduction of the soot content in oil: ∼75% for 1200@13_IP and ∼25% for 3400@13_IP. This suggests that the lower momentum flux achieved by the spray due to the lower injection pressure lead to less penetration and therefore, it minimises the likelihood of soot reaching the oil film in the cylinder walls. For SiE however, the results are initially unexpected. It is known that lower injection pressure, less efficient fuel combustion, favours more soot generation. Figure 6.68 schematises the phenomenon that is taking place: bigger fuel droplets reduce the total contact surface between the oxygen (red sphere) and

fuel (blue sphere), hindering the fuel oxidation while enhancing soot particles nucleation.

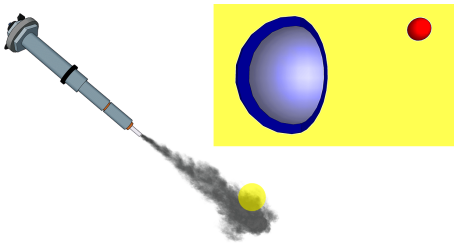

Figure 6.68. *Effect of injection pressure on fuel atomisation.*

This effect can be clearly observed in 1200@13_IP point, where SiE significantly increases, whereas the amount of SiO decreases. However, this effect is not observed in 3400@13_IP when the engine speed is increased. In this case, soot emissions are less sensitive to injection pressure since the values of soot particles at the exhaust are scarcely altered for the same variation of IP.

The next group of parametric tests are related to fuel injection with the purpose of studying its effect on soot generation and its subsequent mixing or not with the lubricant. According to Figure 6.69, this study focuses on two aspects: on the main injection for the conventional combustion and DPF regeneration modes, and on the post injection for only DPF regeneration modes.

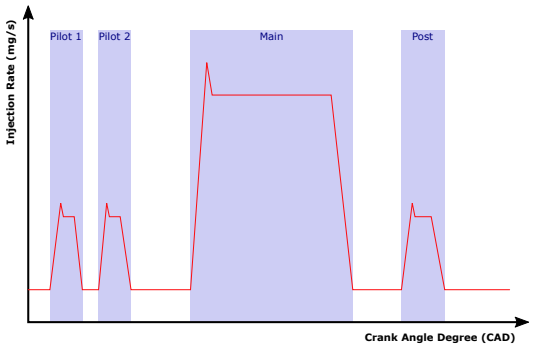

Figure 6.69. *Common injection setup comprising four injections: pilot 1, pilot 2, main and post injection.*

For the first case, the main injection was delayed by 4 CAD for conventional combustion modes for the points: 1200@13_SoI$_{\text{Main}}$ and 3400@13_SoI$_{\text{Main}}$, and 2 CAD for 2000@2_SoI$_{\text{Main}}$ and 2000@10_SoI$_{\text{Main}}$ DPF regeneration mode points. As for post injections, these were advanced by 4 CADs at the following DPF regeneration points: 1200@6_SoI$_{\text{Post}}$, 2000@2_SoI$_{\text{Post}}$ y 1200@6_SoI$_{\text{Post}}$.

In Figure 6.70 the results derived from the main injection delay have been grouped together.

According to the SiO results for point 1200@13_SoI$_{\text{Main}}$ and point 3400@13_SoI$_{\text{Main}}$ in Figure 6.70, there has been a reduction of the soot content in the lubricant in both points (to almost zero in the case of 1200@13_SoI$_{\text{Main}}$). One explanation for these results is the fact that by delaying injection, the piston is more advanced and the exposed lubricant film (located on the cylinder walls) is larger, so that a greater dilution of the soot particles in the exposed lubricant film would be expected. However, the soot particles generated under these combustion conditions are located far away from the cylinder walls, so the particles do not have enough time to migrate towards the cylinder walls, causing most of them to be expelled through the exhaust gases. However, for high engine speed situations, delaying the main injection (towards the expansion stroke) is still a valid strategy to reduce the SiE emissions. But when the engine is at low engine speed conditions, this approach is not effective, because the lower temperature dissipation due to the decreased engine speed favour the soot generation.

As for the response obtained by delaying the main injection at regeneration points, the observed trends are similar to those described for regular combustion points. But there are a number of nuances in these cases: at high load conditions (point 2000@10_SoI$_{\text{Main}}$) the soot concentration in the oil and in the exhaust is considerably reduced (around 58% and 31%, respectively). Whereas if the engine is under low load conditions, such as in point Y, as there are no significant levels of soot in the exhaust (given that SiO is zero), no noticeable changes are seen. In general, for DPF regeneration mode conditions, it is possible to control the amount of soot generated by simply adjusting the time at which the main injection takes place.

To conclude the analysis of injection timing, it is now time to study the effect of altering post injection timing. Figure 6.71 shows the results of SiO and SiE obtained when the post injection timing is modified -4 CAD in 1200@6_SoI$_{\text{Post}}$, 3400@6_SoI$_{\text{Post}}$ points.

Based on the results shown in Figure 6.71, there is a difference in the behaviour of SiO and SiE as a function of engine speed: for low speeds, as post injection is advanced, higher soot levels are achieved, specially in the lubricant

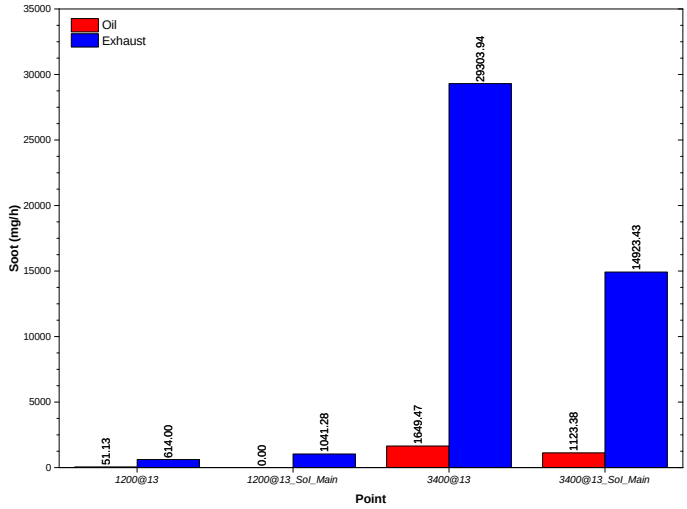

(a) Conventional combustion mode

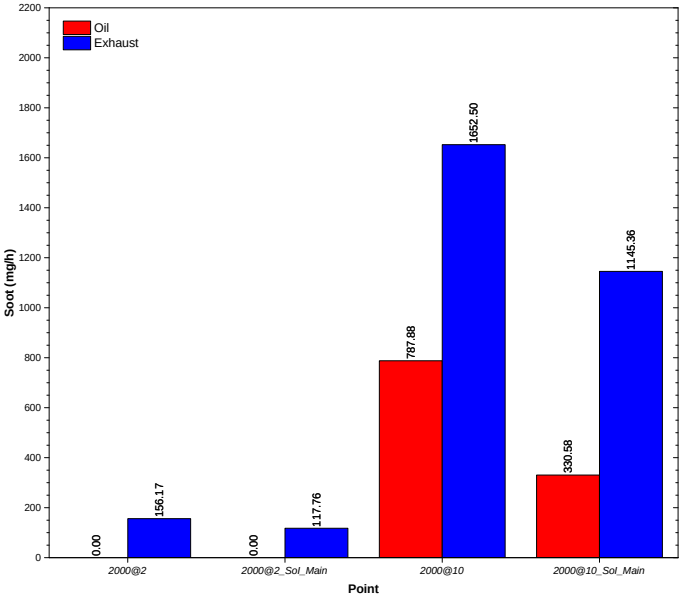

(b) DPF regeneration mode

Figure 6.70. *Influence of main injection delay, +4 CAD, on the soot content in conventional or regular combustion conditions and regeneration conditions.*

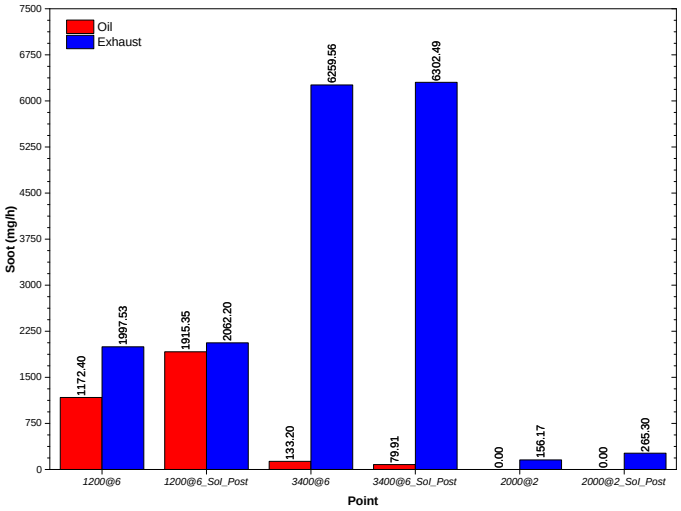

Figure 6.71. *Effect of post injection advance, -4 CAD in relation to its original value, on the soot content for DPF regeneration modes.*

(since for SiE there is practically no variation). However, at medium–high engine speeds, both parameters (SiO and SiE) are excessively non altered. In view of this unique behaviour depending on the engine speed, it leads to the conclusion that the mechanism or process that takes place for the dissolution of the soot particles in the oil film is different depending on the speed considered.

To finish with the parametric tests, the last modification focuses on the amount of fuel injected in the post injection of the regeneration points: 1200@6, 3400@6 and 2000@2. By doing so, the effect of altering the timing and amount of post injection fuel on the DPF regeneration conditions can be tested. As a result of this analysis, Figure 6.72 is generated.

Examination of the results in Figure 6.72 again reveals differences in behaviour between low and medium–high regime conditions. In 1200@6_Fuel the SiO decreases by 80% of its value at origin, while SiE levels are virtually unaffected by changes in the mass of fuel injected (MoI). However, in the 3400@6_Fuel and 2000@2_Fuel points where the post injection was removed, there are no significant changes that are relevant (only a very slight increase in the amount of soot, nothing remarkable).

As for the study involving the reference points, at the end of the parametric engine test points, some verification of the reported soot values is necessary. For this reason, a further analysis of the KV and FT–IR spectra

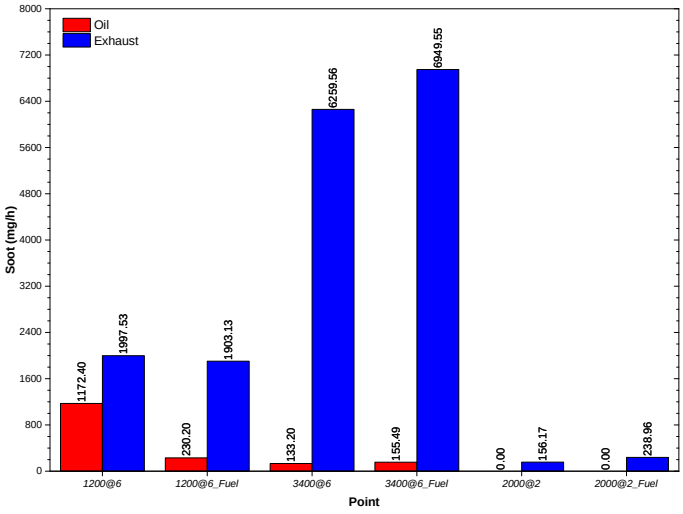

Figure 6.72. *Effect of injected fuel mass (post) on the soot content for DPF regeneration modes.*

of the lubricating oil samples collected during the test will be carried out. Specifically, the points to be studied are those related to the post injection timing and the amount of fuel mass injected when the engine is operating under DPF regeneration conditions since under these conditions, the soot values do not present a logical or consistent trend.

So, by analysing the kinematic viscosity variation at 40 degrees Celsius of the oil samples from the parametric tests (between the beginning and end of all tests performed), Figure 6.73 can be generated. Taking the same confidence interval of $\pm 1.5\%$ of ΔKV@40°C, four points above this limit: 3400@13_EGR, 2000@2_SoI_{Main}, 2000@2_SoI_{Post} and 2000@2_Fuel.

For the first and only case exceeding the confidence interval, 3400@13_EGR point, the increase in SiO content is due to the increase in EGR. This increase in the amount of soot is consistent with the values reported by the BTSA equipment and with the FT–IR spectroscopy (where it was observed that the soot content experienced an increase of 0.203 %). Since the levels of HC in the oil and at the exhaust do not show a significant increment, the fuel dilution can be considered small and this measurement can be considered fully valid. The other three remaining points, derived from the 2000@2 reference point, experience a strong reduction in kinematic viscosity. At each of the three points, the amount of fuel contained in the lubricating oil (analysed by FT–

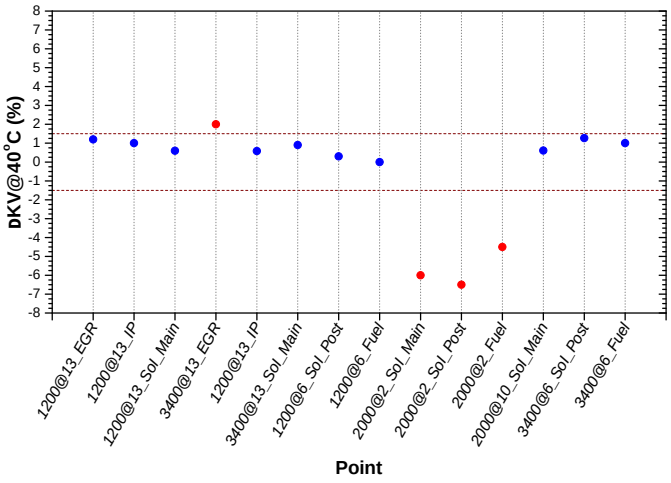

Figure 6.73. *Variation of KV at 40 degrees Celsius of engine oil from testing the parametric test points.*

IR) is considerable: 5.1% for 2000@2_SoI$_{\text{Main}}$, 7.1% for 2000@2_SoI$_{\text{Post}}$ and 2.7% for 2000@2_Fuel.

6.4.4.3 Analysis of numerical simulations

Now, in order to provide a better explanation of the experimental results obtained, the CFD model described above will be used. Thanks to the collaboration of Dr. José M. Pastor and Dr. Ricardo Novella, who carried out and developed the work related to the CFD model implementation, it has been possible to complete this study. With this tool it is possible to analyse the consequences of emission control strategies in the lubricant contamination by soot particles and fuel.

This numerical model has been used as a tool to visualise the phenomenon of lubricating oil contamination, a process that is difficult to follow in an experimental (empirical) way. Thus, two different situations have been chosen to better observe the potential of this tool:

- Firstly, the point 3400@13 has been selected, representative of an engine operating condition under regular combustion
- While, on the contrary, representing the DPF regeneration conditions, the point 2000@2 has been chosen.

These two points are very good candidates for observing divergences in the phenomena occurring inside the engine and are conditioning factors for the final recorded behaviour (as far as soot is concerned: its generation rate and whether it subsequently migrates into the lubricating oil or into the exhaust together with the combustion gases).

For point 3400@13, three modifications were made in relation to its original parameters: EGR, injection pressure and main injection timing. Of these three, those that had the greatest impact in terms of soot were the first (labelled 3400@13_EGR) and the last (3400@13_SoI$_{\text{Main}}$); while the second (3400@13_IP) is not relevant. Figure 6.74 shows a series of snapshots of different phases of the combustion process at each of the above–mentioned points. In order to facilitate the comprehesion of the process to be studied, the trio of captures (at 60, 80 and 90 cad) focused on the final stage of combustion inside the combustion chamber, since this is the stage where soot is mainly generated.

Two important aspects can be seen in Figure 6.74: firstly, the difference in the deposition pattern of soot particles on the cylinder walls, and the soot levels generated by the combustion process can be observed (at a given representative value):

- For 3400@13_EGR in contrast with 3400@13, the soot iso–surfaces have a similar pattern: two main soot clouds. According to the distribution of these iso–surfaces, the soot is generated in two regions: one located close to the centre of the combustion chamber within the piston bow, and other located in the squish region in contact with the cylinder wall. Also, as the EGR is increased, the amount of soot produced is expected to be higher (as a consequence of worse mixing conditions), so the iso–surfaces at this point are higher. Looking at the image at the end of the expansion stroke (90 cad), in this case where the differences are more easily detectable, it can be seen that there is a greater amount of soot near the piston walls, which favours the deposition of more soot particles (SiO increases).

- By reducing the injection pressure at point 3400@13_IP, as observed in the SiO and SiE values in Figure 6.67, no significant changes are observed. In that parametric test the soot levels are the same but the pattern is not. Now the iso–surfaces shape (pattern) is different but the soot levels are the same, consequently, this small changes do not affect enough to the recorded SiO and SiE values.

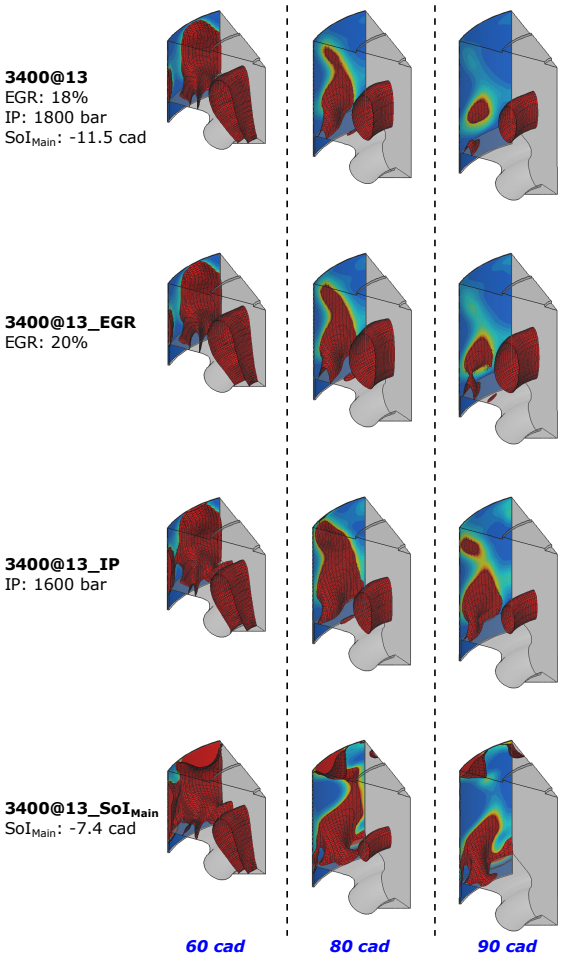

Figure 6.74. *Soot generation (brown iso–surfaces) and soot particles deposition in the lubricant film of the liner wall (contour plot).*

- When the main injection timing is altered, it can be seen that the 3400@13_SoI$_{\text{Main}}$ point differs greatly from the original 3400@13 point. As can be seen in the pictures, the pattern of the iso–surfaces blurs as it goes from 60 to 90 cad, so that all the soot that was located in the centre of the combustion chamber spreads out. When the soot disappears, a completely different pattern is registered, resulting in a reduction of the amount of soot dissolved in the oil.

The 2000@2 point of DPF regeneration conditions is the other analysed example due to its peculiarities. This is a particular situation because in none of the parametric studies, any effect on SiO values has been observed. Because of this, a combustion process tracing has been prepared from the moment the main injection is made until the combustion is completed.

Thus, in Figure 6.75, two aspects involved in the process to be followed have been brought together: in the first line, the soot generation has been represented (under the same guidelines as those used for point 3400@13) and in the second line the evolution of the UHC (unburned hydrocarbons).

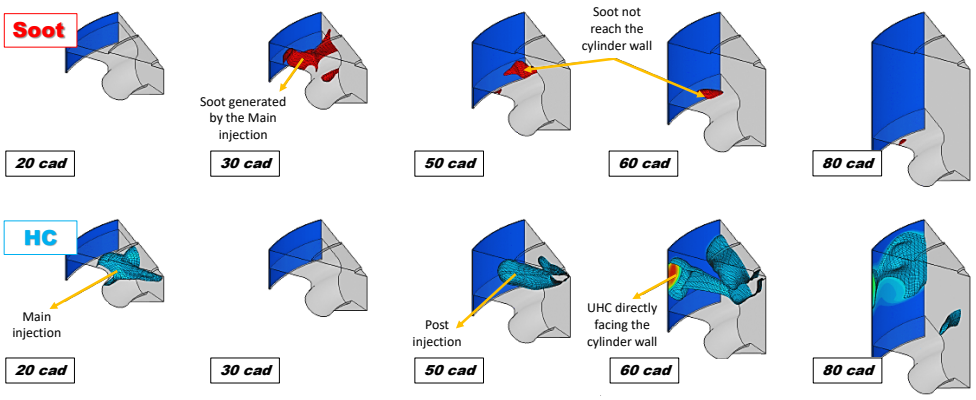

Figure 6.75. *Monitoring and evolution of soot and UHC at point 2000@2.*

These snapshots show the entire sequence from 20 cad to 80 cad. Thanks to this it is possible to observe that the soot particles that are generated do not reach the walls on which the lubricant film is located (soot concentration iso–surfaces become smaller due to the soot particles diffusion), so that SiO mixing is not produced. Moving on to the next family of snapshots, the fuel injected in the main injection is totally consumed (HC iso–surface disappears), which is consistent with its counterpart for soot. However, at 50 cad, the post-injection is performed during the expansion stroke; under these conditions, that amount of fuel is not completely burned (most of the fuel remains inert once the injection is finished whereas no soot is generated), which leads to some of the UHC to reach the cylinder walls and mix with the lubricant (note how in the last picture, where the exhaust valve is open, the amount of UHC in contact with the oil is significant).

6.4.5 Conclusions

Thanks to the combination of experimental measurements and numerical studies, it has been possible to obtain a better understanding of the effect of emission–control strategies on the lubricant oil tribological properties and, in particular, about the mechanism of soot in oil (SiO) and fuel dilution contamination.

In order to better study the different mechanisms that cause or lead to soot and fuel contamination of the lubricant, as a consequence of emission control strategies applied to engines (in particular for diesel engines), on–line (directly from the engine) and off–line (laboratory samples measurements) experimental analysis methodologies have been developed that have been useful for the construction and validation of the CFD model that was developed specifically for this study. As a result, the following events or trends were observed:

- The contamination of the lubricant by soot depends mainly on the operating conditions of the engine: the most demanding conditions (high speeds and high loads) are the most critical. Thus, even though the engine may be operating in high smoke combustion conditions (high soot generation rates), this does not lead to corresponding soot levels in the oil. Whereas, for fuel contamination, the most important parameters are the delayed injections (Post). This behaviour was reflected in the results obtained both experimentally and by means of the numerical model.

- With regard to the emission control strategies studied, several conclusions could be drawn:

  - The EGR is a source of soot contamination in the oil due to its mode of operation. Because the EGR uses the waste or residual gases from the previous combustion in the current combustion, the atmosphere generated inside the combustion chamber is a less reactive atmosphere, which favours the formation of more soot particles.
  - Similarly, when the injection pressure (IP) is altered, soot management is also affected. In fact, if the pressure is increased, both SiO and SiE are enhanced.
  - The change of the injection map is dependent on the engine operating conditions: under regular combustion conditions, it was observed that by delaying the main injection the SiO and SiE values are reduced but, when the timing of the post injection is altered,

under DPF regeneration conditions, the impact is very limited (only a slight increase of SiO is observed if the conditions are: constant level of soot generated at medium load and low engine speed).

  - The amount of fuel injected is not an agent that causes major alterations in the soot generation mechanism.

- Numerical models have shed light on the experimental results obtained by visualising the soot particle generation process, their evolution inside the combustion chamber (migration through convection and diffusion mechanisms) and, finally, the deposition of these particles on the lubricant film on the cylinder walls. Thus, taking advantage of the results provided by these tools, the next facts were found:

  - EGR does not alter the spatial pattern of the soot inside the chamber, but it does alter the overall amount of soot (and consequently SiO).
  - The spatial pattern of the soot particles is dependent on the timing of the injections. It was found that by delaying the main injection, the pattern changed, leading to a situation of decreased SiO.
  - The last conclusion is correlated to the late post injections. This post injections do not contribute to either the soot generation or the SiO. This is due to the poor thermodynamic conditions during the expansion stroke that hinder the complete burning of the fuel, avoiding the soot generation while leading the unburned HC directly to the cylinder wall.

- Both the experimental and the numerical part are subject to improvements which, at the date of the study, there was neither sufficient capacity nor the means to carry them out. This fact is exposed as a consequence of the need to further refine the model improving its sensitivity and simulation capabilities (e.g. when making changes in injection pressure and in the mass quantity of fuel injected in post–injections).

4.A Appendix: Extra information about SiO quantification techniques

4.A.1 IR Spectroscopy

4.A.1.1 Wavenumber for the quantification of soot in oil

The absorbance responses of the oil soot standards used for the calibration of the FT–IR spectrophotometer used in this Thesis are shown below, focusing on the selected wavenumber values: 3800, 3600, 2250, 2000, 1980 and 1870 cm^{-1}. Thus, for each of these wavenumbers, the linearity of the response has been analysed as shown in Figure 4.76.

4.A.2 UV–Vis Spectroscopy

4.A.2.1 Low mileage engine oil samples

This section gathered information about samples of low-use engine lubricating oil, which were collected from a diesel engine set up on a test bench which was running stationary tests for a duration of 4 hours.

In Table 4.12, the absorbance values of these used lubricating oil samples have been compiled for the selected 800 nm wavelength.

Table 4.12. *Absorbances at 800 nm of the different sample sets.*

Abs.@800 nm	Sample 1	Sample 2	Sample 3	Sample 4	Sample 5	Sample 6	Sample 7
0 min.	0.0198	0.0023	0.0017	0.0043	0.0080	0.0026	0.0035
5 min.	0.0202	0.0029	0.0027	0.0046	0.0081	0.0027	0.0037
15 min.	0.0207	0.0031	0.0032	0.0052	0.0088	0.0028	0.0038
30 min.	0.0225	0.0047	0.0037	0.0057	0.0092	0.0030	0.0041
45 min.	0.0237	0.0065	0.0051	0.0060	0.0092	0.0032	0.0044
60 min.	0.0240	0.0088	0.0060	0.0070	0.0097	0.0034	0.0048
240 min.	0.0354	0.0243	0.0154	0.0129	0.0148	0.0067	0.0095

From the absorbance values gathered in Table 4.12, it can be extrapolated to the soot content based on the empirical correlation extracted from the calibration of the UV–Vis spectrophotometer with the soot in oil standards. Thus, in Figure 4.77, the evolution of the soot quantity for each set of samples has been gathered.

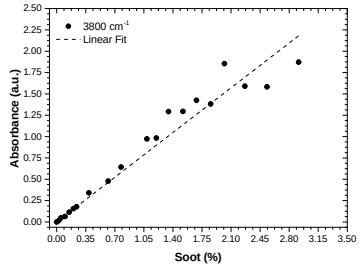

(a) At 3800 cm^{-1}, $R^2 = 0.97629$

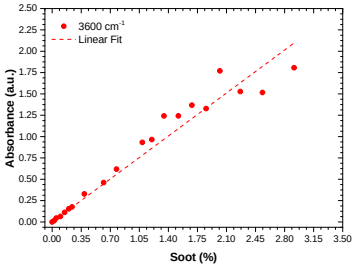

(b) At 3600 cm^{-1}, $R^2 = 0.97669$

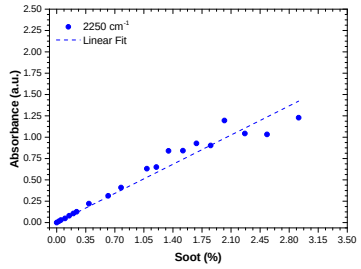

(c) At 2250 cm^{-1}, $R^2 = 0.97767$

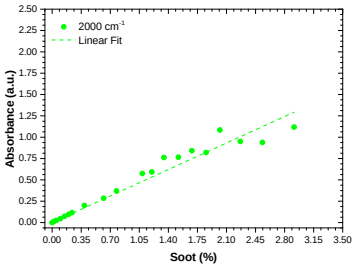

(d) At 2000 cm^{-1}, $R^2 = 0.97791$

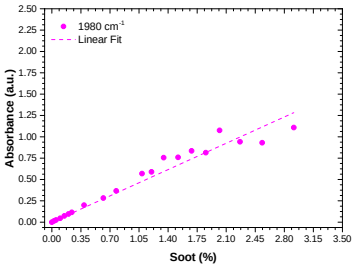

(e) At 1980 cm^{-1}, $R^2 = 0.97787$

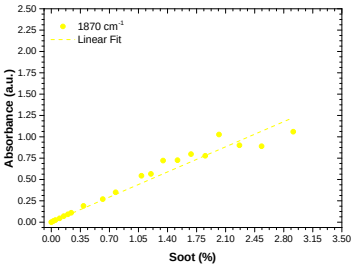

(f) At 1870 cm^{-1}, $R^2 = 0.97801$

Figure 4.76. *Linear trends (represented by the value of R^2) observed when analysing the absorbances of oil soot patterns at agreed wavenumbers.*

As noted, the different trends in the evolution of the soot content in the seven samples, collected from the engine bench test: Sample 1, Sample 2, Sample 3, Sample 4, Sample 5, Sample 6 and Sample 7, follows a clearly linear evolution. Each of these samples has been coloured following the same pattern as in Figure 6.48 in order to facilitate the understanding and monitoring of these trends.

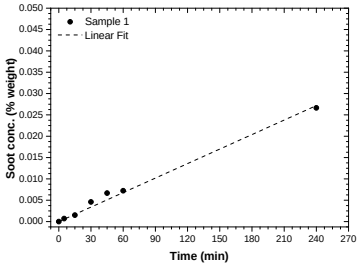

(a) Set 1, $R^2 = 0.99375$

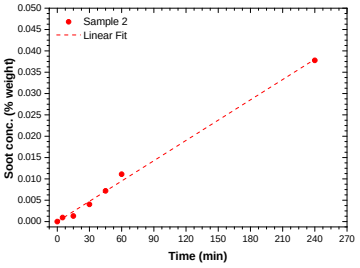

(b) Set 2, $R^2 = 0.99691$

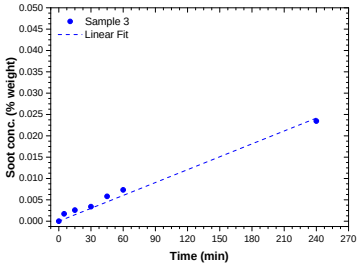

(c) Set 3, $R^2 = 0.98831$

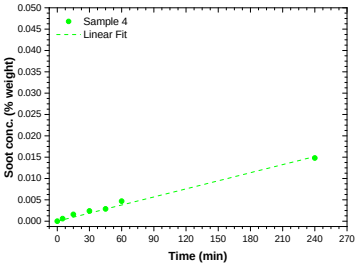

(d) Set 4, $R^2 = 0.99234$

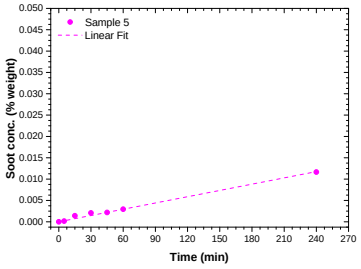

(e) Set 5, $R^2 = 0.99349$

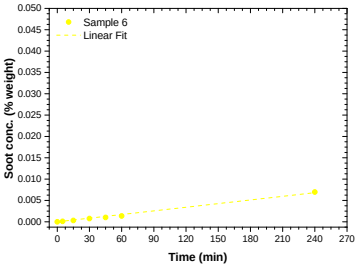

(f) Set 6, $R^2 = 0.99467$

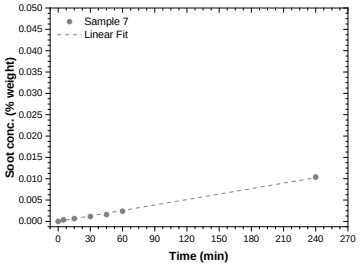

(g) Set 7, $R^2 = 0.99799$

Figure 4.77. *Set of samples and its fit (represented by R^2) to a linear evolution.*

Bibliography

[1] L. B. Abdulqadir, N. F. Mohd Nor, R. Lewis, and T. Slatter. Contemporary challenges of soot build-up in IC engine and their tribological implications. *Tribology-Materials, Surfaces & Interfaces*, 12(3):115–129, 2018.

[2] A. Al Sheikh Omar, F. Motamen Salehi, U. Farooq, A. Morina, and A. Neville. Chemical and physical assessment of engine oils degradation and additive depletion by soot. *Tribology International*, 160:107054, 2021.

[3] H. B. Al-Wakeel, Z. A. Abdul Karim, and H. H. Al-Kayiem. Soot reduction strategy: A review. *Journal of Applied Sciences*, 12(23):2338–2345, 2012.

[4] Inc. Analytical Engineering. *User's manual: Bench top soot analyzer (BTSA)*, 2017.

[5] C. Angelberger, T. Poinsot, and B. Delhay. Improving near-wall combustion and wall heat transfer modelling in SI engine computations. In *International Fuels & Lubricants Meeting & Exposition*. SAE International, oct 1997. doi:10.4271/972881.

[6] S. Antusch, M. Dienwiebel, E. Nold, P. Albers, U. Spicher, and M. Scherge. On the tribochemical action of engine soot. *Wear*, 269(1-2):1–12, 2010.

[7] A. Asango, A. La Rocca, and P. Shayler. Investigating the effect of carbon nanoparticles on the viscosity of lubricant oil from light duty automotive diesel engines. In *World Congress & Exhibition*. SAE International, jan 2014. doi:10.4271/2014-01-1481.

[8] E. A. Bardasz, V. A. Carrick, H. F. George, M. M. Graf, R. E. Kornbrekke, and S. B. Pocinki. Understanding soot mediated oil thickening through designed experimentation Part 4: Mack T-8 test. In *International Spring Fuels & Lubricants Meeting & Exposition*. SAE International, may 1997. doi:10.4271/971693.

[9] H. Bockhorn. Mechanisms and models of soot formation: final discussion and perspectives. In *Soot Formation in Combustion*, pages 577–588. Springer, 1994.

[10] H. Bockhorn. *Combustion generated fine carbonaceous particles: Proceedings of an international workshop*. KIT Scientific publishing, 2009.

[11] H. Bockhorn. *Soot formation in combustion: mechanisms and models*, volume 59. Springer Science & Business Media, 2013.

[12] A. Bredin, A. V. Larcher, and B. J. Mullins. Thermogravimetric analysis of carbon black and engine soot–Towards a more robust oil analysis method. *Tribology international*, 44(12):1642–1650, 2011.

[13] A. Broatch, X. Margot, R. Novella, and J. Gómez-Soriano. Impact of the injector design on the combustion noise of gasoline partially premixed combustion in a 2-stroke engine. *Applied Thermal Engineering*, 119:530–540, 2017.

[14] A. Broatch, R. Novella, J. García-Tíscar, and J. Gómez-Soriano. Potential of dual spray injectors for optimising the noise emission of gasoline partially premixed combustion in a 2-stroke HSDI CI engine. *Applied Thermal Engineering*, 134:369–378, 2018.

[15] A. Bueno-López. Diesel soot combustion ceria catalysts. *Applied Catalysis B: Environmental*, 146:1–11, 2014.

[16] F. Chinas-Castillo and H. A. Spikes. The behavior of diluted sooted oils in lubricated contacts. *Tribology Letters*, 16(4):317–322, 2004.

[17] M. Y. Choi, G. W. Mulholland, A. Hamins, and T. Kashiwagi. Comparisons of the soot volume fraction using gravimetric and light extinction techniques. *Combustion and Flame*, 102(1-2):161–169, 1995.

[18] S. M. Chun. A study on the effect of soot on changes in diesel engine oil's dielectric constant. *Tribology and Lubricants*, 26(2):111–121, 2010.

[19] A. D. H. Clague, J. B. Donnet, T. K. Wang, and J. C. M. Peng. A comparison of diesel engine soot with carbon black. *Carbon*, 37(10):1553–1565, 1999.

[20] P. Colacicco and D. Mazuyer. The role of soot aggregation on the lubrication of diesel engines. *Tribology transactions*, 38(4):959–965, 1995.

[21] O. Colin and A. Benkenida. The 3-zones extended coherent flame model (ECFM3Z) for computing premixed/diffusion combustion. *Oil & Gas Science and Technology*, 59(6):593–609, 2004.

[22] D. Crolla. *Encyclopedia of automotive engineering*. John Wiley & Sons, 2015.

[23] L. Dahlén. *On applied CFD and model development in combustion systems development for DI diesel engines*. PhD thesis, Royal Institute of Technology, Stockholm, Sweden, 2002.

[24] G. Di Liberto. *Mechanisms of soot transfer to oil of an HPCR diesel engine*. PhD thesis, University of Nottingham, 2017.

[25] P. P. Duvvuri, R. K. Shrivastava, S. Sukumaran, and S. Sreedhara. Numerical modelling of thermophoretic deposition on cylinder liner of a diesel engine using a sectional soot model. *Journal of Aerosol Science*, 139:105464, 2020.

[26] P. Eastwood. *Particulate emissions from vehicles*, volume 20. John Wiley & Sons, 2008.

[27] P. F. Flynn, R. P. Durrett, G. L. Hunter, A. O. Zur Loye, O. C. Akinyemi, and et al. Diesel combustion: An integrated view combining laser diagnostics, chemical kinetics, and empirical validation. In *Future Transportation Technology Conference & Exposition*. SAE International, mar 1999. doi:10.4271/1999-01-0509.

[28] M. Frenklach and H. Wang. Detailed modeling of soot particle nucleation and growth. In *Symposium (International) on Combustion*, volume 23, pages 1559–1566. Elsevier, 1991.

[29] M. Frenklach, H. Wang, and H. Bockhorn. Soot formation in combustion: mechanisms and models. *Springer series in chemical physics*, 59:165–192, 1994.

[30] H. Fujita and H. Spikes. The influence of soot on lubricating films. *Tribology Series*, 43:37–43, 2004.

[31] S. George, S. Balla, and M. Gautam. Effect of diesel soot contaminated oil on engine wear. *Wear*, 262(9-10):1113–1122, 2007.

[32] S. George, S. Balla, V. Gautam, and M. Gautam. Effect of diesel soot on lubricant oil viscosity. *Tribology International*, 40(5):809–818, 2007.

[33] B. Giechaskiel, M. Maricq, L. Ntziachristos, C. Dardiotis, X. Wang, and et al. Review of motor vehicle particulate emissions sampling and measurement: From smoke and filter mass to particle number. *Journal of Aerosol Science*, 67:48–86, 2014.

[34] D. Green. *The tribological effects of soot contaminated lubricants on engine components*. PhD thesis, University of Sheffield, 2007.

[35] D. A. Green and R. Lewis. Effect of soot on oil properties and wear of engine components. *Journal of Physics D: Applied Physics*, 40(18):5488, 2007.

[36] D. A. Green and R. Lewis. The effects of soot-contaminated engine oil on wear and friction: a review. *Proceedings of the Institution of Mechanical Engineers, Part D: Journal of Automobile Engineering*, 222(9):1669–1689, 2008.

[37] D. A. Green, R. Lewis, and R. S. Dwyer-Joyce. Wear effects and mechanisms of soot-contaminated automotive lubricants. *Proceedings of the Institution of Mechanical Engineers, Part J: Journal of Engineering Tribology*, 220(3):159–169, 2006.

[38] C. Habchi, F. A. Lafossas, P. Béard, and D. Broseta. Formulation of a one-component fuel lumping model to assess the effects of fuel thermodynamic properties on internal combustion engine mixture preparation and combustion. In *Fuels & Lubricants Meeting & Exhibition*. SAE International, jun 2004. doi:10.4271/2004-01-1996.

[39] A. K. Hasannuddin, J. Y. Wira, S. Sarah, W. M. N. Wan Syaidatul Aqma, A. R. Abdul Hadi, and et al. Performance, emissions and lubricant oil analysis of diesel engine running on emulsion fuel. *Energy conversion and management*, 117:548–557, 2016.

[40] B. S. Haynes and H. G. Wagner. Soot formation. *Progress in energy and combustion science*, 7(4):229–273, 1981.

[41] H. Hiroyasu and T. Kadota. Models for combustion and formation of nitric oxide and soot in direct injection diesel engines. In *Automotive Engineering Congress & Exposition*. SAE International, feb 1976. doi:10.4271/760129.

[42] E. Hu, X. Hu, T. Liu, L. Fang, K. D. Dearn, and H. Xu. The role of soot particles in the tribological behavior of engine lubricating oils. *Wear*, 304(1-2):152–161, 2013.

[43] K. Y. Huh. A phenomenological model of diesel spray atomization. In *Proc. of The International Conf. on Multiphase Flows' 91-Tsukuba*, 1991.

[44] ASTM International. *ASTM D5967-17 Standard test method for evaluation of diesel engine oils in T-8 diesel engine*, 2017. doi:10.1520/D5967-17.

[45] ASTM International. *ASTM D893-14 Standard test method for insolubles in used lubricating oils*, 2018. doi:10.1520/D0893-14R18.

[46] ASTM International. *ASTM D7686-19 Standard test method for field-based condition monitoring of soot in in-service lubricants using a fixed-filter infrared (IR) instrument*, 2019. doi:10.1520/D7686-19.

[47] ASTM International. *ASTM D7899-19 Standard test method for measuring the merit of dispersancy of in-service engine oils with blotter spot method*, 2019. doi:10.1520/D7899-19.

[48] ASTM International. *ASTM D7844-20 Standard test method for condition monitoring of soot in in-service lubricants by trend analysis using Fourier Transform Infrared (FT-IR) Spectrometry*, 2020. doi:10.1520/D7844-20.

[49] R. I. Issa. Solution of the implicitly discretised fluid flow equations by operator-splitting. *Journal of computational physics*, 62(1):40–65, 1986.

[50] T. C. Jao, S. Li, K. Yatsunami, S. J. Chen, A. A. Csontos, and J. M. Howe. Soot characterisation and diesel engine wear. *Lubrication Science*, 16(2):111–126, 2004.

[51] R. Jatoth, S. K. Gugulothu, R. K. S. Gadepalli, B. Burra, and S. Rafiuzzama. Impact of thermophoresis factor on soot particle trajectories near the in-cylinder wall in a diesel engine. *International Journal of Environmental Science and Technology*, pages 1–16, 2021.

[52] H. Jiang, T. Li, Y. Wang, P. He, and B. Wang. The evolution of soot morphology and nanostructure along axial direction in diesel spray jet flames. *Combustion and Flame*, 199:204–212, 2019.

[53] A. Karlsson, I. Magnusson, M. Balthasar, and F. Mauss. Simulation of soot formation under diesel engine conditions using a detailed kinetic soot model. In *International Fuels & Lubricants Meeting & Exposition*. SAE International, feb 1998. doi:10.4271/981022.

[54] I. M. Kennedy. Models of soot formation and oxidation. *Progress in Energy and Combustion Science*, 23(2):95–132, 1997.

[55] A. A. Khaziev, N. N. Sugatov, and A. V. Laushkin. The development of a dependent mathematical model of dielectric properties of an engine oil to the concentration of soot formation. In *IOP Conference Series: Materials Science and Engineering*, volume 1159, page 012094. IOP Publishing, 2021.

[56] R. Khobragade, S. K. Singh, P. C. Shukla, T. Gupta, A. S. Al-Fatesh, and et al. Chemical composition of diesel particulate matter and its control. *Catalysis Reviews*, 61(4):447–515, 2019.

[57] M. R. Kholghy, A. Veshkini, and M. J. Thomson. The core–shell internal nanostructure of soot–A criterion to model soot maturity. *Carbon*, 100:508–536, 2016.

[58] D. Kittelson and M. Kraft. Particle formation and models. *Encyclopedia of Automotive Engineering*, pages 1–23, 2014.

[59] D. B. Kittelson. Engines and nanoparticles: a review. *Journal of aerosol science*, 29(5-6):575–588, 1998.

[60] K. Kondo, J. Takahashi, and T. Aizawa. Morphology analysis of wall-deposited diesel soot particles via transmission electron microscope. *SAE International Journal of Fuels and Lubricants*, 7(3):683–692, 2014.

[61] M. Kraft. Modelling of particulate processes. *KONA Powder and Particle Journal*, 23:18–35, 2005.

[62] K. Kudlaty. *Attenuated total reflection technique for on-line oil monitoring by means of a FTIR fiber-optic probe*. PhD thesis, Technische Universität München, 2004.

[63] O. Laget, L. M. Malbec, J. Kashdan, N. Dronniou, R. Boissard, and P. Gastaldi. Experimental and numerical investigations on the mechanisms leading to the accumulation of particulate matter in lubricant oil. *SAE International Journal of Engines*, 9(4):2030–2043, 2016.

[64] F. Lantos. An unusual twist to the blotter test-the Lantos Method. *Practicing Oil Analysis Magazine*, 2002.

[65] M. Lapuerta, F. J. Martos, and J. Herreros. Effect of engine operating conditions on the size of primary particles composing diesel soot agglomerates. *Journal of aerosol science*, 38(4):455–466, 2007.

[66] G. Lepperhoff. Influences on the particle size distribution of diesel particulate emissions. *Topics in Catalysis*, 16(1):249–254, 2001.

[67] D. O. Lignell, J. H. Chen, P. J. Smith, T. Lu, and C. K. Law. The effect of flame structure on soot formation and transport in turbulent nonpremixed flames using direct numerical simulation. *Combustion and Flame*, 151(1-2):2–28, 2007.

[68] C. Liu, S. Nemoto, and S. Ogano. Effect of soot properties in diesel engine oils on frictional characteristics. *Tribology Transactions*, 46(1):12–18, 2003.

[69] N. Liu, Z. C. Zheng, and G. X. Li. Analysis of the blow-by in piston ring pack of the diesel engine. *Chemical Engineering Transactions*, 46:1045–1050, 2015.

[70] P. Liu and C. Wang. The diesel soot particles fractal growth model and its agglomeration control. In *Kinetic Modelling for Environmental Systems*. IntechOpen, 2018.

[71] F. E. Lockwood, Z. G. Zhang, S. Choi, and W. Yu. Effect of soot loading on the thermal characteristics of diesel engine oils. In *Vehicle Thermal Management Systems Conference & Exposition*. SAE International, jan 2001. doi:10.4271/2001-01-1714.

[72] V. Macián, B. Tormos, S. Ruiz, and A. García-Barberá. An alternative procedure to quantify soot in engine oil by ultraviolet-visible spectroscopy. *Tribology Transactions*, 62(6):1063–1071, 2019.

[73] R. Mainwaring. Soot and wear in heavy duty diesel engines. In *International Spring Fuels & Lubricants Meeting & Exposition*. SAE International, may 1997. doi:10.4271/971631.

[74] Z. A. Mansurov. Soot formation in combustion processes. *Combustion, Explosion and Shock Waves*, 41(6):727–744, 2005.

[75] M. M. Maricq. Chemical characterization of particulate emissions from diesel engines: A review. *Journal of Aerosol Science*, 38(11):1079–1118, 2007.

[76] U. Mathis, M. Mohr, R. Kaegi, A. Bertola, and K. Boulouchos. Influence of diesel engine combustion parameters on primary soot particle diameter. *Environmental science & technology*, 39(6):1887–1892, 2005.

[77] H. A. Michelsen. Probing soot formation, chemical and physical evolution, and oxidation: A review of in situ diagnostic techniques and needs. *Proceedings of the Combustion Institute*, 36(1):717–735, 2017.

[78] S. Mohankumar and P. Senthilkumar. Particulate matter formation and its control methodologies for diesel engine: A comprehensive review. *Renewable and Sustainable Energy Reviews*, 80:1227–1238, 2017.

[79] J. Moldanová, E. Fridell, H. Winnes, S. Holmin-Fridell, J. Boman, and et al. Physical and chemical characterisation of PM emissions from two ships operating in European Emission Control Areas. *Atmospheric Measurement Techniques*, 6(12):3577–3596, 2013.

[80] S. Mosbach, M. S. Celnik, A. Raj, M. Kraft, H. R. Zhang, and et al. Towards a detailed soot model for internal combustion engines. *Combustion and Flame*, 156(6):1156–1165, 2009.

[81] R. Munro. Blow-by in relation to piston and ring features. *SAE Transactions*, pages 2804–2811, 1981.

[82] A. Neer and U. O. Koylu. Effect of operating conditions on the size, morphology, and concentration of submicrometer particulates emitted from a diesel engine. *Combustion and flame*, 146(1-2):142–154, 2006.

[83] R. Nguele, H. S. Al-Salim, and K. Mohammad. Modelling and forecasting of depletion of additives in car engine oils using attenuated total reflectance fast transform infrared spectroscopy. *Lubricants*, 2(4):206–222, 2014.

[84] R. Niessner. The many faces of soot: characterization of soot nanoparticles produced by engines. *Angewandte Chemie International Edition*, 53(46):12366–12379, 2014.

[85] J. Olfert and S. Rogak. Universal relations between soot effective density and primary particle size for common combustion sources. *Aerosol Science and Technology*, 53(5):485–492, 2019.

[86] H. Omidvarborna, A. Kumar, and D. Kim. Recent studies on soot modelling for diesel combustion. *Renewable and Sustainable Energy Reviews*, 48:635–647, 2015.

[87] T. Owen. *Fundamentals of UV-visible spectroscopy*. Agilent Technologies, 2008.

[88] M. Pawlyta and H. Hercman. Transmission electron microscopy (tem) as a tool for identification of combustion products: application to black layers in speleothems. In *Annales Societatis Geologorum Poloniae*, volume 86, 2016.

[89] H. Perkampus. *UV-VIS Spectroscopy and its applications*. Springer Science & Business Media, 2013.

[90] R. Prasad and V. R. Bella. A review on diesel soot emission, its effect and control. *Bulletin of Chemical Reaction Engineering & Catalysis*, 5(2):69, 2010.

[91] S. S. Reham, H. H. Masjuki, M. A. Kalam, I. Shancita, I. M. R. Fattah, and A. M. Ruhul. Study on stability, fuel properties, engine combustion, performance and emission characteristics of biofuel emulsion. *Renewable and Sustainable Energy Reviews*, 52:1566–1579, 2015.

[92] R. D. Reitz and R. Diwakar. Structure of high-pressure fuel sprays. In *International Congress & Exposition*. SAE International, feb 1987. doi:10.4271/870598.

[93] R. D. Reitz, H. Ogawa, R. Payri, T. Fansler, S. Kokjohn, and et al. IJER editorial: The future of the internal combustion engine. *International Journal of Engine Research*, 21(1):3–10, 2020.

[94] İ. A. Reşitoğlu, K. Altinişik, and A. Keskin. The pollutant emissions from diesel-engine vehicles and exhaust aftertreatment systems. *Clean Technologies and Environmental Policy*, 17(1):15–27, 2015.

[95] J. Rissler, M. E. Messing, A. I. Malik, P. T. Nilsson, E. Z. Nordin, and et al. Effective density characterization of soot agglomerates from various sources and comparison to aggregation theory. *Aerosol Science and Technology*, 47(7):792–805, 2013.

[96] T. Rönkkö, T. Lähde, J. Heikkilä, L. Pirjola, U. Bauschke, and et al. Effects of gaseous sulphuric acid on diesel exhaust nanoparticle formation and characteristics. *Environmental science & technology*, 47(20):11882–11889, 2013.

[97] P. R. Ryason, M. J. Hillyer, and T. P. Hansen. Infrared absorptivities of several diesel engine soots; application to the analysis of soot in used engine oils. In *International Fuels & Lubricants Meeting & Exposition*. SAE International, oct 1994. doi:10.4271/942030.

[98] F. Schulz, M. Commodo, K. Kaiser, G. De Falco, P. Minutolo, and et al. Insights into incipient soot formation by atomic force microscopy. *Proceedings of the Combustion Institute*, 37(1):885–892, 2019.

[99] W. W. Seifert and J. B. Desjardins. Measurement of soot in diesel engine lubricating oil. In *International Congress & Exposition*. SAE International, feb 1995. doi:10.4271/951023.

[100] M. Sejkorová, M. Kučera, I. Hurtová, and O. Voltr. Application of FTIR-ATR spectrometry in conjunction with multivariate regression methods for viscosity prediction of worn-out motor oils. *Applied Sciences*, 11(9):3842, 2021.

[101] V. Sharma, D. Uy, A. Gangopadhyay, A. O'Neill, W. A. Paxton, and et al. Structure and chemistry of crankcase and exhaust soot extracted from diesel engines. *Carbon*, 103:327–338, 2016.

[102] D. Siegla. *Particulate carbon: formation during combustion*. Springer Science & Business Media, 2013.

[103] B. R. Stanmore, J. F. Brilhac, and P. Gilot. The oxidation of soot: a review of experiments, mechanisms and models. *carbon*, 39(15):2247–2268, 2001.

[104] STAR-CD. Version 4.22. *Methodology*, 2016.

[105] S. M. Tan, H. K. Ng, and S. Gan. CFD modelling of soot entrainment via thermophoretic deposition and crevice flow in a diesel engine. *Journal of Aerosol Science*, 66:83–95, 2013.

[106] Z. Tang, Z. Feng, P. Jin, X. Fu, and H. Chen. The soot handling ability requirements and how to solve soot related viscosity increases of heavy duty diesel engine oil. *Industrial Lubrication and Tribology*, 2017.

[107] P. A. Tesner. Formation of soot particles. In *Faraday Symposia of the Chemical Society*, volume 7, pages 104–108. Royal Society of Chemistry, 1973.

[108] N. Tokura, K. Terasaka, and S. Yasuhara. Process through which soot intermixes into lubricating oil of a diesel engine with exhaust gas recirculation. In *International Congress & Exposition*. SAE International, feb 1982. doi:10.4271/820082.

[109] E. Tomanik, R. Sobrinho, and R. Zecchinelli. Influence of top ring end gap types at blow-by of internal combustion engines. In *SAE Brasil*. SAE International, oct 1993. doi:10.4271/931669.

[110] B. Tormos, R. Novella, J. Gomez-Soriano, A. García-Barberá, N. Tsuji, I. Uehara, and M. Alonso. Study of the influence of emission control strategies on the soot content and fuel dilution in engine oil. *Tribology International*, 136:285–298, 2019.

[111] D. R. Tree and K. I. Svensson. Soot processes in compression ignition engines. *Progress in energy and combustion science*, 33(3):272–309, 2007.

[112] X. Wang and Y. Cao. Characterizations of absorption, scattering, and transmission of typical nanoparticles and their suspensions. *Journal of Industrial and Engineering Chemistry*, 82:324–332, 2020.

[113] Y. Wang, X. Liang, G. Shu, and L. Dong. Impact of lubricating oil on morphology of particles from a diesel engine. *Energy Procedia*, 75:2388–2393, 2015.

[114] H. E. Wichmann. Diesel exhaust particles. *Inhalation toxicology*, 19(sup1):241–244, 2007.

[115] J. F. Wiedenhoefer and R. D. Reitz. Multidimensional modelling of the effects of radiation and soot deposition in heavy-duty diesel engines. In *World Congress & Exhibition*. SAE International, mar 2003. doi:10.4271/2003-01-0560.

[116] J. Xi and B. J. Zhong. Soot in diesel combustion systems. *Chemical Engineering & Technology: Industrial Chemistry-Plant Equipment-Process Engineering-Biotechnology*, 29(6):665–673, 2006.

[117] V. Yakhot and S. A. Orszag. Renormalization group analysis of turbulence. I. Basic theory. *Journal of scientific computing*, 1(1):3–51, 1986.

Chapter 7

Conclusions and future work

Contents

7.1 Introduction

This chapter, which concludes this Thesis, brings together the main conclusions reached as a result of the research work that has been carried out throughout this process. In addition, a series of study topics are offered that would be interesting to develop in order to keep contributing to the field of study of the engine lubricating oils.

7.2 Discussion

This section brings together, in a clear and concise way, the main achievements of this Thesis as well as the scientific contributions applied to the analysis of engine lubricating oils in three areas: study of the performance behaviour of new lubricating oil formulations in the current automotive field, study of the current problem of soot and its quantification and, finally, the development of new tools to improve the analysis of lubricating oils and to obtain information of interest.

7.2.1 LVEOs monitoring for lubrication performance and OCM

In this study focusing on LVEOs, several aspects were achieved that need to be explained separately:

- The first one involves a more analytical approach. During the experimental measurements of the LVEOs, some limitations or inadequacies of the measurement protocols and equipment were encountered. This is due to the fact that, in spite of trying to generate general protocols, it has been found that it is always necessary to resort to the experience acquired with these systems, in order to obtain the best response that the analysis equipment is capable of providing. For example, thermometric titration for the determination of TAN and TBN of lubricating oil samples. Another example would be the use of the appropriate KF coulometric titrator, since in the course of the study, it was found that a single chamber configuration (frit-free) is more advantageous than the one using two reagents (electrochemical system with porous frit).
- Focusing on the performance of the lubricating oil formulations used in the study: 5W30 API CK–4 (Lube B), 5W30 API FA–4 (Lube C),

10W30 API CK–4 (Lube D) and 10W30 API FA–4 (Lube E), all of them were able to complete the stipulated ODI of 30000 kilometres. However, in all of them it was observed that they suffered a accelerated degradation at the initial stages of the test but then, this degradation slowed down and did not lead to a breakdown of the lubricant. Thus, the use of LVEOs in a vehicle does not lead to damage or problems. These types of lubricants, for what could be classified as normal (non-severe) use conditions, are able to cope with all the demands required by the engine.

7.2.2 Chemometric analysis applied to lubricating oils

In relation to this field of chemometrics, its application to the analysis of engine lubricating oils has been reinforced as a consequence of the results obtained in the first approximation carried out in the Maintenance Engineering research group of the CMT-Motores Térmicos institute.

In this field, two different studies were carried out according to the capabilities available at that time: first, a study was carried out that combined the thermometric analysis (novel technique applied for TAN and TBN determination) with the FT–IR spectroscopy; while in the second work, an investigation was carried out on the capacity of NIR spectroscopy as a technique for predicting the state of a lubricating oil. Therefore, from each of these two studies, the following conclusions were reached:

- Thanks to the development of the thermometry technique applied to lubricants, the TAN and TBN results they reported were of high quality: accurate and repetitive. This led to the idea of taking advantage of this capability and attempt to develop a chemometric procedure applied to FT–IR spectroscopy (since it was a technique available in the laboratory) for the prediction of these two parameters. The result obtained when carrying out this study came to fruition, since it was possible to obtain a generalist procedure capable of accurately predicting both TAN and TBN.

- The most recent incursion into the application of chemometry was the study conducted with NIR spectroscopy, which was developed in the final stretch of the Thesis. With the recent acquisition of a NIR spectrometer and with the database of engine oil samples, it was decided to study whether it was possible or not to be able to determine a series of parameters of the oils: kinematic viscosity, additives

depletion, degradation and acidification. By performing the relevant calculations and data processing, it was possible to achieve a series of chemometric models that allowed predicting the values of the set of selected parameters. Although this was the first study applied to this equipment, the results obtained were very satisfactory, both from an applicability point of view and from a more academic point of view.

Taking into account the results provided by the binomial spectroscopy and chemometrics applied to the field of engine lubricating oils, it is justified the need to further investigate in this field with the final purpose of developing new alternatives that allow to determine the engine oil performance in a simple and fast way, and that does not imply the use of reagents and/or the destruction or loss of samples.

7.2.3 Soot in Oil quantification

As a consequence of the legislative requirements for the reduction of pollutant emissions in ICEs, a collateral effect of the measures implemented in vehicles to comply with the low emission limits, has led to the lubricating oil being adversely affected under certain circumstances.

Soot contamination has been one of the biggest problems, so there was an urgent need to be able to quantify the presence of this pollutant in the lubricant in the best possible way. It is for this reason that in this Thesis, a chapter on this subject has been developed with the aim of improving existing techniques as well as developing new ones of our own.

The following conclusions can be drawn from this research:

- Firstly, TGA requires an improvement of the analysis protocol since new formulations, increasingly focused on achieving a low level of ash generation, make it difficult to stabilise the final signal, so that no reference point can be established from where the soot can be quantified. Accordingly, it would be interesting to develop a joint procedure between TGA and DSC (Differential Scanning Calorimetry) to try to combine the maximum of information from both thermal techniques and put them in common for the case of SiO.

- Apart from the laboratory equipment, it has been shown that there are measurement systems capable of on-line operation, allowing real-time monitoring of the soot content in the lubricant. In the case studied,

the BTSA allowed to obtain accurate and fast values, not only of soot concentration but also ratios (the latter being obtained in very short times, in contrast to the existing traditional procedures). Consequently, the development of new technologies, increasingly miniaturised and specialised, will make it possible to achieve increasingly precise monitoring of the state of the lubricant. Nonetheless, all these developments will always need to be checked since, as with the BTSA, the analysis conditions are not always the most favourable, giving rise to the appearance of phenomena that interfere with or mask the signals used by these new analysis systems, and falsify the real SiO values.

- Finally, during the course of this Thesis, the idea of finding an analytical technique capable of detecting small variations of SiO was raised. After performing a bench mark analysis, it was not possible to find a technique that meet the requirements. For this reason, it was decided to develop a new and in-house method for SiO quantification using UV–Vis spectroscopy. Within the framework of small soot concentrations and low mileage/short period used samples, it was observed that, after designing a valid sample preparation protocol for the type of samples to be analysed, UV–Vis spectroscopy provided very satisfactory results and answers. It allowed to monitor very small increments of soot in samples with a very small use differential (15 minutes), and to obtain generation ratios in record time (for example, in a 1-hour test it is possible to obtain data at: 0 min., 15 min., 30 min., 45 min. and 60 min. with which to track the evolution of the soot).

7.3 Future work

The development of this Thesis has allowed to open several lines of research focused on the new aspects that are taking relevance within the automotive industry. Specifically for the Maintenance Engineering research group at the CMT-Motores Térmicos, of which I am part of, these new lines of research dedicated to the study of engine lubricating oils, are described below,

- Firstly, the future of new lubricating oil formulations is moving towards low-viscosity lubricating oils (according to the SAE viscosity grade): 5W20, 0W20, 0W16, etc. being oils well below what is currently the norm, a 5W30 oil. All this will mean that, with the new thermal and thermo-electric (hybrid) configurations of engines in vehicles already in

production, it will be necessary to study and analyse the engine oil performance under these new working conditions.

- Focusing on hybrid vehicles, these new electromotive configurations require a special encapsulation and cooling system for their battery structures. Specifically, these systems use special oils known as "E–fluids", which are designed to cool the battery system. This imperative need to cool the batteries in the new hybrid vehicles opens a new working environment focused on the study of the performance of these fluids (studying their thermal properties), and on the degradation of the E–fluids as a consequence of the working conditions to which they are subjected. This is a very current topic, so that very little research has been carried out, and it is necessary to focus efforts on getting to know and characterise these new fluids in order to understand more about them.

- Finally, the remaining aspect is the combination of spectroscopic techniques and chemometric procedures applied to the study of engine lubricating oils. This tool, tested in this Thesis for the case of engine lubricating oils, has proved to be very useful in this field. However, this combination of spectroscopy and chemometrics is not exclusive to this type of substance, since it is transferable and applicable to the case of the aforementioned E–fluids. In short, what this binomial allows is to achieve a tool capable of providing a more exhaustive knowledge of a specific system thanks to their capacity of treatment and processing of information. Furthermore, given that this tool allows to work with a big dataset, it is possible to develop a very concise in-depth study of a given subject. Thus, in view of the good progress made in this aspect of the Thesis, it is suggested to continue along this path and to extend the application of this tool to other fields that may be of practical interest to the research line. The next step would be to develop new chemometric analysis protocols and expand their application to the rest of the analytical techniques available in the Fuels and Lubricants laboratory: ICP–OES [8], RULER [1, 5, 6], FT–IR [2–4, 7, 10], UV–Vis [9], etc., in the same way that it is being developed by other laboratories around the world, and that is clearly observed in the trend dictated by the research works published on this topic.

Bibliography

[1] J. B. Ali, B. Chebel-Morello, L. Saidi, S. Malinowski, and F. Fnaiech. Accurate bearing remaining useful life prediction based on weibull distribution and artificial neural network. *Mechanical Systems and Signal Processing*, 56:150–172, 2015.

[2] C. Besser, N. Dörr, F. Novotny-Farkas, K. Varmuza, and G. Allmaier. Comparison of engine oil degradation observed in laboratory alteration and in the engine by chemometric data evaluation. *Tribology International*, 65:37–47, 2013.

[3] A. Borin and R. J. Poppi. Application of mid infrared spectroscopy and iPLS for the quantification of contaminants in lubricating oil. *Vibrational Spectroscopy*, 37(1):27–32, 2005.

[4] J. W. B. Braga, A. A. dos Santos Junior, and I. S. Martins. Determination of viscosity index in lubricant oils by infrared spectroscopy and PLSR. *Fuel*, 120:171–178, 2014.

[5] Y. Du, T. Wu, and V. Makis. Parameter estimation and remaining useful life prediction of lubricating oil with hmm. *Wear*, 376:1227–1233, 2017.

[6] D. Galar-Pascual, L. Berges-Muro, M. P. Lambán-Castillo, J. L. Huertas-Talón, and B. Tormos-Martínez. Cálculo de la vida útil remanente mediante trayectorias móviles entre hiperplanos de máquinas de soporte vectorial. *Interciencia*, 38(8):556–562, 2013.

[7] N. Gracia, S. Thomas, P. Bazin, L. Duponchel, F. Thibault-Starzyk, and O. Lerasle. Combination of mid-infrared spectroscopy and chemometric factorization tools to study the oxidation of lubricating base oils. *Catalysis Today*, 155(3-4):255–260, 2010.

[8] R. Grimmig, S. Lindner, P. Gillemot, M. Winkler, and S. Witzleben. Analyses of used engine oils via atomic spectroscopy–influence of sample pre-treatment and machine learning for engine type classification and lifetime assessment. *Talanta*, 232:122431, 2021.

[9] T. Holland, A. M. Abdul-Munaim, C. Mandrell, R. Karunanithy, D. G. Watson, and P. Sivakumar. Uv-visible spectrophotometer for distinguishing oxidation time of engine oil. *Lubricants*, 9(4):37, 2021.

[10] A. Wolak. TBN performance study on a test fleet in real-world driving conditions using present-day engine oils. *Measurement*, 114:322–331, 2018.

Appendix: Publications

The following publications are the result of the research work developed and presented in this Thesis.

Journal publication

- **Study of the influence of emission control strategies on the soot content and fuel dilution in engine oil**
  Tribology International, 136 (2019) 285-298
  DOI: 10.1016/j.triboint.2019.03.066
  Authors: Bernardo Tormos, Ricardo Novella, Josep Gomez-Soriano, Antonio García-Barberá, Naohide Tsuji, Isshou Uehara, Marcos Alonso
  Abstract: The engine oil contamination by both particulate matter (PM) and fuel is becoming an important problem since strategies to control pollutant emissions in internal combustion engines (ICE) significantly increase their presence in engine oil. As a consequence, the engine oil loses its tribological properties compromising engine lubrication and leading to potential problems in engine such as wear, corrosion, etc. For that reason, the study of the oil degradation and contamination due to these strategies have a special interest to the engine manufacturers and engine oil formulators. In this paper, the engine oil soot content and fuel dilution is analysed under real engine conditions. The study is addressed from two different but complementary points of views. First, on-line measurements at several engine operating conditions are performed in order to further understand how the soot generation correlates with the oil soot content and other derived problems on oil performance. Then, experimental data available after the experimental campaign is used to calibrate a numerical model, based on Computational Fluid Dynamics (CFD), that estimate the amount of soot particles settled in the engine oil. Results show that soot particles are more present in oil when

operating high load-speed conditions and during the Diesel Particulate Filter (DPF) regeneration cycles. Regarding the fuel dilution, delayed post-injections are critical since they significantly increase the amount of fuel in the engine oil. Numerical results also show the relationships between the soot particles generated during combustion and the amount of soot in engine oil, giving an enhanced comprehension of soot-in-oil deposition mechanisms.

- **An alternative procedure to quantify soot in engine oil by Ultraviolet-Visible spectroscopy**
  Tribology Transactions, 62:6, 1063-1071
  DOI: 10.1080/10402004.2019.1645255
  Authors: Vicente Macián, Bernardo Tormos, Santiago Ruiz, Antonio García-Barberá
  Abstract: Due to new pollutant emissions standards, internal combustion engines need several emission control strategies (and related procedures) such as exhaust gas recirculation, diesel/gasoline particulate filters, and selective catalyst reduction that allow them to comply with complete requirements defined on those standards. These strategies result in faster degradation of engine oil, one of the most relevant consequences of which is an increase in soot contamination level. All of these strategies facilitate soot generation. Consequently, soot is one of the most important contaminants present in engine oil. The main technique to measure the content of soot in oil is thermogravimetric analysis (TGA), but this technique has certain limitations. TGA requires a long and specific procedure and has limitations in measuring small concentrations of soot in oil. Therefore, the design of an alternative technique to quantify soot in oil is relevant. One alternative is Fourier transform infrared (FTIR) spectroscopy, but it also has limitations related to low concentrations of soot in oil. This work presents an alternative technique based on ultraviolet-visible (UV-Vis) spectroscopy that allows quantification of small soot contents in used engine oil samples and avoids potential interference from other typical contaminants or those related to measurement processes, such as sample cuvette material.

- **Applying chemometric procedures for correlation the FTIR spectroscopy with the new thermometric evaluation of Total Acid Number and Total Basic Number in engine oils**
  Chemometrics and Intelligent Laboratory Systems, 208 (2021) 104215
  DOI: 10.1016/j.chemolab.2020.104215
  Authors: Vicente Macián, Bernardo Tormos, Antonio García-Barberá, Athanasios Tsolakis
  Abstract: Currently, the main trend is to employ spectroscopic techniques for the condition assessment of used engine oils. That is a consequence of the requirement for increasing the Oil Condition Monitoring (OCM) efficiency. Usually, FTIR (Fourier Transform Infrared) Spectroscopy is employed to achieve the ability of measuring used engine oil and uses the FTIR spectrum to generate a relation between attribute-spectrum. To allow this connection, it is necessary to develop chemometric studies. However, this procedure needs a previous validation to correlate the spectrum with the value of the attribute measured by standardised techniques. One of the potential attribute for study is the acidification of the engine oil by the Total Acid Number (TAN), specially employing the ASTM D8045 standard that measures the TAN level by thermometric titration. The new standard offers a better chemical path to quantify accurately the TAN value of used engine oil. And other basic parameter is the Total Basic Number (TBN) that also is possible to quantify by thermometric determinations. Both of these parameters are correlated, therefore this study is focused on the generation of a mathematical model that describes the condition of the engine oil employing the shape of its FTIR spectrum. Specifically, in this work has been shown the applicability of chemometric procedures in conjunction with thermometric titration for determining TAN and TBN values of an used engine oil.

Congress publication

- **A comparison between FTIR and UV-Vis soot quantification in engine oil**
  Congress publication: IBERTRIVA 2019-X Iberian Conference on Tribology / XI Iberian Vacuum Conference
  Date and location: June 26-28, 2019. Seville, Spain

ISBN: 978-84-09-12421-3
Authors: Vicente Macián, Bernardo Tormos Martínez, Antonio García-Barberá
Abstract: FTIR spectroscopy needs another technique to improve the soot in oil quantification. Mainly, when it is necessary to quantify small increments (after short oil usage periods). UV-Vis spectroscopy is a more sensible technique and is able to detect small variations. Specially, the soot change the opacity of the engine oil and can be measured by UV-VIS. In this initial study, target is to measure spectral differences between samples which differed for a small variation in its oil period use by UV-Vis, which quantification were not possible to appreciate by FTIR.

- **Long-term real-world test for engine oil lubricants: oil performance, engine problems and fuel economy assessment**
Congress publication: 22nd International Colloquium Tribology
Date and location: January 28-30, 2020. Stuttgart/Ostfildern, Germany
ISBN: 978-3-943563-11-5
Authors: Vicente Macián, Bernardo Tormos, Antonio García-Barberá, Tomás Pérez
Abstract: The goal of the study was to analyze the performance of several different engine oil formulations in a selection of diesel and CNG (Compressed Natural Gas) engines in urban bus service and assess their effect in terms of fuel economy on a real world test. This study has been addressed to give answers to those potential end-users of the new low viscosity engine oil formulations in this type of severe service. The whole test has comprised five stages with a duration of one oil drain interval (30000 km) each one, where data of fuel consumption and distance travelled of the buses was recorded in a daily basis; furthermore oil samples were taken in regular predefined periods. Engine oils tested have included commercial formulations and special formulations developed for that test, with different SAE grades, different values of HTHS viscosity, different base oil groups and different SAPS (sulphated ash, phosphorus and sulfur) levels. The bus fleet involved in the test is made up of 48 vehicles: 29 diesel engines and 19 CNG engines; furthermore, these vehicles belong to four different engine technologies allowing to obtain results representative of current vehicles used in urban transport fleets.

- **Correlation between FTIR spectroscopy and thermometric TAN values to allow a more efficient Oil Condition Monitoring**
  Congress publication: Lubmat 2020 - Seventh Congress in Lubrication, Tribology and Condition Monitoring
  Date and location: December 15-17, 2020. Online conference
  Authors: Vicente Macián, Bernardo Tormos, Antonio García-Barberá
  Abstract: The current trend in Oil Condition Monitoring (OCM) is the use of sensors to monitorize the oil performance, based on spectroscopic techniques such as Fourier Transformed Infrared (FTIR) spectroscopy or electrochemical procedures. However, the transition from classical techniques/procedures to new alternatives is not easy due to different factors, such as the requiered number of samples, technical limitations and signal reproducibility. Focused on engine oils, FTIR is one of the most important techniques to determine the performance of the engine oil, thanks to the variety of parameters that this spectroscopy can measure: oxidation, nitration, soot content, etc. According to that, some researchers are developing studies to use the FTIR to detect or quantify other parameters that cannot be determined directly from the spectrum. One of these parameters is the Total Acid Number (TAN), which impact on the etching of specific metals of the engine (like copper and lead) has been corroborated. To get a correlation between FTIR spectra and TAN (according to new ASTM D8045) sometimes are needed a huge number of samples to generate a robust mathematic model. However, this could be a problem, due to the complexity to obtain this information. In this research work, it was necessary to study the spectrum and apply some criteria to reduce the amount of data (without alteraing the spectrum): select those sensible regions that can affect the TAN value and disscard those regions of no (not linked) or low relevance. This in order to equilibrate the FTIR data and the available TAN measurements. Results have shown that it is possible to generate a mathematical model that allows to determine the TAN value and keep a control of its level along the oil drain interval (ODI). Furthermore, the implementation of this methodology in the routine analysis of engine oil, could generate a benefit to the OCM in terms of costs and time for the analysis.

Bibliography

Abd-Alla G. H.
Using exhaust gas recirculation in internal combustion engines: a review.
Energy Conversion and Management, Vol. 43 n^o 8, pp. 1027–1042, 2002. (cited in p. 57)

Abdel-Rahman A. A.
On the emissions from internal-combustion engines: a review.
International Journal of Energy Research, Vol. 22 n^o 6, pp. 483–513, 1998.
(cited in p. 56)

Abdul-Munaim A. M., Holland T., Sivakumar P. and Watson D. G.
Absorption wavebands for discriminating oxidation time of engine oil as detected by FT-IR spectroscopy.
Lubricants, Vol. 7 n^o 3, pp. 24, 2019. (cited in p. 130)

Abdulqadir L. B., Mohd Nor N. F., Lewis R. and Slatter T.
Contemporary challenges of soot build-up in IC engine and their tribological implications.
Tribology-Materials, Surfaces & Interfaces, Vol. 12 n^o 3, pp. 115–129, 2018.
(cited in p. 368)

Adams M. J.
Chemometrics in analytical spectroscopy.
Royal Society of Chemistry, 2004. (cited in p. 298)

Agarwal A. K., Srivastava D. K., Dhar A., Maurya R. K., Shukla P. C. and Singh A. P.
Effect of fuel injection timing and pressure on combustion, emissions and performance characteristics of a single cylinder diesel engine.
Fuel, Vol. 111, pp. 374–383, 2013. (cited in p. 58)

Agarwal D., Singh S. K. and Agarwal A. K.
Effect of Exhaust Gas Recirculation (EGR) on performance, emissions, deposits and durability of a constant speed compression ignition engine.
Applied Energy, Vol. 88 n^o 8, pp. 2900–2907, 2011. (cited in p. 66)

Agoston A., Ötsch C. and Jakoby B.
Viscosity sensors for engine oil condition monitoring: application and interpretation of results.
Sensors and Actuators A: Physical, Vol. 121 n^o 2, pp. 327–332, 2005. (cited in p. 108)

Akochi-Koble E., Pelchat M., Pinchuk D., Pinchuk J. and Dwight S.
Validation of a FTIR spectroscopy method for measuring and monitoring fuel dilution in lubricating oils, 1998. (cited in p. 166)

Al Sheikh Omar A., Motamen Salehi F., Farooq U., Morina A. and Neville A.
Chemical and physical assessment of engine oils degradation and additive depletion by soot.
Tribology International, Vol. 160, pp. 107054, 2021. (cited in p. 370)

Al-Wakeel H. B., Abdul Karim Z. A. and Al-Kayiem H. H.
Soot reduction strategy: A review.
Journal of Applied Sciences, Vol. 12 n^o 23, pp. 2338–2345, 2012. (cited in p. 351)

Aldajah S., Ajayi O. O., Fenske G. R. and Goldblatt I. L.
Effect of exhaust gas recirculation (EGR) contamination of diesel engine oil on wear.
Wear, Vol. 263 n^o 1-6, pp. 93–98, 2007. (cited in p. 66)

Ali J. B., Chebel-Morello B., Saidi L., Malinowski S. and Fnaiech F.
Accurate bearing remaining useful life prediction based on Weibull distribution and artificial neural network.
Mechanical Systems and Signal Processing, Vol. 56, pp. 150–172, 2015. (cited in p. 457)

Alkemade U. G. and Schumann B.
Engines and exhaust after treatment systems for future automotive applications.
Solid State Ionics, Vol. 177 n^o 26-32, pp. 2291–2296, 2006. (cited in p. 56)

Alpert N. L., Keiser W. E. and Szymanski H. A.
IR: theory and practice of infrared spectroscopy.
Springer Science & Business Media, 2012. (cited in p. 122)

Ambs J. L. and McClure B. T.
The influence of oxidation catalysts on NO_2 in diesel exhaust.
In *International Off-Highway & Powerplant Congress & Exposition.* SAE International, sep 1993. (cited in p. 60)

Amirav A. and Muller D.
Arson analysis by GC-MS with cold EI–Fuel fingerprinting by isomer distribution analysis.
`http://blog.avivanalytical.com/2012/11/arson-analysis-by-gc-ms-with-cold-ei.html`, nov 2012. (cited in p. 160)

Analytical Engineering Inc.
User's manual: Bench top soot analyzer (BTSA), 2017. (cited in p. 408)

Angelberger C., Poinsot T. and Delhay B.
Improving near-wall combustion and wall heat transfer modelling in SI engine computations.
In *International Fuels & Lubricants Meeting & Exposition.* SAE International, oct 1997. (cited in p. 417)

Antusch S., Dienwiebel M., Nold E., Albers P., Spicher U. and Scherge M.
On the tribochemical action of engine soot.
Wear, Vol. 269 n^o 1-2, pp. 1–12, 2010. (cited in p. 368)

Asango A., La Rocca A. and Shayler P.
Investigating the effect of carbon nanoparticles on the viscosity of lubricant oil from light duty automotive diesel engines.
In *World Congress & Exhibition.* SAE International, jan 2014. (cited in p. 369)

Aucélio R. Q, de Souza R. M., de Campos R. C., Miekeley N. and da Silveira C. L. P.
The determination of trace metals in lubricating oils by atomic spectrometry.
Spectrochimica Acta Part B: Atomic Spectroscopy, Vol. 62 n^o 9, pp. 952–961, 2007. (cited in p. 154)

Bardasz E. A., Carrick V. A., George H. F., Graf M. M., Kornbrekke R. E. and Pocinki S. B.
Understanding soot mediated oil thickening through designed experimentation Part 4: Mack T-8 test.
In *International Spring Fuels & Lubricants Meeting & Exposition*. SAE International, may 1997. (cited in p. 369)

Bark L. S. and Bark S. M.
Thermometric titrimetry: International series of monographs in analytical chemistry, volume 33.
Elsevier, 2016. (cited in p. 114)

Barthel J. and Wachter R.
Thermometric titrations.
Journal of Chemical Education, Vol. 55 n^o 1, pp. A48, 1978. (cited in p. 114)

Bartsch N.
Lubricating oil analysis according to ASTM D5185 using the Thermo Scientific iCAP 7400 ICP-OES, 2017. (cited in p. 152)

Bartz W. J.
Engine oils and automotive lubrication.
CRC Press, 2019. (cited in p. 31)

Behn A., Feindt M., Matz G., Krause S. and Gohl M.
Fuel transport across the piston ring pack: Measurement system development and experiments for online fuel transport and oil dilution measurements.
SAE Technical Paper, n^o 2015-24-2534, 2015. (cited in p. 81)

Bensaid S., Caroca C. J., Russo N. and Fino D.
Detailed investigation of non-catalytic DPF regeneration.
The Canadian Journal of Chemical Engineering, Vol. 89 n^o 2, pp. 401–407, 2011. (cited in p. 62)

Besser C., Dörr N., Novotny-Farkas F., Varmuza K. and Allmaier G.
Comparison of engine oil degradation observed in laboratory alteration and in the engine by chemometric data evaluation.
Tribology International, Vol. 65, pp. 37–47, 2013. (cited in p. 457)

Bhushan B.
Modern tribology handbook.
CRC Press, 2000. (cited in p. 67)

Bings N. H., Bogaerts A. and Broekaert J. A. C.
Atomic spectroscopy: a review.
Analytical chemistry, Vol. 82 n^o 12, pp. 4653–4681, 2010. (cited in p. 141)

Blanco M. and Villarroya I.
NIR spectroscopy: a rapid-response analytical tool.
TrAC Trends in Analytical Chemistry, Vol. 21 n^o 4, pp. 240–250, 2002. (cited in p. 333)

Blomberg J., Schoenmakers P. J. and Brinkman U. A. T.
Gas chromatographic methods for oil analysis.
Journal of Chromatography A, Vol. 972 n^o 2, pp. 137–173, 2002. (cited in p. 161)

Bockhorn H.
Mechanisms and models of soot formation: final discussion and perspectives.
In *Soot Formation in Combustion*, pp. 577–588. Springer, 1994. (cited in p. 354)

Bockhorn H.
Combustion generated fine carbonaceous particles: Proceedings of an international workshop.
KIT Scientific publishing, 2009. (cited in p. 356)

Bockhorn H.
Soot formation in combustion: mechanisms and models, volume 59.
Springer Science & Business Media, 2013. (cited in p. 352)

Bohnet M.
Ullmann's encyclopedia of industrial chemistry.
Wiley-VCH, 7th edition, 40 volume set edition, 2006. (cited in p. 20)

Bohren C. F. and Huffman D. R.
Absorption and scattering of light by small particles.
John Wiley & Sons, 2008. (cited in p. 192)

Booksh K. S. and Kowalski B. R.
Theory of analytical chemistry.
Analytical Chemistry, Vol. 66 n^o 15, pp. 782A–791A, 1994. (cited in p. 298)

Borin A. and Poppi R. J.
Application of mid infrared spectroscopy and iPLS for the quantification of contaminants in lubricating oil.
Vibrational Spectroscopy, Vol. 37 n^o 1, pp. 27–32, 2005. (cited in p. 457)

Boumans P. W. J. M.
Inductively coupled plasma-atomic emission spectroscopy: its present and future position in analytical chemistry.
Fresenius' Zeitschrift für Analytische Chemie, Vol. 299 n^o 5, pp. 337–361, 1979.
(cited in p. 139)

Braga J. W. B., dos Santos Junior A. A. and Martins I. S.
Determination of viscosity index in lubricant oils by infrared spectroscopy and PLSR.
Fuel, Vol. 120, pp. 171–178, 2014. (cited in p. 457)

Bredin A., Larcher A. V. and Mullins B. J.
Thermogravimetric analysis of carbon black and engine soot–Towards a more robust oil analysis method.
Tribology international, Vol. 44 n^o 12, pp. 1642–1650, 2011. (cited in pp. 373, 376)

Bro R.
Multivariate calibration: what is in chemometrics for the analytical chemist?
Analytica Chimica Acta, Vol. 500 n^o 1-2, pp. 185–194, 2003. (cited in p. 300)

Broatch A., Margot X., Novella R. and Gómez-Soriano J.
Impact of the injector design on the combustion noise of gasoline partially premixed combustion in a 2-stroke engine.
Applied Thermal Engineering, Vol. 119, pp. 530–540, 2017. (cited in p. 417)

Broatch A., Novella R., García-Tíscar J. and Gómez-Soriano J.
Potential of dual spray injectors for optimising the noise emission of gasoline partially premixed combustion in a 2-stroke HSDI CI engine.
Applied Thermal Engineering, Vol. 134, pp. 369–378, 2018. (cited in p. 417)

Broekaert J. A. C.
Atomic emission spectroscopy instrumentation.
Spectrochimica Acta, Vol. 37, pp. 727, 1982. (cited in p. 141)

Brown J. M.
Infrared spectroscopic analysis of petroleum, petroleum products, and lubricants.
ASTM International, 2011. (cited in p. 130)

Brown M. W., Issa K. and Sinclair A. G.
Precise manual enthalpimetric titrations.
Analyst, Vol. 94 n^o 1116, pp. 234–235, 1969. (cited in p. 114)

Brown S. D., Tauler R. and Walczak B.
Comprehensive chemometrics: chemical and biochemical data analysis.
Elsevier, 2020. (cited in p. 302)

Browner R. F. and Boorn A. W.
Sample introduction techniques for atomic spectroscopy.
Analytical Chemistry, Vol. 56 n^o 7, pp. 875A–888A, 1984. (cited in p. 144)

Bueno-López A.
Diesel soot combustion ceria catalysts.
Applied Catalysis B: Environmental, Vol. 146, pp. 1–11, 2014. (cited in p. 360)

Burrington J. D., Pudelski J. K. and Roski J. P.
Challenges in detergents and dispersants for engine oils.
In *Practical Advances in Petroleum Processing*, pp. 579–595. Springer, 2006.
(cited in p. 30)

Carneiro M. J. D., Feres Júnior M. A. and Godinho O. E.S.
Determination of the acidity of oils using paraformaldehyde as a thermometric end-point indicator.
Journal of the Brazilian Chemical Society, Vol. 13 n^o 5, pp. 692–694, 2002.
(cited in p. 119)

Cassap M.
The analysis of used lubrication oils by inductively coupled plasma spectrometry for predictive maintenance.
Spectroscopy Europe, Vol. 20 n^o 1, pp. 17–20, 2008. (cited in p. 154)

Cedergren A. and Jonsson S.
Progress in Karl-Fischer coulometry using diaphragm-free cells.
Analytical chemistry, Vol. 73 n^o 22, pp. 5611–5615, 2001. (cited in p. 178)

Chinas-Castillo F. and Spikes H. A.
The behavior of diluted sooted oils in lubricated contacts.
Tribology Letters, Vol. 16 n^o 4, pp. 317–322, 2004. (cited in p. 370)

Choi M. Y., Mulholland G. W., Hamins A. and Kashiwagi T.
Comparisons of the soot volume fraction using gravimetric and light extinction techniques.
Combustion and Flame, Vol. 102 n^o 1-2, pp. 161–169, 1995. (cited in p. 362)

Chun S. M.
A study on the effect of soot on changes in diesel engine oil's dielectric constant.
Tribology and Lubricants, Vol. 26 n^o 2, pp. 111–121, 2010. (cited in p. 370)

Clague A. D. H., Donnet J. B., Wang T. K. and Peng J. C. M.
A comparison of diesel engine soot with carbon black.
Carbon, Vol. 37 n^o 10, pp. 1553–1565, 1999. (cited in p. 364)

Colacicco P. and Mazuyer D.
The role of soot aggregation on the lubrication of diesel engines.
Tribology transactions, Vol. 38 n^o 4, pp. 959–965, 1995. (cited in p. 370)

Colin O. and Benkenida A.
The 3-zones extended coherent flame model (ECFM3Z) for computing premixed/diffusion combustion.
Oil & Gas Science and Technology, Vol. 59 n^o 6, pp. 593–609, 2004. (cited in p. 417)

Competence Center Titration Metrohm.
Acidity in crude oils and petroleum products by thermometric titration according to ASTM D8045, 2016. (cited in p. 119)

Competence Center Titration Metrohm.
Determination of the total base number in petroleum products, 2016. (cited in p. 119)

Corporation Noria.
How to measure water in oil.
`https://www.machinerylubrication.com/Read/327/water-oil-analysis`, may 2002. (cited in p. 178)

Corporation Noria.
Karl Fischer Coulometric Titration Explained and Illustrated.
`https://www.machinerylubrication.com/Read/594/karl-fischer-coulometric-titration`, mar 2004. (cited in p. 178)

Covitch M. J. and Trickett K. J.
How polymers behave as viscosity index improvers in lubricating oils.
Advances in Chemical Engineering and Science, Vol. 5 n^o 02, pp. 134, 2015. (cited in p. 25)

Crolla D.
Encyclopedia of automotive engineering.
John Wiley & Sons, 2015. (cited in p. 353)

Cui Y., Cai Y., Fan R., Shi Y., Gu L. and et al.
Effects of residual ash on DPF capture and regeneration.
International Journal of Automotive Technology, Vol. 19 n^o 5, pp. 759–769, 2018. (cited in p. 62)

CWG.
Properties of mixture water/glycol - Extract from VDI-Warmeatlas Dd 17- VDI-Verlag GmbH.
`https://detector-cooling.web.cern.ch/data/Table%208-3-1.htm`, aug 1991. (cited in p. 168)

DaCosta H., Shannon C. and Silver R.
Thermal and chemical aging of diesel particulate filters.
In *World Congress & Exposition*. SAE International, jan 2007. (cited in p. 61)

Dahlén L.
On applied CFD and model development in combustion systems development for DI diesel engines.
Royal Institute of Technology, Stockholm, Sweden, 2002. (cited in p. 418)

Dante G.
Motores endotérmicos.
Omega, 3a edición edition, 1989. (cited in p. 52)

Davies A. M. C.
An introduction to near infrared (NIR) spectroscopy.
J. Near Infrared Spectrosc, 2014. (cited in p. 332)

Dey S. and Dhal G. C.
Materials progress in the control of CO and CO_2 emission at ambient conditions: an overview.
Materials Science for Energy Technologies, 2019. (cited in p. 59)

Di Liberto G.
Mechanisms of soot transfer to oil of an HPCR diesel engine.
University of Nottingham, 2017. (cited in p. 368)

Directive EU.
98/69/EC of the European Parliament and of the Council of 13 October 1998 relating to measures to be taken against air pollution by emissions from motor vehicles and amending Council Directive 70/220/EEC.
Official Journal of the European Communities L, Vol. 350 n^o 28, pp. 12, 1998.
(cited in p. 56)

Directive EU.
Directive 2005/55/EC of the European Parliament and of the Council of 28 September 2005 on the approximation of the laws of the Member States relating to the measures to be taken against the emission of gaseous and particulate pollutants from compression-ignition engines for use in vehicles, and the emission of gaseous pollutants from positive-ignition engines fuelled with natural gas or liquefied petroleum gas for use in vehicles.
Official Journal of the European Communities L, Vol. 275, pp. 1–163, 2005.
(cited in p. 56)

Directive EU.
Regulation (EC) No 715/2007 of the European Parliament and of the Council of 20 June 2007 on type approval of motor vehicles with respect to emissions from light passenger and commercial vehicles (Euro 5 and Euro 6) and on access to vehicle repair and maintenance information.
Official Journal of the European Communities L, Vol. 171, pp. 1–16, 2007.
(cited in p. 56)

Directive Council.
91/441/EEC of 26 June 1991 amending Directive 70/220.
EEC on the approximation of the laws of the Member States relating to measures to be taken against air pollution by emissions from motor vehicles, 1991. (cited in p. 56)

Divekar P. S., Chen X., Tjong J. and Zheng M.
Energy efficiency impact of EGR on organizing clean combustion in diesel engines.
Energy Conversion and Management, Vol. 112, pp. 369–381, 2016. (cited in p. 65)

Dorinson A. and Ludema K. C.
Mechanics and chemistry in lubrication, volume 9.
Elsevier, 1985. (cited in pp. 20, 38)

Du Y., Wu T. and Makis V.
Parameter estimation and remaining useful life prediction of lubricating oil with HMM.
Wear, Vol. 376, pp. 1227–1233, 2017. (cited in p. 457)

Duvvuri P. P., Shrivastava R. K., Sukumaran S. and Sreedhara S.
Numerical modelling of thermophoretic deposition on cylinder liner of a diesel engine using a sectional soot model.
Journal of Aerosol Science, Vol. 139, pp. 105464, 2020. (cited in pp. 364, 367)

Eastwood P.
Particulate emissions from vehicles, volume 20.
John Wiley & Sons, 2008. (cited in pp. 356, 358, 365)

Esteban B., Riba J., Baquero G., Rius A. and Puig R.
Temperature dependence of density and viscosity of vegetable oils.
Biomass and bioenergy, Vol. 42, pp. 164–171, 2012. (cited in p. 68)

Fang J., Meng Z., Li J., Pu Y., Du Y. and et al.
The influence of ash on soot deposition and regeneration processes in diesel particular filter.
Applied Thermal Engineering, Vol. 124, pp. 633–640, 2017. (cited in p. 62)

Fassel V. A. and Kniseley R. N.
Inductively coupled plasma. Optical emission spectroscopy.
Analytical Chemistry, Vol. 46 n^o 13, pp. 1110A–1120a, 1974. (cited in p. 141)

Feng X., Ge Y., Ma C., Tan J., Yu L. and et al.
Experimental study on the nitrogen dioxide and particulate matter emissions from diesel engine retrofitted with particulate oxidation catalyst.
Science of the Total Environment, Vol. 472, pp. 56–62, 2014. (cited in p. 63)

Fentress A., Sander J. and Ameye J.
The use of linear sweep voltammetry in condition monitoring of diesel engine oil.
Journal of ASTM International, Vol. 8 n^o 7, pp. 1–10, 2011. (cited in p. 131)

Fialkov A. B., Gordin A. and Amirav A.
Hydrocarbons and fuels analyses with the supersonic gas chromatography mass spectrometry–The novel concept of isomer abundance analysis.
Journal of Chromatography A, Vol. 1195 n^o 1-2, pp. 127–135, 2008. (cited in p. 162)

Fiebig M., Wiartalla A., Holderbaum B. and Kiesow S.
Particulate emissions from diesel engines: correlation between engine technology and emissions.
Journal of Occupational Medicine and Toxicology, Vol. 9 n^o 1, pp. 6, 2014.
(cited in p. 58)

Field L. D., Li H. L. and Magill A. M.
Organic structures from spectra.
John Wiley & Sons, 2020. (cited in p. 126)

Fitch J.
Glycol in lubricating oil - Detection, analysis and removal.
`https://www.machinerylubrication.com/Read/193/oil-glycol`, jul 2001. (cited in p. 183)

Fitch J. C.
Oil analysis for maintenance professional.
Noria Corporation, 1998. (cited in p. 173)

Flynn P. F., Durrett R. P., Hunter G. L., Zur Loye A. O., Akinyemi O. C. and et al.
Diesel combustion: An integrated view combining laser diagnostics, chemical kinetics, and empirical validation.
In *Future Transportation Technology Conference & Exposition*. SAE International, mar 1999. (cited in p. 353)

for Standarization International Organization.
ISO 4406:2021 Hydraulic fluid power–Fluids–method for coding the level of contamination by solid particles, 2021. (cited in p. 193)

Fox M. F., Pawlak Z. and Picken D. J.
Acid-base determination of lubricating oils.
Tribology international, Vol. 24 n^o 6, pp. 335–340, 1991. (cited in p. 112)

Frenklach M. and Wang H.
Detailed modeling of soot particle nucleation and growth.
In *Symposium (International) on Combustion*, volume 23, pp. 1559–1566. Elsevier, 1991. (cited in p. 354)

Frenklach M., Wang H. and Bockhorn H.
Soot formation in combustion: mechanisms and models.
Springer series in chemical physics, Vol. 59, pp. 165–192, 1994. (cited in p. 354)

Fujita H. and Spikes H.
The influence of soot on lubricating films.
Tribology Series, Vol. 43, pp. 37–43, 2004. (cited in p. 370)

Galar-Pascual D., Berges-Muro L., Lambán-Castillo M. P., Huertas-Talón J. L. and Tormos-Martínez B.
Cálculo de la vida útil remanente mediante trayectorias móviles entre hiperplanos de máquinas de soporte vectorial.
Interciencia, Vol. 38 n^o 8, pp. 556–562, 2013. (cited in p. 457)

Galer-Tatarowicz K., Pazikowska-Sapota G., Dembska G. and Stasiek K.
Determination of petroleum compounds in bottom sediments.
Bulletin of the Maritime Institute in Gdansk, Vol. 30, pp. 174–179, 01 2015. (cited in p. 161)

Geochemistry Torkelson.
Examples of chromatograms: regular gasoline, aviation gasoline, aviation spirits, jet fuel, diesel fuel, 10W30 motor oil, crude oil.
`https://torkelsongeochemistry.com/chromatogramexamples.html`, may 2007. (cited in p. 162)

George S., Balla S. and Gautam M.
Effect of diesel soot contaminated oil on engine wear.
Wear, Vol. 262 n^o 9-10, pp. 1113–1122, 2007. (cited in p. 370)

George S., Balla S., Gautam V. and Gautam M.
Effect of diesel soot on lubricant oil viscosity.
Tribology International, Vol. 40 n^o 5, pp. 809–818, 2007. (cited in p. 369)

Ghosh S., Prasanna V. L., Sowjanya B., Srivani P., Alagaraja M. and et al.
Inductively coupled plasma–optical emission spectroscopy: a review.
Asian Journal of Pharmaceutical Analysis, Vol. 3 n^o 1, pp. 24–33, 2013. (cited in p. 141)

Giechaskiel B., Maricq M., Ntziachristos L., Dardiotis C., Wang X. and et al.
Review of motor vehicle particulate emissions sampling and measurement: From smoke and filter mass to particle number.
Journal of Aerosol Science, Vol. 67, pp. 48–86, 2014. (cited in p. 368)

GmbH Grabner Instruments Messteckhnik.
Shipboard flashpoint testing of fuels and lube oils, 2011. (cited in p. 164)

Gollin M. and Bjork D.
Comparative performance of ethylene glycol/water and propylene glycol/water coolants in automobile radiators.
In *International Congress & Exposition*. SAE International, mar 1996. (cited in p. 169)

Gracia N., Thomas S., Bazin P., Duponchel L., Thibault-Starzyk F. and Lerasle O.
Combination of mid-infrared spectroscopy and chemometric factorization tools to study the oxidation of lubricating base oils.
Catalysis Today, Vol. 155 n^o 3-4, pp. 255–260, 2010. (cited in p. 457)

Gras K., Luong J., Lin M., Gras R. and Shellie R. A.
Determination of ethylene glycol in lubricants by derivatization static headspace gas chromatography.
Analytical Methods, Vol. 7 n^o 13, pp. 5545–5550, 2015. (cited in p. 184)

Greaney J. P. and Cozzone G. E.
Comparative performance of aqueous propylene glycol and aqueous ethylene glycol coolants.
In *International Congress & Exposition*. SAE International, mar 1999. (cited in p. 169)

Green D.
The tribological effects of soot contaminated lubricants on engine components.
University of Sheffield, 2007. (cited in p. 370)

Green D. A. and Lewis R.
Effect of soot on oil properties and wear of engine components.
Journal of Physics D: Applied Physics, Vol. 40 n^o 18, pp. 5488, 2007. (cited in p. 368)

Green D. A. and Lewis R.
The effects of soot-contaminated engine oil on wear and friction: a review.
Proceedings of the Institution of Mechanical Engineers, Part D: Journal of Automobile Engineering, Vol. 222 n^o 9, pp. 1669–1689, 2008. (cited in p. 370)

Green D. A., Lewis R. and Dwyer-Joyce R. S.
Wear effects and mechanisms of soot-contaminated automotive lubricants.
Proceedings of the Institution of Mechanical Engineers, Part J: Journal of Engineering Tribology, Vol. 220 n^o 3, pp. 159–169, 2006. (cited in p. 370)

Grimmig R., Lindner S., Gillemot P., Winkler M. and Witzleben S.
Analyses of used engine oils via atomic spectroscopy–Influence of sample pre-treatment and machine learning for engine type classification and lifetime assessment.
Talanta, Vol. 232, pp. 122431, 2021. (cited in p. 457)

Guan B., Zhan R., Lin H. and Huang Z.
Review of state of the art technologies of selective catalytic reduction of NOx from diesel engine exhaust.
Applied Thermal Engineering, Vol. 66 n^o 1-2, pp. 395–414, 2014. (cited in p. 63)

Guan B., Zhan R., Lin H. and Huang Z.
Review of the state-of-the-art of exhaust particulate filter technology in internal combustion engines.
Journal of environmental management, Vol. 154, pp. 225–258, 2015. (cited in p. 61)

Gupta S. V.
Viscometry for Liquids.
Springer, 2016. (cited in p. 101)

Habchi C., Lafossas F. A., Béard P. and Broseta D.
Formulation of a one-component fuel lumping model to assess the effects of fuel thermodynamic properties on internal combustion engine mixture preparation and combustion.
In *Fuels & Lubricants Meeting & Exhibition*. SAE International, jun 2004. (cited in p. 417)

Hall G. and Lightle E.
Determining fuel diluents in lubrication oils.
Practicing Oil Analysis, Vol. 10, pp. 3–4, 2008. (cited in p. 159)

Han L., Hong W. and Wang S.
The key points of inductive wear debris sensor.
In *Proceedings of 2011 International Conference on Fluid Power and Mechatronics*, pp. 809–815. IEEE, 2011. (cited in p. 192)

Harrison G. R.
Massachusetts Institute of Technology wavelength tables: Wavelengths by element, volume 1.
Mit Press, 1969. (cited in p. 140)

Hasannuddin A. K., Wira J. Y., Sarah S., Wan Syaidatul Aqma W. M. N., Abdul Hadi A. R. and et al.
Performance, emissions and lubricant oil analysis of diesel engine running on emulsion fuel.
Energy conversion and management, Vol. 117, pp. 548–557, 2016. (cited in p. 350)

Haynes B. S. and Wagner H. G.
Soot formation.
Progress in energy and combustion science, Vol. 7 n^o 4, pp. 229–273, 1981. (cited in p. 354)

Headquarters Metrohm International.
Quality control of lubricants–Fast and chemical-free determination of the acid number, viscosity, moisture content, and color number of lubricants with NIRS, 2020. (cited in p. 333)

Heredia-Cancino J. A., Ramezani M. and Álvarez-Ramos M. E.
Effect of degradation on tribological performance of engine lubricants at elevated temperatures.
Tribology International, Vol. 124, pp. 230–237, 2018. (cited in p. 68)

Hiroyasu H. and Kadota T.
Models for combustion and formation of nitric oxide and soot in direct injection diesel engines.
In *Automotive Engineering Congress & Exposition*. SAE International, feb 1976. (cited in p. 418)

Holland T., Abdul-Munaim A. M., Mandrell C., Karunanithy R., Watson D. G. and Sivakumar P.
UV-Visible spectrophotometer for distinguishing oxidation time of engine oil.
Lubricants, Vol. 9 n^o 4, pp. 37, 2021. (cited in p. 457)

Hu E., Hu X., Liu T., Fang L., Dearn K. D. and Xu H.
The role of soot particles in the tribological behavior of engine lubricating oils.
Wear, Vol. 304 n^o 1-2, pp. 152–161, 2013. (cited in p. 368)

Hu J., Yang S., Zhang J., Guo L. and Xin Y.
The Determination of lower acidity in several coloured oils by catalyzed thermometric titration.
Petroleum Chemistry, Vol. 57 n^o 12, 2017. (cited in p. 119)

Huh K. Y.
A phenomenological model of diesel spray atomization.
In *Proc. of The International Conf. on Multiphase Flows' 91-Tsukuba*, 1991. (cited in p. 418)

Hull W. C., Robertson C., Mullen J., Stradling J. and Sidwell B.
Analysis of ethylene glycol-based engine coolant as a vehicle fire fuel.
In *Proceedings of the International Symposium on Fire Investigation Science and Technology, National Association of Fire Investigators, Sarasota, FL*, pp. 1–12, 2008. (cited in p. 169)

Institute American Petroleum.
Engine oil licensing and certification system. API 1509 Eighteenth Edition, 2019. (cited in p. 14)

Institute Energy.
IP 449: Petroleum products and lubricants - Determination of acid number - Non-aqueous potentiometric titration method, 2000. (cited in p. 111)

Institute Energy.
IP 417: Determination of base number - Potentiometric titration method, 2004. (cited in p. 111)

Institute Energy.
IP 431: Petroleum products - Determination of acid number - Semi-micro colour-indicator titration method, 2004. (cited in p. 111)

Institute Energy.
IP 139: Petroleum products and lubricants - Determination of acid or base number - Colour-indicator titration method, 2017. (cited in p. 111)

Institute Energy.
IP 276: Petroleum products - Determination of base number - Perchloric acid potentiometric titration method, 2018. (cited in p. 111)

Institute Energy.
IP 177: Determination of weak and strong acid number - Potentiometric titration method, 2019. (cited in p. 111)

Instruments SPECTRO Analytical.
Which spectrometer optical technology offers superior performance? Echelle vs. ORCA, 2020. (cited in p. 150)

International ASTM.
ASTM D6810-13 Standard test method for measurement of hindered phenolic antioxidant content in non-zinc turbine oils by linear sweep voltammetry, 2013. (cited in p. 137)

International ASTM.
ASTM D6971-09(2014) Standard test method for measurement of hindered phenolic and aromatic amine antioxidant content in non-zinc turbine oils by linear sweep voltammetry, 2014. (cited in p. 137)

International ASTM.
ASTM D7590-09(2014) Standard guide for measurement of remaining primary antioxidant content In in-service Industrial lubricating oils by linear sweep voltammetry, 2014. (cited in p. 137)

International ASTM.
ASTM D7593-14 Standard test method for determination of fuel dilution for in-service engine oils by gas chromatography, 2014. (cited in p. 159)

International ASTM.
ASTM D7922-14 Standard test method for determination of glycol for in-service engine oils by gas chromatography, 2014. (cited in p. 184)

International ASTM.
ASTM D2896-15 Standard test method for base number of petroleum products by potentiometric perchloric acid titration, 2015. (cited in pp. 111, 113)

International ASTM.
ASTM D6224-16 Standard practice for in-service monitoring of lubricating oil for auxiliary power plant equipment, 2016. (cited in p. 137)

International ASTM.
ASTM E168-16 Standard practices for general techniques of infrared quantitative analysis, 2016. (cited in p. 127)

International ASTM.
ASTM D3339-12(2017) Standard test method for acid number of petroleum products by semi-micro color indicator titration, 2017. (cited in p. 111)

International ASTM.
ASTM D4291-04 Standard test method for trace ethylene glycol in used engine oil, 2017. (cited in p. 183)

International ASTM.
ASTM D4739-17 Standard test method for base number determination by potentiometric hydrochloric acid titration, 2017. (cited in p. 111)

International ASTM.
ASTM D5967-17 Standard test method for evaluation of diesel engine oils in T-8 diesel engine, 2017. (cited in p. 371)

International ASTM.
ASTM D5984-11(2017) Standard test method for semi-quantitative field test method for base number in new and used lubricants by color-indicator titration, 2017. (cited in p. 111)

International ASTM.
ASTM D8045-17e1 Standard test method for acid number of crude oils and petroleum products by catalytic thermometric titration, 2017. (cited in pp. 111, 120)

International ASTM.
ASTM D5185-18 Standard test method for multielement determination of used and unused lubricating oils and base oils by Inductively Coupled Plasma Atomic Emission Spectrometry (ICP-AES), 2018. (cited in pp. 154, 184, 198)

International ASTM.
ASTM D664-18e2 Standard test method for acid number of petroleum products by potentiometric titration, 2018. (cited in pp. 111, 113)

International ASTM.
ASTM D7412-18 Standard test method for condition monitoring of phosphate antiwear additives in in-service petroleum and hydrocarbon based lubricants by trend analysis using Fourier Transform Infrared (FT-IR) spectrometry, 2018. (cited in p. 131)

International ASTM.
ASTM D7414-18 Standard test method for condition monitoring of oxidation in in-service petroleum and hydrocarbon based lubricants by trend analysis using Fourier Transform Infrared (FT-IR) spectrometry, 2018. (cited in p. 130)

International ASTM.
ASTM D7415-18 Standard test method for condition monitoring of sulfate by-products in in-service petroleum and hydrocarbon based lubricants by trend analysis using Fourier Transform Infrared (FT-IR) spectrometry, 2018. (cited in p. 131)

International ASTM.
ASTM D7527-10(2018) Standard test method for measurement of antioxidant content in lubricating greases by linear sweep voltammetry, 2018. (cited in p. 137)

International ASTM.
ASTM D7624-18 Standard test method for condition monitoring of nitration in in-service petroleum and hydrocarbon-based lubricants by trend analysis using Fourier Transform Infrared (FT-IR) spectrometry, 2018. (cited in p. 130)

International ASTM.
ASTM D7647-10(2018) Standard Test Method for Automatic Particle Counting of Lubricating and Hydraulic Fluids Using Dilution Techniques to Eliminate the Contribution of Water and Interfering Soft Particles by Light Extinction.
2018. (cited in p. 193)

International ASTM.
ASTM D893-14 Standard test method for insolubles in used lubricating oils, 2018.
(cited in p. 381)

International ASTM.
ASTM D92-18 Standard test method for flash and fire points by Cleveland open cup tester, 2018. (cited in p. 164)

International ASTM.
ASTM E2412-10(2018) Standard practice for condition monitoring of in-service lubricants by trend analysis using Fourier Transform Infrared (FT-IR) spectrometry, 2018.
(cited in pp. 130, 156, 166, 181)

International ASTM.
ASTM D2887-19 Standard test method for boiling range distribution of petroleum fractions by gas chromatography, 2019. (cited in p. 44)

International ASTM.
ASTM D4951-14(2019) Standard test method for determination of additive elements in lubricating oils by Inductively Coupled Plasma Atomic Emission Spectrometry, 2019.
(cited in p. 154)

International ASTM.
ASTM D7686-19 Standard test method for field-based condition monitoring of soot in in-service lubricants using a fixed-filter infrared (IR) instrument, 2019. (cited in p. 406)

International ASTM.
ASTM D7899-19 Standard test method for measuring the merit of dispersancy of in-service engine oils with blotter spot method, 2019. (cited in p. 376)

International ASTM.
ASTM D3524-14(2020) Standard test method for diesel fuel diluent in used diesel engine oils by gas chromatography, 2020. (cited in p. 159)

International ASTM.
ASTM D3525-20 Standard test method for gasoline fuel dilution in used gasoline engine oils by wide-bore capillary gas chromatography, 2020. (cited in p. 159)

International ASTM.
ASTM D4378-20 Standard practice for in-service monitoring of mineral turbine oils for steam, gas, and combined cycle turbines, 2020. (cited in p. 136)

International ASTM.
ASTM D5800-20 Standard test method for evaporation loss of lubricating oils by the Noack Method.
West Conshohocken, PA, 2020. (cited in p. 44)

International ASTM.
ASTM D6304-20 Standard test method for determination of water in petroleum products, lubricating oils, and additives by coulometric Karl Fischer titration, 2020.
(cited in p. 178)

International ASTM.
ASTM D7214-20 Standard test method for determination of the oxidation of used lubricants by FT-IR using peak area increase calculation, 2020. (cited in p. 130)

International ASTM.
ASTM D7279-20 Standard test method for kinematic viscosity of transparent and opaque liquids by automated Houillon viscometer, 2020. (cited in p. 98)

International ASTM.
ASTM D7418-20 Standard practice for set-up and operation of Fourier Transform Infrared (FT-IR) spectrometers for in-service oil condition monitoring, 2020. (cited in p. 129)

International ASTM.
ASTM D7844-20 Standard test method for condition monitoring of soot in in-service lubricants by trend analysis using Fourier Transform Infrared (FT-IR) Spectrometry, 2020. (cited in pp. 131, 156, 387)

International ASTM.
ASTM D93-20 Standard test methods for flash point by Pensky-Martens closed cup tester, 2020. (cited in p. 164)

International ASTM.
ASTM D445-21 Standard test method for kinematic viscosity of transparent and opaque liquids (and calculation of dynamic viscosity), 2021. (cited in p. 97)

International ASTM.
ASTM D7042-21 Standard test method for dynamic viscosity and density of liquids by Stabinger viscometer (and the calculation of kinematic viscosity), 2021. (cited in p. 104)

International ASTM.
ASTM D974-21 Standard Test Method for Acid and Base Number by Color-Indicator Titration, 2021. (cited in p. 111)

Issa R. I.
Solution of the implicitly discretised fluid flow equations by operator-splitting.
Journal of computational physics, Vol. 62 n^o 1, pp. 40–65, 1986. (cited in p. 417)

Ivanova P. G. and Aneva Z. V.
Assessment and assurance of quality in water measurement by coulometric Karl-Fischer titration of petroleum products.
Accreditation and quality assurance, Vol. 10 n^o 10, pp. 543–549, 2006. (cited in p. 179)

Iwai Y., Honda T., Miyajima T., Yoshinaga S., Higashi M. and Fuwa Y.
Quantitative estimation of wear amounts by real time measurement of wear debris in lubricating oil.
Tribology International, Vol. 43 n^o 1-2, pp. 388–394, 2010. (cited in p. 191)

Jao T. C., Li S., Yatsunami K., Chen S. J., Csontos A. A. and Howe J. M.
Soot characterisation and diesel engine wear.
Lubrication Science, Vol. 16 n^o 2, pp. 111–126, 2004. (cited in p. 370)

Jatoth R., Gugulothu S. K., Gadepalli R. K. S., Burra B. and Rafiuzzama S.
Impact of thermophoresis factor on soot particle trajectories near the in-cylinder wall in a diesel engine.
International Journal of Environmental Science and Technology, pp. 1–16, 2021. (cited in p. 368)

Jefferies A. and Ameye J.
RULER and used engine oil analysis programs.
Tribology & Lubrication Technology, Vol. 54 n^o 5, pp. 29, 1998. (cited in p. 134)

Jiang H., Li T., Wang Y., He P. and Wang B.
The evolution of soot morphology and nanostructure along axial direction in diesel spray jet flames.
Combustion and Flame, Vol. 199, pp. 204–212, 2019. (cited in p. 359)

Jiaqiang E., Xie L., Zuo Q. and Zhang G.
Effect analysis on regeneration speed of continuous regeneration-diesel particulate filter based on NO_2 assisted regeneration.
Atmospheric Pollution Research, Vol. 7 n^o 1, pp. 9–17, 2016. (cited in p. 63)

Johnson D. W.
Lubrication - Tribology, lubricants and additives.
BoD–Books on Demand, 2018. (cited in p. 135)

Johnson T.
Diesel engine emissions and their control.
Platinum Metals Review, Vol. 52 n^o 1, pp. 23–37, 2008. (cited in p. 57)

Johnson T. and Joshi A.
Review of Vehicle Engine Efficiency and Emissions.
SAE International Journal of Engines, Vol. 11 n^o 6, pp. 1307–1330, 2018.
(cited in p. 56)

Johnson T. V.
Diesel emission control in review.
SAE international journal of fuels and lubricants, Vol. 1 n^o 1, pp. 68–81, 2009.
(cited in p. 57)

Jolliffe I. T. and Cadima J.
Principal component analysis: a review and recent developments.
Philosophical Transactions of the Royal Society A: Mathematical, Physical and Engineering Sciences, Vol. 374 n^o 2065, pp. 20150202, 2016. (cited in p. 328)

JuGer J. J. and Crook R. F.
Heat transfer performance of propylene glycol versus ethylene glycol coolant solutions in laboratory testing.
In *International Congress & Exposition*. SAE International, feb 1999. (cited in p. 169)

Karacan Ö, Kök M. V. and Karaaslan U.
Dependence of thermal stability of an engine lubricating oil on usage period.
Journal of thermal analysis and calorimetry, Vol. 55 n^o 1, pp. 109–114, 1999.
(cited in p. 47)

Karlsson A., Magnusson I., Balthasar M. and Mauss F.
Simulation of soot formation under diesel engine conditions using a detailed kinetic soot model.
In *International Fuels & Lubricants Meeting & Exposition*. SAE International, feb 1998.
(cited in p. 418)

Kauffman R. E.
Rapid, portable voltammetric techniques for performing antioxidant, total acid number (TAN) and total base number (TBN) measurements.
Tribology & Lubrication Technology, Vol. 54 n^o 1, pp. 39, 1998. (cited in pp. 109, 132)

Kemp W.
Organic spectroscopy.
Macmillan International Higher Education, 2017. (cited in p. 123)

Kennedy I. M.
Models of soot formation and oxidation.
Progress in Energy and Combustion Science, Vol. 23 n^o 2, pp. 95–132, 1997.
(cited in p. 354)

Khaziev A. A., Sugatov N. N. and Laushkin A. V.
The development of a dependent mathematical model of dielectric properties of an engine oil to the concentration of soot formation.
In *IOP Conference Series: Materials Science and Engineering*, volume 1159, pág. 012094. IOP Publishing, 2021. (cited in p. 370)

Khobragade R., Singh S. K., Shukla P. C., Gupta T., Al-Fatesh A. S. and et al.
Chemical composition of diesel particulate matter and its control.
Catalysis Reviews, Vol. 61 n^o 4, pp. 447–515, 2019. (cited in p. 351)

Kholghy M. R., Veshkini A. and Thomson M. J.
The core–shell internal nanostructure of soot–A criterion to model soot maturity.
Carbon, Vol. 100, pp. 508–536, 2016. (cited in p. 354)

Kittelson D. and Kraft M.
Particle formation and models.
Encyclopedia of Automotive Engineering, pp. 1–23, 2014. (cited in p. 361)

Kittelson D. B.
Engines and nanoparticles: a review.
Journal of aerosol science, Vol. 29 n^o 5-6, pp. 575–588, 1998. (cited in p. 352)

Knecht W.
Diesel engine development in view of reduced emission standards.
Energy, Vol. 33 n^o 2, pp. 264–271, 2008. (cited in p. 56)

Koch M., Tenbohlen S., Hoehlein I. and Blennow J.
Reliability and improvements of water titration by the Karl Fischer technique.
In *Proceedings of the XVth International Symposium on High Voltage Engineering, ISH, Ljubljana, Slovenia*, volume 1, pág. 2, 2007. (cited in pp. 174, 175)

Kokot S., Grigg M., Panayiotou H. and Phuong T. D.
Data interpretation by some common chemometrics methods.
Electroanalysis: An International Journal Devoted to Fundamental and Practical Aspects of Electroanalysis, Vol. 10 n^o 16, pp. 1081–1088, 1998. (cited in p. 299)

Kondo K., Takahashi J. and Aizawa T.
Morphology analysis of wall-deposited diesel soot particles via transmission electron microscope.
SAE International Journal of Fuels and Lubricants, Vol. 7 n^o 3, pp. 683–692, 2014. (cited in p. 360)

Kraft M.
Modelling of particulate processes.
KONA Powder and Particle Journal, Vol. 23, pp. 18–35, 2005. (cited in p. 354)

Kramida A., Ralchenko Y., Reader J. and Team NIST ASD.
Atomic spectra database - NIST standard reference database 78, Version 5.8, 2020. (cited in p. 140)

Kudlaty K.
Attenuated total reflection technique for on-line oil monitoring by means of a FTIR fiber-optic probe.
Technische Universität München, 2004. (cited in p. 389)

Ladommatos N., Abdelhalim S. and Zhao H.
The effects of exhaust gas recirculation on diesel combustion and emissions.
International Journal of Engine Research, Vol. 1 n^o 1, pp. 107–126, 2000. (cited in p. 65)

Ladommatos N., Abdelhalim S. M., Zhao H. and Hu Z.
The dilution, chemical, and thermal effects of exhaust gas recirculation on diesel engine emissions - Part 2: Effects of carbon dioxide.
In *International Fuels & Lubricants Meeting & Exposition*. SAE International, may 1996. (cited in p. 66)

Ladommatos N., Abdelhalim S. M., Zhao H. and Hu Z.
The dilution, chemical, and thermal effects of exhaust gas recirculation on diesel engine emissions - Part 3: Effects of water vapour.
In *International Spring Fuels & Lubricants Meeting & Exposition*. SAE International, may 1997. (cited in p. 66)

Ladommatos N., Abdelhalim S. M., Zhao H. and Hu Z.
The dilution, chemical, and thermal effects of exhaust gas recirculation on diesel engine emissions - Part 4: Effects of carbon dioxide and water vapour.
In *International Spring Fuels & Lubricants Meeting & Exposition*. SAE International, may 1997. (cited in p. 66)

Ladommatos N., Abdelhalim S. M., Zhao Hua and Hu Z.
The dilution, chemical, and thermal effects of exhaust gas recirculation on diesel engine emissions - Part 1: Effect of reducing inlet charge oxygen.
In *International Fuels & Lubricants Meeting & Exposition*. SAE International, may 1996. (cited in p. 66)

Laget O., Malbec L. M., Kashdan J., Dronniou N., Boissard R. and Gastaldi P.
Experimental and numerical investigations on the mechanisms leading to the accumulation of particulate matter in lubricant oil.
SAE International Journal of Engines, Vol. 9 n^o 4, pp. 2030–2043, 2016. (cited in p. 365)

Lantos F.
An unusual twist to the blotter test-the Lantos Method.
Practicing Oil Analysis Magazine, 2002. (cited in p. 380)

Lanz M., De Caro C. A., Rüegg K. and De Agostini A.
Coulometric Karl-Fischer titration with a diaphragm-free cell: cell design and applications.
Food chemistry, Vol. 96 n^o 3, pp. 431–435, 2006. (cited in p. 179)

Lapuerta M., Martos F. J. and Herreros J.
Effect of engine operating conditions on the size of primary particles composing diesel soot agglomerates.
Journal of aerosol science, Vol. 38 n^o 4, pp. 455–466, 2007. (cited in p. 359)

Lattimore T., Wang C., Xu H., Wyszynski M. L. and Shuai S.
Investigation of EGR effect on combustion and PM emissions in a DISI engine.
Applied Energy, Vol. 161, pp. 256–267, 2016. (cited in p. 66)

Lavine B. and Workman J.
Chemometrics.
Analytical chemistry, Vol. 80 n^o 12, pp. 4519–4531, 2008. (cited in p. 297)

Leet J. A., Friesen T. and Shadbourne A.
EGR's effect on oil degradation and intake system performance.
SAE transactions, pp. 347–354, 1998. (cited in p. 66)

Lepperhoff G.
Influences on the particle size distribution of diesel particulate emissions.
Topics in Catalysis, Vol. 16 n^o 1, pp. 249–254, 2001. (cited in p. 360)

Levermore D. M., Josowicz M., Rees W. S. and Janata J.
Headspace analysis of engine oil by gas chromatography/mass spectrometry.
Analytical chemistry, Vol. 73 n^o 6, pp. 1361–1365, 2001. (cited in p. 162)

Liang Z., Chen L., Alam M. S., Rezaei S. Z., Stark C., Xu H. and Harrison R. M.
Comprehensive chemical characterization of lubricating oils used in modern vehicular engines utilizing GC× GC-TOFMS.
Fuel, Vol. 220, pp. 792–799, 2018. (cited in p. 162)

Lignell D. O., Chen J. H., Smith P. J., Lu T. and Law C. K.
The effect of flame structure on soot formation and transport in turbulent nonpremixed flames using direct numerical simulation.
Combustion and Flame, Vol. 151 n^o 1-2, pp. 2–28, 2007. (cited in p. 354)

Lindon J. C., Tranter G. E. and Koppenaal D.
Encyclopedia of spectroscopy and spectrometry.
Academic Press, 2016. (cited in p. 332)

Liu C., Nemoto S. and Ogano S.
Effect of soot properties in diesel engine oils on frictional characteristics.
Tribology Transactions, Vol. 46 n^o 1, pp. 12–18, 2003. (cited in p. 370)

Liu N., Zheng Z. C. and Li G. X.
Analysis of the blow-by in piston ring pack of the diesel engine.
Chemical Engineering Transactions, Vol. 46, pp. 1045–1050, 2015. (cited in p. 366)

Liu P. and Wang C.
The diesel soot particles fractal growth model and its agglomeration control.
In *Kinetic Modelling for Environmental Systems.* IntechOpen, 2018. (cited in p. 360)

Ljubas D., Krpan H. and Matanović I.
Influence of engine oils dilution by fuels on their viscosity, flash point and fire point.
Nafta: exploration, production, processing, petrochemistry, Vol. 61 n^o 2, pp. 73–79, 2010. (cited in p. 81)

Lloyd A. C. and Cackette T. A.
Diesel engines: environmental impact and control.
Journal of the Air & Waste Management Association, Vol. 51 n^o 6, pp. 809–847, 2001. (cited in p. 56)

Lockwood F. E., Zhang Z. G., Choi S. and Yu W.
Effect of soot loading on the thermal characteristics of diesel engine oils.
In *Vehicle Thermal Management Systems Conference & Exposition.* SAE International, jan 2001. (cited in p. 369)

Luong J., Gras R., Cortes H. J. and Shellie R. A.
Determination of trace ethylene glycol in industrial solvents and lubricants using phenyl boronic acid derivatization and multidimensional gas chromatography.
Analytica Chimica Acta, Vol. 805, pp. 101–106, 2013. (cited in p. 184)

Macián V., Tormos B., Bastidas S. and Pérez T.
Improved fleet operation and maintenance through the use of low viscosity engine oils: Fuel economy and oil performance.
Eksploatacja i Niezawodność, Vol. 22 n^o 2, 2020. (cited in p. 3)

Macián V., Tormos B., Bermúdez V. and Ramírez L.
Assessment of the effect of low viscosity oils usage on a light duty diesel engine fuel consumption in stationary and transient conditions.
Tribology International, Vol. 79, pp. 132–139, 2014. (cited in p. 3)

Macián V., Tormos B., García-Barberá A. and Tsolakis A.
Applying chemometric procedures for correlation the FTIR spectroscopy with the new thermometric evaluation of Total Acid Number and Total Basic Number in engine oils.
Chemometrics and Intelligent Laboratory Systems, Vol. 208, pp. 104215, 2021.
(cited in p. 332)

Macián V., Tormos B., Miró G. and Pérez T.
Assessment of low-viscosity oil performance and degradation in a heavy duty engine real-world fleet test.
Proceedings of the Institution of Mechanical Engineers, Part J: Journal of Engineering Tribology, Vol. 230 n^o 6, pp. 729–743, 2016. (cited in p. 3)

Macián V., Tormos B., Ruiz S. and García-Barberá A.
An alternative procedure to quantify soot in engine oil by ultraviolet-visible spectroscopy.
Tribology Transactions, Vol. 62 n^o 6, pp. 1063–1071, 2019. (cited in pp. 398, 403)

Macián V., Tormos B., Ruíz S. and Miró G.
Low viscosity engine oils: Study of wear effects and oil key parameters in a heavy duty engine fleet test.
Tribology International, Vol. 94, pp. 240–248, 2016. (cited in p. 3)

Macián V., Tormos B., Ruiz S., Miró G. and Pérez T.
Evaluation of low viscosity engine wear effects and oil performance in heavy duty engines fleet test.
In *International Powertrain, Fuels & Lubricants Meeting*. SAE International, jan 2014.
(cited in p. 3)

Macián V., Tormos B., Ruíz S. and Ramírez L.
Potential of low viscosity oils to reduce CO_2 emissions and fuel consumption of urban buses fleets.
Transportation Research Part D: Transport and Environment, Vol. 39, pp. 76–88, 2015.
(cited in p. 3)

Mackosko C. W.
Rheology: principles, measurements and applications.
Wiley-VCH, 1994. (cited in p. 94)

Mainwaring R.
Soot and wear in heavy duty diesel engines.
In *International Spring Fuels & Lubricants Meeting & Exposition*. SAE International, may 1997. (cited in p. 369)

Malkin A. Y. and Isayev A. I.
Rheology: concepts, methods, and applications.
Elsevier, 2017. (cited in p. 94)

Mang T. and Dresel W.
Lubricants and lubrication.
John Wiley & Sons, 2007. (cited in pp. 16, 94)

Mansurov Z. A.
Soot formation in combustion processes.
Combustion, Explosion and Shock Waves, Vol. 41 n^o 6, pp. 727–744, 2005.
(cited in p. 352)

Maricq M. M.
Chemical characterization of particulate emissions from diesel engines: A review.
Journal of Aerosol Science, Vol. 38 n^o 11, pp. 1079–1118, 2007. (cited in p. 363)

Mark H. and Workman J.
Chemometrics in spectroscopy.
Elsevier, 2010. (cited in p. 301)

Martin J., Boehman A., Topkar R., Chopra S., Subramaniam U. and Chen H.
Intermediate combustion modes between conventional Diesel and RCCI.
SAE International Journal of Engines, Vol. 11 n^o 6, pp. 835–860, 2018.

Marx N., Fernández L., Barceló F. and Spikes H.
Shear thinning and hydrodynamic friction of viscosity modifier-containing oils. Part I: shear thinning behaviour.
Tribology Letters, Vol. 66 n^o 3, pp. 92, 2018. (cited in pp. 40, 41)

Marzban M., Packirisamy M. and Dargahi J.
3D suspended polymeric microfluidics (SPMF3) with flow orthogonal to bending (FOB) for fluid analysis through kinematic viscosity.
Applied Sciences, Vol. 7 n^o 10, pp. 1048, 2017. (cited in p. 108)

Mathis U., Mohr M., Kaegi R., Bertola A. and Boulouchos K.
Influence of diesel engine combustion parameters on primary soot particle diameter.
Environmental science & technology, Vol. 39 n^o 6, pp. 1887–1892, 2005. (cited in p. 360)

Michelsen H. A.
Probing soot formation, chemical and physical evolution, and oxidation: A review of in situ diagnostic techniques and needs.
Proceedings of the Combustion Institute, Vol. 36 n^o 1, pp. 717–735, 2017.
(cited in p. 354)

Miller J. and Miller J. C.
Statistics and chemometrics for analytical chemistry.
Pearson Education, 2018. (cited in p. 297)

Miró Mezquita G., Tormos B., Allmaier H. and Knauder C.
Current trends in ICE wear detection technologies: from lab to field.
ASRO Journal of Applied Mechanics, Vol. 2 n^o 1, pp. 32–41, 2017. (cited in p. 192)

Mohan B., Yang W. and kiang Chou S.
Fuel injection strategies for performance improvement and emissions reduction in compression ignition engines–A review.
Renewable and Sustainable Energy Reviews, Vol. 28, pp. 664–676, 2013. (cited in p. 57)

Mohankumar S. and Senthilkumar P.
Particulate matter formation and its control methodologies for diesel engine: A comprehensive review.
Renewable and Sustainable Energy Reviews, Vol. 80, pp. 1227–1238, 2017.
(cited in p. 351)

Moldanová J., Fridell E., Winnes H., Holmin-Fridell S., Boman J. and et al.
Physical and chemical characterisation of PM emissions from two ships operating in European Emission Control Areas.
Atmospheric Measurement Techniques, Vol. 6 n^o 12, pp. 3577–3596, 2013.
(cited in p. 363)

Moore G. L.
Introduction to inductively coupled plasma atomic emission spectrometry.
Elsevier, 2012. (cited in p. 139)

Mortier R. M., Orszulik S. T. and Fox M. F.
Chemistry and technology of lubricants, volume 107115.
Springer, 2010. (cited in p. 15)

Mosbach S., Celnik M. S., Raj A., Kraft M., Zhang H. R. and et al.
Towards a detailed soot model for internal combustion engines.
Combustion and Flame, Vol. 156 n^o 6, pp. 1156–1165, 2009. (cited in p. 354)

Munro R.
Blow-by in relation to piston and ring features.
SAE Transactions, pp. 2804–2811, 1981. (cited in p. 365)

Murtagh F. and Heck A.
Multivariate data analysis, volume 131.
Springer Science & Business Media, 2012. (cited in p. 300)

Muthuvel P., George B. and Ramadass G. A.
Magnetic-capacitive wear debris sensor plug for condition monitoring of hydraulic systems.
IEEE Sensors Journal, Vol. 18 n^o 22, pp. 9120–9127, 2018. (cited in p. 192)

Myle B. and Kauffman R.
The use of cyclic voltammetric antioxidant analysis for proactive engine oil condition monitoring program.
In *Spring Fuels & Lubricants Meeting & Exposition*. SAE International, jan 2000.
(cited in p. 134)

Nadkarni R. A. K. and Lane J. L.
Determination of kinematic viscosity of used lubricating oils using Houillon viscometer.
Journal of ASTM International, Vol. 8 n^o 7, pp. 1–11, 2011. (cited in p. 99)

Næs T., Isaksson T., Fearn T. and Davies T.
A user-friendly guide to multivariate calibration and classification, volume 6.
NIR Chichester, 2002. (cited in p. 299)

Neer A. and Koylu U. O.
Effect of operating conditions on the size, morphology, and concentration of submicrometer particulates emitted from a diesel engine.
Combustion and flame, Vol. 146 n^o 1-2, pp. 142–154, 2006. (cited in p. 360)

Nguele R., Al-Salim H. S. and Mohammad K.
Modelling and forecasting of depletion of additives in car engine oils using attenuated total reflectance fast transform infrared spectroscopy.
Lubricants, Vol. 2 n^o 4, pp. 206–222, 2014. (cited in p. 390)

Niculescu R., Iorga-Simăn V., Trică A. and Clenci A.
Study on the engine oil's wear based on the flash point.
IOP Conference Series: Materials Science and Engineering, Vol. 147 n^o 1, pp. 012124, aug 2016. (cited in p. 164)

Niessner R.
The many faces of soot: characterization of soot nanoparticles produced by engines.
Angewandte Chemie International Edition, Vol. 53 n^o 46, pp. 12366–12379, 2014. (cited in p. 357)

Nordmark U. and Cedergren A.
Conditions for accurate Karl-Fischer coulometry using diaphragm-free cells.
Analytical chemistry, Vol. 72 n^o 1, pp. 172–179, 2000. (cited in p. 178)

of Standards National Insitute and Technology.
NIST Chemistry WebBook, SRD 69: Water.
`https://webbook.nist.gov/cgi/cbook.cgi?ID=C7732185&Type=IR-SPEC&Index=1`, oct 2021. (cited in p. 181)

O'Haver T.
A pragmatic introduction to signal processing.
University of Maryland at College Park, 2021. (cited in p. 299)

Olfert J. and Rogak S.
Universal relations between soot effective density and primary particle size for common combustion sources.
Aerosol Science and Technology, Vol. 53 n^o 5, pp. 485–492, 2019. (cited in p. 362)

Omidvarborna H., Kumar A. and Kim D.
Recent studies on soot modelling for diesel combustion.
Renewable and Sustainable Energy Reviews, Vol. 48, pp. 635–647, 2015. (cited in p. 354)

Otto M.
Chemometrics: statistics and computer application in analytical chemistry.
John Wiley & Sons, 2016. (cited in pp. 297, 298)

Owen T.
Fundamentals of UV-visible spectroscopy.
Agilent Technologies, 2008. (cited in p. 394)

Pawlak Z.
Tribochemistry of lubricating oils.
Elsevier, 2003. (cited in p. 20)

Pawlyta M. and Hercman H.
Transmission electron microscopy (TEM) as a tool for identification of combustion products: application to black layers in speleothems.
In *Annales Societatis Geologorum Poloniae*, volume 86, 2016. (cited in p. 360)

Payri F. and Desantes J. M.
Motores de combustión interna alternativos.
Editorial Universitat Politècnica de València, 2011. (cited in p. 50)

Peng Y., Wu T., Wang S. and Peng Z.
Wear state identification using dynamic features of wear debris for on-line purpose.
Wear, Vol. 376, pp. 1885–1891, 2017. (cited in p. 192)

Perkampus H.
UV-VIS Spectroscopy and its applications.
Springer Science & Business Media, 2013. (cited in p. 393)

Phelps III F. M.
MIT wavelength tables. Second Edition, Volume 2: Wavelengths by element.
Cambridge: Massachusetts Institute of Technology (MIT) Press, 1982. (cited in p. 140)

Piloyan G. O. and Dolinina Y. V.
On the theory of thermometric titration.
Talanta, Vol. 21 n^o 9, pp. 975–978, 1974. (cited in p. 114)

Pirro D. M., Webster M. and Daschner E.
Lubrication fundamentals, revised and expanded.
CRC Press, 2016. (cited in p. 16)

Prasad R. and Bella V. R.
A review on diesel soot emission, its effect and control.
Bulletin of Chemical Reaction Engineering & Catalysis, Vol. 5 n^o 2, pp. 69, 2010.
(cited in p. 351)

Regulation EC.
Regulation (EC) No 595/2009 of the European Parliament and of the Council of 18 June 2009 on type-approval of motor vehicles and engines with respect to emissions from heavy duty vehicles (Euro VI) and on access to vehicle repair and maintenance information and amending Regulation (EC) No 715/2007 and Directive 2007/46/EC and repealing Directives 80/1269/EEC, 2005/55/EC and 2005/78/EC.
Official Journal of the European Communities L, Vol. 188, 2009. (cited in p. 56)

Reham S. S., Masjuki H. H., Kalam M. A., Shancita I., Fattah I. M. R. and Ruhul A. M.
Study on stability, fuel properties, engine combustion, performance and emission characteristics of biofuel emulsion.
Renewable and Sustainable Energy Reviews, Vol. 52, pp. 1566–1579, 2015.
(cited in p. 350)

Reitz R. D. and Diwakar R.
Structure of high-pressure fuel sprays.
In *International Congress & Exposition*. SAE International, feb 1987. (cited in p. 418)

Reitz R. D., Ogawa H., Payri R., Fansler T., Kokjohn S. and et al.
IJER editorial: The future of the internal combustion engine.
International Journal of Engine Research, Vol. 21 n^o 1, pp. 3–10, 2020. (cited in p. 350)

Reşitoğlu İ. A., Altinişik K. and Keskin A.
The pollutant emissions from diesel-engine vehicles and exhaust aftertreatment systems.
Clean Technologies and Environmental Policy, Vol. 17 n^o 1, pp. 15–27, 2015.
(cited in p. 351)

Richter W. and Tinner U.
Practical aspects of modern titration, 2004. (cited in pp. 111, 113)

Rinkinen J. and Elo L.
Clean components of fluid power system reduce maintenance costs.
In *International conference on maintenance, condition monitoring and diagnostics, and maintenance performance measurement and management*, pp. 81–88, 2015.
(cited in p. 193)

Rissler J., Messing M. E., Malik A. I., Nilsson P. T., Nordin E. Z. and et al.
Effective density characterization of soot agglomerates from various sources and comparison to aggregation theory.
Aerosol Science and Technology, Vol. 47 n^o 7, pp. 792–805, 2013. (cited in p. 362)

Rönkkö T., Lähde T., Heikkilä J., Pirjola L., Bauschke U. and et al.
Effects of gaseous sulphuric acid on diesel exhaust nanoparticle formation and characteristics.
Environmental science & technology, Vol. 47 n^o 20, pp. 11882–11889, 2013.
(cited in p. 364)

Rubinson K. A. and Rubinson J. F.
Análisis instrumental.
Pearson Publications Company, 2001. (cited in p. 123)

Rudnick L. R.
Synthetics, mineral oils, and bio-based lubricants: chemistry and technology.
CRC press, 2005. (cited in p. 16)

Rudnick L. R. and Shubkin R. L.
Synthetic lubricants and high-performance functional fluids, revised and expanded.
CRC Press, 1999. (cited in p. 19)

Ruppel T. D. and Hall G.
Determination of ethylene glycol in used engine oil by headspace-gas chromatography.
PerkinElmer Life and Analytical Sciences, 2005. (cited in p. 184)

Russell A. and Epling W. S.
Diesel oxidation catalysts.
Catalysis Reviews, Vol. 53 n^o 4, pp. 337–423, 2011. (cited in p. 59)

Ryason P. R., Hillyer M. J. and Hansen T. P.
Infrared absorptivities of several diesel engine soots; application to the analysis of soot in used engine oils.
In *International Fuels & Lubricants Meeting & Exposition*. SAE International, oct 1994.
(cited in p. 387)

Sánchez R.l, Todolí J. L., Lienemann C. and Mermet J.
Determination of trace elements in petroleum products by inductively coupled plasma techniques: a critical review.
Spectrochimica Acta Part B: Atomic Spectroscopy, Vol. 88, pp. 104–126, 2013.
(cited in p. 139)

Schlemmer G., Balcaen L., Todolí J. L. and Hinds M. W.
Elemental analysis: An introduction to modern spectrometric techniques.
Walter de Gruyter GmbH & Co KG, 2019. (cited in p. 141)

Schulz F., Commodo M., Kaiser K., De Falco G., Minutolo P. and et al.
Insights into incipient soot formation by atomic force microscopy.
Proceedings of the Combustion Institute, Vol. 37 n^o 1, pp. 885–892, 2019.
(cited in p. 358)

Scientific Spectro.
Guide to measuring fuel dilution in lubricating oil, 2017. (cited in p. 167)

Scientific Spectro.
Guide to measuring water in oil, 2017. (cited in p. 170)

Seifert W. W. and Desjardins J. B.
Measurement of soot in diesel engine lubricating oil.
In *International Congress & Exposition*. SAE International, feb 1995.
(cited in pp. 373, 380)

Sejkorová M., Kučera M., Hurtová I. and Voltr O.
Application of FTIR-ATR spectrometry in conjunction with multivariate regression methods for viscosity prediction of worn-out motor oils.
Applied Sciences, Vol. 11 n^o 9, pp. 3842, 2021. (cited in p. 390)

Severa L., Havlíček M. and Kumbár V.
Temperature dependent kinematic viscosity of different types of engine oil.
Acta Universitatis Agriculturae et Silviculturae Mendelianae Brunensis, Vol. 57 n^o 4, pp. 95–102, 2009. (cited in pp. 68, 102)

Severa L., Havlíček M. and Kumbár V.
Temperature dependent kinematic viscosity of different types of engine oils.
Acta Universitatis Agriculturae et Silviculturae Mendelianae Brunensis, Vol. 57 n^o 4, pp. 95–102, 2014. (cited in p. 38)

Sharma B. and Gandhi O. P.
Reliability analysis of engine oil using "polygraph approach".
Industrial Lubrication and Tribology, 2008. (cited in p. 94)

Sharma V., Uy D., Gangopadhyay A., O'Neill A., Paxton W. A. and et al.
Structure and chemistry of crankcase and exhaust soot extracted from diesel engines.
Carbon, Vol. 103, pp. 327–338, 2016. (cited in p. 364)

Sherman F. B.
Determination of water with a modified Karl-Fischer reagent–Stability and the mechanism of reaction with water.
Talanta, Vol. 27 n^o 12, pp. 1067–1072, 1980. (cited in p. 175)

Siegla D.
Particulate carbon: formation during combustion.
Springer Science & Business Media, 2013. (cited in p. 356)

Smith B. C.
Fundamentals of Fourier Transform Infrared Spectroscopy.
CRC press, 2011. (cited in p. 120)

Smith T.
Practical thermometric titrimetry, 2006. (cited in p. 119)

Sneddon J.
Sample introduction in atomic spectroscopy.
Elsevier, 2012. (cited in p. 143)

Song B. and Choi Y.
Investigation of variations of lubricating oil diluted by post-injected fuel for the regeneration of DPF and its effects on engine wear.
Journal of mechanical science and technology, Vol. 22 n^o 12, pp. 2526–2533, 2008. (cited in p. 63)

Spearot J. A.
High-temperature, high-shear (HTHS) oil viscosity: measurement and relationship to engine operation, volume 1068.
ASTM International, 1989. (cited in p. 211)

Speight J. G.
The chemistry and technology of petroleum.
CRC press, 2014. (cited in p. 14)

Squaiella L. L. F., Martins C. A. and Lacava P. T.
Strategies for emission control in diesel engine to meet Euro VI.
Fuel, Vol. 104, pp. 183–193, 2013. (cited in p. 57)

Stachowiak G. W. and Batchelor A. W.
Engineering tribology.
Butterworth-Heinemann, 2013. (cited in p. 35)

Stanmore B. R., Brilhac J. F. and Gilot P.
The oxidation of soot: a review of experiments, mechanisms and models.
carbon, Vol. 39 n^o 15, pp. 2247–2268, 2001. (cited in p. 354)

STAR-CD. Version 4.22.
Methodology, 2016. (cited in p. 417)

Stehouwer D. M. and Hudgens R. D.
Coolant contamination of diesel engine oils.
In *International Congress & Exposition*. SAE International, jan 1987. (cited in pp. 170, 172)

Stepina V. and Vesely V.
Lubricants and special fluids, volume 23.
Elsevier, 1992. (cited in pp. 16, 20, 38)

Stuart B. H.
Infrared spectroscopy: fundamentals and applications.
John Wiley & Sons, 2004. (cited in pp. 120, 123)

Tan S. M., Ng H. K. and Gan S.
CFD modelling of soot entrainment via thermophoretic deposition and crevice flow in a diesel engine.
Journal of Aerosol Science, Vol. 66, pp. 83–95, 2013. (cited in p. 366)

Tang Z., Feng Z., Jin P., Fu X. and Chen H.
The soot handling ability requirements and how to solve soot related viscosity increases of heavy duty diesel engine oil.
Industrial Lubrication and Tribology, 2017. (cited in p. 369)

Taylor R. I. and de Kraker B. R.
Shear rates in engines and implications for lubricant design.
Proceedings of the Institution of Mechanical Engineers, Part J: Journal of Engineering Tribology, Vol. 231 n^o 9, pp. 1106–1116, 2017. (cited in p. 40)

Tesner P. A.
Formation of soot particles.
In *Faraday Symposia of the Chemical Society*, volume 7, pp. 104–108. Royal Society of Chemistry, 1973. (cited in p. 354)

Timm D., Kurowski C., Grummisch U., Meyhack U. and Grunewald H.
Applications of near infrared spectroscopy for qualification of lubricants and other mineral oil products.
Journal of Near Infrared Spectroscopy, Vol. 6 n^o A, pp. A243–A246, 1998.
(cited in p. 333)

Tissot B. P. and Welte D. H.
Petroleum formation and occurrence.
Springer Science & Business Media, 2013. (cited in p. 14)

Tokura N., Terasaka K. and Yasuhara S.
Process through which soot intermixes into lubricating oil of a diesel engine with exhaust gas recirculation.
In *International Congress & Exposition*. SAE International, feb 1982.
(cited in pp. 364, 365)

Tomanik E., Sobrinho R. and Zecchinelli R.
Influence of top ring end gap types at blow-by of internal combustion engines.
In *SAE Brasil*. SAE International, oct 1993. (cited in p. 366)

Toms A. M., Powell J. R. and Dixon J.
The utilization of FT-IR for Army oil condition monitoring, 1998. (cited in p. 165)

Torbacke M., Rudolphi Å. K. and Kassfeldt E.
Lubricants: introduction to properties and performance.
John Wiley & Sons, 2014. (cited in p. 29)

Tormos B.
Diagnóstico de motores diesel mediante el análisis del aceite usado.
Reverté, 2005. (cited in pp. 94, 156)

Tormos B., Novella R., Gomez-Soriano J., García-Barberá A., Tsuji N., Uehara I. and Alonso M.
Study of the influence of emission control strategies on the soot content and fuel dilution in engine oil.
Tribology International, Vol. 136, pp. 285–298, 2019. (cited in p. 413)

Tormos B., Pla B., Bastidas S., Ramírez L. and Pérez T.
Fuel economy optimization from the interaction between engine oil and driving conditions.
Tribology International, Vol. 138, pp. 263–270, 2019. (cited in p. 3)

Tormos B., Ramírez L., Johansson J., Björling M. and Larsson R.
Fuel consumption and friction benefits of low viscosity engine oils for heavy duty applications.
Tribology International, Vol. 110, pp. 23–34, 2017. (cited in p. 3)

Torregrosa A., Olmeda P., Martín J. and Romero C.
A tool for predicting the thermal performance of a diesel engine.
Heat transfer engineering, Vol. 32 n^o 10, pp. 891–904, 2011. (cited in p. 53)

Tree D. R. and Svensson K. I.
Soot processes in compression ignition engines.
Progress in energy and combustion science, Vol. 33 n^o 3, pp. 272–309, 2007.
(cited in p. 354)

Tripathi A. and Vinu R.
Characterization of thermal stability of synthetic and semi-synthetic engine oils.
Lubricants, Vol. 3 n^o 1, pp. 54–79, 2015. (cited in p. 47)

van de Voort F. R., Sedman J., Cocciardi R. and Juneau S.
An automated FTIR method for the routine quantitative determination of moisture in lubricants: An alternative to Karl-Fischer titration.
Talanta, Vol. 72 n^o 1, pp. 289–295, 2007. (cited in p. 182)

Van De Voort F. R., Sedman J., Cocciardi R. A. and Pinchuk D.
FTIR condition monitoring of in-service lubricants: ongoing developments and future perspectives.
Tribology Transactions, Vol. 49 n^o 3, pp. 410–418, 2006. (cited in p. 130)

Van Loon J. C.
Analytical atomic absorption spectroscopy: selected methods.
Elsevier, 2012. (cited in p. 141)

Varmuza K. and Filzmoser P.
Introduction to multivariate statistical analysis in chemometrics.
CRC press, 2016. (cited in p. 299)

Verhoef J. C. and Barendrecht E.
Mechanism and reaction rate of the Karl-Fischer titration reaction: Part I. Potentiometric measurements.
Journal of Electroanalytical Chemistry and Interfacial Electrochemistry, Vol. 71 n^o 3, pp. 305–315, 1976. (cited in p. 175)

Viswanath D. S., Ghosh T. K., Prasad D. H. L., Dutt N. V. K. and Rani K. Y.
Viscosity of liquids: theory, estimation, experiment, and data.
Springer Science & Business Media, 2007. (cited in p. 95)

Wakiru J., Pintelon L., Chemweno P. and Muchiri P.
Analysis of lubrication oil contamination by fuel dilution with application of cluster analysis.
In *Proceedings of the XVII International Scientific Conference on Industrial Systems, University of Novi Sad, Novi Sad, Serbia*, pp. 4–6, 2017. (cited in p. 166)

Wakiru J. M., Pintelon L., Muchiri P. N. and Chemweno P. K.
A review on lubricant condition monitoring information analysis for maintenance decision support.
Mechanical Systems and Signal Processing, Vol. 118, pp. 108–132, 2019. (cited in p. 192)

Wang H., Ge Y., Tan J., Hao L., Wu L. and et al.
Ash deposited in diesel particular filter: a review.
Energy Sources, Part A: Recovery, Utilization, and Environmental Effects, Vol. 41 n^o 18, pp. 2184–2193, 2019. (cited in p. 62)

Wang Q. J. and Chung Y.
Encyclopedia of tribology.
Springer, 2013. (cited in pp. 16, 21)

Wang X. and Cao Y.
Characterizations of absorption, scattering, and transmission of typical nanoparticles and their suspensions.
Journal of Industrial and Engineering Chemistry, Vol. 82, pp. 324–332, 2020. (cited in p. 394)

Wang Y., Liang X., Shu G. and Dong L.
Impact of lubricating oil on morphology of particles from a diesel engine.
Energy Procedia, Vol. 75, pp. 2388–2393, 2015. (cited in p. 360)

Wattrus M.
Fuel property effects on oil dilution in diesel engines.
SAE International Journal of Fuels and Lubricants, Vol. 6 n^o 3, pp. 794–806, 2013. (cited in p. 81)

Wei H., Wenjian C., Shaoping W. and Tomovic M. M.
Mechanical wear debris feature, detection, and diagnosis: A review.
Chinese Journal of Aeronautics, Vol. 31 n^o 5, pp. 867–882, 2018. (cited in p. 191)

Wen S. and Huang P.
Principles of tribology.
John Wiley & Sons, 2012. (cited in p. 35)

Wichmann H. E.
Diesel exhaust particles.
Inhalation toxicology, Vol. 19 n^o sup1, pp. 241–244, 2007. (cited in p. 363)

Wiedenhoefer J. F. and Reitz R. D.
Multidimensional modelling of the effects of radiation and soot deposition in heavy-duty diesel engines.
In *World Congress & Exhibition*. SAE International, mar 2003. (cited in p. 418)

Winge R. K., Peterson V. J. and Fassel V. A.
Inductively coupled plasma-atomic emission spectroscopy: prominent lines.
Applied Spectroscopy, Vol. 33 n^o 3, pp. 206–219, 1979. (cited in p. 140)

Wolak A.
TBN performance study on a test fleet in real-world driving conditions using present-day engine oils.
Measurement, Vol. 114, pp. 322–331, 2018. (cited in p. 457)

Wolak A., Zajac G. and Slowik T.
Measuring kinematic kiscosity of engine oils: a comparison of data obtained from four different devices.
Sensors, Vol. 21 n^o 7, pp. 2530, 2021. (cited in p. 108)

Xi J. and Zhong B. J.
Soot in diesel combustion systems.
Chemical Engineering & Technology: Industrial Chemistry-Plant Equipment-Process Engineering-Biotechnology, Vol. 29 n^o 6, pp. 665–673, 2006. (cited in pp. 353, 358)

Xinkun C.
Atomic Emission Spectroscopy.
Chinese Journal of Analysis Laboratory, Vol. 4, 1991. (cited in p. 141)

Yakhot V. and Orszag S. A.
Renormalization group analysis of turbulence. I. Basic theory.
Journal of scientific computing, Vol. 1 n^o 1, pp. 3–51, 1986. (cited in p. 417)

Yeung V., Miller D. D. and Rutzke M. A.
Atomic absorption spectroscopy, atomic emission spectroscopy, and inductively coupled plasma-mass spectrometry.
In *Food Analysis*, pp. 129–150. Springer, 2017. (cited in p. 141)

Zamora D., Blanco M., Bautista M., Mulero R. and Mir M.
An analytical method for lubricant quality control by NIR spectroscopy.
Talanta, Vol. 89, pp. 478–483, 2012. (cited in p. 334)

Zenchelsky S. T.
Thermometric Titration.
Analytical Chemistry, Vol. 32 n^o 5, pp. 289–292, 1960. (cited in p. 119)

Zhan H., Song Y., Zhao H., Gu J., Yang H. and Li S.
Study of the sensor for on-line lubricating oil debris monitoring.
Sensors & Transducers, Vol. 175 n^o 7, pp. 214, 2014. (cited in p. 192)

Zhan R., Huang Y. and Khair M.
Methodologies to control DPF uncontrolled regenerations.
SAE Transactions, pp. 431–444, 2006. (cited in p. 62)

Zheng M., Reader G. T. and Hawley J. G.
Diesel engine exhaust gas recirculation—-a review on advanced and novel concepts.
Energy conversion and management, Vol. 45 n^o 6, pp. 883–900, 2004. (cited in p. 65)

Zhu X., Zhong C. and Zhe J.
Lubricating oil conditioning sensors for online machine health monitoring–A review.
Tribology International, Vol. 109, pp. 473–484, 2017. (cited in p. 192)

Zoller U.
Handbook of detergents, Part E: applications.
Surfactant Science. Taylor & Francis, 2008. (cited in p. 32)